The Roles of Hsp70 Proteins in Antigen Processing and Presentation

Christopher Charles Winchester,

St. Catherine's College.

A thesis submitted for the degree of Doctor of Philosophy

Trinity Term, 1997.

MRC Immunochemistry Unit,

Department of Biochemistry,

Oxford University.

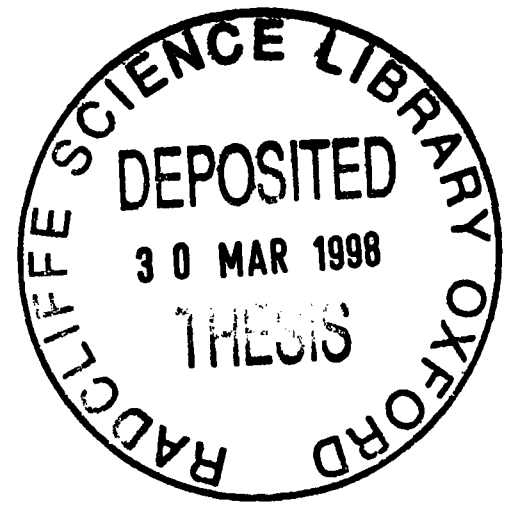

ACKNOWLEDGEMENTS

I would like to thank Caroline Milner and Duncan Campbell for their supervision over the last four years, for helpful discussions and for the care they took correcting my thesis. I would like to thank the following enthusiastically for their help, without which much of the work described in this thesis would not have happened:

Caroline Milner for technical help throughout my research and for the TK143B cells expressing tagged hsp70hom and BiP; Suzanne Jenkins for the purified C-terminal region of hsp70hom; Tony Willis for N-terminal sequencing, amino-acid analysis and help with HPLC and preparation of the pigeon cytochrome c peptide; Guy Stuart for help with plate binding studies and ELISAs; Tony Gascoyne for oligonucleotide synthesis; Andras Purczel, Graeme Shaw and Iain Campbell for NMR spectroscopy; Brian Marsden for the model of the C-terminal region of hsp70hom with bound peptides; Vilmos Fulop for crystallisation trials; Robin Aplin for mass spectrometry; Sheena Radford for help with circular dichroism; Richard Copley for help with the alignment of 166 hsp70s; Claire Thomas, Derek McCusker, Jethro Herberg and John Trowsdale for help with subcellular fractionation, immunoprecipitations and 2-D gel electrophoresis, and for antibodies, Larry Hightower for the peptide FYQLALT for trial binding studies, Lois Greene and Evan Eisenberg for hsc70 purified from bovine brain.

Personal thanks go to members of the lab, unit and department, past and present, for their friendship, advice and technical assistance. I would particularly like to thank Anu, Begona, Caroline, Gloria, Helene, Jo, John, Mark, Matt, Mohamed, Ruth and Suzanne in the lab; Alison, Alvaro, Bing-Bing, Bob, Guy, Ken, Nicky, Sheila, Tim, Viv, Wendy in the rest of the Unit and Ash, Hilke, Stuart and Tony in the department. Many apologies to the people I have forgotten at the last minute.

ABSTRACT:

The Roles of Hsp70 Proteins in Antigen Processing and Presentation

The ability of members of the hsp70 family to bind to peptides *in vivo* and *in vitro* suggests that they may be involved in the processing of antigens for binding to Major Histocompatibility (MHC) class I and/or class II molecules. The aims of this thesis have been to provide evidence for the involvement of hsp70s in antigen processing and to characterise the binding of peptides by hsp70s by structural and functional studies.

Firstly, the peptide-binding domains of two hsp70s, hsp70hom and PBP74, were expressed in isolation from the rest of the molecule for structure determination. Both of these hsp70s were implicated in antigen processing: hsp70hom in the class I pathway, due to its cytoplasmic localisation and constitutive expression, and the presence of its gene in the MHC; and PBP74 in the class II pathway because published work indicated that it was localised to endosomes and that antibodies against it inhibited antigen processing. The expression and purification of both peptide-binding domains was very successful, and one dimensional NMR experiments indicated that they were folded. However, it was not possible to determine their structures by NMR spectroscopy or X-ray crystallography because they aggregated in solution at high concentrations.

Instead, the structure of the C-terminal region of hsp70hom, which includes its peptide-binding domain, was modelled based on the known structure of the equivalent portion of dnaK, the hsp70 of *E.coli*. The structure of hsp70hom is predicted to be very similar to that of dnaK, and modelling studies suggest that it is likely to bind peptides in a closely related fashion. The modelling of complexes between hsp70hom and two peptides suggest that the peptide-binding groove is very versatile, accounting for the broad peptide-binding specificity of hsp70s.

The interactions of hsp70hom and PB74 with peptides were investigated using plate binding assays and isothermal titration calorimetry. A biotinylated peptide bound to the peptide-binding domain of hsp70hom, immobilised in plastic wells, with a Kd of <25 μM, which is within the range of Kds reported for other hsp70-peptide complexes (0.1-100 μM). In solution, isothermal titration calorimetry showed that the binding of peptides to the peptide-binding domains of hsp70hom and PBP74 was likely to be entropically rather than enthalpically driven, and, therefore, the interactions involved are likely to be predominantly hydrophobic.

Secondly, PBP74, an hsp70 thought to be involved in the class II antigen processing pathway in endosomes, was localised by immunofluorescence microscopy. It was shown to be a mitochondrial protein, and is, therefore, unlikely to be involved in antigen processing. The presence of other members of the hsp70 family in lysosomes purified from a B cell line by Percoll density gradient centrifugation was investigated using antibodies that reacted with many different members of the hsp70 family. No hsp70s were detected in these late endocytic compartments, even after heat shock or serum starvation. However, the presence of an hsp70 in endosomes, or of a member of this family not detected by the antibodies used, in lysosomes, cannot be ruled out.

A third approach investigated the induction of the three hsp70 genes found in the MHC by four cytokines. The hsp70-1 and hsp70-2 genes are induced at the mRNA level by IFN-γ and IL-1, while TNF induces hsp70-2 alone. This data supports a role for the heat-inducible hsp70 in MHC class I antigen processing, as it appears to be coregulated with known members of this antigen processing pathway. The expression of hsp70hom was unaffected by any of the four cytokines examined. In addition, the mitochondrial hsp70 (which is not encoded in the MHC) appears to be induced by IFN-γ at the protein level.

The research presented in this thesis provides a greater understanding of the peptide-binding properties of two hsp70s. Further work is necessary to show conclusively whether any of the hsp70s is involved in antigen processing.

Christopher Charles Winchester,
St. Catherine's College, Oxford.

Thesis submitted for D.Phil degree, Trinity Term 1997.

Contents

Abbreviations

Å	angstrom
aka	also known as
APC	class II-expressing antigen presenting cell
ATP	adenosine triphosphate
ATPase	ATP hydrolysing
BCA	bicininchoninic acid
BiP	Immunoglobulin heavy-chain Binding Protein
bp	base pairs
BSA	bovine serum albumin
cDNA	complementary DNA
CDR	complementarity determining region
CLIP	class II-associated invariant chain peptide
CMV	cytomegalovirus
cpm	counts per minute
CSA	C3H-strain specific antigen
Da	dalton
DM	HLA-DM
DMEM	Dulbecco's modified Eagle's medium
DNA	deoxyribonucleic acid
dnaJ	hsp40 of *E. coli*
dnaK	hsp70 of *E. coli*
dNTP	deoxynucleotide triphosphate
EDTA	Ethylenediaminetetraacetic acid
ER	endoplasmic reticulum
FCS	foetal calf serum
gp96	the ER-resident hsp90 (aka grp94)
grp78	78 kDa glucose-regulated protein (BiP)
grpE	ADP/ATP exchange factor of *E. coli*
GST	glutathione-S-transferase
Hip	hsc70-interacting protein
HOM-C	the C-terminal region of hsp70hom
HOM-P	the peptide-binding domain of hsp70hom
Hop	hsp70/hsp90 organising protein
HPLC	high performance liquid chromatography

hsc70	70 kDa heat shock cognate (aka hsp73, hsc73 or prp73)
hsp40	40 kDa heat shock protein
hsp70	70 kDa heat shock protein (aka hsp72)
hsp70hom	hsp70 homologue
hsp90	90 kDa heat shock protein
IFN	interferon
Ii	invariant chain
IL	interleukin
IPTG	isopropyl-ß-thiogalactopyranoside (IPTG)
K_m	Michaelis-Menten constant
LMP	low molecular weight protein
MHC	major histocompatability complex
mIg	membrane-immunoglobulin
MIIC	MHC class II loading compartment
mt	mitochondrial
NMR	nuclear magnetic resonance
OD_{***}	optical density at *** nm
pA28	proteasome associated 28 kDa protein
PAGE	polyacrylamide gel electrophoresis
PBP-P	the peptide-binding domain of PBP74
PBP74	74 kDa peptide-binding protein (aka mt hsp70, CSA, mortalin)
PBS	phosphate buffered saline
RNA	ribonucleic acid
S	Svedberg
SDS	sodium dodecylsulphate
$ß_2m$	$ß_2$-microglobulin
SV40	Simian Virus 40
TAP	Transporter associated with Antigen Processing
TEMED	N,N,N',N'-tetramethylethylenediamine
TNF	Tumour necrosis factor
Tris	Tris(hydroxymethyl)-aminomethane
U	units
Ubc	ubiquitin-conjugating enzyme
X-gal	5-bromo 4-chloro 3-indolyl-ß-galactopyranoside

Chapter 1: Introduction

The Seventy-Kilodalton Heat Shock Proteins

The 70-kDa heat shock proteins (hsp70s) are a family of highly conserved and ubiquitous proteins. They have an essential role in the cell, being involved in folding, unfolding, transporting and degrading other proteins. They are particularly important in situations where environmental stresses cause denatured proteins to accumulate. Members of the hsp70 family were first discovered as being induced by heat shock, although other members of the family are expressed constitutively (reviewed by Tavaria *et al.*, 1996). In humans, there are two heat-induced members of the hsp70 family: hsp70 (which is also expressed constitutively at a low level) (Milner and Campbell, 1990) and hsp70B' (Leung *et al.*, 1990). These, together with the constitutive proteins, hsc70 (Dworniczak and Mirault, 1987), hsp70hom (Milner and Campbell, 1990) and hsp70A2 (Bonnycastle *et al.*, 1994), are expressed in the cytoplasm. In addition, BiP is found in the endoplasmic reticulum (ER) (Ting and Lee, 1988) and mt hsp70 is localised in the mitochondrion (Leustek *et al.*, 1989).

The hsp70 family is remarkably conserved in all organisms studied. For example, human hsp70 is 50% identical to dnaK, its homologue in *Escherichia coli*, and this similarity has been conserved for at least 2 billion years, since before the divergence of the earliest eukaryotes (Boorstein *et al.*, 1994). The human cytoplasmic hsp70s are >75% identical to each other, while the hsp70s found in other organelles are more divergent; BiP is 62-66% identical to the cytoplasmic hsp70s and the mitochondrial hsp70 is 49-50% identical to all the others (Figure 1-1).

% Identity	hsp70-1	hsp70hom	hsp70A2	hsc70	hsp70B'	BiP	PBP74
hsp70-1	100	89 (93)	84 (84)	86 (89)	82 (84)	64 (63)	49 (58)
hsp70hom		100	82 (81)	83 (85)	79 (80)	64 (64)	50 (56)
hsp70A2			100	86 (88)	78 (78)	63 (62)	50 (59)
hsc70				100	77 (80)	66 (64)	50 (60)
hsp70B'					100	62 (58)	49 (55)
BiP						100	49 (55)
PBP74							100

Figure 1-1. A table displaying the sequence identities between members of the hsp70 family in humans. The percentage identities are given for the whole proteins (excluding the leader sequences of PBP74 and BiP) and, in brackets, the peptide-binding domains alone (defined in Chapter 3). The peptide-binding domains are defined as the sequences equivalent to amino acids 384-554 of hsp70hom. The amino acid sequences of hsp70-1 (Milner and Campbell, 1990), hsp70A2 (Bonnycastle *et al.*, 1994), hsp70B' (Leung *et al.*, 1990), hsc70 (Dworniczak and Mirault, 1987), BiP (Ting and Lee, 1988) and PBP74 (Domanico *et al.*, 1993) were obtained from the Swiss Prot protein sequence database (GCG) and the hsp70hom sequence, which differs from the published sequence (Milner and Campbell, 1990) at two positions, V508A and P525T, was obtained from Dr. C. Milner. The identities between the different sequences [excluding the leader peptides of BiP (amino acids 1-22) and PBP74 (amino acids -46 to -1)] were calculated using the program Best Fit (GCG).

Molecular Chaperones

Hsp70s are molecular chaperones, which prevent improper interactions between proteins. Molecular chaperones were originally defined as a group of unrelated proteins that mediate the correct assembly of other proteins, without themselves being part of the final functional structures (Ellis, 1987). It is now clear that molecular chaperones are involved in a far broader range of cellular processes, and this has led to the definition being extended to proteins that bind to and stabilise an otherwise unstable conformation of another protein and, by controlled binding and release, facilitate its correct fate *in vivo* (Hendrick and Hartl, 1993).

The properties of molecular chaperones are best understood in the context of folding nascent proteins and refolding denatured proteins. They recognise unfolded protein substrates through characteristic features such as stretches of unstructured polypeptide chain or exposed hydrophobic residues. Different chaperones recognise different features, allowing them to co-operate efficiently. They generally function through cycles of substrate binding and release, driven by ATP binding and hydrolysis. To understand how chaperones help proteins to fold, we must consider protein folding in their absence.

Anfinsen first observed that a denatured protein (ribonuclease A) can refold spontaneously *in vitro* (Anfinsen, 1973), indicating that all the information necessary for a polypeptide to attain its native state is contained within its amino acid sequence. This conclusion has since been reached for many other proteins, including multi-subunit complexes (Jaenicke, 1987). Protein refolding proceeds through a number of parallel interconnecting pathways during which elements of secondary structure form transiently and become progressively stabilised by the formation of tertiary interactions between them (Creighton, 1990). The discovery of molecular chaperones implies that protein folding inside cells is more complex than in a test-tube. The challenge has been to identify a role for molecular chaperones in which they do not give the folding chain information as to

what its folded structure should be, since Anfinsen showed that the polypeptide 'knows' that already. Two models have been proposed:

1. Molecular chaperones work by preventing the aggregation of intermediates in protein folding with other proteins and with each other. The cytoplasm is crowded with macromolecules (Zimmerman and Trach, 1991) and the concentration of nascent chains in polysomes is very high (Ellis and Hartl, 1996). Molecular chaperones provide an environment in which folding intermediates are protected from aggregating with each other, by coating them or binding them in cavities (Creighton, 1991). Binding by the chaperone anchors the substrate in place, while folding occurs predominantly during the periods of release.

2. Chaperones may play a more active role. Some chaperones can dissolve aggregates of denatured proteins. In this model, chaperones unfold non-productive folding intermediates, which can be seen as intramolecular aggregates (Hubbard and Sander, 1991).

The Functions of Hsp70s

The ability of hsp70s to interact with unfolded and incompletely folded proteins has equipped them to carry out a broad range of related functions in the cell. Hsp70s help proteins that have been newly synthesised in the cytoplasm or newly translocated into an organelle to attain their correct three-dimensional conformation (Hartl, 1996), as discussed above. Furthermore, hsp70s protect denatured proteins from aggregating and dissolve any aggregates that do form, refolding the denatured proteins if possible, or else targetting them for degradation (Gething and Sambrook, 1992). Cytoplasmic hsp70s also play a role in the post-translational translocation of proteins from the cytoplasm into other organelles, such as mitochondria and the endoplasmic reticulum in eukaryotes (Brodsky, 1996) and the prokaryotic periplasm (Phillips and Silhavy, 1990). These proteins are generally

synthesised as precursors with additional amino acids at the N-terminus that are not part of the mature protein. Such a 'leader sequence' allows the protein to be recognised by the appropriate organelle and prevents it from folding prematurely in the cytoplasm. The association of precursor proteins with hsp70s in the cytoplasm helps them to maintain an unfolded and disaggregated state so that they can pass easily through membrane pores. Finally, hsp70s can interact with non-functional proteins and prevent their activation. Thus, steroid hormone receptors form complexes with hsc70 and hsp90 in the cytoplasm. Once the hormone binds, the chaperones are released, allowing the receptor to diffuse to the nucleus to activate gene transcription (Zeigelhoffer *et al.*, 1996; Frydman and Höhfeld, 1997). The immunosuppressant drug deoxyspergualin, which binds to both hsc70 and hsp90 (Nadeau *et al.*, 1994), is thought to prevent steroid hormone receptor activation.

The Hsp70 Reaction Cycle

Hsp70s recognise unfolded proteins through regions of unstructured polypeptide (DeLuca-Flaherty *et al.*, 1990) which they bind in an extended conformation (Palleros *et al.*, 1991; Landry *et al.*, 1992; Langer *et al.*, 1992). They can also bind to peptides (see Chapter 5). Hsp70s bound to ADP form a stable complex with their polypeptide substrates, and ATP binding (but not hydrolysis*) is required for substrate release (Munro and Pelham, 1986; Palleros *et al.*, 1993; Theyssen *et al.*, 1996).

Two models have been proposed for the ATP-driven binding and release of polypeptide and peptide substrates by hsp70s. The affinity model proposes that hsp70s bound to ATP have low affinity for polypeptides while their ADP form has high affinity (Palleros *et al.*, 1993). In this case, substrates bind to the ADP form of hsp70s, and ATP binding triggers substrate release. However, it is a kinetic model that has more experimental support. In

* The fact that binding of the non-hydrolysable ATP analogues ATPγS and AMP-PNP to hsp70s does not induce them to release peptides was thought to mean that the hydrolysis of bound ATP is required for peptide dissociation, until it was discovered that these analogues stabilise hsp70s in an ADP-bound conformation (Palleros *et al.*, 1993).

contrast to the affinity model, it proposes that ATP and ADP-bound hsp70 have the same affinity for substrates, with the ATP form allowing rapid polypeptide binding and release (Schmid *et al.*, 1994) while the ADP form restricts polypeptide exchange (Farr *et al.*, 1995). In this model, substrates bind to the ATP-bound conformation of hsp70s, but only form a stable complex once ATP is hydrolysed. This complex dissociates once the resulting bound ADP is exchanged for ATP. Upon release, the polypeptide substrate has the option of folding, interacting with a different chaperone system or rebinding to the hsp70, depending on its folded state.

These two models imply different conformational changes in hsp70s during polypeptide binding and release. The affinity model implies that the peptide-binding site dissolves upon ATP binding and reforms after ATP hydrolysis. The kinetic model suggests that the binding site itself remains unchanged during the ATPase cycle, but access to and from it is controlled so that peptides can only enter and leave the binding site when ATP is bound.

During the folding of substrate proteins, dnaK (the *E. coli* hsp70) co-operates with two cofactors: dnaJ (a member of the hsp40 chaperone family) and the nucleotide-exchange factor grpE. DnaJ recognises substrates with exposed hydrophobic surfaces and targets them to ATP-bound dnaK (Langer *et al.*, 1992). DnaJ may be released when ADP dissociates from dnaK. Several dnaJ (hsp40) homologues have been described in eukaryotic cells (Cyr *et al.*, 1994), as well as the 42 kDa hsc70-interacting protein (Hip) which, like dnaJ, binds to unfolded proteins and hsp70s, stabilising the latter in the ADP-bound state (Zeigelhoffer *et al.*, 1996; Frydman and Höhfeld, 1997). DnaK co-operates with a second cofactor, grpE, which promotes the dissociation of ADP from dnaK and the subsequent binding of ATP (Liberek *et al.*, 1991). In eukaryotes, no grpE homologues have been discovered outside mitochondria and chloroplasts (Rassow *et al.*, 1995), but the eukaryotic cytoplasm contains hsp70/hsp90 organising protein (Hop) which, like grpE, promotes ADP/ATP exchange (Frydman and Höhfeld, 1997). Hsp70s are regulated by

phosphorylation (Leustek *et al.*, 1992; Panagiotidis *et al.*, 1994) which increases substrate binding (Sherman and Goldberg, 1993). In addition, hsc70 interacts with calmodulin, although the significance of this is not clear (Stevenson and Calderwood, 1990).

The Structure of Hsp70s

Hsp70s consist of an N-terminal ATP-hydrolysing (ATPase) domain (44 kDa, ~380 amino acids) and a C-terminal domain (28 kDa, ~250 amino acids) responsible for binding to unfolded protein substrates. The structure of the ATPase domain of bovine hsc70 (Flaherty *et al.*, 1990) and the C-terminal domain of *E.coli* dnaK (lacking 31 amino acids at its C-terminus) (Zhu *et al.*, 1996) have been solved by X-ray crystallography.

The C-terminal domain consists of a eight ß-strands arranged in two ß-sheets (the ß-subdomain, 110 amino acids) with a long α-helical segment (the α-subdomain, 110 amino acids) towards its C-terminus (Figure 1-2a). The C-terminal domain of dnaK was crystallised with a peptide (NRLLLTG), which was shown to bind to the first four ß-strands and two of the intervening loops, through hydrophobic interactions, hydrogen bonds and van der Waals contacts. The α-helical segment, which lies over the top of the peptide-binding site in the ß-subdomain, may act as a lid, that opens to release the polypeptide substrate from its binding site. In other words, although the α-subdomain forms no contacts with the peptide, it may increase the stability of the complex by sterically hindering the egress of the polypeptide substrate. This explains why peptides are able to bind to an N-terminal 18 kDa (160 amino acids) segment of the C-terminal domain that includes all of the ß-subdomain, known as the peptide-binding domain (Chappell *et al.*, 1987; Wang *et al.*, 1993) (see Chapter 3).

The structure of the ATPase domain of hsc70 (Figure 1-2b) is topologically equivalent to that of hexokinase (Flaherty *et al.*, 1990) and actin (Flaherty *et al.*, 1991). Mg^{2+}-ATP is bound in a cleft between two subdomains which, by analogy with hexokinase, may open

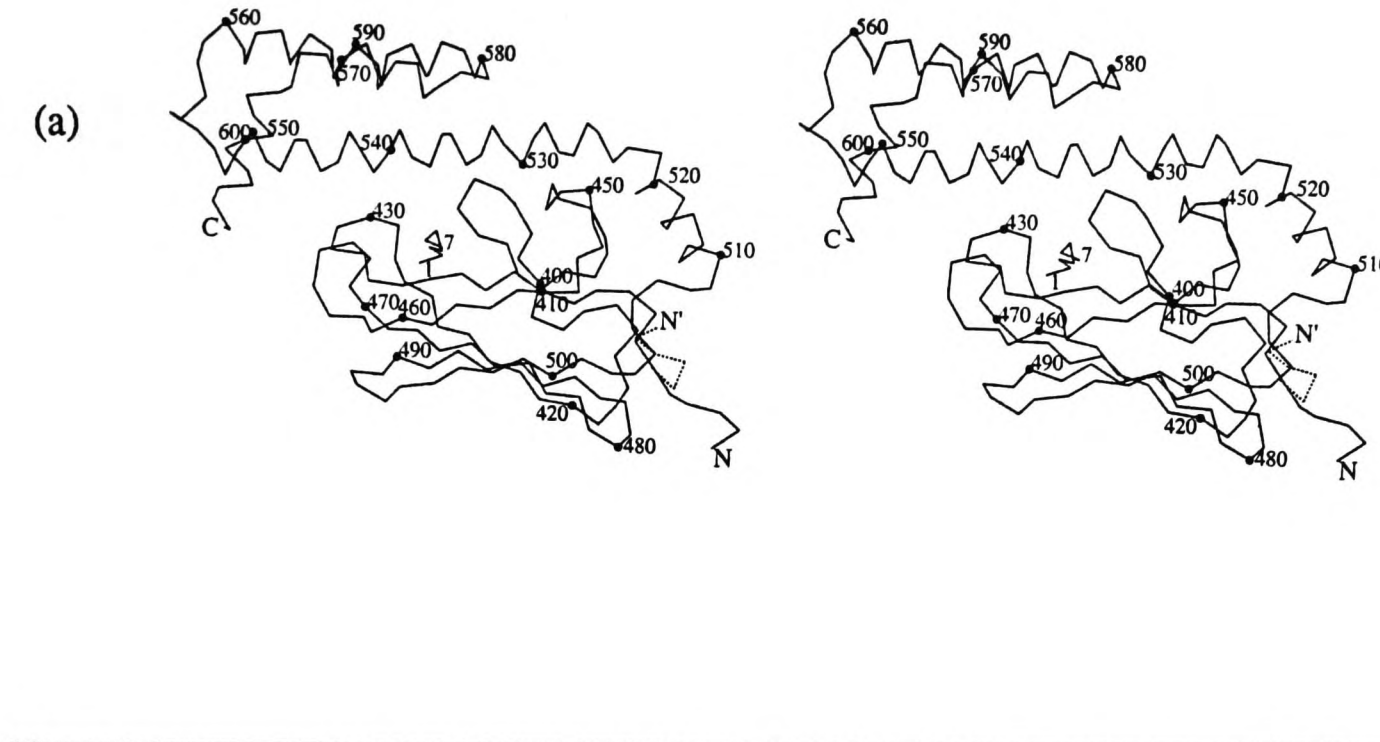

Figure 1-2: The structures of (a) the peptide-binding domain of dnaK complexed with the peptide NRLLLTG and (b) the ATPase domain of hsc70 bound to Mg^{2+}-ATP. The structures were solved by X-ray crystallography at 2.0 Å and 2.2 Å resolution, respectively. The stereo views are reproduced from Zhu *et al.* (1996) and Flaherty *et al.* (1991). A stereoviewer is provided at the end of this thesis.

and close about a central hinge. Binding of ATP would push the two subdomains apart, while ATP hydrolysis and the subsequent loss of inorganic phosphate would allow them to close again. Opening of the two halves of the ATPase domain upon ATP binding may force the α-helical lid of the C-terminal region to open to reveal the peptide-binding site in the ß-subdomain and allow substrate exchange.

A fuller understanding of the structural basis of the hsp70 reaction cycle will depend on determining how conformational changes are transmitted between the ATPase domain and the peptide-binding C-terminal domain. This process involves the C-terminal ~30 amino acids of hsp70s, whose structure is unknown. This C-terminal sequence is the most variable part of the molecule, but ends with a conserved EEVD motif in the eukaryotic cytoplasmic hsp70s. Hsp70 with even one of these amino acids exchanged for alanine (Freeman *et al.*, 1995) or hsc70 from which the C-terminal 10 kDa has been removed by proteolysis (Chappell *et al.*, 1987) have the same defect. Both are able to bind to substrates and hydrolyse ATP, but are unable to co-ordinate ATP binding with substrate release.

Antigen Presentation

T lymphocytes recognise foreign protein antigens as peptides bound to Major Histocompatibility Complex (MHC) molecules on the surface of a cell (reviewed by Abbas *et al.*, 1996). The display of peptides complexed with MHC molecules is called antigen presentation. Two classes of T lymphocytes recognise antigens bound to two structurally distinct families of MHC molecules: cytotoxic T cells recognise antigen bound to MHC class I molecules and helper T cells recognise antigen bound to the related group of MHC class II molecules. MHC class I molecules are found on almost all cells and display antigens derived from inside the cell. Cytotoxic T cells are activated to kill cells carrying foreign antigens complexed with class I molecules by lysis or apoptosis. They are an essential part of antiviral and antitumour immunity. Class II molecules, in contrast, are expressed by specialised antigen presenting cells such as dendritic cells, macrophages and B lymphocytes. They present peptides derived from proteins present in the endocytic pathways of these cells, including antigens taken up from outside the cell. Recognition of antigen by helper T cells leads to the activation of humoral or cell-mediated immunity, such as antibody production or activation of macrophages and neutrophils.

Antigen presentation is constitutive, ensuring that a selection of all available proteins is presented by MHC molecules. Discrimination between self and non-self is determined by the T cell repertoire, which is established during T cell development. Each T cell has a single T cell receptor specificity, which is generated by random genetic recombination to ensure the broadest T cell repertoire. T cells that recognise self are then deleted during their development in the thymus.

The Structure of MHC Molecules

MHC molecules (reviewed by Germain, 1994) are transmembrane glycoproteins consisting of an N-terminal peptide-binding domain supported by two membrane-proximal immunoglobulin domains and anchored by one (class I) or two (class II) transmembrane regions followed by short cytoplasmic domains. The peptide-binding domain comprises two parallel α-helices lying across an antiparallel ß-sheet of eight ß-strands (Figure 1-3). The peptide binds in an extended conformation, in a cleft between the two helices. The MHC molecule binds to the peptide backbone through hydrogen bonds and binds its side chains in deep specificity pockets via hydrogen bonds, electrostatic interactions and Van der Waals contacts.

MHC class I and class II molecules both consist of two subunits, but differ from each other in the arrangement of their domains between these two subunits. The peptide-binding domain of class I molecules, one immunoglobulin domain and the transmembrane and cytoplasmic regions are formed by the α (heavy) chain, which associates with a single soluble immunoglobulin domain, $ß_2$-microglobulin ($ß_2$m). In class II molecules, the two chains (α and ß) each contribute a cytoplasmic region, a transmembrane helix, an immunoglobulin domain and half of the peptide-binding domain (one α-helix and four ß-strands each). In addition, the two classes differ subtly in their peptide-binding groove. A major source of binding energy for class I molecules is through contacts with the N- and C-termini of the peptide. This limits the length of the bound peptide to usually 8-12 amino acids, depending on the class I allotype. In contrast, the binding grooves of class II molecules have open ends and do not restrict the length of peptides that may bind; typically these are 12-24 amino acids long (Rudensky *et al.*, 1991; Chicz *et al.*, 1992; Hunt *et al.*, 1992). Class I molecules generally bind to the peptide through two of its side-chains (known as anchor positions), one, usually a hydrophobic amino acid, at the C-terminus of the peptide, and the other, whose character depends on the class I allotype, near its N-terminus (usually the second amino acid of the peptide). Such an arrangement allows

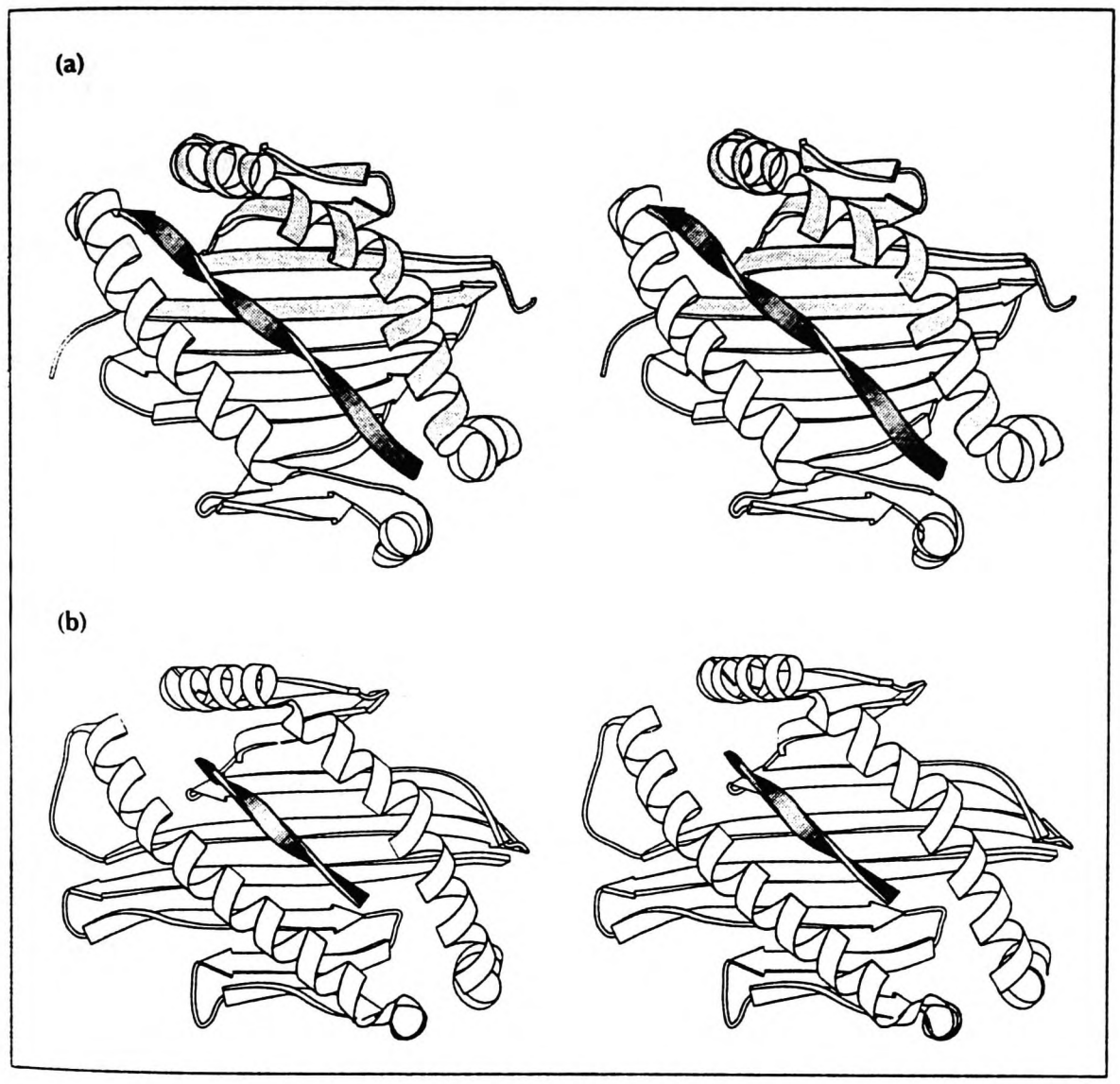

Figure 1-3: The structure of the peptide-binding domains of (a) MHC class I and (b) MHC class II molecules complexed with peptides. The MHC class I molecule is H-2K^b in complex with the peptide FAPGNYLPAL (Fremont *et al.*, 1992) and the MHC class II molecules is HLA-DR1 in complex with the peptide PKYVKQNTLKLAT (Stern *et al.*, 1994). The figures are stereoviews reproduced from Stanfield and Wilson (1995).

amino acids in the centre of the peptide to bulge out of the groove (Fremont *et al.*, 1992; Guo *et al.*, 1992; Madden *et al.*, 1993; Fahnestock *et al.*, 1995); the exceptions are H-2K^b and H-2D^b which anchor their peptides at the centre through a tyrosine or arginine at position 5. The peptide-binding grooves of MHC class II molecules also have pockets that bind specific anchor residues in the peptide, but these are less well defined than for class I molecules. It is interesting to note that the peptide-binding groove of MHC molecules is flexible, so its structure is influenced by the peptides it binds (Madden *et al.*, 1993; Freeman *et al.*, 1995).

T Cell Receptor Structure

T cell recognition of MHC-peptide complexes involves many different interactions. The T cell receptor is made up from two polypeptide chains (α and ß) which are joined by a disulphide bond. Each consists of two immunoglobulin domains, a transmembrane helix and a cytoplasmic tail. The membrane-distal immunoglobulin domains contact the MHC-peptide complex and determine the antigenic specificity of the T cell. It is these domains that vary from receptor to receptor.

The structures of two T cell receptor-MHC class I peptide complexes have recently been determined by X-ray crystallography (Garboczi *et al.*, 1996; Garcia, 1996). They show that the T cell receptor contacts the MHC molecule as well as the antigenic peptide, to generate a strong enough interaction between the T cell and its target. The membrane-distal variable domains of the T cell receptor each provide three loops, known as complementarity determining regions (CDRs), which specify the interaction with MHC-peptide complexes. The variability between T cell receptors is concentrated in these loops, particularly in the CDR3s. The T cell receptor lies diagonally across the MHC-peptide complex so that the two CDR1s lie over the termini of the peptide, the CDR2s contact the α-helices of the MHC molecules and the CDR3s bind to the exposed central portion of the peptide.

T Cell Activation

For a T cell to be activated, its receptors must recognise several hundred identical MHC-peptide complexes (Srinivasan *et al.*, 1991). The T cell receptors aggregate at the site of contact with its target cell and trigger a signalling cascade within the T cell. T cell receptor aggregation may be aided by the ability of T cell receptor-peptide-MHC class I molecule complexes to oligomerise *in vitro* (Reich *et al.*, 1997) and MHC class II molecules to dimerise, as seen in the crystal structure of HLA-DR (Brown *et al.*, 1993).

T cells must contact MHC molecules through a second cell surface molecule (CD4 or CD8) in addition to their T cell receptors before they can become activated. CD4 is expressed on T helper cells and binds to class II molecules, while CD8 is expressed on cytotoxic T cells and binds to class I molecules. Thus, these molecules restrict T cell recognition so that T helper cells are activated only by class II molecule-peptide complexes whereas cytotoxic T cells are only activated by peptides complexed with class I molecules.

Additional costimulatory signals are required to activate naïve T cells (T cells which have never before encountered their antigen). This is provided by B7, a cell surface molecule found on certain antigen presenting cells (see below), which binds to CD28 or CTLA-4 on the T cell surface. In the absence of this second signal, the MHC-peptide signal alone inactivates the T cell (anergy) or kills it (apoptosis). This 'two signal' mechanism is thought to be essential to maintain self-tolerance.

Antigen Processing

Antigen processing describes the degradation of intracellular or extracellular proteins to peptides that form complexes with MHC molecules which are expressed at the cell surface. Although both MHC class I and II molecules are synthesised in the ER, antigen processing is carefully controlled so that, with only a few exceptions, intracellular antigens are presented by class I molecules and extracellular or endocytic antigens by class II molecules. The class I antigen processing pathway is summarised in Figure 1-4.

The Class I Pathway of Antigen Processing

The Generation of Antigenic Peptides

The class I antigen processing pathway begins with the degradation of a selection of cytoplasmic proteins into peptides. This is thought to be the work of the proteasome, a large multi-proteolytic complex in the cytoplasm. The 20S proteasome consists of four stacked rings, each consisting of seven subunits. The catalytic subunits (ß-family) make up the two inner rings, while the function of the outer rings of α-subunits is not known. In humans, each ring (α or ß) contains 7 different subunits (Seemuller *et al.*, 1995).

The structure of the 20S proteasome of archaebacteria (Lowe *et al.*, 1995), which consists of 14 identical α-subunits and 14 identical ß-subunits, and of yeast, which consists of 7 types of α-subunit and 7 types of ß-subunit (Groll *et al.*, 1997), have been determined by X-ray crystallography. Both structures show the catalytic sites of the ß-subunits lining the inside of a secluded central cavity. In the archaebacterial proteasome, this cavity is accessible through openings 13 Å wide at either end of the complex. These narrow openings prevent the proteasome from degrading normal, folded proteins, but allow unfolded proteins to enter the catalytic cavity (Wenzel and Baumeister, 1995). In the

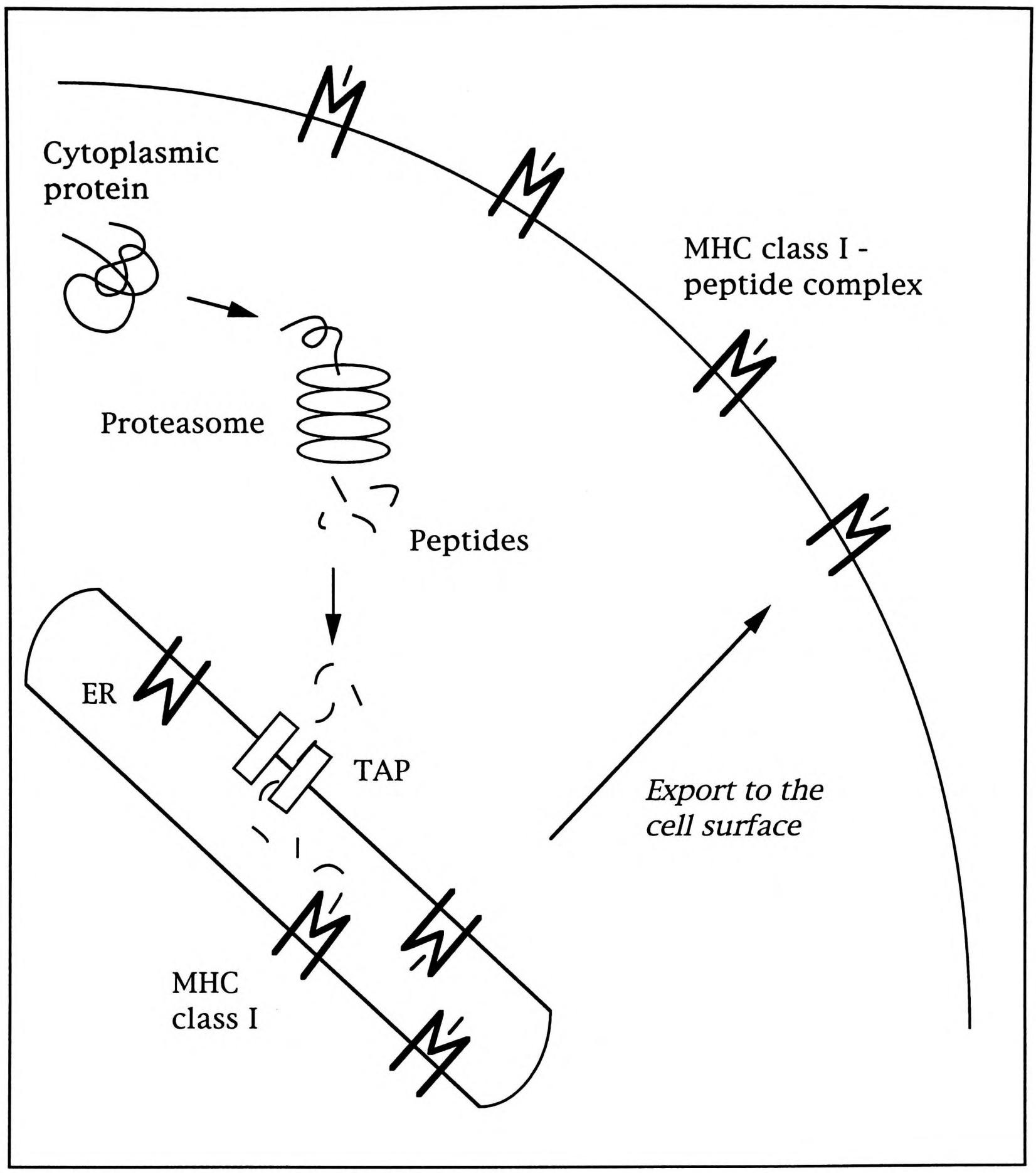

Figure 1-4: The class I pathway of antigen processing. A selection of cellular proteins is degraded by the proteasome to produce peptides. These enter the ER through TAP, where they associate with MHC class I molecules. The resulting class I molecule-peptide complexes are exported to the cell surface where they can be surveyed by circulating cytotoxic T cells.

yeast 20S proteasome, these openings appear to be completely blocked (Groll *et al.*, 1997), although, in solution, there seems to be sufficient structural flexibility for unfolded substrates to gain access to the active sites and be degraded (Gregori *et al.*, 1997).

Each ß-subunit of the archaebacterial proteasome contains a catalytic site of the N-terminal nucleophile family of proteases. These sites are spaced 28 Å apart around each ß-ring, poised to cleave a polypeptide bound in an extended conformation every 8 amino acids or so. However, in eukaryotes, only three of the seven different ß-subunits contain functional N-terminal nucleophile active sites. Two of these subunits (ß1 and ß2) are adjacent, and so could generate peptides of a suitable length to bind to MHC class I molecules, but the third is on the far side of the ß-ring. However, the structure of the yeast proteasome revealed the existence of an additional active site found in every ß-subunit, that is important in their post-translational processing and assembly. This active site is poised to cleave bound polypeptide substrates 8-9 amino acids from the N-terminal nucleophile site. However, its importance in degrading proteasome substrates is unknown, as all the known proteasome inhibitors bind to the N-terminal nucleophile site. While the N-terminal nucleophile site of each subunit has a specificity pocket equipped to select cleavage sites that will generate peptides with defined C-termini, the second active site in the eukaryotic proteasome is thought to be non-selective.

The evidence that the proteasome produces antigenic peptides from cytoplasmic proteins is strong, though not conclusive. *In vitro,* 20S proteasomes generate peptides of approximately the right size to bind to MHC class I molecules (5-15 amino acids) (Kuckelkorn *et al.*, 1995; Wenzel and Baumeister, 1995) and can degrade unfolded fragments of proteins to antigenic peptides identical to those found complexed with MHC class I molecules (Dick *et al.*, 1994). Furthermore, in cultured cells, various protease inhibitors has been shown to reduce antigen processing in proportion to their ability to inhibit the proteasome (reviewed by Groettrup *et al.*, 1996c). The production of the epitope by the proteasome *in vitro* and the antigen processing pathway *in vivo* are altered

in proportion to each other if the sequences flanking the epitope are changed (Niedermann *et al.*, 1995). In addition, interferon-γ (IFN-γ), a potent antiviral cytokine that stimulates production of other members of the MHC class I antigen processing pathway, has two tantalising effects on the proteasome. Firstly, it induces three proteasome subunits, LMP2, LMP7 and MECL-1 (Nandi *et al.*, 1996; Groettrup *et al.*, 1996a), which replace the constitutive catalytic ß-family subunits δ, MB-1 and z (Belich *et al.*, 1994; Hisamatsu *et al.*, 1996). The yeast homologues of these three pairs of subunits are the only subunits to contain active N-terminal nucleophile active sites (Groll *et al.*, 1997). It has long been thought that the interferon-induced proteasome subunits may alter the specificity of the proteasome to favour the production of antigenic peptides, but the evidence for this hypothesis thus far is weak (reviewed by Groettrup *et al.*, 1996c). Replacement of δ by LMP2 changes the character of its specificity pocket, although substitution of LMP7 or MECL-1 for MB-1 and z does not (Groll *et al.*, 1997). However, while some studies using fluorogenic tri- and tetrapeptide substrates suggested that proteasomes purified from IFN-γ-treated cells generate more peptides with charged or hydrophobic C-termini, which bind better to MHC class I (Driscoll *et al.*, 1993; Gaczynska *et al.*, 1993), others have failed to demonstrate such a difference (Ustrell *et al.*, 1995). Nevertheless, it is interesting that LMP7 (though not LMP2) knockout mice show decreased expression of MHC class I molecules on certain immune cell types (Fehling *et al.*, 1994; VanKaer *et al.*, 1994).

IFN-γ also induces production of a proteasome-associated 11S regulator composed of two subunits, pA28α and ß, arranged in a heptameric or hexameric ring (Ahn *et al.*, 1996b). Expression of pA28 in fibroblasts at levels similar to those found after interferon-γ treatment enhances the presentation of two viral proteins by MHC class I molecules (Groettrup *et al.*, 1996b). pA28 activates the 20S proteasome and also increases the cooperativity of its different subunits so that peptides of 7-8 amino acids are produced by co-ordinated dual cleavages (Dick *et al.*, 1996).

What determines which proteins are degraded by the proteasome? Many of the substrates of the proteasome are selected as a result of being ubiquitinated. Ubiquitin is a small protein of only 76 amino acids which can be covalently attached to lysines in a target protein. This complex process is best understood in yeast, where it involves any one of 12 ubiquitin-conjugating enzymes (Ubcs or E2s) (for a review, see Jentsch, 1992). Some Ubcs are involved in selecting specific proteins for degradation, for example cyclins during cell cycle progression. Ubc2p co-operates with Ubr1p to ubiquitinate certain short-lived proteins. Ubr1p (a ubiquitin ligase or E3 enzyme) recognises proteins with acidic or basic N-terminal amino acids (the N-end rule) (Varshavsky, 1992), but most proteins resist this pathway because they have acetylated N-termini. Two essential ubiquitin-conjugating enzymes, Ubc4p and Ubc5p, mediate general protein turnover. Rather than selecting proteins at random, it seems likely that they select old and worn-out substrates that are partly unfolded and unable to refold, so remaining complexed with chaperones for a long time. Evidence for this suggestion is circumstantial. Ubc4p, Ubc5p and ubiquitin are induced by heat-shock, presumably to degrade irreversibly heat-denatured proteins (Finley *et al.*, 1987; Müller-Taubenberger *et al.*, 1988; Seufert and Jentsch, 1990). *ubc4 ubc5* mutant cells constitutively activate the heat shock response due to an accumulation of denatured proteins, and are hypersensitive to factors that cause proteins to unfold, such as heat shock and amino acid analogues (Seufert and Jentsch, 1990). Ubiquitination may also be necessary for the degradation of a small number of rapidly degraded proteins that contain PEST sequences: regions enriched in proline, glutamate, serine and threonine uninterrupted by positively-charged residues (Rechsteiner and Rogers, 1996).

Ubiquitinated substrates are degraded by the 26S proteasome, which consists of the 20S proteasome with a 19S complex bound at one end. This 19S cap recognises and deubiquitinates substrates and its requirement for ATP suggests that it may unfold them as well. The 26S proteasome can also degrade short-lived non-ubiquitinated substrates, such as ornithine carboxylase (Murakami *et al.*, 1992).

The evidence that the ubiquitin pathway of degradation selects antigens for entry into the antigen processing pathway is mixed. Ubiquitin fusion proteins are able to overcome an epitope-specific block in antigen processing imposed by vaccinia virus infection (Townsend *et al.*, 1988). Only for two proteins containing intramolecular disulphide bonds has antigen processing been shown to depend on ubiquitin conjugation (Michalek *et al.*, 1993; Grant *et al.*, 1995; Michalek *et al.*, 1996), and one group saw enhanced presentation when ubiquitin conjugation was prevented (Cox *et al.*, 1995). It is very unlikely that proteins need to be ubiquitinated before they can be processed for presentation by MHC class I molecules, since proteins which do not contain a single lysine to which ubiquitin could be conjugated are still presented by class I molecules (Lehner and Cresswell, 1996) and the IFN-γ-induced 11S proteasome regulator is unable to bind to the 26S proteasome complex that recognises ubiquitinated proteins (Ahn *et al.*, 1996b). Therefore, it seems likely that the 20S proteasome when complexed with the 11S regulator requires another factor besides the 19S cap to unfold its substrates.

How are antigens in compartments outside the cytoplasm degraded? Nuclear proteins are synthesised in the cytoplasm and a proportion may be degraded there, but the proteasome is also found in the nucleus (Peters *et al.*, 1994) and the peptides that it produces may be able to reach the cytoplasm through the nuclear pores. Peptides from proteins resident in the ER may be generated by ER proteases (Hammond *et al.*, 1993; Gueguen *et al.*, 1994; Lee *et al.*, 1996b), but surprisingly the peptides from several ER and plasma membrane proteins seem to be generated in the cytoplasm, as their presentation is dependent on being transported into the ER by TAP (see below) (Hammond *et al.*, 1995; Hombach *et al.*, 1995). It has been suggested that membrane proteins enter the class I antigen processing pathway when they are synthesised errantly in the cytoplasm, but a different mechanism may be responsible. Incorrectly folded or unassembled proteins that are unable to exit the ER by vesicular transport are exported to the cytoplasm and rapidly

degraded by the ubiquitin-proteasome pathway (Brodsky and McCracken, 1997). Proteins may pass into the cytoplasm through the ER import channel, the Sec61p complex. The export of proteins from the ER is ATP-dependent, implicating chaperones in unfolding the proteins in the ER and/or acting as 'molecular rachets' (Schneider *et al.*, 1994) in the cytoplasm, pulling proteins through by co-operative binding to the protein-in-transit. Once in the cytoplasm, the proteins are likely to be ubiquitinated by Ubc6p, an ER transmembrane protein with its active site in the cytoplasm, and degraded by proteasomes, which are found on the cytoplasmic face of the ER. This pathway may account for the ATP-dependent transport of glycosylated peptides from the ER to the cytoplasm (Romisch and Schekman, 1992; Roelse *et al.*, 1994).

Most mitochondrial proteins are encoded in the nucleus and synthesised as precursors in the cytoplasm, where they are accessible to the MHC class I processing pathway, but it is a mystery how proteins that are encoded and synthesised in the mitochondrial matrix are processed and loaded onto non-classical MHC class I molecules. For example, N-formylated peptides derived from two mitochondrial proteins, maternally transmitted factor (mtf) (Shawar *et al.*, 1990) and cytochrome oxidase subunit 1 (Morse *et al.*, 1996), give rise to minor histocompatibility antigens presented by the non-classical class I molecule, H2-M3. It is likely that peptides from other mitochondrial proteins are presented by class I molecules, and the similarity of proteins from mitochondria and prokaryotic infectious organisms has led to speculation that they may be potent antigens in the development of autoimmunity. Interest has focused on the highly-conserved mitochondrial heat shock proteins hsp60 and mt hsp70, homologues of groEL and dnaK, respectively (Kauffman, 1990).

Transport of Antigenic Peptides into the ER

Once peptides have been produced in the cytoplasm, they are transported into the endoplasmic reticulum to encounter newly synthesised MHC class I molecules by the transporter associated with antigen processing, TAP (reviewed by Koopmann *et al.*, 1997). TAP is a dimer of two closely-related subunits which are members of the ATP-binding cassette family of transmembrane transporters. Peptides bind to the cytoplasmic face of TAP and are then driven through a transmembrane pore by ATP hydrolysis in the cytoplasmic domain. Cell lines deficient in TAP show greatly reduced expression of MHC class I molecules at the cell surface; although class I molecules are synthesised normally, most fail to leave the ER and are degraded (Raposo *et al.*, 1995). Those molecules that do reach the cell surface carry peptides generated in the ER from signal sequences.

Peptides bind to TAP in an ATP-independent manner (VanEndert *et al.*, 1994) with micromolar affinities (Koopmann *et al.*, 1996), correlating with the micromolar Michaelis constant (K_m) for peptide transport (Yang and Braciale, 1995). These relatively low affinities are surprising, since cytoplasmic peptide concentrations are thought to be 1 nM at most (Yang and Braciale, 1995). TAP molecules from various species preferentially transport peptides of 8-12 amino acids (Androlewicz and Cresswell, 1994; Heemels and Ploegh, 1994; Momburg *et al.*, 1994; Koopmann *et al.*, 1996), that are of the optimal size to bind to class I. Peptides of up to 40 amino acids can be carried into the ER (Koopmann *et al.*, 1996), where they are trimmed to the optimal length. ER trimming has been shown to occur efficiently from the N-terminus, but not the C-terminus (Eisenlohr *et al.*, 1992; Snyder *et al.*, 1994; Elliott *et al.*, 1995), thus the correct C-termini of antigenic peptides need to be generated in the cytoplasm. TAP has some sequence selectivity: glutamic acid at positions 6 or 7 enhances transport whereas proline at position 2 or 3 prevents it (Neefjes *et al.*, 1995). Nevertheless, peptides that have proline at position 2 or 3 are presented by MHC class I molecules and, therefore, must have been transported as longer precursors and N-terminally trimmed in the ER. Species-specific differences in TAP specificity have

been observed. While human TAP and the rat *cim*^{a} allelic variant are relatively indiscriminate regarding the C-terminal amino acid, the mouse transporter and rat *cim*^{b} prefer to transport peptides with aromatic or aliphatic C-termini (Heemels *et al.*, 1993; Momburg *et al.*, 1994; Schumacher *et al.*, 1994).

Once in the ER, peptides are able to bind to MHC class I molecules. Newly synthesised class I molecules are retained in the ER by chaperones such as calnexin, calreticulin and BiP until they have bound to peptide, which is essential for folding of the $\alpha\beta_2$m complex to be completed (reviewed by Koopmann *et al.*, 1997). Many class I alleles bind to TAP (Ortmann *et al.*, 1994) through the bridging molecule tapasin (Sadasivan *et al.*, 1996), and it is easy to imagine this increasing the efficiency of peptide transfer. A mutant MHC class I molecule that is unable to associate with tapasin is unable to present endogenous antigens, despite being capable of binding to peptides and β_2m (Peace-Brewer *et al.*, 1996). However, not all class I alleles associate with TAP and in the absence of TAP, class I is able to present peptides expressed in the ER (Bacik *et al.*, 1994; Elliott *et al.*, 1995), including signal sequences.

The MHC class I peptide-binding groove must undergo significant conformational changes to allow peptides to bind so deeply within its structure. One such change may involve the part of the α_2-helix that contacts the C-terminus of the peptide (Smith *et al.*, 1996). Such a movement, or even simply a reorientation of the amino acid side chains of class I molecules (Collins *et al.*, 1994) may allow peptides that are longer than optimal to bind via their N-termini and exit the groove at the C-termini (Urban *et al.*, 1994). These longer peptides may then be trimmed by ER peptidases to generate peptides that bind to class I molecules with both ends (Roelse *et al.*, 1994; Snyder *et al.*, 1994; Elliott *et al.*, 1995).

Viral Interference with the Presentation of Antigens by Class I Molecules

Many viruses inhibit antigen presentation in infected cells (reviewed by Smith, 1994 and Ehrlich, 1995). Adenovirus 12 E1A protein inhibits transcription of genes encoding the interferon-induced components of the MHC class I pathway, such as TAP, LMP-2 and 7 and class I itself, by inhibiting the MHC class I transcriptional enhancer (Rotem-Yehudar *et al.*, 1996). In addition, adenovirus E3 (19K) protein binds to MHC class I molecules in the ER and blocks their transport to the cell surface (Rawle *et al.*, 1989). Herpes simplex virus encodes a small cytoplasmic protein, ICP47, that blocks the peptide-binding site of TAP (Tomazin *et al.*, 1996; Ahn *et al.*, 1996a). Human cytomegalovirus (CMV) produces two ER proteins, US2, which retains MHC class I molecules in the ER (Ahn *et al.*, 1996c), and US11 which targets them for degradation by the proteasome (Wiertz *et al.*, 1996); murine CMV prevents transport of peptide-loaded MHC molecules from the ER to the Golgi (DelVal *et al.*, 1992); and poxviruses such as vaccinia, ectromelia and myxoma reduce cell-surface MHC class I expression by means as yet unknown. However, a non-specific strategy to inhibit antigen presentation by MHC class I molecules has its dangers, as natural killer cells destroy cells that do not express class I on their surface. Therefore, human and murine CMVs encode UL18, an MHC class I heavy chain-like molecule that binds to $ß_2$-microglobulin and endogenous peptides (Fahnestock *et al.*, 1995), protecting CMV-infected cells from destruction by natural killer cells (Farrell *et al.*, 1997; Reyburn *et al.*, 1997).

Viruses also have mechanisms for preventing specific proteins from entering the antigen processing pathway. During latency, many cells infected with Epstein-Barr virus express only one protein, the nuclear antigen EBNA-1. It contains a glycine-alanine repeat region that prevents the protein being processed and presented to T cells (Levitskaya *et al.*, 1995). Phosphorylation of human CMV immediate early protein, which is induced by the matrix protein pp65, plays the same role (Gilbert *et al.*, 1993).

The Class II Pathway of Antigen Processing

MHC class II molecules display peptides derived from endocytic compartments. The twin purposes of the class II antigen processing pathway are to produce peptides from endocytosed antigens and bring them together with peptide-receptive MHC class II molecules. This pathway is summarised in Figure 1-5.

MHC class II Molecule Synthesis and Transport

Like MHC class I molecules, class II molecules are synthesised in the ER. Newly synthesised α and β chains associate with the invariant chain (Ii) as a trimer of trimers: $(\alpha\beta Ii)_3$. Invariant chain is an extended type II transmembrane protein with two major functions (reviewed by Wubbolts *et al.*, 1997). Firstly, it occupies the peptide-binding groove of class II molecules, preventing peptides and folding intermediates of newly synthesised proteins from binding to class II molecules in the ER. Secondly, a dileucine motif in its cytoplasmic tail is responsible for diverting the class II-Ii complex to the endocytic compartments. Human invariant chain is produced in four forms as a result of alternative transcriptional initiation and mRNA splicing. These forms differ from each other in the presence or absence of an N-terminal ER retention signal (that is masked by binding of MHC class II molecules) or a domain that inhibits endosomal proteases, especially cathepsin L (Bevec *et al.*, 1996).

The route that MHC class II-Ii complexes follow to endocytic compartments is unclear as they are found throughout the endocytic pathway (Castellino and Germain, 1995). Invariant chain has been shown to divert class II molecules from the *trans* Golgi network directly to the endocytic pathway, but other researchers have seen class II-Ii complexes travelling to the plasma membrane before being internalised into endocytic vesicles (reviewed by Wubbolts *et al.*, 1997). It is possible that both routes are used in parallel.

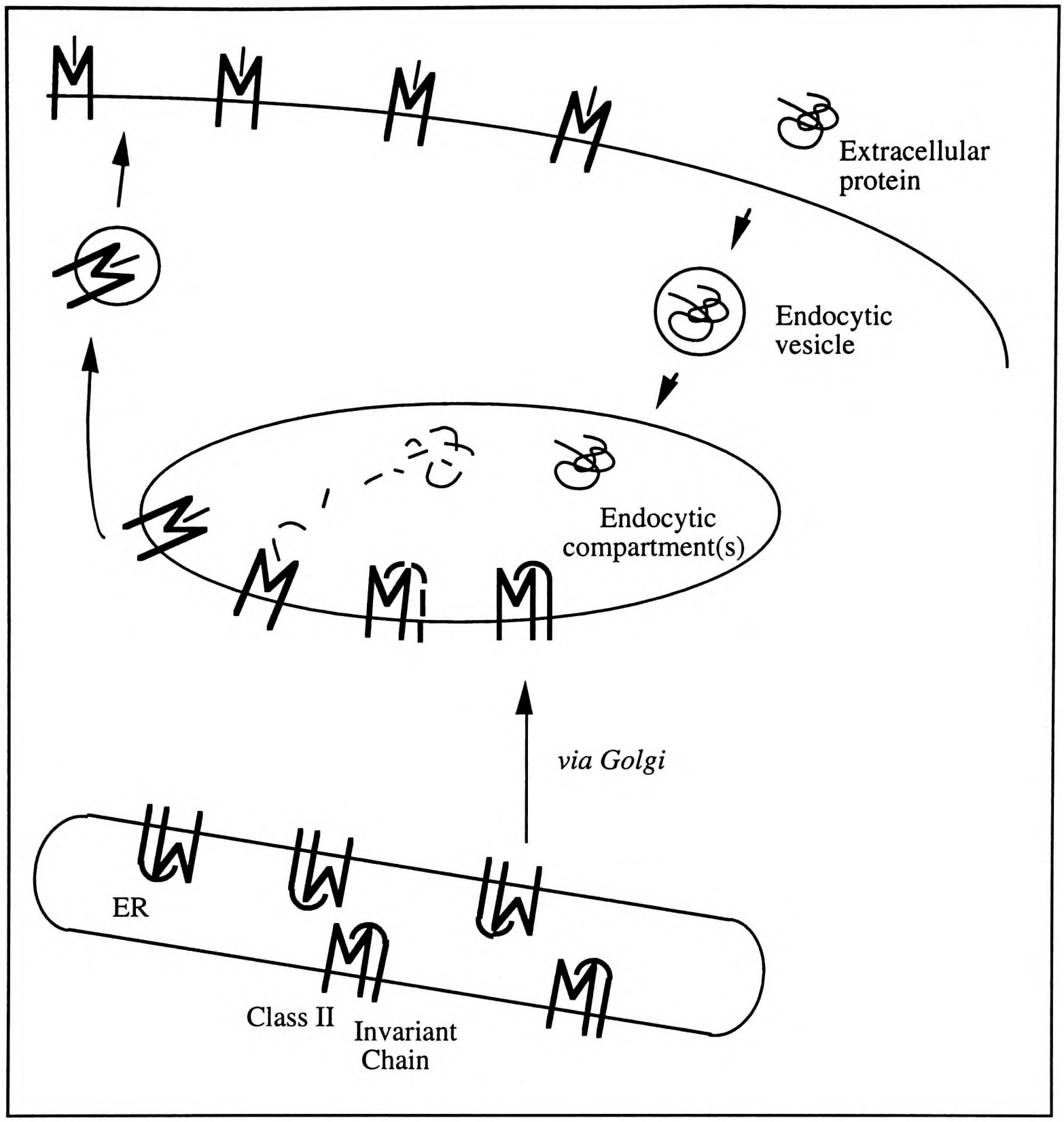

Figure 1-5: The class II pathway of antigen processing. MHC class II molecules are synthesised in the endoplasmic reticulum, where they associate with the invariant chain. Class II molecule-invariant chain complexes are transported to endocytic compartments, where the invariant chain is degraded and peptides can bind. The resulting class II molecule-peptide complexes are exported to the cell surface for inspection by circulating helper T cells.

Once in the endocytic pathway, most of the invariant chain is removed from the MHC class II αβ complex by proteolytic degradation, for which cathepsins B (Xu *et al.*, 1994) and S (Riese *et al.*, 1996) are essential. The part of the invariant chain bound in the peptide-binding groove is inaccessible to proteases and becomes the class II-associated invariant chain peptide (CLIP). Although CLIP seems to be able to release itself from certain class II allotypes at low pH (Kropshofer *et al.*, 1995), its dissociation from most allotypes requires the action of a class II-related molecule, HLA-DM (reviewed by Kropshofer *et al.*, 1997). Mutant cells lacking DM present antigens ineffectively, as most of their class II molecules remain associated with CLIP. At acidic pH, DM promotes the exchange of CLIP for antigenic peptides, although it does not bind to peptides itself. It is thought to stabilise an unstable conformation of class II molecules as CLIP is released. In fact, the action of DM is not confined to CLIP, as it promotes the dissociation of a range of antigenic peptides from class II molecules (Sloan *et al.*, 1995). This is not surprising, as CLIP does not bind to class II molecules in a manner that is structurally distinct from the binding of antigenic peptides (Ghosh *et al.*, 1995). Instead, DM appears to enhance the dissociation of any unstable complexes to favour the formation of long-lived ones, irrespective of their affinity (Kropshofer *et al.*, 1997). This activity is known as molecular proof-reading.

MHC class II molecules only bind stably to peptides at acidic pH (Brodsky, 1992). Since the peptide-binding clefts of class II molecules are open at each end, they can bind to unfolded proteins as well as peptides (Sette *et al.*, 1989), thus protecting the epitopes they bind to from degradation. Subsequent trimming of the bound protein would yield the shorter peptides usually eluted from class II *in vivo*.

Antigen Uptake and Degradation

Endocytosed antigens are degraded in the endocytic pathway, which can be considered as three increasingly acidic and proteolytic compartments: early endosomes (pH 6-6.5), late endosomes (pH 5-6) and lysosomes (pH 4.5-5) (reviewed by Brodsky, 1992 and Berg *et al.*, 1995). Early endosomes are primarily sorting compartments, in which some receptors dissociate from their ligands and recycle to the cell surface. They contain some degradative enzymes that begin to digest the endocytosed antigens, and can degrade some antigens completely. Late endosomes have greater proteolytic power, since they contain lysosomal enzymes which are carried there by mannose-6-phosphate receptors prior to entry into lysosomes. However, these enzymes may not be fully active at the less acidic pH of late endosomes. Lysosomes are the terminal degradative compartments. They complete the degradation of endocytosed material to its basic components (such as sugars, amino acids and fats), which can be transported into the cytoplasm and metabolised.

Much interest has focused on the proteases of the endocytic pathway, which will influence the peptide epitopes that are produced. In addition, disulphide bond reduction (Collins *et al.*, 1991) and deglycosylation (Aronson and Kuranda, 1989) may be required before certain epitopes can be generated, although some T cells recognise glycopeptides (Harding *et al.*, 1993; Dudler *et al.*, 1995). The endosomal and lysosomal proteases are called cathepsins and fall into two different families: the aspartic proteases (cathepsins D and E) and the cysteine proteases (cathepsins B, C, H, L and S). In macrophages, interferon-γ induces cathepsins H (Lafuse *et al.*, 1995), B and L (Lah *et al.*, 1995), and cathepsin S is constitutively expressed at high levels (Shi *et al.*, 1994). Inhibition of the neutral protease cathepsin E, which has an endosomal localisation and is upregulated late in B cell development (Sealy *et al.*, 1996), prevents processing of exogenously added ovalbumin (Bennett *et al.*, 1992). *In vitro* studies have shown that cathepsin D, an acid protease found in both endosomes and lysosomes, liberates antigenic peptides from

ovalbumin (Diment, 1990). However, the aspartic proteases (cathepsins D and E) are not needed to generate three different epitopes from myoglobin (Takahashi *et al.*, 1989).

Peptide Loading of MHC Class II Molecules

The site at which MHC class II molecules are loaded with peptide is still controversial as virtually every endocytic compartment has been implicated (for reviews, see Brodsky, 1992 and Wubbolts *et al.*, 1997). However, interest has been particularly focused on novel multivesicular and multilamellar structures whose synthesis depends on continuous synthesis of class II molecules (Calafat *et al.*, 1994), termed MHC class II loading compartments (MIIC) (reviewed by Xu and Pierce, 1995). DM is confined to these late endocytic compartments, and it is here that Ii is cleaved and mature antigenic peptide-class II complexes form. However, the loading of MHC class II molecules with peptide has also been described in endosomes (Amigorena *et al.*, 1994).

Class II molecules may gain access to much of the endocytic pathway when they recycle from the plasma membrane through the endosomes (Brodsky, 1992). Empty class II molecules can be transported to the cell surface (Germain and Hendrix, 1991) and they will have the opportunity to bind peptides present in compartments other than the MIIC when they recycle through the endocytic pathway. The presentation of certain antigens, such as influenza haemagglutinin, myelin basic protein and ribonuclease A appears to depend on recycling class II molecules (Pinet *et al.*, 1995).

Antigen Presenting Cells

MHC class II molecules are expressed on the functionally diverse group of cells called antigen presenting cells (APCs). While the general scheme of class II antigen processing is the same in these cells, the details, particularly in relation to the uptake of antigens, differ.

The dendritic cell is the initiator of adaptive immune responses (reviewed by Cella *et al.*, 1997) because it has access to naïve T cells and constitutively expresses the costimulatory molecules necessary to activate them. Dendritic cells begin life as precursors in the peripheral tissues, such as Langerhans cells in the skin. These are specialised antigen processing cells that take up antigens from the extracellular fluid by non-specific pinocytosis, innate recognition mechanisms such as carbohydrate binding and antibody-binding Fc receptors. They migrate to secondary organs such as lymph nodes, specialised mucosal sites or the spleen, where they differentiate into dendritic cells. Migration occurs constitutively at a low level, and is stimulated by formylated peptides, the complement component C5a (Sozzani *et al.*, 1995) and cytokines such as granulocyte-monocyte colony stimulating factor. Mature dendritic cells express MHC class II molecules and the costimulatory molecules necessary to activate resting T cells, but are no longer capable of ingesting and processing antigen, so they represent a snapshot of the antigenic content of the extracellular fluid of the tissue they resided in as precursors. In the secondary lymphoid organs, the dendritic cells come into contact with naïve T cells, which are restricted to the blood and lymph and cannot enter the peripheral tissues.

Tissue macrophages (such as Kupfer cells in the liver) and monocytes (their circulating precursors) phagocytose and destroy large, particulate antigens, such as bacteria, viruses and immune complexes. They link innate and adaptive immunity by recognising, processing and presenting antigens that carry prokaryotic sugar groups or that are coated with complement fragments. In addition, they present antigens opsonised with antibodies, thus amplifying the adaptive immune response. Like dendritic cells, they are capable of activating naïve T cells (DeBruijn *et al.*, 1995). Antigens are degraded in phagosomes and phagolysosomes, which acquire contents such as proteases and class II molecules by fusion with endosomes and lysosomes (reviewed by Harding, 1995).

B lymphocytes endocytose antigen that has bound to their membrane-immunoglobulin (mIg). Thus, a peptide antigen bound to class II molecules on a B cell indicates the

specificity of its mIg to activated helper T cells, which can then activate the B cell. Activated B cells proliferate, secrete soluble forms of their mIg as antibodies and express costimulatory molecules that allow them to activate naïve T cells. Receptor-mediated endocytosis by B cells is more efficient for antigens carrying several identical epitopes, which cross-link their mIg molecules. The mIg specificity of a B cell may influence which peptide epitopes are produced from the degradation of bound antigen (Davidson and Watts, 1989). Two mIg-associated subunits modulate the trafficking of mIg-antigen complexes: Igα targets antigen to MIICs, whereas Igß directs it to early endosomes (Bonnerot *et al.*, 1995).

In addition to the constitutive antigen presenting cells described above, certain cells such as endothelial cells and fibroblasts, are induced to express class II molecules by interferon-γ. During a sustained inflammatory response, they may play an important role in stimulating already active T cells.

Cross-Talk

The separation of the class I and class II antigen processing pathways described above is not inviolable. Although most cells use MHC class I molecules to present peptides from exclusively endogenous peptides, class II-presenting cells (primarily dendritic cells and macrophages) can use class I molecules to present exogenous antigens, a process called cross-talk. This ability was first seen as cross-priming; in transplantation, recipient T cells are activated against peptides derived from donor cytoplasmic proteins complexed with recipient MHC class I alleles (Bevan, 1976).

Cross-talk has now been demonstrated for many different antigens (Harding, 1995; Rock, 1996) and it may be vital for the initiation of a cytotoxic immune response. As previously described, two signals are required to activate naïve or resting T cells: MHC-peptide complexes and a costimulatory signal provided only by dendritic cells, activated B

cells and macrophages. So how are cytotoxic T cells activated against a virus that does not infect these specialised antigen presenting cells? The answer appears to be that dendritic cell precursors and macrophages route some of the antigen they pick up from the extracellular fluid (which will include the contents of cells lysed by virus, for example) to bind to class I molecules, which can then be presented at the cell surface together with the appropriate costimulatory molecules to activate naïve cytotoxic T cells.

In general, antigen injected in particulate form can efficiently activate a cytotoxic T cell response. There appear to be two mechanisms for loading class I molecules with exogenous antigen. One does not require newly-synthesised class I molecules, since it is resistant to brefeldin A which prevents proteins from leaving the ER; it apparently involves class I molecules that have been recycled through the endocytic pathway and bound to peptides generated there (reviewed by Harding *et al.*, 1993 and Bachmann *et al.*, 1995). The second pathway is inhibited by Brefeldin A, proteasome inhibitors and mutations in TAP, suggesting that antigens are transferred from endocytic compartments into the cytoplasm, where they are degraded by the proteasome and transported into the ER (reviewed by Rock, 1996). Chloroquine, which raises the pH of endocytic compartments, has no effect on this pathway, implying that proteolysis need not begin outside the cytoplasm. However, it is surprising that phagocytic cells risk transporting whole antigenic proteins into the cytoplasm. Transfer of antigens to the cytoplasm may occur by rupture of phagocytic vesicles or involve a specific transmembrane transporter.

Cross-talk can also occur in the opposite direction, resulting in endogenous peptides being presented by class II molecules (Malnati *et al.*, 1992). The mechanism of this process has not been explored, but lysosomes are known to be involved in the degradation of intracellular macromolecules as well as extracellular ones (reviewed by Dunn, 1994). Cellular proteins are delivered to lysosomes by secretory vesicles (crinophagy), hsc70-mediated transport (described in detail below) or envelopment of regions of cytoplasm by the lysosomal membrane (autophagy). Autophagy is responsible for the degradation of

large complexes such as ribosomes and proteasomes (Cuervo *et al.*, 1995) and, like hsc70-mediated transport, is induced by nutrient or serum starvation.

MHC Association

Many of the proteins involved in the presentation of antigens to T cells are encoded in a relatively small region of the genome, called the Major Histocompatibility Complex (MHC) on chromosome 6. This was discovered as the major genetic determinant of rejection of tissues transplanted between individuals (Counce *et al.*, 1956). Tissue rejection is a result of the recipient's T cells recognising the donor MHC class I molecules as foreign and killing the donor cells. This is a consequence of the extra-ordinary polymorphism of MHC molecules. In the MHC there are three class I genes (HLA-A, B and C) and three class II loci (HLA-DP, DQ and DR; HLA-DR encodes between 2 and 4 genes, depending on the individual). In addition, there are less polymorphic non-classical class I genes, such as H2-M3 in mouse, that encode proteins involved in the presentation of microbial N-formylated peptides (Shawar *et al.*, 1991). The amount of polymorphism at each locus varies. The number of alleles found at different class I and class II loci varies greatly, from HLA-DRA, which has only two known alleles, to HLA-DRB1, which has at least 106 different alleles (Bodmer *et al.*, 1994). The polymorphic amino acids are usually found in the peptide-binding cleft, where they alter the specificity of the MHC molecules for peptides by altering the pockets that bind to peptide anchor residues. Why are MHC molecules so polymorphic? In a non-polymorphic population, there will be selection for pathogens whose proteins do not provide peptides that can bind to MHC molecules, and this will drive selection of individuals whose MHC molecules have unusual binding specificities (Hill *et al.*, 1992) and who are heterozygotes (Hughes and Nei, 1989). Since the shared ancestors of *Xenopus* and man had MHC molecules, the current extensive

polymorphism in the human population has evolved over millions of years (reviewed by Potts and Wakeland, 1993).

Why are the genes encoding MHC class I and II molecules clustered together? Their related structure and sequence suggest that they arose by duplication of an ancestral gene through unequal crossing over, which would leave the copies side by side in the genome. However, members of other equally ancient gene families are now distributed over many chromosomes, and members of the MHC superfamily that have lost the function of antigen presentation, such as the neonatal IgG transporter FcRn (Burmeister *et al.*, 1994), are no longer encoded in the MHC (Kandil *et al.*, 1996). Even related subunits of the same protein are rarely encoded in close proximity, for example, the immunoglobulin light and heavy chain genes. When we consider that molecules which have no homology to MHC molecules, but share a function in antigen processing, are also encoded in the MHC, it becomes clear that there must be an important reason for this clustering.

The genes encoding MHC class I and class II molecules, DM, the two TAP subunits, the proteasome subunits LMP 2 and 7, and perhaps tapasin (Grandea *et al.*, 1995) may be clustered together because of their shared function coupled with their polymorphism, past or present. Functional polymorphisms have been detected in the MHC molecules of all species studied and in rat TAP. The proximity of these polymorphic genes in the MHC allows particular alleles of different genes to be coinherited in what is known as an extended haplotype. Such coinheritance is aided by the unusually low levels of recombination that occur in the MHC (Martin *et al.*, 1995), so that, for example, particular MHC class I alleles will be more often inherited with LMP and TAP alleles that produce and transport them. Thus mouse class I molecules exclusively bind peptides with hydrophobic C-termini (Rammensee *et al.*, 1993), so mouse TAP preferentially transports peptides with aromatic or aliphatic C-termini. In rats, the RT1A^a class I allotype, which bind peptides with arginine at their C-terminus, is usually coinherited with the more permissive *cim*^{a} TAP allotype (Powis *et al.*, 1996). The alternative allotype of TAP, *cim*^{b},

which has a specificity more like mouse TAP, is unable to transport peptides that bind to RT1A^a class I molecules. These considerations beg the question, why not have a non-specific pathway for antigen processing and presentation that is able to transport and present all possible peptide epitopes. Apart from the fact that side chain specific interactions may be necessary to generate high affinity interactions between peptides and MHC molecules or TAP, it may not be advantageous to present every possible peptide. Given that there is a threshold number of identical MHC-peptide complexes necessary to activate a T cell and the number of MHC molecules is limited, the greatest sensitivity will be achieved if each antigen produces only one peptide. This would maximise the number of identical peptide-MHC complexes produced from an antigen.

It is possible to understand how functional polymorphisms in components of an antigen processing pathway will favour them being positioned close together in the genome so that they can be co-inherited. However, it is more difficult to explain why inheriting class I and class II alleles together is advantageous, since the proteins they encode co-operate only in the broadest sense. This is also true for the large number of genes in the MHC encoding other important immunoregulatory molecules, such as complement factors, cytokines and intracellular signalling molecules (Campbell and Trowsdale, 1997). These genes have a shared function in only the broadest sense, but may be clustered for the purpose of shared regulation. Proteins of both the class I and class II presentation pathways are induced by interferon-γ, for example. However, other components of these pathways, such as the proteasome subunit MECL-1 (Larsen *et al.*, 1993) and the invariant chain (Genuardi and Saunders, 1988) are not encoded in the MHC and this does not affect their coregulation.

There is particular interest in genes in the MHC because this region of the genome is associated with susceptibility to a large number of autoimmune diseases (reviewed by Campbell and Milner, 1993); indeed, it has been suggested that all autoimmune diseases will be linked to the MHC. The mechanisms for such predispositions are not yet known, but their determination will open new avenues for diagnosis, treatment and, one day, cure.

Hsp70s and Antigen Processing

Hsp70 genes are linked with the MHC of vertebrates from *Xenopus laevis* to man. Three genes for hsp70s are found in the human MHC class III region, between the complement component C2 and tumour necrosis factor (TNF) genes. Two genes code for the heat-inducible hsp70 and one encodes the constitutive hsp70hom (Milner and Campbell, 1990). This fact and the unique properties of hsp70s have lead to speculation about the roles of hsp70s in antigen processing.

Hsp70s and the Class I Pathway of Antigen Processing

Hsp70s may be involved in selecting substrates for degradation by the proteasome. They might feed proteins directly into the 20S proteasome or co-operate with ubiquitin-conjugating enzymes in identifying proteins for degradation by the 26S proteasome (Mellins *et al.*, 1990). In yeast, the degradation by the ubiquitin-proteasome pathway of short-lived and abnormal proteins (Lee *et al.*, 1996a) and cyclin 3 (Yaglom *et al.*, 1996), though not N-end rule substrates (Lee *et al.*, 1996a), depends on an hsp70 accessory protein, the hsp40, Ydj1p. Ydj1p may be acting as a cofactor in the ubiquitination of denatured proteins by Ubc4p and Ubc5p. In the ER, proteins such as isolated immunoglobulin light chains (Knittler *et al.*, 1995) or HLA-DRß chains (Cotner and Pious, 1995) associate with BiP prior to degradation, transport into the cytoplasm and degradation by the proteasome. In mitochondria, mt hsp70 co-operates with the PIM1 protease to degrade dihydrofolate reductase that is targeted to the matrix rather than the intermembrane space (Wagner *et al.*, 1994). In *E. coli*, proteins bind to dnaK and grpE before they are destroyed (Sherman and Goldberg, 1991). Normally long-lived proteins that are destabilised by the insertion of unstructured regions, associate with hsp70 and other chaperones and are rapidly degraded (Yang *et al.*, 1994) and mutations in chaperones

including dnaK increase the stability of short-lived proteins (Straus *et al.*, 1988; Sherman and Goldberg, 1992).

Hsp70s might transfer peptides from the proteasome to TAP, protecting them from rapid degradation in the cytoplasm (Roelse *et al.*, 1994), preventing them binding to other cellular proteins and overcoming the relatively low affinity of TAP for peptides by increasing the local peptide concentration. BiP may play an analogous role in the ER, shuttling peptides between TAP and class I molecules. Such a role has been shown for gp96, the ER-resident hsp90, which has been cross-linked to antigenic peptides transported by TAP (Lammert *et al.*, 1997), although the fact that BiP is not cross-linked in this way suggests that it is not involved. These roles have been suggested by the ability of hsp70s to bind to peptides *in vitro* and the fact that they can bind to antigenic peptides *in vivo* (Udono and Srivastava, 1993).

There are several lines of evidence supporting the involvement of hsp70s in class I antigen processing. The expression of class I molecules at the cell surface is reduced by deoxyspergualin treatment (N. Blachere and P. Srivastava, personal communication in (Koopmann *et al.*, 1997)), which binds to hsc70 and hsp90 and inhibits peptide binding (Nadler *et al.*, 1992), or the expression of antisense hsp70-1 RNA (D. Mathioudakis, L. Heine and E. Gunther, personal communication). However, heat shock decreases cell surface expression of MHC class I molecules by murine lymphoma cells (Mehdi *et al.*, 1984). Nevertheless, heat shock increases the cell surface expression of transfected Qa-1 (Imani and Soloski, 1991), a non-classical class I molecule that presents peptides in a TAP-dependent fashion (Aldrich *et al.*, 1994), perhaps by increasing the peptide supply.

Hsp70s and the Class II Pathway of Antigen Processing

Hsp70s may also play a role in MHC class II antigen processing and presentation. They could help to degrade endocytosed substrates by unfolding them and preventing them

from aggregating and may also protect peptides from complete degradation and shuttle them to peptide-receptive class II molecules.

Hoeger and colleagues (1994) showed that deoxyspergualin inhibits tetanus toxoid processing by monocytes without reducing cell surface expression of class II, although Nikolic-Paterson *et al.* (1995) saw reduced cell surface expression of class II molecules after deoxyspergualin treatment. In addition, there have been two reports of antibodies against hsp70s inhibiting the class II pathway of antigen processing (Lakey *et al.*, 1987; Manara *et al.*, 1993). The effects of heat shock are also confusing, as it enhances the processing of some exogenous antigens but not others. Heat shock enhances the ability of B cells to activate helper T cells specific for influenza (Rees *et al.*, 1991) and cytochrome c (Cristau *et al.*, 1994) against both the intact antigen and synthetic peptides derived from it, and increases the presentation by human monocytes of diphtheria toxoid, though not tetanus toxoid (Mariethoz *et al.*, 1994). Heat shock has no effect on the presentation of ovalbumin by class II molecules, except when it is synthesised in the cytoplasm of the antigen presenting cell (Michalek *et al.*, 1992). In addition, heat shock has been shown to stimulate the costimulatory function of B cells (Rees *et al.*, 1991), inhibit it (Kuperberg *et al.*, 1991) or leave it unchanged (Malnati *et al.*, 1992; Mariethoz *et al.*, 1994), as judged by the ability to stimulate a mixed lymphocyte reaction.

A rather bizarre role has been proposed for hsc70 in class II processing. Auger *et al.* (1996) showed that hsc70 binds to the DRß chains of two MHC class II allotypes that are associated with rheumatoid arthritis but does not interact with non-associated allotypes. These two allotypes, HLA-DRB1*0401 and HLA-DRB1*1001, have in common what is known as the 'shared epitope' in the same position in their peptide-binding grooves (QKRAA in HLA-DRB1*0401 and RRAAA in HLA-DRB1*1001). This interaction is not specific to hsc70, however, as it also takes place with dnaK. By pulse-chase and immunoprecipitation, complexes between the DRβ chain of HLA-DRB*0401 allele and DRα, the invariant chain and hsc70 were detected immediately after its synthesis, in

subcellular fractions containing lysosomes. The authors suggest that this association occurs in the ER and results in the class II molecule being targeted to dense endocytic vesicles unusually rapidly, but it is unclear how this would cause susceptibility to rheumatoid arthritis. However, hsc70 has never been observed in the ER, although it has been detected by electron microscopy in the lysosomes of rat liver after prolonged starvation (Cuervo and Dice, 1996), and in the lysosomes of serum-starved human fibroblasts by a combination of subcellular fractionation and protease-protection studies (S. Terlecky and F. Dice, unpublished data quoted in (Terlecky, 1994)), so it is possible that the association between hsc70 and HLA-DRB*0401 takes place here. The presence of hsc70 in endocytic compartments is supported by evidence that peptides bound to class II molecules include those derived from hsc70 (Newcomb and Cresswell, 1993) and hsp70 (Nelson *et al.*, 1992) and that a heterogeneous preparation of hsp70s carries peptides derived from extracellular proteins (P. Srivastava, unpublished data quoted in (Srivastava, 1994)). Alternatively, the interaction between hsc70 and HLA-DRB*0401 may occur only after the ER and lysosomal membranes are lysed *in vitro*. The significance of the interaction hsc70 with HLA-DRB1*0401 and HLA-DRB1*1001 in increasing the susceptibility to rheumatoid arthritis of people inheriting these allotypes is therefore unclear.

The best evidence for the involvement of hsp70s in antigen processing was related to a novel member of the hsp70 family, PBP74. PBP74 was localised to early endosomes (VanBuskirk *et al.*, 1991) and antibodies against it were shown to inhibit antigen presentation by MHC class II molecules (Lakey *et al.*, 1987).

Hsp70s and Cross-talk

Hsp70s may fulfil a crucial role in initiating immune responses by directing exogenous antigenic peptides to MHC class I molecules of antigen presenting cells (reviewed by

Srivastava *et al.*, 1994). The work of Srivastava and colleagues has shown that hsp70s and an ER-resident hsp90 called gp96 carry antigenic peptides *in vivo,* and that complexes between these chaperones and antigenic peptides efficiently transfer immunity against methylcholanthrene-induced (Meth A) sarcomas in mice (Udono and Srivastava, 1993). Immunisation with chaperone-peptide complexes is more efficient than with the peptides alone, suggesting that a subset of macrophages have specific receptors to take up hsp70s and gp96 so that the peptides they carry can be transferred to class I molecules (Suto and Srivastava, 1995). *In vivo*, chaperone-peptide complexes are released by cell lysis, due to viral infection for example. The chaperone molecules will act to protect the peptides from degradation and target them to antigen presenting cells, where they can be presented by class I molecules together with the costimulatory molecules necessary to activate naïve cytotoxic T cells. If the macrophage chaperone receptors recognise the related prokaryotic chaperones too, they may account for the adjuvancy of mycobacterial and *E. coli* hsp70 in activating helper T cell responses (Perraut *et al.*, 1993; Barrios *et al.*, 1994; Roman and Moreno, 1996) and even the induction of inflammatory cytokine production in macrophages by exogenous mycobacterial hsp70 (Retzlaff *et al.*, 1994).

As discussed earlier, the hsc70-mediated targeting of cytoplasmic proteins to lysosomes may lead to their processing and presentation by MHC class II molecules. Dice and colleagues have shown that serum-starved tissue culture cells (Chiang *et al.*, 1989) and liver cells in starved rats (Cuervo *et al.*, 1995) degrade specific cytoplasmic proteins in lysosomes, including certain glycolytic enzymes and ribonuclease A. The proteins to be degraded share a degenerate KFERQ-like motif recognised by hsc70 (Terlecky *et al.*, 1992) which transports them to a receptor in the lysosomal membrane called LAMP-2 (Cuervo and Dice, 1996). The means of transporting proteins across the lysosomal membrane is unknown, but presumably they have to be unfolded by hsc70. It seems likely that there is a lysosomal transmembrane protein transporter, which might be related to the transporter that carries phytochelatin peptides into yeast vacuoles (Ortiz *et al.*, 1995). An analysis of

the structures of KFERQ-containing proteins showed that these motifs are generally located at the surface near the end of an α-helix (Gorinsky *et al.*, 1996). As hsc70 cannot interact with polypeptide substrates containing secondary structure, this explains how proteins containing KFERQ motifs can coexist with hsc70 in cells under normal conditions without being degraded in lysosomes. It also implies that, following serum starvation, another factor is responsible for unfolding proteins containing KFERQ motifs so that they can be recognised by hsc70. Since heat shock enhances the presentation of a cytoplasmic antigen by class II molecules in B cells (Michalek *et al.*, 1992), heat induced hsp70s may also be involved in this process.

An unusual finding related to these observations concerns the ability of MHC class I molecules to present peptides derived from truncated forms of simian virus 40 large-T antigen. When these fragments are expressed in the cytoplasm of TAP-deficient cells, the presentation of peptides derived from them is correlated with their association with hsc70 and is inhibited by chloroquine and NH_4Cl, which block endosomal and lysosomal proteolysis (Schirmbeck and Reimann, 1994). This provides the first evidence that hsc70 transports cytoplasmic protein antigens to lysosomes for degradation and presentation, but it is surprising that the resulting peptides are presented by class I molecules; whether or not they were also presented by class II molecules was not investigated.

Aims of the Project

The aim of the project has been to investigate possible roles for hsp70s in the class I and class II pathways of antigen processing and presentation:

1. To determine the involvement of PBP74 in the processing of antigens to peptides that bind to class II molecules

A good case has been made for this, as PBP74 was initially localised in early endosomes (VanBuskirk *et al.*, 1991) and antibodies raised against PBP74 inhibited the class II pathway of antigen processing. However, later work has suggested other localisation patterns for this protein, either in the cytoplasm (Wadhwa *et al.*, 1993c), or the mitochondrion (Bruschi *et al.*, 1993; Michikawa *et al.*, 1993b). Given this controversy, the first stage of elucidating the possible involvement of PBP74 in antigen processing was to determine its precise intracellular location. This research was extended to look for members of the hsp70 family in lysosomes.

2. To investigate the specificity of hsp70hom for peptides and the structural basis for this specificity

A candidate for involvement in the class I pathway of antigen processing is the constitutive MHC-encoded hsp70, hsp70hom. Other experiments in our laboratory are examining the possibility that hsp70hom binds to peptides in the cell and if so, which. To complement these *in vivo* data, a recombinant peptide-binding domain from hsp70hom could be used for nuclear magnetic resonance spectroscopy (NMR) studies to determine the structural basis of peptide binding to hsp70hom, and hsp70s in general. Such a domain

might be useful for peptide-binding studies *in vitro*, to enable conclusions to be drawn about the specificity of hsp70hom that might be applied more broadly than the *in vivo* data.

3. To determine whether hsp70s are induced during an immune response

Circumstantial evidence for the involvement of the MHC-encoded hsp70s in the presentation of antigens by class I molecules would be provided if they were found to be coregulated with other members of the processing pathway. Three proteasome subunits, the two TAP subunits and MHC class I molecules themselves are all induced by interferon-γ, and MHC class I molecules and TAP are also induced by tumour necrosis factor. Investigation of the effects of a panel of cytokines on various cell types will answer this question.

Chapter 2: Methods

General laboratory chemicals were obtained from Sigma or BDH, apart from Tris (Ultrol grade), which was obtained from Nova Biochem. The pH of solutions was adjusted with HCl or NaOH, except that acetic acid was used for sodium acetate solutions.

A. Cell Culture

A1 Bacterial Culture

All solutions for bacterial culture were steam-sterilised by autoclaving, unless otherwise stated, and some solutions were filter sterilised by passage through a 0.22 μm filter (Millipore). Bacterial cultures were grown from single colonies or 5 μl of glycerol stock, in L broth [1% (w/v) Bacto tryptone (Difco), 1% (w/v) NaCl, 0.5% (w/v) yeast extract (Oxoid)] unless otherwise stated, in an incubator shaking at 150-200 revolutions per minute at 37 °C. *Escherichia coli* transformed with plasmids carrying the Amp^R gene were grown in L broth (Sigma) supplemented with 50 μg/ml ampicillin (from a 20 mg/ml filter sterile frozen stock in 1 M $NaHCO_3$). Colonies were selected on agar plates made from L broth with 1.5% (w/v) Bacto agar (Difco), supplemented when appropriate with 50 μg/ml ampicillin. Bacterial stocks, comprising 450 μl of culture mixed with 50 μl of 10 x Hogness solution [40% (v/v) glycerol, 10 mM $MgSO_4$, 36 mM K_2HPO_4, 13 mM KH_2PO_4, 20 mM Tris-sodium citrate, pH 7.4], were stored at -70 °C.

The *E. coli* strains used were: NM554, for general use (Raleigh *et al.*, 1988); TG1, for producing single-stranded DNA (Sambrook *et al.*, 1989); and BL21, for protein

expression, since it is deficient in the proteases OmpT and Lon and grows in minimal medium (Phillips *et al.*, 1984).

A2 Preparation of Competent Bacterial Cells

Competent cells of *E.coli* strain NM554 (for general use) or BL21 (for expression studies, see Section E7) were prepared for transformation [Section C8] as follows. 20 ml of TYM broth [2% (w/v) Bacto tryptone, 0.5% (w/v) Yeast extract, 0.1 M NaCl, 10 mM $MgSO_4$] was inoculated with a single colony of the appropriate bacterial strain, grown to mid-log phase (OD_{600}=0.3-0.5) and diluted in 100 ml of TYM broth in a 2 l flask. When the OD_{600} of this culture reached 0.5-0.9, it was diluted with a further 400 ml of TYM and grown until its OD_{600} reached ~0.6, when it was rapidly cooled on ice. The cells were then pelleted by centrifugation at 625 g for 20 minutes (4 °C), and resuspended in 100 ml of ice-cold filter sterilised TfB-1 buffer [100 mM KCl, 50 mM $MnCl_2$, 30 mM potassium acetate, 10 mM $CaCl_2$, 15% (v/v) glycerol, pH 7] by gently shaking on ice. The cells were pelleted as before and gently resuspended in 20 ml ice-cold filter sterilised buffer TfB-II [75 mM $CaCl_2$, 10 mM KCl, 15% (v/v) glycerol, 10 mM MOPS, pH adjusted to 5.8 with acetic acid]. The cell suspension was then aliquoted into prechilled sterile 1.5 ml tubes, frozen on dry ice and stored at -70 °C.

For use in the preparation of single-stranded DNA [Section C14], competent cells of *E.coli* strain TG1 were prepared as follows. 1 ml of an overnight culture grown in TYM broth was diluted 100-fold in a 1 litre conical flask with TYM broth, grown until the OD_{600} was ~0.5 and centrifuged at 625 g for 15 minutes at 4 °C. The pellet was gently resuspended in 33 ml of filter sterilised buffer RF1 [100 mM RbCl, 50 mM $MnCl_2$, 30 mM potassium acetate, 10 mM $CaCl_2$, 15% (v/v) glycerol, pH 5.8], incubated on ice for 15 minutes and centrifuged at 625 g for 15 minutes at 4 °C. The pellet gently resuspended in 8 ml filter sterilised RF2 buffer [75 mM $CaCl_2$, 10 mM RbCl, 15% (v/v) glycerol, 10

mM MOPS, pH 6.8] and incubated on ice for 15 minutes. The cell suspension was aliquoted into prechilled 1.5 ml microfuge tubes, frozen on dry ice and stored at -70 °C.

A3 Mammalian Cell Culture

Tissue culture cells were grown in flasks (Nunc) at 37 °C under a 5% (v/v) CO_2 atmosphere, unless otherwise stated. Culture media were supplemented with 10% (v/v) foetal calf serum (TCS) that had been heat-inactivated by incubation at 55 °C for 30 minutes. The media used were Dulbecco's modified Eagle's medium (DMEM, Sigma) (Jelachich *et al.*, 1984) supplemented with 4 mM glutamine (Sigma), RPMI 1640 medium (Gibco) and L-15 Liebovitz medium (Gibco) (see Figure 2-1). Adherent cells were detached by treatment with 0.5% (w/v) trypsin, 0.2% (w/v) EDTA (Sigma) for 2-5 minutes at 37 °C, after they had been washed with PBS (phosphate-buffered saline, without Mg^{2+} and Ca^{2+}, Gibco). New flasks were seeded by dilution of an appropriate quantity of the detached cells in fresh culture medium.

Recombinant human cytokines were obtained from Boehringer (IFN-γ) and Advanced Protein Products (TNF, IL-1 and IL-6). They were stored in aliquots at -70 °C.

Cell Line	Origin	Culture Medium
HeLa	epitheloid carcinoma	DMEM
HepG2	hepatocellular carcinoma	DMEM
TK143B	osteosarcoma	DMEM
HT1080	fibrosarcoma	DMEM
SW620	colon adenocarcinoma	Liebovitz
Raji	Burkitt's lymphoma	RPMI
LCL721.45	B lymphoblastoid cell	RPMI
COS7	SV40-tranformed kidney cell	DMEM

Figure 2-1: Cell lines. All the cell lines used are of human origin, with the exception of COS7, which is derived from a Green African Monkey.

B. General Nucleic Acid Techniques

B1 Organic Extraction

DNA and RNA were purified from proteins by organic extraction, with an equal volume of 50% (v/v) phenol (Camlab), 48% (v/v) chloroform, 2% (v/v) propan-2-ol. The samples were mixed vigorously by vortexing and after centrifugation at 12 000 g, the upper aqueous layer containing the nucleic acids was collected leaving the aggregated proteins at the interface with the organic phase.

B2 Ethanol Precipitation

DNA and RNA were precipitated from aqueous solution by addition of 2-3 volumes of ethanol and 0.1 volume of 3 M sodium acetate, pH 7, chilled at -70 °C for 10 minutes and centrifuged at 12 000 g for 5 minutes. 1 ml of 70% (v/v) ethanol was added to the pellet, centrifuged at 12 000 g for 5 minutes and discarded. The pellet was allowed to dry in air and was resuspended in 50 µl TE (0.1 mM EDTA, 10 mM Tris, pH 7.4).

B3 Determination of Nucleic Acid Concentration

Quantities of DNA and RNA were calculated from their OD_{260} in aqueous solution, using the formula $OD=\varepsilon cl$, where c is the concentration (g/l), ε is the extinction coefficient (25000 l/g/cm for nucleic acid at 260 nm) and l is the path length of the spectrophotometer (1 cm). In other words, a 40 µg/ml solution of nucleic acid will produce an OD_{260} of 1. Alternatively, plasmid DNA was digested with restriction enzymes [C2] and separated by agarose gel electrophoresis [C3] so that the quantity of DNA could be judged by eye against the 1 kilobase (kb) standards (Gibco), in which the concentration of each fragment is 100 ng/µl.

C. DNA Techniques

C1 Preparation of Plasmid DNA

The plasmids used were pBluescript-KS$^+$ (Stratagene), pcDNA3 (Invitrogen) and pGEX-2T (Pharmacia) and carried the ampicillin resistance gene Amp^R. Preparation of plasmid DNA was generally carried out by a modified alkaline lysis method (Birnboim and Doly, 1979). A 5 ml culture of *E. coli* transformed with the appropriate plasmid was grown overnight [A1] and the cells harvested by centrifugation at 625 g for 5-10 minutes. The pellet of cells was resuspended in 200 µl lysis buffer (50 mM glucose, 10 mM EDTA, 25 mM Tris, pH 8), transferred to a 1.5 ml microfuge tube and mixed thoroughly with 400 µl of freshly prepared 0.2 M NaOH, 1% (w/v) SDS and then 300 µl of 3 M sodium acetate, pH 4.8. After incubation on ice for 5 minutes, the genomic DNA and cell debris were pelleted by centrifugation at 12 000 g for 5 minutes. The plasmid DNA in the supernatant was precipitated upon addition of 600 µl propan-2-ol, incubation at -70 °C for 10 minutes and centrifugation at 12 000 g for 5 minutes. The pellet was resuspended in 200 µl of 0.3 M sodium acetate, pH 7 and the DNA was purified by phenol/chloroform extraction and precipitated with 600 µl propan-2-ol as before. The pellet was washed by addition of 1 ml of 70% (v/v) ethanol and centrifugation at 12 000 g for 5 minutes and resuspended in 50 µl TE. RNA was removed from the plasmid preparation by incubation at 37 °C for 30 minutes with 2 µg of RNase A, which had previously been heated at 80 °C for 10 minutes to inactivate any DNase present. The DNA was stored at -20 °C and the yield of DNA was typically 25-50 µg [B3].

Large scale preparations of plasmid DNA were performed using the Wizard maxiprep DNA purification system (Promega). A 10 ml culture was grown for ~3 hours at 37 °C and used to inoculate a 500 ml overnight culture in a 2 litre conical flask. The cells were pelleted at 2 000 g for 15 minutes and the DNA prepared according to the manufacturer's

instructions. The DNA was stored at 4 °C and the yield of DNA was typically 2.5-5 mg [B3].

Large scale preparations of plasmid DNA for mammalian cell transfection experiments were carried out by caesium chloride gradient centrifugation (Sambrook *et al.*, 1989). Two 2 l flasks containing 500 ml of medium were inoculated with 5 ml of an overnight culture and grown overnight. The cells were harvested by centrifugation at 2 000 g for 15 minutes, resuspended in 20 ml of lysis buffer (50 mM glucose, 10 mM EDTA, 25 mM Tris, pH 8) and mixed with 40 ml of 0.2 M NaOH, 1% (w/v) SDS and then 30 ml of 3 M sodium acetate, pH 4.8. After a 30 minute incubation on ice, genomic DNA was pelleted by centrifugation at 12 000 g for 10 minutes, and plasmid DNA was precipitated from the supernatant by addition of 2 volumes of ethanol and incubation at -70 °C for 20 minutes. The DNA was recovered by centrifugation at 12 000 g for 10 minutes, dried and resuspended in 6 ml of SET buffer (150 mM NaCl, 5 mM EDTA, 50 mM Tris, pH 8). 0.016 % (w/v) ethidium bromide and 7 g of caesium chloride (optical grade, Sigma) were added and the density was checked by weighing, to ensure that it was close to 1.6 g/ml. The solution was overlaid with paraffin and centrifuged for 16 hours at 200 000 g (55 000 rpm in a 70.1 Ti rotor) at 18 °C in a sealed tube. The gradient was allowed to relax at 140 000 g (45 000 rpm in a 70.1 Ti rotor) for 1 hour and the rotor was slowed without using the brake. The band of closed circular plasmid DNA was removed with a syringe needle and the ethidium bromide present was extracted with five equal volumes of water-saturated butanol. The sample was mixed with 3 volumes of water and 8 volumes of ethanol and chilled at -70 °C for 2 hours. The plasmid DNA was recovered by centrifugation at 12 000 g for 10 minutes, resuspended in 400 µl of 0.3 M sodium acetate, pH 7 and reprecipitated with 1 ml of ethanol at -70 °C for 30 minutes. The DNA was pelleted by centrifugation as before, resuspended in 100 µl of TE and stored at 4 °C. The yield was typically 0.5-1 mg [B3].

C2 Restriction Enzyme Digestion

Restriction enzymes were obtained from Promega, with the exceptions of *Ava* I (Gibco), *Bam*H I (Amersham), *Nae* I (New England Biolabs), *Not* I (CP Labs), *Sma* I (Boehringer) and *Sst* I (Gibco). Restriction digests were carried out in buffers recommended by the manufacturer. For analytical digests, ~1 µg DNA was digested with 1-5 U enzyme in 10 µl reactions at 37°C for 2 hours, while large scale digests (usually containing ~15 µg of DNA) were performed in 150 µl reactions with 15-50 U enzyme. Spermidine (5 mM final concentration) was added to digests performed in buffers containing more than 50 mM NaCl.

C3 Agarose Gel Electrophoresis

DNA fragments produced by restriction digestion [C2] were separated by agarose gel electrophoresis (Southern, 1975). Submerged horizontal slab gels (10 x 10 x 0.5 cm) were prepared by melting 0.8%-1.5% (w/v) agarose (SeaKem HGT, Flowgen) in TBE buffer (90 mM Tris, 1 mM EDTA, 90 mM boric acid) containing 0.001% (w/v) ethidium bromide. Samples (5-10 µl) were mixed with 0.1 volume of glycerol dyes [30% (v/v) glycerol, 0.1% (w/v) bromophenol blue, 0.1% (w/v) xylene cyanol, 5 mM EDTA, pH 8] and loaded in the wells alongside one well containing 1 kb Ladder (Gibco) as standards. Electrophoresis was carried out at 80 mA in TBE for 1-2 hours. DNA was visualised on an ultraviolet transilluminator (UVP).

C4 Gel Purification

To purify DNA fragments of a particular size from restriction digests, they were separated by agarose gel electrophoresis [C3] and excised from the gel with a clean razor blade. The DNA was recovered by one of two methods.

For cloning, DNA was recovered by electroelution. Gel slices were placed into the chambers of a unidirectional electroelution apparatus (International Biotechnologies) filled with 50 mM NaCl, 4 mM EDTA, 200 mM Tris, pH 8. The V-chamber beneath each gel slice was filled with 80 µl of 7.5 M ammonium acetate, 0.01% (w/v) bromophenol blue and electrophoresis was carried out for 30 minutes at 100 V. The ammonium acetate buffer containing the DNA was carefully removed in excess (250 µl) and the DNA was precipitated with an equal volume of propan-2-ol for 30 minutes on ice. The precipitate was pelleted at 12 000 g for 5 minutes, washed with 1 ml of 70% (v/v) ethanol and resuspended in 10 µl of TE.

For use as a labelled probe [D6], DNA was extracted from agarose gel slices using the Qia-quick gel extraction kit (Qiagen), following the manufacturer's instructions. DNA samples were eluted in 30-50 µl 10 mM Tris, pH 7.4. Alternatively, the slice was simply melted at 50 °C in 3 volumes of water (if the gel was prepared with low rather than high gelling temperature agarose) and an aliquot was added directly to labelling reactions.

C5 Klenow End-Filling of Recessed 3' Termini

Many restriction enzymes generate recessed 3' termini, which can be treated with the Klenow fragment of DNA polymerase I to generate blunt ends. These blunt ends can be ligated together with other blunt ends generated by end-filling or by digestion with certain restriction enzymes (e.g. *Sma* I). Each DNA sample (10-15 µg) was precipitated and resuspended in Klenow buffer (50 mM NaCl, 10 mM $MgCl_2$, 10 mM DTT, 10 mM Tris, pH 7.4) containing 250 µM of each dNTP and 2U of Klenow enzyme (Amersham), and incubated at 37 °C for 30 minutes. The DNA was then purified by organic extraction [B1] and ethanol precipitation [B2].

C6 Dephosphorylation

A vector that has been digested with restriction enzymes can be prevented from ligating back together if the phosphate groups are removed from its 5' ends. Vectors were dephosphorylated by incubation with 0.01 U calf intestinal alkaline phosphatase (Boehringer) per pmol of 5' ends, for 30 minutes at 37 °C in 50 µl of the recommended buffer. Reactions were terminated and the enzyme inactivated by heating at 80 °C for 10 minutes. The vector DNA was then purified by organic extraction [B1] and ethanol precipitation [B2].

C7 Ligation

Inserts for ligation were prepared by restriction digestion [C2], purified by agarose gel electrophoresis [C3] and recovered by electroelution [C4]. Ligations were performed at room temperature for 5 hours, in a volume of 10 µl containing equal quantities of vector and insert DNA (5-20 ng of each), 1U of T4 DNA ligase (Amersham), 1 mM ATP, 10 mM $MgCl_2$, 20 mM DTT, 50 µg/ml BSA, 1 mM spermidine and 50 mM Tris, pH 7.4. Ligations were also set up with only vector DNA to determine how efficiently it had been dephosphorylated. In ligations using blunt-ended vector DNA, 10 ng of *Alu* I-cut pBluescript DNA was used as a positive control insert. The ligated plasmid DNA was used to transform competent cells [C8], and colonies containing the correct plasmid insert were identified in one of a number of ways [C10].

C8 Transformation

Plasmid DNA (~10 ng or the products of one ligation) was mixed with 50 µl of thawed competent *E.coli* cells [A2], incubated on ice for 20 minutes and then heat shocked at 37 °C for 5 minutes. L broth (150 µl) was added and the samples were incubated for a further 30

minutes at 37 °C before being spread onto L plates containing ampicillin and incubated at 37°C overnight. When transforming ligation reactions, the restriction-digested vector DNA was used as a negative control to indicate how much uncut vector it contained. Circular pBluescript vector (10 ng) was used as a positive control.

C9 Identification of Recombinant Clones

Transformed cells were screened for plasmids containing the correct inserts primarily by preparing plasmid DNA [C1] from colonies picked at random and restriction digestion [C2] to see if fragments of the expected size were produced. In pBluescript, recombinant clones could be identified by blue/white selection, because insertion of DNA into this vector's multiple cloning site disrupts the *lac* Z gene, which encodes ß-galactosidase. Cells transformed with pBluescript were spread onto agar plates containing 0.01% (w/v) 5-bromo-4-chloro-3-indolyl ß-galactopyranoside (X-Gal, Nova Biochem), a chromogenic ß-galactosidase substrate, and 1 mM IPTG, to induce expression of *lac* Z. Colonies transformed with vector containing inserts stayed white, and were screened by restriction digestion.

C10 Oligonucleotides

Oligonucleotides were synthesised using an Applied Biosystems 381A automated DNA synthesiser by Mr. A. Gascoyne. They were released from the column by incubation at room temperature with four 500 µl volumes of 35% (v/v) ammonia solution for 15 minutes each. The eluted oligonucleotides were deprotected by further incubation at 55 °C for ~16 hours, ethanol precipitated [B2] and resuspended in water. Their concentrations were determined spectrophotometrically [B3], using the approximation that the molecular weight of 1 nucleotide is 330.

The sequences of oligonucleotide primers used for PCR [C13] and sequencing [C15] did not contain palindromic sequences or long tracts of any one nucleotide. Primers used for PCR or sequencing of cloned DNA were not complementary to other sequences in the vector or insert, and primers used for PCR from first strand cDNA did not have significant identity to other sequences known to be expressed in humans (as determined by a FastA search of the GenEMBL database). The primers in a pair were designed to have the same annealing temperature for template DNA (~60 °C). The annealing temperatures (°C) of duplexes less than 25 base pairs (bp) were calculated by multiplying the number of G:C base pairs by four and adding this to the number of A:T base pairs multiplied by two.

C11 Labelling of Oligonucleotides

Some primers were phosphorylated with γ-[^{32}P] ATP (Amersham) to assess their purity by denaturing acrylamide electrophoresis. Each oligonucleotide (10 ng) was mixed with 10 μCi of γ-[^{32}P] ATP (3000 mCi/mmol) and 1 U of polynucleotide kinase (Boehringer) in buffer provided by the manufacturer. The products of the reaction were incubated at 37 °C for 30 minutes, mixed with an equal volume of formamide dyes [98% deionised formamide, 10 mM EDTA (pH 8), 0.025% (w/v) xylene cyanol, 0.025% (w/v) bromophenol blue], separated on a 12% (v/v) acrylamide denaturing gel [C16] and detected by autoradiography.

C12 Polymerase Chain Reactions (PCR)

DNA was amplified from plasmid DNA [C1] or first strand cDNA [D2] by polymerase chain reaction (PCR) (Erlich *et al.*, 1991). PCR was performed in 100 μl volumes using either Biotaq (Bioline), *Taq* polymerase (Promega) or *Tli* polymerase (Promega), in buffers supplied by the manufacturers. The reactions included 1 μM primers (Figure 2-2a), 1.5 mM $MgCl_2$, 1 mM of each dNTP (Promega) and 1U enzyme, and were overlaid

Primer	Position	Template	Sequence (5'-3')
5' HOM-P	2108-2127	hsp70hom	CGGGATCCGGGGACAAGTCTGAGAAGG
3' HOM-P	2625-2645	hsp70hom	CGGAATTC**A**GCCCTTCAAACCTTCATCAC
5' PBP	89-109	PBP74	TAGGATCCATGATAAGTGCCAGCCGAG
3' PBP	2098-2128	PBP74	TTCTGCTCCATGGACTGTTTTTCCTCCTTTTG
5' Actin	45-64	Actin	GATGATGATATCGCCGCGCT
3' Actin	610-629	Actin	GCGCTCGGTGAGGATCTTCA

Figure 2-2a: Primers used to amplify and clone the sequences encoding the hsp70hom peptide-binding domain and PBP74 by PCR. The engineered restriction sites are underlined (*Bam*H I in 5' HOM-P and 5' PBP, *Eco*R I in 3' HOM-P and *Nco* I in 3' PBP). An A nucleotide introduced to generate a stop codon in 3' HOM-P is shown in bold. The nucleotides of hsp70hom are numbered according to Milner and Campbell (1990), those of PBP74 according to Domanico *et al.* (1993) and those of actin according to Ponte *et al.* (1984).

Primer pair	Cycle parameters
5' and 3' HOM-P	94 °C for 1 min, 58 °C for 1 min and 72 °C for 1 min
5' and 3' PBP	94 °C for 2 min, 58 °C for 3 min and 72 °C for 3 min
5' and 3' actin	94 °C for 1 min, 62 °C for 1 min and 72 °C for 45 s

Figure 2-2b: PCR conditions used to amplify and clone the sequences encoding the peptide-binding domains of hsp70hom and PBP74. The reactions were carried out with thirty cycles of the conditions described above, preceded by an incubation at 94 °C for 5 minutes and followed by an incubation at 72 °C for 10 minutes.

with 3 drops of paraffin. PCR was carried out with 30 cycles of denaturation at 94 °C, annealing at 58 °C and extension at 72 °C (Figure 2-2b) followed by a 10 minute incubation at 72 °C. The reaction products were analysed by agarose gel electrophoresis [C3].

C13 Preparation of Single-Stranded DNA

Single-stranded DNA is easier to sequence [C15] than double-stranded DNA and can be prepared from pBluescript vectors. A colony of *E. coli* strain TG1 transformed with pBluescript was inoculated into 1.5 ml of TY medium [1.6% (v/v) Bacto tryptone, 1% (v/v) yeast extract, 0.5% (v/v) NaCl] containing 10^7 plaque forming units per ml of M13K07 helper bacteriophage and grown for 1 hour, after which 40 µg/ml kanamycin was added. The culture was incubated overnight, transferred to microfuge tubes and centrifuged at 12 000 g for 10 minutes. The supernatant was mixed with 200 µl of 20% (v/v) PEG 4000 and incubated on ice for 30 minutes. Single stranded DNA was harvested by centrifugation at 12 000 g for 10 minutes, resuspended in 150 µl water, purified by organic extraction [B1] and ethanol precipitation [B2], and resuspended in 20 µl water. The yield [B3] was generally ~20 ng DNA.

C14 Sequencing

Sequencing reactions were performed by dideoxy chain termination (Sanger *et al.*, 1977), using Sequenase version 2.0 (United States Biochemical), according to the manufacturer's instructions (Tabor and Richardson, 1987; Tabor and Richardson, 1989). Double-stranded plasmid DNA (~5 ng) [C1] was denatured for 30 minutes before use in 0.2 M NaOH, 0.2 mM EDTA at 37 °C, neutralised with 0.1 volume 3M sodium acetate, pH 4.8 and ethanol precipitated [B2]. The pellet was resuspended in 7 µl sterile water and used for sequencing. Single-stranded DNA templates (~0.5 ng) [C13] were used directly.

Primer	Position	Template	Sequence (5'-3')
M13 universal		pBluescript	TGACCGGCAGCAAAATG
H4	2280-2298	hsp70hom	CTGATCCAGGTGTATGAGG
PBPso1	332-350	PBP74	CTGAAGGTGCCAGAACCAC
PBPso2	652-671	PBP74	AATGCTGTGATCACAGTCCC
PBPso3	969-989	PBP74	GACAGGGGTTGATTTGACTAA
PBPso4	1276-1295	PBP74	TTTGATTGGAATTCCACCAGC
PBPso5	1602-1622	PBP74	TTTGATTGGAATTCCACCAGC
PBPso6	1901-1920	PBP74	CTGCTGATGAGTGCAACAAG

Figure 2-3: Primers used to sequence the cloned PCR products encoding the hsp70hom peptide-binding domain and PBP74. The numbering is according to the sequences of Milner and Campbell (1990) (for hsp70hom) and Domanico *et al.* (1993) (for PBP74).

Sequencing was carried out using 3 ng of primers (Figure 2-3) and completed sequencing reactions were separated by 6% (v/v) denaturing acrylamide gel electrophoresis [C16].

C15 Denaturing Acrylamide Gel Electrophoresis

Denaturing acrylamide gel electrophoresis was used to separate the products of sequencing reactions [C15] and phosphorylated oligonucleotides [C12]. The samples were heated for 5 minutes at 80 °C (sequencing) or 55 °C (oligonucleotides) and 3 µl was loaded immediately on 0.4 mm thick denaturing acrylamide gels [6% or 12% (v/v) acrylamide (National Diagnostics: Accugel 40), TBE, 42% (w/v) urea, polymerised with 400 µl 10% (w/v) APS, 40 µl Tetramethyl ethylene diamine (TEMED), 50 ml total volume] using a sharks-tooth comb (Gibco BRL). The front plate was treated with Gel Slick (AT Biochem) before the gel was poured to prevent it sticking when the apparatus was disassembled. Electrophoresis was carried out in TBE buffer at 30 mA.

When separating sequencing reactions, 0.3 M sodium acetate was added to the lower reservoir when the dye front had travelled three quarters of the way down the gel, to slow the progress of the shorter DNA fragments. Gels were fixed in 10% (v/v) methanol, 10% (v/v) acetic acid and dried on 3MM paper (Whatman) using a heated vacuum gel drier (BioRad). Autoradiography was carried out at room temperature for 1-3 days, using X-ray film (X-OMAT S, Kodak), which was developed with a Kodak ME-1 automatic processor.

When separating γ-[^{32}P]-labelled oligonucleotides, electrophoresis was carried out until the slow blue dye was half way down the gel. The gel was left on the bottom glass plate, covered in Saran Wrap and autoradiographed at room temperature. Unlabelled oligonucleotides were treated in the same way, but detected by ultraviolet shadowing, in which the gel was placed onto a thin layer chromatography plate and illuminated with an ultraviolet lamp (Camag).

D. RNA Techniques

D1 Preparation of RNA

All solutions for RNA procedures were autoclaved where possible, or made with autoclaved water in autoclaved glassware, to avoid contamination with RNases. RNA was prepared from cultured cell lines [A3] using RNAzol B (Biogenesis), according to the manufacturer's instructions. The RNA was resuspended in water, quantified spectrophotometrically [B3] and stored in 70% (v/v) ethanol, 0.3 M sodium acetate, pH 7 at -20 °C (Chomczynski and Sacchi, 1987). Before use, it was recovered by centrifugation at 12 000 g for 5 minutes and resuspended in water. Approximately 20 µg of RNA could be purified from 10^6 cells, depending on the cell line.

D2 First Strand cDNA Synthesis

First strand cDNA was synthesised by reverse transcription of ~1 µg total RNA [D1] with AMV reverse transcriptase, using the First Strand cDNA Synthesis Kit (Promega). It was ethanol precipitated [B2] for storage at -20 °C, and resuspended in water before use.

D3 Separation of RNA by Agarose Gel Electrophoresis

RNA was separated according to size by agarose gel electrophoresis (Fourney *et al.*, 1988). Horizontal slab gels (20 x 20 x 0.5 cm) were prepared by melting 1% (w/v) high gelling temperature agarose in MOPS buffer (5 mM sodium acetate, 1 mM EDTA, 20 mM MOPS, pH 7) and adding deionised formaldehyde to the gel at 55 °C to a final concentration of 1.9% (v/v). Total RNA (20 µg) was resuspended in 5 µl RNase-free water and denatured by heating at 65 °C with 25 µl of sample buffer [50% (v/v) formamide, 5.9% (v/v) formaldehyde, 4% (v/v) glycerol in MOPS buffer , 0.005% (w/v)

bromophenol blue] for 5 minutes. It was then chilled on ice for 2 minutes, mixed with 0.03% (w/v) ethidium bromide and loaded onto the gel. Samples were electrophoresed overnight at 45 mA in MOPS buffer and visualised on an ultraviolet transilluminator. Prior to Northern blotting [D4], the positions of the major bands (the 18S and 28S ribosomal RNAs) was noted. Formaldehyde [37% (v/v) stock] and formamide were deionised by mixing with Duolite MB 6113 mixed resin (Sigma) for 30 minutes, and then filtered through filter paper (Whatman #50).

D4 Northern Blotting of RNA

RNA was transferred from agarose gels to nitrocellulose by Northern blotting (Fourney *et al.*, 1988). An agarose gel containing separated RNA samples [D3] was washed once in 1 x SSC, 0.5 M NaOH and twice in 10 x SSC at room temperature, for 20 minutes each. It was placed onto three sheets of 3MM filter paper (Whatman) on top of a 1 cm layer of sponges (J. Sainsbury), all soaked in 10 x SSC. A Hybond-C extra nitrocellulose membrane (Amersham) was prewetted in 10 x SSC and placed on top of the gel, without introducing bubbles. Three sheets of prewetted 3MM paper (Whatman) were placed on top of the membrane, followed by a stack of paper towels and a weight. The transfer proceeded by capillary action overnight, with 10 x SSC as the transfer buffer. The RNA was fixed to the membrane by baking at 80 °C for 2 hours. Solutions containing SSC were made from a 20 x stock containing 3 M NaCl and 0.3 M sodium citrate, pH 7.

D5 Slot Blotting of RNA

RNA [D1] was applied directly to nitrocellulose membranes by slot blotting (Sambrook *et al.*, 1989). A 6 x 22 cm sheet of nitrocellulose (Hybond-C extra) was soaked for 1 hour in 20 x SSC and placed on the vacuum unit of a Minifold II (Schleicher & Shuell), on top of two sheets of 3MM paper (wetted in 20 x SSC). The apparatus was clamped together

and the slots were twice filled with 10 x SSC and emptied by applying gentle suction. The RNA samples (4 µg of each) were prepared by being incubated at 68 °C for 15 minutes in 50% (v/v) formamide, 7% (v/v) formaldehyde, 1 x SSC. They were mixed with two volumes of 20 x SSC and loaded immediately in the slots, drawn onto the nitrocellulose by gentle suction and washed twice with 1 ml of 10 x SSC. Suction was continued for 5 minutes, after which the nitrocellulose was removed from the apparatus, allowed to dry completely and baked for 2 hours at 80 °C.

D6 Probing RNA Blots with Radiolabelled DNA

DNA probes were labelled by random hexanucleotide priming (Feinberg and Vogelstein, 1984). Between 20 and 50 ng of gel purified DNA (in aqueous solution or in melted agarose) [C4] was diluted to 30 µl with water, boiled for 5 minutes and cooled on ice (or to 37 °C for those preparations containing agarose). The DNA was mixed with 10-50 µCi of α-[^{32}P] dCTP (3 000 mCi/mmol, Amersham), random hexanucleotide primers, the nucleotides dATP, dGTP and dTTP and Klenow DNA polymerase (all from the Multiprime system, Amersham). After incubation at room temperature overnight or at 37 °C for 1 hour, unincorporated nucleotides were removed by desalting the labelled probe through a Sephadex G-50 nick column (Pharmacia) with TE, according to the manufacturer's instructions. Typical specific activities obtained were 10^7-10^9 counts per minute (cpm) per µg DNA.

Hybridisation of radiolabelled DNA to RNA bound to nitrocellulose membranes was carried out as follows. The blots were washed with 50 ml prewash buffer [1 M NaCl, 0.1% (w/v) SDS, 1 mM EDTA, 50 mM Tris, pH 7.4] for 30 minutes at 42 °C, in a rotating hybridisation oven (Hybaid). Salmon sperm DNA (100 µg/ml in TE, stored at -20 °C) was prepared by being boiled for 5 minutes, cooled and passed several times through a 19G1.5 needle. It was mixed with hybridisation buffer [50% (v/v) formamide,

1 M NaCl, 10% (w/v) dextran sulphate (Pharmacia), 0.2% (w/v) BSA, 0.2% (w/v) Ficoll 400 (Pharmacia), 0.2% (w/v) polyvinylpyrrolidone, 0.1% (w/v) sodium pyrophosphate, 0.1% (w/v) SDS, 50 mM Tris, pH 7.4], boiled for 5 minutes, cooled to 42 °C and incubated overnight at 42 °C with the blots. The next morning, radiolabelled probes were boiled in hybridisation buffer ($\geq 10^6$ cpm/ml), cooled to 42 °C and mixed with the blots for 24 hours at 42 °C.

Following hybridisation, the nitrocellulose membranes were washed in 2 x SSC, 0.1% (w/v) SDS for 20 minutes at 42 °C followed by two high stringency washes for 30 minutes at 65 °C, in 0.2 x SSC, 0.1% (w/v) SDS (for Northern blots) or in 0.1 x SSC, 0.1% SDS (for slot blots). The blots were allowed to dry partially, wrapped in Saran Wrap and autoradiographed at -70 °C using sensitised X-ray film and two tungstate intensifying screens. Alternatively, the hybridised probe was detected using phosphor screens (Molecular Dynamics) and a Storm 860 Imager (Molecular Dynamics) and analysed using ImageQuaNT software (Molecular Dynamics). Signals on slot blots were quantified in columns using the Peak Finder and Area Report commands.

After detection, hybridised probes were removed from RNA blots by incubation in 0.5% (w/v) SDS. The blot was left for 10 minutes in SDS solution that had been brought to the boil and removed from the heat. The blot was then washed in 2 x SSC at room temperature for 5 minutes. Prior to adding a different probe, the efficacy with which the probe had been stripped from the blot was confirmed by autoradiography.

E. Protein Techniques

E1 SDS-Polacrylamide Gel Electrophoresis

Proteins were separated by sodium dodecyl sulphate-polyacrylamide gel electrophoresis (SDS-PAGE) (Laemmli, 1970). 10% (w/v) or 12% (w/v) polyacrylamide minigels (6 cm x 9 cm) were prepared as follows. The resolving gel [10% or 12% (w/v) acrylamide (Protogel, National Diagnostics), 0.025% (w/v) SDS, 0.375 M Tris-HCl, pH 8.8, polymerised with 0.05% (w/v) APS and 0.05% (v/v) TEMED] was poured to within 2 cm of the top of the lower plate, overlaid with water or water-saturated butanol (to ensure a very sharp boundary) and allowed to set. The stacking gel [5% (w/v) acrylamide, 0.025% (w/v) SDS, 125 mM Tris, pH 6.8, polymerised as before] was then poured and combs containing 10 or 15 teeth were inserted. Samples and prestained molecular weight standards (low or high molecular weight, Gibco) were boiled with an equal volume of 2 x protein sample buffer [4% (w/v) SDS, 1.4 M 2-mercaptoethanol, 20% (v/v) glycerol, 0.025% (w/v) bromophenol blue, 0.12 M Tris, pH 6.8] for 5 minutes and loaded into the wells in the stacking gel with duck-billed tips. Electrophoresis was performed at 150 V in 192 mM glycine, 0.1% (w/v) SDS, 25 mM Tris, pH 9, using a mini-Protean II apparatus (BioRad). The proteins in the gel were then detected by Coomassie blue staining [E3] or Western blotting [E4, E5].

E2 Native Gel Electrophoresis

The formation of complexes between proteins can be detected by native gel electrophoresis (Fourie *et al.*, 1994). For each potential interaction, the proteins were incubated together for two hours at room temperature, in 10 µl of an appropriate buffer. As a control, each protein was incubated alone under identical conditions. The reactions

were mixed with an equal volume of 10% (v/v) glycerol, 0.01% (w/v) bromophenol blue, 120 mM Tris, pH 6.8 and loaded on a native polyacrylamide gel. The resolving gel consisted of 6% (w/v) acrylamide, 0.4 M Tris, pH 8.8 and the stacking gel of 4.5% (w/v) acrylamide, 0.12 M Tris, pH 6.8, polymerised as above [E1]. The gel was run at 100V in running buffer (192 mM glycine, 25 mM Tris, pH 8.3) and stained with Coomassie blue [E3].

E3 Staining Protein Gels

Proteins in gels [E1] were stained with Coomassie blue [0.05% (w/v) Coomassie Brilliant Blue (BioRad), 40% (v/v) methanol, 10% (v/v) acetic acid] for 15-30 minutes at room temperature, and destained overnight in 7% (v/v) methanol, 5% (v/v) acetic acid at room temperature, with shaking. Where indicated, gels were subsequently stained with silver stain (BioRad) to visualise weak bands.

E4 Western Blotting of Proteins

Proteins were transferred from SDS-PAGE gels [E1] to polyvinyl difluoride membrane (Hybond-PVDF, Amersham) by western blotting, using a BioRad transblot apparatus. The transblot cassette was assembled with a 6 x 9 cm sheet of 3MM paper (Whatman), the gel (washed in transfer buffer, q.v.), the PVDF membrane (6 x 9 cm, wet in methanol) and another sheet of 3MM paper. All dry components were wet first in transfer buffer and care was taken not to introduce bubbles between the layers. The cassette was placed in the chamber with the gel next to the negative electrode, the chamber was filled with transfer buffer [0.221% (w/v) 3-(cyclohexylamino)-1-propanesulphonic acid (CAPS), 10% (v/v) methanol] and an ice block was added. Electrophoresis was carried out at 100 V for 1.5 hours.

E5 Detection of Proteins on Western Blots

Blotted proteins [E4] were reversibly stained with 0.1% (v/v) Ponceau S (Sigma) in 1% (v/v) acetic acid for 1 minute and destained in water or phosphate buffered saline (PBS, Difco) containing 0.1% (v/v) Tween 20 (Sigma) (PBS-0.1% Tween) to check that the transfer had been even. Specific proteins were detected with antibodies (Figure 2-4). Blots were first blocked for 2 hours in 10% (w/v) skimmed milk powder (J. Sainsbury) in PBS-0.1% Tween, to prevent non-specific interactions between the antibodies and the membrane or bound proteins. Antibodies were then added to the blots in 10 ml of 1% (w/v) milk in PBS-0.1% Tween, at the dilutions indicated in Figure 2-4. After 1 hour, they were washed three times with 100 ml of PBS-0.1% Tween, once for 5 seconds and twice for 20 minutes each. To detect bound primary antibodies, secondary antibodies against mouse IgG that were conjugated with alkaline phosphatase or horse radish peroxidase (2°-AP or 2°-HRP) were added in 10 ml of 1% (w/v) milk in PBS-0.1% Tween for one hour and then washed as before.

The secondary antibody conjugated with horseradish peroxidase (2°-AP, Sigma) was detected by enhanced chemiluminescence (ECL). Blots were partially dried and 3 ml of each ECL substrate (Amersham) was added for one minute. Excess liquid was shaken off and the blots were wrapped in Saran Wrap and exposed to X-ray film for 1 minute-2 hours at room temperature.

The secondary antibody conjugated with alkaline phosphatase was detected by enhanced chemifluorescence (ECF). Blots were partially dried and 1 ml of each Vistra ECF substrate (Amersham) was added for 1 minute. Excess liquid was shaken off and the blots were wrapped in Saran Wrap and left at room temperature for 20 min-2 hours. The formation by alkaline phosphatase of a fluorescent product was detected with a Storm 860 Imager (Molecular Dynamics). The collected data was analysed using ImageQuaNT software (Molecular Dynamics). Boxes (of identical dimensions where possible) were

Antibody	Specificity	Source	Dilution
3A3	hsp70, hsc70, mt hsp70	Affinity Bioreagents (MA3-006)	1 : 3 000
5A5	hsp70, hsc70, BiP	Affinity Bioreagents (MA3-007)	1 : 2 000
4G4	hsp70	Affinity Bioreagents (MA3-009)	1 : 5 000
346.42.2	hsp70hom	Dr. P. van Endert	1 : 2 000
1B5	class II molecules (DR)	Dr. J. Trowsdale	1 : 2 000
HC10	class I molecules (heavy chain)	Dr. J. Trowsdale	1 : 2 000
5B1	HLA-DM (alpha chain)	Dr. J. Trowsdale	1 : 2 000
AC-40	actin	Sigma	1 : 3 000
2°-AP	mouse IgG	BioRad	1 : 3 000
2°-HRP	mouse IgG	Sigma	1 : 10 000

Figure 2-4: Antibodies used in the detection of proteins on Western blots. All are monoclonal mouse IgG, with the exception of 2°-AP and 2°-HRP, which are polyclonal goat and rabbit antibodies, respectively.

drawn around the bands and the intensity of the signal within the boxes was calculated with the Volume Report command, using a box around an empty area of the blot (Object Average) to calculate the background.

Antibodies could be stripped from western blots by incubation in 0.1 M 2-mercaptoethanol, 2 % (w/v) SDS, 62.5 mM Tris, pH 6.8 for 30 minutes at 50 °C, with shaking. The stripped blots were probed with the secondary antibody to confirm that the primary antibodies had been removed.

E6 Determination of Protein Concentration

The concentrations of purified proteins were determined using the bicinchoninic acid (BCA) assay (Pierce) (Smith *et al.*, 1985). Protein samples of unknown concentration were incubated at varying dilutions with the BCA reagent at 37 °C for 30 minutes. Bovine serum albumin standards (50 µg/ml, 100 µg/ml, 200 µg/ml, 400 µg/ml and 600 µg/ml) were incubated with the BCA reagent at the same time. The OD_{562} of the BSA standards were measured and plotted against concentration , allowing the concentration of the protein samples to be estimated from their OD_{562}.

E7 Expression of Glutathione-S-Transferase Fusion Proteins

The recombinant peptide-binding domains of hsp70hom and PBP74 were expressed as glutathione-S-transferase fusion proteins using the vector pGEX-2T (Smith and Johnson, 1988). The method described here is the optimised large-scale method; some conditions were varied as described in Chapter 3. A 25 ml culture of *Escherichia coli* strain BL21 transformed with pGEX-PBP or pGEX-HOM in L-broth and 50 µg/ml ampicillin was grown overnight in a 50 ml tube (Falcon) and used to inoculate a 2 l baffled flask containing 500 ml of medium. This was induced in log phase growth (OD_{600} 0.35-0.5) by

addition of IPTG to a final concentration of 100 μM, and incubated for 24 hours at 37 °C. The bacteria were harvested by centrifugation at 2 000 g for 15 minutes, resuspended in 25 ml MTPBS (150 mM NaCl, 16 mM Na_2HP0_4, 4 mM NaH_2P0_4, pH 7.3) containing 1% (v/v) Triton X100 (Sigma) and sonicated on ice at 14 μm for 5 x 30 s. Following centrifugation at 2 000 g for 10 minutes, the supernatant was mixed with 2.5 ml (bed volume) glutathione agarose (Sigma) at 4 °C for 2-6 hours. The glutathione agarose was then washed four times with 50 ml MTPBS, resuspended in an equal volume of 1 mM EDTA, 50 mM Tris, pH 8 and incubated with 25 U of thrombin (~1 U/mg fusion protein) for 6 hours at room temperature with constant mixing, to release the peptide-binding domain. This glutathione agarose suspension was centrifuged at 2 000 g for 10 minutes, and the supernatant was collected and filtered through a 0.4 μm filter (Millipore) to remove all traces of glutathione agarose.

After thrombin cleavage, the glutathione agarose could be regenerated by mixing with an equal volume of 10 mM reduced glutathione, 0.5 M NaCl, 50 mM Tris, pH 8, to elute the glutathione-S-transferase. The glutathione agarose was then washed extensively with MTPBS and an aliquot was run on a gel [E1] to check that the elution had been successful. To prevent cross-contamination, each batch of glutathione agarose was used to purify only one protein.

E8 Protein Expression in Minimal Medium

A culture of *E.coli* strain BL21 transformed with pGEX-PBP was grown overnight in L-broth and 50 μg/ml ampicillin. The cells were collected by centrifugation at 2 000 g for 10 minutes and resuspended in ten times the original culture volume (20 ml) of minimal medium [0.6% (w/v) Na_2HPO_4, 0.3% (w/v) KH_2PO_4, 0.5% (w/v) NaCl, 0.1 mM $CaCl_2$, 1 mM $MgSO_4$, 0.052% (w/v) NH_4Cl, 0.05%-0.4% (w/v) glucose] containing 50 μg/ml ampicillin, in a 50 ml tube. The minimal medium was made from an autoclaved 10 x stock

of M8 salts [6% (w/v) Na_2HPO_4, 3% (w/v) KH_2PO_4 and 5% (w/v) NaCl] and supplemented with filter sterile stocks of 1 mM $CaCl_2$, 1 mM $MgSO_4$ and 0.52% (w/v) NH_4Cl and an autoclaved stock of 20% (w/v) glucose. The cells were induced in log phase growth (OD_{600} 0.35-0.5) by addition of 100 µM IPTG and 200 µl aliquots were harvested after 24-48 hours. These were resuspended in 20 µl of water to which 20 µl of 2 x protein sample buffer was added, and separated by SDS-PAGE [E1].

E9 Reverse phase High Performance Liquid Chromatography (HPLC)

Solvents for HPLC were made up with acetonitrile (optical grade, Labscan), trifluoroacetic acid (TFA, Pierce) and fresh deionised water (MilliQ), and degassed with helium bubbles for 5 minutes each morning. Solvent A was 0.1% (v/v) TFA and solvent B was 80% (v/v) acetonitrile, 0.1% (v/v) TFA. The pumps and detector (Beckman) were controlled by System Gold software (Beckman). Samples were mixed with an equal volume of solvent A and loaded on a C4 or C8 column equilibrated in 90% solvent A, 10% solvent B. These conditions were maintained for 5 minutes after loading and then proteins were eluted with a linear gradient reaching 100% solvent B after 30-40 minutes. The OD_{280} was continuously monitored, and major peaks were collected from the point at which the OD_{280} started to rise, until it fell to less than a quarter of its maximum, avoiding related species that sometimes eluted at a similar concentration of acetonitrile. After use, the column was stored in 50% (v/v) methanol.

E10 Lyophilisation

Proteins that had been purified by HPLC were lyophilised. The relevant fractions were frozen in liquid nitrogen and left under vacuum overnight in a freeze drier, so that the water, acetonitrile and trifluoroacetic acid sublimed.

E11 N-Terminal Sequencing

Amino-terminal protein sequencing (Hewick *et al.,* 1981) was carried out on an Applied Biosystems 470A protein sequencer with an on-line phenyl thiohydantoin analyser (Perkin-Elmer), by Mr. A.C. Willis (MRC Immunochemistry Unit). Liquid samples were applied to a glass-fibre disc pretreated with polybrene and run using the standard 03CPTH program (Applied Biosystems). Data were analysed using Waters Expert Ease software (Millipore).

E12 Amino Acid Analysis

Amino acid analysis was carried out by Mr. A.C. Willis. The samples were hydrolysed at 110 °C for 22 hours and applied to an ABI 420A derivatiser/analyser (Perkin-Elmer), in which the amino acids react with phenylisothiocyanate to form phenylthiocarbamyl amino acids. The samples were automatically sampled to a narrow-bore HPLC system [E9], and peak intensities quantified by an ABI 920A Data Analysis System.

E13 Mass Spectrometry

Electrospray ionisation mass spectra (Fitzgerald and Siuzdak, 1996) were acquired with a Micromass BioQ-II triple quadrupole atmospheric pressure ionisation mass spectrometer equipped with an electrospray interface (Micromass UK Ltd), by Dr. R. Applin (Oxford Centre for Molecular Sciences). Samples (10 µl), at a concentration of 10 pmol/µl in 50% (v/v) acetonitrile, 0.2% (v/v) formic acid, were injected into the electrospray source at a flow rate of 10 µl/min (Applied Biosystems model 140A dual syringe pump). The mass spectrometer was scanned over the mass range 700-1600 Da

and calibrated with horse heart myoglobin (16951.48 kDa). Molecular weights were compared with those predicted by the Peptide Interpretation Program (Staden).

E14 NMR Spectroscopy

Protein samples (10-20 mg) were resuspended in 0.6 ml 10% (v/v) deuterated water (D_2O, Sigma) containing 0.02% (w/v) sodium azide as a preservative, and the pH was adjusted with NaOH or HCl. In some cases, 10% (v/v) deuterated acetonitrile (Sigma) or 50 mM NaCl were added to try to improve solubility. Care was taken when filling the sample tube to avoid introducing bubbles.

NMR spectroscopy was carried out by Dr. A. Perczel and Dr. G. Shaw in the laboratory of Prof. I.D. Campbell (Department of Biochemistry), using an Omega 500 MHz spectrometer. Spectra were measured at 25 °C, unless otherwise stated. Two dimensional nuclear Overhaüser effect spectroscopy (2-D NOESY) was carried out with 64 scans and 512 increments in the T1 direction, and the mixing time was 150 ms, unless otherwise stated. Proton chemical shifts are referenced to H_2O at 4.8 parts per million (ppm).

E15 Crystallisation

Crystallisation trials were carried out using the hanging drop method at 2 °C and 20 °C, by Dr. V. Fulop (Laboratory of Molecular Biophysics). One hundred different buffer conditions were tested, including pH gradients (pH 5-9 in increments of 0.5) in the presence of varying concentrations of ammonium sulphate (0.2-0.5% saturation) or 2-methyl-2,4-pentanediol (MPD) (10-70% saturation). Additionally, the Sparse Matrix crystallisation screening kit (Crystal Screen) was used (Jancarik and Kim, 1991).

E16 Preparation of Peptides

The pigeon cytochrome c peptide (81-104) was derived from the native protein by cyanogen bromide cleavage (Solinger *et al.*, 1979), by Mr. A.C. Willis. To remove its haem group, pigeon cytochrome c (5 mg, Sigma) was dissolved in 250 µl of water and added dropwise to 5 ml of acetone containing 2% (v/v) HCl at 0 °C. The resulting apocytochrome c precipitated and was collected by centrifugation at 2 000 g for 10 minutes. It was washed twice with cold acetone, dried under a stream of argon, redissolved in 1 ml of water and lyophilised. The apocytochrome c was then incubated at 5 mg/ml in 0.1 M HCl with 0.3 mg/ml (a 40-fold molar excess over methionine) of cyanogen bromide (Sigma) for half an hour in the dark. The digested protein was lyophilised twice from water to remove any traces of cyanogen bromide and dissolved in 0.1% (v/v) TFA. HPLC separation was performed with a C4 column (Brownlee Aquapore BU300, Perkin-Elmer) equilibrated in 0.1% (v/v) TFA, 2% (v/v) acetonitrile (3 ml/min flow rate). A linear gradient of 2-50% (v/v) acetonitrile was applied over 50 minutes and a further gradient of 50-90% acetonitrile over 18 minutes. The pumps and detector (Severn Analytical) were controlled by Flowmaster software (Severn Analytical). Detection was carried out at OD_{215} and data was collected using Waters Expert Ease software (Millipore). The major peaks were collected, lyophilised, resuspended in water and identified by N-terminal sequencing.

FYQLALT for initial studies was generously supplied by Dr. L. Hightower (University of Connecticut, USA). Further stocks were synthesised using fluorenyl-methoxycarbonyl (fmoc) chemistry (Genosys), purified by reverse phase HPLC using a 0.1% (v/v) TFA/acetonitrile gradient [10-90% (v/v) acetonitrile over 34 minutes, 1.5 ml/min] and a C8 column (Vydac) and analysed by mass spectrometry.

E17 Peptide Biotinylation

The peptide FYQLALT [E16] was biotinylated using N-hydroxysuccinimidobiotin (NHSd-biotin, Sigma). FYQLALT (13 mg) and a 5-fold molar excess of NHSd-biotin (27 mg) were dissolved in 3.3 ml of dimethysulphoxide, to which 0.9 ml of water and 4.2 ml of 0.2 M $NaHCO_3$ (pH 8.8) were added. The reaction was incubated for one day at room temperature, stopped by mixing with two volumes of 0.1% (v/v) TFA and centrifuged at 12 000 g for 5 minutes to remove any precipitated hydrolysed biotin. The biotinylated peptide was purified from the unbiotinylated form by HPLC [E9].

E18 Plate Binding Assay

The peptide-binding proteins were bound onto wells in a 96 well plate (Nunc Immuno Plate: PolySorb surface) by incubation overnight at room temperature in 20 mM Na_2CO_3, pH 9.3 (200 µl per well). The wells were washed three times in phosphate buffered saline (PBS, Difco) containing 0.05% (v/v) Tween 20 (Sigma) (PBS-Tween) and unused binding sites on the plate were blocked by filling each well with 1% (w/v) bovine serum albumin (BSA) in PBS-Tween for 90 minutes. Empty wells were blocked with BSA for use as a negative control. The wells were washed and dilutions of peptide were added in 200 µl of PBS-Tween. After 2 hours at room temperature, the wells were washed and avidin-alkaline phosphatase conjugate (Sigma) was diluted 1:10 000 in PBS-Tween and added for 30 minutes. After washing, 200 µl Sigma Fast phosphatase substrate (p-nitrophenyl phosphate) was added and alkaline phosphatase activity was measured by monitoring the OD_{405}. Readings were taken after 1-24 hours at room temperature.

E19 Isothermal Titration Calorimetry

Isothermal titration calorimetry (Ladbury and Chowdhry, 1996) was carried out by Dr. J. Ladbury (University College, London), using an MCS Type isothermal titration calorimeter (MicroCal), at 25 °C or 20 °C. The peptide-binding domains (250 μM) were dissolved in 0.5 x PBS and added incrementally in sixteen 15 μl aliquots to 1.3 ml of cytochrome c peptide (25 μM) in 0.5 x PBS. Alternatively, HOM-P [100 μM in 0.2% (v/v) DMSO, 0.5 x PBS] was added in fifteen 15 μl aliquots to 1.3 ml of 10 μM FYQLALT in 0.2% (v/v) DMSO, 0.5 x PBS. To determine the heat of dilution, the experiment was repeated with the peptide replaced by 0.5 x PBS [±0.2% (v/v) DMSO] alone. Heat changes were measured at 25 °C and 20 °C.

E20 Calculation of Dissociation Constants

For an equilibrium, P + L <--> PL,

$$Kd = \frac{[P][L]}{[PL]}$$

where P = a protein, L = its ligand and Kd = the dissociation constant for the interaction. The dissociation constant can be calculated from the concentration of ligand required for half of the protein to be bound to it. At this point, [P] = [PL], so Kd = [L]. [L] is the concentration of free ligand, but if the ligand is added in excess over the protein, the proportion of total ligand that is bound to the protein will be insignificant, and the concentration of free ligand can be approximated to the total concentration of ligand added. In other words, the Kd is the amount of ligand that must be added for half the binding sites on a protein to be occupied.

F. Subcellular Localisation Techniques

F1 Transient Transfection of a Eukaryotic Cell Line

The adherent cell line COS7, was seeded onto 21.6 x 45.7 mm chamber slides and cultured for 20 hours to achieve ~50% confluency. The vector pcDNA-PBPtag (0.1 μg) [C1] was mixed with 500 μl of culture medium containing 0.1 mM chloramphenicol and 0.04% (w/v) diethylaminoethyl (DEAE)-dextran, and added to cells which had been washed three times in medium without serum. After 2 hours, the transfection mix was replaced with 10% (v/v) dimethysulphoxide in PBS for two minutes. The cells were then washed and returned to culture medium for 48 hours.

F2 Immunofluorescence Microscopy

Immunofluorescence was carried out on slides carrying COS7 cells that had been transfected [A4] with pcDNA3-PBPtag and cultured for 48 hours. The cells were washed with PBS and fixed to the slides by incubation for 10 minutes with 3% (w/v) paraformaldehyde in PBS. After quenching in 50 mM ammonium sulphate for 15 minutes the cells were washed with PBS and permeabilised for 15 minutes with 0.2% (w/v) gelatin, 0.05% (w/v) saponin (Calbiochem) in PBS (GSP). The primary monoclonal antibody (Figure 2-5) was added for 30 minutes at a dilution of 1:1600 in GSP, and the cells were then washed with 0.05% (w/v) saponin in PBS. In the dark, the slides were incubated with the secondary antibody, a goat anti-mouse IgG antibody conjugated with fluorescein-isothiocyanate (FITC, Sigma) at a dilution of 1:130 in 10% (v/v) goat serum, 0.2% (w/v) gelatin, 0.05% (w/v) saponin (Calbiochem) in PBS. After half an hour, they were washed with 0.05% (w/v) saponin in PBS followed by PBS alone, and mounted in Vectashield (Vector Labs). The slides were viewed on a Zeiss Axioscop microscope,

Antibody	Specificity	Source
T7.Tag	T7 epitope	Novagen
Tubulin	alpha-tubulin	Sigma
1B5	35-60 kDa late endocytic proteins	Dr. M. Marsh
2C2	~100 kDa lysosomal protein	Dr. M. Marsh

Figure 2-5: Primary antibodies used in immunofluorescence microscopy. All antibodies were added to the permeabilised cells at a dilution of 1:1600 in GSP.

using an FITC filter to view the antibody. Photographs were taken with a Zeiss microscope camera (MC100) using Fujichrome 1600 Provia film.

A mitochondrial stain, Mitotracker (oxidised rhodamine conjugate, Molecular Probes), was used to visualise mitochondria by fluorescence microscopy. Cells were washed in culture medium and incubated for one hour with 100 nM Mitotracker in 500 µl of medium. The cells were fixed, permeabilised and incubated with antibodies, if desired, as described above. The slides were viewed on a Zeiss Axioscop microscope, using a rhodamine isothiocyanate (RITC) filter to view the Mitotracker fluorescence.

F3 Percoll Gradient Ultracentrifugation

For each gradient, a maximum of 10^8 cells (200 ml of well-grown suspension culture) was harvested by centrifugation at 2 000 g for 10 minutes and washed with 50 ml PBS followed by 10 ml homogenisation buffer (HB: 0.25 M sucrose, 1 mM EDTA, 10 mM acetic acid, 10 mM triethanolamine, pH 7.4). The cells were resuspended in 2.5 ml of HB+, homogenisation buffer containing the protease inhibitors phenylmethylsulphonyl fluoride (1 mM from a 100 mM stock in propan-2-ol), leupeptin (10 µg/ml) and iodoacetic acid (5 mM from a 500 mM stock in acetone). Generally, 80 strokes with a tight-fitting Dounce homogeniser were used to lyse the cells, but 20-160 strokes, 10 passes through a ball-bearing homogeniser (H&Y Enterprise, Redwood City, California), or 10-50 passes through a 0.6 x 25 mm syringe needle (Microlance, 23G1 no. 16) were also tested. Nuclei, mitochondria, plasma membrane sheets and unlysed cells were removed by centrifugation at 2 000 g for 10 minutes. The post-nuclear homogenate was loaded on top of 10 ml of 20% (v/v) Percoll (Pharmacia) in HB+ and centrifuged for 20 minutes at 25 000 g (19 000 rpm in a 70.1 Ti rotor). Fractions (12 x 1 ml unless otherwise stated) were collected from the bottom of the tube using a capillary tube, flexible plastic tubing and a peristaltic pump. The whole procedure was carried out at 4 °C.

An optional step allowed the cellular vesicles to be purified from the soluble cytoplasmic contents. To do this, the post-nuclear homogenate was made up to 10 ml with HB+ and centrifuged for 1 hour at 100 000 g (37 000 rpm in a Ti 70.1 rotor). The pelleted vesicles were then resuspended in 3 ml of HB+ and loaded onto the preparation of 20% (v/v) Percoll.

The gradient fractions were assayed for ß-hexosaminidase activity [F4], and Western blotted [E4] and probed with various antibodies [E5].

F4 ß-Hexosaminidase Assay

The ß-hexosaminidase activity of fractions from Percoll density gradients was assayed in 96 well plates with a chromogenic substrate (Marsh *et al.*, 1987). Each sample (25 µl) was incubated at 37 °C for 2-3 hours with an equal volume of 1.7 mg/ml p-nitrophenyl N-acetyl-ß-D-glucosaminide in 0.5% (v/v) nonidet-P40, 50 mM sodium citrate, pH 4.8. The reaction was stopped by adding 200 µl of 84 mM NaCl, 166 mM glycine, 104 mM Na_2CO_3, pH 10.7 and the OD_{405} measured. Control measurements were made with buffer HB+ [F3].

F5 Preparation of Microsomes

ER microsomes were prepared from Raji cells according to the method of Nigam *et al.* (1994). ~10^9 cells (2 l of well grown culture) were harvested by centrifugation at 2 000 g for 10 minutes and washed with 100 ml PBS followed by 10 ml homogenisation buffer (HB2: 0.25 M sucrose, 150 mM NaCl, 1 mM DTT, 20 mM Tris, pH 8). The cells were resuspended in 3 ml of HB2 and lysed with 80 strokes of a tight-fitting Dounce homogeniser. The homogenate was diluted to 10 ml with HB2 and unlysed cells, nuclei, mitochondria, plasma membrane sheets, lysosomes and other large organelles were

removed by centrifugation for 30 minutes at 20 000 g (17 000 rpm in a JA20 rotor), twice. The remaining vesicles were collected from the supernatant by centrifugation for 1 hour at 100 000 g (37 000 rpm in a 70.1 Ti rotor), resuspended in an equal volume of HB2 and stored if necessary at -20 °C. The whole procedure was carried out at 4 °C.

F6 Unfolded Protein Affinity Chromatography

Fetuin agarose (2 ml bed volume, Sigma) was denatured by incubation in an equal volume of 6 M urea, 1 M 2-mercaptoethanol for 1 hour, with constant mixing. The fetuin agarose was collected by centrifugation at 2 000 g for 5 minutes and washed five times with 8 ml of wash buffer (WB: 150 mM NaCl, 1 mM DTT, 20 mM Tris, pH 8). The fetuin agarose was then transferred into a column and washed with 20 ml of WB containing 2.5 mM EDTA and 1 mM EGTA.

Microsomes (~5 μg) were mixed with an equal volume of solubilisation buffer [1% (v/v) Triton X100, 5 mM EDTA, 2 mM EGTA, 2 mM DTT, 20 mM Tris, pH 8] and applied to the column immediately. The flow through was collected and the column was washed with 10 ml of WB containing 2.5 mM EDTA and 1 mM EGTA, followed by 10 ml of WB containing 2 mM $MgCl_2$, 0.5 mM $CaCl_2$. Putative ER chaperones were eluted with 5 ml of 1 mM ATP in WB containing 2 mM $MgCl_2$, 0.5 mM $CaCl_2$, and collected in 1 ml fractions. The column was then washed with 5 ml of 0.1 M acetic acid. The proteins from different fractions were precipitated by addition of 0.5 volume of 30% (v/v) trichloroacetic acid (TCA), washed with acetone and dissolved in 20 μl of water.

Alternatively, ER fractions from Percoll density gradients were pooled and mixed with 0.5 volume of solubilisation buffer 2 [1.5 % (v/v) Triton X100, 6 mM EDTA, 3 mM EGTA, 3 mM DTT, 30 mM Tris, pH 8] to lyse the vesicles. The Percoll in the fractions was then pelleted by centrifugation for 20 minutes at 100 000 g (37 000 rpm in a 70.1 Ti rotor). The supernatant was collected and added to the fetuin agarose column as before.

G. Molecular Modelling

G1 Molecular Modelling of the C-terminal Region of Hsp70hom

The sequences of hsp70hom and dnaK were aligned using AMPS (Barton and Sternberg, 1987; Barton, 1990) Twenty independent models were generated from this alignment using the program Modeller, version 3 (Sali and Blundell, 1993). Their backbones were overlaid and compared, so that models which had unusual backbone configurations could be discarded. The remaining models were analysed using Procheck (Lawkowski *et al.*, 1993) and Whatcheck (part of the Whatif package) (Vriend, 1990) to identify the model with the best packing, bond angles, bond lengths and planarity of cyclic side chains. This model was further refined by energy minimisation and molecular dynamics [G2].

G2 Refinement of the Model

The best model was then refined using XPlor (pre-release version 3.851) on a Sun Ultra 1 workstation. The hydrogen atoms were built onto the model using XPlor and their positions optimised by energy minimisation, using the Powell gradient algorithm and the Charmm22 force field (Brooks *et al.*, 1983) in a vacuum. This was carried out with the rest of the molecule being fixed. A second round of energy minimisation was then carried out with the amino acid side chains allowed to move. The electrostatic component of the energy term was neglected, so that the lower energy structure was arrived at only by repulsion of atoms that were too close together. The minimisation was terminated when the gradient of the energy function was less than 0.1 kcal/mol/Å. To improve unfavourable bond angles, residues containing a bond angle more than 10° from its optimum value (defined in the parameter files), and the residues on either side, were exposed to 20 ps of

molecular dynamics followed by energy minimisation, with the other amino acids remaining fixed. This step was repeated for any remaining unfavourable bond angles. Next, the positions of the amino acid side chains were energy minimised with the main chain atoms fixed and electrostatic forces taken into account. The weight of the electrostatic energy term was 1. This allowed hydrogen bonds to form, at the expense of poorer packing, bond angles and bond lengths. To improve these, another round of molecular dynamics was carried out to improve the geometry of the molecule, using the Shake-and-Bake iterative method (Miller *et al.*, 1993; Weeks *et al.*, 1993). Then the amino acid side chain positions were optimised by energy minimisation as before, but with the weight of the electrostatic energy term reduced to 0.1, to retain the hydrogen bonds and electrostatic interactions that formed while allowing the side chain (though not the main chain) atoms to move. This energy minimisation was repeated with all the atoms (main chain and side chain) free to move. The molecule was then solvated with a 10 Å layer of water, using Insight 2.3 (Biosym) and the solvent layer was energy minimised. Finally, the whole system was energy minimised with all atoms (protein and water) free to move. To offset the large electrostatic contribution from the water molecules, the electrostatic energy term was reduced to 0.01.

G3. Modelling Complexes of the C-terminal Region of Hsp70hom with Peptides

The conformation of the peptide FYQLALT was created using the backbone of NRLLLTG and mutating the residues using Insight 2.3 (Biosym). The peptides (NRLLLTG and FYQLALT) were placed in the model of the peptide-binding cleft of the C-terminal portion of hsp70hom using Molmol (Koradi *et al.*, 1996). The configuration of the peptide was energy minimised with a purely repulsive force field, which pushed it away from the protein and into the hole. This procedure was repeated several times, with the peptide rotated in the cleft to a different position each time. The peptide configuration for

which the overall energy of the complex (determined using the purely repulsive force field) was lowest was chosen. Its energy was within 5% of the total energy of the protein alone.

To allow interactions to form between hsp70hom and the peptide, molecular dynamics and energy minimisation were carried out on the complex. In general, all the atoms of the peptide were given freedom of movement, while only residues comprising the peptide-binding site of the C-terminal region of hsp70hom were allowed to move. Flexibility was introduced into the binding site for two reasons. Firstly, the binding site may have real flexibility and, secondly, as the binding site was modelled in the absence of peptide, it is likely to need readjusting to accommodate the peptide successfully.

To introduce electrostatic interactions and hydrogen bonds into the complex, energy minimisation was carried out in a full Charmm22 force field, with all energy terms set to 1 and allowing the side chains of all residues within 5 Å of the peptide to move. A further energy minimisation was carried out with the backbone atoms of all residues within 4 Å also allowed to move. Next, the peptide and peptide-binding site were subjected to molecular dynamics, using simulated annealing. This involved promoting movement in the peptide, the side chain atoms of residues of hsp70hom within 5 Å of the peptide and all atoms of residues within 4 Å, with molecular dynamics at 1000 K for 15 ps. The temperature was then reduced in increments of 10 K over 7.5 ps to 100 K, allowing interactions between the peptide and peptide-binding site to form. Finally, the conformation of these atoms was energy minimised in a full force-field, but with the electrostatic energy term reduced to 0.01, so that it did not overwhelm the other energies. The modelling was carried out in a simulated vacuum.

Twenty independent models were produced as described above and analysed using Procheck, Whatcheck and molecular graphics. Models with very high energies or whose backbones did not follow the general consensus were rejected. The remaining models were averaged to generate a mean structure which was energy minimised again. This energy

minimisation was carried out with the electrostatic energy term for peptide-protein and peptide-peptide interactions set to 100 times its value for protein-protein interactions, in order to favour the formation of electrostatic interactions and hydrogen bonds between the two components of the complex without distorting the structure of the protein.

Chapter 3: The Expression and Characterisation of the Peptide-Binding Domains of Two Divergent Hsp70s

Introduction

As discussed in Chapter 1, hsp70s have been implicated as components of the antigen processing pathways. Therefore, their substrate-binding specificities may influence the presentation of peptide antigens by MHC molecules. Hsp70s bind to antigenic peptides *in vivo* (Srivastava *et al.*, 1994), and currently the binding properties of individual human hsp70s are being investigated in our laboratory. To complement this approach, *in vitro* peptide-binding and structural studies have been carried out with the isolated peptide-binding domains of two hsp70s. The two hsp70s chosen were PBP74: an hsp70 which had been described to have an endosomal localisation and implicated in class II antigen processing (Lakey *et al.*, 1987; VanBuskirk *et al.*, 1991); and hsp70hom, a constitutive, cytoplasmic hsp70 encoded in the MHC class III region and potentially involved in the class I antigen processing pathway (Milner and Campbell, 1990). The peptide-binding domains of these two molecules were expressed in isolation from the rest of the molecule to make it possible to determine their structure by nuclear magnetic resonance spectroscopy (NMR), the current size limit of which is ~20 kDa. Such a 'dissect and build' approach to structure determination has been used successfully for a wide range of proteins, including components of the extracellular matrix, complement system and intracellular signalling cascades (Baron *et al.*, 1991; Campbell and Downing, 1994). The most important stage in a dissect and build strategy to protein structure is deciding on the boundaries of the chosen domain. The extent of the hsp70 peptide-binding domain was determined with help from secondary structure prediction methods, proteolysis studies and sequence alignments.

Results

.c.Predicting the Secondary Structure of the Hsp70 Peptide-Binding Domain

Several studies have suggested that the hsp70 peptide-binding domain has a structure similar to the peptide-binding groove of MHC class I and class II molecules (Flajnik *et al.*, 1991; Rippmann *et al.*, 1991). Although the peptide-binding regions of hsp70s and MHC class I molecules share only limited amino acid sequence identity (~24% between human hsc70 and the peptide-binding groove of *Xenopus laevis* class I molecules) (Flajnik *et al.*, 1991), they have a similar hydrophobicity profile (Flajnik *et al.*, 1991)and the secondary structure of the hsc70 peptide-binding domain was predicted to be similar to the MHC class I peptide-binding groove (Rippmann *et al.*, 1991), using the Chou-Fasman and Garnier-Osguthorpe-Robson methods. Based on these observations, the tertiary structure of the peptide-binding domain of the hsp70 family has been modelled on the peptide-binding groove of MHC class I molecules.

The Chou-Fasman (Chou and Fasman, 1978) and Garnier-Osguthorpe-Robson (Garnier *et al.*, 1978) methods used by Rippmann and colleagues (1991) predict secondary structures in proteins based on amino acid composition. A more sophisticated method, called Predict Protein, is based on an alignment of the protein with its relatives (Rost and Sander, 1993; Rost and Sander, 1994). It uses a neural network to predict secondary structure based on the pattern of amino acid conservation and the positions of gaps/insertions in the alignment, as well as using the amino acid composition. Therefore, Predict Protein predicts the secondary structure of a whole family of proteins and displays it beneath the amino acid sequence of one family member.

The secondary structure of the complete amino acid sequence of PBP74 (Domanico *et al.*, 1993) was predicted by the Predict Protein program of PHDsec (EMBL) and the Chou-Fasman and Garnier-Osguthorpe-Robson indices from the Peptide Structure program of

the University of Wisconsin's Genetics Computer Group (GCG) (Pearson and Lipman, 1988) (Figure 3-1). Predict Protein generated its prediction from an alignment of 121 hsp70s which share more than 40% identity with PBP74.

The accuracy of the prediction methods was assessed using the ATPase domain of the hsp70 family, the secondary structure of which has been determined by X-ray crystallography for hsc70 (Flaherty *et al.*, 1990). This domain contains both α-helices and ß-sheets, and was not one of the structures used to train the Predict Protein neural network (Rost and Sander, 1993). Predict Protein (PP in Figure 3-1) predicted the secondary structure of the ATPase domain (DEF in Figure 3-1) with great accuracy, including all the elements of secondary structure more than 3 amino acids long with the exception of a ß-strand (amino acids 295-301) at the N-terminus of a long α-helical segment, two short ß-strands (amino acids 104-114) and the 3_{10} helices (amino acids 74-76, 331-333 and 341-344). The extent of the secondary structural elements was usually predicted to within one or two amino acids. However, this method incorrectly predicted the existence of two α-helices three amino acids long at the C-termini of two ß-strands (amino acids 385-387 and 204-206). Predict Protein was more accurate than either the Chou-Fasman (CF) or the Garnier-Osguthorpe-Robson (GOR) methods, which tended to predict ß-sheets as α-helices (Figure 3-1).

The C-terminal half of PBP74 (amino acids 383-633) was predicted to consist of a segment rich in ß-sheet followed by a predominantly α-helical segment by all three methods. However, the Chou-Fasman and Garnier-Osguthorpe-Robson methods predict that the ß-rich segment contains one or two long α-helices, respectively, which might form the central helix in the ββββαββββα arrangement of MHC molecules. In contrast, Predict Protein does not predict an MHC-like secondary structure. While there is an α-helix predicted in the ß-rich segment, it is only three amino-acids long, is not in the right place and is not predicted when the sequence of the C-terminal half of PBP74 is submitted to the program without the sequence of the ATPase domain (data not shown). The greater

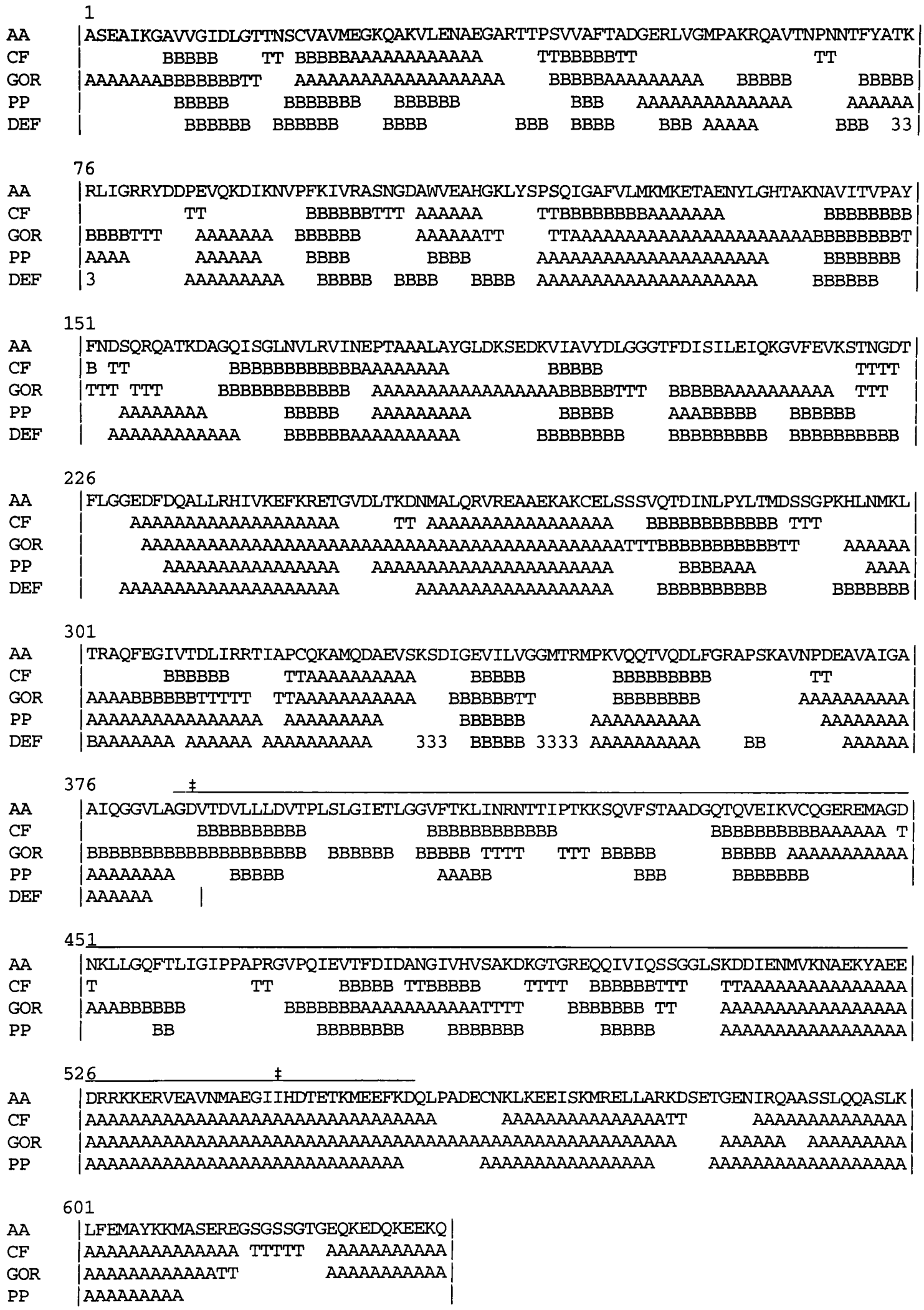

Figure 3-1: The predicted secondary structure of PBP74. The amino-acid sequence of PBP74 (AA) (Domanico*et al.*, 1993) is displayed with the secondary structure predicted by the Chou-Fasman (CF), Garnier-Osguthorpe-Robson (GOR) and PredictProtein (PP) methods beneath. The secondary structure of the ATPase domain of hsc70, as determined by X-ray crystallography (Flaherty*et al.*, 1990), is shown beneath the equivalent amino-acids of PBP74 (DEF). Alpha-helix (A), beta-sheet (B), beta-turns (T) and 3_{10} helices (3) are shown. The sites equivalent to the chymotryptic cleavage sites in hsc70 are marked with ‡ and the extent of the peptide-binding domain expressed in pGEX-2T is overlined.

accuracy and sophistication of the Predict Protein approach and the tendency of the other two methods to predict ß-sheets as α-helices made the structure of hsp70 modelled on MHC class I molecules seem unlikely, and suggested that the C-terminus of hsp70s consists of six or more ß-sheets followed by three long α-helices.

The Boundaries of the Peptide-Binding Domain

The extent of the hsp70 peptide-binding domain was inferred from proteolytic studies and sequence alignment. Chymotryptic digestion of bovine hsc70 (amino acids 1-646) produces a 60 kDa fragment (amino acids 3-546) that is subsequently degraded to a 44 kDa fragment (amino acids 3-384) (Chappell *et al.*, 1987). Like intact hsc70, the 60 kDa fragment can bind to clathrin baskets (though it is no longer able to disassemble them). The 44 kDa fragment cannot bind to clathrin, and is a complete, functional ATPase domain; its structural homology to the ATPase domains of hexokinase and actin (Flaherty *et al.*, 1990; Flaherty *et al.*, 1991) suggests that it does not include any peptide-binding determinants. Therefore, amino-acids 385 to 546 of hsc70 must include the whole of its peptide-binding domain. Indeed, this region (amino acids 384-543) binds to peptides with the same affinity as native hsc70 when expressed as a GST fusion protein (Wang *et al.*, 1993), and it was possible to determine the secondary structure of this region by NMR, when it was expressed as a hexahistidine fusion protein (Morshauser *et al.*, 1995). This structure was very similar to that predicted here using the Predict Protein program. These conclusions are supported by examining an alignment of members of the hsp70 family (Figure 3-2). In evolution, deletions or insertions are rarely accommodated in regions of conserved secondary structure and occur more often in the flexible segments between domains. Gaps or insertions occur in the alignment at or near the chymotryptic cleavage sites (‡ in Figure 3-2), at positions equivalent to amino acids 385 and 555 of hsc70.

```
hsp70      M A - - K A A A I G I D L G T T Y S C V G V F Q H G K V E I I A N D Q G N R T T P S Y V A F T - D T E R L I G    52
hsp70hom   . . T A . G I . . . . . . . . . . . . . . . . . . . . . . . . . . . . . . . . . . . . . . . - . . . . . .    54
hsp70A2    M S - A R G P . . . . . . . . . . . . . . . . . . . . . . . . . . . . . . . . . . . . . . . - . . . . . .    53
hsc70      . S - - . G P . . . . . . . . . . . . . . . . . . . . . . . . . . . . . . . . . . . . . . . - . . . . . .    52
hsp70-B'   . Q A P R E L . V . . . . . . . . . . . . . . . . Q . R . . . L . . . . . . . . . . . . . . - . . . . . V .    54
BiP        K K E D V G T V V . . . . . . . . . . . . . . . K N . R . . . . . . . . . . . I . . . . . . . P E G . . . . .    59
PBP74      S E A I . G . V V . . . . . . N . . . A N M E G K Q A K V L E . A E . A . . . . . V . . . . A . G . . . V .    56

hsp70      D A A K N Q V A L N P Q N T V F D A K R L I G R K F G D P V V Q S D M K H W P F Q V I N D G D K P K V Q V S Y   107
hsp70hom   . . . . . . . . . . . . . . . . . . . . . . . . . . . . . . . . . . . . . . . . . . . . . . E . G . . . . L . . .   109
hsp70A2    . . . . . . . . M . . T . . I . . . . . . . . . . . E . A T V . . . . . . . . . R . V S E . G K P . . . . E .   108
hsc70      . . . . . . . . M . . T . . . . . . . . . . . . . . R . D . A . . . . . . . . . M . . . . A G R . . . . . E .   107
hsp70B'    . . . . S . A . . . . H . . . . . . . . . . . . . . . A . T T . . . . . . . . . R . V S E . G . . . . P . . .   109
BiP        . . . . . L T S . . E . . . . . . . . . . . . . . T W N . . S . . Q . I . F L . . K . V E K K T . . Y I . . D I   114
PBP74      M P . . R . A V T . . N . . F Y A T . . . . . . R Y D . . E . . K . I . N V . . K I V R A S N - - - G D A W V   108

hsp70      K G - E T K A F Y P E E I S S M V L T K M K E I A E A Y L G Y P V T N A V I T V P A Y F N D S Q R Q A T K D A   161
hsp70hom   . . - . N . . . . . . . . . . . . . . . . L . . T . . . F . . H . . . . . . . . . . . . . . . . . . . . .   163
hsp70A2    . . - . . . . T . F . . . . . . . . . . . . . . . . . . . G K . H S . . . . . . . . . . . . . . . . . . .   162
hsc70      . . - . . . . S . . . . . V . . . . . . . . . . . . T . . . . . K T . . . . . V . . . . . . . . . . . . . .   161
hsp70B'    R . - . D . T . . . . . . . . . . . . . S . . . . T . . . . . . Q . . K H . . . . . . . . . . . . . . . . .   163
BiP        G . G Q . . T . A . . . . . A . . . . . . . . . . T . . . . . . K K . . H . . V . . . . . . . . . A . . . . . .   169
PBP74      E A - H G . L Y S . S Q . G A F . . M . . . . T . . N . . . H T A K . . . . . . . . . . . . . . . . . . . .   162

hsp70      G I F E V K A T A G D T H L G G E D F D N R L V N H F V E E F K R K H K K D I S Q N K R A V R R L R T A C E R   269
hsp70hom   . . . . . . . . . . . . . . . . . . . . . . . . . . . . . . . . . . . . . . S . . . . . . . . . . . . . . .   271
hsp70A2    . . . . . . S . . . . . . . . . . . . . . . . . . M . S . L A . . . . . . . . . . . G P . . . . . . . . . .   272
hsc70      . . . . . . S . . . . . . . . . . . . . . . . . . M . . . . I A . . . . . . . . . . E . . . . . . . . . . .   270
hsp70-B'   . V . . . . . . . . . . . . . . . . . . . . . . . . . . . . M . . . R . . . G . . L . G . . . . L G . . . . . .   271
BiP        . V . . . V . . N . . . . . . . . . . . . . . . Q . V M E . . I K L Y . K . T G . . V R K D N . . . Q K . . R E V . K   276
PBP74      . V . . . . S . N . . . F . . . . . . . . Q A . L R . I . K . . . . E T G V . L T Y D N M . L Q . V . E . A . K   268

hsp70      A K R T L S S S T Q A S L E I D S L - - - - F E G I D F Y T S I T R A R F E E L C S D L F R S T L E P V E K A   320
hsp70hom   . . . . . . . . . . . N . . . . . . . . - - - - Y . . . . . . . . . . . . . . . . . A . . . . G . . . . . . .   322
hsp70A2    . . . . . . . . . . . I . . . . . . . . - - - - Y . . V . . . . . . . . . . . . . . N A . . . . G . . . . . . .   323
hsc70      . . . . . . . . . . . I . . . . . . . . - - - - Y . . . . . . . . . . . . . . . . . N A . . . . G . . D . . . . .   321
hsp70-B'   . . . . . . . . . . T . . . . . . . . - - - - . . . V . . . . . . . . . . . . . . . . . . . . . . . . . . . .   322
BiP        . K - A . . . Q H . . R I . . E . F - - - - Y . . E . . S E T L . . . K . . . . N M . . . . . . M K . . Q . V   326
PBP74      . . C E . . . . V . T D I N L P Y . T M D S S G P K H L N M K L . . . Q . . G I V T . . I . R . I A . C Q . .   323
```

```
hsp70      L R D A K L D K A Q I H D L V L V G G S T R I P K V Q K L L Q D F F N G R D L N K S I N P D E A V A Y G A A V  375
hsp70hom   . . . . . M . . . K . . . . . . . . . . . . . . . . . R . . . . Y . . . . . . . . . . . . . . . . . .  377
hsp70A2    . . . . . G . . Q E I . . . . . . . . . . . . I Q K L . . . . . . K E . . . . . . . . . . . . . . . . .  378
hsc70      . . . . . S . . . . I . . . . . . . . . . . . I . . . . . . . . . K E . . . . . . . . . . . . . . . . .  376
hsp70-B'   . . . . . V . . . . . . . . . . . . . . . . . . . . . . . . . . K E . . . . . . . . . . . . . . . . .  377
BiP        M E . S D . K . S D . D E I . . . . . . . . . . . . I . Q . V K E . . . . K E P S R G . . . . . . . . . . . . . .  381
PBP74      . Q . . E V S . S D . G E V I . . . . M . . M . . . . Q T V . . L . - . . A P S . A V . . . . . . . I . . . I  377

                                  ‡
hsp70      Q A A I L M G D K S E N V Q D L L L L D V A P L S L G L E T A G G V M T A L I K R N S T I P T K Q T Q I F T T  430
hsp70hom   . . . . . . . . . . K . . . . . . . . . . . . . . . . . . . . . . . . . . . . . . . . . . . . . . . . .  432
hsp70A2    . . . . . I . . . . . . . . . . . . . . T . . . . . I . . . . . . . . P . . . . . T . . . . . . . . T . . .  433
hsc70      . . . . . S . . . . . . . . . . . . . . T . . . . . I . . . . . . . . V . . . . . T . . . . . . . . . . .  431
hsp70-B'   . . . V . . . . . C . K . . . . . . . . . . . . . . . . . . . . . . . . . . . . . . . . . . . . . . . .  432
BiP        . . G V . S . . - - Q D T G . . V . . H . C . . T . . I . . V . . . . . K . . P S . T V V . . . N S . . . S .  444
PBP74      . G G V . A . . - - - - - . T . V . . . . T . . . . I . . L . . . F . K . . N . . T . . . . . K S . V . S .  428

hsp70      Y S D N Q P G V L I Q V Y E G E R A M T K D N N L L G R F E L S G I P P A P R G V P Q I E V T F D I D A N G I  485
hsp70hom   . . . . . . . . . . . . . . . . . . . . . . . . . . . . . . . . . . . . . . . D . T . . . . . . . . . . .  487
hsp70A2    . . . . . S S . . V . . . . . . . . . . . . . . . . . . . . . . . . K . D . T . . . . . . . . . . . . . . . . .  488
hsc70      . . . . . . . . . . . . . . . . . . . . . . . . . . . . . . . . . . . K . . . T . . . . . . . . . . . . . . . . .  486
hsp70-B'   . . . . . F . . . . . . . . . . . . . . . . . . . . . . . . . . . . . . . . . . . . . . . . . . . . . . . .  487
BiP        A . . . . . T . T . K . . . . . P L . . . . H . . . T . D . T . . . . . . . . . . . . . . . . . . . . E . . V . . .  489
PBP74      A A . G . T Q . E . K . C Q . . . E . A G . . K . . . Q . T . I . . . . . . . . . . . . . . . . . . . . . . .  483

hsp70      L N V T A T D K S T G K A N K I T I T N D K G R L S K E E I E R M V Q E A E K Y K A E D E V Q R E R V S A K N  540
hsp70hom   . . . . . . . . . . . V . . . . . . . . . . . . . . . . . . . . . . . . L . . . . . . . . . . . K I A . . .  542
hsp70A2    . . . . . A . . . . . E . . . . . . . . . . . . . . . . D D . D . . . . . . . R . . S . . . A N . D . . A . . .  543
hsc70      . . . S . V . . . . . E . . . . . . . . . . . . . . . . D . . . . . . . . . . . . . . . K . . . K . . S . .  541
hsp70-B'   . S . . . . . R . . . . . . . . . . . . . . . . . . . . V . . . H . . . Q . . . . . A . . D . . A . . .  542
BiP        . R . . . E . . G . . N K . . . . . . . . Q N . . T P . . . . . N D . . . F A E . . K K L K . . I D T R .  544
PBP74      V H . S . K . . G . . R E Q Q . V . - Q S S . G . . . D D . . N . . K N . . . . A E . . R R K K . . . E . V .  537

                    ‡
hsp70      A L E S Y A F N M K S A V E D - E G L K G K I S E A D K K K V L D K C Q E V I S W L D A N T L A E K D E F E H  594
hsp70hom   . . . . . . . . . . V . S . - . . . . . . . . . S . . N . I . . . . N . L L . . . E V . Q . . . . . . D .  596
hsp70A2    . . . . . T Y . I . Q T . . . . - . K . R . . . . . Q . . N . I . . . . . . . . . N . . . R . Q M . . . . . Y . .  597
hsc70      S . . . . . A T . . . . - . K . Q . . . N D E . . Q . I . . . . N . I . N . . . K . Q T . . . E . . . . .  595
hsp70-B'   S . . A H V . H V . G S L Q E - . S . R D . . P . E . R R . M Q . . . R . . L A . . E H . Q . . . . E . Y . .  596
BiP        E . . . . . Y S L . N Q I G . K . K . G . . L . S E . . E T M E K A V E . K . E . . E S H Q D . D I E D . K A  599
PBP74      M A . G I I H D T E T K M . E - - - F . D Q L P A D E C N . L K E E I S K M R E L . A R K D S E T G E N I R Q  589

hsp70      K R K E L E Q V C N P I I S G L Y Q G A G G P G P G - - - - - G F G A Q G P K G G S G S G P T I E E V D        641
hsp70hom   . . . . . M . . . . . T K . . . . G C T G P A C - - - - - - - - G T G Y V P . R P A T . . . . . .        641
hsp70A2    . Q . . . . R . . . . . . . K . . . . G P . G - - - - - - - - - - S G . G G S . A S G . . . . . .        639
hsc70      . Q . . . . K . . . . . . T K . . . S A . . M P G . M P G G F P G . G A P . S . . A . . . . . . . .        647
hsp70-B'   Q K R . . . . I . R . . F . R . . G . P . V . . G S S C - - - - - - . T . A R Q . D P S T . . I . . . . .        642
BiP        . K . . . . E I V Q . . . . K . . G S A . P . P T . E E D T A E K D E L                                  645
PBP74      A A S S . Q . A S L K L F E M A . K K M A S E R E G S G S S G T G E Q G E D Q K E E K Q                  633
```

Figure 3-2: An alignment of the amino acid sequences of members of the human hsp70 family. Identities with the hsp70 sequence are indicated with dots (.) and amino acids that differ from hsp70 are shown. Gaps inserted to optimise the alignment are indicated with dashes (-). The chymotryptic cleavage sites in hsc70 (Chappell *et al.*, 1987) are indicated with ‡ and the extent of hsp70hom and PBP74 expressed as fusions with glutathione-S-transferase is overlined. The sequences were aligned sequentially using the program Best Fit, as described in Figure 1-1.

In summary, amino acids 385-555 of hsc70 will include its peptide-binding domain, and this is equivalent to amino acids 386-557 of hsp70hom and amino acids 386-552 of PBP74. These boundaries fall between elements of secondary structure predicted by Predict Protein (Figure 3-1).

Cloning of the Peptide-Binding Domains

The peptide-binding domains of PBP74 and hsp70hom (PBP-P and HOM-P) were expressed in *E. coli* using the vector pGEX-2T (Smith and Johnson, 1988), as described in detail in Chapter 2 [Section E7]. In this system, the recombinant protein is expressed as a fusion with glutathione-S-transferase (GST), allowing its purification by glutathione-affinity chromatography. The domains can then be released from the GST moiety by digestion with the protease thrombin. Transcription of this fusion protein is controlled by the *lac* Z promoter which is induced by isopropyl-ß-thiogalactopyranoside (IPTG).

A sequence encoding the peptide-binding domain of PBP74 (amino-acids 384-554) was excised from the full-length PBP74 coding sequence using fortuitously located restriction sites and cloned in-frame with the 3' end of the GST coding sequence. pBluescript KS+ clone 32 (see Chapter 6) was digested [Chapter 2, Section C2] with *Ava* II and *Nae* I and end-filled using the Klenow fragment of DNA polymerase I [C5]. The 513 bp fragment (comprising nucleotides 1378-1891) was gel purified [C4], and ligated [C7] into pGEX-2T that had been digested with *Eco*R I, Klenow-end-filled and dephosphorylated [C6], to create clone pGEX-PBP. The orientation of the ligated fragments with respect to each other was shown by digestion with *Sty* I and *BamH* I. The correct orientation yielded 225 bp and 5.2 kb fragments, while the incorrect orientation produced 315 bp and 5.2 kb fragments. The correct orientation of the insert was further confirmed when a fusion protein of the correct size was induced by IPTG (see below). The multiple cloning site of pGEX-2T encodes an additional five amino-acids (Gly-Ser-

Pro-Gly-Ile) at the N-terminus of the domain after thrombin cleavage and three (Asp-Ser-Ser) at its C-terminus.

The sequence encoding the equivalent amino-acids of hsp70hom (384-561) was amplified by polymerase chain reaction (PCR) and cloned in-frame with the 3' end of the GST coding sequence. Nucleotides 2108-2645 of hsp70hom were amplified from cloned genomic DNA (pBluescript clone BS4.0-H: Milner and Campbell, 1990) using the primers 5' HOM-P and 3' HOM-P and Biotaq DNA polymerase [C12]. The 5' primer contains an engineered *Bam*H I site and the 3' primer an engineered *Eco*R I site, followed by an additional A nucleotide to introduce a stop codon (TGA). The PCR product was digested with *Bam*H I and *Eco*R I, gel purified and ligated into pBluescript KS+ that had been digested with the same enzymes, dephosphorylated and gel purified. Three clones were analysed by single-stranded sequencing using the primers H4, H13 and M13 [C14]. The insert was removed from an error-free clone by digestion with *Bam*H I and *Eco*R I and gel purified. Clone pGEX-Hom was created by ligating the insert into pGEX-2T that had been digested with the same enzymes, dephosphorylated and gel purified. The multiple cloning site of pGEX introduces two amino-acids (Gly-Ser) at the N-terminus of the domain after thrombin cleavage.

Expression of the Peptide-Binding Domains

Initial experiments to optimise the expression and purification of the glutathione-S-transferase fusion proteins were carried out using pGEX-PBP. Small scale cultures of transformed colonies were treated with IPTG [E7] to see if a fusion protein was induced (Figure 3-3). Cells that contain pGEX-2T with the insert in the correct orientation expressed a 45 kDa protein in the presence of IPTG (lane 2) that was not seen in uninduced cells (lane 1). This protein is the right size to be a fusion of GST (26 kDa) and the peptide binding domain (19 kDa). When the insert is in the wrong orientation, the induced cells

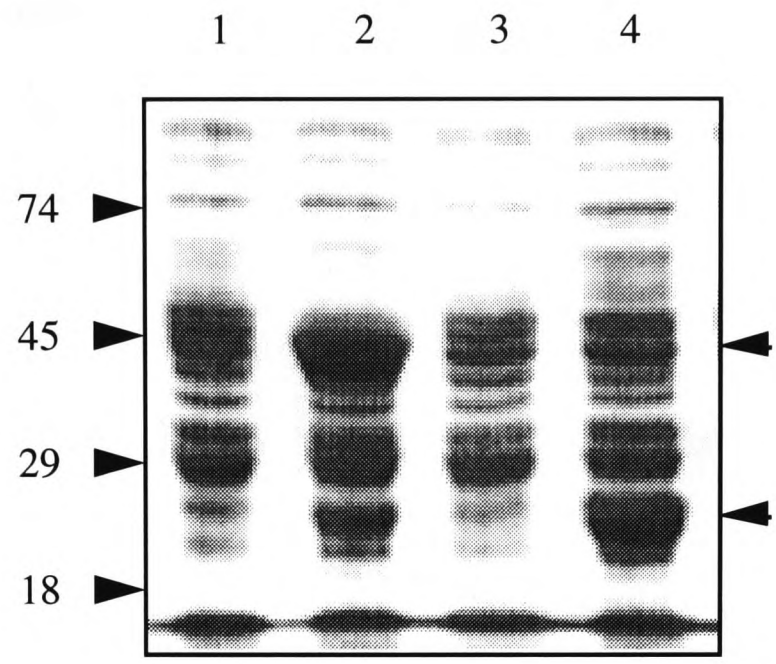

Figure 3-3: Expression of the peptide-binding domain of PBP74 as a fusion with glutathione-S-transferase. Overnight cultures of *E.coli* strain NM554 transformed with pGEX-2T clones of the sequence encoding the PBP74 peptide-binding domain in the correct (pGEX-PBP; lanes 1 and 2) or incorrect (lanes 3 and 4) orientation were diluted tenfold in 5 ml fresh medium and grown to mid log-phase [E7]. Each culture was split into two, and half (lanes 2 and 4) was treated with 100 μM IPTG for 4 hours. Cells from all four cultures (200 μl) were harvested by centrifugation at 12 000 g for 1 minute, resuspended in 20 μl of water and 10 μl aliquots were analysed by SDS-PAGE on a 10% (v/v) acrylamide gel [E1]. Proteins were visualised by Coomassie blue staining and the positions of the size markers is indicated on the left hand side. The proteins produced when the sequence encoding the PBP74 peptide-binding domain was cloned in the correct (top arrow) and incorrect (bottom arrow) directions are indicated.

express an ~26 kDa protein that is likely to correspond to GST with a few additional amino acids at its C-terminus (lane 4).

The production of the fusion protein from a given volume of bacterial culture was maximised by varying the point at which the cells were treated with IPTG and when they were harvested. IPTG was added to small scale cultures when their OD_{600}s had reached 0.2, 0.4, 0.6 or 0.8, and aliquots were harvested 2, 4, 6 or 14-18 hours after induction (Figure 3-4). This showed that inducing the culture at a higher OD_{600} and harvesting the cells later increased the amount of fusion protein produced. However, in large scale 0.5-1 l cultures, the efficiency of induction was reduced if the OD_{600} was greater than 0.6 when IPTG was added (data not shown). Therefore, large scale cultures were treated with IPTG when there OD_{600}s reached 0.4-0.6, for 16-20 hours.

These first experiments were carried out with *E. coli* strain NM554, but expression of proteins in the BL21 strain has several advantages. The BL21 strain is deficient in the OmpT and Lon proteases (Phillips *et al.*, 1984), reducing the likelihood of the fusion protein being degraded in the *E. coli* cytoplasm. Furthermore, it can grow in minimal medium, which can be supplemented with ^{13}C-glucose and ^{15}N-ammonium chloride. This allows isotopic labelling of recombinant proteins for structure determination by NMR spectroscopy. The plasmids pGEX-PBP and pGEX-Hom were therefore transformed into competent BL21 cells [C8].

Small-scale expression of the PBP74 fusion protein was the same in *E. coli* strain BL21 as in the NM554 strain (data not shown), so large-scale cultures of BL21 transformed with pGEX-PBP and pGEX-Hom were prepared for expression and purification of the hsp70hom and PBP74 peptide-binding domains [E7]. An overnight culture of *E. coli,* transformed with the appropriate pGEX plasmid, was diluted tenfold in fresh L broth and induced with a final concentration of 100 μM IPTG during log-phase growth. The cells were harvested 18-20 hours later and lysed by sonication in the presence

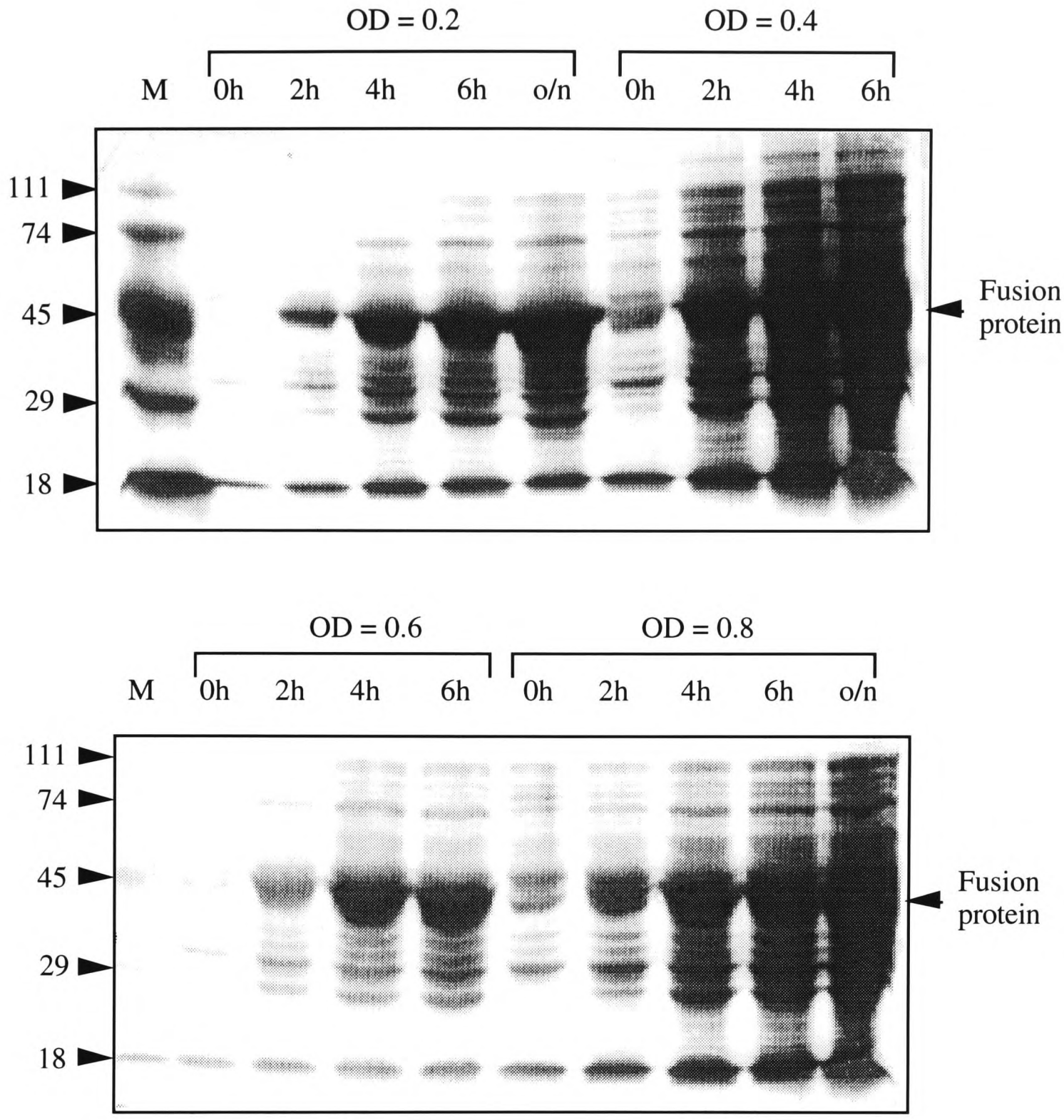

Figure 3-4: Time course of fusion protein expression. Overnight cultures of *E. coli* strain NM554 transformed with pGEX-PBP were diluted tenfold in 5 ml of fresh medium and induced at OD_{600} = 0.2, 0.4, 0.6 or 0.8. Aliquots (200 µl) were harvested 2, 4, 6 or 14-18 hours after induction, by centrifugation at 12 000 g for 1 minute. The cells were resuspended in 20 µl of water, and 10 µl of each sample was analysed by SDS-PAGE on a 10% (w/v) acrylamide gel [E1]. Proteins were visualised by Coomassie blue staining. Lane M contains high molecular weight standards. The top gel was photographed with an exposure time of 240 µs, and the bottom gel with an exposure time of 180 µs.

of 1% (v/v) Triton X100. Glutathione agarose was mixed with the soluble fraction of the cell lysate for 6 hours, washed extensively and incubated with thrombin at room temperature for 6 hours. This strategy for the expression and purification of the peptide-binding domains proved very successful (see Figure 3-5). The fusion proteins are expressed in abundance (lane 3), are soluble following cell lysis (lane 4) and bind to glutathione agarose, from which other *E.coli* proteins are removed easily by washing (lane 6). Thrombin efficiently frees the peptide-binding domains from the GST moieties, thus releasing them from the glutathione agarose into solution, without degrading them (lane 7). A proportion of each domain remains associated with the glutathione agarose after thrombin cleavage (lane 8) but can be efficiently removed by washing (lane 9). At this stage, the peptide-binding domains are already very pure.

The most inefficient step in the purification procedure is when the fusion protein binds to the glutathione agarose (lanes 4 and 5). However, varying the amount of glutathione agarose added to the soluble cell lysate from 20% to 50% or 100% (v/v) bed-volume, changing the time or temperature of incubation (carried out for 15 minutes, 30 minutes, 1 hour, 6 hours or 16 hours, at 4 °C or 24 °C), or titrating the concentration of detergent used to lyse the cells (0%, 0.1%, 1% Triton) had no effect on the amount of binding observed (data not shown). Another inefficient step is cell lysis by sonication, particularly in large-scale purifications. The yield of fusion protein could be increased by resuspending the insoluble fraction of the cell lysate (2 000 g pellet) in MTPBS containing 1% (v/v) Triton X100 and sonicating it again. The soluble material (2 000 g supernatant) released by this second sonication was pooled with the supernatant after the first sonication and mixed with glutathione agarose as before.

Thrombin cleavage was carried out at room temperature to reduce the likelihood of the peptide-binding domains being degraded by thrombin or traces of *E. coli* proteases. The amount of thrombin used to digest the fusion protein was titrated (data not shown). The fusion protein from 10 ml of culture was completely digested in two hours by 1 or 2 units

(a) PBP74

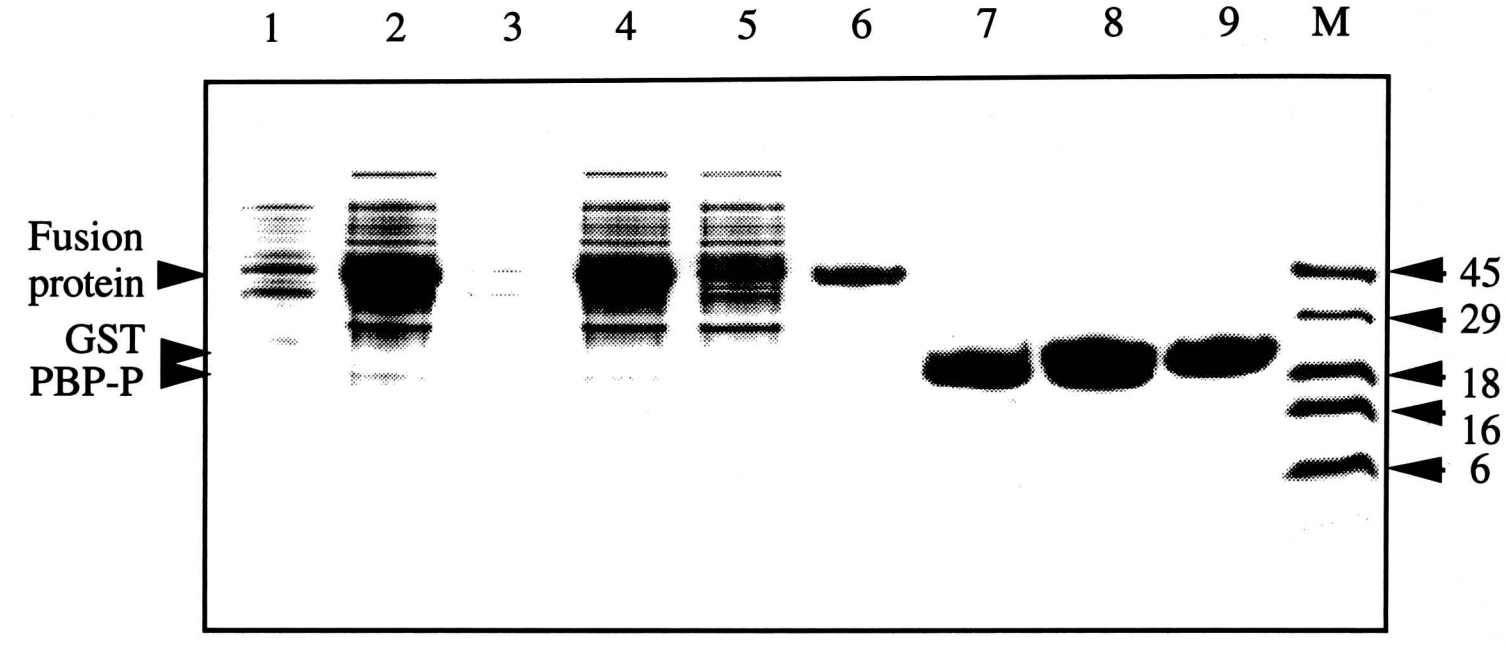

(b) Hsp70hom

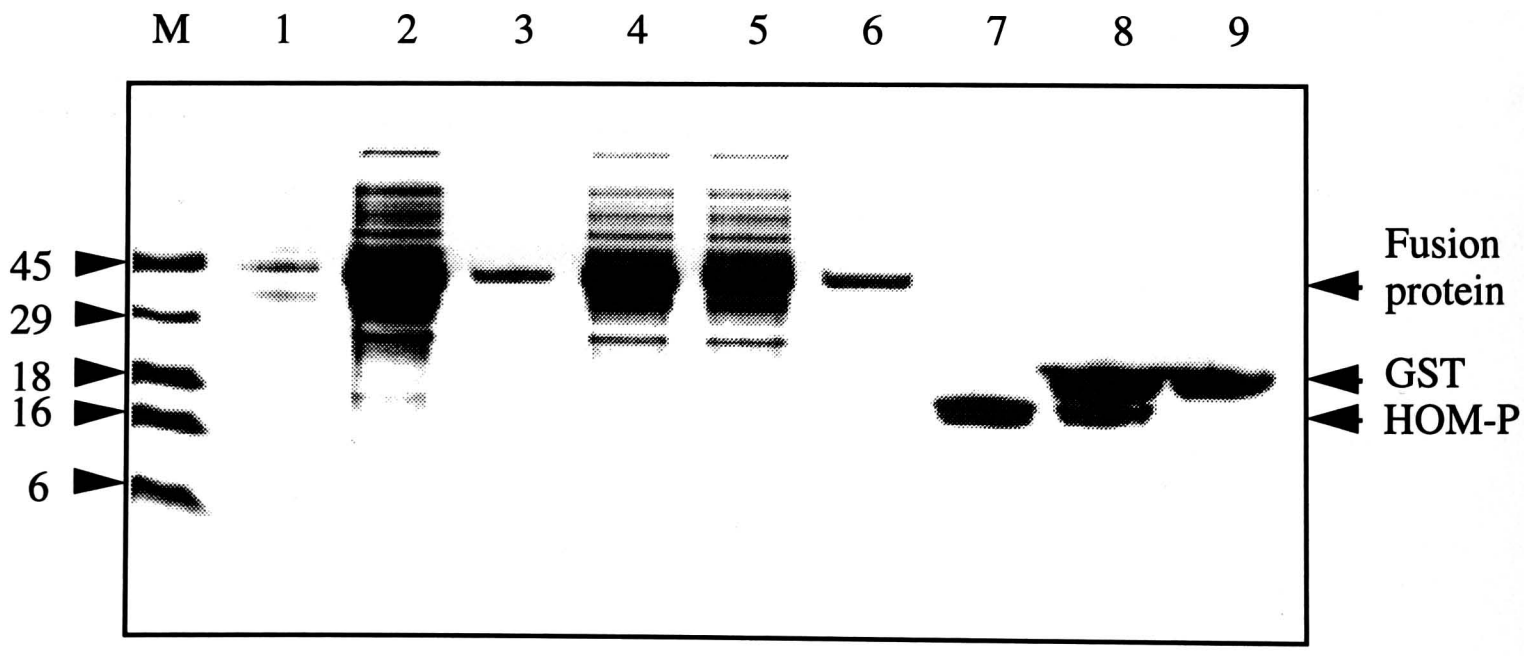

Figure 3-5: Expression and purification of the peptide-binding domains of (a) PBP74 and (b) hsp70hom as fusions with glutathione-S-transferase.

LANES:

1 Uninduced cells after 20 hours of culture

2 Cells induced by incubation with 100 μM IPTG (final concentration) for 20 hours: the fusion protein can be seen at ~45 kDa

3 Material from the induced cell lysate that is insoluble in 1% Triton X100

4 Material from the induced cell lysate that is soluble in 1% Triton X100

5 Material from the induced cell lysate that is not bound to glutathione agarose

6 Material from the induced cell lysate that is bound to glutathione agarose

7 Soluble material after thrombin digestion of the fusion protein bound to glutathione agarose: the peptide-binding domain (~19 kDa) is the sole visible species.

8 Material associated with glutathione agarose after thrombin cleavage: includes the glutathione-S-transferase moiety of the fusion protein (~23 kDa) and some of the peptide-binding domain

9 Material bound to glutathione agarose after washing with MTPBS: glutathione-S-transferase alone remains bound

The fusion proteins can be seen at ~45 kDa in lanes 2-6, the peptide-binding domain at ~19 kDa in lanes 7 and 8 and GST at ~26 kDa in lanes 8 and 9. Lane M contains 5 μg of low molecular weight standards (Gibco BRL). Lanes 1-6 contain 5 μl from 25 ml samples, lane 7 contains 2.5 μl from 2.5 ml and lanes 8 and 9 contain 5 μl from 5 ml of 50% (v/v) glutathione agarose. Thus, the protein loaded in lanes 1-6 is derived from the equivalent of 100 μl of the 500 ml induced culture, and lanes 7-9 contain protein from 500 μl of the culture.

of thrombin and approximately half was digested by 0.1 unit. Very little was digested after incubation with 0.01 unit for 2 hours. Therefore, for large scale purifications, the fusion protein from 500 ml of culture was treated with 25 -50 units of thrombin (0.1-0.05 units per 10 ml of culture) with an extended incubation period of 6 hours (Figure 3-5). If the fusion protein was not cleaved after this time, the glutathione agarose was simply incubated with thrombin again.

Each domain was purified from the supernatant after thrombin cleavage by reverse phase high performance liquid chromatography (HPLC) [E9] on a C8 column using a 0.1% (v/v) trifluoroacetic acid (TFA)/acetonitrile gradient (8-80% acetonitrile, 1.8%/min, 3 ml/min flow rate), and was eluted from a C4 column by ~60% acetonitrile in each case (Figure 3-6). The fractions containing each peptide-binding domain were pooled, lyophilised and resuspended in water. The yield of protein was calculated using the bicinchoninic acid (BCA) assay [E6] and the purified domains characterised by N-terminal sequencing [E11] and mass spectrometry [E13]. The N-terminal sequence obtained for each protein indicated that thrombin cleavage occurred at the correct site (GSPGIGDVTDVLLLDV for PBP-P and GSGDKSEKNVQ for HOM-P). Mass spectrometry (Figure 3-7) showed that the purifications were extremely successful and confirmed that the sequences of the domains were correct, since the mass of PBP-P was 19471±3, compared to a predicted mass of 19469, and the mass of HOM-P was 19692±7 compared to a predicted mass of 19688. Species seen with masses of approximately 19491 and 19507 in PBP-P, and 19710 and 19726 in HOM-P, represented the sodium and potassium salts of the proteins, respectively. The yield of purified protein was greater than 10 mg per litre of culture. The two domains are soluble at concentrations of up to 20 mg/ml (1 mM) in water, making them suitable for NMR studies.

In preparation for isotopic labelling for NMR studies, the ability of *E. coli* strain BL21 to express PBP-P in minimal medium was investigated [E8] (Figure 3-8). Cultures were grown in the presence of 0.05, 0.1, 0.2 and 0.4% (w/v) glucose, induced with IPTG at

(a) PBP-P

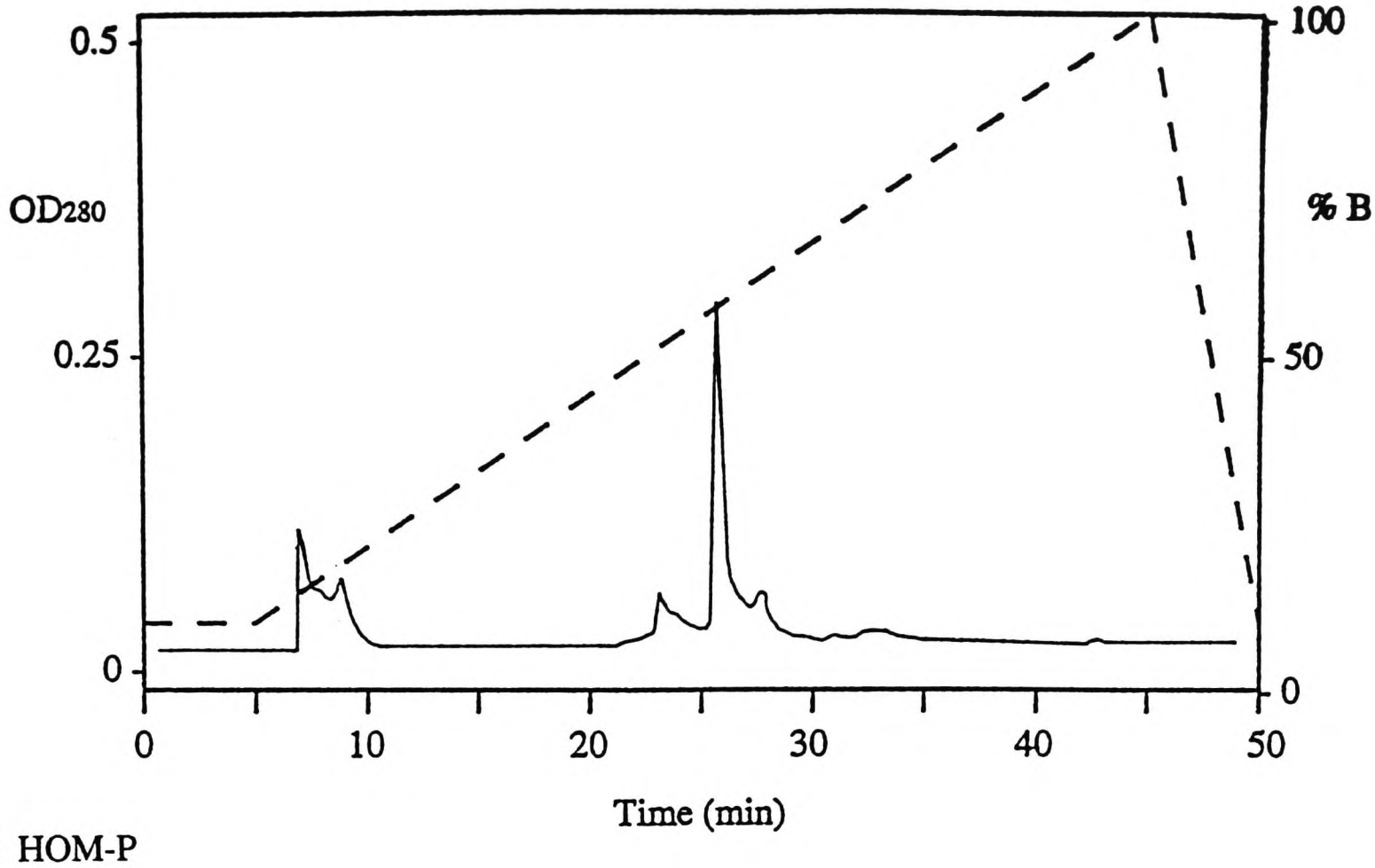

(b) HOM-P

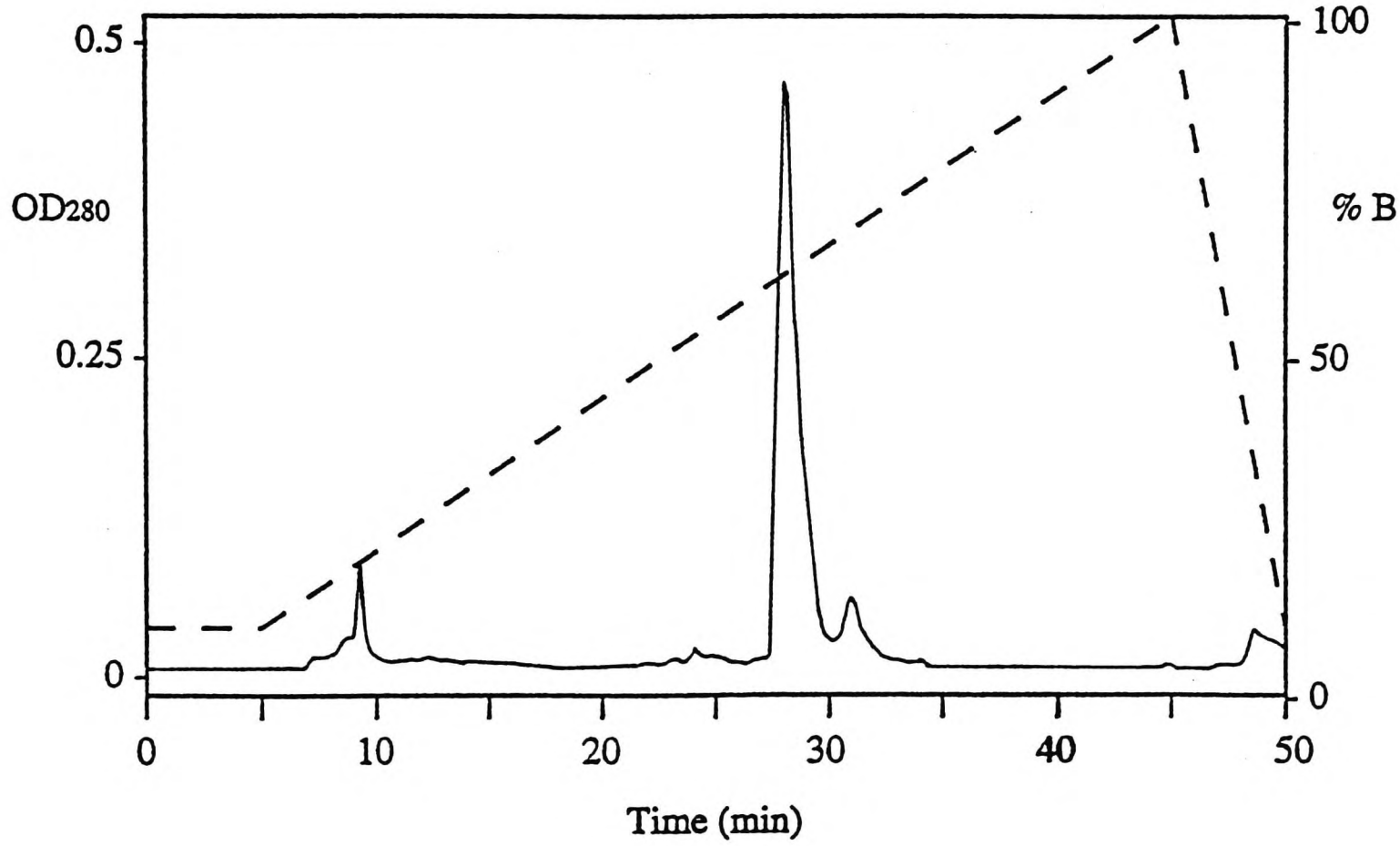

Figure 3-6: Purification of (a) PBP-P and (b) HOM-P by reverse-phase HPLC. Up to 5 ml of the soluble fraction after thrombin cleavage (Figure 3-5, lane 7) pooled with the washings from the glutathione agarose after thrombin cleavage (Figure 3-5, lane 8) and mixed with 0.1% (v/v) TFA. This was loaded onto a C8 column (Dynamax-300A) that had been equilibrated with 90% (v/v) solvent A [0.1% (v/v) TFA], 10% (v/v) solvent B [80% (v/v) acetonitrile, 0.1% (v/v) TFA]. These conditions were continued for 10 minutes, with the proportion of solvent B (- - -) then rising to 100% (v/v) over 40 minutes. The proportion of solvent B returned to 10% (v/v) over five minutes. In each case, the largest peak was collected, from as soon as the OD_{280} (___) started to rise until it fell below about a fifth of its highest value. PBP-P was eluted by ~41% (v/v) acetonitrile and HOM-P by ~37% (v/v) acetonitrile.

(a) PBP-P

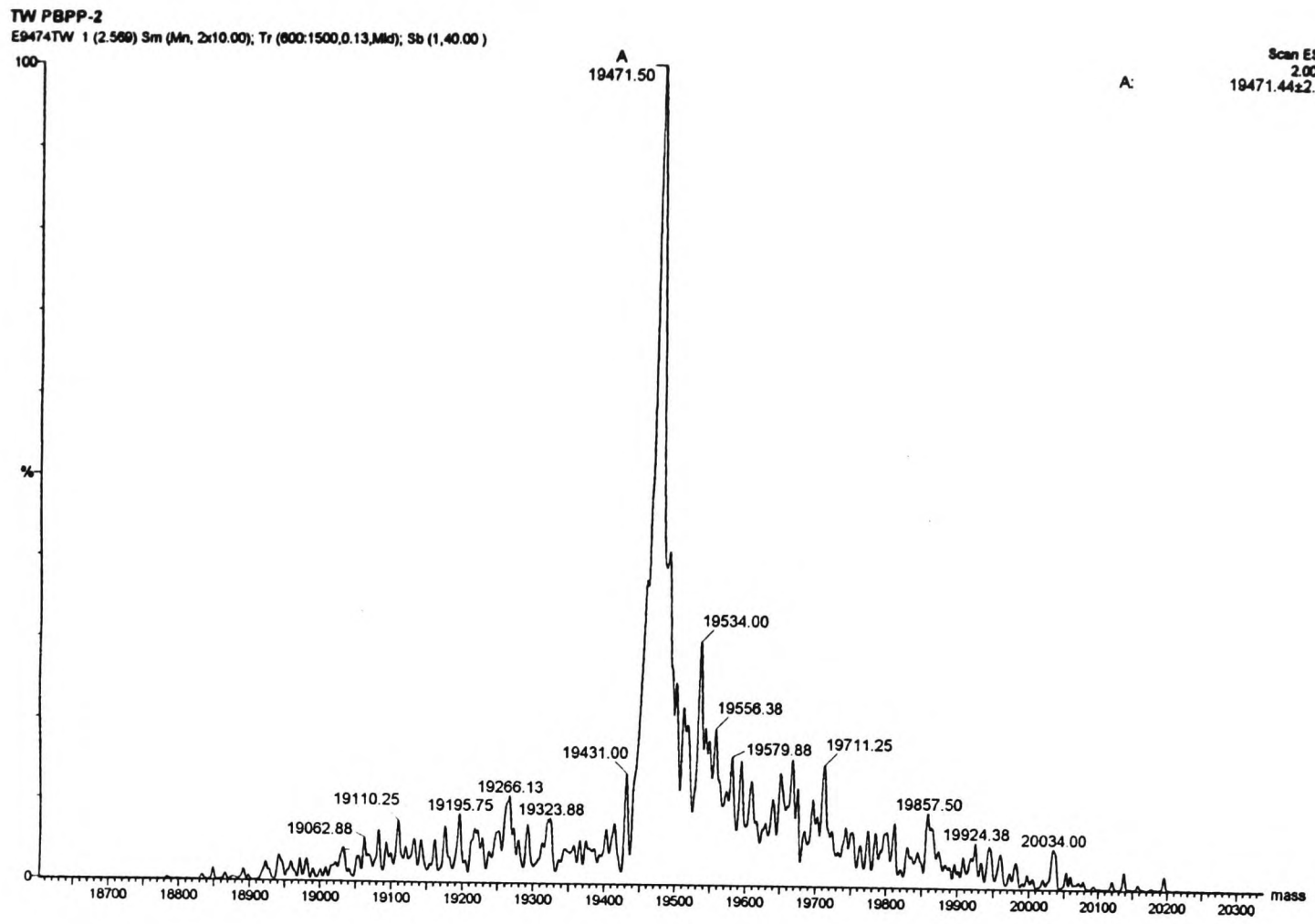

(b) HOM-P

Figure 3-7: Electrospray mass spectrometry of (a) PBP-P and (b) HOM-P after purification by HPLC. In each case, 1 nmol of protein (50 µl of a 25 µM solution in water) was used and peak A represents the peptide-binding domain. The molecular masses determined by electrospray mass spectrometry are close to the masses predicted from the amino acid sequences of the two proteins (19469 for PBP-P and 19688 for HOM-P).

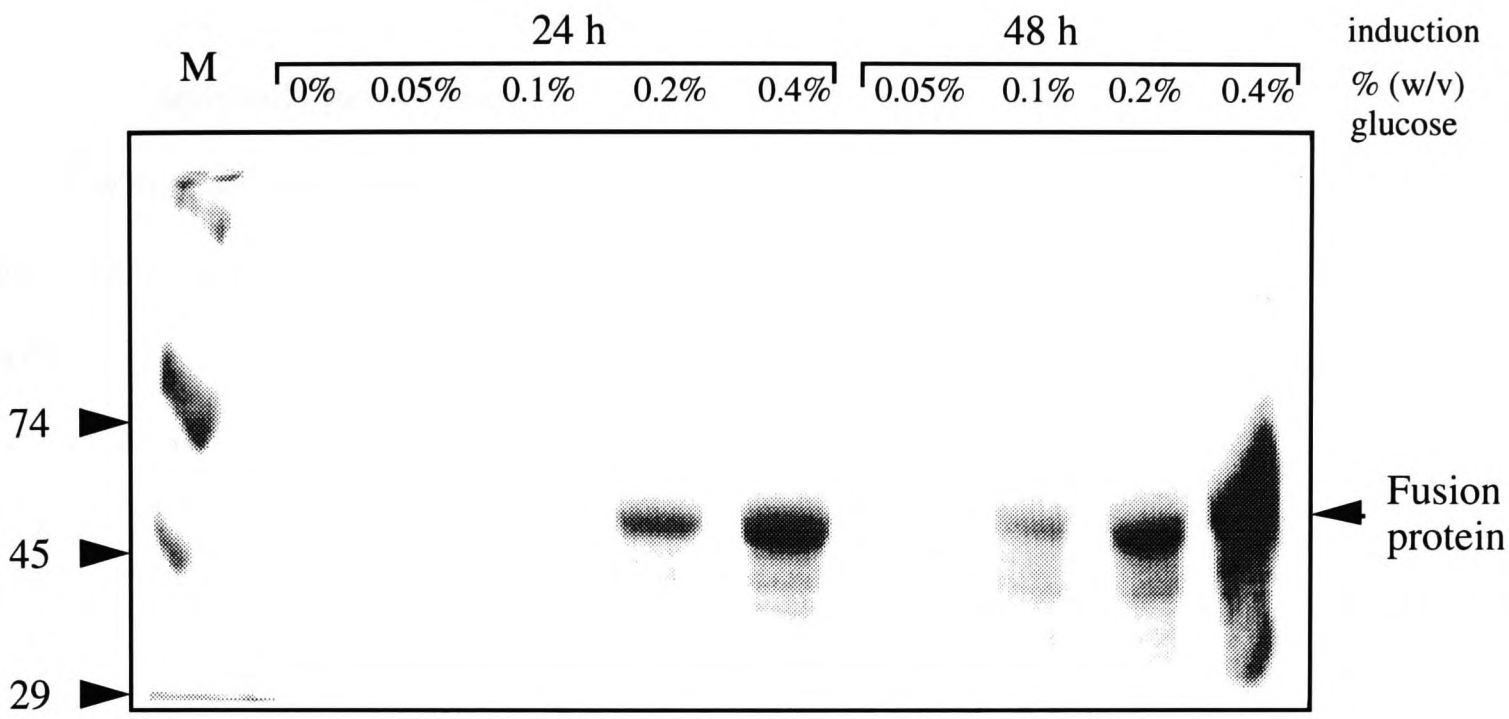

Figure 3-8: Expression of the peptide-binding domain of PBP74 in minimal medium. An overnight culture of*E.coli* strain BL21 transformed with pGEX-PBP was grown in L-broth and 50 µg/ml ampicillin. The cells were collected by centrifugation at 2 000 g for 10 minutes and resuspended in 20 ml (ten times the original culture volume) of minimal medium supplemented with glucose at 0.05% (w/v) (lanes 2 and 6), 0.1% (w/v) (lanes 3 and 7), 0.2% (w/v) (lanes 4 and 8) and 0.4% (w/v) (lanes 1, 5 and 9). The cells were induced in log phase growth and aliquots were harvested after 24 hours (lanes 2-5) and 48 hours (lanes 6-9). Lane 1 contains uninduced cells grown in 0.4% (w/v) glucose and harvested after 24 hours. Cells from each culture (200 µl) were harvested by centrifugation at 12 000 g for 1 minute, resuspended in 20 µl of water and 10 µl was separated by SDS-PAGE on a 10% (v/v) acrylamide gel [E1]. The proteins were visualised with Coomassie blue stain. Lane M contains high molecular weight standards.

OD_{600} = 0.5 and aliquots were harvested after 24 and 48 hours. The fusion protein is expressed strongly in minimal medium, and is more abundant when the growth medium is supplemented with increasing concentrations of glucose (lanes 4, 5, 8 and 9) and when the cells are harvested after 48 hours rather than 24 hours (lanes 8 and 9). The point at which IPTG was added was also varied (data not shown). When IPTG was added at OD_{600} = 0.7, rather than 0.5, more of the fusion protein was produced, but when IPTG was added at OD_{600} = 1, which is near the maximum growth achieved in the 50 ml tubes used (see below), the induction was much less efficient. The addition of glucose increases fusion protein expression by stimulating bacterial growth as well as increasing the amount of protein each bacterium produces. While the cultures supplemented with different concentrations of glucose grew at similar rates to begin with, reaching OD_{600} = 0.5 at much the same time, the cultures containing more glucose grew more quickly after IPTG was added (data not shown). Thus, in the presence of 0.05% (v/v) glucose, the OD_{600} remained unchanged at 0.5 after 24 and 48 hours, while in the presence of 0.4% (v/v) glucose, the OD_{600} rose to 0.7 after 24 hours and 1.0 after 48 hours. In comparison, the OD_{600} of cultures grown in L-broth rise more quickly, but do not reach a significantly higher maximum; in half-filled 50 ml tubes, the maximum OD_{600} was 1.1, which was reached within 6 hours. In baffled flasks, the OD_{600} reached 1.5 after culture overnight in L broth, indicating that aeration, as well as the richness of the medium, is an important factor influencing bacterial reproduction.

NMR Spectroscopy

Nuclear magnetic resonance (NMR) spectroscopy [E14] is a powerful technique for determining the structure of molecules (Evans, 1995). It makes use of a property called spin, possessed by certain atoms, such as hydrogen (^{1}H), and rare isotopes of carbon (^{13}C), nitrogen (^{15}N) and phosphorus (^{31}P). This spin gives each atom a magnetic dipole,

which is influenced by the environment of the atom. In an NMR experiment, the sample is placed in a magnetic field to orient the spins of the different atoms in the same direction. When a pulse of electromagnetism covering a broad frequency range is applied, each atomic dipole resonates at a frequency that depends on the environment of the atom and the conditions of the experiment. This resonance is detected and displayed as a graph of intensity against frequency. Since hydrogen atoms have spin, naturally occurring molecules resonate in NMR experiments. Protons attached to nitrogen, carbon and oxygen have characteristic resonance ranges and the protons in water appear as a large central peak. To make molecules, such as acetonitrile, invisible to NMR, their hydrogen atoms must be replaced with deuterium (^2H). In contrast, to detect carbon, nitrogen or phosphorus spectra, molecules must be synthesised from the rare isotopes ^{13}C, ^{15}N or ^{31}P.

One dimensional (1-D) spectra were determined for PBP-P and HOM-P at pH 3.5, 5.5, 6.5 and 7, by Dr. G. Shaw. At pH 3·5, the spectrum for PBP-P contains only a few, very broad resonance peaks (Figure 3-9a). This shows that the domain is unfolded; its protons differ only in their covalent environment so their resonances overlap. At higher pHs, above the isoelectric points of the proteins (pI = 4.7 for PBP-P and 4.88 for HOM-P)*, the resonances are more dispersed and the spectra contain sharply defined peaks indicative of folded structure (Figure 3-9b, 3-10). In particular, the amide proton region has spread out (5-10 ppm), with resonances appearing in the ß-sheet NH region (5-6 ppm), and there are some clear chemically-shifted methyl proton resonances (0-1 ppm). The effect of temperature on the 1-D spectra was investigated, since increasing the temperature of the sample can enhance the resolution of NMR spectra by increasing the rate at which molecules tumble. However, the resonance line-widths did not change significantly as the temperature of the sample was increased from 25 °C to 30 °C, 35 °C or 42 °C (data not shown).

---

* Isoelectric points (the pH at which a protein has no net charge) were calculated using the Isoelectric program of GCG.

(a) HOM-P

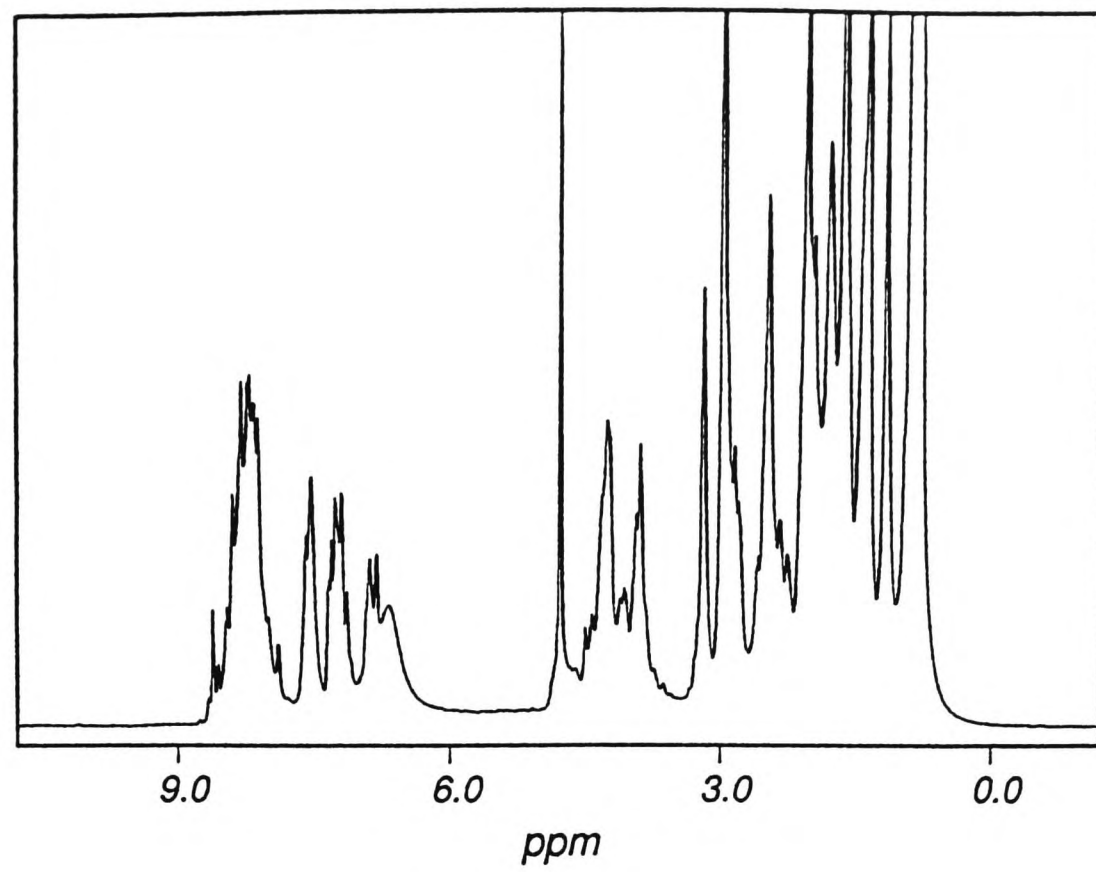

(b) PBP-P

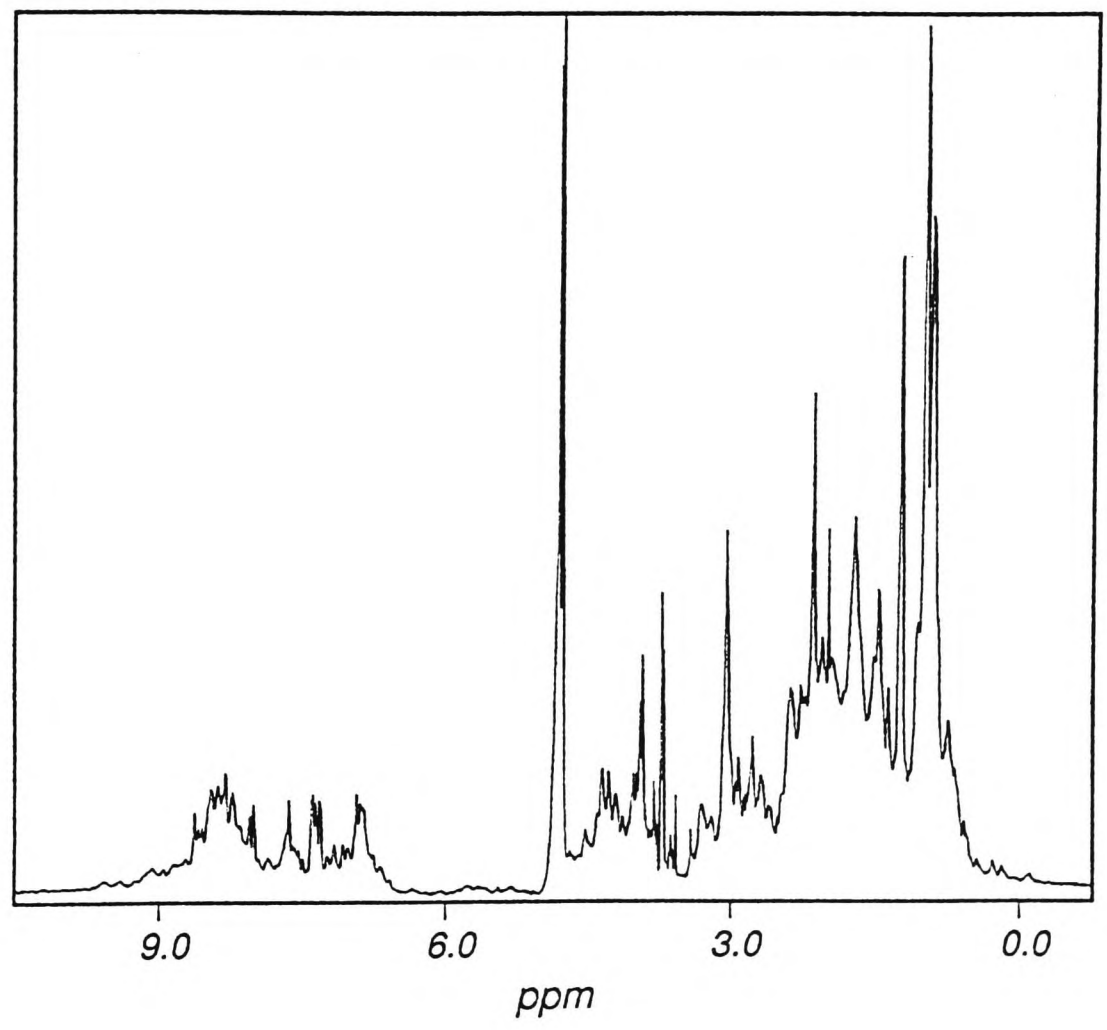

Figure 3-9: 1-D NMR spectra of PBP-P at (a) pH 3.5 and (b) pH 5.5. The sample concentration was 0.5 mM. Resonances of PBP-P can be detected from amide protons (5-10 ppm), hydroxyl protons (3.5-5 ppm) and aliphatic (-CH_2- or -CH_3) protons (0-3.5 ppm). The large peak at 4.8 ppm is produced by the protons in H_2O. The spectra were determined at 25 °C with an Omega 500 MHz spectrometer.

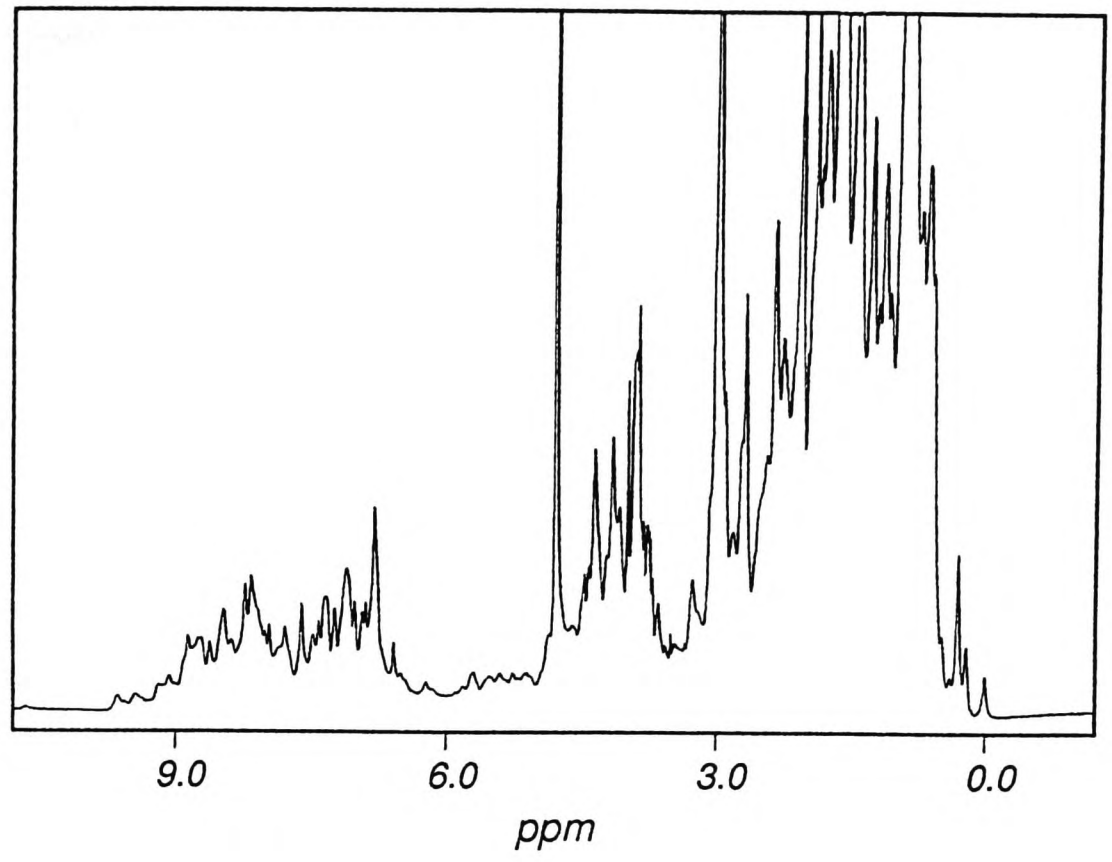

Figure 3-10: 1-D NMR spectra of HOM-P at pH 6.5. The sample concentration was 0.5 mM. Resonances of PBP-P can be detected from amide protons (5-10 ppm), hydroxyl protons (3.5-5 ppm) and aliphatic (-CH_2- or -CH_3) protons (0-3.5 ppm). The large peak at 4.8 ppm is produced by the protons in H_2O. The spectra were determined at 25 °C with an Omega 500 MHz spectrometer.

More information can be provided by two-dimensional (2-D) NMR spectroscopy, in which an additional pulse of electromagnetic radiation is applied soon after the first. By varying the interval between the two pulses, magnetic resonance is allowed to pass between atoms that interact, a phenomenon called relaxation. In the resultant spectra, the 1-D spectrum appears as a diagonal line, with interactions between protons appearing as cross-peaks on either side. Nuclear Overhaüser effect spectroscopy (NOESY) detects interactions between protons that are close together in space, and is used to determine the three dimensional structure of a protein, whereas correlated spectroscopy (COSY) detects interactions between atoms that are close together in the polypeptide chain and is used to assign NOESY resonances to specific atoms.

The 2-D NOESY spectra of 1 mM HOM-P at pH 5·5 (not shown), pH 6 (not shown) and pH 6.5 (Figure 3-11a), determined by Dr. A. Perczel, contained a number of cross-peaks, indicating that the domain is folded. However, only a few resonances can be detected above background noise, and these signals are weaker than would be expected from a sample at this concentration. This suggests that HOM-P is aggregating in solution. Aggregation reduces the intensity of a spectrum because large molecular aggregates tumble slowly in solution and resonate over a broader frequency range, causing the peaks to become more diffuse. The intensity of the spectrum was not altered by doubling the concentration of the sample from 0.5 mM to 1 mM, suggesting that the amount of HOM-P in the monomeric form is saturated. Addition of 10% (v/v) deuterated acetonitrile to the sample appeared to reduce the amount of aggregation, as it slightly improved the 2-D spectrum of HOM-P (Figure 3-11b). Acetonitrile has been shown to improve markedly the stability of the peptide-binding domain of hsc70 against denaturation, aggregation and precipitation, in a buffer containing 50 mM sodium phosphate, pH 7 (Morshauser *et al.*, 1995). Addition of 50 mM NaCl had no effect on the aggregation of HOM-P (data not shown). The spectra shown in Figure 3-11 were measured using a mixing time of 150 ms,

(a) Without acetonitrile

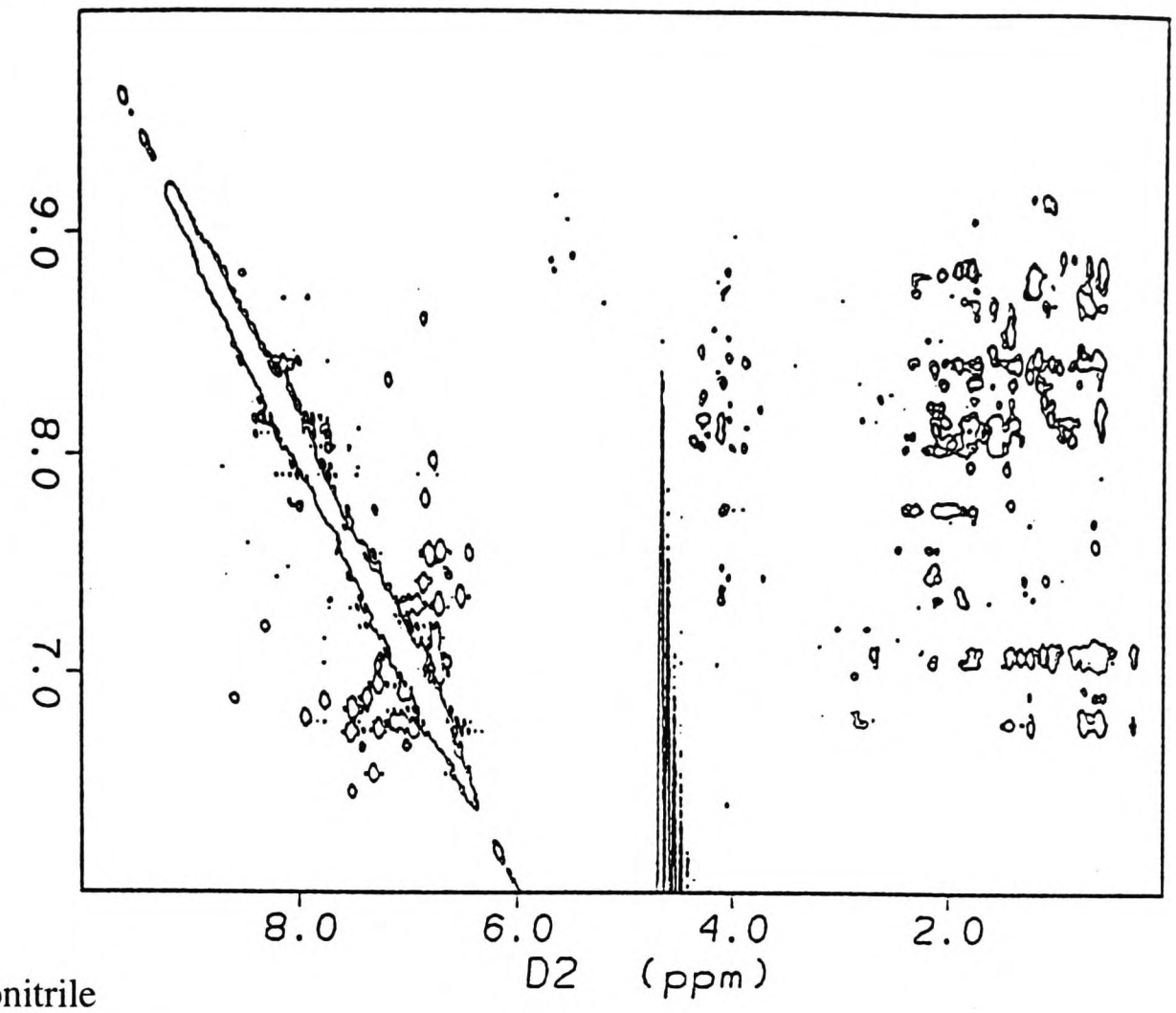

(b) + 10% (v/v) acetonitrile

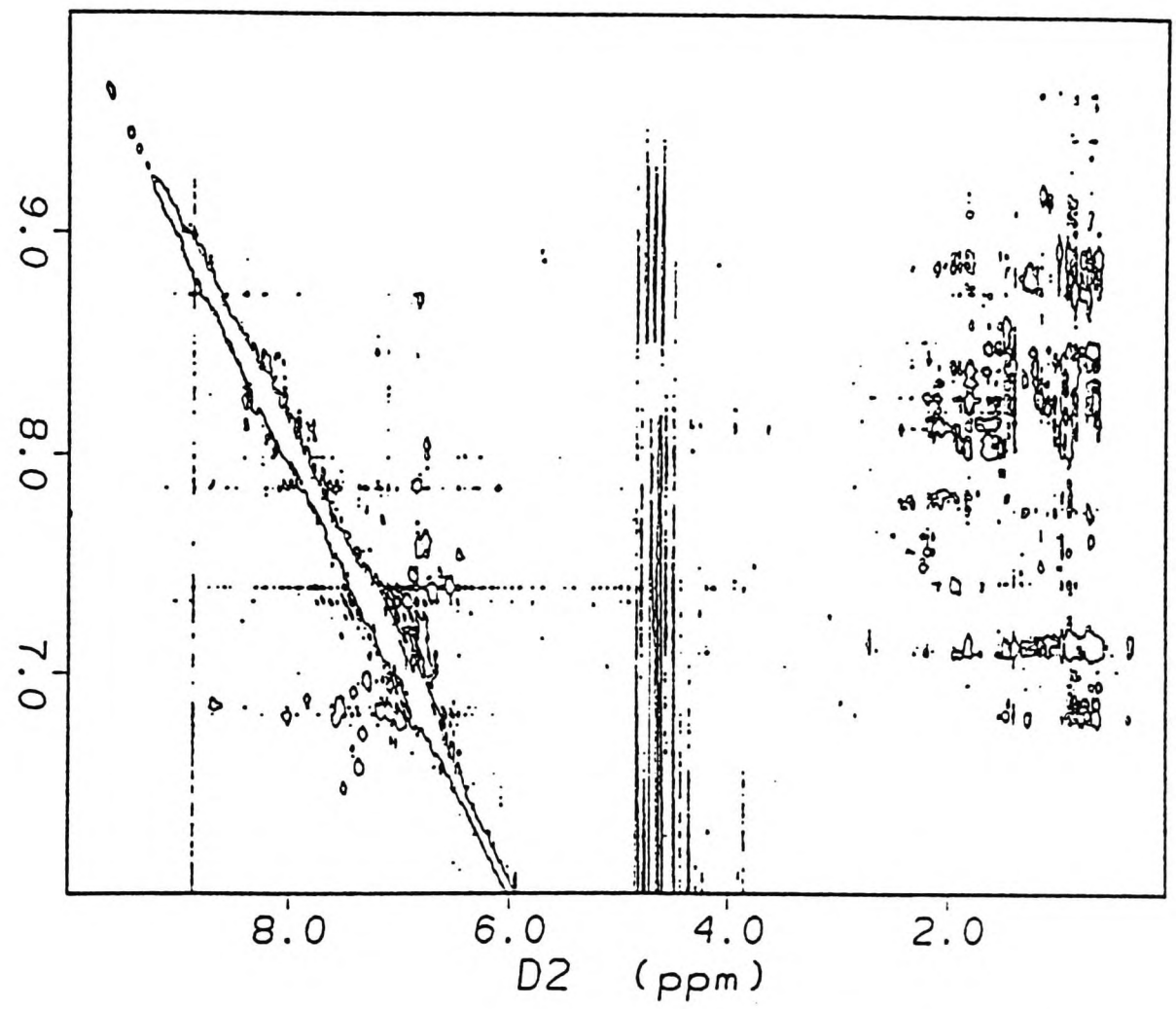

Figure 3-11: The fingerprint regions from 2-D NOESY spectra of HOM-P at pH 6.5, (a) in the absence or (b) in the presence of 10% (v/v) deuterated acetonitrile as a cosolvent. The sample concentration was 1 mM and the mixing time was 150 ms. These spectra show interactions between amide protons (6-9 ppm) on the vertical axis and other amide protons (6-9 ppm) and methyl protons (0-4.5 ppm) on the horizontal axis. Water forms the line at ~5 ppm on the horizontal axis.

which gave better results than a mixing time of 80 ms (data not shown), because it optimised the time for interactions between atoms to occur.

Extensive spectroscopy was not carried out with PBP-P because no cross-peaks could be detected in a 2-D NOESY spectrum of a 1 mM sample at pH 5·5 (data not shown) and after storage for one month at 4 °C, a 1-D spectrum indicated that PBP-P had unfolded (data not shown).

X-ray crystallography

Crystallisation trials of HOM-P were carried out using the hanging drop method at 2 °C and 20 °C, by Dr. V. Fulop. One hundred different buffer conditions were tested, including pH gradients (pH 5-9 in increments of 0.5) in the presence of varying concentrations of ammonium sulphate (0.2-0.5% saturation) or 2-methyl-2,4-pentanediol (MPD) (10-70% saturation). Additionally, the Sparse Matrix crystallisation screening kit (Crystal Screen) was used (Jancarik and Kim, 1991).

It was not possible to crystallise the peptide-binding domain of hsp70hom, because it precipitates quickly before it can form crystals. This supports the idea that HOM-P aggregates in solution. Using reverse phase HPLC and lyophilisation to purify proteins for crystallography is not recommended by crystallographers because HPLC denatures the proteins which must, therefore, refold when resuspended in water. Nevertheless, single domain proteins are commonly purified by HPLC for NMR spectroscopy, and the NMR spectra showed that the domains, prepared as described above, were folded.

Discussion

The strategy chosen for expressing the peptide-binding domains of PBP74 and hsp70hom was very successful. Both domains were produced as glutathione-S-transferase fusion proteins at high levels, without modification or degradation. Their purification by glutathione-affinity chromatography was straightforward, and they were efficiently released from the fusion protein by thrombin digestion without being degraded. A single round of HPLC was sufficient to remove any contaminants that remained. The final yield of the domains was greater than 10 mg per litre.

The domains were highly soluble and could be prepared at concentrations of at least 20 mg/ml. NMR spectroscopy showed that the expressed domains are folded and so they should be suitable for functional studies investigating their ability to bind to peptides. However, the domains aggregated at the high sample concentrations necessary for NMR, lessening the signal strength and precluding structural determination. This was disappointing, because it has been possible to determine the secondary structure of the peptide-binding domain of hsc70 by NMR under similar conditions [1-1.4 mM protein in 50 mM sodium phosphate buffer, pH 7 containing 10% (v/v) deuterated acetonitrile and 0.02 % (w/v) sodium azide, at 25 °C] (Morshauser *et al.*, 1995). However, this domain also had a strong tendency to aggregate and precipitate, and it was not possible to determine its complete three-dimensional structure. It is difficult to account for the different behaviours of the hsp70hom and hsc70 peptide-binding domains in NMR experiments, because they differ by only 4 non-conservative and 12 conservative amino acid substitutions in 160 amino acids. However, HOM-P includes 16 more amino acids at its C-terminus than the hsc70 domain, and although these are predominantly polar residues, they may increase the tendency of the domain to aggregate. In addition, HOM-P

lacks the hexahistidine tag expressed at the N-terminus of the hsc70 domain, which may have increased its solubility.

The aggregation of HOM-P in solution also prevented its structure from being determined by X-ray crystallography, since the protein precipitated rather than forming crystals. This appears to be a general feature of the peptide-binding domains of hsp70s (Rüdiger *et al.*, 1997b). However, the aggregation of the C-terminal half of dnaK could be reversed by binding peptide (X. Zhao, personal communication). This suggests that the peptide-binding domain of hsp70s is relatively flexible in the absence of peptides, and that peptide binding induces it to adopt a stable conformation that is suitable for crystallisation. Therefore, a complex of HOM-P with a peptide might be able to form crystals, or to maintain a sufficiently high concentration of monomer in solution, for its structure to be determined by X-ray crystallography or NMR respectively. However, it is first necessary to identify a peptide that binds to HOM-P, and this work is described in Chapter 5.

Chapter 4: A Model of the Peptide-Binding Domain of Hsp70hom

Introduction

The proposed role of hsp70s in antigen processing suggests that their specificity for peptides may influence the repertoire of peptide antigens presented by MHC molecules. As discussed in Chapter 1, hsp70s may be involved in the MHC class I pathway of antigen processing, shuttling peptides through the cytoplasm from the proteasome, where they are generated, to TAP, which transports them into the ER to meet newly synthesised class I molecules. Furthermore, peptides complexed to hsp70s are efficiently endocytosed by antigen presenting cells and presented in association with MHC class I molecules (Srivastava *et al.*, 1994).

A key to understanding the broad, but not unlimited, specificity of hsp70s for peptides and other substrates is the structure of their peptide-binding domains. The peptide-binding domains of hsp70hom and PBP74 were expressed in isolation from the rest of the molecule for structural studies, as described in Chapter 3. Unfortunately, their structures could not be determined by NMR or X-ray crystallography, because they aggregate in solution at high concentrations. Therefore, it was decided to model the peptide-binding domain of hsp70hom, based on the structure of the C-terminal region of the *E. coli* hsp70, dnaK (amino acids 389-607) complexed with a peptide (NRLLLTG), which has been determined recently by X-ray crystallography (Zhu *et al.*, 1996). The model generated should be reliable because the C-terminal regions of hsp70hom and dnaK share 42% amino acid sequence identity. Hsp70hom, a constitutively-expressed cytoplasmic hsp70, is of particular interest from the point of view of antigen processing because it is encoded in the

MHC (Milner and Campbell, 1990), an area of the genome containing many genes involved in antigen processing and presentation, as well as genes involved in other immune functions. A model of the C-terminal region of hsp70hom will also provide insights into the specificity of the other cytoplasmic human hsp70s, with which it shares at least 80% amino acid identity (Figure 1-1).

The Structure of the C-terminal Region of DnaK bound to the Peptide NRLLLTG

The C-terminal region of dnaK (Zhu *et al.,* 1996) consists of two subdomains, an N-terminal ß-subdomain (amino acids 389-501), which consists of eight ß-strands arranged as two layers of antiparallel ß-sheet, and a C-terminal α-subdomain (503-611) which contains five α-helices (Figure 1-2a). The peptide is bound in an extended conformation, by residues found in the first four ß-strands and the loops between the first and second strands ($L_{1,2}$) and third and fourth strands ($L_{3,4}$). The α-subdomain does not contact the peptide, and is thought to function as a lid over the peptide-binding site.

The interactions between dnaK and the peptide NRLLLTG have been analysed by Zhu *et al.* (1996). We carried out our own analysis of these interactions using the program Naomi (Brocklehurst and Perham, 1993), with slightly different results. An additional hydrogen bond was detected, between Thr 403 of dnaK and Arg 2 of the peptide, which are also in Van der Waals contact. No additional Van der Waals interactions were seen, and three such interactions identified by Zhu and colleagues were not found in our analysis (Val 407-Arg 2, Thr 409-Arg 2, and Ser 427-Leu 3). The differences between these analyses are likely to be due to differences in the parameters (such as distance) used by Zhu *et al.* (1996) and Naomi. Interactions detected in both analyses are included in the discussion below.

The peptide NRLLLTG is bound by dnaK through hydrophobic interactions and hydrogen bonds (Figure 4-1). Six of its seven side chains are in contact with a total of 13

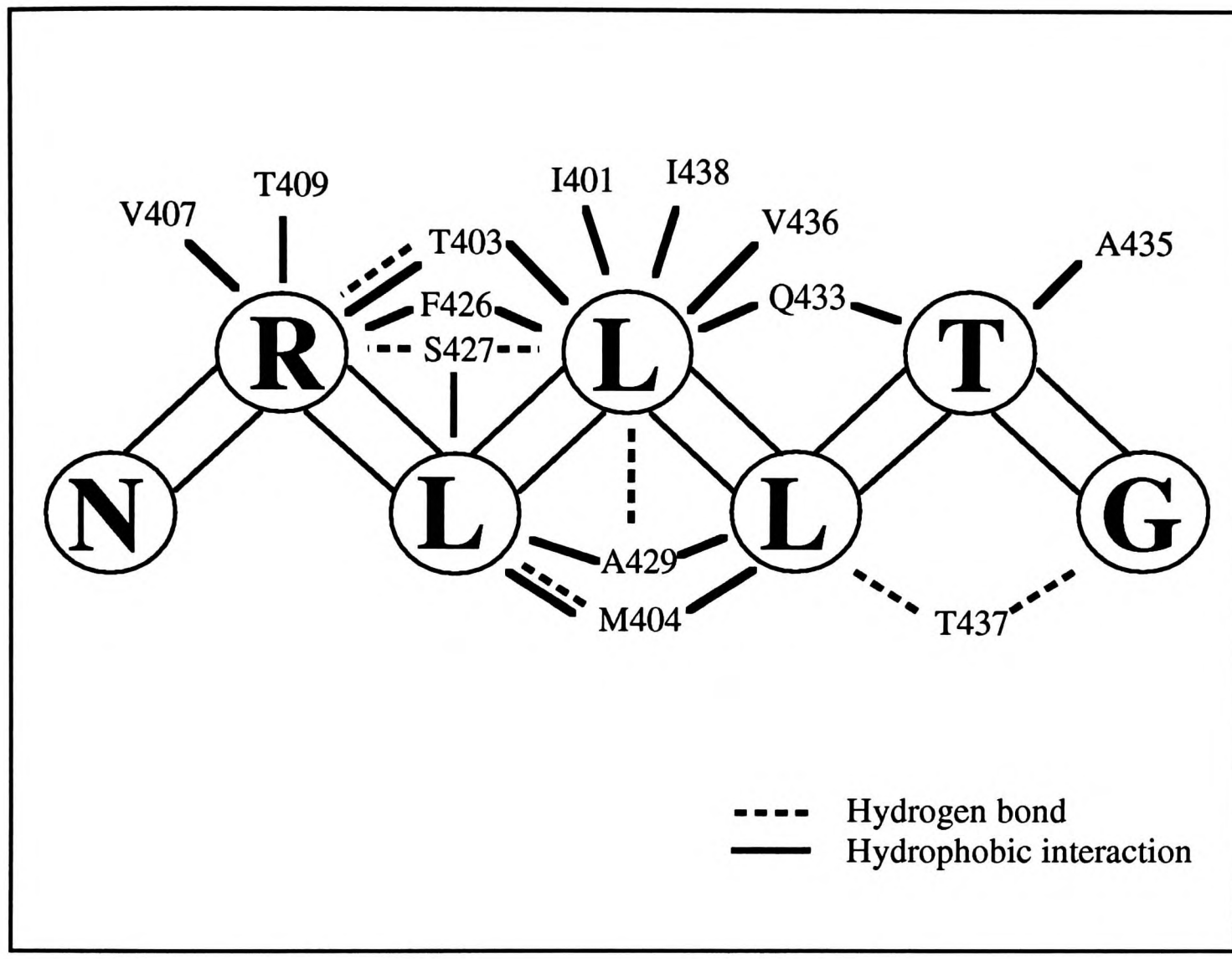

Figure 4-1: The contacts between dnaK and peptide NRLLLTG. The contacts shown are those derived from the co-ordinates of Zhu *et al.* (1996) by them, and by ourselves using the program Naomi (Brocklehurst and Perham, 1993). The peptide is bound through hydrogen bonds and hydrophobic interactions. The hydrogen bond between Arg 2 and Thr 403 was identified only by ourselves, while three hydrophobic interactions were detected only by Zhu and colleagues (Arg 2-Val 407, Arg 2-Thr 409, and Leu 3-Ser 427).

side chains of dnaK. The interactions between dnaK and the peptide are predominantly hydrophobic, involving ten amino acids of dnaK and the five central residues of the peptide, notably the central leucine. This residue (Leu 4) binds in a deep hydrophobic pocket in the centre of the peptide-binding cleft. The peptide has no secondary structure, so its main chain carbonyl and amide groups are available to form hydrogen bonds with dnaK. Six hydrogen bonds anchor the peptide backbone at residues 2-5, while a seventh hydrogen bond, formed with Gly 7 of the peptide is poorly ordered and, therefore, questionable (Zhu *et al.,* 1996). In addition, there is one hydrogen bond between a side chain of the peptide, Arg 2, and dnaK (the side chain of Thr 403). The significance of a hydrophobic interaction (a Van der Waals contact between hydrophobic residues) depends on the area of hydrophobic surface that is buried when the two amino acids interact. In contrast, the contribution to binding of a hydrogen bond, while dependent on the distance between the two atoms, is less variable. It is interesting that electrostatic interactions are not involved in the binding of this peptide by dnaK.

This information tells us how dnaK binds to one peptide, but without knowing the relative contributions of the different interactions to the overall binding affinity, it is difficult to use this structural information to speculate on the sequence specificity of dnaK for different peptides. The hydrogen bonds with the main chain atoms of a bound peptide will be able to form irrespective of its amino acid sequence. However, interactions with the peptide side chains are likely to be essential for high affinity binding and will determine the sequence specificity of dnaK. In the case of the dnaK-NRLLLTG complex, with the exception of the hydrogen bond with the side chain of Arg 2, all the interactions involving the peptide side chains are hydrophobic. It should be noted that the specificity will be determined as much by which amino acids are prevented from binding (by steric or electrostatic repulsion, for example) as by the formation of favourable interactions.

Results

Alignment of the Amino Acid Sequences of Hsp70hom and DnaK

The first stage of modelling the C-terminal region of hsp70hom on the structure of the equivalent region of dnaK is to align their sequences (Figure 4-2). Hsp70hom and dnaK share 49% amino acid identity overall and 42% in their C-terminal regions (amino acids 389-607 of dnaK). Their ß-subdomains, which are thought to contain all the residues that interact with the peptide, share 65% identity, while the α-subdomains, which form a lid over the peptide-binding site, have very little identity with each other (24%). The C-terminal portion of hsp70hom contains three amino acid insertions compared to dnaK. One (Arg 511) is between amino acids equivalent to 506 and 507 of dnaK, in the loop between the final ß-strand of the ß-subdomain and the first α-helix of the α-subdomain. A second insertion (Leu 560 and Lys 561) is between amino acids equivalent to 554 and 555 of dnaK, in the loop between the second and third α-helices of the α-subdomain. The third (Asn 586, Gln 587 and Leu 588) is between amino acids equivalent to 579 and 580 of dnaK, between the third and fourth α-helices of the α-subdomain. The fact that the insertions are not in the peptide-binding ß-subdomain or in elements of secondary structure means that they are unlikely to affect the topology of the peptide-binding site.

Modelling the C-Terminal Region of Hsp70hom

The structure of the C-terminal domain of hsp70hom (amino acids 393-617) was modelled on the basis of the structure of the equivalent region of dnaK (Zhu *et al.*, 1996) by Mr. B. Marsden (Department of Biochemistry), using the program Modeller (Sali and Blundell, 1993). This program models the three-dimensional structure of a target protein by satisfaction of spatial restraints derived from the known structure of a homologous

```
  1 MGKIIGIDLGTTNSCVAIMDGTTPRVLENAEGDRTTPSIIAYTQDGETLV 50
  5 KGIAIGIDLGTTYSCVGVFQHGKVEIIANDQGNRTTPSYVAFT.DTERLI 53

 51 GQPAKRQAVTNPQNTLFAIKRLIGRRFQDEEVQRDVSIMPFKII.AADNG 99
 54 GDAAKNQVAMNPQNTVFDAKRLIGRKFNDPVVQADMKLWPFQVINEGGKP 103

100 DAWVEVKGQKMA..PPQISAEVLKKMKKTAEDYLGEPVTEAVITVPAYFN 147
104 KVLVSYKGENKAFYPEEISSMVLTKLKETAEAFLGHPVTNAVITVPAYFN 153

148 DAQRQATKDAGRIAGLEVKRIINEPTAAALAYGLDKGT.GNRTIAVYDLG 196
154 DSQRQATKDAGVIAGLNVLRIINEPTAAAIAYGLDKGGQGERHVLIFDLG 203

197 GGTFDISIIEIDEVDGEKTFEVLATNGDTHLGGEDFDSRLINYLVEEFKK 246
204 GGTFDVSILTIDDG....IFEVKATAGDTHLGGEDFDNRLVSHFVEEFKR 249

247 DQGIDLRNDPLAMQRLKEAAEKAKIELSSAQQTDVNLPYITADATGPKHM 296
250 KHKKDISQNKRAVRRLRTACERAKRTLSSSTQANLEIDSLYEGI....DF 295

297 NIKVTRAKLESLVEDLVNRSIEPLKVALQDAGLSVSDIDDVILVGGQTRM 346
296 YTSITRARFEELCADLFRGTLEPVEKALRDAKMDKAKIHDIVLVGGSTRI 345

347 PMVQKKVAEFF.GKEPRKDVNPDEAVAIGAAVQGGVLTGD....VKDVLL 391
346 PKVQRLLQDYFNGRDLNKSINPDEAVAYGAAVQAAILMGDKSEKVQDLLL 395

392 LDVTPLSLGIETMGGVMTTLIAKNTTIPTKHSQVFSTAEDNQSAVTIHVL 441
396 LDVAPLSLGLETAGGVMTALIKRNSTIPTKQTQIFTTYSDNQPGVLIQVY 445

442 QGERKRAADNKSLGQFNLDGINPAPRGMPQIEVTFDIDADGILHVSAKDK 491
446 EGERAMTKDNNLLGRFDLTGIPPAPRGVPQIEVTFDIDANGILNVTATDK 495

492 NSGKEQKITIKASSG.LNEDEIQKMVRDAEANAEADRKFDELVQTRNQGD 540
496 STGKVNKITITNDKGRLSKEEIERMVLDAEKYKAEDEVQREKIAAKNALE 545

541 HLLHSTRKQVEEAG..DKLPADDKTAIESALTALETALKG...EDKAAIE 585
546 SYAFNMKSVVSDEGLKGKISESDKNKILDKCNELLSWLEVNQLAEKDEFD 595

586 AKMQELAQVSQKLMEIAQQQHAQQQTAGADASANNAKDDDVVDAEFEEVK 635
596 HKRKELEQMCNPIITKLYQGGCT....GPACGTGYVPGRPATGPTIEEVD 641
```

Figure 4-2: An alignment of the amino acid sequences of dnaK and hsp70hom. The sequences (Figure 1-1) of dnaK (top) and hsp70hom (bottom) were aligned using the program AMPS (Barton and Sternberg, 1987; Barton, 1990). Identities (|) and similarities (:) and gaps inserted to optimise the alignment (.) are indicated. The segment of dnaK crystallised by Zhu *et al.* (1996) is overlined.

protein (the template). These spatial restraints, which take the form of interatomic distances and dihedral angles, are applied to the target using an alignment of its amino acid sequence with that of the template. The degree of flexibility allowed in the spatial restraints has been derived empirically from a comparison of many pairs of homologous structures (Sali and Overington, 1994), and is expressed as a conditional probability density function (pdf). Molecular dynamics at 300 K and energy minimisation of the target polypeptide are carried out using these restraints, with the structure with the lowest energy being the one which best conforms to the restraints. Molecular dynamics and energy minimisation differ in the ways that they allow a polypeptide chain to explore the infinite number of different conformations These can be thought of as an energy landscape of peaks and troughs, with some conformations having a lower energy than others. Energy minimisation helps to move a protein to a local energy minimum, while molecular dynamics gives it additional, kinetic energy to overcome energy barriers and search for a global energy minimum. In the energy minimisation programs used, electrostatic forces cause hydrogen bonds to be formed.

Twenty independent models of the C-terminal region of hsp70hom were made, using the protocol summarised in Figure 4-3 [Chapter 2, Section G1]. Their backbones were overlaid and compared, so that models with unusual backbone configurations could be discarded. The remaining models were analysed using the programs Procheck (Lawkowski *et al.*, 1993) and Whatcheck (Vriend, 1990) to identify which model had the best packing, bond angles, bond lengths and planarity of cyclic side chains. This model was further refined by energy minimisation and molecular dynamics, using XPlor [G2]. Since X-ray crystallography does not detect protons, models based on crystallographic structures, as in this case, are proton free. Therefore, hydrogen atoms were added to the model using the program XPlor and positioned by energy minimisation (in a vacuum), with the other atoms in the model remaining fixed. Then a second round of energy minimisation was carried out, allowing the amino acid side chains to move without electrostatic forces

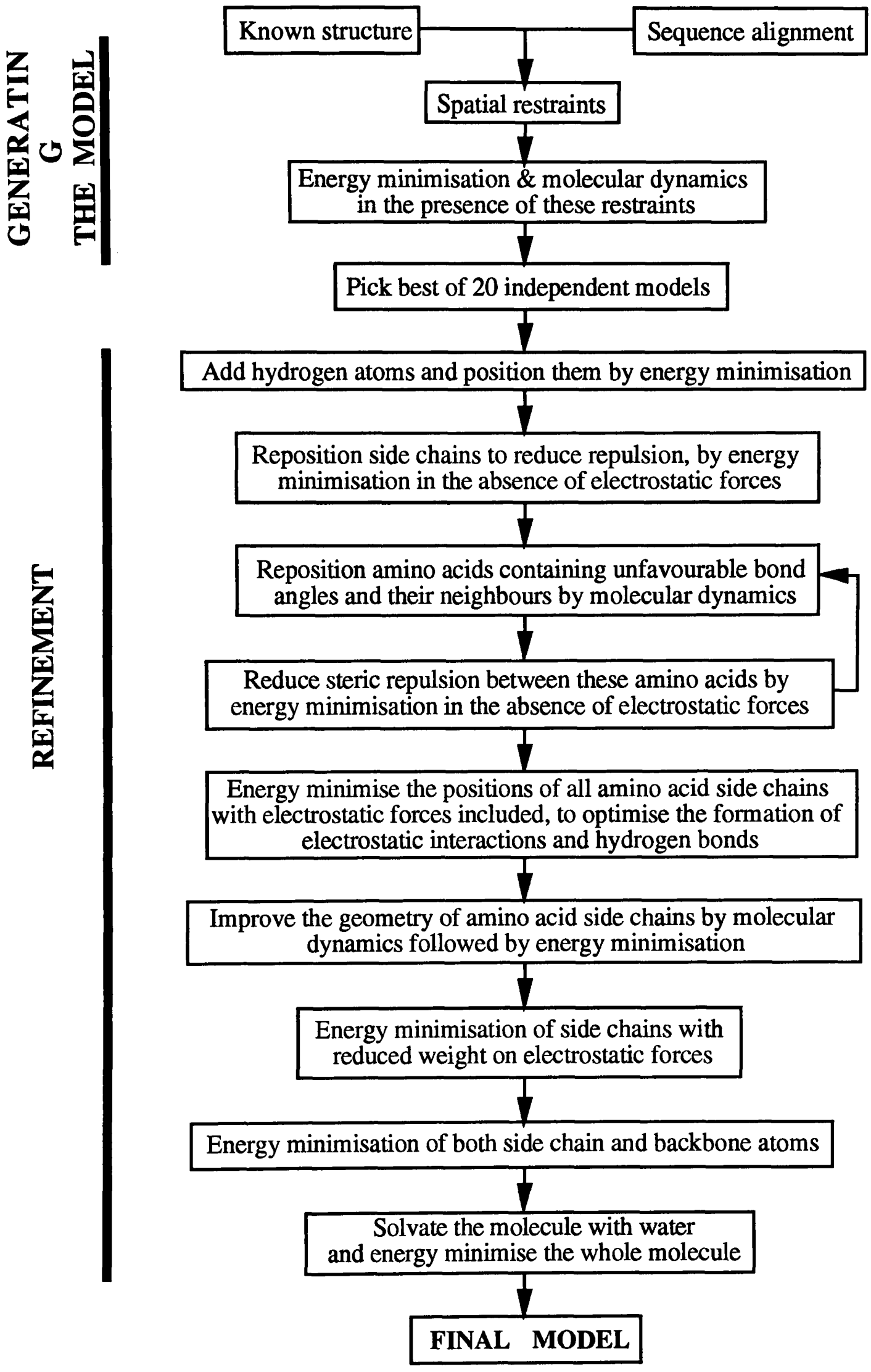

Figure 4-3: A flow diagram of the modelling of the C-terminal region of hsp70hom on the basis of the structure of the equivalent region of dnaK. The model was generated using Modeller (Sali and Blundell, 1993) and refined using Xplor.

being taken into account, so that the model attained a lower energy structure only by repulsion of side chain atoms that were too close together. Residues containing unfavourable bond angles were identified and they, together with residues either side of them (±1), were exposed to molecular dynamics for 20 picoseconds (ps), followed by energy minimisation. This step was repeated until all the bond angles were within 7.5° of their most favoured value. Next, the positions of the amino acid side chains were energy minimised with the main chain atoms fixed and electrostatic forces taken into account. This allowed hydrogen bonds to form, at the expense of poorer packing, bond angles and bond lengths. To improve these, another round of molecular dynamics was carried out. Then the amino acid side chain positions were optimised by energy minimisation as before, but with the contribution from electrostatic forces reduced to 10% of their previous values, to retain the hydrogen bonds and electrostatic interactions that have formed while allowing the side chains (though not the main chains) to move. This energy minimisation was repeated with all the atoms (main chain and side chain) free to move. A 10 Å layer of water was then added to the molecule and energy minimised using the Optimised Parameters for Liquid Simulation (OPLS) force field (Jorgensen and Tirado-Rives, 1988). Finally, the whole system was energy minimised with all atoms (protein and water) free to move. To offset the large electrostatic contribution from the water molecules, the electrostatic energy term was reduced further, to 1% of its original value.

The progress of the refinement was monitored after each step using Procheck and Whatcheck and by monitoring the energy terms calculated by XPlor.

The Model of the C-Terminal Region of Hsp70hom

The final model of the C-terminal region of hsp70hom is shown in Figure 4-4. The model is very similar to the structure of the same region of dnaK, as can be seen when the structures of their polypeptide backbones are overlaid (Figure 4-5) and the extent of the

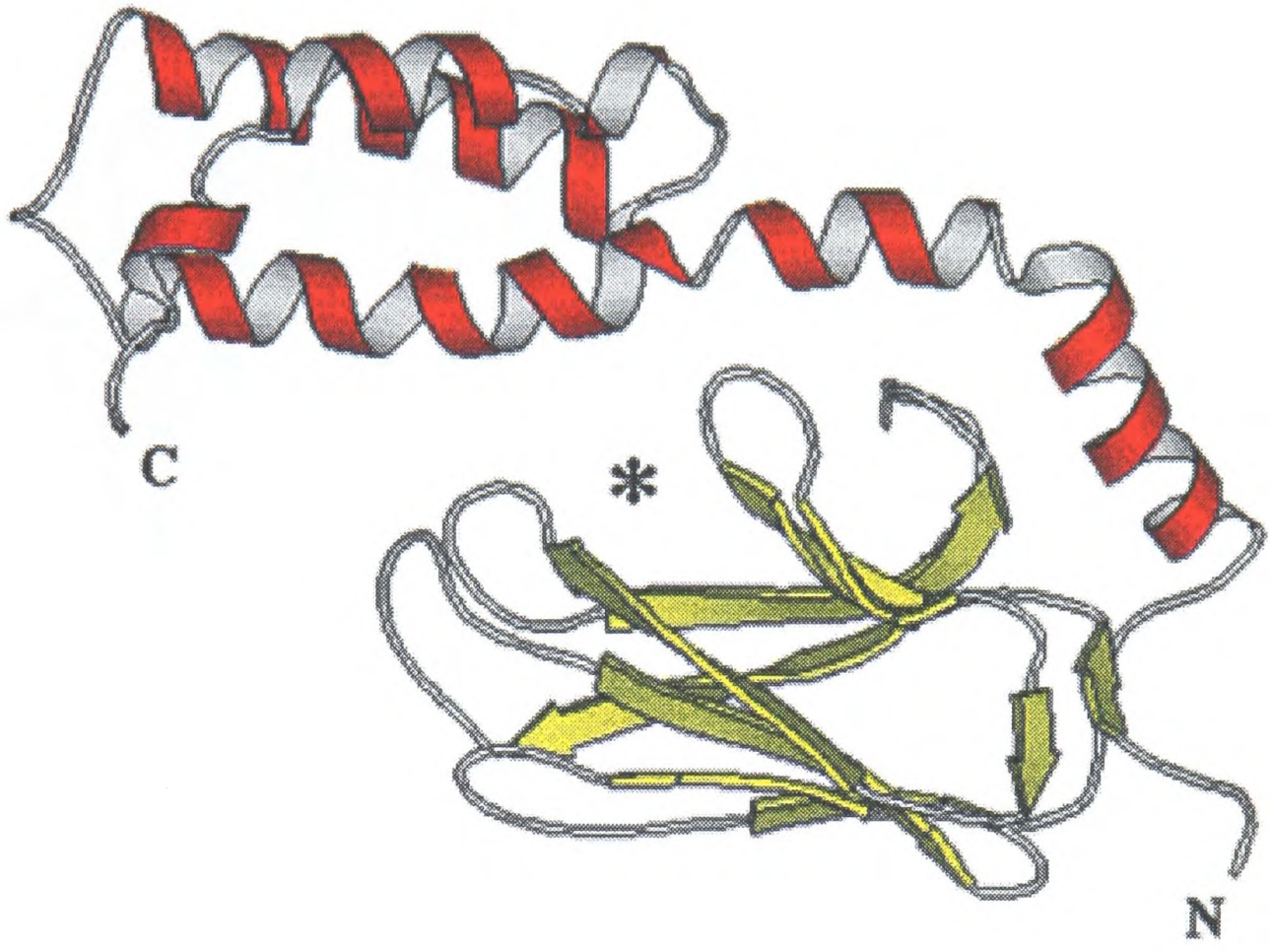

Figure 4-4: A model of the C-terminal region of hsp70hom. The model was generated by the program Modeller based on the structure of the C-terminal half of dnaK (Zhu *et al.,* 1996) and an alignment of its amino acid sequence with residues 393-616 of hsp70hom (Figure 4-2). The co-ordinates of the structure of the C-terminal half of dnaK were kindly provided by Dr. X. Zhu, and are now available from the Protein Data Bank (code 1DKX). The secondary structure of the model was assigned using DSSP (Kabsch and Sander, 1983) and displayed using Molscript (Kraulis, 1991). The peptide-binding site is indicated with an asterisk.

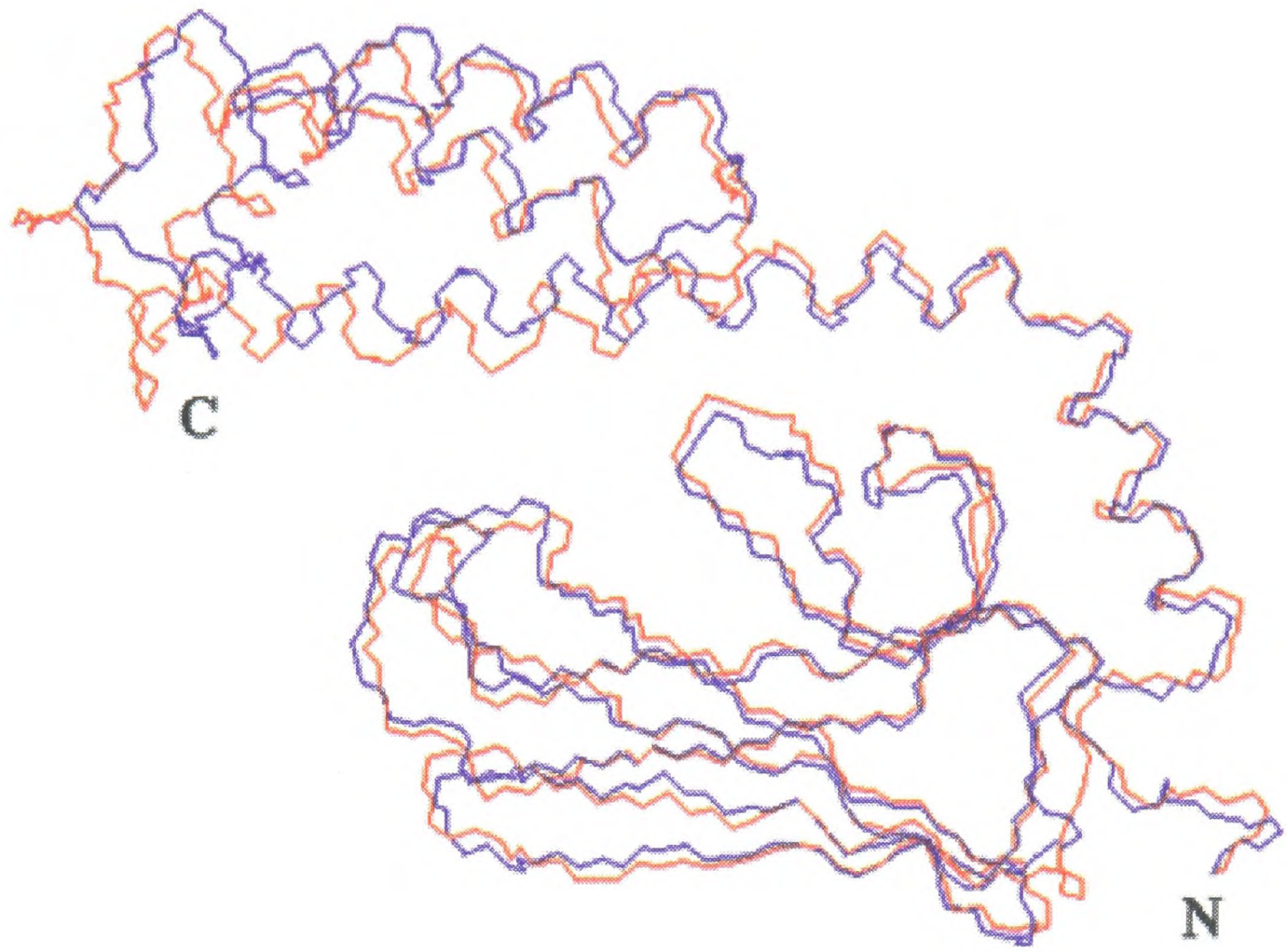

Figure 4-5: An overlay of the polypeptide backbones of the C-terminal regions of hsp70hom (red) and dnaK (blue). The Cα traces of the model of the C-terminal region of hsp70hom and the X-ray crystal structure of the equivalent region of dnaK (Zhu *et al.*, 1996) are displayed using Molmol (Koradi *et al.*, 1996).

individual secondary structural elements is compared (Figure 4-6). The peptide-binding ß-subdomains overlay each other closely, while the α-subdomains are displaced slightly, reflecting flexibility at the junction between the two subdomains. The most significant difference in the modelled secondary structure of the C-terminal region of hsp70hom is the breakage of the long α-helix (αB) by Glu 536 and Lys 537 (Figures 4-4 and 4-6). The model has excellent main chain bond lengths and angles: in the Ramachandran plot (Figure 4-7), 85% of residues are in 'most favoured' configurations and no residues are in the generously allowed' or 'disallowed' regions of the plot.

The surface potential of the C-terminal region of hsp70hom is generally negatively charged (red) (Figure 4-8a), in agreement with its isoelectric point, which at 4.8, is relatively acidic. Looking at the 'front' of the domain (with the hinge between the α- and ß-subdomains on the right), there are three charges near the hole that is the peptide binding site, two negative charges (Glu 545 in the α-subdomain and Glu 477 in the ß-subdomain) and one positive charge (Lys 495 in the ß-subdomain). The 'back' of the domain contains more charges around the peptide-binding site. Lys 541, Glu 545, Glu 584 and Arg 471 form a patch of mixed charges above the peptide-binding site, and Glu 406, Arg 460 and Asp 462 form a charged patch beneath it, in the ß-subdomain. The surface charge of the model of the C-terminal region of hsp70hom is similar to that of dnaK (Figure 4-8b), which has an isoelectric point of 4.65. However, the distribution of charges around the peptide binding site is different, with only one of these charges being conserved between the two molecules (Glu 545 of hsp70hom and Asp 540 of dnaK are equivalent). Two positive charges (Lys 548 and Arg 467) appear at the front of the domain of dnaK, to the left of the hole, while from the back, three negative charges (Glu 402, Asp 540 and Glu 530) are clustered above the hole and Asp 460 and Lys 495 are found at some distance beneath it.

The peptide-binding site of hsp70hom is clearly uncharged, and is predominantly hydrophobic (data not shown), as in dnaK (Zhu *et al.,* 1996). The Leu 4 pocket is highly

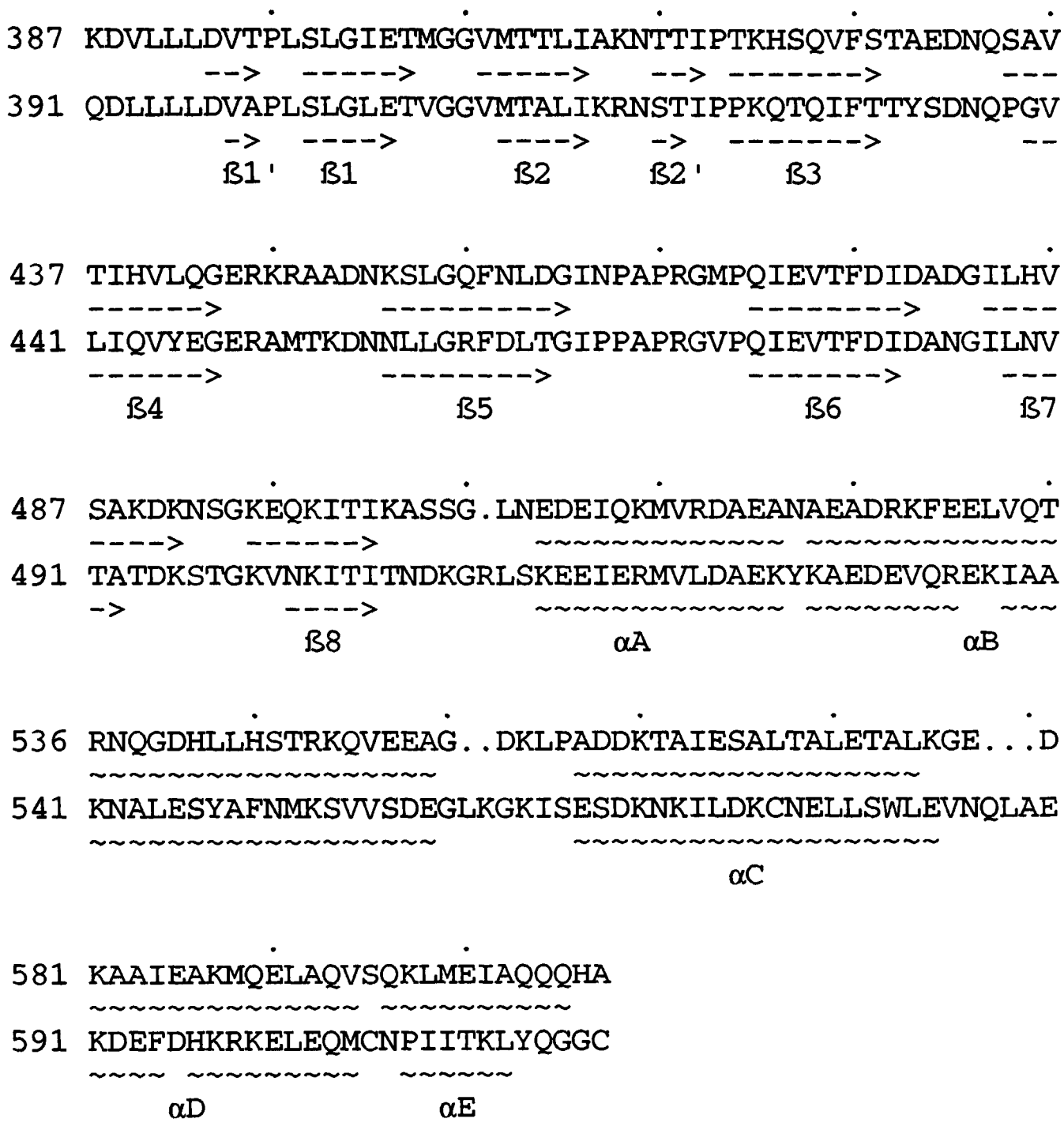

Figure 4-6: A comparison of the secondary structure of the C-terminal regions of dnaK and hsp70hom. The amino acid sequences of the C-terminal regions of dnaK (387-607; top) and hsp70hom (391-617; bottom) (Figure 4-2) are displayed with the secondary structure of C-terminal regions of dnaK (Zhu *et al.*, 1996) and hsp70hom (modelled), comprising 8 ß-strands and 5 α-helices, shown underneath. Alpha helices (~~~) and beta sheets (-->) are indicated.

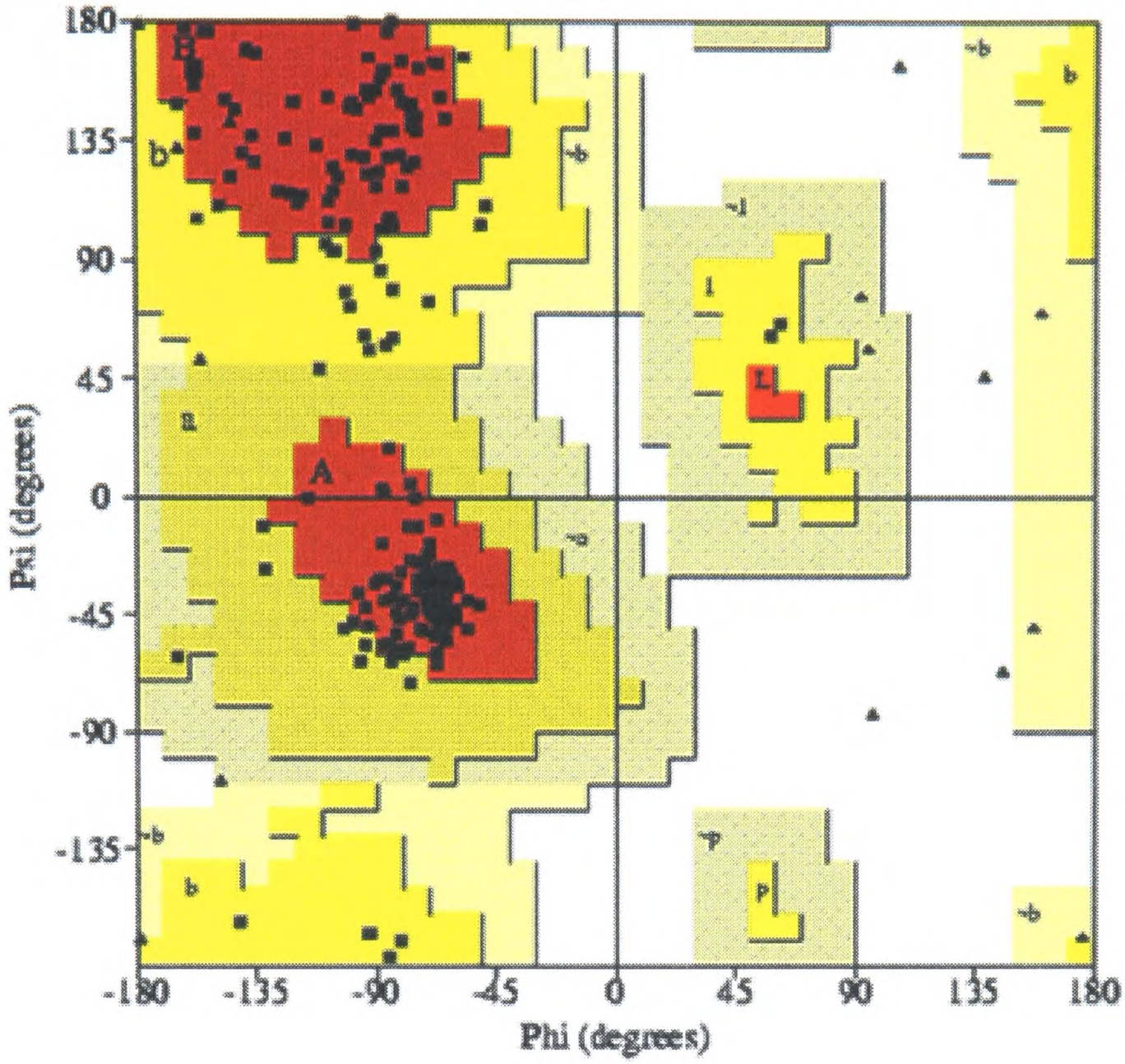

Figure 4-7: A Ramachandran plot of the main chain bond angles in the model of hsp70hom. A Ramachandran plot is a plot of the dihedral angle phi (the angle of rotation at the bond between the nitrogen and α-carbon atoms of the main chain) against psi (the angle of the bond between the α-carbon and carbonyl carbon atoms) for each residue in a protein. 85.5% of the residues in the model of hsp70hom are in most favoured' regions of the plot (A, B, L). 14.5% are in 'additional allowed' regions (a, b, l, p) and no residues are in the 'generously allowed' (~a, ~b, ~l, ~p) or 'disallowed' regions. Glycine, proline and the N- and C-terminal residues were excluded from the statistics. Glycine residues are plotted as triangles and all other residues, except proline, are plotted as squares. The plot and statistics were generated by the program Procheck (Lawkowski *et al.,* 1993).

(a) hsp70hom

Front

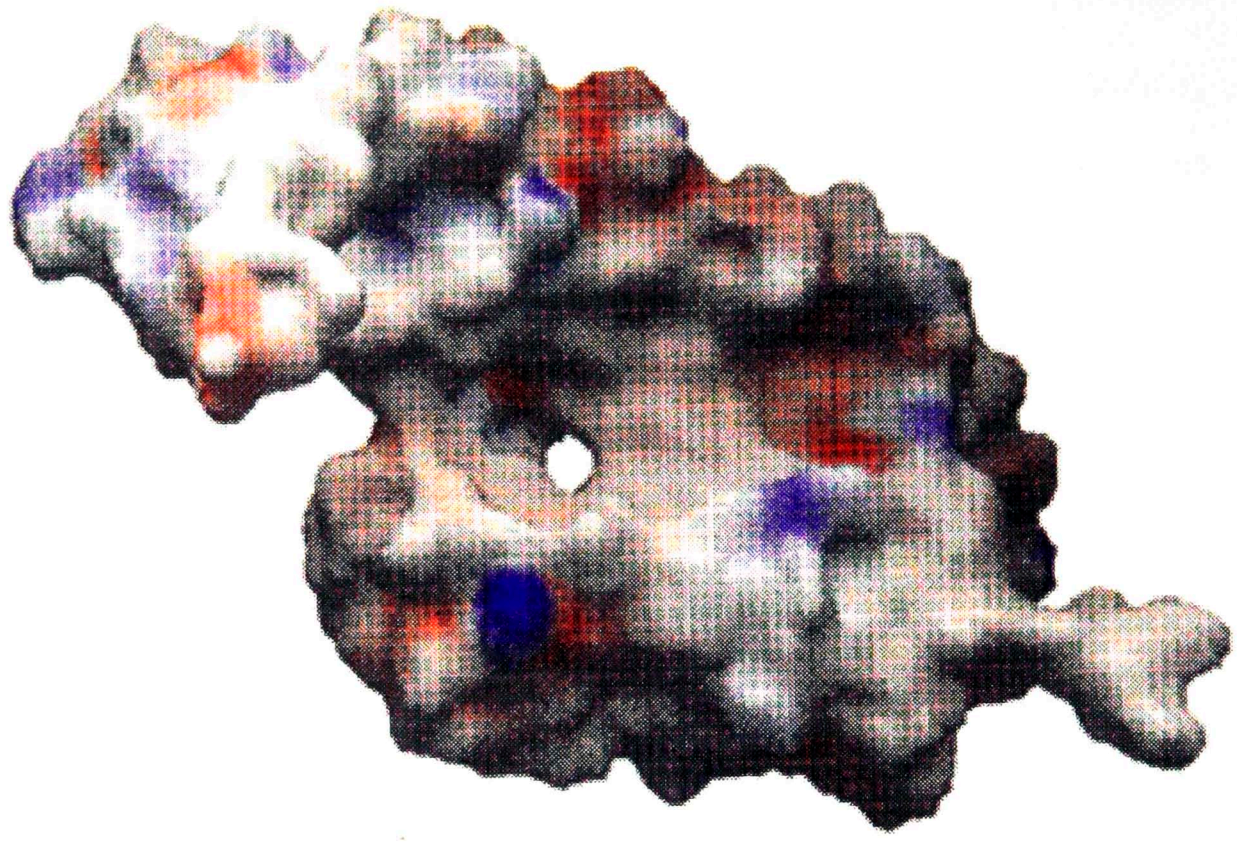

Back

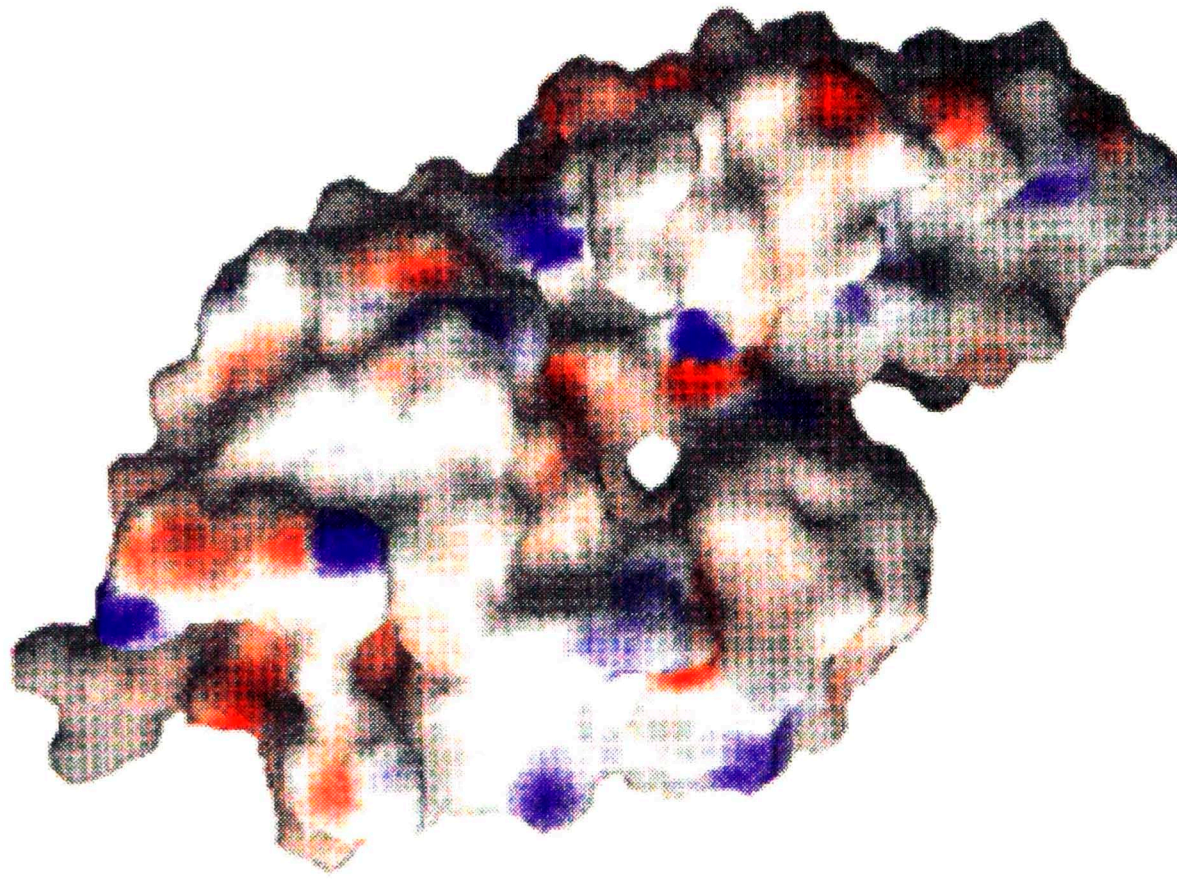

(b) dnaK

Front

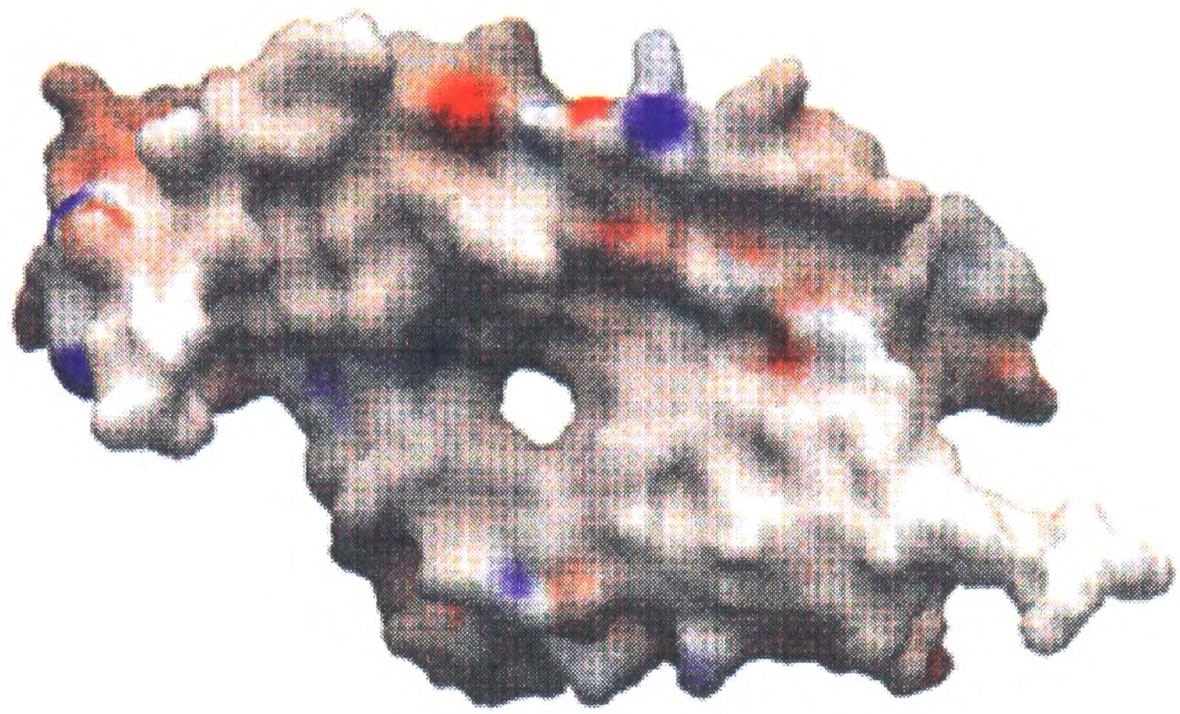

Back

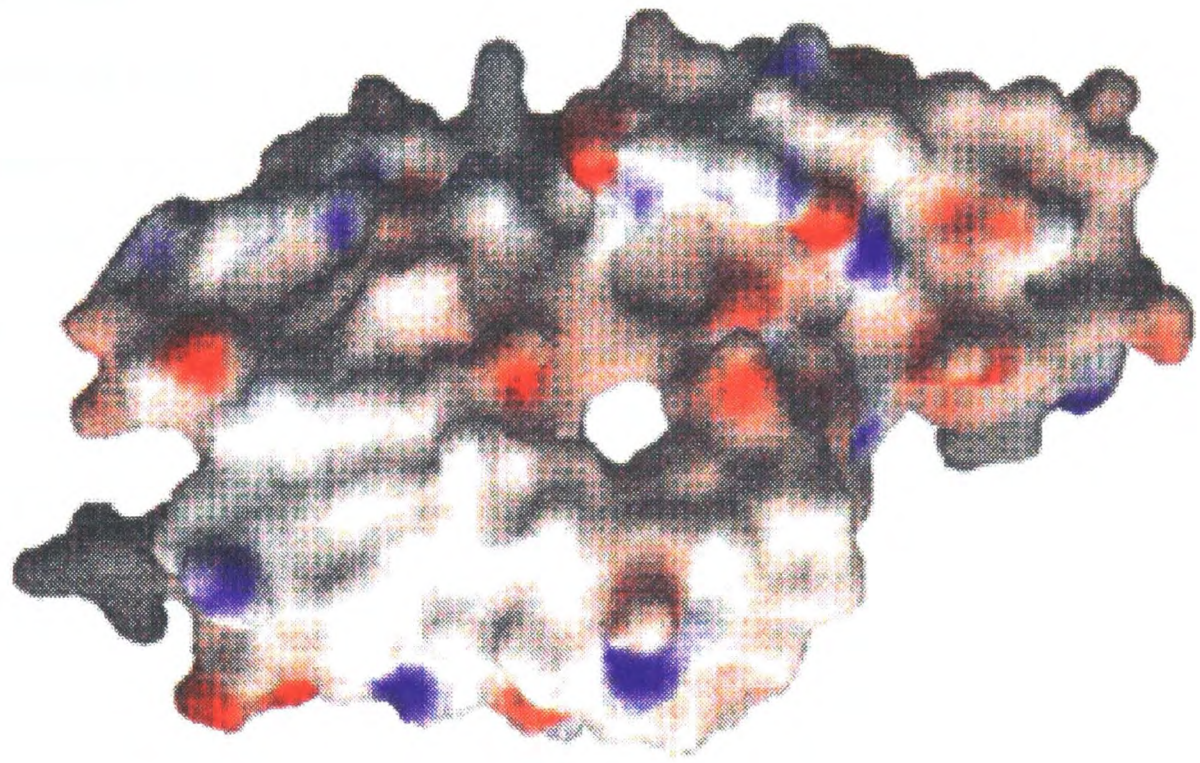

Figure 4-8: The surface charges of the C-terminal regions of (a) hsp70hom and (b) dnaK. The figures were generated from the model of the C-terminal region of hsp70hom and its structure in dnaK using Grasp (Nicholls *et al.*, 1991). The surface is coloured according to electrostatic potential, ranging from dark blue (most positive, 23.1 kT) to deep red (most negative, -24.36 kT). White is uncharged (0 kT).

conserved, especially in its hydrophobic character (see below). Although the surface charges of the two molecules are neither located near the peptide-binding site nor conserved, they may nevertheless have functional significance, in binding to substrates or cofactors. Indeed, the significance of negative surface charges in peptide-binding by hsp70s has been suggested by several studies which have shown that hsp70s prefer to bind peptides containing basic amino acids (Takenaka *et al.*, 1995; DeCrouy-Chanel *et al.*, 1996) (reviewed in Chapter 5).

Modelling of Peptide

The binding of peptides to the C-terminal region of hsp70hom was investigated by molecular modelling [G2]. The first peptide modelled in a complex with the C-terminal region of hsp70hom was NRLLLTG, which was co-crystallised with the equivalent region of dnaK (Zhu *et al.,* 1996) and is known to bind to several hsp70s including hsc70 (Gragerov and Gottesman, 1994). The amino acid sequence of the peptide-binding ß-subdomain of hsp70hom differs from that of hsc70 by two conservative substitutions (Asp 462 Glu, Thr 464 Ser) and one non-conservative substitution (Val 500 Ala) (Figure 3-1). In dnaK, none of these positions is involved in peptide binding, so it seems likely that these changes will not differentiate the peptide-binding specificities of hsc70 and hsp70hom.

The peptide was placed in the model of the peptide-binding cleft of the C-terminal portion of hsp70hom using molecular graphics. Its configuration was energy minimised with a purely repulsive force field, which pushed the peptide away from the protein and into the hole. This procedure was repeated several times, with the peptide rotated in the cleft to a different position each time. The peptide configuration for which the overall energy of the complex (determined using the purely repulsive force field) was lowest was chosen. Its energy was within 5% of the total energy of the protein alone.

To allow interactions to form between hsp70hom and the peptide, simulated annealing and energy minimisation were performed upon the complex. In general, all the atoms of the peptide were given freedom of movement, while only the atoms constituting the peptide-binding site of hsp70hom were allowed to move. Flexibility was introduced into the binding site for two reasons. Firstly, the binding site may have real flexibility and, secondly, as the binding site was modelled in the absence of peptide, it is likely to need readjusting to accommodate the peptide successfully.

To introduce electrostatic interactions and hydrogen bonds into the complex, energy minimisation was carried out in a full force field (Charmm22) with the side chains of all residues within 5 Å of the peptide allowed to move. A further energy minimisation was carried out with the backbone atoms of all residues within 4 Å also allowed to move. Next, the peptide and peptide-binding site were subjected to a simulated annealing protocol. This involved promoting movement in the peptide, the backbone atoms of residues of hsp70hom within 5 Å of the peptide and all atoms of residues within 4 Å, with molecular dynamics at a high temperature (1000 K) for 15 ps. The temperature was then reduced slowly, over 7.5 ps to a low temperature (100 K), allowing stable interactions between the peptide and peptide-binding site to form. Finally, the conformation of these atoms was energy minimised in a full force field. The modelling was carried out in the absence of water molecules. The presence of water would have been unlikely to change the structure of the complex, because the peptide-binding site is hydrophobic and does not contain water in the structure of the dnaK-peptide complex.

Twenty independent models were produced as described above and analysed using Procheck, WhatCheck and molecular graphics. Models with very high energies or whose backbones did not follow the general consensus were rejected. The remaining models were averaged to generate a mean structure which was energy minimised again. This energy minimisation was carried out with the electrostatic energy term for peptide-protein and peptide-peptide interactions set at 1, to favour the formation of electrostatic interactions and

hydrogen bonds between the two components of the complex, while its value for protein-protein interactions was 1% of this (i.e. at the same level as was used to generate the final model), to avoid distorting the structure of the protein.

The model of the peptide NRLLLTG bound to hsp70hom (Figure 4-9) is similar to the structure of this peptide bound to dnaK (Figure 1-2) (Zhu *et al.*, 1996). The peptide backbone is predicted to have a similar conformation when bound to hsp70hom to that adopted when associated with dnaK, except that Asn 1 of the peptide bends round the side of the ß-subdomain of the former (Figure 4-10a). The side chains of the three central leucines superimpose very well in the two conformations, whereas the side chains of Asn 1 and Arg 2 have quite different configurations. Nevertheless, the peptide is contacted by many of the same amino acids in the modelled complex with hsp70hom (Figure 4-11) as in the structure determined for dnaK (Figure 4-1). The peptide is bound by four hydrogen bonds between main chain atoms: Leu 3-Ala 408, Leu 4-Tyr 433, Leu 5-Glu 406 and Leu 5-Gln 443. Furthermore, there are four side chain-side chain hydrogen bonds, one between Asn 1 and Glu 428, two between Arg 2 and Thr 407 and one between Thr 6 and Tyr 433. In addition, eleven hydrophobic amino acids are in Van der Waals contact with residues 3 and 6 of the peptide. Leu 3 is contacted by Ala 408, Thr 431 and Arg 471; Leu 4 is contacted by Leu 405, Phe 430, Tyr 433, Val 440 and Ile 442; Leu 5 is contacted by Glu 406, Ala 408 and Tyr 433; and Thr 6 is contacted by Tyr 433 and Leu 441. In total, six amino acids of the heptameric peptide interact with a total of 15 amino acids of hsp70hom.

Many of the interactions between hsp70hom and the peptide NRLLLTG (Figure 4-11) are identical to those seen in the X-ray structure of dnaK, which forms a total of 7 hydrogen bonds and 16 hydrophobic interactions with this peptide (Figure 4-1). In dnaK, the peptide is contacted by residues from the first two ß-strands and the intervening loop (ß1, ß2, $L_{1,2}$), as well as ß3, ß4 and $L_{3,4}$. In the model of hsp70hom, the same regions are involved in peptide binding, with the exception of ß2, which in dnaK interacts with Arg

(a)

(b)

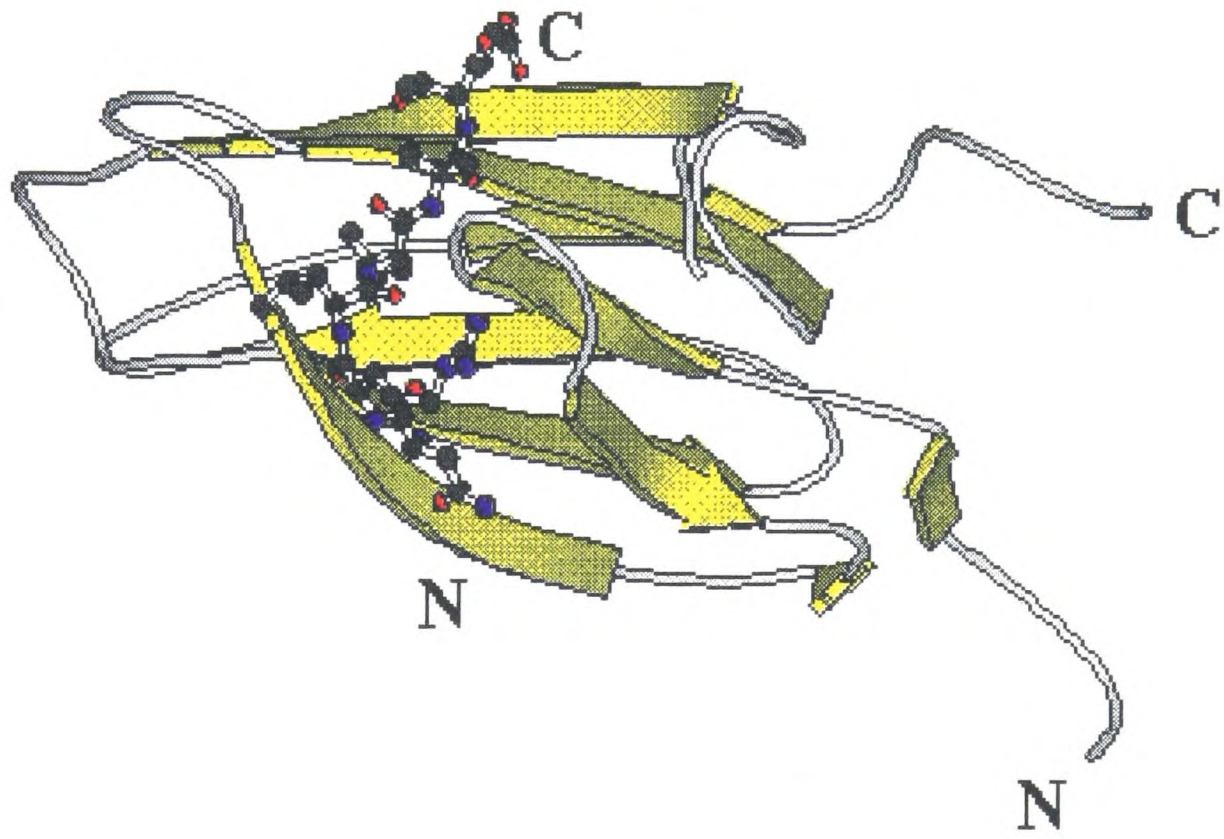

Figure 4-9: A model of a complex between the peptide NRLLLTG and (a) the whole C-terminal region of hsp70hom or (b) the ß-subdomain alone. The ß-subdomain is rotated through -60° about the y axis compared to the whole domain. The secondary structure of the model of hsp70hom was assigned using DSSP (Kabsch and Sander, 1983) and displayed using Molscript (Kraulis, 1991). The peptide, in the same conformation as binds to dnaK (Zhu *et al.,* 1996), was placed in the peptide binding site using Molmol (Koradi *et al.,* 1996). It was positioned by energy minimisation using repulsive forces alone, and then molecular dynamics was performed on it together with the amino acids constituting the binding site. Finally, hydrogen bonds and electrostatic interactions were introduced by energy minimisation.

(a) Peptide main chains

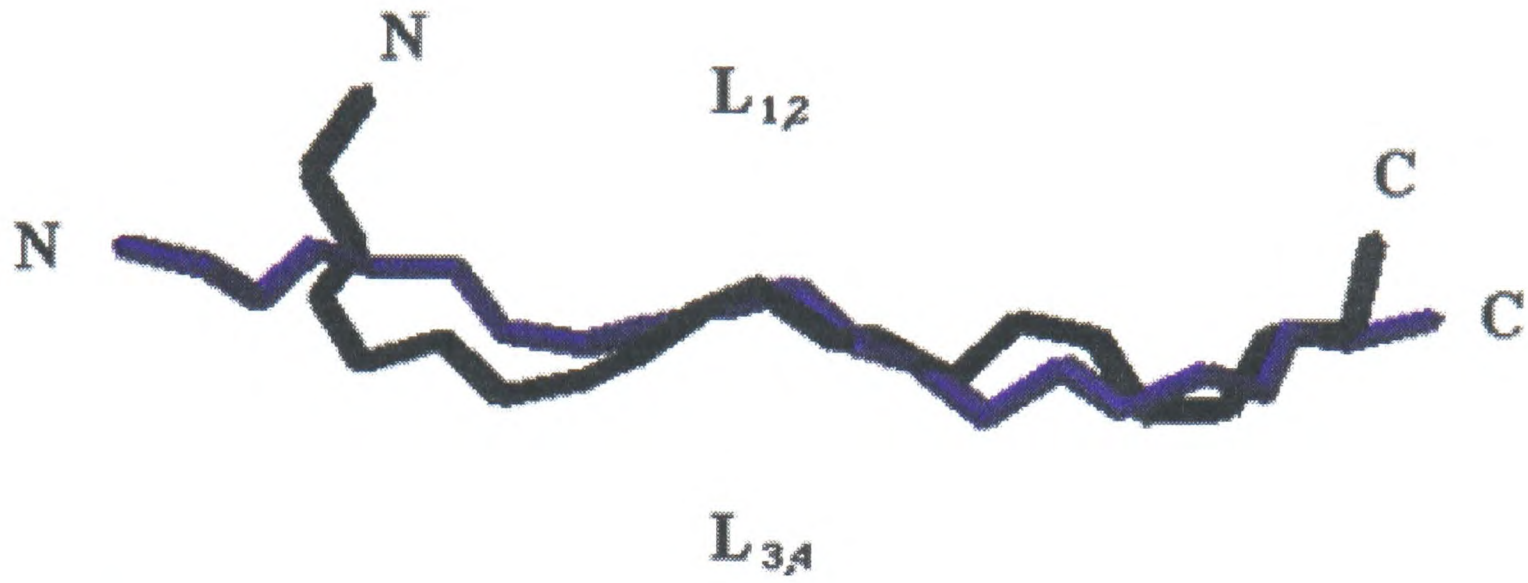

(b) Peptide side chains

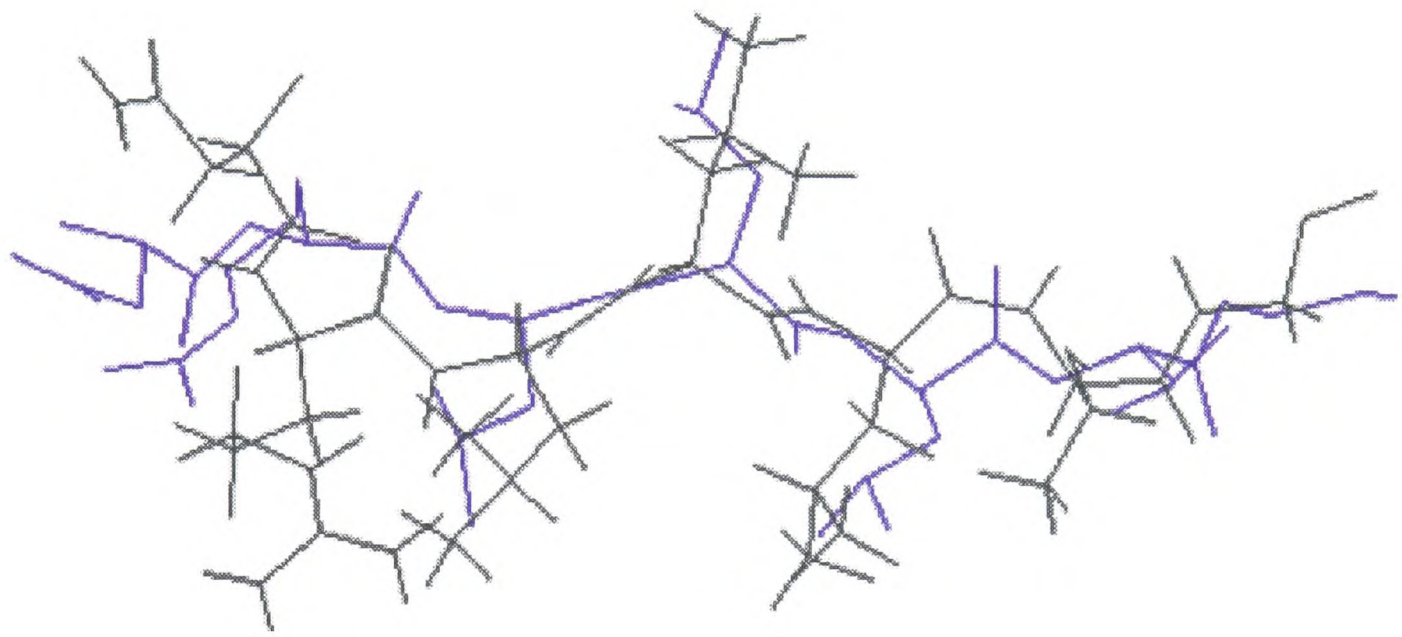

Figure 4-10: A model of NRLLLTG bound to hsp70hom (black) overlayed on the structure of the same peptide bound to dnaK (blue), displayed (a) as backbone only and (b) with side chains. The main chains of the two peptide conformations were overlayed and displayed using Molmol (Koradi *et al.*, 1996).

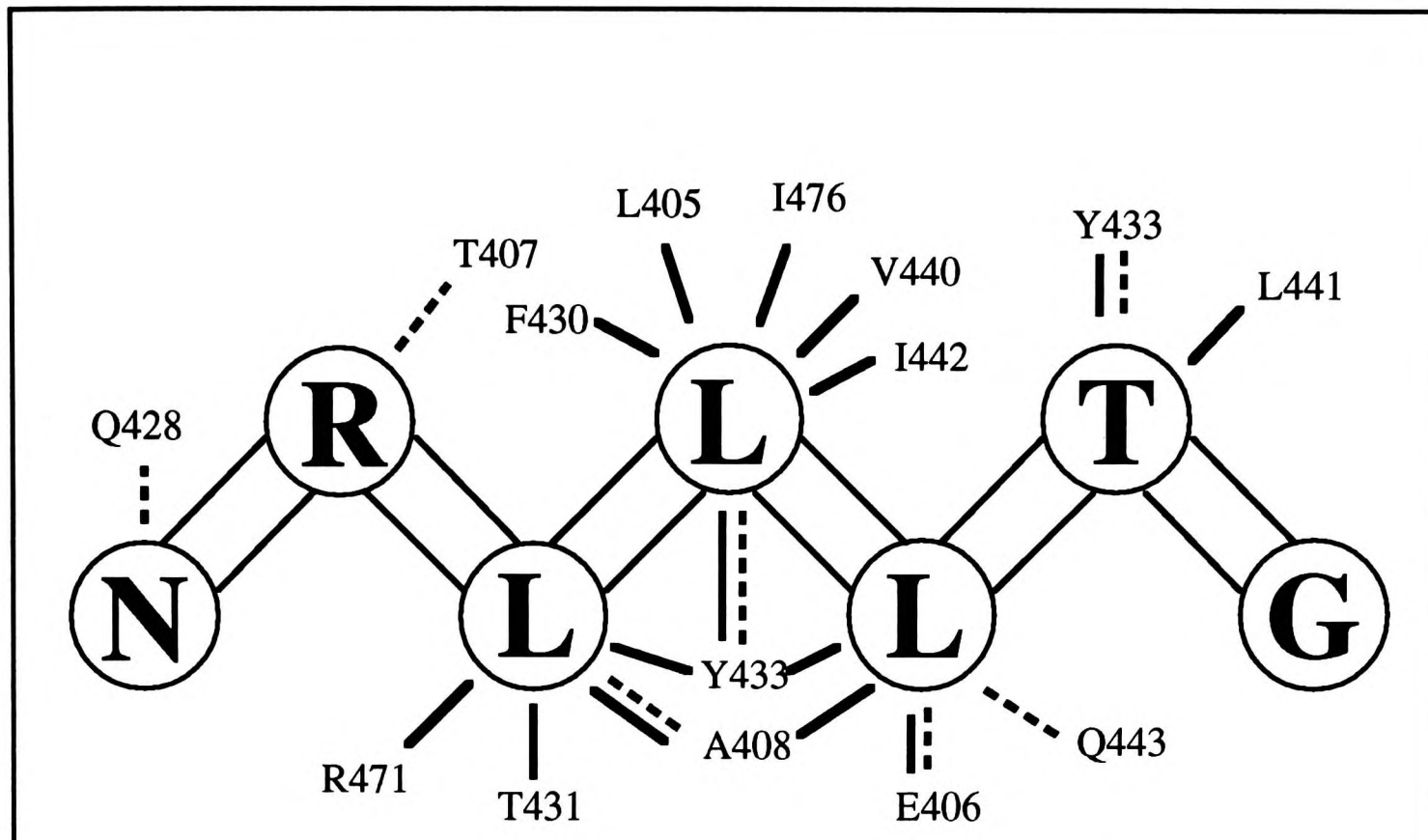

Figure 4-11: The predicted contacts between hsp70hom and peptide NRLLLTG. The results of the modelling predict that hsp70hom binds to the peptide predominantly through hydrogen bonds and hydrophobic interactions, in a very similar manner to dnaK (Figure 4-1). Tyr 433, which contacts Leu 3, Leu 4, Leu 5 and Thr 6, is marked on the figure twice, for the sake of clarity. The interactions were analysed using Naomi (Brocklehurst and Perham, 1993).

2 of the peptide. However, in the hsp70hom model, two amino acids from the second half of the ß-subdomain, Arg 471 ($L_{5,6}$) and Ile 476 (ß6), form hydrophobic contacts with Leu 3 and Leu 4 of the peptide. Ile 476 is buried and forms part of the Leu 4 pocket, whereas Arg 471 is a surface residue and contacts Leu 3.

Two amino acids in the ß-subdomain of dnaK, Met 404 and Ala 429, form a bridge over the peptide. In hsp70hom, their equivalents, Ala 408 and Tyr 429 form the same peptide contacts, despite their lack of conservation. In the hsp70hom model, Tyr 433 also contacts Leu 4 and Thr 6. It is able to contact four peptide residues because its large, flat side chain runs along the peptide-binding site, parallel with the peptide backbone. Therefore, it prevents Gln 437 (the equivalent of Gln 433 in dnaK) from interacting with Leu 4 and Thr 6 of the peptide.

Another important feature of the peptide-binding site of dnaK is the pocket in which Leu 4 of NRLLLTG is buried. This is largely conserved in hsp70hom, where it is formed by Leu 405 (Ile 401 in dnaK), Phe 430 (Phe 426), Ile 442 (Ile 438) and Val 440 (Val 436). In addition, Tyr 433 and Ile 476 of hsp70hom and Thr 403 of dnaK contact Leu 4.

Asn 1 of the peptide is predicted to be hydrogen bonded by Gln 428 of the hsp70hom model, causing the N-terminus of the peptide to loop around the domain. As Asn 1 of the peptide does not contact dnaK at all, even though glutamine at this position is conserved, it seems unlikely that this interaction is real. It may be introduced during the modelling because it decreases the energy of the complex, and therefore would not necessarily be seen in an X-ray or NMR structure. Arg 2 of the peptide is only bound by one amino acid of hsp70hom (Thr 407), through a hydrogen bond. In the complex with dnaK, another hydrogen bond and four hydrophobic interactions are seen in addition to this interaction.

Leu 3 of the peptide makes the same interactions with the model of hsp70hom (Ala 408, Tyr 433, Thr 431) as with dnaK (Ser 427, Met 404, Ala 429) and forms an additional interaction with Arg 471. Leu 5 forms hydrophobic contacts with equivalent amino acids

in the hsp70hom model (Ala 408 and Tyr 433) and in dnaK (Met 404 and Ala 429). Additionally, each protein forms a hydrogen bond with the main chain of Leu 5, through Gln 433 of hsp70hom or Thr 437 of dnaK. Also, Glu 406 of hsp70hom contacts this residue hydrophobically and through a hydrogen bond.

The amino acids that interact with Thr 6 of the peptide are different in the two complexes. In the model of hsp70hom, it is contacted by Tyr 433 and Leu 441, whereas in dnaK, it interacts with Gln 433 and Ala 435. The hsp70hom model does not interact with Gly 7 of the peptide. In the complex with dnaK, Gly 7 is weakly hydrogen bonded to the side chain of Thr 437, but in hsp70hom the corresponding residue is Leu 441 and, therefore, the equivalent interaction cannot form.

In summary, the peptide NRLLLTG is predicted to bind to hsp70hom through the same sorts of interactions as to dnaK (Zhu *et al.,* 1996). In the model of the complex, the peptide forms a total of 15 hydrophobic interactions with 11 amino acids of hsp70hom, compared to the 17 hydrophobic contacts it forms with 12 amino acids of dnaK. The interactions with the three central leucines are conserved between the two hsp70s, even when the amino acid side chains at a given position are different. In particular, the Leu 4 pocket is highly conserved. The peptide is also bound by seven hydrogen bonds in each complex. These are created by seven side chains of hsp70hom or five of dnaK. Neither dnaK nor the model of hsp70hom interacts with the peptide electrostatically. The energy of this conformation of NRLLLTG bound to hsp70hom (i.e. the energy of the peptide and all its interactions with the protein) is -421 kcal/mol (Figure 4-12).

A Model of Peptide FYQLALT complexed with hsp70hom

Modelling was carried out with a second peptide, that is known to bind to hsp70hom (see Chapter 5). The model of the complex between FYQLALT and the C-terminal domain of hsp70hom was created using the same protocol as described above for NRLLLTG. The

	Hsp70hom complexed with		
Orientation:	NRLLLTG forward	FYQLALT forward	FYQLALT reverse
<u>Energy (kcal/mol)</u>			
Bond length	10.6	9.3	7.5
Bond angle	32.2	37.7	26.7
Dihedral angle	33.4	38.7	35.6
Improper angles	0.52	1.50	0.79
Van der Waals	-59.3	-11.9	-22.7
Electrostatic	-439	-236	-326
TOTAL	-421	-160	-278
<u>No. of interactions:</u>			
Hydrogen bonds	8	7	6
Hydrophobic contacts	11	11	12

Figure 4-12: The energies of three models of peptides bound to the C-terminal region of hsp70hom. The energies of peptide-peptide and protein-peptide interactions are shown.

conformation of the peptide FYQLALT was created using the backbone of NRLLLTG and changing the side chains. Since the structure of only one hsp70-peptide complex is known, it is not clear whether peptides can bind in either orientation, or only in one. DnaK does not interact with the N- and C-termini of the peptide NRLLLTG, presumably because its substrates are usually longer polypeptides, so it will not determine peptide orientation in this way. However, the formation of hydrogen bonds with the main chain of the peptide may favour one orientation over the other. Therefore, to determine which way round the peptide may prefer to bind in the cleft, both orientations were modelled.

(a) The Forward Orientation

The model shows that FYQLALT binds to hsp70hom in a very different manner to NRLLLTG, even though it is in the same orientation (Figure 4-13a). The peptide is shifted in the groove by the equivalent of between 1 or 2 amino acids towards its C-terminus (to the left in Figure 4-14). This may be because the hydrophobic side chains of Phe 1 and Tyr 2 occupy the groove, whereas the equivalent side chains of NRLLLTG predominantly point away from the peptide-binding site. Even taking this into account, the backbone orientation is not equivalent to that of NRLLLTG.

In the forward orientation, FYQLALT is predicted to bind to the model of hsp70hom through 7 hydrogen bonds and 10 hydrophobic interactions, involving a total of 11 amino acids (Figure 4-15). Many of the amino acids that contact the 'forward' orientation of FYQLALT also interact with NRLLLTG, such as Thr 407, Ala 408, Phe 430, Thr 431, Tyr 433, although they often play a different role. For example, Thr 431 contacts one amino acid of NRLLLTG hydrophobically (Leu 3), whereas it contacts three amino acids of FYQLALT (Tyr 2, Gln 3 and Leu 4), through hydrophobic contacts and/or hydrogen bonds.

(a) forward

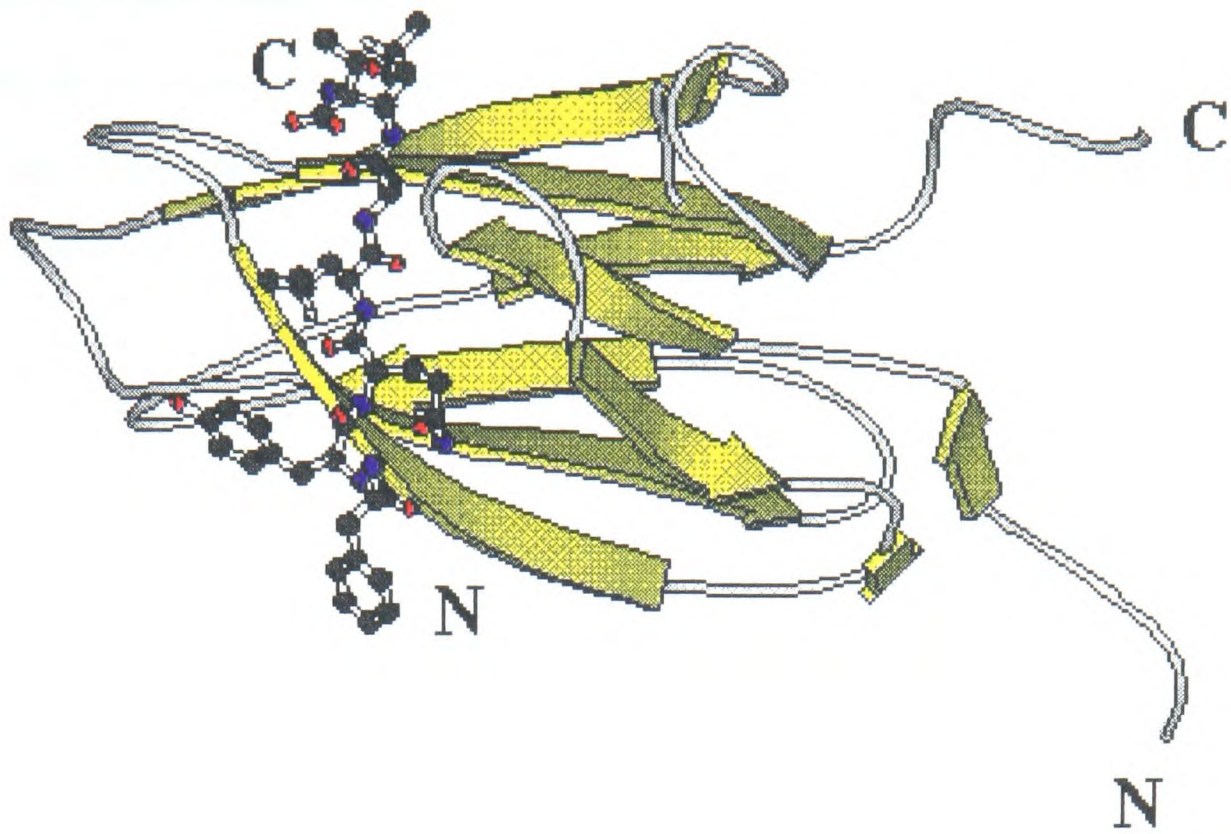

(b) reverse

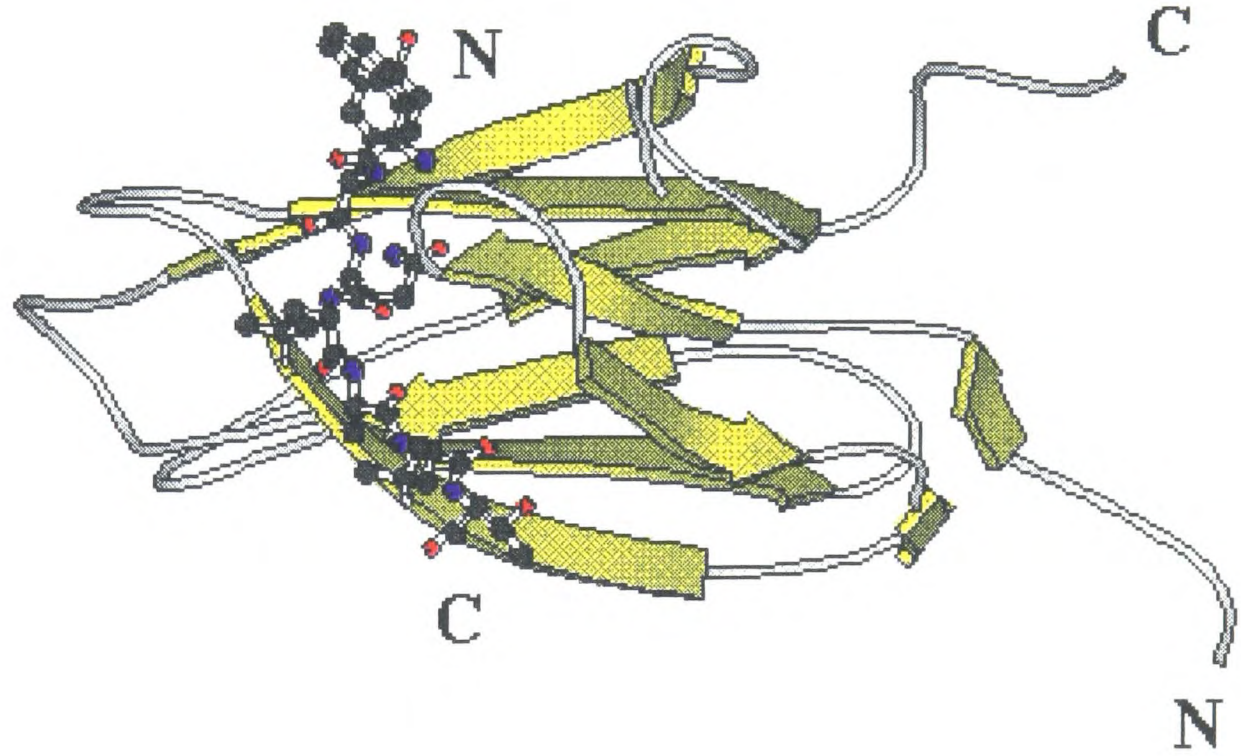

Figure 4-13: Models of the peptide FYQLALT bound to hsp70hom in (a) the forward and (b) the reverse orientation. The secondary structure of the model of hsp70hom was assigned using DSSP (Kabsch and Sander, 1983) and displayed using Molscript (Kraulis, 1991). The peptide was created using the backbone conformation of NRLLLTG bound to dnaK (Zhu *et al.,* 1996), by replacing the side chains using Molmol (Koradi *et al.,* 1996). The model of the complex was then generated as described in Figure 4-9.

The arrangement of the amino acid side chains is sufficiently different that it is not possible to equate amino acid positions in FYQLALT with positions in NRLLLTG. Binding to the central Leu 4 pocket is lost, because the Ala 5 is positioned over this pocket but is too small to fill it. Most of the interactions involve amino acids 1-3 of the peptide. Phe 1 points out of the end of the peptide-binding cleft whereas Tyr 2 and Gln 3 run over the surface of the domain. Leu 4 and Thr 7 point upwards, towards the α-domain, and Leu 6 points down over the side of the domain. This peptide, in this orientation, contains an intrapeptide hydrogen bond, between the backbone of Phe 1 and the side chain of Gln 3. The complex of hsp70hom with this conformation of FYQLALT is less energetically favourable than its complex with NRLLLTG, as the total energy of the peptide and all its interactions with the protein is -160 kcal/mol, less than half the equivalent energy for the hsp70hom-NRLLLTG complex (-421 kcal/mol) (Figure 4-12).

(b) The Reverse Orientation

When modelled in the reverse orientation, FYQLALT occupies much the same position in the binding cleft of hsp70hom as it does in the forward orientation, i.e. shifted lengthways in the cleft relative to NRLLLTG, in this case towards its N-terminus (Figure 4-14). Thirteen amino acids of hsp70hom anchor the peptide through 6 hydrogen bonds and 12 hydrophobic interactions involving every position of the peptide except Leu 6 (Figure 4-16). The Leu 4 pocket contains Gln 3, which it binds through Leu 405, Phe 430 and Val 440. The side chain of glutamine is not large enough to contact Ile 442 and Ile 476 in the same way as Leu 4 of NRLLLTG. Like NRLLLTG, the two terminal residues of FYQLALT in the reverse orientation wrap themselves around strands ß1 and ß2. This is especially true for the C-terminal threonine.

The total energy of the interactions between the reverse orientation of FYQLALT and hsp70hom (i.e. the energy of the peptide and all its interactions with the protein) is -278

(a)

(b)

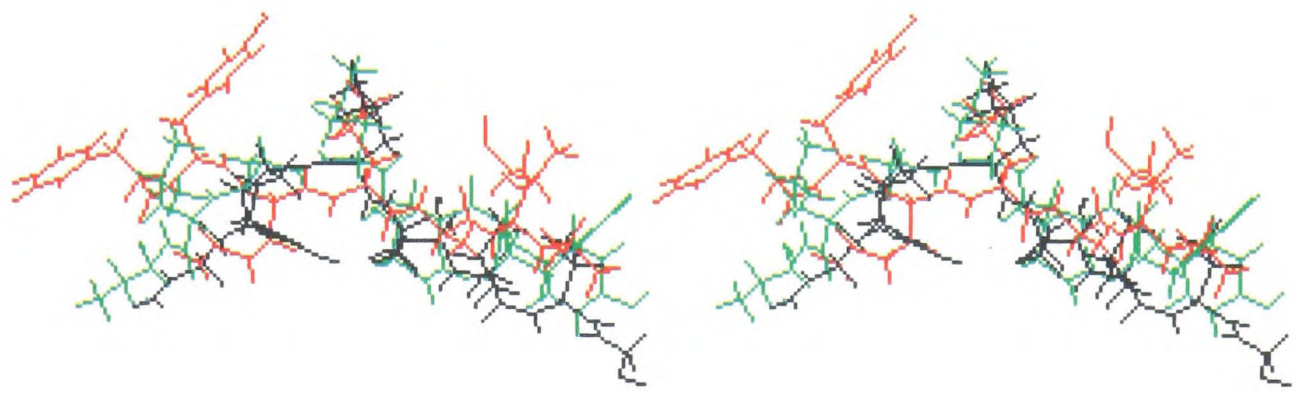

Figure 4-14: The predicted conformations of peptides NRLLLTG (black) and FYQLALT in the same (red) and opposite (blue) orientations when bound to hsp70hom: (a) the main chain atoms and (b) all atoms. The figure was created using Molmol (Koradi *et al.*, 1996).

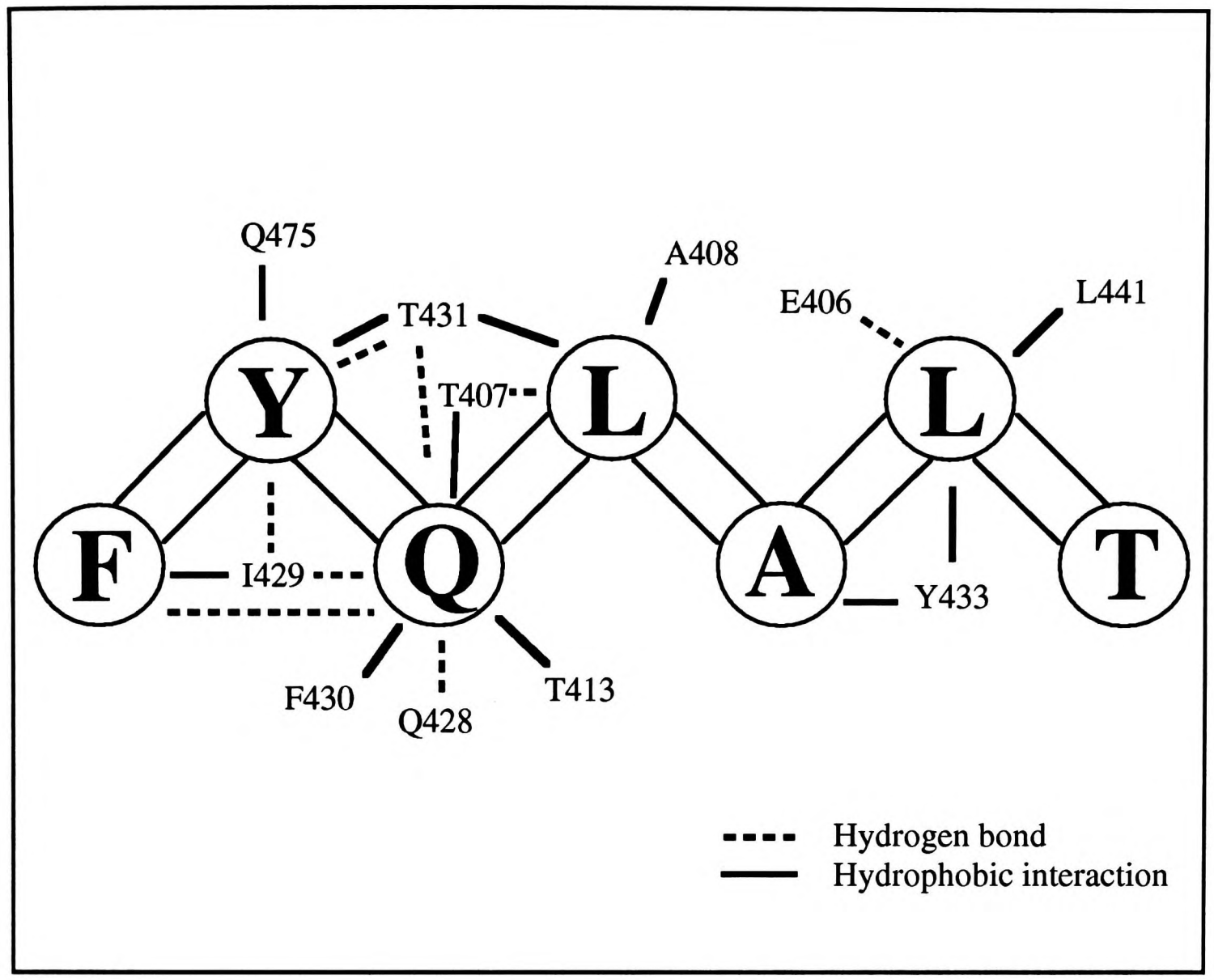

Figure 4-15: The predicted contacts between hsp70hom and peptide FYQLALT in the same orientation as NRLLLTG binds to dnaK. The interactions were analysed using Naomi (Brocklehurst and Perham, 1993).

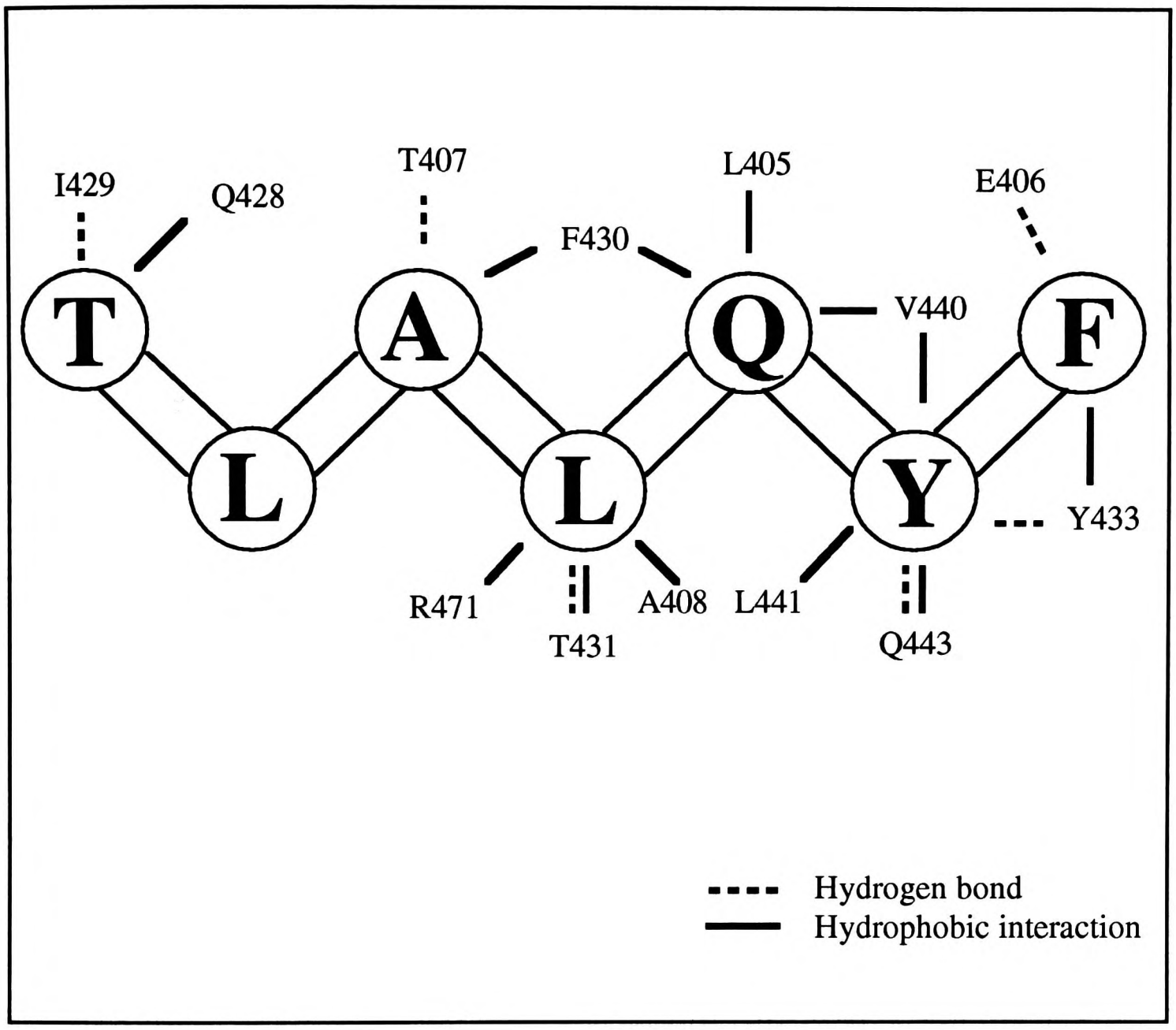

Figure 4-16: The predicted contacts between hsp70hom and peptide FYQLALT in the reverse orientation. The interactions were analysed using Naomi (Brocklehurst and Perham, 1993).

kcal/mol, two thirds of the energy of the complex between NRLLLTG and hsp70hom (Figure 4-12). This orientation of the peptide is, therefore, likely to be more favoured than the forward orientation.

Summary of the Modelling of Bound Peptides

Three peptides were modelled binding to the C-terminal domain of hsp70hom. The complex of hsp70hom with NRLLLTG appears to be the most reliable model. It has the lowest energy, and shows the clearest relation to the structure of the dnaK-peptide complex determined by X-ray crystallography. It was not possible to determine which orientation of the FYQLALT peptide was correct, but as modelled here, the reverse orientation has the lower energy. Even with a relatively constricted peptide-binding groove, the modelling of bound peptides has proved challenging. The most significant problem is that the groove does not have defined ends and, therefore, the position of the peptide within it is uncertain. While many of the same amino acids of hsp70hom are involved in the three complexes modelled here, they often have very different roles. Furthermore, the paucity of contacts with the terminal amino and carboxyl groups of the peptides prevents assumptions being made about the orientation of a peptide in the cleft. However, these properties are advantageous to a molecular chaperone, which primarily has to deal with long polypeptide substrates without accessible termini, and with many different amino acid sequences. The peptide-binding site of hsp70s is likely to be very versatile and this causes modellers problems. Nevertheless, the modelled hsp70hom-peptide complexes reinforce the idea that the α-subdomain of the hsp70 family is not involved in peptide binding (Zhu *et al.,* 1996), although it does seem to be required for binding to larger unfolded substrates (Freeman *et al.*, 1995; Hu and Wang, 1996) (see Chapter 5).

Amino Acid Sequence Conservation in the Hsp70 Family

The amino acid sequences of the C-terminal regions of 166 members of the hsp70 family were aligned using AMPS (Barton and Sternberg, 1987; Barton, 1990). All the

proteins had more than 40% identity with the C-terminal region of hsp70hom. The alignment was displayed in a graphic form using Sequence Logo (Schneider and Stephens, 1990) (Figure 4-17). The hsp70 family is clearly more conserved in the ß-subdomain (amino acids 391-505) than in the α-subdomain (amino acids 505-615). Surprisingly, the amino acid sequence is no more conserved in elements of secondary structure than in the loops between them, suggesting that most of these loops are functionally important, either in interacting with peptide or polypeptide substrates and cofactors, or in the conformational changes that couple ATP binding to peptide release. The pattern of conservation is displayed on the model of the three-dimensional structure of hsp70hom in Figure 4-18. Again, the α-subdomain is clearly less conserved than the ß-subdomain. Only a small number of amino acids in the α-subdomain have an information content of greater than 3 bits (blue). Lys 563 and Tyr 613 both face out from the end of the α-subdomain, towards the ~25 amino acids at the very C-terminus of the hsp70 family, whose structure is not known. This region, which is relatively unconserved apart from an EEVD motif at the very terminus of eukaryotic cytoplasmic hsp70s, is important in coupling the activity of the C-terminal peptide-binding region with that of the N-terminal ATPase domain (Freeman *et al.*, 1995). Tyr 613 and Lys 563 (which has the opposite charge to the EEVD motif) may be involved in this function. Leu 601 points into the centre of the α-subdomain, whereas Glu 545 forms a hydrogen bond with Arg 471 of the ß-subdomain. The side chains of Asn 542 of hsp70hom and Arg 2 of NRLLLTG are predicted to lie very close in the model. However, the peptide is further from the side chain of the equivalent amino acid of dnaK (Asn 537) in the crystal structure. Nevertheless, the location of these conserved residues suggests that the α-subdomain may interact with the peptide. Lys 541 of hsp70hom lies above Asn 542, pointing out of the α-subdomain, parallel to the peptide. The other most conserved amino acids in the α-subdomain are Leu 544, which forms part of the hydrophobic core of the α-subdomain, and Asp 531 of αB, which may interact with the loop between α-helices C and D.

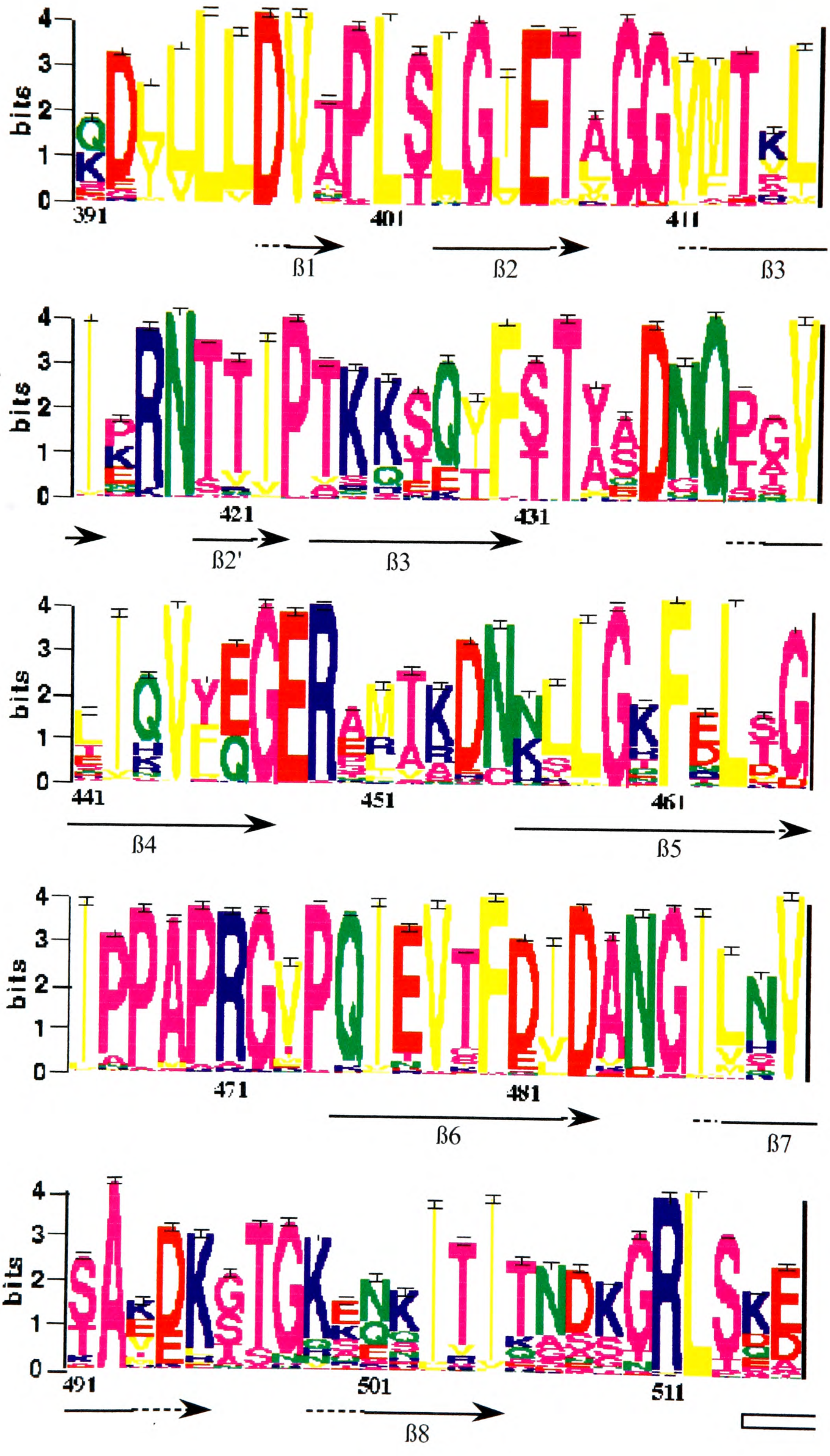
bits
391
401
411
ß1
ß2
ß3
421
431
ß2'
ß3
441
451
461
ß4
ß5
471
481
ß6
ß7
491
501
511
ß8

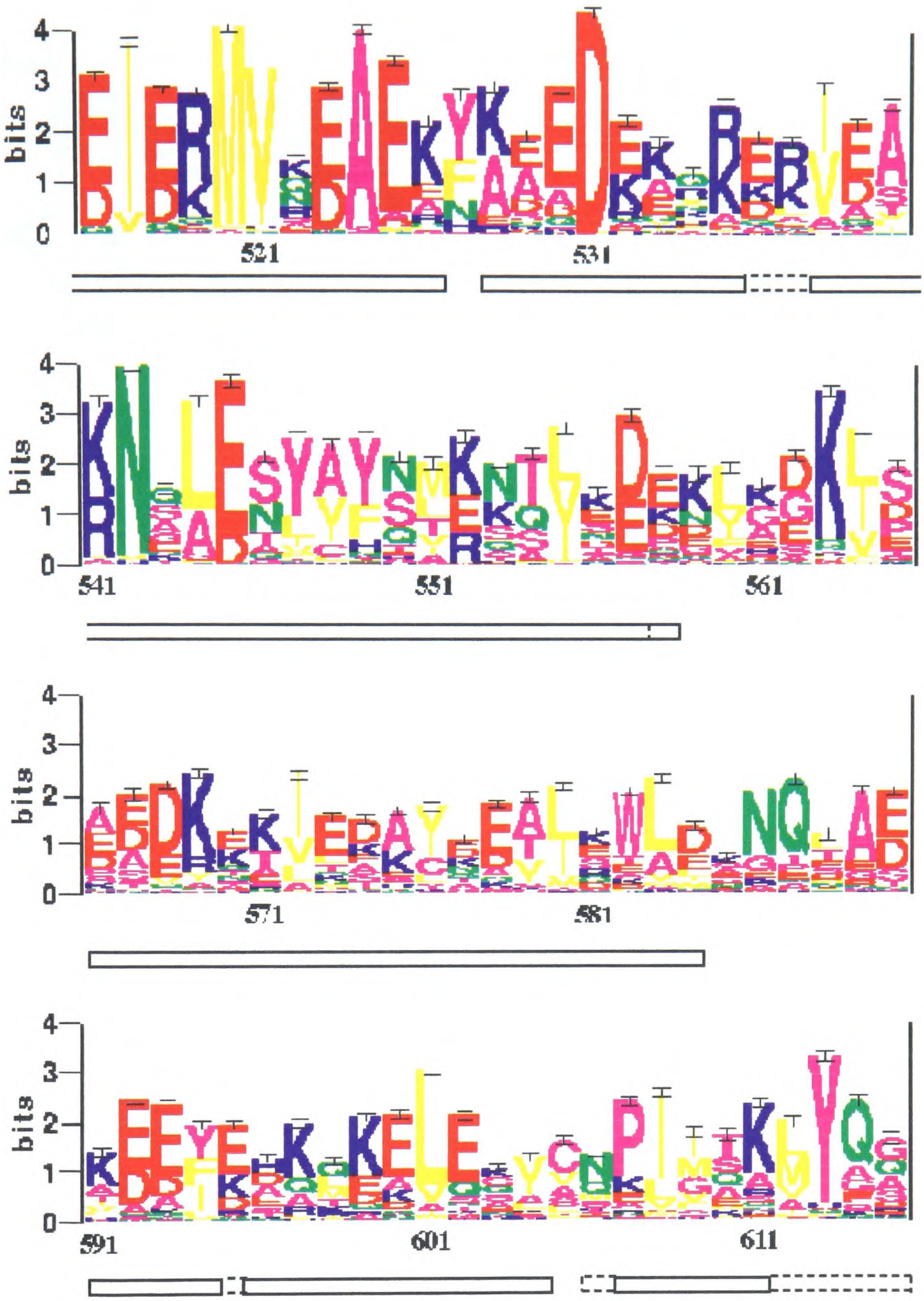

Figure 4-17: A sequence logo of the C-terminal region of the hsp70 family. The amino acid sequences of 166 different hsp70s were aligned using Multalign (Barton and Sternberg, 1987; Barton, 1990) and analysed using WebLogo (Schneider and Stephens, 1990). Sequence logos are a graphical method for displaying the patterns in a set of aligned sequences. The characters representing the amino acids present at a position in the alignment are stacked on top of each other, with the height of each letter proportional to the frequency of the corresponding amino acid. The height of the entire stack represents the information content (conservation) at that position. The non-polar amino acids (F, L, I, V and M) are shown in yellow, the positively charged amino acids (K, R and H) in blue, the negatively-charged amino acids (D, E) in red, the other polar residues (N and Q) in green and the ambivalent amino acids (S, T, C, A, G, P, Y and W) in pink. The numbering is according to the sequence of hsp70hom. The secondary structure of the model of hsp70hom is shown underneath, with additional secondary structure determined for dnaK shown in dotted lines (see Figure 4-6). ß-strands are shown as arrows and α-helices as boxes.

(a) Front

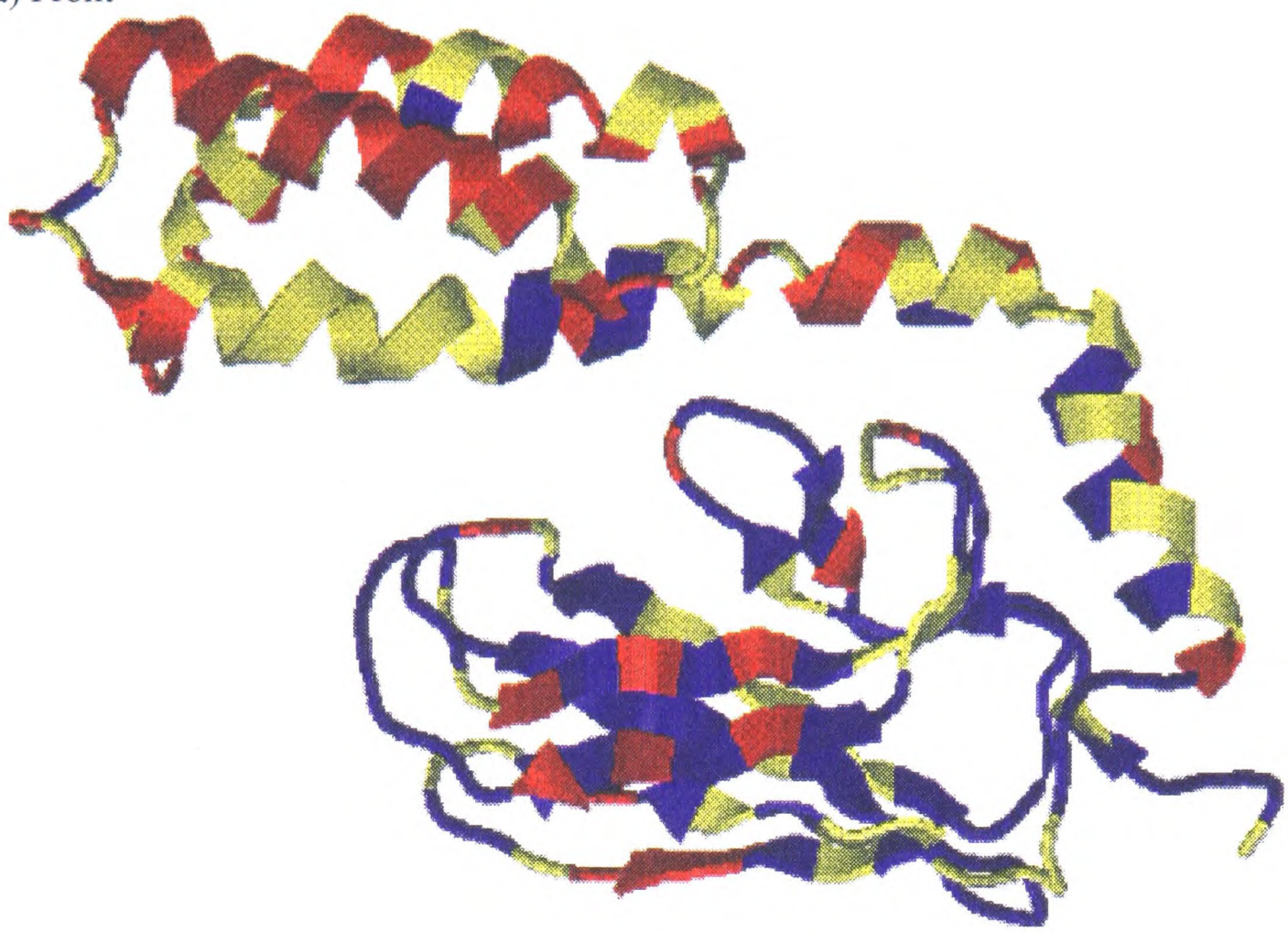

(b) Back

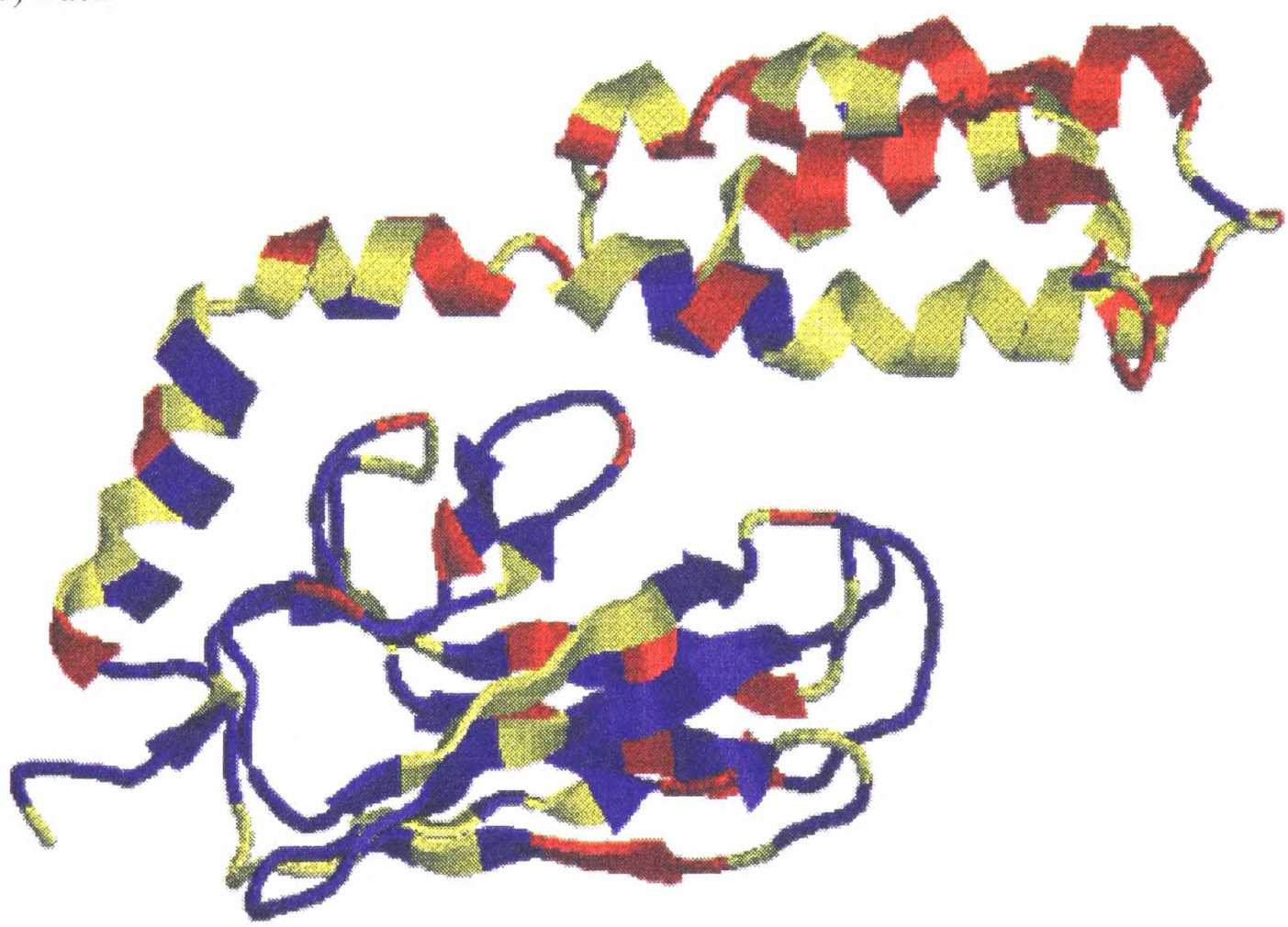

Figure 4-18: Amino acid sequence conservation in the C-terminal region of the hsp70 family. The information content (conservation) at each position was calculated from a sequence logo representing an alignment of 166 different hsp70s (Figure 4-17) and displayed on the model of the C-terminal region of hsp70hom using Molscript (Kraulis, 1991). Positions with information content of 0-2 bits are coloured red, 2-3 bits are coloured yellow and more than 3 bits are coloured blue.

The rest of the conserved amino acids in the α-subdomain are in contact with the ß-subdomain, near the hinge between the two. Val 521, Ala 524, Glu 525, Met 530 and Asp 531 contact $L_{4,5}$ and may be important in transferring conformational change between the peptide-binding site and the α-subdomain. Ser 513 and Glu 516 are interesting because they point out from the hinge, at the back of the C-terminal region. They may interact with cofactors that regulate the peptide-binding activity of hsp70s, such as dnaJ and its homologues (Cyr *et al.*, 1994; Zeigelhoffer *et al.*, 1996).

The ß-subdomain is predominantly very highly conserved between members of the hsp70 family. However, as suggested by the alignment of hsp70hom and dnaK, this conservation is not particularly concentrated in the peptide-binding site or in internal amino acids. On the one hand, many amino acids on the surface of the ß-subdomain are conserved, while on the other, several amino acids in the peptide-binding site are not. Positions 408 and 433 (hsp70hom numbering), which form a bridge over the peptide-binding site, are variable. In the alignment of 166 different hsp70s, position 408 is variable, containing 49% alanine, 22% leucine, 13% valine and only 6% methionine. Position 433 is essentially either tyrosine (59% of hsp70s) or alanine (37% of hsp70s). These amino acids are very different (alanine has a simple methyl side chain while tyrosine contains a bulky phenol ring), yet the modelling of the complex of NRLLLTG with a peptide-binding site containing Ala 408 and Tyr 433 (that of hsp70hom) suggests that it is remarkably similar to the structure of the same peptide complexed with the C-terminal region of dnaK (Zhu *et al.*, 1996), which contains Met and Ala at the equivalent positions.

Amino Acid Conservation in the Human Cytoplasmic Hsp70s

The model of hsp70hom may be helpful in understanding why there are at least five different hsp70s in the human cytoplasm. There are two possible explanations. Firstly, duplicated hsp70 genes may allow the proteins the encode to be differentially expressed. For instance, hsp70 is heat-inducible, hsc70 is constitutively expressed in all tissues and hsp70A2 is only expressed in certain tissues. In this model, the cytoplasmic human hsp70s may have the same functions, which are not affected by differences in their amino acid sequences. Alternatively, the human cytoplasmic hsp70s may have different functions, due to the differences in their amino acid sequences. These may affect peptide-binding specificity or interactions with cofactors. It may be possible to distinguish between the two models by looking at the patterns of amino acid sequence conservation between the different hsp70s.

The differences in the C-terminal regions of hsp70hom and the other cytoplasmic human hsp70s are displayed using the model of hsp70hom (Figure 4-19). Hsp70hom is most similar to hsp70, followed by hsp70A2, hsc70 and hsp70B' (Figure 1-1). Hsp70hom does not differ from any of the cytoplasmic hsp70s in its peptide-binding site, and while there are some differences in the ß-subdomain, most non-conserved amino acids are seen in the α-subdomain. Thus the distribution of amino acid conservation in the human cytoplasmic hsp70s is very similar to that seen for the whole hsp70 family (Figure 6-18). However, each hsp70 has its own pattern of amino acid conservation. Hsp70hom differs from all the hsp70s at certain positions, most noticeably at the C-terminal ends of α-helices αB, αC and αD. However, none of the hsp70s differ from hsp70hom in an easily distinguished patch of unique amino acids. A possible exception is hsp70A2, which has less conserved amino acids along the solvent exposed face of α-helices αA and αB. It may be that the different cytoplasmic hsp70s interact with distinct, but related, cofactors. These could bind to the same site on hsp70hom and be distinguished through only one or two amino acid changes.

(a) hsp70

(b) hsp70A2

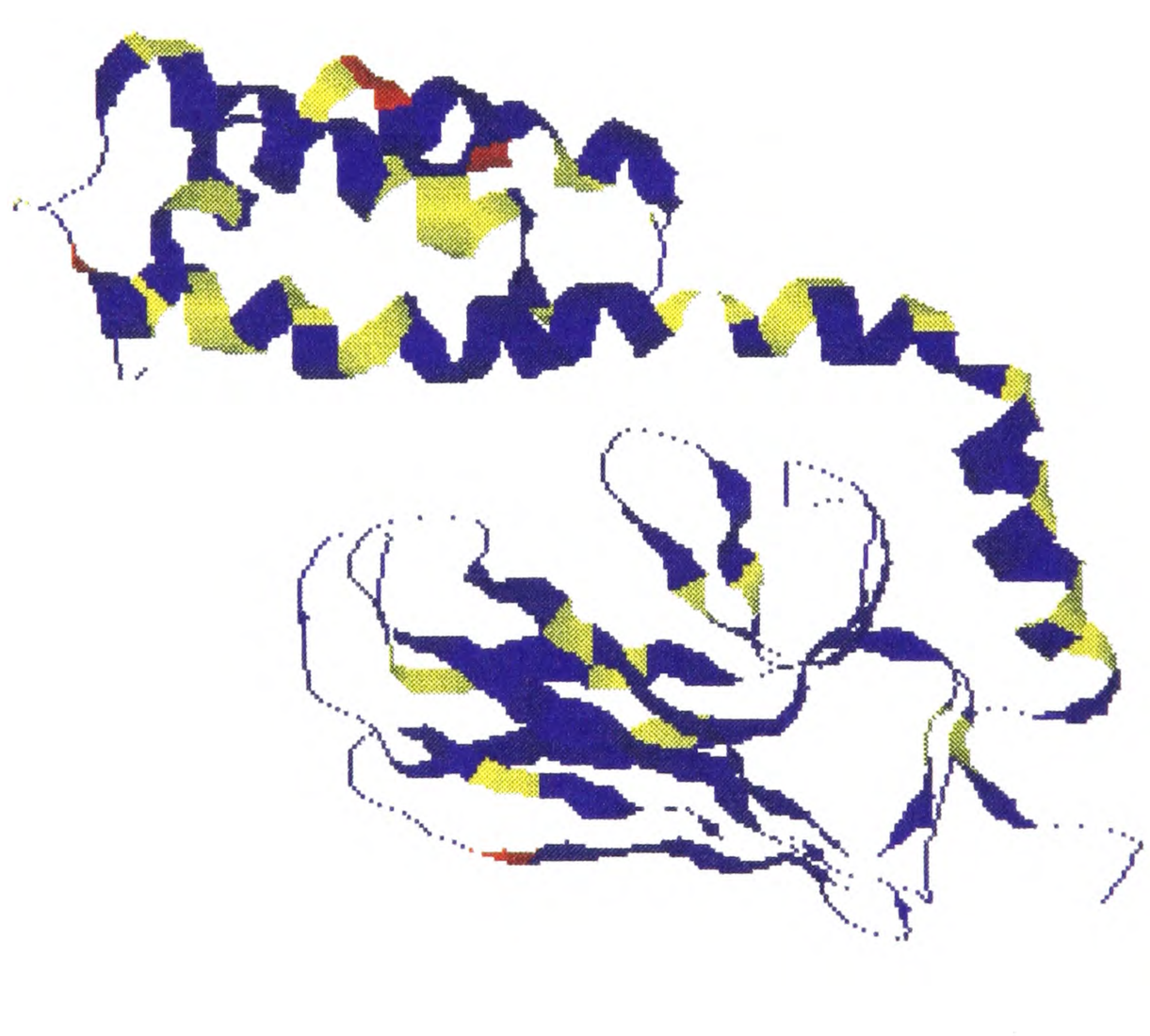

(c) hsc70

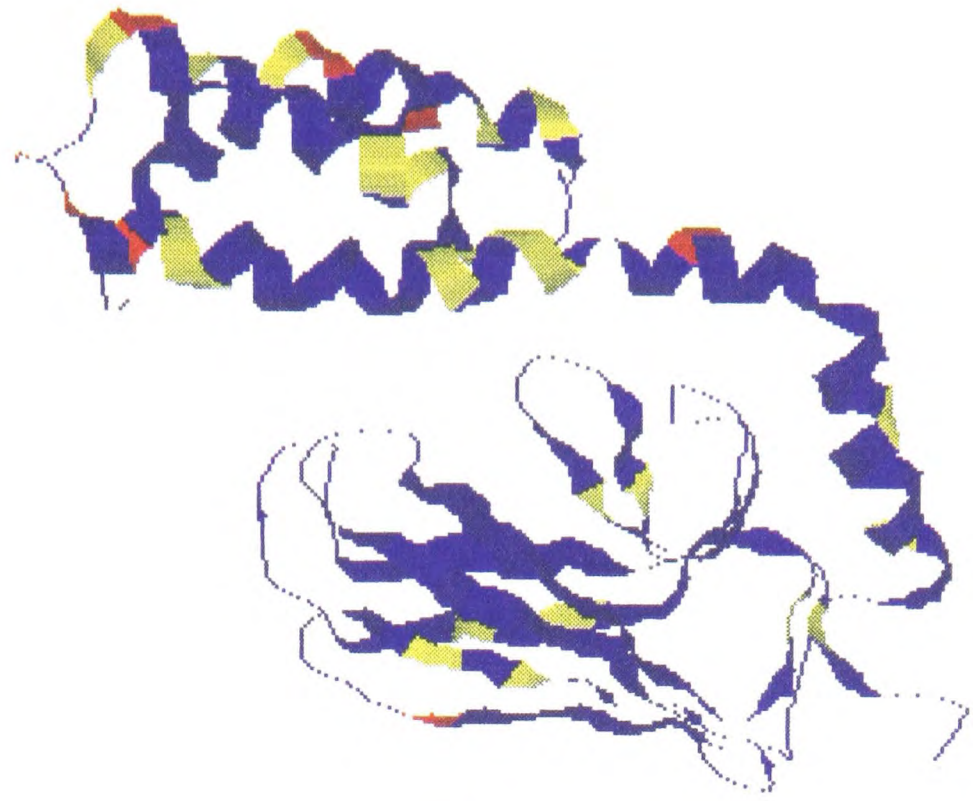

(d) hsp70B'

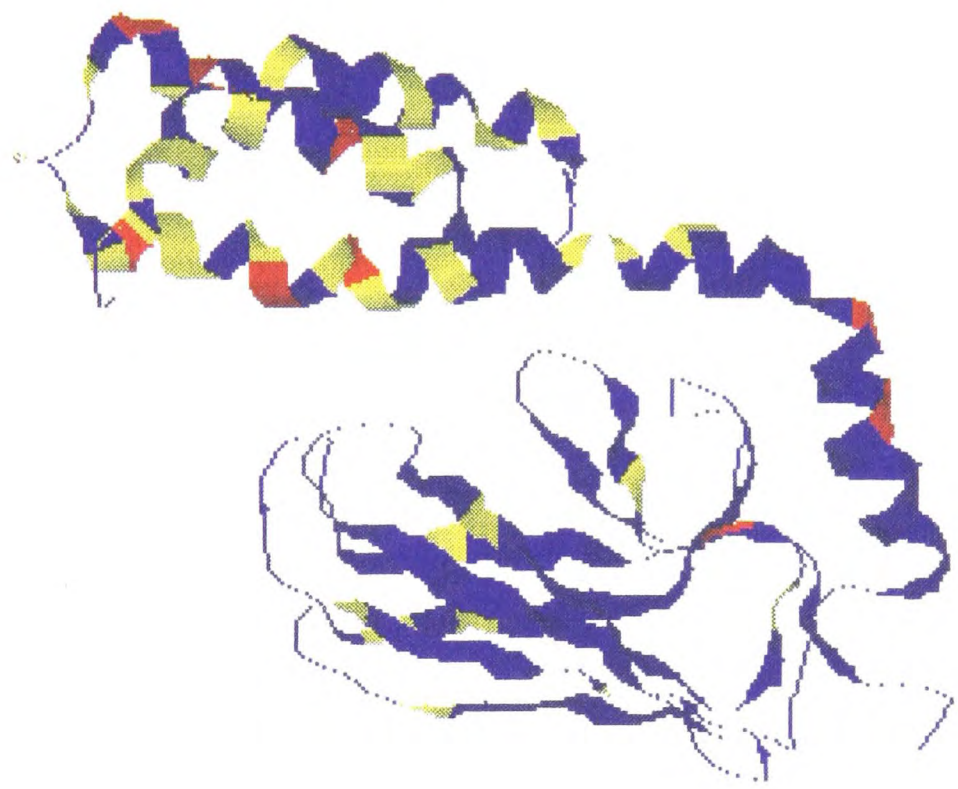

Figure 4-19: Amino acid conservation between hsp70hom and (a) hsp70, (b) hsp70A2, (c) hsc70 and (d) hsp70B'. Amino acids that are the conserved in each pair of proteins are coloured blue; gained, lost or reversed charges are coloured red and other non-conserved amino acids are coloured yellow. This conservation is displayed on the model of the C-terminal region of hsp70hom, using Rasmol (Sayle *et al.,* 1995).

The Structure of HOM-P and PBP-P

The model sheds light on the expression of the peptide-binding domains alone from hsp70hom and PBP74, as described in Chapter 3. The peptide-binding domains as expressed using pGEX-2T (equivalent to amino acids 384-554 of hsp70hom) comprise the ß-subdomain (393-505 of hsp70hom) and 49 amino acids of the α-subdomain, including the long α-helix (αB) that runs across the top of the peptide-binding site. Therefore, the expressed peptide-binding domains include all the residues involved in peptide-binding, confirming the conclusions drawn from proteolysis of hsc70 (Chappell *et al.*, 1987). However, the additional α-helical region may be responsible for the expressed domains aggregating at high concentrations. It is rich in hydrophobic amino acids, and those in the C-terminal half, which usually interact with the rest of the α-domain, will be exposed. These hydrophobic surfaces may interact with each other to form aggregates, and if unstructured, they might even interact with the peptide-binding site of another domain. Nevertheless, it is possible that, like the C-terminal region of dnaK (Zhu *et al.*, 1996), the peptide-binding domains of hsp70hom and PBP74 will not aggregate once they are bound to a peptide.

Assessing the Secondary Structure Prediction for the C-Terminal Region of PBP74

This is an appropriate point to discuss the accuracy of the different methods used to predict the secondary structure of PBP74 (Chapter 3). In Figure 4-20, these predictions are displayed together with the structure determined for the C terminus of dnaK by X-ray crystallography (Zhu *et al.*, 1996). All three prediction methods (Chou-Fasman, Garnier-Osguthorpe-Robson and Predict Protein) correctly predicted that the N-terminal half of the PBP74 peptide binding domain would be rich in ß-sheet, while the C-terminal half of the domain would consist almost entirely of α-helices. All three methods had predicted the ß-sheets fairly accurately, but only the Predict Protein method avoided predicting incorrectly

```
          1
AA        |ASEAIKGAVVGIDLGTTNSCVAVMEGKQAKVLENAEGARTTPSVVAFTADGERLVGMPAKRQAVTNPNNTFYATK|
CF        |       BBBBB    TT BBBBBAAAAAAAAAAAA     TTBBBBBTT                TT       |
GOR       |AAAAAAABBBBBBBTT   AAAAAAAAAAAAAAAAAA    BBBBBAAAAAAAAA   BBBBB      BBBBB|
PP        |        BBBBB     BBBBBBB   BBBBBB         BBB   AAAAAAAAAAAAA     AAAAAA|
DEF       |         BBBBBB  BBBBBB    BBBB        BBB  BBBB    BBB AAAAA       BBB  33|

         76
AA        |RLIGRRYDDPEVQKDIKNVPFKIVRASNGDAWVEAHGKLYSPSQIGAFVLMKMKETAENYLGHTAKNAVITVPAY|
CF        |          TT          BBBBBBTTT AAAAAA     TTBBBBBBBBBAAAAAAA          BBBBBBBB|
GOR       |BBBBTTT   AAAAAAA  BBBBBB     AAAAAATT    TTAAAAAAAAAAAAAAAAAAAAAABBBBBBBBT|
PP        |AAAA      AAAAAA    BBBB       BBBB       AAAAAAAAAAAAAAAAAAAAA     BBBBBBB |
DEF       |3         AAAAAAAAA   BBBBB  BBBB   BBBB  AAAAAAAAAAAAAAAAAAAA     BBBBBB   |

        151
AA        |FNDSQRQATKDAGQISGLNVLRVINEPTAAALAYGLDKSEDKVIAVYDLGGGTFDISILEIQKGVFEVKSTNGDT|
CF        |B TT          BBBBBBBBBBBBAAAAAAAA          BBBBB                        TTTT |
GOR       |TTT TTT     BBBBBBBBBBBB  AAAAAAAAAAAAAAAAAABBBBBTTT  BBBBBAAAAAAAAAA  TTT  |
PP        |   AAAAAAAA        BBBBB   AAAAAAAAA         BBBBB     AAABBBBB   BBBBBB     |
DEF       |  AAAAAAAAAAAA     BBBBBBAAAAAAAAAA        BBBBBBBB    BBBBBBBBB  BBBBBBBBBB |

        226
AA        |FLGGEDFDQALLRHIVKEFKRETGVDLTKDNMALQRVREAAEKAKCELSSSVQTDINLPYLTMDSSGPKHLNMKL|
CF        |    AAAAAAAAAAAAAAAAAA      TT AAAAAAAAAAAAAAAA   BBBBBBBBBBBB TTT       |
GOR       |     AAAAAAAAAAAAAAAAAAAAAAAAAAAAAAAAAAAAAAAAAAAAAAATTTBBBBBBBBBBBBTT    AAAAAA|
PP        |       AAAAAAAAAAAAAAAA   AAAAAAAAAAAAAAAAAAAA      BBBBAAA          AAAA|
DEF       |   AAAAAAAAAAAAAAAAAAAA       AAAAAAAAAAAAAAAAAA    BBBBBBBBBB      BBBBBB|

        301
AA        |TRAQFEGIVTDLIRRTIAPCQKAMQDAEVSKSDIGEVILVGGMTRMPKVQQTVQDLFGRAPSKAVNPDEAVAIGA|
CF        |       BBBBBB     TTAAAAAAAAAA     BBBBB        BBBBBBBBB          TT       |
GOR       |AAAABBBBBBTTTTT  TTAAAAAAAAAAA   BBBBBBTT       BBBBBBBB          AAAAAAAAAA|
PP        |AAAAAAAAAAAAAAAA  AAAAAAAAA       BBBBBB      AAAAAAAAAA          AAAAAAAA|
DEF       |BAAAAAAA AAAAAA AAAAAAAAAA    333  BBBBB 3333 AAAAAAAAAA    BB       AAAAAA|

        376      _‡_____________________________________________________________________
AA        |AIQGGVLAGDVTDVLLLDVTPLSLGIETLGGVFTKLINRNTTIPTKKSQVFSTAADGQTQVEIKVCQGEREMAGD|
CF        |           BBBBBBBBBB             BBBBBBBBBBBB                BBBBBBBBBBAAAAAA T|
GOR       |BBBBBBBBBBBBBBBBBBB  BBBBBB  BBBBB TTTT   TTT BBBBB      BBBBB AAAAAAAAAA|
PP        |AAAAAAAA     BBBBB              AAABB              BBB      BBBBBBB          |
DEF       |AAAAAA    |       BBB  BBBBBB   BBBBBB   BBB BBBBBBBB      BBBBBBBBBB       |

        451_____________________________________________________________________________
AA        |NKLLGQFTLIGIPPAPRGVPQIEVTFDIDANGIVHVSAKDKGTGREQQIVIQSSGGLSKDDIENMVKNAEKYAEE|
CF        |T               TT      BBBBB TTBBBBB    TTTT  BBBBBBTTT   TTAAAAAAAAAAAAAAA|
GOR       |AAABBBBBB          BBBBBBBAAAAAAAAAAATTTT    BBBBBBB TT    AAAAAAAAAAAAAAAA|
PP        |      BB              BBBBBBBB    BBBBBBB       BBBBB      AAAAAAAAAAAAAAAA|
DEF       | BBBBBBBBBB         BBBBBBBBB   BBBBBBBBB   BBBBBBB       AAAAAAAAAAAAA AAA|

        526_________________‡____________
AA        |DRRKKERVEAVNMAEGIIHDTETKMEEFKDQLPADECNKLKEEISKMRELLARKDSETGENIRQAASSLQQASLK|
CF        |AAAAAAAAAAAAAAAAAAAAAAAAAAAAAAA      AAAAAAAAAAAAAAATT      AAAAAAAAAAAAA|
GOR       |AAAAAAAAAAAAAAAAAAAAAAAAAAAAAAAAAAAAAAAAAAAAAAAAAAAAAAA    AAAAAA  AAAAAAAAA|
PP        |AAAAAAAAAAAAAAAAAAAAAAAAAAAA       AAAAAAAAAAAAAAAA     AAAAAAAAAAAAAAAAA|
DEF       |AAAAAAAAAAAAAAAAAAAAAAAAAAAAA     AAAAAAAAAAAAAAAAA    AAAAAAAAAAAAA AAAAA|

        601
AA        |LFEMAYKKMASEREGSGSSGTGEQKEDQKEEKQ|
CF        |AAAAAAAAAAAAAA TTTTT  AAAAAAAAAAA|
GOR       |AAAAAAAAAAAATT        AAAAAAAAAAA|
PP        |AAAAAAAAA                        |
DEF       |AAAAA  |
```

Figure 4-20: The predicted secondary structure of PBP74. The amino-acid sequence of PBP74 (AA) (Domanico *et al.*, 1993) is displayed with the secondary structure predicted by the Chou and Fasman (CF), Garnier, Osguthorpe and Robson (GOR) and Predict Protein (PP) methods beneath. The secondary structure of the ATPase domain of hsc70 (Flaherty *et al.*, 1990) and the C-terminus of dnaK (Zhu *et al.*, 1996), as determined by X-ray crystallography, are displayed beneath the equivalent amino-acids of PBP74 (DEF). Alpha-helices (A), ß-sheet (B), ß-turns (T) and 3_{10} helices (3) are shown. The sites equivalent to the chymotryptic cleavage sites in hsc70 (Chappell *et al.*, 1987) are marked with ‡ and the extent of the peptide-binding domain expressed in pGEX-2T is overlined.

the presence of one or more α-helices in the ß-subdomain. The Garnier-Osguthorpe-Robson method also predicted slightly too much α-helix in the C-terminal α-subdomain.

Functional Implications of Polymorphisms in Hsp70hom

As discussed in Chapter 1, susceptibility to many autoimmune diseases is linked to the MHC. Therefore, it is interesting that in humans, hsp70hom has several allelic variants, with polymorphisms at Thr 493 Met (Milner and Campbell, 1992) and Glu 602 Lys (S. Jenkins, personal communication). In the model of hsp70hom, Thr 493 is located towards the C-terminus of the seventh ß-strand, at the opposite side of the ß-subdomain to the peptide-binding site. This position is relatively unconserved in the hsp70 family, consisting of 27% lysine, 25% glutamate, 22% valine, 8% threonine and only 4% methionine in the 166 members considered here. Thr 493 is equivalent to Lys 489 of dnaK, which is partially accessible to solvent (Zhu *et al.,* 1996). Glu 602 lies towards the C-terminus of the fourth α-helix of the α-subdomain. This position is more highly conserved among hsp70s, consisting of 62% glutamate, 14% glutamine, 2% lysine, 2% alanine. Ala 592 of dnaK, which occupies this position is fully solvent accessible.

These polymorphisms in hsp70hom are not at positions that are predicted to contact the bound peptide, so they are unlikely to alter the peptide-binding specificity of the protein. The relative lack of conservation of these residues in the hsp70 family and the solvent accessibility of the equivalent residues in dnaK suggests that they are not important in the structure of hsp70s and, therefore, polymorphisms at these positions are unlikely to diminish the activity of hsp70hom by destabilising its structure. However, somewhat conserved, solvent accessible amino acid side chains may be involved in binding to cofactors and polymorphisms may alter the activity of hsp70hom by interfering with such interactions. Several examples of mutations that affected the ability of the C-terminus of dnaK to bind to substrates have been identified (Burkholder *et al.*, 1996). Of 15 single

amino acid mutations, all but one of them map to the peptide-binding ß-subdomain, outside the peptide binding site. However, it is interesting that the single mutation in the α-subdomain (Gly 539 Asp) lies directly above the substrate binding site, suggesting that the introduction of a long, charged amino acid at this position (Leu 544 in hsp70hom) may sterically hinder the binding of peptides to the ß-subdomain.

Discussion

A model of the C-terminal region of hsp70hom has been generated on the basis of the structure of the same region of the hsp70 of *E.coli*, dnaK. This model should be a good likeness of the true structure, because of the high degree of sequence conservation between the two molecules (42% identity in the C-terminal region) and the existence of only three insertions (six amino acids) in hsp70hom. The secondary and tertiary structures of the hsp70hom model are very similar to those of dnaK and, more interestingly, the nature and positions of the amino acids of the peptide binding cleft are highly conserved. This allowed the peptide NRLLLTG, which was co-crystallised with the C-terminal region of dnaK, to be modelled as a complex with hsp70hom. The peptide is able to bind to the hsp70hom model in much the same way as it binds to dnaK, with conserved contacts being focused on the central leucine of the peptide, which fits into the 'Leu 4 pocket. Modelling of another peptide, FYQLALT, which is known to bind to the C-terminal region of hsp70hom (see Chapter 5) was less successful. The peptide was modelled bound in the peptide-binding cleft in both orientations, in the absence of evidence to suggest which orientation was correct. A lower energy complex was formed when FYQLALT bound in the reverse orientation (opposite to NRLLLTG binding). However, it is far from conclusive that this model represents the correct orientation. However, at least their energies were not significantly higher, which is likely to be an advantage of allowing flexibility in the peptide-binding site during complex formation.

The modelling of bound peptide is the least certain part of the work described in this chapter. More reliable models could be created if the modelling procedure was repeated 100 rather than 20 times, since in general only 20% of models (4 out of 20) were accepted for use in generating the mean, and therefore the final, structure. This made it difficult to distinguish a consensus structure for the bound peptides. It would also be preferable to

generate several independent models from peptides that have been rotated around their axis or moved laterally in the binding groove. Finally, an important measure of the reliability of the peptide modelling procedure would be to test whether it can recreate the structure of the complex of NRLLLTG with the C-terminus of dnaK. However, ultimately, a model needs to be validated experimentally, ideally through structure determination by nuclear magnetic resonance spectroscopy or X-ray crystallography.

Chapter 5: Peptide-Binding Studies

Introduction

Hsp70s interact with unfolded proteins and aid their folding, help transport them across membranes or target them for degradation (see Chapter 1). They have to be able to interact with a wide range of different protein substrates and yet be able to distinguish the unfolded conformation of a protein from its folded form. Hsp70s recognise unfolded proteins through stretches of extended polypeptide chain (DeLuca-Flaherty *et al.*, 1990), which they in an extended conformation (Landry *et al.*, 1992), which has allowed short peptides to be used as model substrates (Flynn *et al.*, 1989). They prefer to bind substrates through exposed hydrophobic amino acids (discussed below), another feature of unfolded proteins.

The substrate specificity of hsp70s has been investigated using two complementary approaches, described below. One has been to measure the binding affinity of defined peptide substrates, while the other uses hsp70s to select substrates from a pool of random peptides and identifies those that have bound by amino acid sequencing. A development of the latter approach has been peptide phage display, in which the random peptides are expressed on the surface of a bacteriophage coat protein and sequenced at the level of the phage DNA (Allen *et al.*, 1995).

Measuring Peptide Binding to Hsp70s

Since polypeptide substrates stimulate the ATPase activity of hsp70s, ATP hydrolysis can be used as a measure of peptide binding (Flynn *et al.*, 1989). ATPase assays use thin layer chromatography to measure the conversion of tritiated ATP to ADP (Flynn *et al.*, 1989), or the release of radiolabelled inorganic phosphate from ATP (DeLuca-Flaherty *et*

al., 1990; Gragerov *et al.*, 1994). However, peptide binding does not always correlate with ATPase stimulation: short peptides are much less effective at stimulating ATP hydrolysis than they are at binding (Flynn *et al.*, 1991), and basic peptides that bind to hsc70 are inefficient stimulators of its ATPase activity (Takenaka *et al.*, 1995). Nevertheless, this is in a sense a functional assay, because it detects peptide binding to the site involved in chaperone function.

Binding of peptides to hsp70s can be detected more directly if they are labelled. Amino groups can be biotinylated (Roman *et al.*, 1994) or tritiated by reductive methylation (Flynn *et al.*, 1989; Gragerov and Gottesman, 1994; Takenaka *et al.*, 1995). Peptide-hsp70 complexes can be separated from free peptide by native gel electrophoresis (Roman *et al.*, 1994) or gel filtration (Flynn *et al.*, 1989; Gragerov and Gottesman, 1994; Takenaka *et al.*, 1995). Such assays may be more reliable when the binding of unlabelled peptides is measured by their competition with a well-characterised substrate such as a labelled peptide (Gragerov and Gottesman, 1994) or the permanently unfolded protein, reduced carboxymethylated α-lactalbumin (RCMLA) (Fourie *et al.*, 1994). Alternatively, interactions can be measured semiquantitatively by immobilising peptides on nitrocellulose filters and detecting bound hsp70s through a biotin label (Blond-Elguindi *et al.*, 1993) or with antibodies (Rüdiger *et al.*, 1997a). This approach allows the binding of hydrophobic peptides to be measured more easily, since it avoids the problem of their tendency to aggregate and precipitate in solution.

The interaction of peptides with hsp70s can be followed in solution in real time using fluorescent labels. The binding of fluorescein-conjugated peptides can be detected by monitoring fluorescence anisotropy (Endo *et al.*, 1996) and that of peptides conjugated to the environmentally-sensitive fluorophore dansyl chloride by measuring fluorescence (Farr *et al.*, 1995).

In addition, peptide binding can be detected, if not quantified, by sequencing of bound peptides (Flynn *et al.*, 1991) or bacteriophage inserts (Blond-Elguindi *et al.*, 1993; Gragerov *et al.*, 1994; Takenaka *et al.*, 1995), by two dimensional NMR (Landry *et al.*, 1992), by X-ray crystallography (Zhu *et al.*, 1996) and by peptide cross-linking (Zhang and Walker, 1996). Substrate binding has even been measured by its ability to protect hsp70s from protease digestion (DeLuca-Flaherty *et al.*, 1990; Freeman *et al.*, 1995).

The Specificity of Hsp70s for Peptides

The size of the hsp70 peptide-binding site has been investigated using peptides with defined lengths and random sequences. While peptides of four or five amino acids can bind to BiP or dnaK, they must be 7 or 8 amino acids long to bind with high affinity (Flynn *et al.*, 1991; Jordan and McMacken, 1995). However, in the crystal structure of the C-terminal domain of dnaK, the heptameric peptide (NRLLLTG) is bound through only six of its residues, with the majority of the interactions through its four central amino acids, RLLL (Zhu *et al.*, 1996).

The sequence specificity of BiP has been investigated using a panel of 42 synthetic peptides 7-18 amino acids long (Flynn *et al.*, 1989; Fourie *et al.*, 1994). Most peptides bound with affinities ranging from 10 μM to 1 mM, but about a fifth did not bind at all. High affinity peptides tended to be rich in large hydrophobic residues, such as leucine and tryptophan, and had few acidic amino acids. Similar preferences were seen when random 7-mer peptides were bound to BiP, eluted and pool sequenced (Flynn *et al.*, 1991). Aliphatic amino acids were enriched at all positions whereas polar and charged amino acids and proline were disfavoured, except that positive amino acids were slightly enriched at the C-terminus. In phage display, the 8-mer and 12-mer inserts of BiP-binding phage were enriched in the large hydrophobic amino acids tryptophan, phenylalanine and leucine, and to a lesser extent the amino acids glutamine, cysteine, methionine and isoleucine; lysine

was strongly disfavoured (Blond-Elguindi *et al.*, 1993). The authors propose that the hydrophobic amino acids (Hy) are arranged in an alternating pattern of Hy(W/X)HyXHyXHy (where X = any amino acid and W = tryptophan), forming a hydrophobic face to the peptide if it adopts an extended conformation like a ß-strand.

In summary, the presence of large hydrophobic amino acids, especially leucine, favours binding to BiP. While charged amino acids are disfavoured in peptide selection experiments with BiP (Flynn *et al.*, 1991; Blond-Elguindi *et al.*, 1993), many peptides that bind strongly to BiP do contain positively charged amino acids (Flynn *et al.*, 1989; Fourie *et al.*, 1994).

DnaK preferentially bound to peptides containing large hydrophobic (leucine, isoleucine and tryptophan) and also basic amino acids in phage display (Gragerov *et al.*, 1994). Basic amino acids were particularly enriched at the N-terminus of the selected hexameric peptide inserts, while large hydrophobic amino acids were more often found in the middle. The importance of basic amino acids in binding to dnaK was shown with synthetic peptides; replacing arginine in the peptide NRLLLTG with alanine or glutamic acid reduced and abolished binding, respectively. Shuffling the central leucines to the ends of the peptide also abolished binding. DnaK showed similar preferences when binding to overlapping 13-mer peptides, comprising the complete sequences of 6 proteins (Rüdiger *et al.*, 1997a). Binding was favoured by aliphatic (leucine, isoleucine and valine), aromatic (phenylalanine and tyrosine), and basic amino acids, while negatively charged residues strongly deterred binding. The majority of the good dnaK binding sites corresponded to regions of ß-sheet in the native protein. DnaK-binding peptides had affinities as strong as 0.1 μM, the strongest reported for any hsp70.

Some of the most straightforward data on the specificity of hsp70s comes from the binding of single amino acids to dnaK (Richarme and Kohiyama, 1993; DeCrouy-Chanel *et al.*, 1996). Amino acids bind to dnaK with low affinities (500 μM at most), but

nevertheless stimulate its ATPase activity and compete with unfolded proteins for binding. Large hydrophobic amino acids (isoleucine, leucine, valine, phenylalanine and tryptophan) and threonine bind strongly, and positively charged amino acids also bind, albeit with lower affinity. DnaK seems to have several amino acid binding sites because when its ATPase activity has been maximally stimulated with a single amino acid, it can be further stimulated by addition of another amino acid of a different class (aliphatic, aromatic or basic). In summary, dnaK binds most strongly to peptides containing hydrophobic and, to a lesser extent, basic amino acids.

Phage display has also been used to investigate the binding specificity of hsc70. The 15-mer peptide inserts bound by hsc70 were significantly enriched in lysine, and to a lesser extent arginine, histidine, glutamine and glutamate, with most containing a stretch of 2-5 basic amino acids (Takenaka *et al.*, 1995). Thus, in contrast to dnaK and BiP, basic rather than hydrophobic residues favoured binding to hsc70. Peptides were synthesised with sequences corresponding to the inserts of bound phage, and shown to bind with affinities in the range 3-300 μM. Although they compete with previously characterised hydrophobic peptides for binding to hsc70, they seem to bind differently, as they fail to stimulate its ATPase activity and cause it to migrate differently on native gels. The phage from which these basic peptides were derived were eluted from hsc70 by acid rather than ATP, so it is possible that they were binding elsewhere than the substrate-binding site. Such an alternative site might interact with other basic motifs known to interact with hsc70, such as nuclear localisation signals, KFERQ motifs and basic dnaJ-homologues (Takenaka *et al.*, 1995).

A constitutive cytoplasmic hsp70 of yeast, Ssa1p, binds to peptides derived from mitochondrial presequences with affinities that are proportional to their hydrophobicity, as measured by their retention time during reverse-phase HPLC (Endo *et al.*, 1996). The peptides with highest affinity for Ssa1p were rich in leucine and arginine residues, again suggesting that hydrophobic and basic amino acids favour binding.

The studies described above suggest that different members of the hsp70 family have similar peptide-binding specificities, preferring to bind to hydrophobic side chains of their peptide substrates, with the possible exception of hsc70. Positively charged amino acids seem to favour the binding of a peptide to dnaK, hsc70 and possibly BiP. The inherent variability between studies that can be seen when comparing different investigations of the same hsp70 precludes judging whether different hsp70s have genuine differences in specificity. Differences in methods of detecting complexes, buffers and, in phage display, elution method and flanking sequences, may account for the apparent lack of consistency between studies. It is therefore more informative to consider studies that investigate the binding of the same set of peptides to different hsp70s.

A study of 50 overlapping 20-mer peptides from three proteins binding to mycobacterial hsp70 and BiP showed that 7.5% bound to BiP alone, 2.5% bound to mycobacterial hsp70 alone and 22.5% bound to both; 67.5% did not bind at all (Roman *et al.*, 1994). However, the peptides used were too long to distinguish potential BiP or mycobacterial hsp70 binding sites clearly. Fourie and colleagues measured the binding of 53 peptides to dnaK, BiP and hsc70 (Fourie *et al.*, 1994). The majority of these randomly-selected peptides bound to all three hsp70s, although more peptides bound strongly to BiP than to the other two. Few peptides had a similar affinity for all three hsp70s, however, those that bound strongly to all three were rich in large hydrophobic and basic amino acids and had few acidic residues. Amino acid substitutions in one heptameric peptide showed that a central large hydrophobic residue (defined as position 0) was important for binding to all three hsp70s, while substitutions at +2 and -2 often caused hsp70-specific differences in affinity. Substitutions at +1 and -1 had little effect, supporting the model of alternating anchor residues proposed for BiP by Blond-Elguindi and colleagues (1993). Hsp70-specific differences in peptide binding have also been demonstrated by Gragerov and Gottesman (1994), who showed that an acidic amino acid substitution in a heptameric peptide reduced its binding to all three hsp70s, having most effect on binding to dnaK and

least for binding to BiP. It is important to note that these studies clearly show that the effect of a particular amino acid substitution on hsp70 binding is influenced by the nature of the neighbouring amino acids.

To summarise, hsp70s (exemplified by dnaK, hsc70 and BiP) bind to their peptide substrates through interactions with hydrophobic side chains. Negatively charged residues interfere with peptide binding, while positively charged amino acids seem to favour it. However, each hsp70 has its own preferences, and single amino acid substitutions in a peptide can change its affinity for some hsp70s and not others. It is worth noting that dnaJ has been reported to alter the peptide-binding specificity of dnaK (DeCrouy-Chanel *et al.*, 1996), and that dnaJ co-operates with dnaK in capturing substrates (see Chapter 1). It is interesting that some peptides do not bind to hsp70s at all, often despite have one or more large hydrophobic amino acids. This suggests that the context of favourable amino acids may influence peptide binding, for example by steric hindrance. In addition, peptides, some as short as 6 amino acids, can adopt ordered structures in solution (Dyson and Wright, 1991; Yao *et al.*, 1994; Dyson and Wright, 1995), which would prevent hsp70 binding. This may explain why some shorter peptides bind more strongly to hsp70s than the longer ones they are derived from (Roman *et al.*, 1994): truncating the peptide may abolish the inhibition of binding caused by the formation of secondary structure.

Functional Specificity of Hsp70s

If hsp70s have very similar peptide-binding specificities, why do eukaryotes need so many different members of the family? A single hsp70 in *E. coli* is capable of performing all the known functions of hsp70s, but yeast contains at least 14 different hsp70s divided into 5 sub-families, and human cells contain at least 7 hsp70s (Figure 3-2). This may in part be accounted for by the division of the eukaryotic cell into many different compartments: it is rare for a protein to be expressed in more than one cellular organelle

(Danpure, 1995), so different hsp70s are needed with alternative targeting signals to reach the various compartments. Nevertheless, hsp70s in different compartments differ in more than their targeting signals and, as a result, they are not functionally equivalent. Thus, BiP and hsc70 cannot substitute for each other in translocating polypeptides into the ER (Brodsky *et al.*, 1993; Wiech *et al.*, 1993) or lysosomes (Terlecky *et al.*, 1992). In addition, hsp70s found in the same cellular compartment are not functionally equivalent. Strikingly, the yeast hsp70s Ssa1p (constitutively expressed) and Ssa2p (heat-induced) exhibit significant differences in their clathrin-uncoating ability (Gao *et al.*, 1991), despite their amino acid sequences being 97% identical. Furthermore, cytoplasmic hsp70s such as hsp70 and hsc70 are unable to substitute for hsp70A2, despite their sharing 89% and 83% identity, respectively, since targeted disruption of its homologue in mouse, hsp70-2, results in male infertility (Dix *et al.*, 1996).

Are these examples of the functional specificity of hsp70s due to different specificities for polypeptides? It would be surprising if the failure of BiP to substitute for hsc70 in microsomal import were a result of differing peptide-binding affinity, as they deal with the same polypeptides on opposite sides of the ER membrane. In addition, dnaK must have a very broad specificity to be able to aid the folding of every *E. coli* protein and many recombinant ones, yet it cannot substitute for hsc70 in promoting polypeptide import into mammalian microsomes (Wiech *et al.*, 1993) or lysosomes (Terlecky *et al.*, 1992). The question was addressed for Ssa1p and Ssb1p, cytoplasmic proteins that perform different roles in yeast, by domain swapping. The conclusions were complex, but it was shown that neither hsp70 required its own peptide-binding domain to function correctly (James *et al.*, 1997). Therefore, it seems likely that the functions of different hsp70s are determined more by their association with various cofactors than by their peptide-binding specificities.

Peptide-Binding by Hsp70hom and PBP74

The peptide-binding specificities of hsp70hom and PBP74 are likely to be similar to each other and to dnaK, hsc70 and BiP, with subtle differences. The peptide-binding domains of these hsp70s were expressed in isolation and shown to be folded by NMR spectroscopy (Chapter 3). This chapter examines their ability to bind to two different peptides and a permanently unfolded polypeptide. Experiments were also carried out with the entire C-terminus of hsp70hom (HOM-C), comprising amino acids 384-641, which was generously provided by Miss. S. Jenkins (MRC Immunochemistry Unit). Like the isolated peptide-binding domains, HOM-P and PBP-P, this was expressed as a fusion with GST. The peptide-binding domain of PBP74 (PBP-P) was used in only a few experiments, because it is relatively unstable in solution (see Chapter 3) and, therefore, had to be freshly prepared each time. Hsc70 purified from bovine brain (the kind gift of L. Greene and E. Eisenberg, National Institutes of Health, Bethesda, USA) was used as a positive control. Like HOM-P and PBP-P, HOM-C and hsc70 ran as single bands on SDS-PAGE [Chapter 2, Section E1] (data not shown).

The ability of hsp70hom to bind to peptides was not previously known, so the choice of a peptide to test that HOM-P and HOM-C can bind to peptides required some thought. Such a peptide could then be used as a positive control in competition studies. Peptides that bind to several different hsp70s (preferably including another cytoplasmic hsp70) are likely to bind to hsp70hom too. Hsc70, dnaK and BiP bind to the peptides FYQLALT and WIFPWIQL with very high affinities (Kds <5 μM for FYQLALT) (Fourie *et al.*, 1994). NRLLLTG also binds strongly to these three hsp70s (Gragerov and Gottesman, 1994), binding to dnaK with an affinity of 11 μM (Burkholder *et al.*, 1996), and a peptide from pigeon cytochrome c (Pc 81-104) binds to hsc70 (Takenaka *et al.*, 1995), BiP (Domanico *et al.*, 1993), PBP74 (Lakey *et al.*, 1987) and hsp70 from *Mycobacterium tuberculosis* (Roman *et al.*, 1994). The Kd of the interaction of Pc 81-104 with hsc70 is 8 μM (Takenaka *et al.*, 1995), but its affinity for the other hsp70s has not been quantified.

Results

The Binding of Immobilised Peptide-Binding Proteins to Biotinylated Peptides

It has been shown that immobilised hsp70s can bind to peptides displayed on phage (Blond-Elguindi *et al.*, 1993; Takenaka *et al.*, 1995) and that biotinylation of peptides does not prevent them from binding to hsp70s (Roman *et al.*, 1994). Therefore, a peptide binding assay was established using peptide-binding proteins immobilised on the surface of plastic wells and a peptide labelled by biotinylation, in which a biotin group is attached via amino groups on the peptide. The chosen peptide was FYQLALT because it binds to dnaK, hsc70 and BiP with very high affinity, and it has no side chain amino groups which could become biotinylated and interfere with binding. The bulky biotin ring was, therefore, attached to the amino terminus of the peptide through a 12-carbon aliphatic linker to reduce steric hindrance. Biotinylated peptide bound to a peptide-binding protein on the plate can then be detected with avidin conjugated to alkaline phosphatase. The interaction between avidin and biotin is very specific and high-affinity (Kd = 10^{-15} M), making it a powerful tool for research. The associated alkaline phosphatase can be detected because it cleaves p-nitrophenyl phosphate to p-nitrophenol, which can be measured spectrophotometrically at 405 nm.

The binding studies were carried out in PBS, since peptide-binding to hsp70s is not dependent on ionic strength or other solutes (Wang *et al.*, 1993). Studies that assay ATPase activity use complex buffers containing ATP, Mg^{2+}, K^{+} and Hepes, pH 7-8, but peptides can bind to hsp70s in 50 mM Tris, pH 7.5 (Roman *et al.*, 1994) or PBS (Terlecky *et al.*, 1992). A non-ionic detergent [0.05% (v/v) Tween 20] was included in the buffer to reduce non-specific interactions, including that between FYQLALT and plastic (Dr. L. Hightower, personal communication).

The peptide FYQLALT [E16] was biotinylated with N-hydroxysuccinimidobiotin [E17] and purified by reverse phase HPLC [E9], using a C8 column and an 8-80% acetonitrile gradient (1.8%/min, 3 ml/min flow rate) (Figure 5-1). There were two major peaks, one eluted by ~30% (v/v) acetonitrile, and the other by ~40% (v/v) acetonitrile. The unbiotinylated peptide alone is eluted by ~30% (v/v) acetonitrile, so the peak eluting at ~40% is likely to be the biotinylated peptide. To confirm this, fractions from both peaks were lyophilised [E10], resuspended in dimethylsulphoxide and analysed by mass spectrometry (Figure 5-2). The mass of the peak which eluted at ~30% (v/v) acetonitrile (855) corresponds to the predicted mass of unbiotinylated FYQLALT (853), while the mass of the peak that eluted at ~40% (v/v) acetonitrile (1105) was approximately the same as that predicted for the biotinylated peptide (1081). The biotinylation and purification were then repeated on a large scale and the concentration of the biotinylated peptide determined by amino acid analysis [E12].

The binding of biotinylated FYQLALT to HOM-P, HOM-C, hsc70 and BSA immobilised in plastic wells was measured [E18]. Briefly, a small quantity of each protein was bound onto the surface of wells in a 96 well plate overnight and unused binding sites were then blocked with a solution of 1% (w/v) bovine serum albumin (BSA). Empty wells were also blocked with BSA for use as a negative control. The solution of biotinylated peptide was added to the wells for two hours at room temperature, unbound peptide was washed away and the avidin-alkaline phosphatase conjugate was added for 30 minutes. Unbound alkaline phosphatase was removed by washing and a solution of p-nitrophenyl phosphate was added. The production of p-nitrophenol by the bound alkaline phosphatase was detected at OD_{405}.

In preliminary experiments, the biotinylated peptide (50 μM) bound more strongly to wells coated with 50 μg of HOM-P, HOM-C and hsc70 than to empty wells blocked with BSA (data not shown). The amount of these proteins added to the wells was reduced to 1 μg of HOM-P and HOM-C and 0.5 μg of hsc70 without reducing the amount of peptide

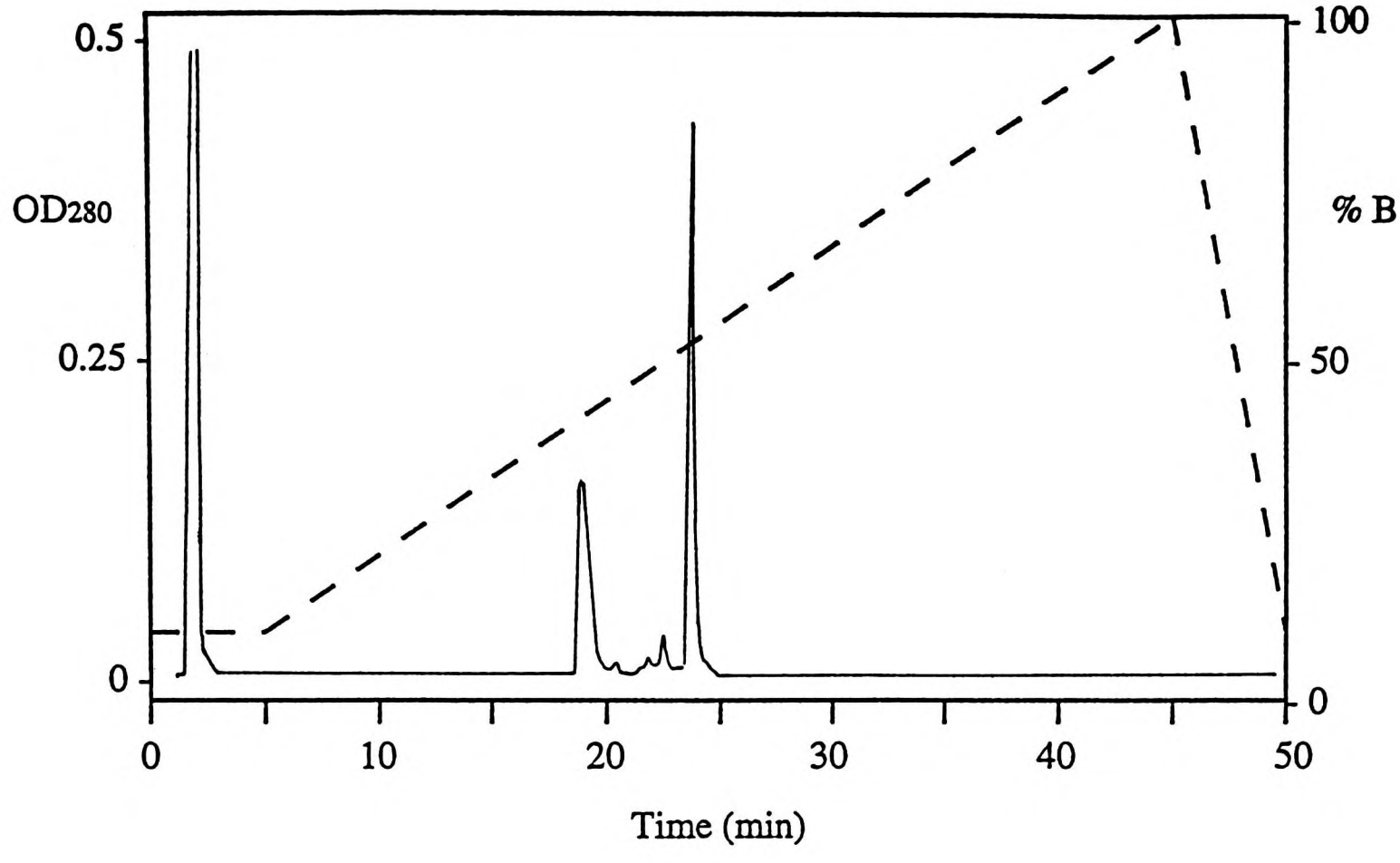

Figure 5-1: Purification of biotinylated peptide FYQLALT by reverse phase HPLC [E9]. The products of the biotinylation reaction were mixed with an equal volume of 0.1% (v/v) TFA, centrifuged at 2,000 g for 10 minutes and loaded onto a C8 reverse phase column (Dynamax-300A) equilibrated with 90% (v/v) solvent A [0.1% (v/v) TFA], 10% (v/v) solvent B [80% (v/v) acetonitrile, 0.1% (v/v) TFA]. These conditions were continued for 10 minutes, with the proportion of solvent B then rising to 100% (v/v) over 30 minutes. The proportion of solvent B was then returned to 10% (v/v) over five minutes. The two largest peaks were collected, from as soon as the OD_{280} started to rise until it fell below about a fifth of its highest value.

(a)

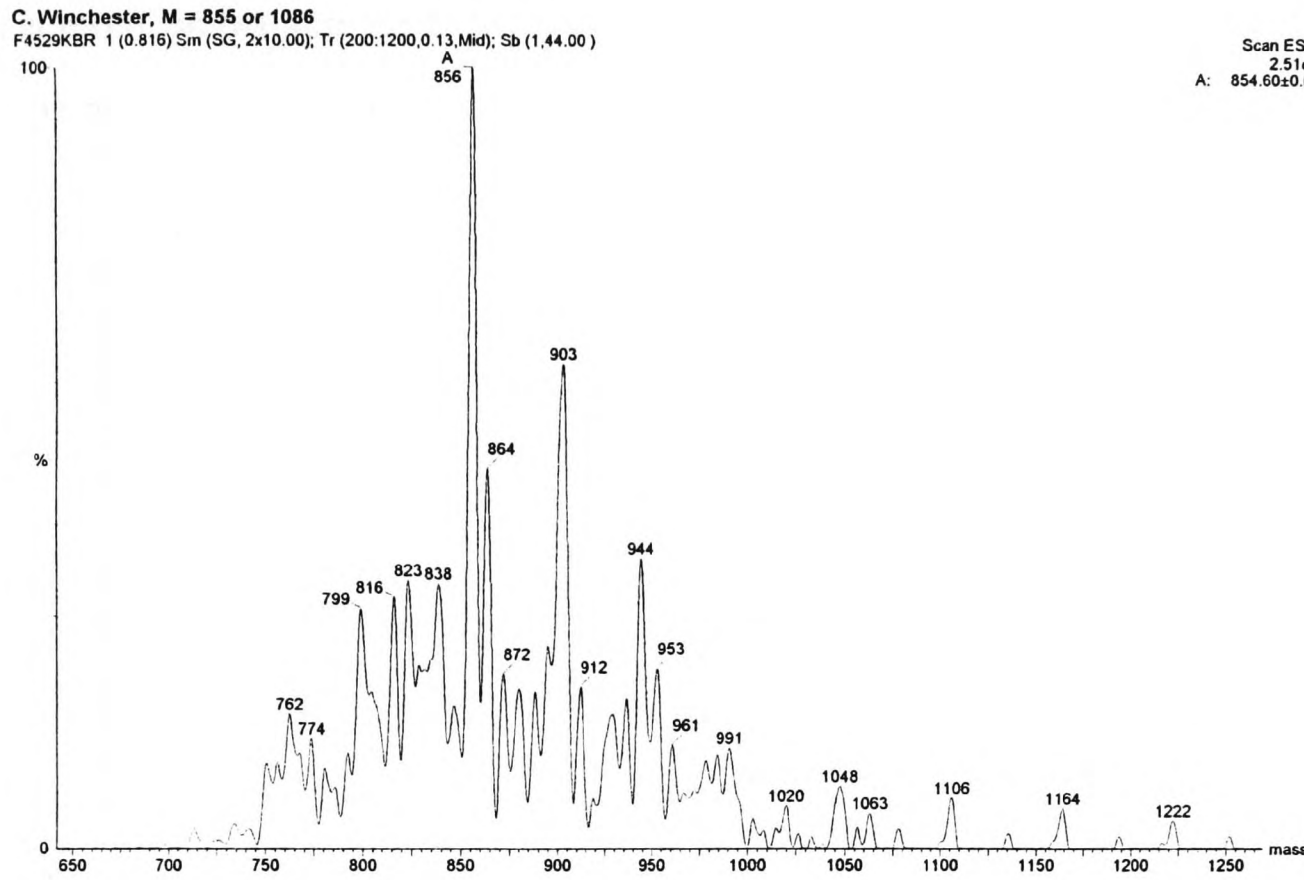

(b)

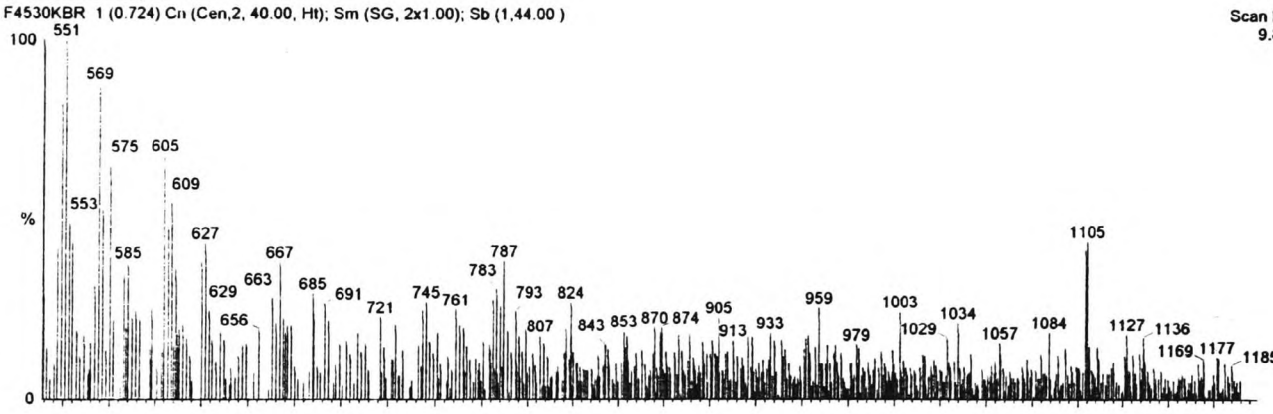

Figure 5-2: Mass spectrometry of (a) unbiotinylated and (b) biotinylated FYQLALT (the first and second peaks from HPLC respectively). ~1 nmol of biotinylated peptide (50 µl of a 25 µM solution in DMSO) and ~0.3 nmol (50 µl of a ~10 mM solution in DMSO) was analysed in each case. The unbiotinylated peptide appears as a peak at a mass of 856 Da (a), and the biotinylated peptide as a peak of 1105 Da in (b).

that bound, showing that the wells were still saturated with these quantities of protein. Similar levels of peptide binding were seen when it was added at 37 °C for 1 hour rather than at room temperature for 2 hours (data not shown). The concentration of avidin-alkaline phosphatase conjugate was varied (1:1 000, 1:10 000, 1:30 000 and 1: 100 000 dilutions), to maximise the detection of bound peptide and minimise any non-specific interactions. The highest concentration of avidin-alkaline phosphatase conjugate (1:1 000) bound more to BSA than the other three concentrations, which bound at similar levels (data not shown); therefore the dilution of 1:10 000 was used, as recommended by the manufacturer.

A titration of biotinylated FYQLALT binding to HOM-P (1 μg), HOM-C (1 μg), hsc70 (0.5 μg) and BSA was carried out, to determine the affinities of its interactions with these three proteins (Figure 5-3). The biotinylated peptide binds fairly strongly to the wells containing peptide-binding proteins and also binds more weakly to wells containing BSA. Therefore, a certain amount of the peptide detected in the wells containing HOM-P, HOM-C or hsc70 is likely to be bound non-specifically to the plastic or the BSA used as a blocking agent. To calculate the amount of peptide that has bound specifically to the peptide-binding proteins, its non-specific binding to the empty wells must, therefore, be subtracted (Figure 5-4). The resulting data clearly show that the two recombinant fragments of hsp70hom and hsc70 bind to biotinylated FYQLALT in a manner that is specific, because the number of binding sites are limited and the binding is, therefore, saturable. Because the binding becomes saturated in the concentration range of peptide used, dissociation constants (Kds) for the interactions between the proteins and the peptide can be calculated [E20]. The dissociation constant (Kd) is the concentration of peptide at which half the specific peptide-binding sites are occupied, and it is less than 25 μM for each protein. Unfortunately, it is not easy to determine their values more accurately than this from the data shown. Nevertheless, these Kds calculated for the binding of hsp70hom and hsc70 to biotinylated FYQLALT are similar to those determined for the

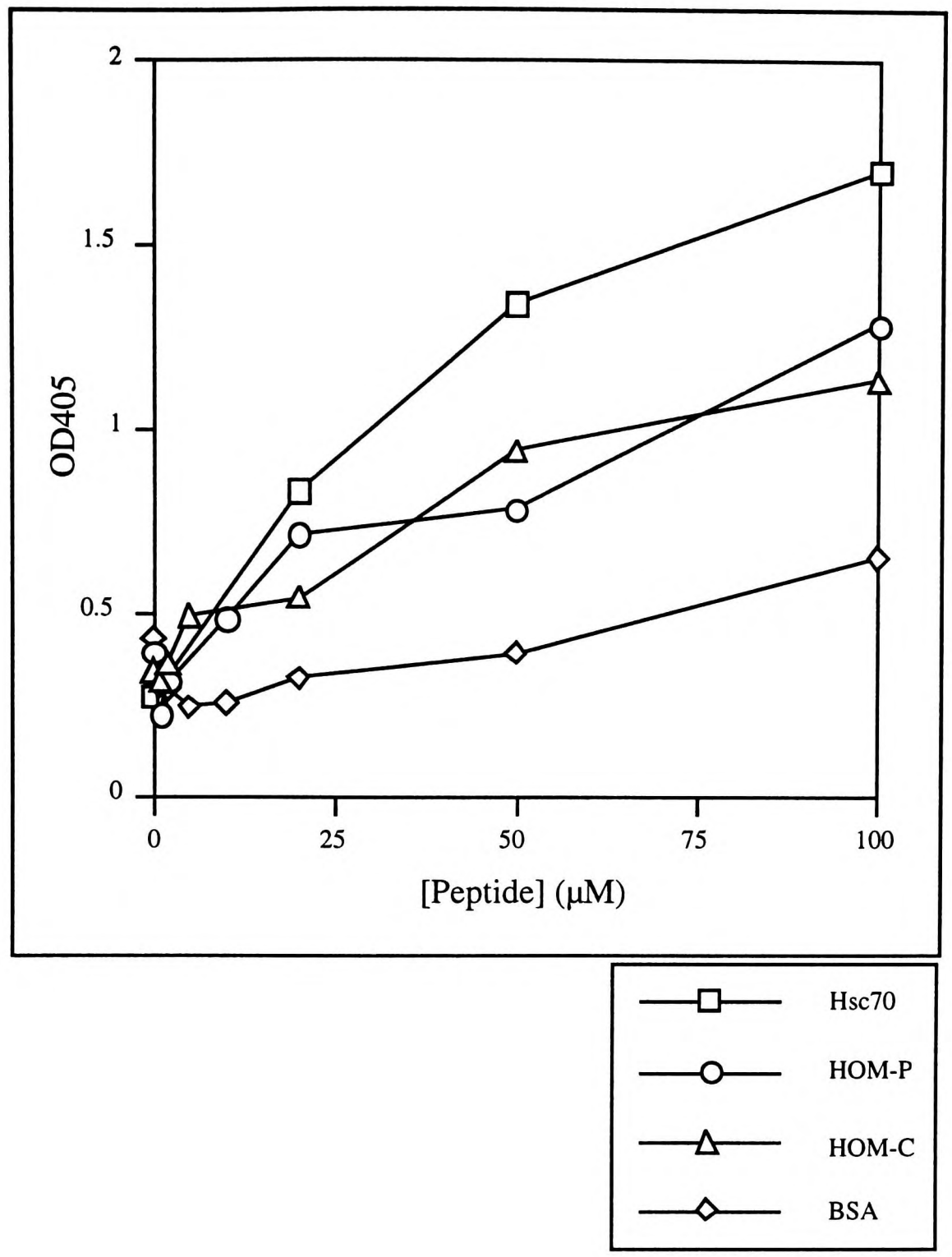

Figure 5-3: The binding peptide FYQLALT to HOM-P, HOM-C and hsc70. 1 μg each of HOM-P and HOM-C and 0.5 μg of hsc70 were bound onto plastic wells overnight and the wells were then blocked with BSA. A range of concentrations (0, 1, 2, 5, 10, 20, 50 and 100 μM) of peptide were added to the bound proteins, in duplicate. The bound peptide was detected with avidin-alkaline phosphatase conjugate and p-nitrophenyl phosphate. The OD_{405} values shown here were measured after 20 hours and averaged for each peptide value. HOM-P and HOM-C were purified by glutathione-affinity chromatography and thrombin cleavage [E7] and hsc70 was purified by ATP-affinity chromatography, by Dr. L. Greene and Dr. E. Eisenberg, University of Connecticut. All ran as single bands on SDS-PAGE.

(a) HOM-P

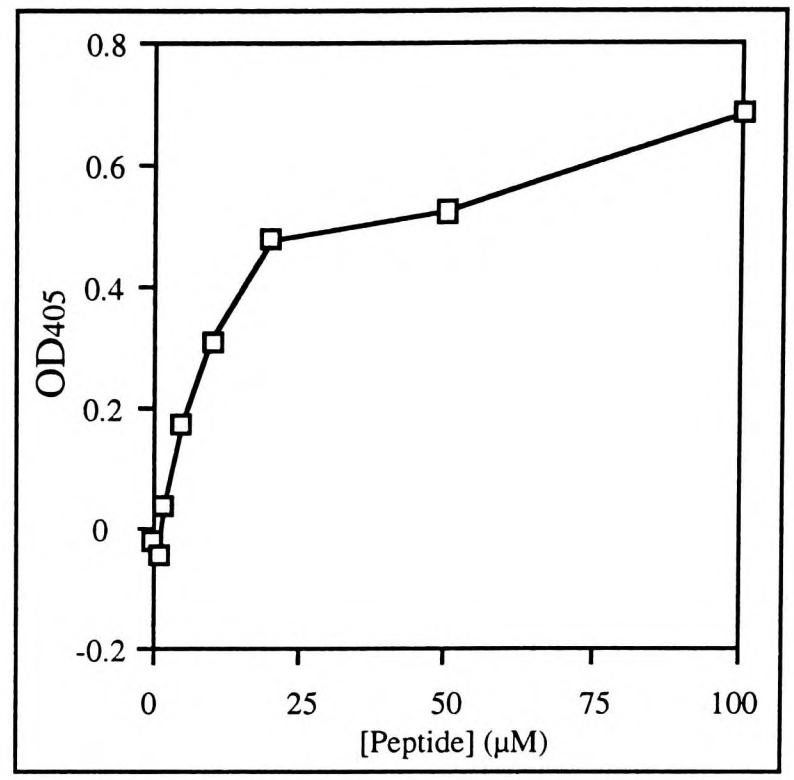
0.8
0.6
0.4
0.2
0
-0.2
OD405
0
25
50
75
100
[Peptide] (μM)

(b) HOM-C

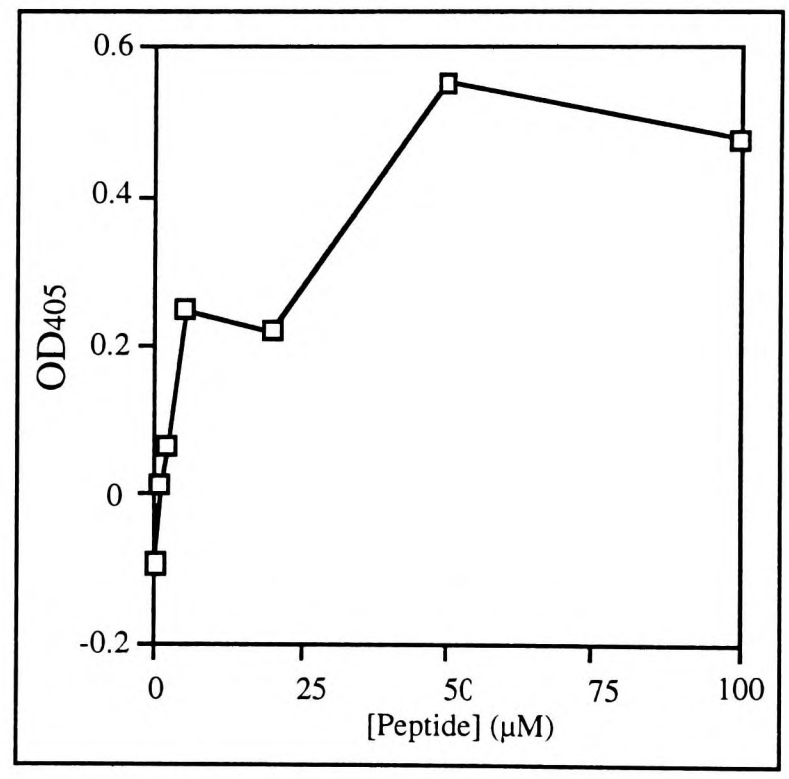
0.6
0.4
0.2
0
-0.2
OD405
0
25
50
75
100
[Peptide] (μM)

(c) hsc70

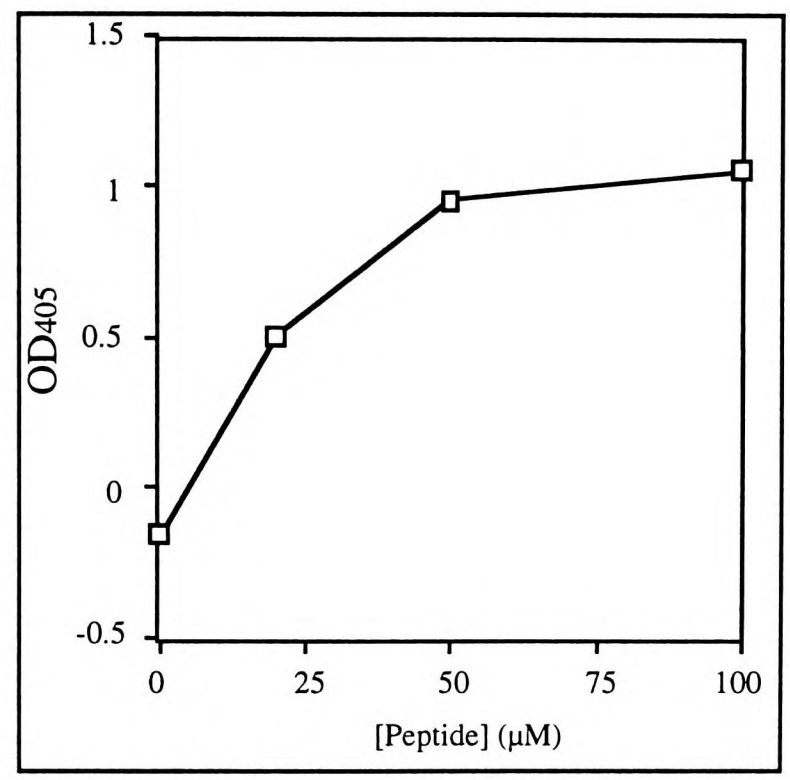

Figure 5-4: Binding of biotinylated FYQLALT to (a) HOM-P, (b) HOM-C and (c) hsc70 immobilised on 96 well plates. The data shown in Figure 5-3 was corrected for non-specific peptide binding by subtracting the OD_{405} values for empty wells blocked with BSA from the values for wells containing HOM-P, HOM-C and hsc70, which had also been blocked with BSA.

binding of the radiolabelled peptide to hsc70, dnaK and BiP (Kds < 5 μM) (Fourie *et al.*, 1994).

When using a biotinylated ligand, it is necessary to show that the interaction between the ligand and its binding protein is specific to the ligand rather than the biotin group. Therefore, it was necessary to show that binding of the biotinylated peptide to the peptide-binding proteins could be reduced by competition with unlabelled peptide. The amount of labelled peptide was kept constant (50 μM) and the amount of competing unlabelled peptide was varied (Figure 5-5). In the absence of competing peptide, the biotinylated peptide binds strongly to HOM-P. Addition of an equal quantity of unlabelled peptide reduces its binding by approximately half, as expected. This shows that the biotinylated peptide interacts with HOM-P through its peptide moiety, rather than through its biotin group. However, increasing the concentration of unlabelled peptide further does not increase its competition of the labelled peptide, and when the molar excess of the competing peptide is very high, the biotinylated peptide binds as strongly as in the absence of competing peptide. This is likely to be because the peptide FYQLALT is so hydrophobic that it tends to aggregate and precipitate at high concentrations; at high molar excesses, the biotinylated and non-biotinylated peptides are probably aggregating with each other and precipitating in the wells where the labelled peptide is detected by avidin-alkaline phosphatase.

The expressed fragments of hsp70hom, HOM-P and HOM-C, appear to bind as strongly to FYQLALT as hsc70, as indicated by their Kds. However, the production of pNPP by bound alkaline phosphatase indicates that wells containing HOM-P (19 kDa) and HOM-C (28 kDa) bind less peptide than wells containing hsc70 (70 kDa) (Figure 5-3), despite having a greater number of binding sites per milligram of protein. This suggests either that the hsc70 binds to the plate more efficiently, or that while equal quantities of protein bind in each case, more of the bound hsc70 is able to bind to the peptide. This could be because hsc70 is a larger molecule, so it is more likely to bind to the plate through a part of the molecule that is not essential for peptide binding, the ATPase domain for

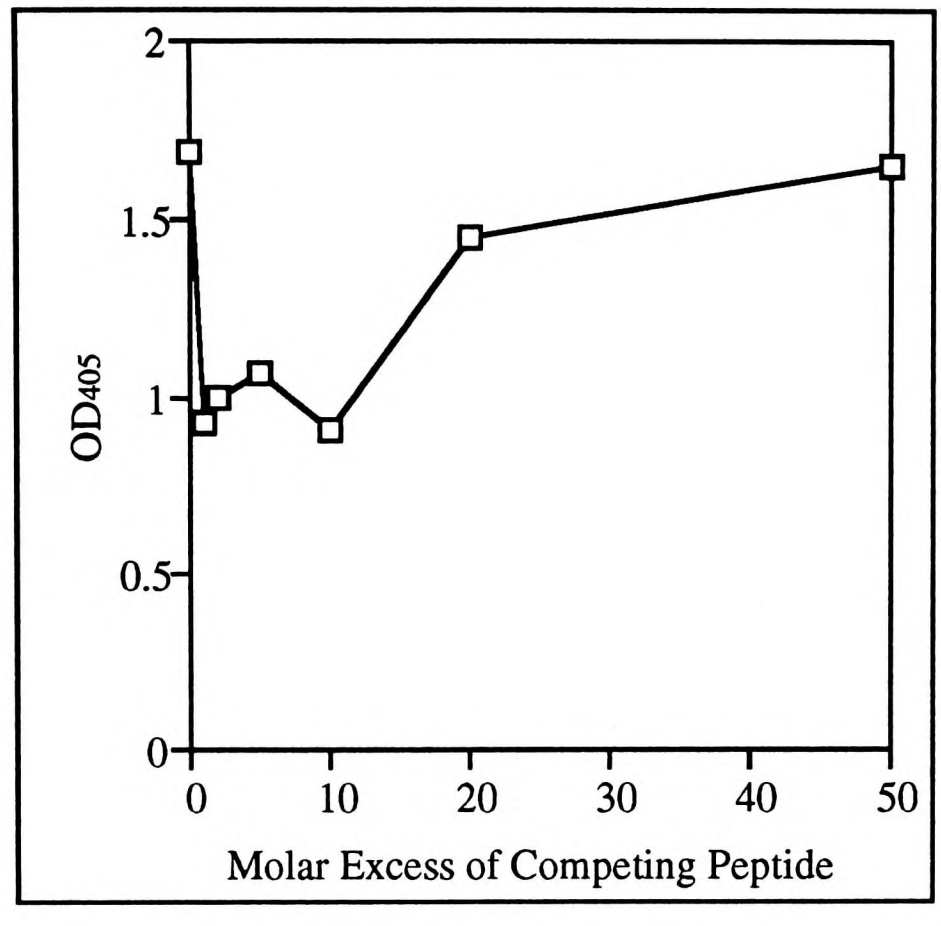

Figure 5-5: Unbiotinylated peptide competes with biotinylated FYQLALT for binding to HOM-P. Plastic wells were coated overnight with 0.2 μg of HOM-P and blocked with BSA. 50 μM biotinylated peptide was mixed with 0-50 fold molar excesses (0, 50, 100, 250, 500, 1000, 2500 μM) of unbiotinylated peptide and added to the wells in duplicate. The bound peptide was detected with avidin-alkaline phosphatase conjugate and p-nitrophenyl phosphate. The OD_{405} values shown here were measured after 24 hours and represent the average value for each set of conditions. HOM-P was purified by glutathione-affinity chromatography and thrombin cleavage [E7] and ran as a single band on SDS-PAGE.

example. Since the expressed proteins bind less peptide than hsc70, the OD_{405} values they produce are less high above the background seen with BSA, and therefore are less reliable than the values obtained for hsc70.

This system is not ideal for peptide-binding studies, because biotinylated FYQLALT binds to empty wells blocked with BSA to produce OD_{405} values that are 30%-50% of those for binding to hsc70, HOM-P and HOM-C. In addition, because the values are small, there is sufficient variation between duplicate wells to make it difficult to interpret studies that compare the binding of different peptides by competition with biotinylated FYQLALT. Part of the problem may be that FYQLALT is so hydrophobic that it tends to stick to plastic surfaces, including the wells. This also makes it difficult to biotinylate and purify.

Native gel electrophoresis

To avoid some of the problems with the binding of biotinylated FYQLALT to immobilised peptide-binding proteins, an alternative approach was developed. This was to detect the binding of the proteins to the permanently unfolded chaperone substrate, reduced and carboxymethylated α-lactalbumin (RCMLA) by native gel electrophoresis (Fourie *et al.*, 1994). This method can be developed to look at peptide binding in a competition assay, in which peptides compete with RCMLA for binding to the peptide-binding proteins.

The ability of HOM-P, HOM-C and hsc70 to form complexes with RCMLA was tested by this method. HOM-P, HOM-C and hsc70 were mixed with RCMLA in PBS containing 0.05% (v/v) Tween 20 (the buffer in which they bound to the biotinylated peptide FYQLALT) for two hours at room temperature and then separated by native gel electrophoresis. A sample of each protein alone was mixed with the same buffer and treated in the same way. The formation of a complex between the peptide-binding protein

and RCMLA is indicated by the appearance of a new species that is not present in either the chaperone or RCMLA alone.

In gel electrophoresis, larger molecules generally travel more slowly, and the smallest protein, RCMLA (14.6 kDa), travelled at the dye-front (Figure 5-6: lanes 2, 4, 6 and 7). HOM-C (28 kDa) forms two bands on native gels (lanes 5 and 6), despite migrating as a single band during denaturing (SDS) PAGE. These two bands are therefore likely to correspond to two different conformations of the protein. In contrast, HOM-P (19 kDa) exists in only one conformation (lanes 3 and 4), so the two conformations of HOM-C are probably caused by the additional 10 kDa of hsp70hom sequence expressed at the C-terminus of the latter. It has been proposed that this segment forms a lid over the top of the peptide-binding site, which opens and closes in response to ATP binding and hydrolysis in the ATPase domain (Zhu *et al.*, 1996), so the two differently migrating forms of HOM-C may correspond to the open and closed conformations.

A complex between RCMLA and HOM-C can be detected, since two bands can be seen clearly when the species are mixed (lane 6) which are not seen with either protein alone (lanes 5 and 7). While it may seem surprising that a complex should migrate more quickly than one of constituents when it must be larger than either, the C-terminal fragment of dnaK migrates more quickly in the presence of peptide NRLLLTG (Burkholder *et al.*, 1996), and some hsc70-peptide complexes run faster than hsc70 alone (Fourie *et al.*, 1994; Takenaka *et al.*, 1995). This may be explained if the domain adopts a more compact conformation when it binds to its substrate.

There is no indication that HOM-P binds to RCMLA (lane 4) as HOM-C is able to. This is surprising, as both are able to bind to biotinylated FYQLALT. This suggests that the C-terminal 10 kDa of hsp70hom is required for its interaction with RCMLA, but not with peptides. This agrees with the results of other studies with fragments of other hsp70s. While both hsp70 and hsc70 can bind to RCMLA, the peptide-binding domain of

hsp70 (amino acids 386-567 or 386-578) (Freeman *et al.*, 1995) and the 60 kDa fragment of hsc70 (amino acids 3-546) (Hu and Wang, 1996) which lack the C-terminal 10 kDa of the native proteins, could not, even though they can bind to peptides. However, the C-terminal segment (amino acids 386-641) is unable to interact with RCMLA when it is expressed in isolation (Hu and Wang, 1996), suggesting that its role is to stabilise the interactions between RCMLA and the peptide-binding domain, perhaps by closing as a lid over the peptide-binding site (Zhu *et al.*, 1996).

Hsc70 forms a faint smear with several bands in native polyacrylamide gels (lanes 1 and 2), despite forming a single strong band during denaturing gel electrophoresis (data not shown). Therefore, it is not possible to detect binding to RCMLA (lane 2). This result is surprising, as others have detected hsc70, purified in the same manner as the material used here, binding to RCMLA by native PAGE under apparently identical conditions (Fourie *et al.*, 1994).

The detection of complexes between HOM-C and RCMLA by native gel electrophoresis is not ideal for investigating the peptide-binding specificity of hsp70hom: the interaction of hsp70s with RCMLA is not well understood, and differs from their interaction with peptides in its requirement for their C-terminal 10 kDa (Hu and Wang, 1996). Therefore, experiments using peptides to compete with RCMLA for binding to HOM-C would be difficult to interpret. Furthermore, it would only be possible to measure the binding of RCMLA to HOM-C and its subsequent competition by different peptides semiquantitatively (Fourie *et al.* 1994).

Isothermal Titration Calorimetry

To detect peptide binding directly and avoid the problems associated with detecting binding to immobilised peptide-binding proteins, a third technique was used. Isothermal titration calorimetry is a powerful technique that detects intermolecular interactions as they

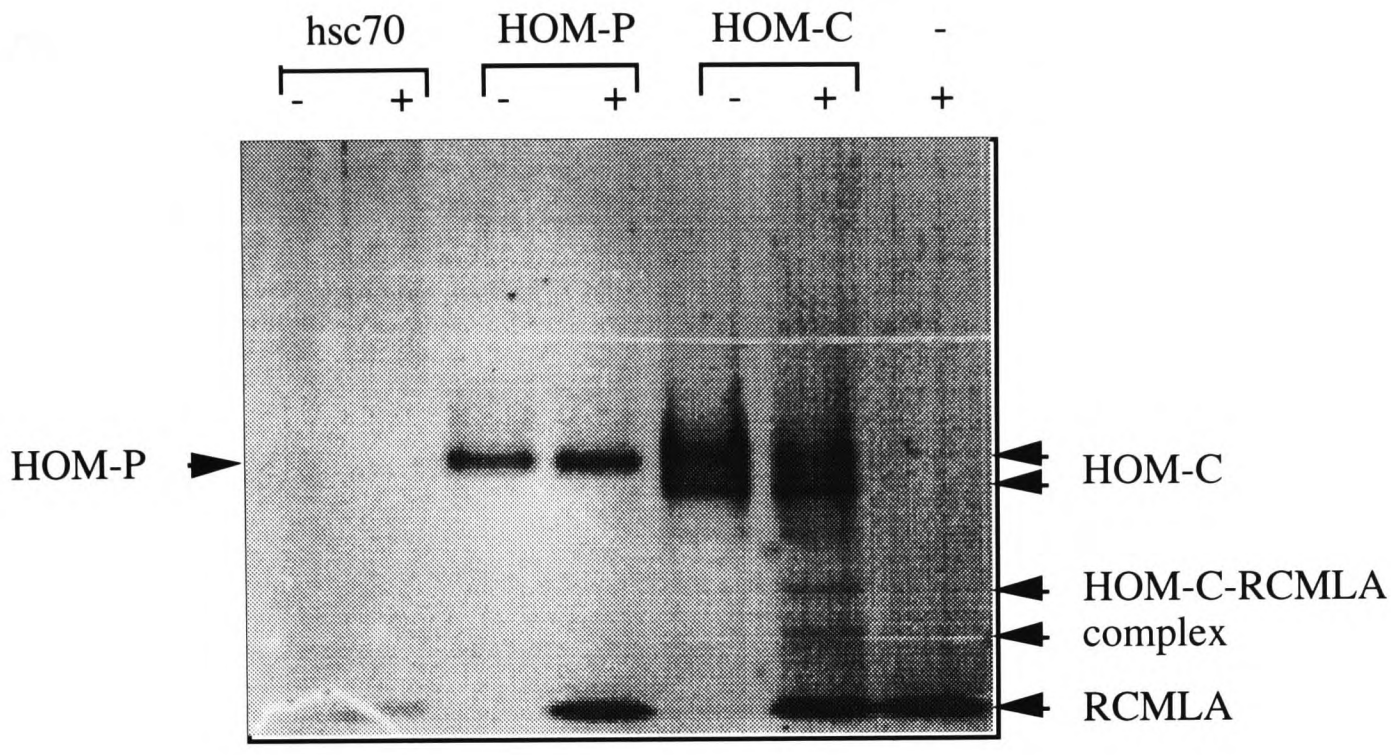

Figure 5-6: Native gel electrophoresis of hsc70, HOM-P and HOM-C mixed with RCMLA. 0.5 μg hsc70 (1.4 μM, lanes 1 and 2), 1 μg HOM-P (5 μM, lanes 3 and 4) or 3 μg HOM-C (3 μM, lanes 5 and 6) alone or mixing with 60 μg RCMLA (40 μM, lanes 2, 4, 6 and 7) were incubated for two hours at room temperature and separated by gel electrophoresis under non-denaturing conditions [E2]. The HOM-P and HOM-C samples used were purified by reverse-phase HPLC [E9] and were pure according to mass spectrometry analysis [E13]. Hsc70 was purified by ATP-affinity chromatography and ran as a single band on SDS-PAGE [E1] (data not shown).

happen in solution, and can determine the thermodynamics of binding (Ladbury and Chowdhry, 1996). It measures the heat released or absorbed as molecules bind (ΔH), allowing binding to be detected and a dissociation constant measured. The dissociation constant can be used to calculate the free energy change (ΔG) of binding and from this together with the value for ΔH, the change in entropy, or disorder, (ΔS) can be calculated. These parameters can indicate which sorts of intermolecular interactions provide the driving force for the binding reaction.

Isothermal titration calorimetry [E19] was first used to follow the binding of a peptide from pigeon cytochrome c, (Pc 81-104) to the peptide-binding domains of hsp70hom and PBP74. This peptide (IFAGIKKKAERADLIAYLKQATAK) has already been shown to bind to PBP74 (Lakey *et al.*, 1987) as well as several other hsp70s, including hsc70 (Takenaka *et al.*, 1995), BiP (Domanico *et al.*, 1993) and hsp70 from *Mycobacterium tuberculosis* (Roman *et al.*, 1994). It was made by removing the haem group from pigeon cytochrome c and cleaving the resulting apocytochrome c with cyanogen bromide (Solinger *et al.*, 1979) [E16]. Peptide 81-105 was then purified from the other cleavage products and remaining intact protein by reverse phase HPLC (Figure 5-7). The contents of the different peaks were identified by N-terminal sequencing [E11]. The second major peak, which eluted after 45 minutes, had the N-terminal sequence IFAGI, indicating that it corresponded to peptide 81-105. It was lyophilised, resuspended in 0.5 x PBS and quantified by amino acid analysis [E12]. The total yield was 101 nmol, i.e. approximately one quarter of the maximum possible yield from 5 mg (400 nmol) of pigeon cytochrome c.

The peptide-binding domains (250 μM) were added incrementally in sixteen 15 μl aliquots to 1.3 ml of cytochrome c peptide (25 μM) in 0.5 x PBS, or, as a control to determine the heat of dilution, to 0.5 x PBS alone. The binding of both PBP-P (Figure 5-7) and HOM-P (data not shown) to the pigeon cytochrome c peptide could be detected at 25 °C. The heat change measured when PBP-P is added to the peptide (bottom trace) is at least twice that measured when the peptide is diluted with buffer alone (top trace).

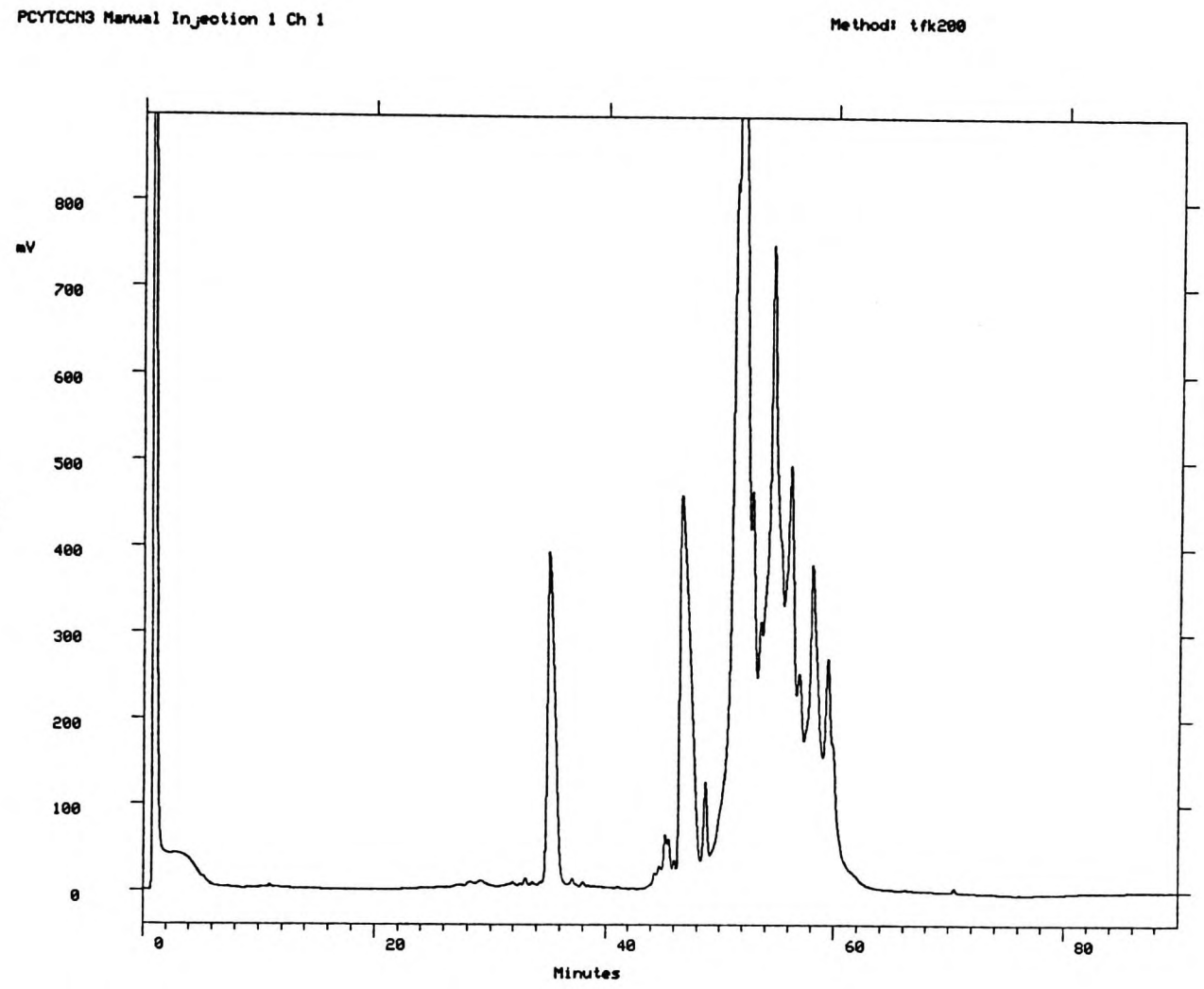

OD_{215}

Figure 5-7: Purification of the pigeon cytochrome c peptide 81-104 by reverse-phase HPLC [E9]. Pigeon apocytochrome c was cleaved with cyanogen bromide [E16] and loaded onto a C4 column equilibrated in 0.1% (v/v) TFA, 2% (v/v) acetonitrile (3 ml/min flow rate). A linear gradient of 2-50% (v/v) acetonitrile was applied over 50 minutes and a further gradient of 50-90% acetonitrile over 18 minutes. All the major peaks were collected and identified by N-terminal sequencing.

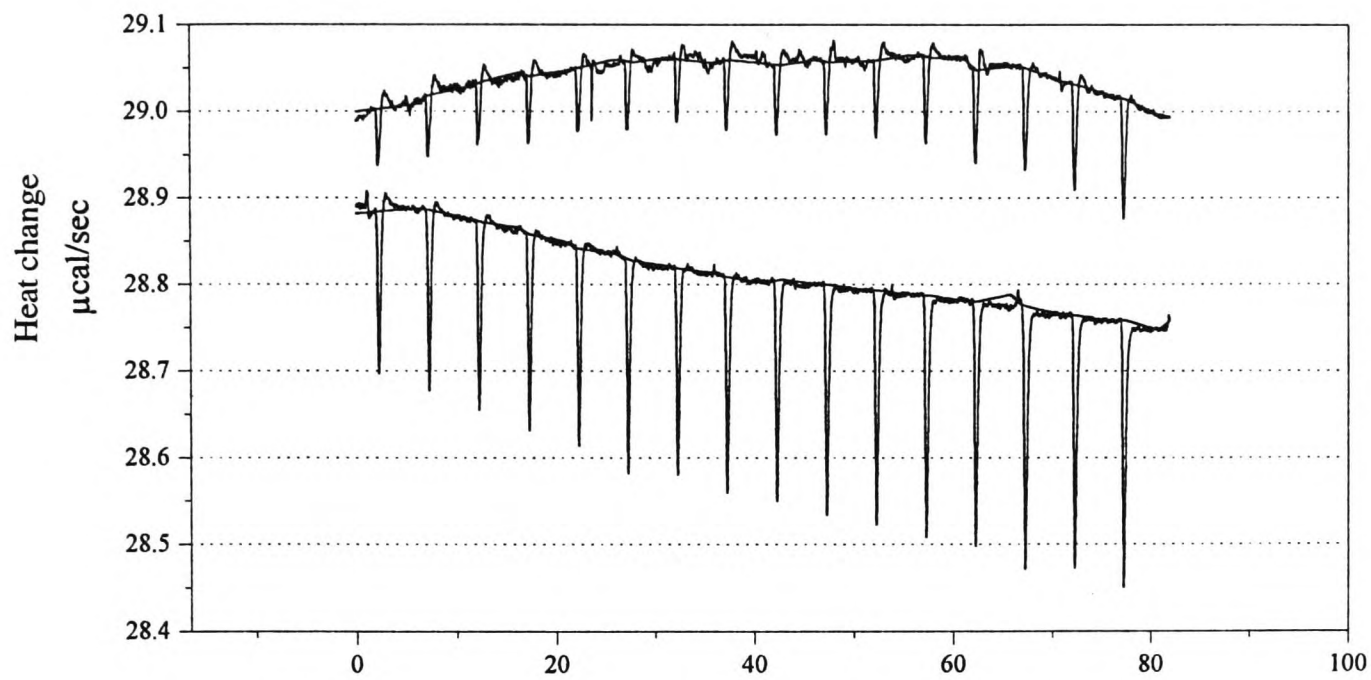

Figure 5-8: Detection of PBP-P binding to the pigeon cytochrome c peptide 81-104 by isothermal titration calorimetry. The peptide-binding domain of PBP74 (250 µM) was added in sixteen 15 µl aliquots to 1.3 ml of cytochrome c peptide (25 µM) in 0.5 x PBS (bottom trace), or, as a control, to 0.5 x PBS alone (top trace). As heat is released during binding (bottom) or dilution (top and bottom), the amount of heat (µcal/s) necessary to maintain a constant temperature in the calorimeter falls, producing a trough. The area of the trough is therefore proportional to the amount of heat released. The experiment was carried out at 25 °C, using an MCS Type isothermal titration calorimeter (MicroCal).

However, this heat change is too weak to make it possible to determine the dissociation constant for the reaction. Since the heat change of interactions is temperature-dependent, the experiment was repeated at 20 °C, but the heat change of binding was not significantly different at this temperature (data not shown). The heat change (ΔH) of binding at 25 °C was approximately -3 μCal per injection in both experiments.

Since each injection of peptide-binding domain (15 μl of 250 μM) contained 37.5 pmol, the ΔH is -800 Cal/mol = -3 kJ/mol. In combination with the dissociation constant of the interaction, the other thermodynamic parameters can be calculated. The second law of thermodynamics states that a favourable process releases 'free energy' (G), which is a combination of enthalpy or heat (H), and entropy or disorder (S):

$$\Delta G = \Delta H - T\Delta S,$$

where free energy, enthalpy and entropy are measured in kJ/mol and the temperature in Kelvin (°C + 273).

When ΔG is negative, a process is energetically favourable, and the size of ΔG determines the equilibrium constant:

$$\Delta G = -RT\ln K$$

The dissociation constant for the interaction of the pigeon cytochrome c peptide with hsc70 is 8 μM (Takenaka *et al.,* 1995). Its interaction with PBP74 is likely to be similar and, therefore, the binding constant (K_B), which is the reciprocal of the dissociation constant, will be assumed to be 10^5 M. Thus, the free energy of binding,

$$\Delta G_B = -RT\ln K_B = -8.31 \times 298 \times \ln (10^5) = -28 \text{ kJ/mol},$$

and the entropy change of binding,

$$\Delta S_B = (\Delta H_B - \Delta G_B)/T = 83 \text{ J/mol/K}.$$

The entropy term ($T\Delta S_B$) at 25 °C (298 K) is therefore 25 kJ/mol, which is much larger than the enthalpy term (ΔH_B), which is 3 kJ/mol. Therefore, the interaction of the peptide

with the peptide-binding domain of PBP74 appears to be entropically driven. Formation of non-covalent bonds, such as electrostatic or hydrogen bonds, releases heat energy, while hydrophobic interactions are entropically-driven, because they remove water from the hydrophobic surfaces involved. This is because water molecules cannot hydrogen bond with non-polar surfaces, so they adopt a very ordered arrangement to maximise the number of hydrogen bonds with each other. Thus, when two hydrophobic surfaces are brought together and water is released, disorder or entropy increases. The importance of hydrophobic peptide side chains in binding to hsp70s has been indicated by the experiments reviewed in the introduction to this chapter, and this is supported by the results of isothermal titration calorimetry. The X-ray structure of dnaK bound to the peptide NRLLLTG shows that several hydrogen bonds are formed with the peptide backbone, and these are likely to be conserved in the interaction between PBP74 and the cytochrome c peptide (see Chapter 5). It is likely to be the heat change as these are formed that is detected by isothermal titration calorimetry.

The interaction of the peptide-binding domain of hsp70hom with the peptide FYQLALT was also measured by isothermal calorimetry. HOM-P (100 μM), or 0.5 x PBS alone, were added to 10 μM peptide in fifteen 15 μl aliquots at 25 °C. The heat change (ΔH_B) was measured as before, and was approximately 10 kJ/mol (data not shown). In this case, ΔS_B=60 J/mol/K, assuming a K_B of 10^5. Therefore, the thermodynamics of hsp70hom binding to FYQLALT are very similar to those of binding to the peptide from pigeon cytochrome c. As the enthalpy term (ΔH_B) is somewhat higher, the entropy term ($T\Delta S_B$) at 25 °C is slightly lower (18 kJ/mol). Nevertheless, the binding is still entropically driven and is likely to involve similar interactions between the peptide-binding domain and the peptide.

It might be profitable to repeat the isothermal titration calorimetry experiments with the peptide and the peptide-binding domain at higher concentrations. However, the heat of

dilution of the peptide would also increase, so it may be difficult to overcome the small heat of binding for the interaction.

Discussion

This study is the first to demonstrate that hsp70hom binds to peptides. The recombinant peptide-binding domain of hsp70hom, with (HOM-C) or without (HOM-P) the C-terminus of the protein, binds to biotinylated FYQLALT with high affinity (Kd < 25 μM). This binding can be reduced by competition with unbiotinylated peptide, showing that the interaction is not dependent on labelling with the biotin group. The formation of a complex between the unfolded protein RCMLA and the C-terminal half of hsp70hom (HOM-C), but not the peptide-binding domain alone (HOM-P), can be detected by native gel electrophoresis, in agreement with experiments using other members of the hsp70 family (Freeman *et al.*, 1995; Hu and Wang, 1996). This suggests that the C-terminal 10 kDa of hsp70hom is necessary for its interaction with RCMLA. Interactions between the peptide-binding domain of hsp70hom and FYQLALT, and between the peptide-binding domains of hsp70hom or PBP74 and a peptide from pigeon cytochrome c (81-104) (a peptide which has been shown to bind to PBP74 (Lakey *et al.*, 1987) and many other members of the hsp70 family by a variety of techniques*) were also detected by isothermal titration calorimetry. This is the first study to investigate the thermodynamics of peptide-binding to hsp70s, using isothermal titration calorimetry. It suggests that the interaction is driven predominantly by an increase in entropy caused by bringing hydrophobic surfaces together, rather than by the release of enthalpy (heat energy) during the formation of non-covalent bonds. This work supports the structure of the complex between the C-terminal region of dnaK and the peptide NRLLLTG (Zhu *et al.*, 1996) and the model of hsp70hom binding to two peptides (NRLLLTG and FYLQLALT) (see Chapter 5), which demonstrate the importance to the interaction of hydrophobic amino acids being brought together by weak Van der Waals forces. Unfortunately, because the heat of binding was small relative

---

* For example, immobilising the peptide (Lakey *et al.*, 1987; Domanico *et al.*, 1993) or labelling it, with tritium (Takenaka *et al.*, 1995) or biotin (Roman *et al.*, 1994).

to the heat of dilution, it was not possible to determine a dissociation constant for the binding of the pigeon cytochrome c peptide to either of the peptide-binding domains.

None of the assays used is ideal for studying the peptide-binding affinity of hsp70s, so a better peptide-binding assay needs to be developed. It might be possible to improve the plate-binding assay by immobilising the GST fusion proteins rather than the isolated domains on the plate, to make a larger proportion of the peptide-binding sites accessible to peptide binding. However, the GST part of the molecule could bind peptides itself, producing artefactual results. Such considerations also apply to the use of the fusion proteins immobilised on glutathione agarose. Isothermal titration calorimetry might be more successful if the concentration of the peptide and peptide-binding domains were increased. It would be interesting to compare the thermodynamics of several peptides binding to the PBP74 and hsp70hom peptide-binding domains. If they differed from one another only in single amino acids, it would be possible to relate thermodynamics to the properties of particular amino acids in, say, heptameric peptides. It would also be interesting to try shorter peptides and even single amino acids.

A reliable peptide-binding assay would be useful to examine the affinity of hsp70hom for a panel of short peptides, which would indicate whether its specificity is broadly similar to that of the well-characterised hsp70s. Mutagenesis of binding peptides could be used to examine the contribution of different positions (Fourie *et al.*, 1994; Gragerov *et al.*, 1994). HOM-P and HOM-C could be used for phage display (Fourie *et al.*, 1994; Gragerov *et al.*, 1994; Takenaka *et al.*, 1995) or selection of random peptides (Flynn *et al.*, 1991). However, in these studies the phage or peptides would have to be eluted with acid rather than ATP, because the proteins do not include the ATPase domain. Therefore, peptides bound elsewhere than to the peptide-binding site might be released to produce misleading results. These studies should be repeated with the known allelic variants of hsp70hom, to determine what effects a mutation in the peptide-binding domain (Milner and Campbell, 1992) and the C-terminal lid (Miss. S. Jenkins, personal communication) may have on

peptide binding by hsp70hom. Expression of the mutant proteins or their peptide-binding domains for peptide-binding studies will be a key step in examining a possible functional role for these mutations.

Chapter 6: Hsp70s in Endocytic Compartments

Subcellular Localisation of PBP74

Hsp70s have been implicated in the processing of antigens for presentation by MHC class II molecules by a range of evidence (reviewed in Chapter 1). In particular, a role has been suggested for a constitutive human hsp70 called PBP74 in the class II pathway of antigen processing, because antibodies against it inhibit antigen presentation by MHC class II molecules (Lakey *et al.*, 1987). PBP74 was localised to early endosomes (VanBuskirk *et al.*, 1991) and cytoplasmic vesicles that were not part of mitochondria, the plasma membrane or the nucleus (Domanico *et al.*, 1993), suggesting that it might be involved in unfolding endocytosed antigens and preventing antigenic peptides from being degraded to amino acids. However, other researchers have suggested alternative localisations for this protein. PBP74 has been independently discovered as mortalin, a protein involved in immortalisation, that has been shown to be localised to the cytoplasm of mortal fibroblast cells and the perinuclear region of immortal fibroblasts (Wadhwa *et al.*, 1993a; Wadhwa *et al.*, 1993b). It also corresponds to the murine C3H-strain specific antigen (CSA) (Michikawa *et al.*, 1993b), which was first described as uniformly dispersed in the cytoplasm (Kusabe *et al.*, 1988) and has since been localised to the mitochondrion (Michikawa *et al.*, 1993b). In addition, mortalin has been detected in mitochondria by subcellular fractionation and N-terminal sequencing during tetrafluoroethyl-cysteine-mediated nephrotoxicity (Bruschi *et al.*, 1993). Therefore, the first stage of understanding the role of PBP74 in antigen processing has been to determine its intracellular location unambiguously.

It was decided to determine the intracellular localisation of PBP74 by immunofluorescence microscopy, which requires minimal manipulation of the cells and

yields clear answers, when used in combination with controls of known localisation. Several other studies looking at the localisation of PBP74 have used immunofluorescence microscopy, with contradictory results (VanBuskirk *et al.*, 1991; Domanico *et al.*, 1993; Michikawa *et al.*, 1993b; Wadhwa *et al.*, 1993b). These studies may be unreliable because, with the exception of Michikawa *et al.* (1993), polyclonal antibodies were used, and even monoclonal antibodies against an hsp70 may recognise an epitope shared by several members of the family. To overcome this problem, PBP74 was expressed in cultured cells with a C-terminal peptide epitope tag, so that it could be detected with a specific monoclonal antibody. To achieve this, the complete PBP74 coding sequence was amplified by PCR and cloned into the vector BS-Tag, in-frame with a sequence encoding the T7 peptide epitope tag.

Construction of BS-Tag Vector

The vector BS-Tag was derived from pBluescript [Chapter 2, Section C1] by inserting a sequence encoding the T7 tag, an epitope from the leader sequence of bacteriophage T7 gene 10 (Lutz-Freyermuth *et al.*, 1990; Tsai *et al.*, 1992), at its multiple cloning site. The tag sequence is flanked by an *Nco* I site at its 5' end and a *Bam*H I site at its 3' end, so that protein coding sequences can be cloned with the tag in-frame at either their N- or C-termini (see Figure 6-1).

The sequence encoding the T7 tag was synthesised as two complementary oligonucleotides which were annealed together and ligated into pBluescript. Two oligonucleotides, oligonucleotide 44 (ATGGCTAGCATGACTGGTGGACAGCAAATGGGTCGGGATCCATA) and oligonucleotide 48 (GATCTATGGATCCCGACCCATTTGCTGTCCACCAGTCATGCTAGCCAT) were synthesised [Chapter 2, section C10] and partially purified by reverse phase HPLC (Figure

M A S M T G G Q Q M G R D P *

CAGCCCATGGCTAGCATGACTGGTGGACAGCAAATGGGTCGGGATCCATA**GATCCAC**

GTCGGGTACCGATCGTACTGACCACCTGTCGTTTACCCAGCCCTAGGTATCTAG**GTG**

Figure 6-1. Cloning site of BS-Tag. The sequence derived from the oligonucleotides 44 and 48 is in plain text and the sequence from pBluescript KS+ is shown in bold. The *Nco* I (5') and *Bam*H I (3') restriction sites that flank the T7 tag sequence are underlined. The amino acid sequence of the T7 tag is also shown and the stop codon is indicated with a star.

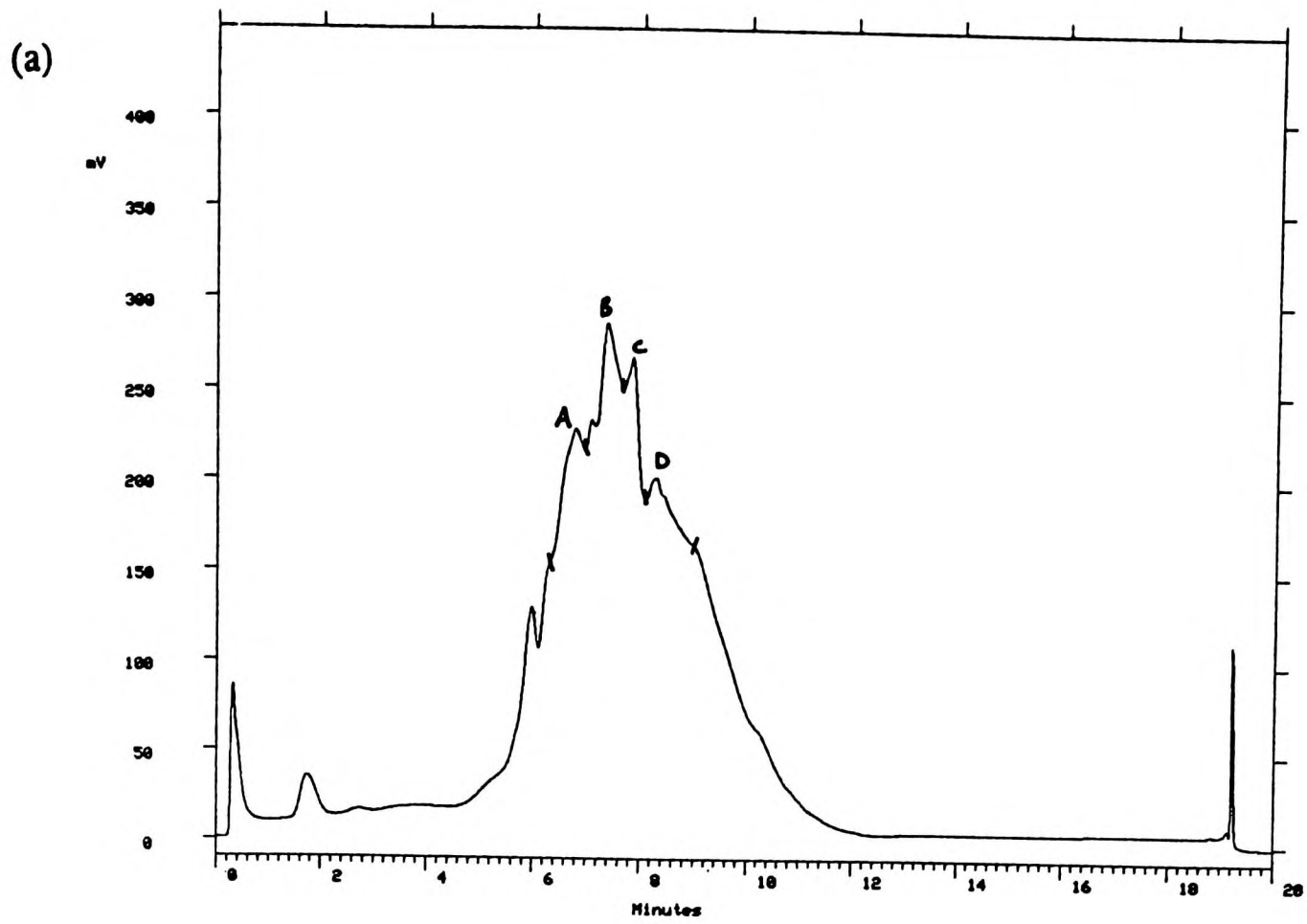

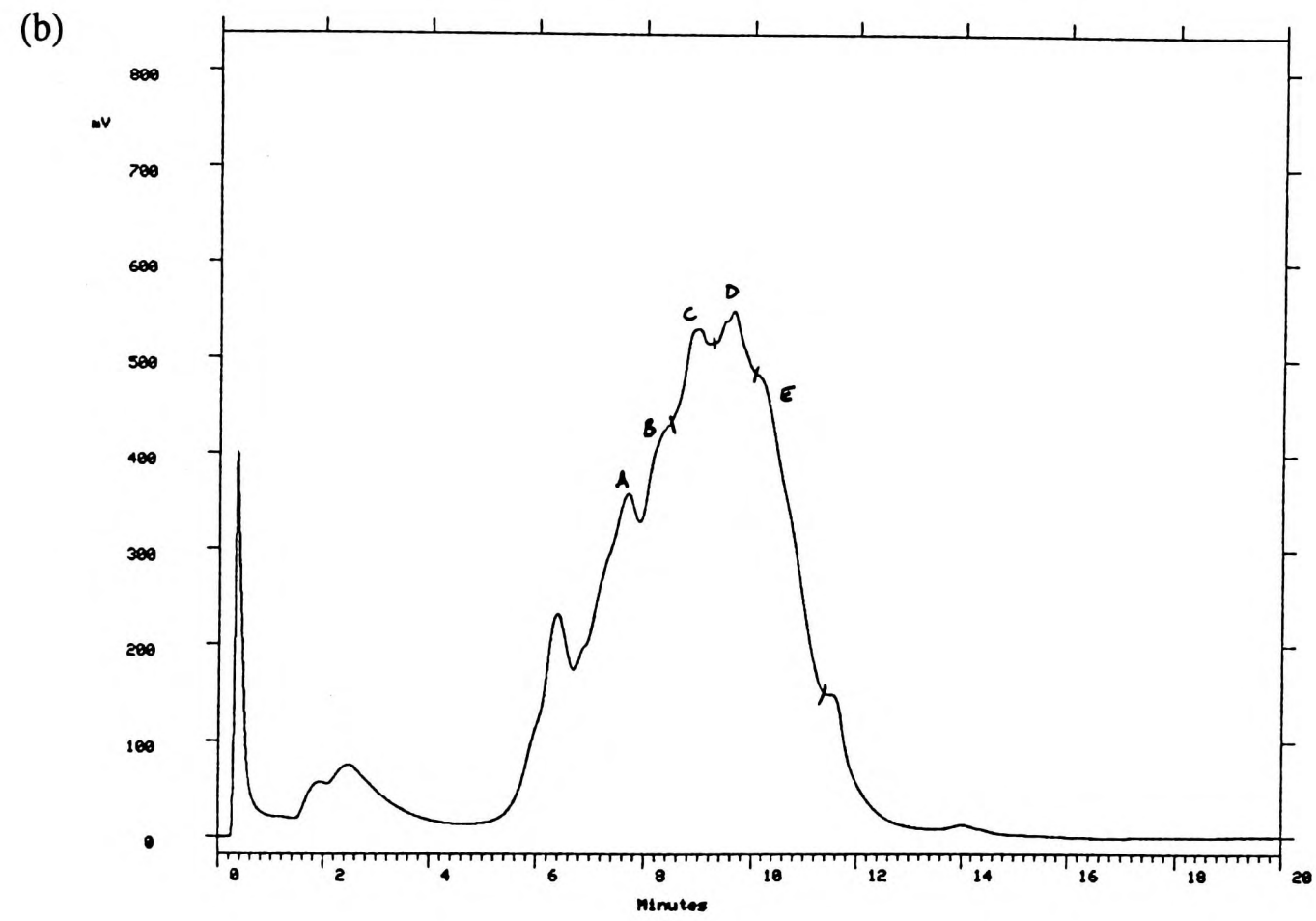

Figure 6-2: Purification of oligonucleotides (a) 44 and (b) 48 by reverse phase HPLC. Samples were mixed with 0.1% (v/v) TFA and loaded onto a Poros R/H reverse phase column (100 x 2 mm) that had been equilibrated with 100% (v/v) solvent A [0.1% (v/v) TFA]. These conditions were continued for 2 minutes, and then the proportion of solvent B [80% (v/v) acetonitrile, 0.1% (v/v) TFA] was increased to 100% (v/v) over 14 minutes. After 1 minute at 100 % (v/v) solvent B, the proportion of solvent B was returned to 0% (v/v) over five minutes. The peaks were collected as indicated.

6-2). Aliquots of the oligonucleotides in the HPLC fractions were labelled by phosphorylation with γ-[^{32}P] ATP [C11] and separated by 12% (w/v) acrylamide denaturing gel electrophoresis [C15], and oligonucleotides of known length were used as controls (data not shown). The full length oligonucleotides were identified in fraction C in both cases (Figure 6-3, lanes 4 and 7), so the full length oligonucleotides were purified from these fractions by 12% (w/v) acrylamide gel electrophoresis. The DNA was visualised by placing the gel on a thin layer chromatography plate and illuminating it with an ultraviolet lamp (ultraviolet shadowing). The highest molecular weight band in each lane was excised, and the oligonucleotides were eluted overnight at 37 °C, in 0.1% (w/v) SDS, 0.5 M ammonium acetate, 10 mM magnesium acetate, with shaking. The eluted oligonucleotides were ethanol precipitated [B2], resuspended in water, quantified spectrophotometrically [B3] and phosphorylated to allow them to be cloned. Prior to phosphorylation, the oligonucleotides (40 pmol of each) were heated at 90 °C for two minutes to remove any secondary structure and cooled rapidly on ice. They were then incubated for 1 hour at 37 °C with 20 U polynucleotide kinase (Boehringer) in the buffer recommended by the manufacturer containing 40 pmol of ATP. The solutions of oligonucleotides were combined, heated at 65 °C for 2 minutes and cooled slowly to room temperature to allow the phosphorylated primers to anneal together. The resulting double-stranded fragment has one blunt end and one *Bam*H I end, enabling it to be ligated into pBluescript KS$^+$ [C7] that had been digested with *Sma* I and *Bam*H I [C2], dephosphorylated [C6] and gel purified [C3]. Three of the clones obtained were analysed by double-stranded sequencing with the M13 universal primer [C14] and shown to contain the correct sequence.

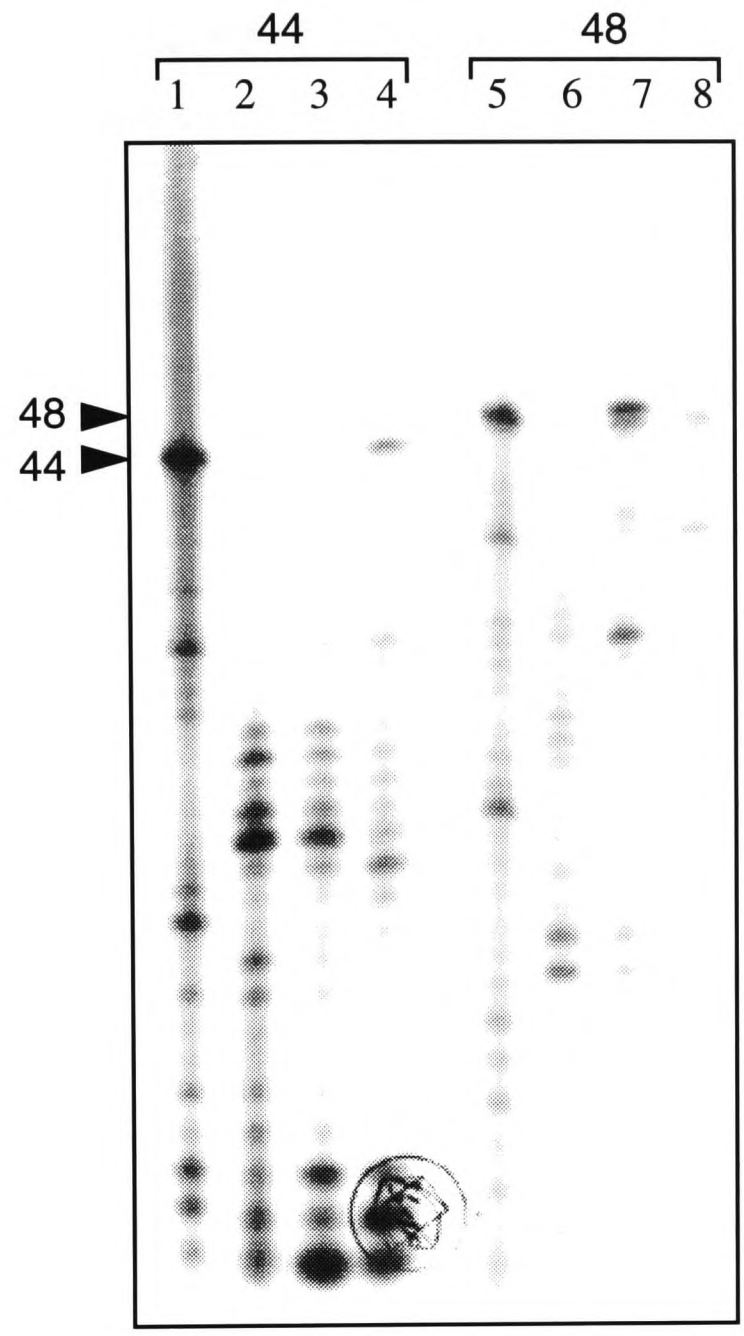

Figure 6-3: Separation of partially purified oligonucleotides by denaturing gel electrophoresis. Oligonucleotides 44 and 48 were partially purified by reverse phase HPLC (Figure 6-2). The unpurified oligonucleotides (lanes 1 and 5) and the HPLC fractions [fractions A (lane 2), B (lane 3) and C (lane 4) for oligonucleotide 44, and fractions B (lane 6), C (lane 7) and D (lane 8)] were labelled with γ-[^{32}P] ATP [C11] and separated by 12% (w/v) acrylamide denaturing gel electrophoresis [C15] to identify the fractions containing the full length oligonucleotides. The positions of the full length oligonucleotides are indicated with arrows.

Cloning and Epitope-Tagging of the PBP74 Coding Sequence

The complete PBP74 coding sequence (nucleotides 89-2128) (Domanico *et al.*, 1993) was amplified from first strand Raji cell cDNA [D2] by polymerase chain reaction (PCR), using primers 5' PBP and 3' PBP [C12]. Initially, PCR was carried out using the proof-reading enzyme *Tli* (Promega), but this did not yield a product of the correct size, even though the concentration of $MgCl_2$ was titrated (50 mM-250 mM) and the annealing temperature was varied (56 °C-68 °C). Hot-start PCR, in which the enzyme is added only after the template and primers had been denatured by incubation at 94 °C for 5 minutes, did not improve the PCR either. The sequence was successfully amplified using *Taq* DNA polymerase (Promega), which does not have proof-reading activity. The product contained an engineered *Bam*H I site at its 5' end and an engineered *Nco* I site at its 3' end. This was digested with *Nco* I (Promega) [C2], Klenow end-filled [C5], digested with *Bam*H I and gel purified [C3]. It was ligated [C7] into pBluescript KS+ that had been digested with *Bam*H I and *Hinc* II (Promega), dephosphorylated [C6] and gel purified. The cloned PBP74 coding sequence then had a *Bam*H I site at its 5' end and a regenerated *Nco* I site at its 3' end.

Single-stranded DNA from seven pBluescript clones containing the amplified PBP74 coding sequence was sequenced using primers PBPso1-so6 and the M13 universal primer [C14]. All of the clones were found to contain errors introduced during PCR, at a rate of approximately 1 in 500 base pairs. Two clones contained only one non-conservative point mutation each, at nucleotide 2033 (T>C) in clone 24 and at nucleotide 333 (T>C) in clone 28. Both clones were digested with *Sst* I, to generate a 1896 bp fragment (containing nucleotides 89 to 1953 of the PBP74 coding sequence and 32 bp of pBluescript) and a 3060 bp fragment (consisting of nucleotides 1953 to 2128 of the PBP74 sequence and the remaining 2885 bp of pBluescript). The 1896 bp fragment of clone 24 and the 3060 bp fragment of clone 28 were gel purified and ligated together. The orientation of the two fragments with respect to each other in the clones was checked by digestion with *Ava* I; the

correct orientation yielded a 1991 bp and a 2965 bp fragment, while the incorrect orientation produced a 267 bp and a 4689 bp fragment. A clone in the correct orientation, pBluescript clone 32, was confirmed to contain an error-free PBP74 sequence by single-stranded sequencing [C14].

The PBP74 coding sequence was then sub-cloned into the vector BS-Tag, by digesting pBluescript clone 32 with *Not* I, end-filling using Klenow and then digesting with *Nco* I. The 2058 bp fragment containing the PBP74 sequence and 19 bp of pBluescript was isolated by gel purification and ligated into BS-Tag digested with *Nco* I and *Hinc* II, joining the T7 tag to the 3' end of the PBP74 coding sequence. The tag was attached at the C-terminus of PBP74 because its N-terminus includes a leader peptide of 46 amino acids that is cleaved from the mature protein. The sequence encoding PBP74 plus the tag was excised from BS-Tag by digestion with *Bam*H I, end-filled using Klenow enzyme, gel purified and sub-cloned into the eukaryotic expression vector pcDNA3 that had been digested with *Eco*R V, for transient transfection experiments. The vector pcDNA3 uses the CMV promoter to express the protein of interest in any of a wide range of mammalian cell types, and can replicate as a plasmid in *E. coli* cells. The resultant clone was called pcDNA-PBPtag.

Immunofluorescence Microscopy

The localisation of the tagged PBP74 in mammalian cells was then investigated by immunofluorescence microscopy [F2]. A monkey kidney cell line (COS7) was transiently transfected [F1] with pcDNA3-PBPtag. Two days post-transfection, the cells were fixed, permeabilised with a mild detergent and incubated with the anti-tag monoclonal antibody or control antibodies. These antibodies were detected using a second antibody conjugated to a fluorescent molecule, which was visualised using a fluorescent microscope.

The pattern of fluorescence detected using the anti-tag antibody suggested that tagged PBP74 is localised in mitochondria (Figure 6-4a). This localisation was confirmed by staining transfected cells with Mitotracker, a membrane-soluble fluorescent molecule that is taken up by mitochondria and retained there by reacting with the thiol groups of mitochondrial proteins. Mitotracker fluoresces in the red spectrum while the secondary antibody used to detect PBP74 fluoresces green, so both can be detected independently in the same cell. Strong PBP74 staining is seen in a proportion of cells, representing those that were successfully transfected, while untransfected cells demonstrate weak vesicular staining with the anti-tag antibody (Figure 6-4a). Mitotracker stained both transfected and untransfected cells (Figure 6-4b), and in transfected cells, the patterns of PBP74 and Mitotracker fluorescence were identical. The localisation pattern of PBP74 was distinct from those of two antibodies kindly supplied by Dr. M. Marsh (University College, London), 1B5 and 2C2, that recognise markers of the endocytic pathway (data not shown). Thus, PBP74 is exclusively a mitochondrial protein. This finding has been confirmed by another study using tagged PBP74 (Dahlseid *et al.*, 1994), and cloning of the gene for mitochondrial hsp70 in rats and humans has shown that it is identical to PBP74 (Webster *et al.*, 1994; Bhattacharyya *et al.*, 1995). These results, therefore, support the earlier studies by Michikawa *et al.* (1993) and Bruschi *et al.* (1993).

Analysis of the Amino Acid Sequence of PBP74

A mitochondrial localisation for PBP74 is also suggested by analyses of its amino acid sequence. Comparison of the PBP74 amino acid sequence with protein sequences in the SwissProt and National Biomedical Research Foundation (NBRF) databases using the FastA program (GCG) show that it is most similar to the putative mitochondrial hsp70 of *Drosophila melanogaster* (78.7% identity), the mitochondrial hsp70s of yeast (65.2% identity with Ssc1p) and the cytoplasmic hsp70s of prokaryotes (60.1% identity with dnaK

(a)

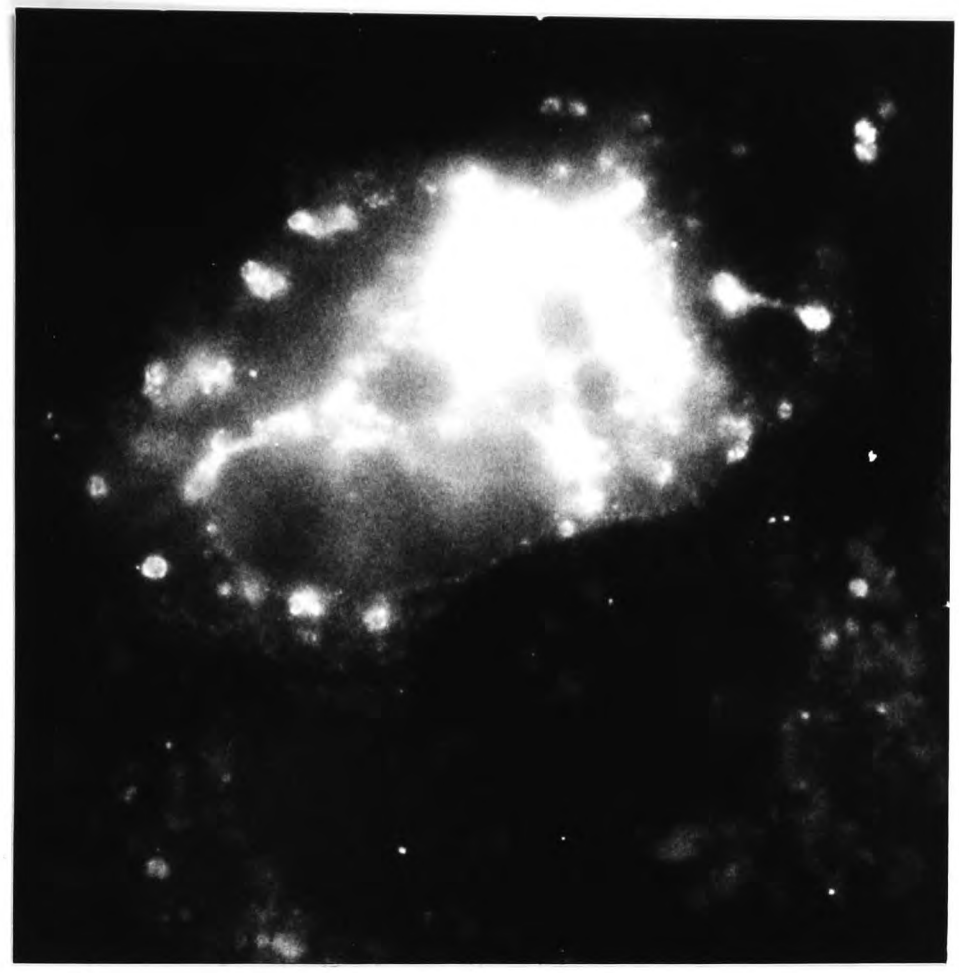

(b)

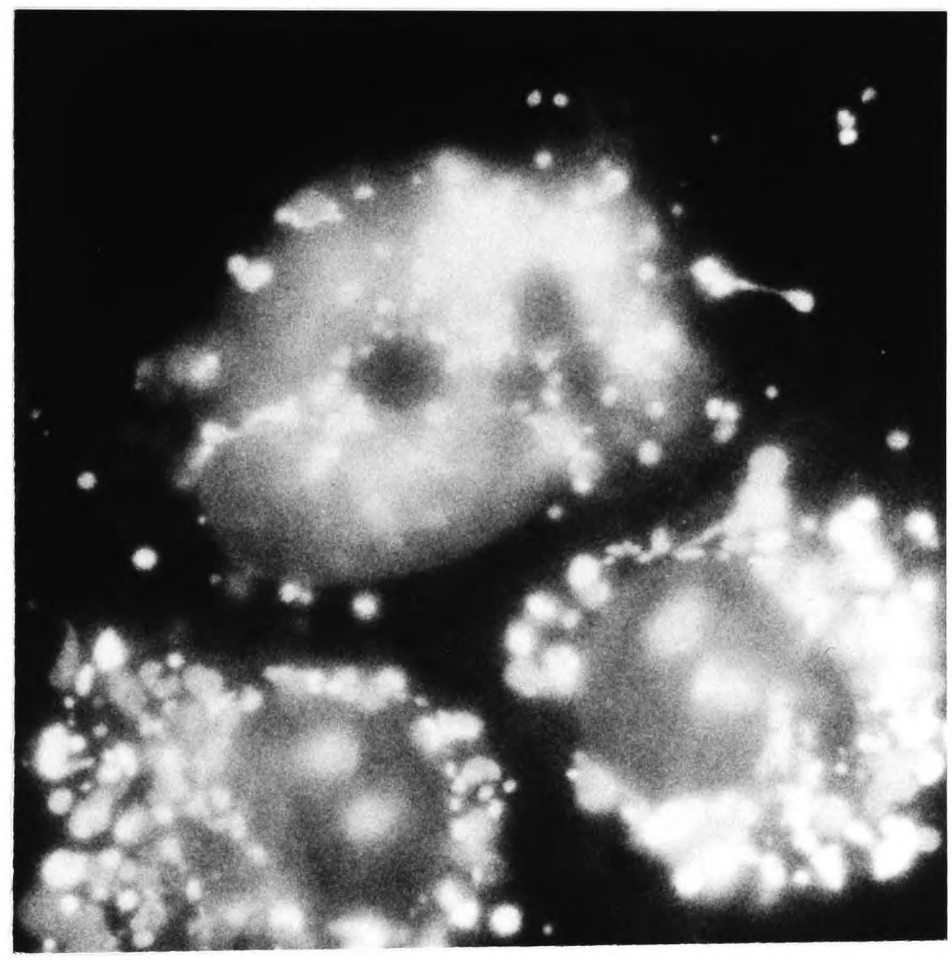

Figure 6-4: (a) Immunofluorescent localisation of PBP74 and (b) localisation of mitochondria in COS7 cells. Cells transfected with a vector expressing PBP74 with a C-terminal antigenic tag were treated with antibody against the tag and a mitochondrial stain, Mitotracker. The antibody was detected with an FITC-labelled secondary antibody that fluoresces green, while Mitotracker fluoresces red, enabling both to be detected independently in the same cell. Fluorescence was visualised with a Axioscop microscope (Zeiss).

of *E. coli)*. It is surprising that PBP74 is more similar to a protein found in prokaryotes than to other hsp70s in man (see Figure 6-5). This is additional evidence that it is a mitochondrial protein, because mitochondria are thought to have originated as a symbiotic prokaryotic organism endocytosed by an ancestor of eukaryotic cells.

The N-terminal leader sequence of PBP74 is not a typical mitochondrial targeting signal, which usually consists of a positively-charged amphiphilic α-helix 7-20 amino acids long (VonHeijne, 1988). In contrast, the leader sequence of PBP74 is 46 amino acids long, and using the Peptide Structure program (GCG), only the first 16 amino-acids of PBP74 are predicted to form an α-helix by both the Chou-Fasman and Garnier-Osguthorpe-Robson indices (Chou and Fasman, 1978; Garnier *et al.*, 1978) (data not shown). These 16 amino-acids include only three positive charges (the amino-terminus and two arginine residues) which are shown to be fairly evenly distributed around the putative helix by a helix-wheel plot created using the program Pepwheel (GCG; data not shown). Nevertheless, it clearly does function as a mitochondrial targeting signal (Dahlseid *et al.*, 1994; Bhattacharyya *et al.*, 1995).

Since PBP74 is the mitochondrial hsp70, it is unlikely to have a role in MHC class II antigen processing, despite evidence that antibodies raised against it can inhibit this process. Nevertheless, PBP74 may be involved in the processing of mitochondrial proteins for binding to MHC class I-related molecules (Shawar *et al.*, 1990), as mitochondrial hsp70 has been implicated in the ATP-dependent proteolytic degradation of misfolded proteins in the mitochondrial matrix by the protease PIM1 (Wagner *et al.*, 1994). It is not known how mitochondrial peptides are transported into the cytoplasm and thence to the ER (see Chapter 1).

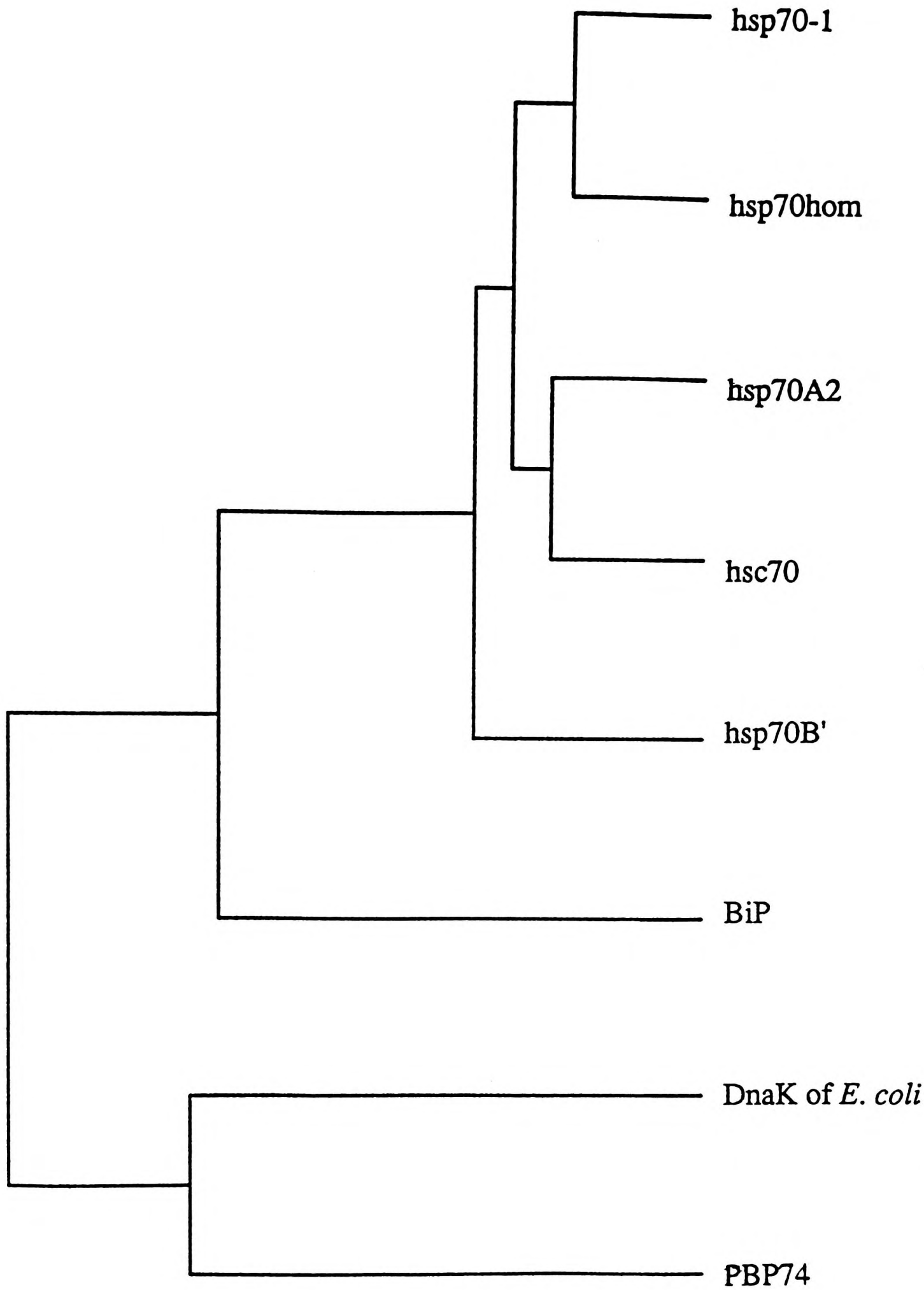

Figure 6-5. A dendrogram depicting the amino acid similarities between members of the human hsp70 family (see Figure 1-1) **and dnaK** (Bardwell and Craig, 1984). The distance on the horizontal axis is proportional to the difference between sequences. The dendrogram was plotted using the Pile Up program of GCG.

Other Hsp70s in Endocytic Compartments

Although PBP74, an hsp70 implicated in antigen processing in endocytic compartments, has turned out to be the mitochondrial hsp70, several lines of evidence suggest that other members of the hsp70 family may be involved in the generation of class II molecule-peptide complexes: antibodies against hsp70s inhibit the class II pathway of antigen processing (Lakey *et al.*, 1987; Manara *et al.*, 1993) and preliminary results from Pierce and colleagues indicate that a 70 kDa protein immunologically related to PBP74 can be immunoprecipitated from the MHC class II loading compartment (MIIC) (unpublished data quoted in Dahlseid *et al.,* 1994); heat shock stimulates the presentation of certain antigens by class II molecules (Cristau *et al.*, 1994; Mariethoz *et al.*, 1994); hsc70 may be involved in the transport of certain class II allotypes through the endocytic pathway (Auger *et al.*, 1996); and the fact that peptides derived from hsc70 are presented by class II molecules supports the idea that hsc70 has access to the class II antigen processing pathway (Newcomb and Cresswell, 1993). Therefore, it was important to determine whether members of the hsp70 family are present in endocytic compartments. A strategy was adopted that used antibodies to detect hsp70s in endocytic compartments purified from antigen presenting cells. The chosen antibodies recognise many different members of the hsp70 family, and this means that they are also likely to recognise any undiscovered hsp70s. Any hsp70s detected by these antibodies in endocytic compartments could then be immunoprecipitated and identified by N-terminal sequencing. A novel endocytic hsp70 could be cloned, and its role in antigen processing investigated further.

Density Gradient Centrifugation

B cells were chosen as a model antigen presenting cell because their pathways of endocytosis and antigen processing by B cells are well characterised (Amigorena *et al.*, 1994; West *et al.*, 1994; Xu and Pierce, 1995) and their endocytic compartments have been purified successfully from cell lysates by Percoll density gradient centrifugation (Davidson and Watts, 1989; Qiu *et al.*, 1994; Castellino and Germain, 1995). Percoll was chosen as the gradient medium for several reasons: being a large molecule, it forms density gradients rapidly during centrifugation; it has a low viscosity, so organelles adopt their positions in the gradients quickly; its very low osmolarity means that it does not absorb water from vesicles and change their density during centrifugation; and since it is chemically inert, it does not interfere with enzymatic assays or SDS-polyacrylamide gel electrophoresis.

Percoll density gradient centrifugation was carried out as follows [F3]. Raji cells (a cell line derived from a human Burkitt's lymphoma) were lysed by homogenisation in an iso-osmotic solution containing sucrose, rather than salts which cause subcellular particles to aggregate. The homogenate was first centrifuged at a low speed (2 000 g for 10 minutes), to separate vesicles according to their size, so that large organelles such as nuclei, mitochondria and plasma membrane sheets which sediment quickly could be discarded. The resulting post-nuclear supernatant contains the smaller organelles of interest and was layered onto homogenisation buffer containing 20% (v/v) Percoll and centrifuged at 25 000 g for 20 minutes to separate the vesicles on the basis of density. During the centrifugation, the vesicles adopt their position in the gradient as it is established, while soluble molecules in the homogenate will remain in the layer at the top of the gradient.

Percoll density gradients were fractionated and characterised by enzymatic assay and western blotting [E4]. ß-hexosaminidase, a deglycosylating enzyme found in endosomes

and lysosomes, was assayed using a fluorogenic substrate, p-nitrophenyl N-acetyl-ß-D-glucosaminide [F4] (Marsh *et al.*, 1987). An antibody against HLA-DM (Sanderson *et al.*, 1996), was used to detect the rough endoplasmic reticulum (ER), where DM is synthesised, and a dense lysosome-like compartment called the MHC class II loading compartment (MIIC), to which it is transported, while an antibody against MHC class I (Stam *et al.*, 1986) showed the position of the rough ER and the plasma membrane. The differences between the localisation patterns of class I molecules and HLA-DM, therefore, allow the ER, plasma membrane and MIIC to be distinguished from each other.

Ball Bearing Homogenisation

Several methods of homogenisation were investigated. Initially, a ball-bearing homogeniser (provided by Dr. J. Trowsdale, Imperial Cancer Research Fund Laboratories, London) was used (Amigorena *et al.*, 1994; West *et al.*, 1994) and the fractions were analysed by ß-hexosaminidase assay (Figure 6-6) and western blotting with antibodies against MHC class I molecules and HLA-DM (Figure 6-7). The results are displayed with fractions from the top of the gradient which contain the less dense vesicles at the left-hand side of the gradient, and fractions from the bottom of the gradient, containing the denser vesicles, on the right. ß-hexosaminidase activity is concentrated in the least dense and most dense fractions of the gradient (especially fractions 4 and 13), which contain endosomes and lysosomes respectively. MHC class I and DM molecules are found predominantly in fractions 3 and 4, while DM is also present in fractions 12-13. Therefore, fractions 12 and 13 contain the dense lysosome-like MIIC, while fractions 3 and 4 contain the ER and plasma membrane. Vesicles derived from the plasma membrane appear to have a wider range of densities than ER vesicles, because the distribution of class I molecules (fractions 2-5) is broader than that of DM (fractions 3-4) in this region. This procedure is not an effective means of separating the ER from endosomes and plasma

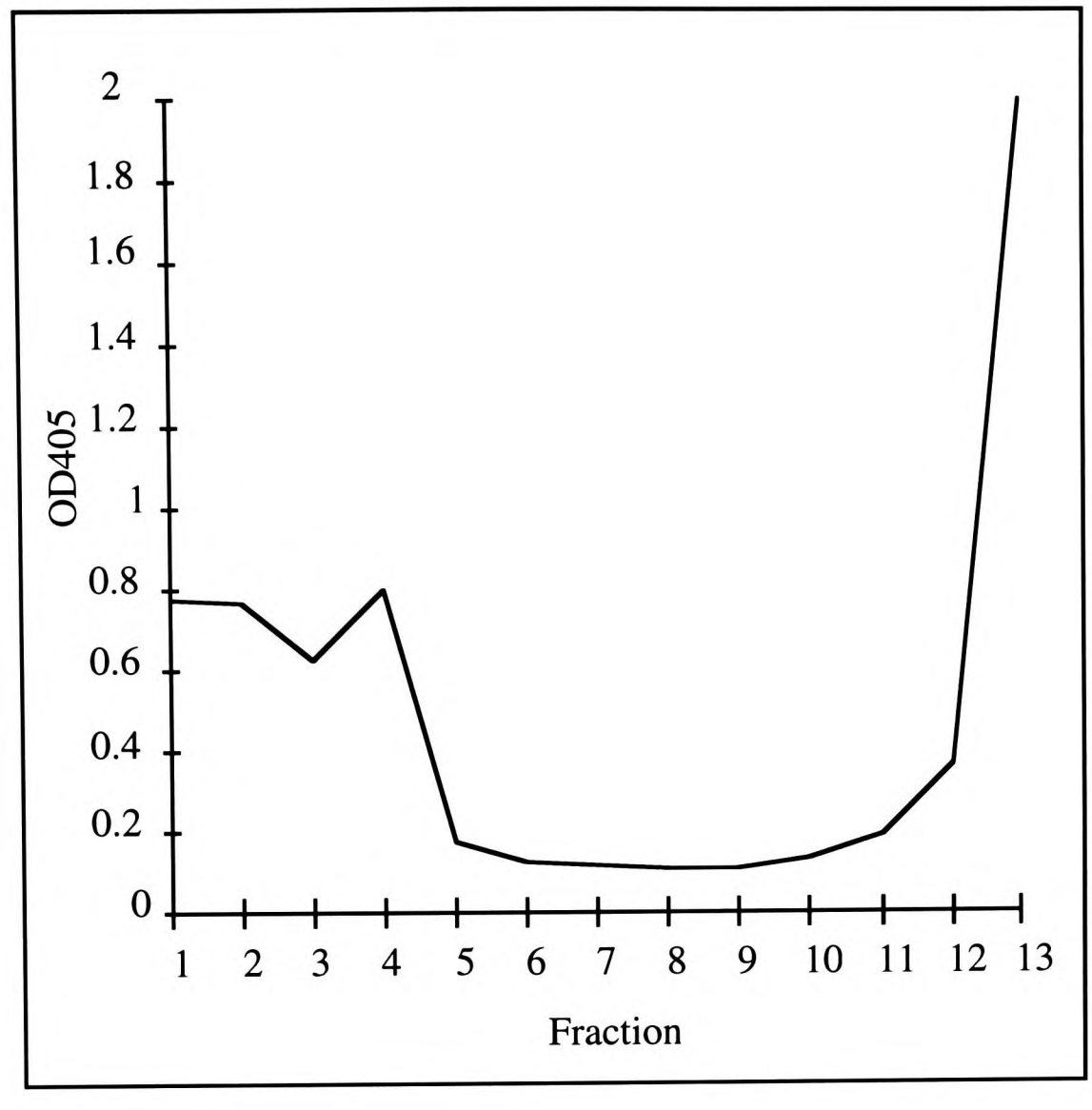

Figure 6-6: ß-hexosaminidase assay of a density gradient of ball-bearing homogenised Raji cells. 10^9 Raji cells were harvested, washed once with PBS and homogenised by ten passes through a ball bearing homogeniser. A post-nuclear supernatant was prepared by centrifugation at 2 000 g for 10 minutes and layered onto a solution of 20% (v/v) Percoll. This was centrifuged at 25 000 g for 20 minutes to establish a density gradient. The resulting gradient was fractionated in thirteen 1 ml fractions. 25 µl of each fraction was mixed with 25 µl of a 1.7 mg/ml solution of p-nitrophenyl N-acetyl-ß-D-glucosaminide in 0.5% (v/v) nonidet-P40, 50 mM sodium citrate, pH 4.8. Homogenisation buffer containing 20% (v/v) Percoll was used as a blank. After 2.5 hours, the reaction was stopped by addition of 200 µl of 84 mM NaCl, 166 mM glycine, 104 mM Na_2CO_3, pH 10.7. The OD_{405} was measured and the results are displayed with the top of the gradient (the less dense fractions) at the left-hand side and the bottom of the gradient (denser fractions) on the right. ß-hexosaminidase was detected [F4] in endosomes (fractions 3-5) and lysosomes (fractions 12 and 13), as well as in fractions containing only soluble proteins (fractions 1 and 2, see Figure 6-12).

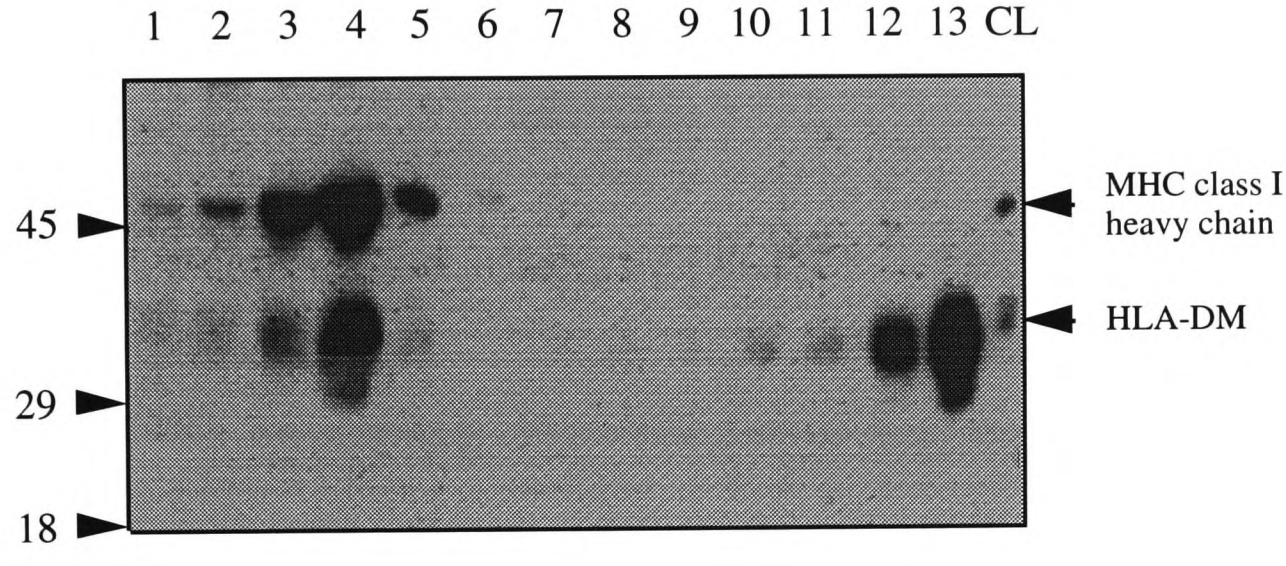

Figure 6-7: A density gradient of ball-bearing homogenised Raji cells probed with antibodies against MHC class I heavy chain and DM. 10 µl of each fraction from the gradient assayed for ß-hexosaminidase activity in Figure 6-6 (lanes 1-13), and 10 µl of crude cell lysate diluted five fold in homogenisation buffer (lane CL) were separated by SDS-PAGE on a 10% (w/v) polyacrylamide gel [E1], western blotted [E4] and probed [E5] with antibodies against MHC class I heavy chain (46 kDa) and HLA-DM α-chain (35 kDa) [E4]. These antibodies were detected by enhanced chemiluminescence using an anti-mouse IgG antibody conjugated to horse radish peroxidase (2°-HRP). MHC class I molecules are detected in fractions 3-5 (plasma membrane and ER) and DM is found in fraction 4 (ER) and fractions 12-13 (lysosomes). The positions of the molecular weight standards are indicated on the left hand side, in kDa.

membrane, but does efficiently separate lysosomes from these organelles. The position of the plasma membrane, early endosomes and lysosomes in these gradients agrees with the reported densities of these organelles (Figure 6-8), so changing the centrifugation conditions to establish a gradient that spans a smaller density range in a larger number of fractions would not improve the separation of these organelles.

Dounce Homogenisation

The fractionation protocol developed using a ball bearing homogeniser was then adapted for use with a method of homogenisation available in our laboratory. Homogenates of Raji cells were prepared with 20, 40, 80 or 160 strokes of either of two Dounce homogenisers (Qiu *et al.*, 1994), or with 10 or 50 passes through a syringe needle (Tulp *et al.*, 1994). The density gradients obtained were very similar to each other and to those obtained using a ball bearing homogeniser, with the distributions of class I, DM and ß-hexosaminidase being almost identical in each case (data not shown). By a small margin, 80 strokes with a Dounce homogeniser was optimal and these conditions were used in further experiments. The ß-hexosaminidase profile of density gradients of cells lysed by Dounce homogenisation (Figures 6-9) is similar to that from cells lysed with a ball bearing homogeniser (Figure 6-6), with activity concentrated in fractions 1-3 and 13. The distributions of class I molecules (which are concentrated in fractions 3-6) and DM (concentrated in fractions 3-5 and 12-13) are also very similar (Figure 6-10 and Figure 6-7), except that each molecule can be detected to some extent in every fraction of the gradient. This may reflect an overloading of the gradient. The protein content of the different fractions was assayed with bicinchoninic acid (BCA) [E6], which showed that proteins are fairly evenly distributed across the gradient, and are most abundant in the three least dense fractions (Figure 6-11).

Organelle	Density (g/cm^3)
Smooth ER	1.03-1.07
Golgi	1.03-1.08
Endosomes	1.05-1.10
Plasma membrane (vesicles)	1.05-1.12
Lysosomes	1.10-1.15
Plasma membrane (sheets)	1.12-1.15
Mitochondria	1.15-1.20
Peroxisome	1.19-1.22
Nucleus	1.21-1.24

Figure 6-8: The density of subcellular particles in low osmolarity media (Dealtry and Rickwood, 1992). The densities of rough ER and nuclear membrane have not been determined.

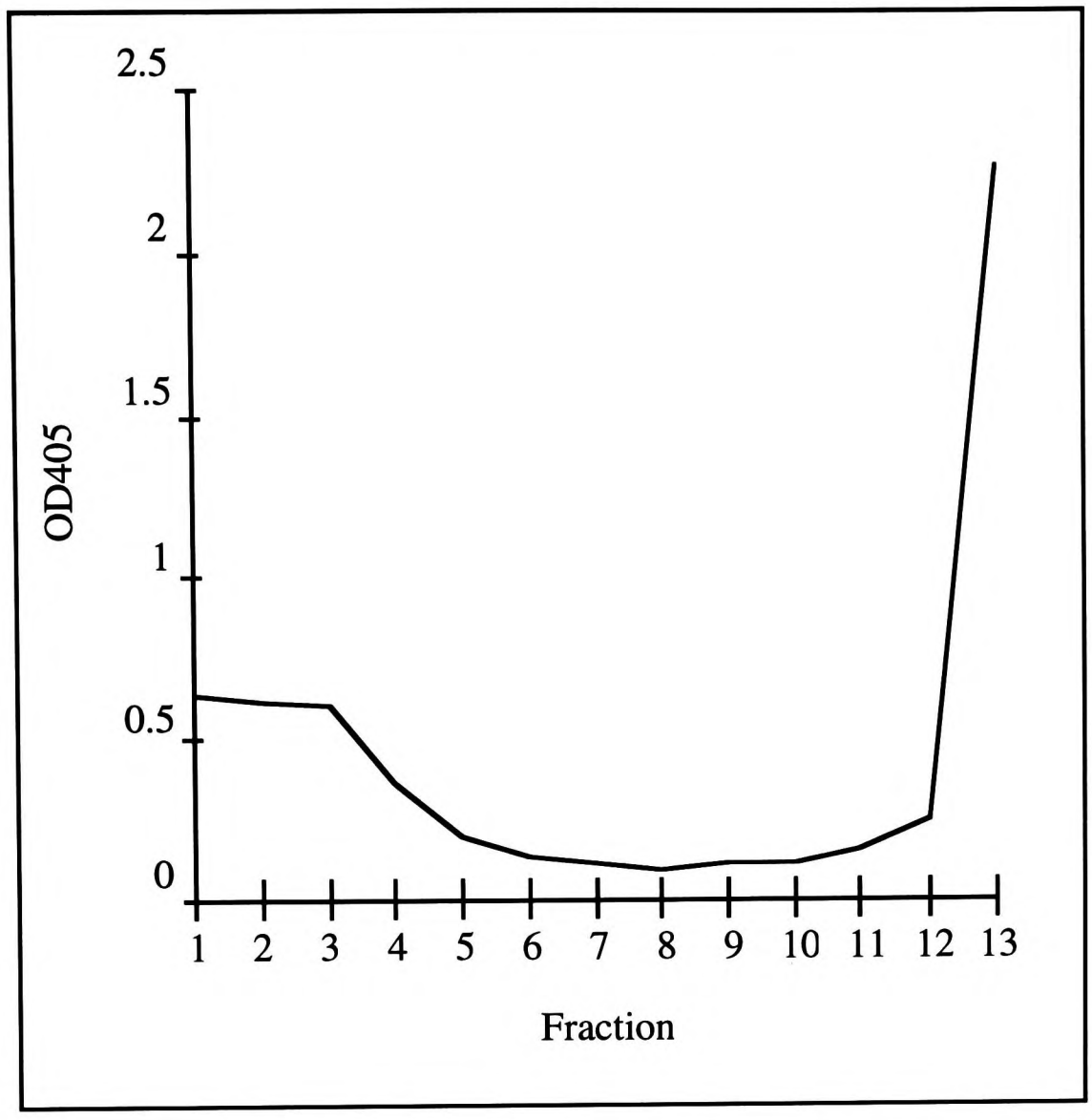

Figure 6-9: ß-hexosaminidase assay of a density gradient of Dounce homogenised Raji cells. A homogenate of 5 x 10^8 Raji cells was prepared by 80 strokes of a Dounce homogeniser and fractionated by Percoll density gradient centrifugation as described in Figure 6-6 [F3]. ß-hexosaminidase activity (assayed as described in Figure 6-6) is present in endosomes (fractions 3 and 4) and lysosomes (fractions 12 and 13), as well as in fractions containing only soluble proteins (fractions 1 and 2, see Figure 6-12) [F4].

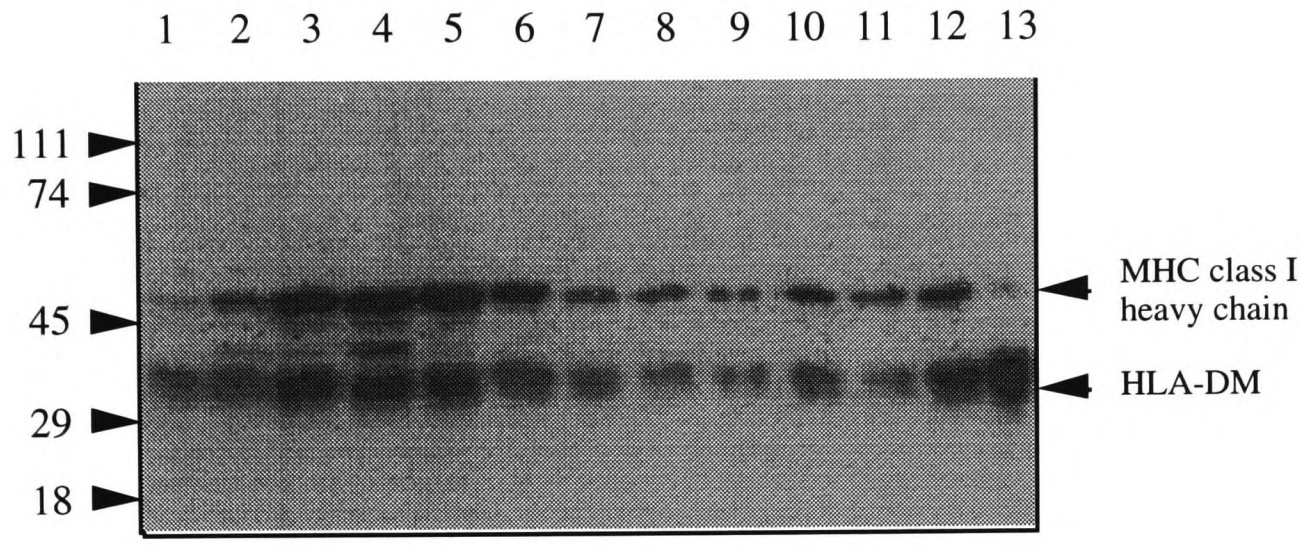

Figure 6-10: A density gradient of Dounce homogenised Raji cells probed with antibodies against class I heavy chain and DM. The fractions assayed for ß-hexosaminidase activity in Figure 6-9 were separated by electrophoresis through a 10% (w/v) polyacrylamide gel [E1], blotted [E4] and probed [E5] with antibodies against class I heavy chain and DM [E4]. MHC class I molecules are detected predominantly in fractions 3-6 (plasma membrane and ER) and DM is predominantly in fractions 3-5 (ER) and fractions 12 and 13 (lysosomes). The bound antibodies were detected by enhanced chemiluminescence (ECL). The positions of the molecular weight standards are indicated on the left hand side, in kDa.

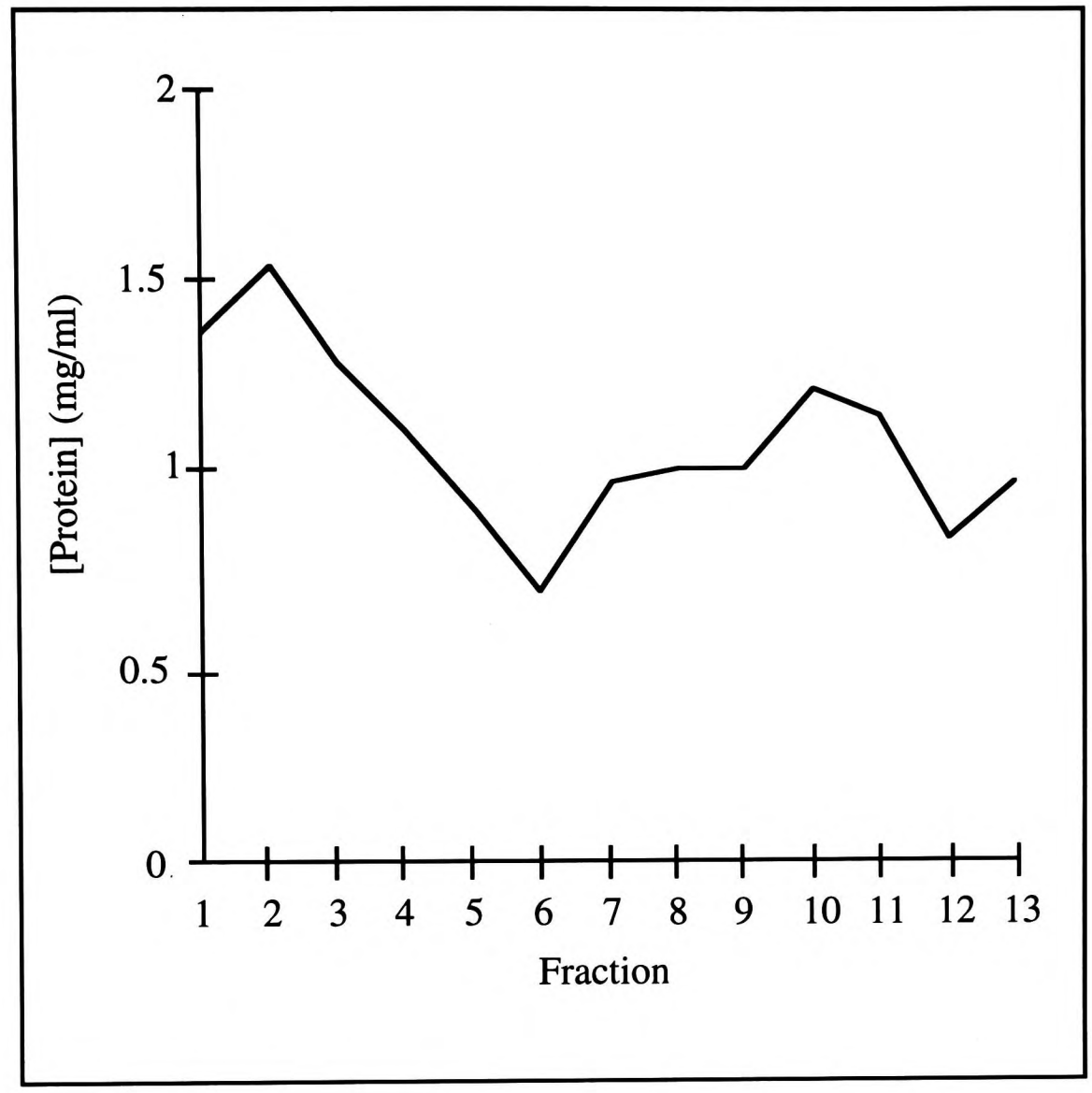

Figure 6-11: Protein content of a density gradient of Dounce homogenised Raji cells. The concentration of protein in the fractions assayed for ß-hexosaminidase activity in Figure 6-9 was determined using the BCA assay [E6]. 5 µl of each fraction was mixed with 200 µl of BCA reagent and the OD_{562} was measured after incubation at 37 °C for 30 minutes. The standards were solutions of BSA, and homogenisation buffer containing 20% (v/v) Percoll was used as a blank. Proteins are detected throughout the gradient, and especially in fractions 1-3, which include soluble proteins (see Figure 6-14).

The number of cells used for each density gradient was reduced from 10^8 to 5 x 10^7 or 2.5 x 10^7 cells without changing the resolution of the different subcellular compartments (data not shown). However, the recovery of ß-hexosaminidase, class I and DM molecules is less efficient in samples containing large numbers of cells. Nevertheless, these results demonstrate that subcellular fractionation by density gradient centrifugation is a robust technique that is little influenced by the conditions of homogenisation.

Density Gradient Centrifugation of Purified Vesicles

The protocol was modified to remove the soluble components of the homogenate from the post-nuclear supernatant by centrifugation at high speed (100 000 g for 1 hour). The supernatant was discarded and the pelleted vesicles (including those derived from plasma membrane, ER, endosomes and lysosomes) were gently resuspended in fresh homogenisation buffer and separated by density as before. Under these conditions, the ß-hexosaminidase activity is concentrated in fractions 4-5 and 12-13 (Figure 6-12), while in contrast to density gradients of post-nuclear supernatants ('whole homogenates'), there is little ß-hexosaminidase activity in fractions 1-3. This shows that ß-hexosaminidase activity found in fractions 1-3 is soluble rather than vesicular, and must have been released by endosomes and lysosomes during homogenisation. Thus the distribution of endosomes is more restricted (fractions 4-5) than was suggested by experiments using whole homogenates. The detection of class I and DM molecules is weak, and both are detected somewhat higher in the gradient than before: class I molecules are exclusively detected in fraction 4 and DM is found in fractions 3-4 and 11-13 (Figure 6-13). This is more likely to result from differences in layering the homogenate onto the gradient or collecting the fractions than to reflect a difference in the density of plasma membrane and ER vesicles prepared by the two methods. A BCA assay shows that the distribution of proteins in the gradient is changed dramatically by removing the soluble components of the homogenate

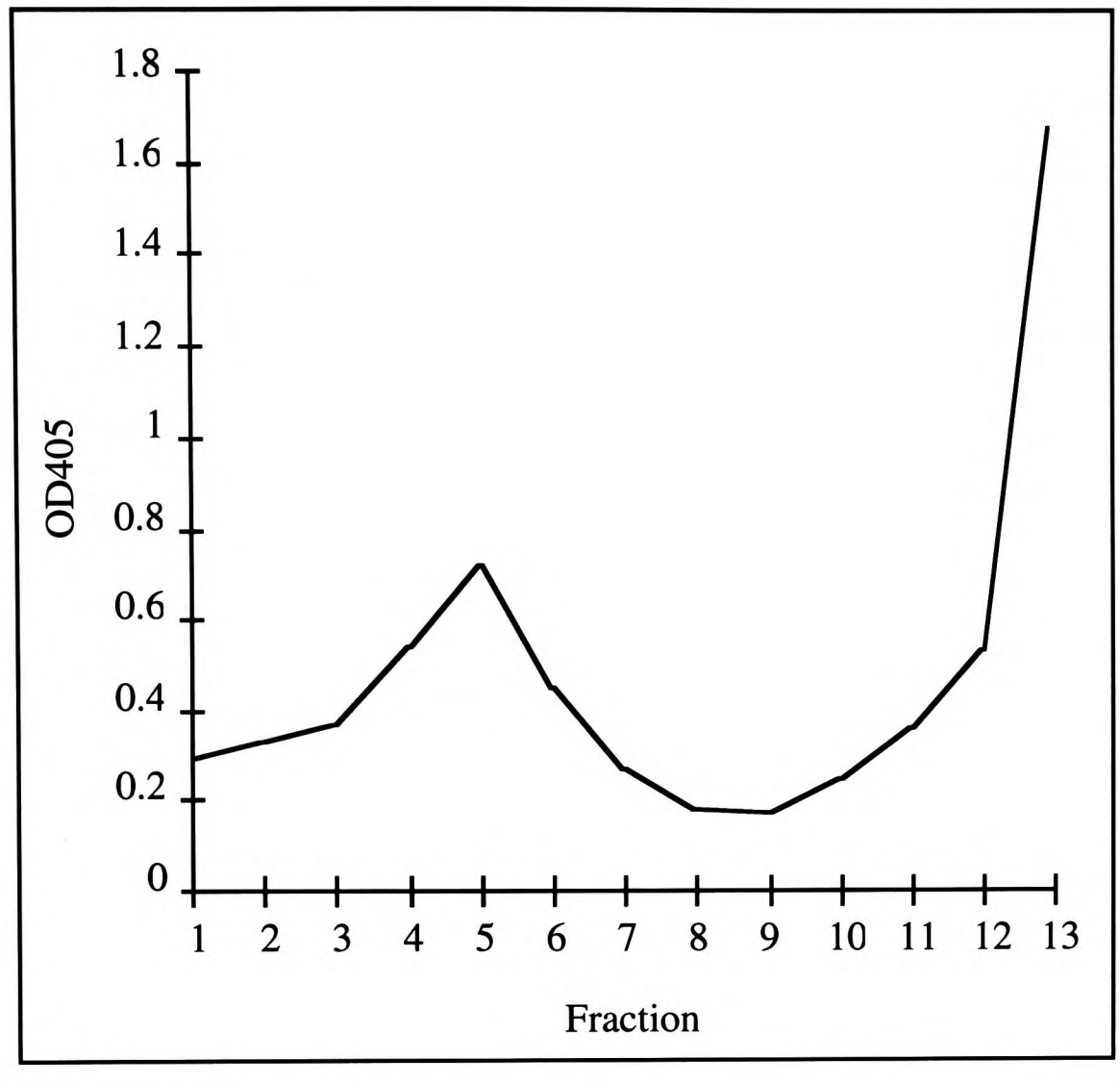

Figure 6-12: ß-hexosaminidase assay of a density gradient of vesicles from Raji cells. ~3 x 10^8 Raji cells were lysed by Dounce homogenisation and a post-nuclear supernatant prepared as described in Figure 6-9 [F3]. This supernatant was centrifuged at 100 000 g for 1 hour and its supernatant was discarded. The pellet of vesicles (including those derived from ER, plasma membrane, endosomes and lysosomes) was resuspended in homogenisation buffer and fractionated by Percoll density gradient centrifugation as described in Figure 6-6. ß-hexosaminidase activity [F4] is present predominantly in endosomes (fractions 4-6) and lysosomes (fractions 12 and 13), and is no longer detected in fractions that, in gradients of whole homogenates, contain soluble proteins (fractions 1 and 2).

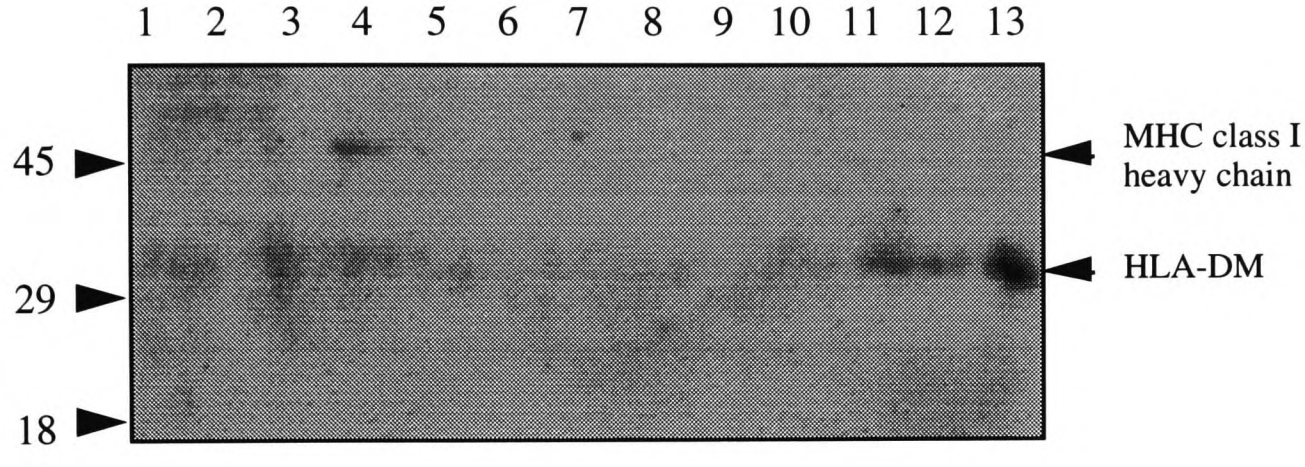

Figure 6-13: A density gradient of vesicles from Raji cells probed with antibodies against class I heavy chain and DM. The fractions assayed for ß-hexosaminidase activity in Figure 6-12 were separated by electrophoresis through a 10% (w/v) polyacrylamide gel [E1], blotted and probed with antibodies against class I heavy chain and DM [E4]. MHC class I molecules are detected in fraction 4 (plasma membrane and ER) and DM is found in fraction 3-4 (ER) and fractions 11-13 (lysosomes). The positions of the molecular weight standards are indicated on the left hand side, in kDa.

before density gradient centrifugation (Figure 6-14, compared to Figure 6-11). The gradient contains significantly less protein overall, especially at the very top and in the centre of the gradient, and there are two sharp peaks of protein concentration, in fractions 3-5 and 12-13. Assuming that different vesicles contain a similar number of proteins, this BCA assay is a good indication of the distribution of vesicles in the gradient.

Detection of Hsp70s in Gradients of Whole Homogenates

The presence of hsp70s in density gradients was detected with two monoclonal antibodies, 3A3 (Bhattacharyya *et al.*, 1995) and 5A5 [E4]. Both of these antibodies recognise hsp70 and hsc70 from humans (Figure 6-15), as well as hsp70s from chicken, frog, fish, fruit fly, wheat and yeast, though not from *E. coli.* Therefore, they are likely to recognise hsp70A2, hsp70B' and hsp70hom as well. In addition, antibody 3A3 reacts with the mitochondrial hsp70 (PBP74) and antibody 5A5 recognises BiP.

The subcellular localisation of hsp70s was examined in density gradients of whole Raji cell homogenate prepared with a ball bearing homogeniser. The distributions of ß-hexosaminidase (Figure 6-16), class I and DM molecules (Figure 6-17) in these gradients were the same as previously observed (Figures 6-9 and 6-10). Hsp70s are concentrated in the four fractions at the top of the gradient (Figures 6-17 and 6-18), showing a very similar distribution to the soluble ß-hexosaminidase activity released from endosomes and lysosomes during homogenisation (see above). Therefore, the hsp70s detected at the top of the gradient are likely to be predominantly soluble molecules. Antibody 5A5 (which recognises the ER-resident hsp70 BiP) detects hsp70s no more strongly than antibody 3A3 (which does not recognise BiP) in fractions containing ER vesicles (fractions 3-4), suggesting that this hsp70 is of low abundance in Raji cells compared to the cytoplasmic hsp70s (Figure 6-17), which are detected by both antibodies with equal efficiency in the first two fractions of the gradient.

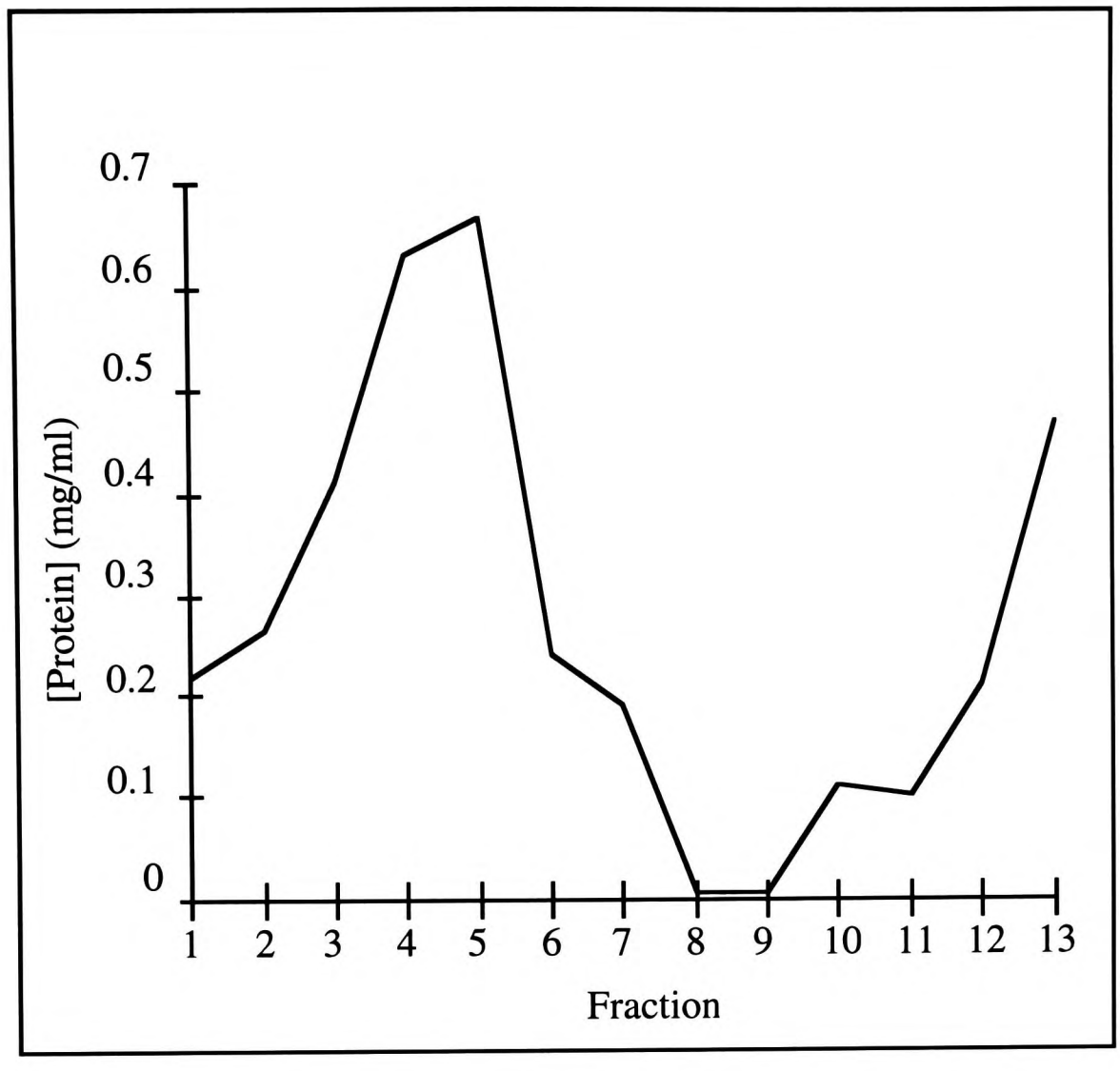

Figure 6-14: Protein content of a density gradient of vesicles from Raji cells. The concentration of protein of each sample assayed for ß-hexosaminidase activity in Figure 6-12 was determined using the BCA assay [E6]. The standards were solutions of BSA, and homogenisation buffer containing 20% (v/v) Percoll was used as a blank. Proteins are detected predominantly in fractions 3-6 (plasma membrane, ER and endosomes) and 12 and 13 (lysosomes).

(a) 3A3

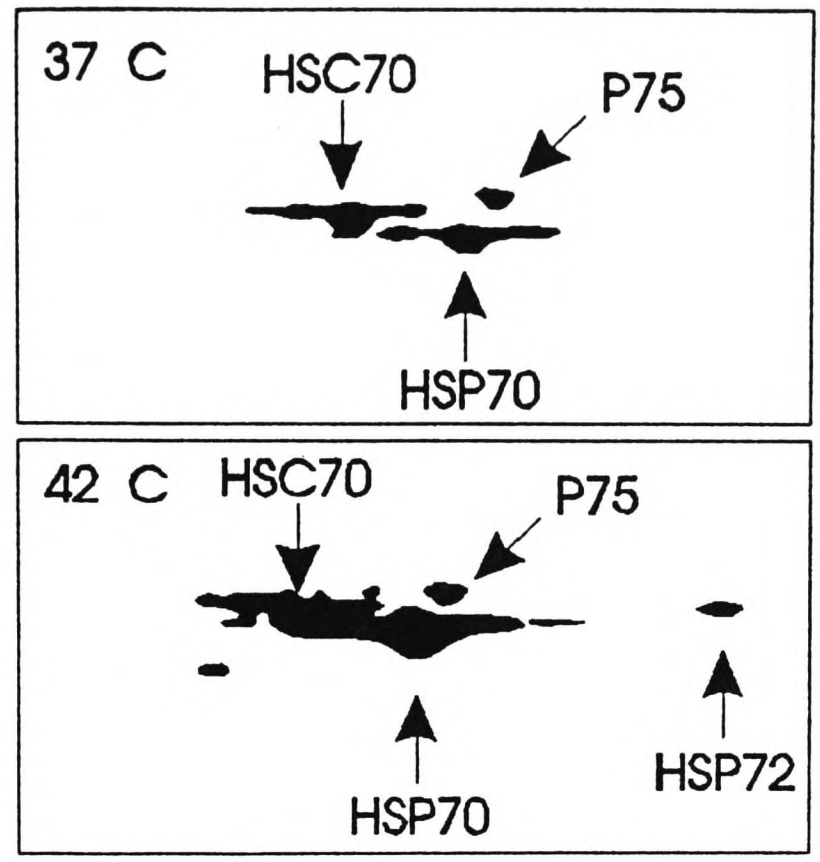

(b) 5A5

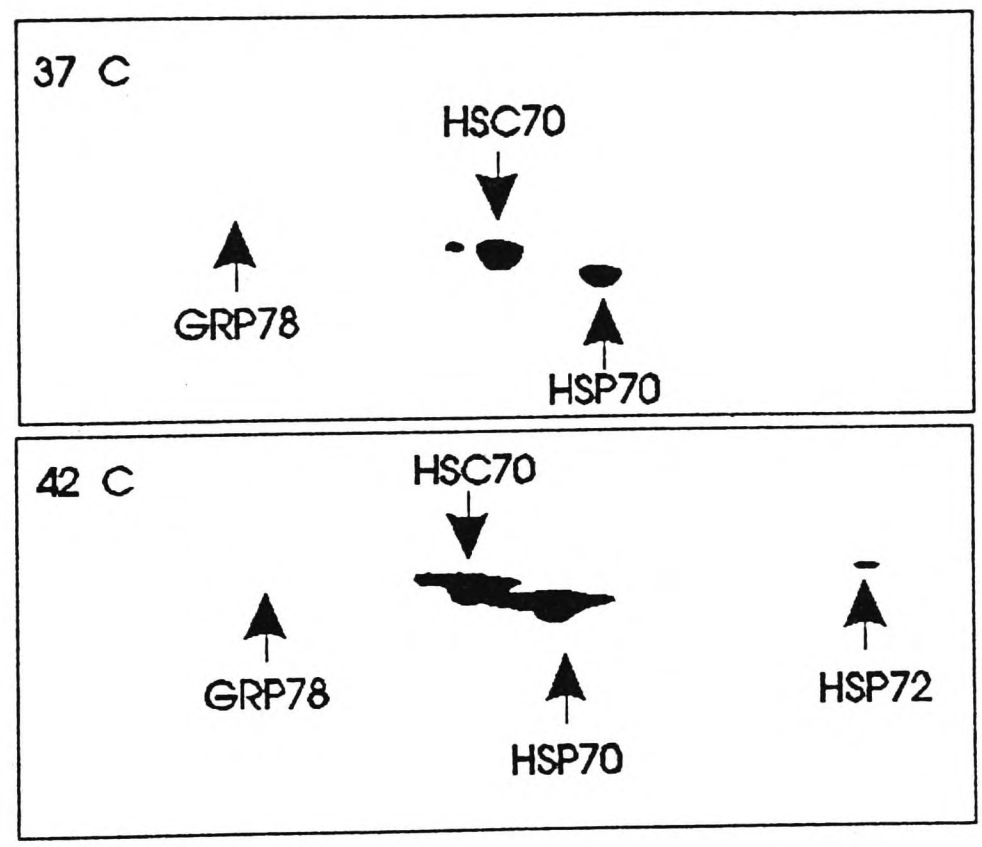

Figure 6-15: The specificity of antibodies 3A3 and 5A5 on two-dimensional gels. Proteins from HeLa cells before (37 °C) or after heat shock at 42 °C for two hours were separated by two-dimensional gel electrophoresis [by charge in the horizontal direction (by isoelectric focusing) and by size vertically (by SDS-PAGE)] western blotted and probed with (a) antibody 3A3 (Bhattacharyya *et al.,* 1995) or (b) antibody 5A5 (S.P.Murphy and R.I. Morimoto, unpublished). P75 is mt hsp70 and hsp72 is hsp70B' (Figures reproduced from the Affinity Bioreagents catalogue.)

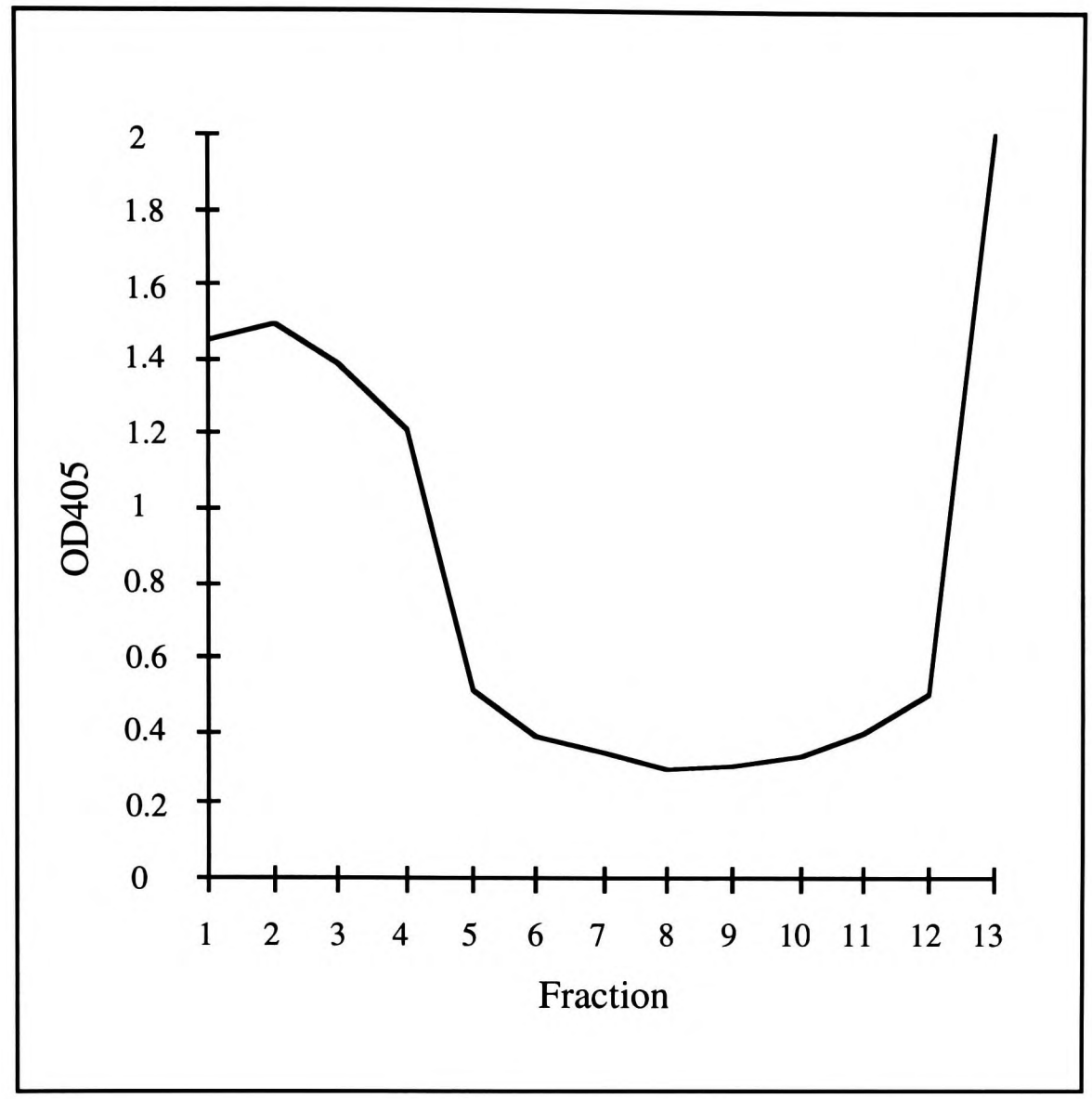

Figure 6-16: ß-Hexosaminidase assay of a density gradient of ball-bearing homogenised Raji cells. A density gradient of a homogenate of 10^8 Raji cells was prepared as described in Figure 6-9 [F3]. ß-hexosaminidase activity [F4] is present in endosomes (fractions 3 and 4) and lysosomes (fraction 13), as well as in fractions containing only soluble proteins (fractions 1 and 2). The positions of the molecular weight standards are indicated on the left hand side, in kDa.

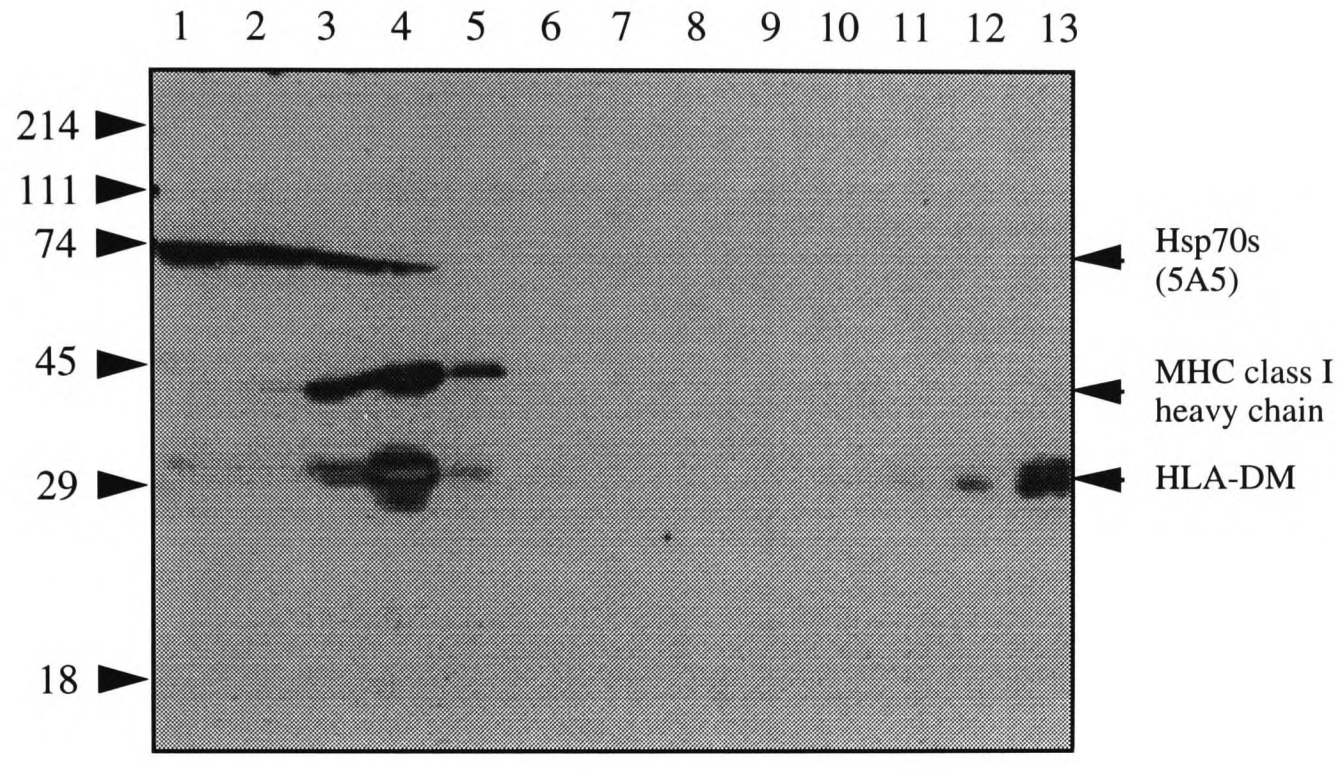

Figure 6-17: A density gradient of ball-bearing homogenised Raji cells probed with antibodies against class I heavy chain, DM and hsp70s (antibody 5A5). MHC class I molecules can be detected in fractions 3-5 (plasma membrane and ER) of the gradient described in Figure 6-16 and DM is present in fractions 3-5 (ER) and 13 (lysosomes). Hsp70s can be detected in the first four fractions of the gradient, which contain soluble proteins. The positions of the molecular weight standards are indicated on the left hand side, in kDa.

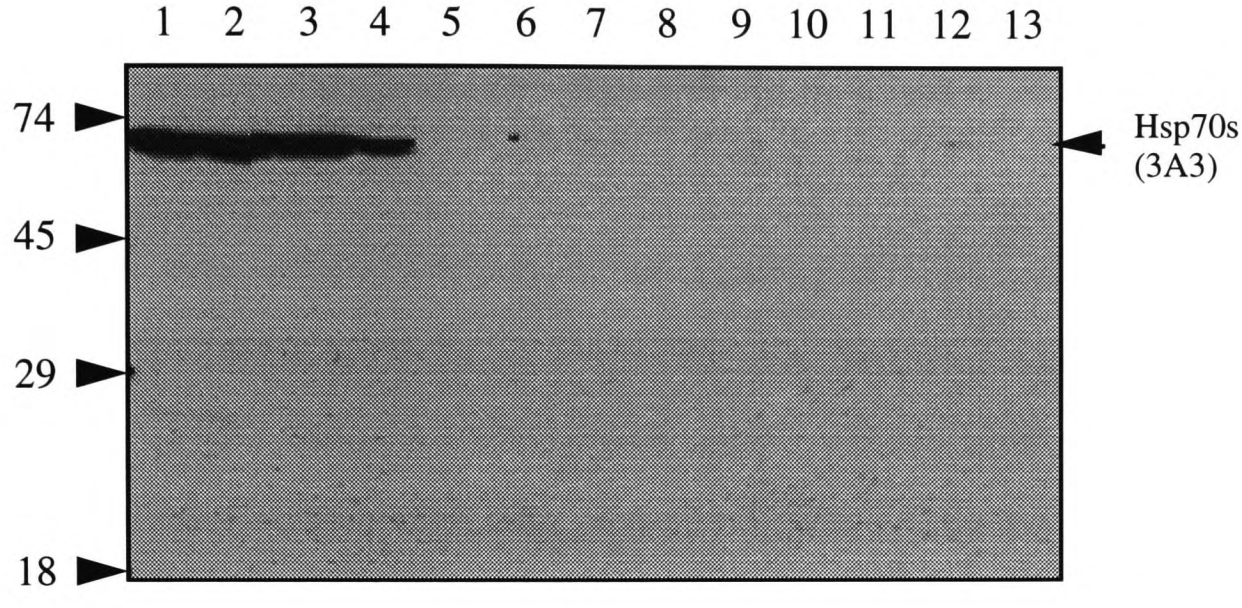

Figure 6-18: A density gradient of ball-bearing homogenised Raji cells probed with an antibody against hsp70s (3A3). Hsp70s can be detected in every fraction of the gradient (described in Figure 6-16), but are found predominantly in fractions 1-4 (soluble proteins). The positions of the molecular weight standards are indicated on the left hand side, in kDa.

No hsp70s were detected with either antibody in the dense fractions at the bottom of the gradient. Since both the antibodies used have very broad specificities, their failure to detect hsp70s makes it extremely unlikely that any member of the hsp70 family resides in dense, endocytic compartments, including lysosomes and the MIIC. It also confirms that mitochondria, which contain an hsp70 recognised by antibody 3A3 and are extremely dense (Figure 6-8), were efficiently removed from the homogenate before it was applied to the density gradient.

The results using antibody 3A3 are similar to those previously reported when a discontinuous Percoll and metrizamide density gradient of a post-nuclear supernatant of HeLa cells was probed with this antibody (Bhattacharyya *et al.*, 1995). Hsp70 and hsc70, which could be resolved from each other, were concentrated at the top of the gradient. However, Bhattacharyya and colleagues found that these cytoplasmic hsp70s could be detected faintly throughout the gradient, and were slightly more abundant in the densest fractions than in the medium density fractions. Their gradients included mitochondria, and the mitochondrial hsp70 was detected as a separate upper band at the bottom of the gradient.

Detection of Hsp70s in Gradients of Purified Vesicles

To confirm that the hsp70s detected in the low density fractions of density gradients are soluble rather than vesicle-associated, density gradient centrifugation was carried out with purified vesicles, from which the soluble proteins had been removed by centrifugation at 100 000 g. The distributions of ß-hexosaminidase (Figure 6-12), class I and DM molecules (Figures 6-13 and 6-19) and protein (Figure 6-14) in these gradients are described above.

Hsp70s recognised by antibody 5A5 were resolved into two bands (Figure 6-19) when gels were prepared by overlaying the resolving gel with water-saturated butanol, rather

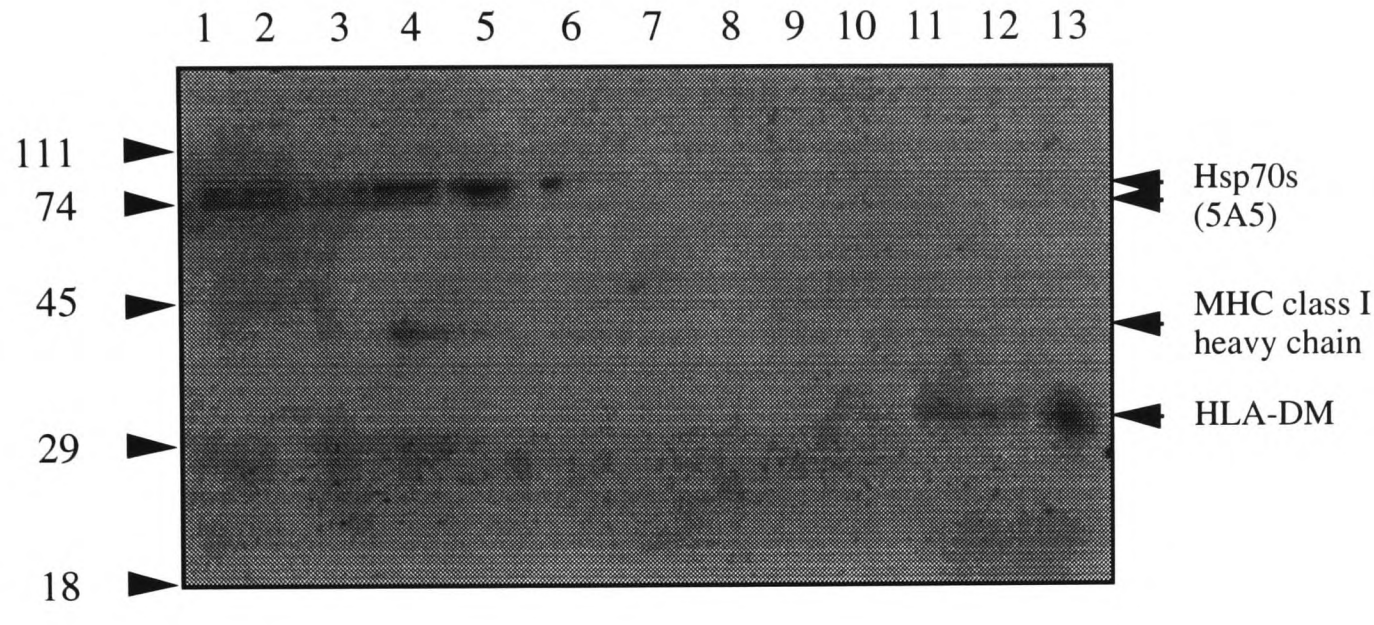

Figure 6-19: A density gradient of vesicles from Raji cells probed with antibodies against class I heavy chain, DM and hsp70s (antibody 5A5). The density gradient is the same as that described in Figure 6-12. MHC class I molecules can be detected in fraction 4 (plasma membrane and ER) and DM is present in fractions 3-4 (ER) and 13 (lysosomes). Hsp70s are detected in fractions 1-5, and BiP (the upper band recognised by antibody 5A5) is predominantly found in fractions 4 and 5.

than water, as it set [E1] so that its junction with the stacking gel was extremely sharp. The stronger upper band (~78 kDa) recognised by antibody 5A5 is BiP (Figure 6-15), which resides in the ER and is therefore predominantly located in fractions 4 and 5, which contain both class I molecules and DM. There is some weak BiP reactivity in the first three fractions of the gradient, representing soluble BiP that was probably released from the ER when the cells were homogenised or the purified vesicles were resuspended.

The lower band recognised by antibody 5A5 in fractions 1-5 (Figure 6-19) is the same as the band recognised by antibody 3A3 (Figure 6-20) and represents the cytoplasmic hsp70s. It is surprising that the cytoplasmic hsp70s are present in gradients of vesicles purified by centrifugation, and this suggests that they are associated with low density vesicles. However, fractions 1-2 contain insignificant amounts of ß-hexosaminidase (endosomes and lysosomes), class I molecules (plasma membrane and rough ER) and DM (MIIC and rough ER), so the identity of any vesicles these fractions contain is not clear. Vesicles derived from the Golgi and the smooth ER have not been located in these gradients and are thought to be less dense than vesicles derived from endosomes, plasma membrane and rough ER, but the low protein content of fractions 1-2 (Figure 6-14) makes it unlikely that they contain any vesicles at all. In any case, it is difficult to imagine what roles hsp70s might play in the smooth ER and Golgi, as proteins are not known to be synthesised, folded or degraded in either location. Therefore, it seems likely that hsp70s were pelleted with the vesicular fraction of the homogenate for another reason than being contained within vesicles or associated with their cytoplasmic face. It is possible that they became associated with protein aggregates generated during homogenisation which were large enough to be pelleted by centrifugation at 100 000 g for 1 hour. Once resuspended, these aggregates would remain near the top of the density gradient, as it was only centrifuged at 25 000 g for 20 minutes.

The distribution of hsp70s detected by antibody 3A3 in gradients of purified vesicles (Figure 6-20) differs from that seen in density gradients of whole homogenates (Figure 6-

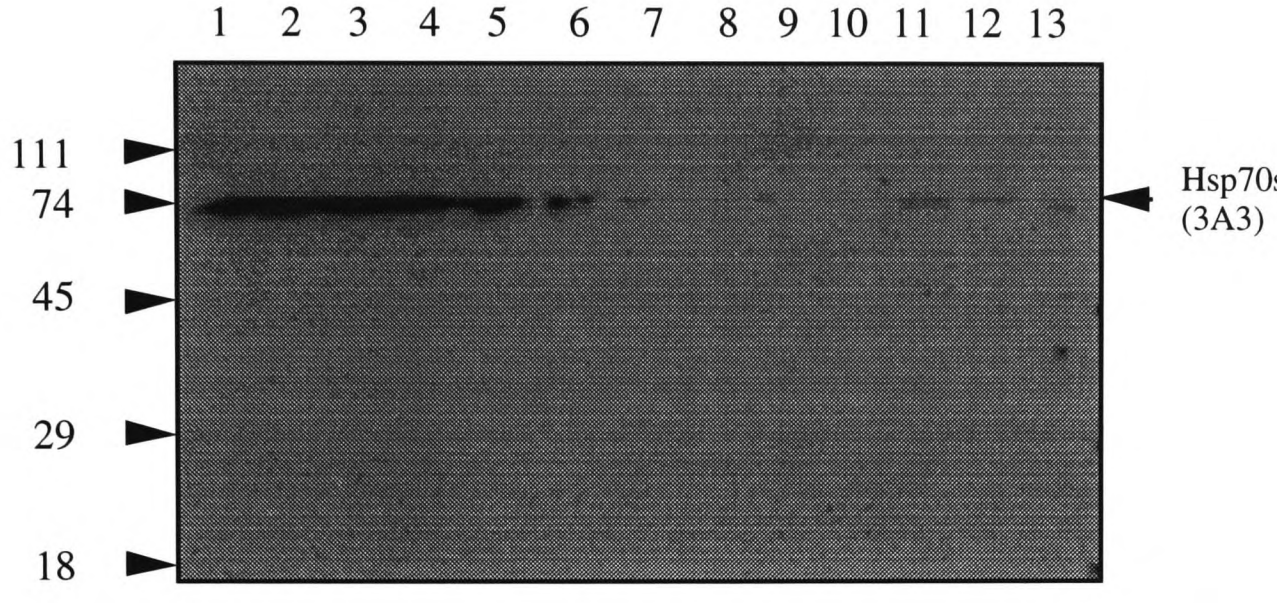

Figure 6-20: A density gradient of vesicles from Raji cells probed with antibody 3A3. Hsp70s are found predominantly in fractions 1-6, but can be detected in every fraction of the gradient. This blot was stripped and probed with the antibodies described in Figure 6-19. The positions of the molecular weight standards are indicated on the left hand side, in kDa.

18) because, although hsp70s are most abundant in fractions 106, they can be detected faintly in every fraction of the gradient. Hsp70s are present in fractions 12-13, which contain lysosomes, as well as fractions 7-11, which contain little or no protein (Figure 6-14) and, therefore, are unlikely to contain any vesicles. The distribution of hsp70s in every fraction, including lysosomes is likely to be an artefact of the loading (or overloading) of this gradient, as it was not seen in other gradients.

Distribution of Hsp70s in Serum-Starved Cells

In human fibroblasts starved of serum (Terlecky, 1994) or the hepatocytes of starved rats (Cuervo *et al.*, 1995), hsc70 becomes associated with lysosomes. Hsc70 is also involved in transporting proteins containing KFERQ motifs to lysosomes for degradation during serum starvation, but the two processes are not necessarily linked (see Chapter 1). The effects of starvation and serum starvation on antigen processing cells have not previously been investigated, yet they may cause cytoplasmic proteins to enter the MHC class II processing pathway and, if hsc70 actually enters the lysosomes, alter the processing of endocytosed antigens. Therefore, the distribution of hsp70s was examined in Raji cells before and after serum starvation.

Raji cells were cultured in RPMI medium lacking foetal calf serum for 24 hours (data not shown), 60 hours (data not shown) or 110 hours (Figure 6-21, 6-22 and 6-23) and homogenised with a Dounce homogeniser. The vesicles were purified from soluble components of the homogenate by centrifugation and separated by density gradient centrifugation. The distribution of ß-hexosaminidase (Figure 6-21), class I molecules and DM (Figure 6-22) was the same in vesicles from serum starved cells as in vesicles from cells which were grown in parallel in the presence of 10% (v/v) foetal calf serum (Figures 6-12 and 6-13). Likewise, the distribution of hsp70s detected with antibody 3A3 or 5A5 was the same whether cells were cultured in the absence (Figure 6-22, 6-23) or presence

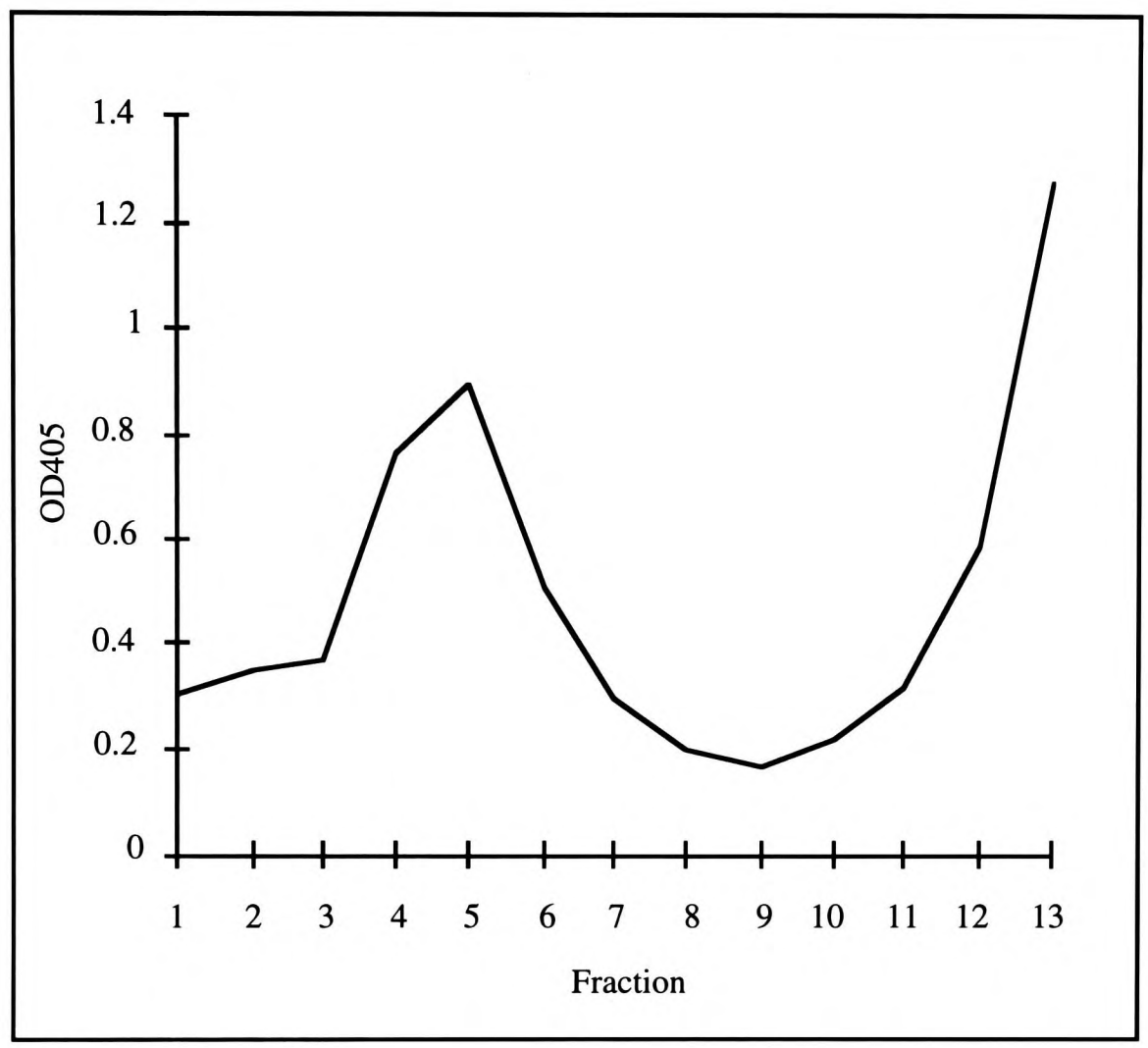

Figure 6-21: ß-hexosaminidase assay of a density gradient of vesicles from Raji cells cultured in the absence of foetal calf serum for 110 hours. The density gradient was prepared as described in Figure 6-12, from 3 x 10^8 cells that had been starved of serum for 48 hours. ß-hexosaminidase activity [F4] is present in endosomes (fractions 3 and 4) and lysosomes (fraction 13), and is absent from fractions containing only soluble proteins (fractions 1 and 2).

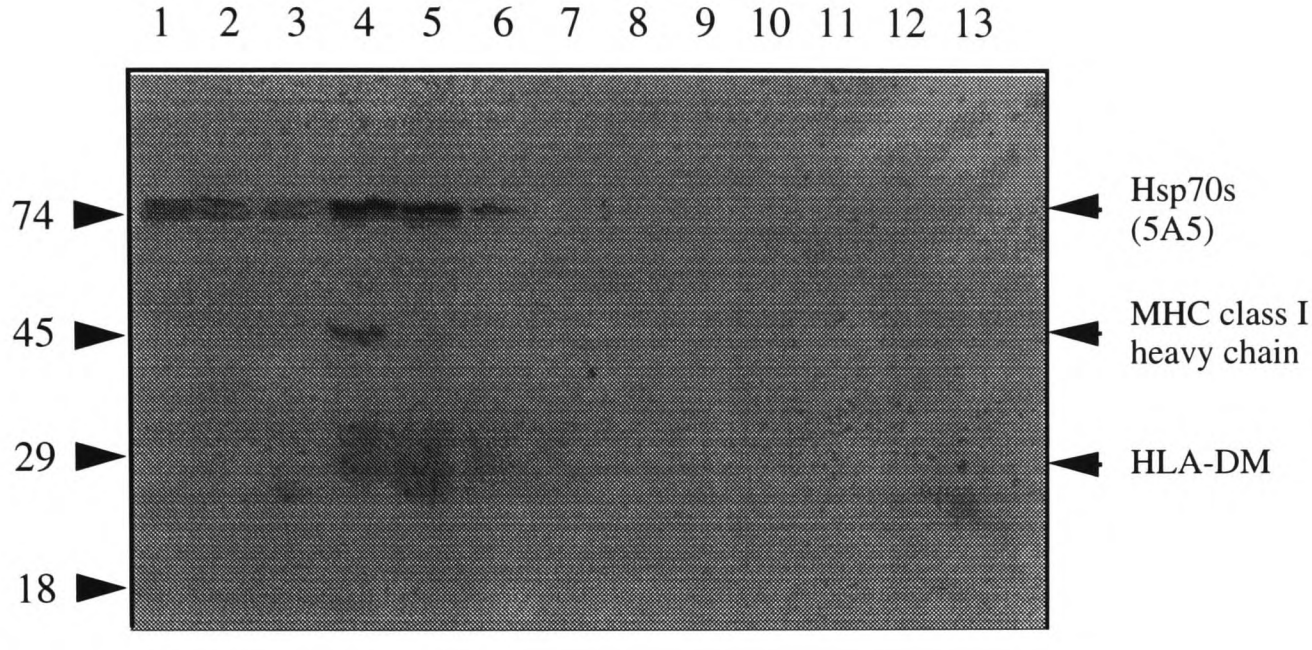

Figure 6-22: A density gradient of vesicles from Raji cells cultured in the absence of foetal calf serum for 110 hours probed with antibodies against class I heavy chain, DM and hsp70s (5A5). The fractions shown are the same as those described in Figure 6-21. MHC class I molecules can be detected in fraction 4 (plasma membrane and ER) and DM is present in fractions 4-6 (ER) and 13 (lysosomes). Hsp70s are detected in fractions 1-5, and BiP (the upper band recognised by antibody 5A5) is predominantly found in fractions 4 and 5. The positions of the molecular weight standards are indicated on the left hand side, in kDa.

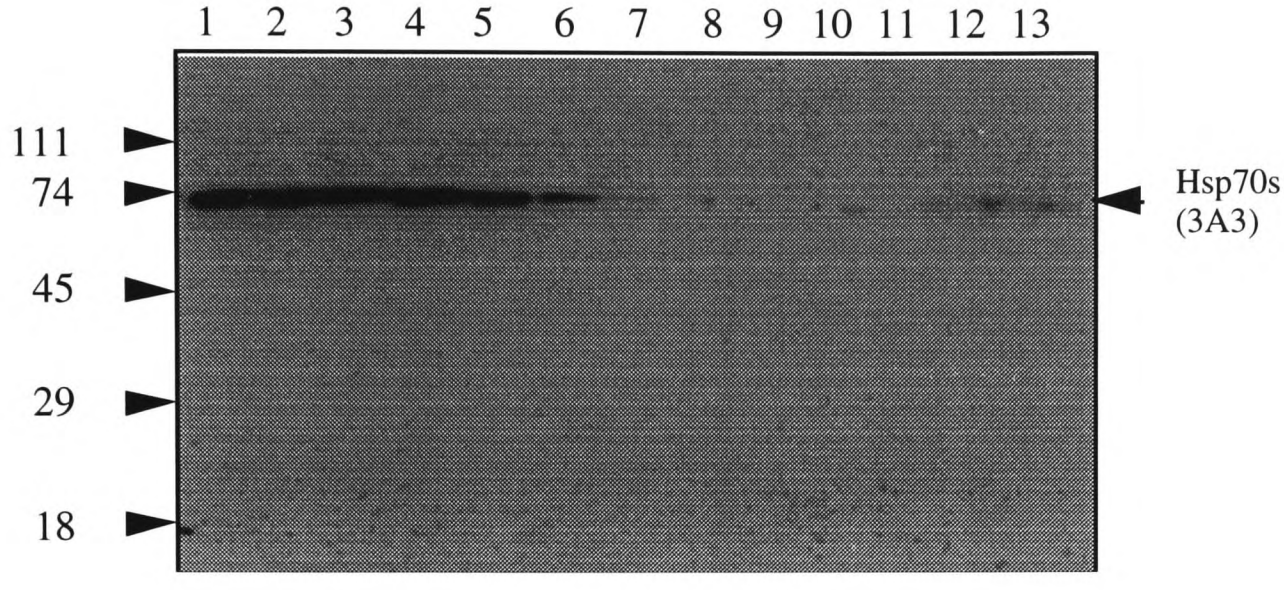

Figure 6-23: A density gradient of vesicles from Raji cells cultured in the absence of foetal calf serum for 110 hours probed with antibody 3A3. The blot is the same as that in Figure 6-22, which was stripped and reprobed with antibody 3A3. Hsp70s are found predominantly in fractions 1-6, but can be detected in every fraction of the gradient. The positions of the molecular weight standards are indicated on the left hand side, in kDa.

(Figures 6-19 and 6-20) of serum. Hsp70s can be detected faintly in every fraction of these gradients, including the dense fractions containing lysosomes, but as discussed before, they are unlikely to be associated with vesicles.

Distribution of Hsp70s in Heat Shocked Cells

The effects of heat shock on the subcellular distribution of hsp70s was also investigated. Raji cells were grown under normal conditions (37 °C) or heat shocked at 42 °C for 2 hours and the whole homogenate (post-nuclear supernatant) was separated by density gradient centrifugation. The gradient was collected in 0.5 ml rather than 1 ml fractions to see if the resolution of different organelles could be improved. The gradients from heat shocked cells show reduced ß-hexosaminidase activity in the early fractions (1-5) of the gradient (Figure 6-24) but the distributions of class I molecules and DM are not greatly changed. Collecting 0.5 ml rather than 1 ml fractions did not improve the resolution of the plasma membrane from the ER. There are more hsp70s in each fraction of the gradient from heat shocked cells (Figures 6-26 and 6-28) than cells grown under normal conditions (Figures 6-25 and 6-27), but there is no change in their distribution. As before, the cytoplasmic hsp70s can be detected in all fractions of the gradient, but in this case, with antibody 5A5 (Figures 6-25 and 6-26), rather than antibody 3A3 (Figures 6-27 and 6-28), which detected them in two earlier gradients (Figures 6-20 and 6-23). This indicates that both antibodies can detect the broadly distributed hsp70s, reinforcing the conclusion that they originated in the cytoplasm rather than in mitochondria or the ER.

The fractions from non-heat shocked cells were probed with an antibody against actin (Figure 6-29). Actin is a component of the cytoskeleton, but as this is a dynamic structure, actin also exists in the cytoplasm as a soluble monomer. Polymerised actin will be removed by the initial centrifugation of the homogenate, leaving monomeric actin in the post-nuclear supernatant. Actin is detected in the first eight of the 0.5 ml fractions of the

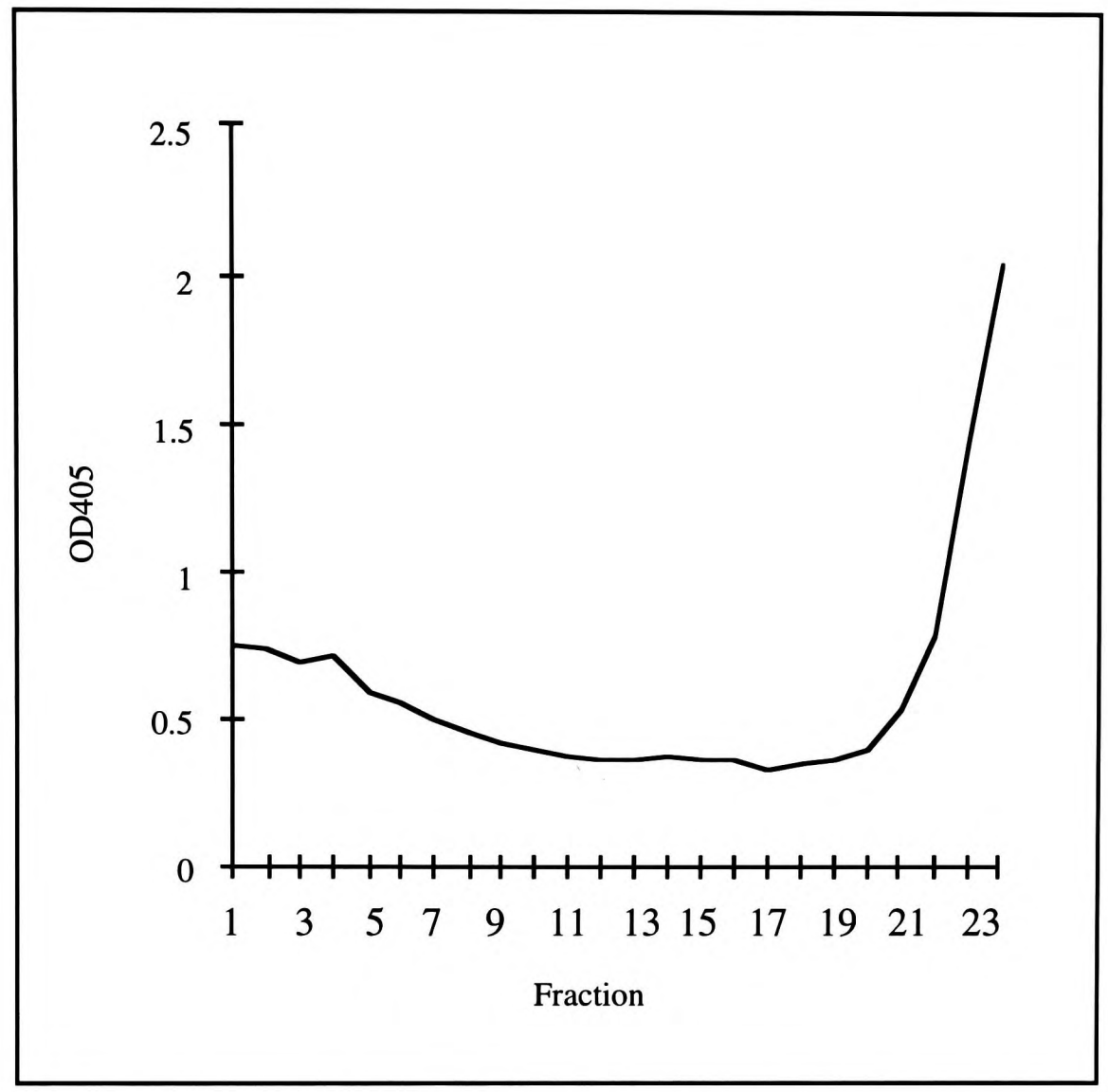

Figure 6-24: ß-hexosaminidase assay of a density gradient from heat shocked Raji cells. Raji cells (~5 x 10^8) were incubated for 2 hours at 42 °C (or as a control, 37 °C) and Dounce homogenised [F3]. A density gradient was prepared as described in Figure 6-9, except that twenty-four 0.5 ml fractions, rather than twelve 1 ml fractions, were collected. ß-hexosaminidase activity [F4] is present in endosomes (fractions 4 and 5) and lysosomes (fraction 22-24), and fractions containing soluble proteins (fractions 1-3).

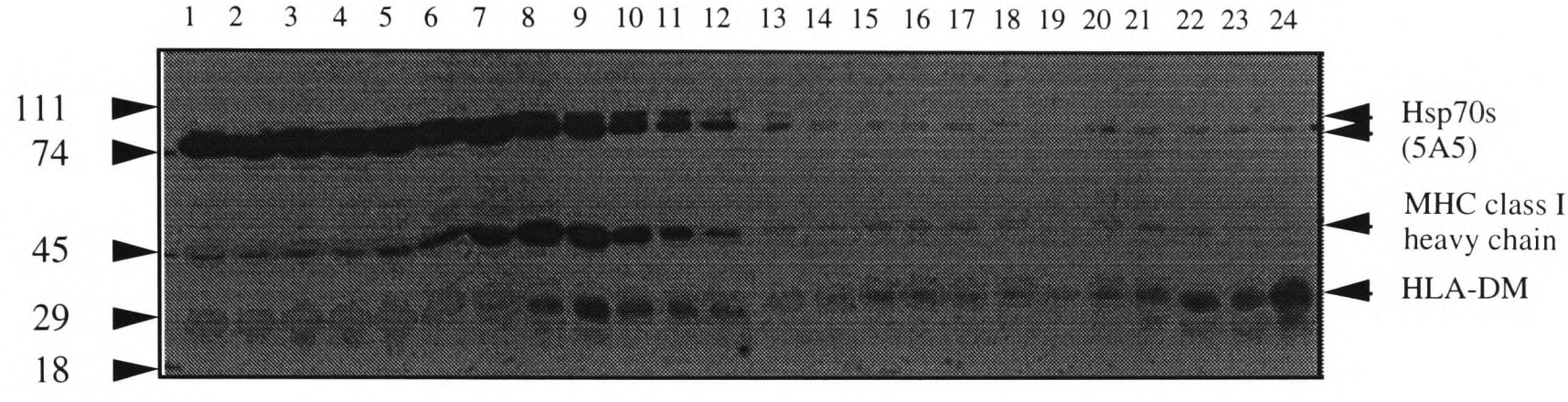

Figure 6-25: A density gradient of non-heat shocked Raji cells probed with antibodies against class I heavy chain, DM and hsp70s (5A5). The preparation of this density gradient is described in Figure 6-24. MHC class I molecules can be detected predominantly in fractions 5-12 (plasma membrane and ER), DM molecules in fractions 8-10 (ER) and 22-24 (lysosomes), and hsp70s in fractions 1-12 (soluble proteins, plasma membrane and ER). The positions of the molecular weight standards are indicated on the left hand side, in kDa.

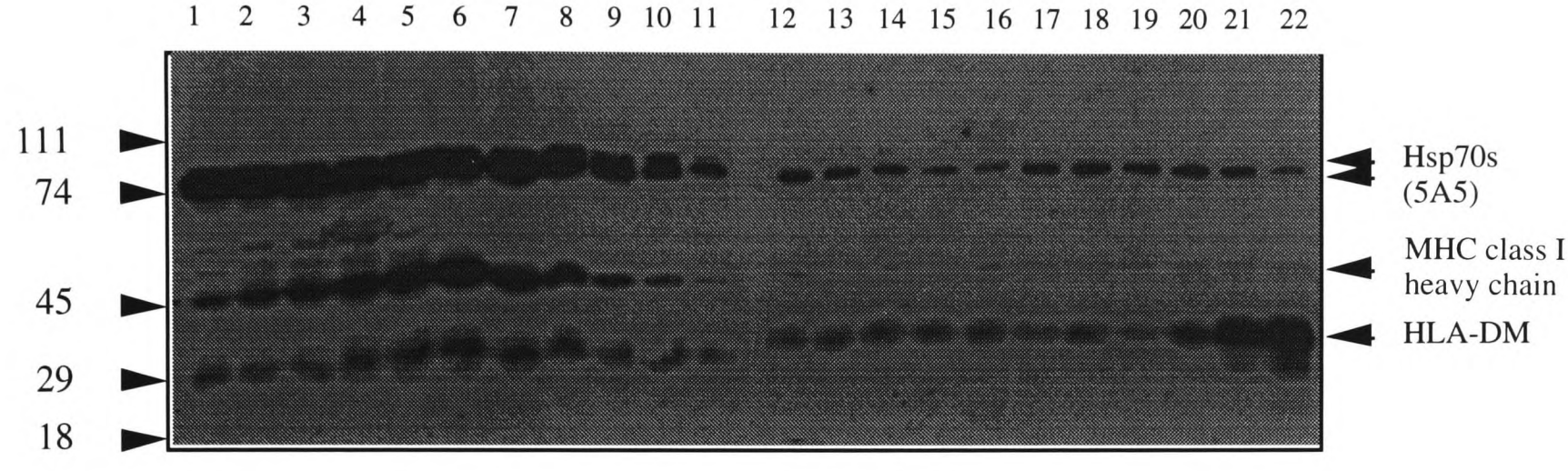

Figure 6-26: A density gradient of heat shocked cells probed with antibodies against class I heavy chain, DM and hsp70s (5A5). The fractions are the same as those described in Figure 6-24. MHC class I molecules can be detected predominantly in fractions 3-9 (plasma membrane and ER), DM molecules in fractions 4-8 (ER) and 20-22 (lysosomes), and hsp70s in fractions 1-10 (soluble proteins, plasma membrane and ER). The positions of the molecular weight standards are indicated on the left hand side, in kDa.

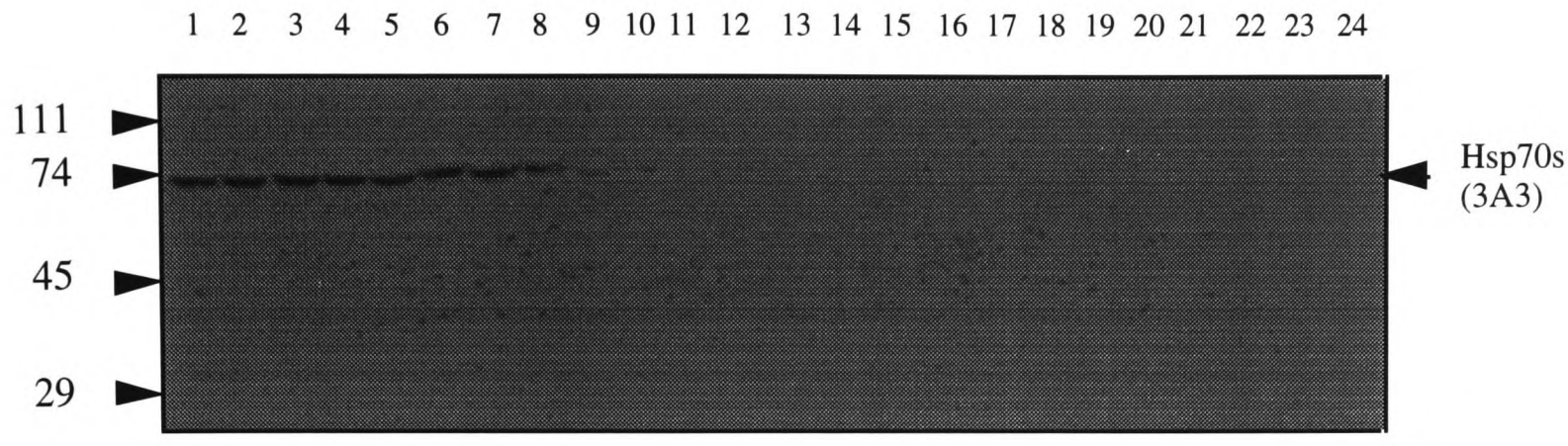

Figure 6-27: A density gradient of non-heat shocked Raji cells probed with antibody 3A3. The blot described in Figure 6-25 was stripped [E5] and probed with antibody 3A3 which detects hsp70s in fractions 1-10 of the gradient.The positions of the molecular weight standards are indicated on the left hand side, in kDa.

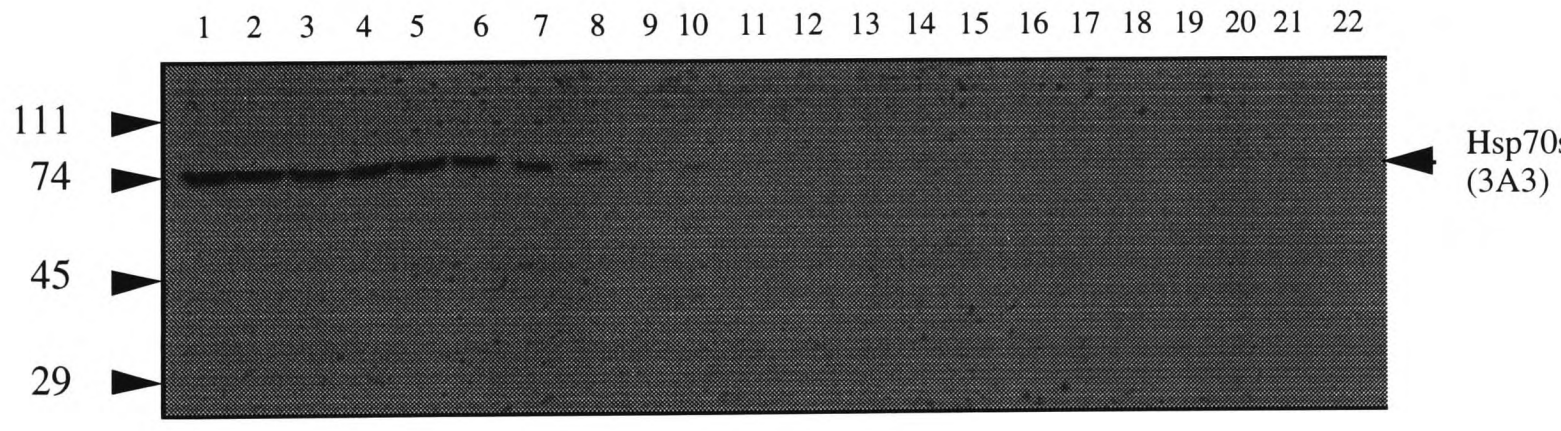

Figure 6-28: A density gradient of heat shocked Raji cells probed with antibody 3A3. The blot described in Figure 6-26 was stripped and probed [E5] with antibody 3A3, which detects hsp70s in fractions 1-8 of the gradient. The positions of the molecular weight standards are indicated on the left hand side, in kDa.

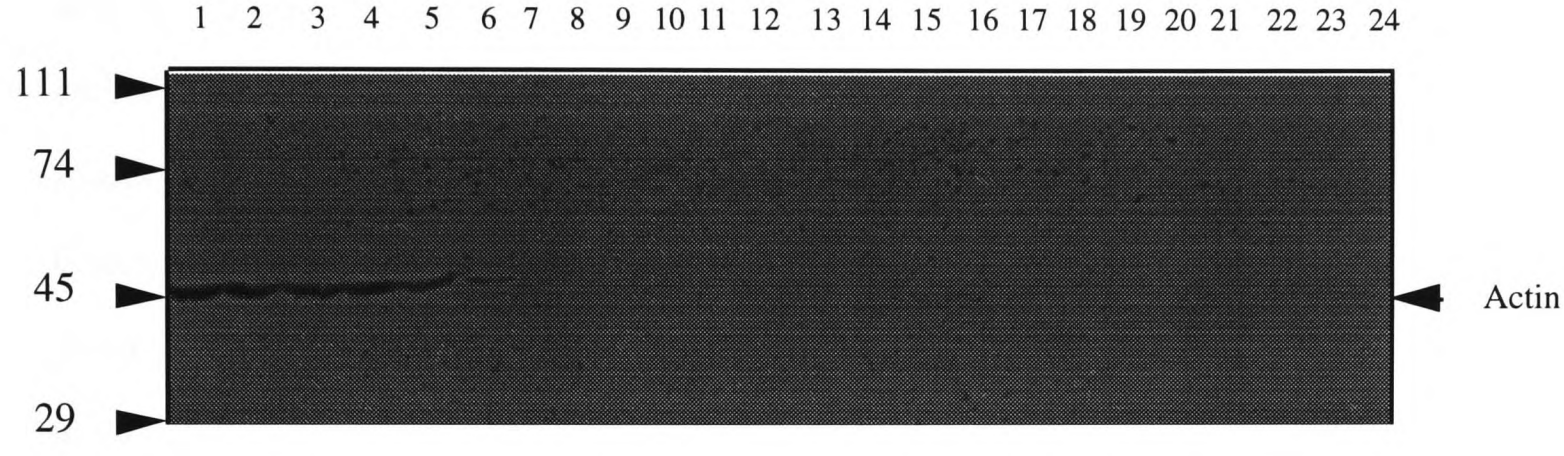

Figure 6-29: A density gradient of non-heat shocked Raji cells probed with an antibody against actin. The blot described in Figure 6-25 was stripped and probed [E5] with an antibody against actin (45 kDa), which can be detected in the first five fractions of the gradient. The positions of the molecular weight standards are indicated on the left hand side, in kDa.

density gradient, a pattern that is very similar to that of the cytoplasmic hsp70s. These results therefore support the conclusion that hsp70s in these less dense fractions are soluble rather than vesicle associated.

Distribution of Tagged Hsp70s in Osteosarcoma Cells

The distribution of specific members of the hsp70 family in Percoll density gradients was investigated by tagging them with the T7 epitope. The coding sequences of hsp70hom and BiP were tagged with a sequence encoding the T7 epitope by Dr. C. Milner (MRC Immunochemistry Unit), using the BS-Tag vector (see above). The tag was attached to the C-terminus of hsp70hom, as for PBP74. However, it could not be added to the N-terminus of BiP, which has a signal sequence that is removed from the mature protein, or to its C-terminus, which has the motif KDEL which retains the protein in the ER (Munro and Pelham, 1987). Therefore, to avoid altering the subcellular distribution of the protein, the tag was inserted close to the C-terminus (Figure 6-30), in a region that is not conserved among members of the hsp70 family (Figure 3-2). The sequences encoding the tagged hsp70s were then cloned into pcDNA3 and used to stably transfect TK143B human osteosarcoma cells.

TK143B cells expressing either tagged hsp70hom or tagged BiP (kindly provided by C. Milner) were Dounce homogenised and their vesicular contents were separated by density gradient centrifugation. The distribution of ß-hexosaminidase in these osteosarcoma cells (Figure 6-31) is similar to that of Raji cells, with activity concentrated in fractions 3-5 and 12-13, but there is more ß-hexosaminidase activity in endosomes (fractions 3-5) than lysosomes (fractions 12-13) in these cells, whereas in Raji cells, its activity is concentrated in lysosomes (Figure 6-12). Class I molecules and DM could not be detected in these gradients (data not shown), suggesting that TK143B cells do not express DM or class I molecules recognised by the antibody HC10. However, in the case

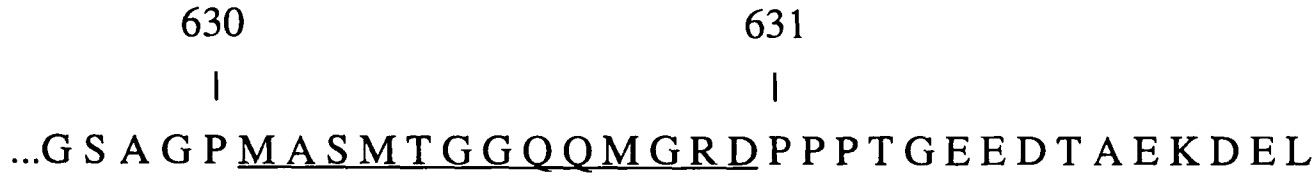

Figure 6-30: The epitope tagging of BiP. The T7 tag (underlined) was inserted between amino acids 630 and 631 of BiP, in a region that is relatively unconserved between different members of the hsp70 family. This enabled the subcellular distribution of BiP to be determined in cells expressing the tagged protein.

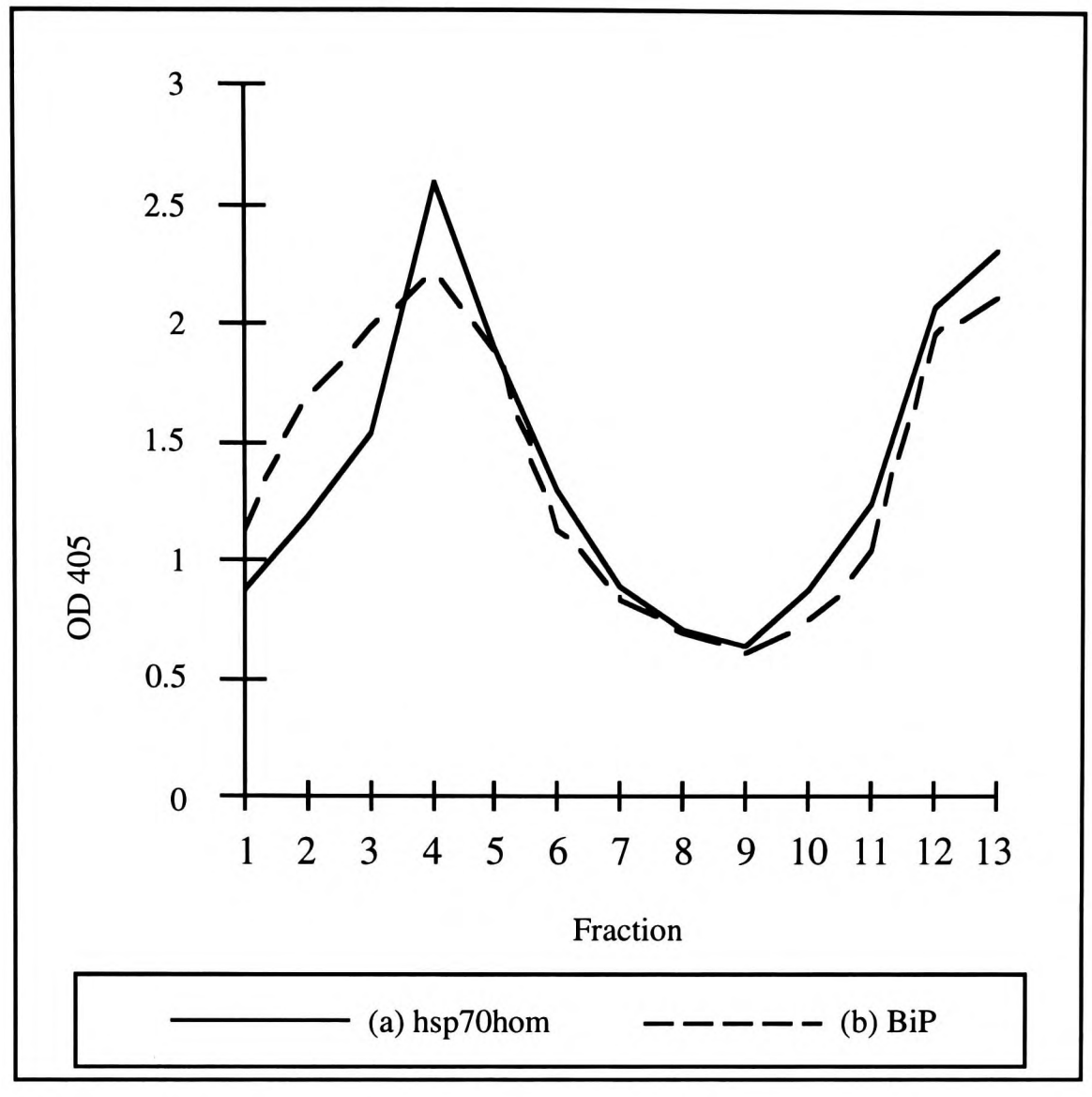

Figure 6-31: ß-hexosaminidase assay of density gradients of vesicles from TK143B cells expressing tagged BiP or hsp70hom. ~5 x 10^7 TK143B cells were harvested by trypsinisation [A3] and Dounce homogenised [F3]. The post-nuclear supernatant was centrifuged at 100 000 g for 1 hour and the pelleted vesicles were resuspended and fractionated by density gradient centrifugation (see Figure 6-12). ß-hexosaminidase activity [F4] is present in endosomes (fractions 4-6) and lysosomes (fractions 12 and 13), and is not detected in fractions that, in density gradients of whole homogenates, contain soluble proteins (fractions 1 and 2).

of the class I molecules, it is perhaps more likely that they were degraded by the trypsin used to harvest the cells. ER and plasma membrane vesicles of TK143B cells are likely to have the same densities as in Raji cells. Indeed, tagged BiP (~78 kDa) is detected in fractions 2-5 with the anti-tag antibody (Figure 6-32), and BiP is detected faintly in fractions 3-4 with antibody 5A5 (Figures 6-33 and 6-34). Tagged hsp70hom (~70 kDa) is predominantly soluble and cytoplasmic (Figure 6-35, lane S) and its distribution in the gradients (Figure 6-35) is essentially the same that of the cytoplasmic hsp70s detected by antibodies 3A3 (Figures 6-36 and 6-37) and 5A5 (Figures 6-33 and 6-34, lower band). Hsp70hom seems to be particularly abundant in fraction 4, where the bulk of the ER is (based on the distribution of tagged BiP). This suggests that it might be involved in the translocation of proteins into the ER, since hsc70 is associated with the outer face of the ER membrane via translocating proteins (Gething and Sambrook, 1992). However, the association with the ER of hsp70s detected by antibody 3A3 has never been detected in Raji cells (Figures 6-20 and 6-23), so this pattern may be unique to hsp70hom.

The localisation of BiP to the ER is not altered by the insertion of the T7 tag near its C-terminus and the localisation of hsp70hom to the cytoplasm is as expected for a protein without a signal sequence. This means that the tagged proteins are likely to be useful in investigating their roles in antigen processing.

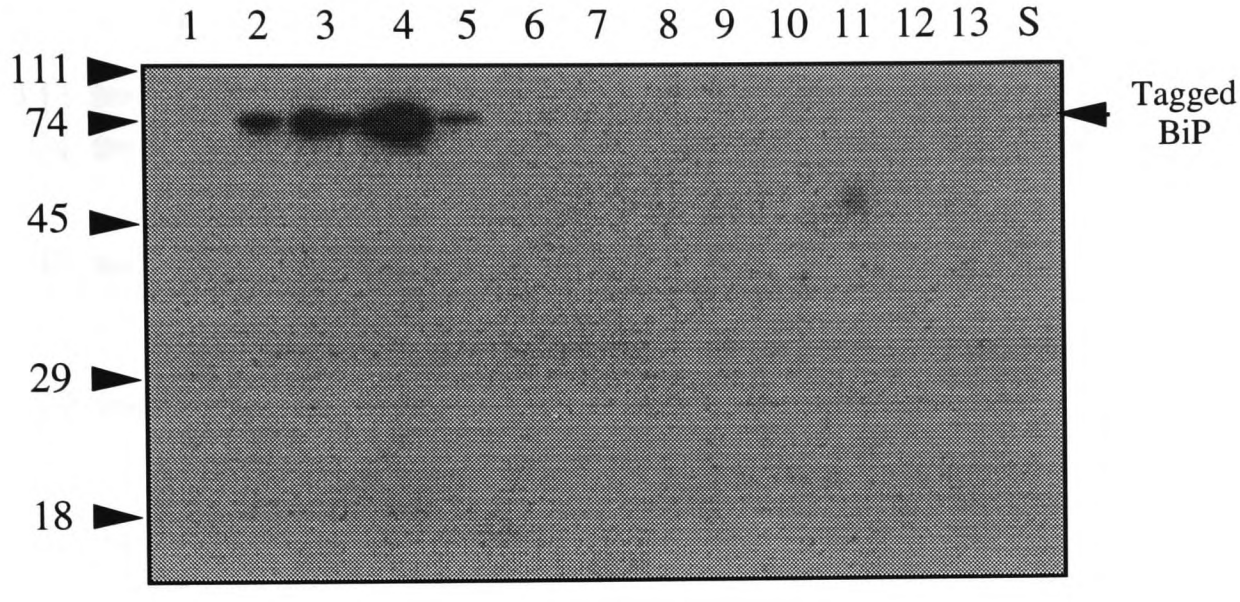

Figure 6-32: Density gradient of vesicles from TK143B cells expressing tagged BiP probed with an antibody against the T7 tag. The fractions described in Figure 6-31, and an aliquot of the post-nuclear supernatant (S), were separated on a 10% (v/v) polyacrylamide gel [E1], blotted [E4] and probed with an antibody against the T7 tag. Tagged BiP is detected in fractions 2-5 of the gradient. The positions of the molecular weight standards are indicated on the left hand side, in kDa.

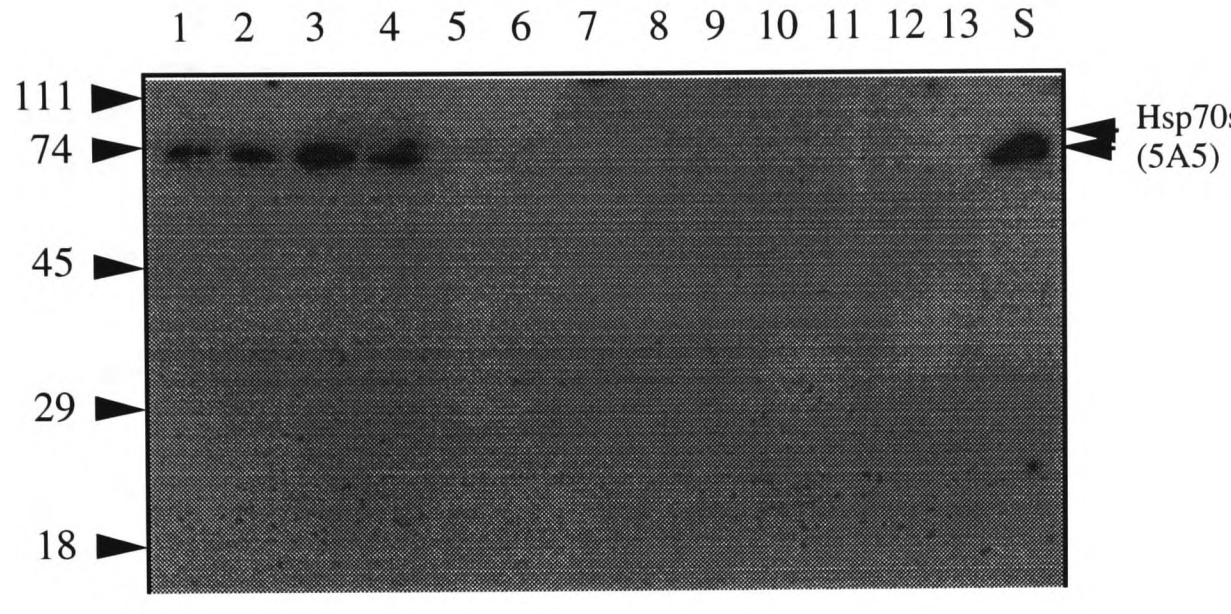

Figure 6-33: Density gradient of TK143B cells expressing tagged BiP probed with antibody 5A5. The blot described in Figure 6-33 was stripped and reprobed [E5], with antibody 5A5. Hsp70s are detected in the 100 000 g supernatant (S) and fractions 1-4 of the gradient. The upper band corresponding to BiP is detected faintly in lanes 3 and 4. The positions of the molecular weight standards are indicated on the left hand side, in kDa.

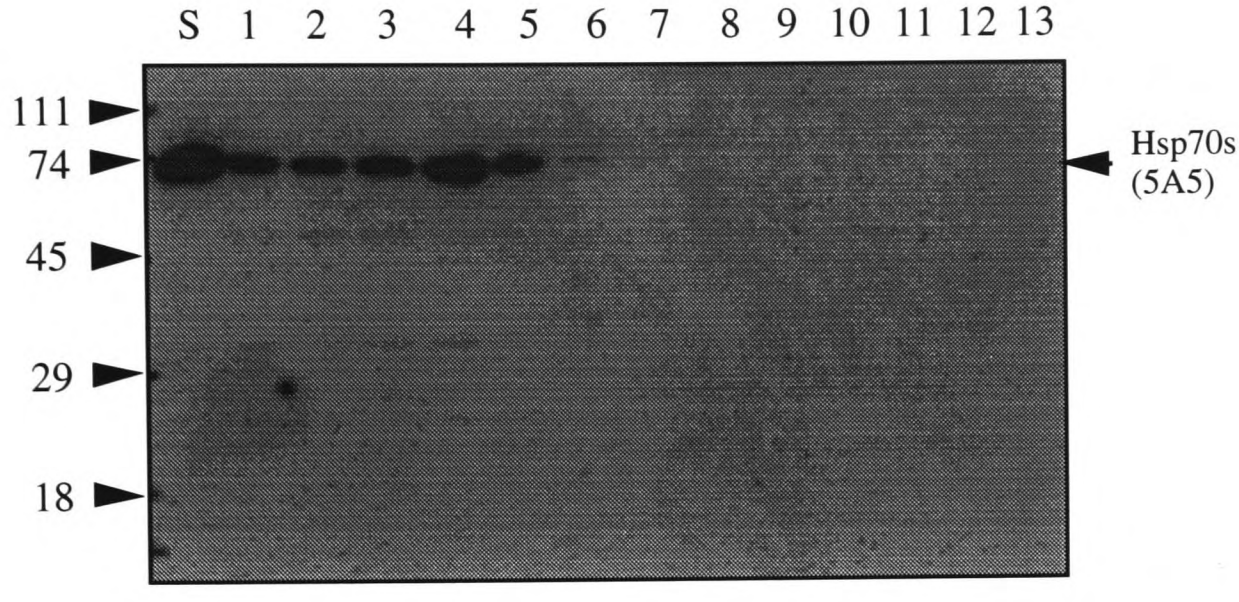

Figure 6-34: Density gradient of TK143B cells expressing tagged hsp70hom probed with antibody 5A5. The fractions described in Figure 6-31 were blotted and probed [E5] as described in Figure 6-32. Hsp70s are found in the 100 000 g supernatant (S) and fractions 1-5 of the gradient, especially fractions 4 and 5 (ER). The positions of the molecular weight standards are indicated on the left hand side, in kDa.

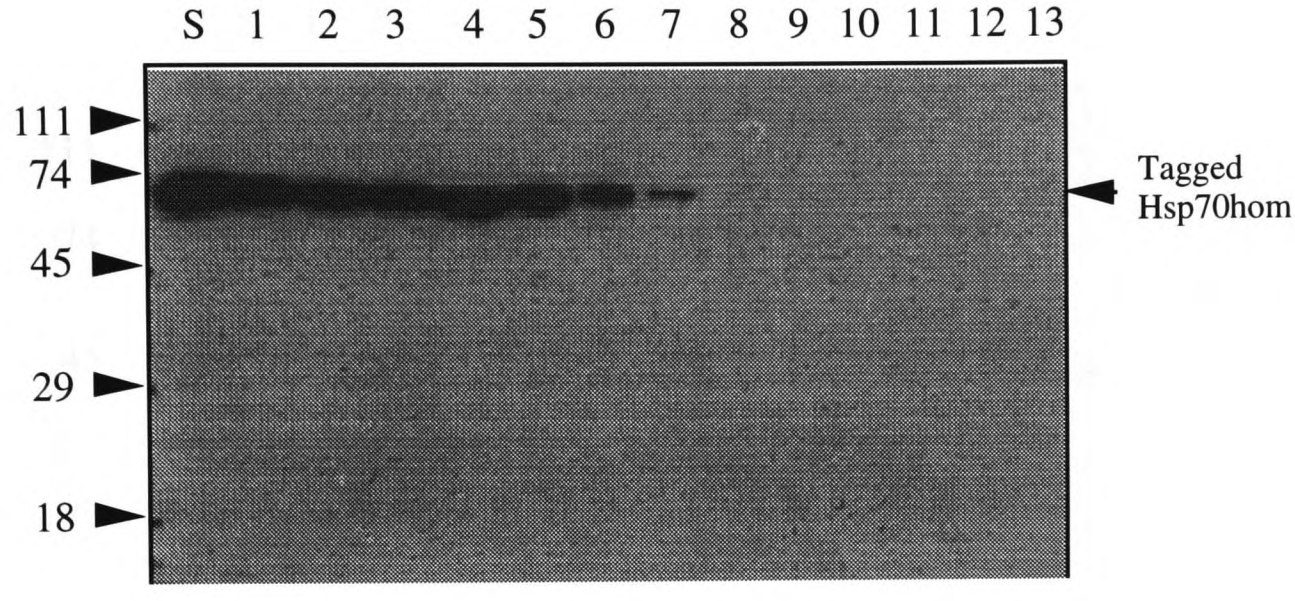

Figure 6-35: Density gradient of vesicles from TK143B cells expressing tagged hsp70hom probed with an antibody against the T7 tag. This blot was afterwards stripped and probed with antibody 5A5 (see Figure 6-34) [E5]. Tagged hsp70hom is detected in of the 100 000 g supernatant (S) and fractions 1-7 of the gradient. The positions of the molecular weight standards are indicated on the left hand side, in kDa.

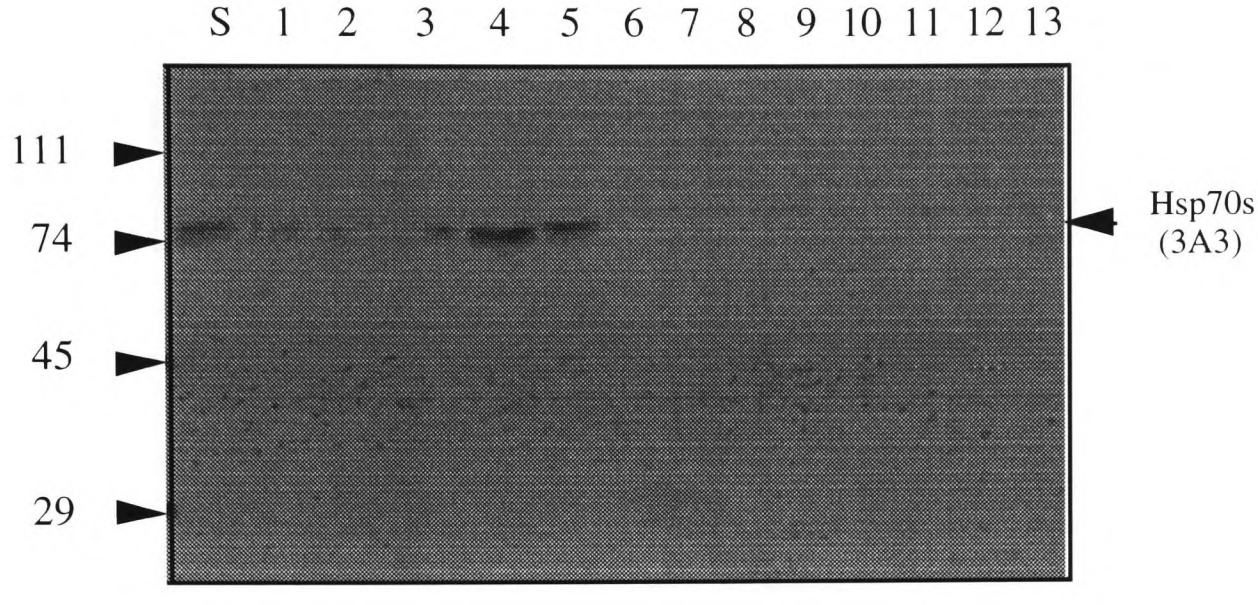

Figure 6-36: Density gradient of TK143B cells expressing tagged hsp70hom probed with antibody 3A3. This is the same blot as in Figure 6-34 after stripping and reprobing with antibody 3A3, which detects hsp70s in the 100 000 g supernatant (S) and fractions 1-5 of the gradient. The positions of the molecular weight standards are indicated on the left hand side, in kDa.

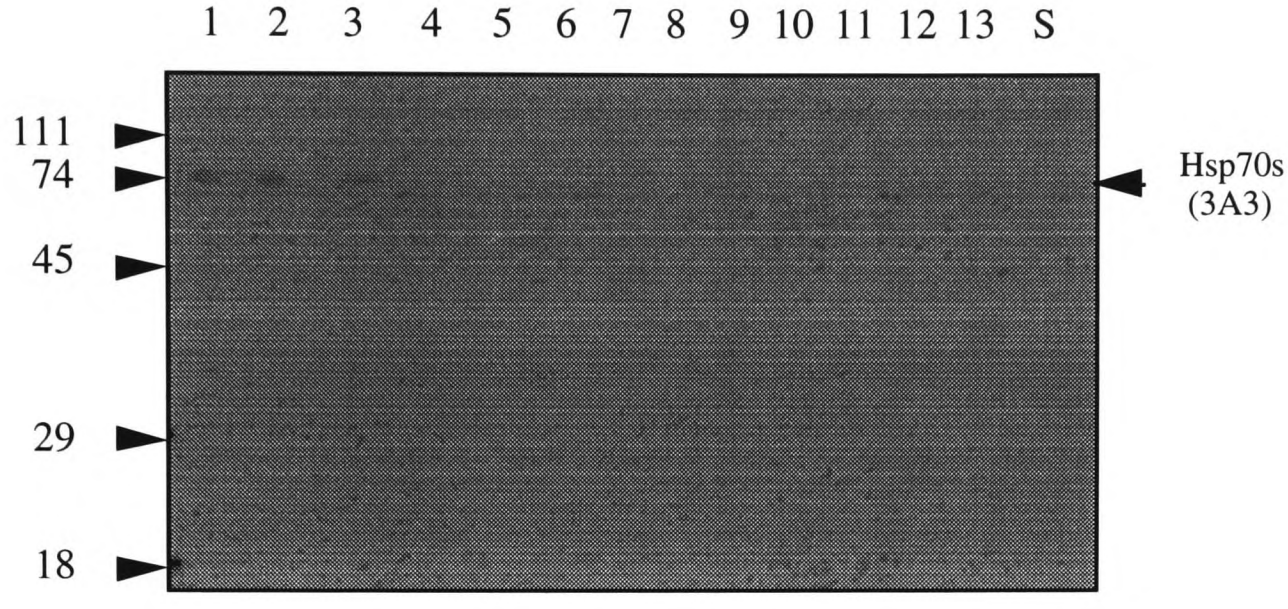

Figure 6-37: Density gradient of TK143B cells expressing tagged BiP probed with antibody 3A3. This is the same blot described in Figure 6-32 after stripping and probing with antibody 3A3, which detects hsp70s in fractions 1-3 of the gradient. The positions of the molecular weight standards are indicated on the left hand side, in kDa.

Unfolded Protein Affinity Chromatography

A broader strategy for isolating molecular chaperones from endocytic compartments is to identify proteins that bind to unfolded proteins by unfolded protein affinity chromatography. Such an approach has been used to purify ER chaperones (Nigam *et al.*, 1994); the contents of ER microsomes from rat liver were mixed with a number of different denatured proteins that were attached to agarose or sepharose beads and bound proteins were eluted with ATP, in the presence of Mg^{2+} and Ca^{2+}. In this study, a number of chaperones were purified, including some that do not depend on binding to ATP to release their unfolded protein substrates. Presumably the ATP-independent chaperones were released by ATP because they rely on forming a complex with both their substrate and ATP-dependent chaperones. Nigam *et al.* (1994) successfully purified BiP, grp94 (gp96), protein disulphide isomerase (56 kDa), calreticulin (55 kDa), ERp72 and p50, and also identified a novel ER ATP-binding chaperone, p46. Another ER-resident molecular chaperone, calnexin (88 kDa), was not eluted by ATP and could only be released from the column by acidic pH.

The possibility of identifying molecular chaperones in endocytic compartments purified by Percoll density gradient centrifugation by this method was investigated. Firstly, it was necessary to adapt the method of Nigam and colleagues (1994) to identify chaperones in ER microsomes of Raji cells. Then the method was adapted to purify chaperones from ER fractions prepared by Percoll density gradient centrifugation. Finally, the method would be applied to fractions of the density gradient containing lysosomes.

ER microsomes were prepared from ~10^9 Raji cells, weighing ~2 g [F5]. The cells were lysed by Dounce homogenisation and the homogenate was centrifuged at 20 000 g to remove whole cells, nuclei, mitochondria and lysosomes. The smaller ER microsomes remain in the supernatant under these conditions, and were pelleted by centrifugation at 100

000 g for 1 hour. The yield of microsomes was judged by resuspending them in the homogenisation buffer and measuring the protein concentration with a BCA assay [E6]. The yield was 5 μg of protein.

The microsomes were lysed with 0.5% (v/v) Triton X100 and loaded onto a column of fetuin agarose that had been denatured with 6 M urea, 1 M 2-mercaptoethanol [F6]. After washing, bound chaperones were eluted with 1 mM ATP in a buffer containing 2 mM Mg^{2+} and 0.5 mM Ca^{2+}. This was followed by an elution with 0.1 M acetic acid. In both cases, eluted proteins were collected in 1 ml fractions and samples were separated by SDS-PAGE [E1].

Several microsomal proteins were eluted from the denatured fetuin agarose column by ATP (Figure 6-38, lanes 5-7). A ~40 kDa protein is the predominant species, but potential chaperones can also be detected at approximately 110 kDa, 90 kDa, 75 kDa, 50 kDa, 45 kDa, 32 kDa and 16 kDa. Some of the 40 kDa protein appears to dissociate from the column in the presence of Mg^{2+} and Ca^{2+} alone (lane 4), while some remains bound to the column in the presence of ATP and is only eluted by acetic acid (lane 8). Some of the eluted species may correspond to grp94 (gp96), BiP (grp78), P5 (p50) and p46 as identified by Nigam *et al.* (1994), but the ~110 kDa, 40 kDa, 32 kDa and 16 kDa species appear to be novel. Therefore, the spectrum of molecular chaperones in the ER of rat liver and human B cells appears to differ.

Next, microsomes were prepared as before [F5] from 10^9 Raji cells, resuspended in 5 ml of HB+ and fractionated by Percoll density gradient centrifugation. Fractions were assayed for ß-hexosaminidase activity (Figure 6-39) and the locations of class I molecules, DM and hsp70s were determined by western blot analysis (Figure 6-40). ER fractions, containing both class I molecules and DM (fractions 3 and 4), were pooled from 2 gradients (Figure 6-41, lane 1). The vesicles were lysed with 0.5% (v/v) Triton X100 and the Percoll was pelleted by centrifugation at 100 000 g for 20 minutes (lane 2) to prevent it

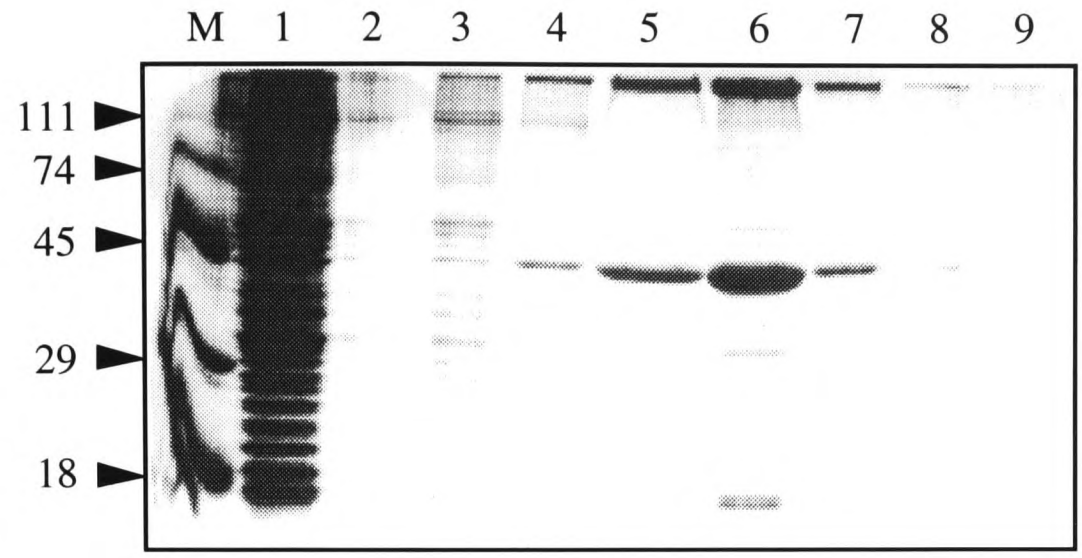

Figure 6-38: Unfolded protein affinity chromatography of microsomal proteins from Raji cells [F6]. Microsomes (5 µg) [F5] were prepared from a post-nuclear supernatant by centrifugation at 100 000 g for 1 hour [F5], resuspended and lysed in a total volume of 700 µl, and applied to a column of denatured fetuin agarose. Lane 1 contains 10 µl of this microsome preparation and lane 2 contains 10 µl of the 700 µl of flow-through from the column. The column was then washed with 10 ml of washing buffer (150 mM NaCl, 1 mM DTT, 20 mM Tris, pH 8) (lane 3 contains 10 µl of 10 ml of washings) and then 10 ml of washing buffer containing 2 mM $MgCl_2$ and 0.5 mM $CaCl_2$ (lane 4 contains 10 µl of the first 1 ml of these washings). Bound chaperones were then eluted with ten 1 ml aliquots of 1 mM ATP in washing buffer containing 2 mM $MgCl_2$ and 0.5 mM $CaCl_2$. Lanes 5, 6 and 7 contain half of the first three ATP-eluted fractions (after TCA precipitation). The column was then washed with ten 1 ml aliquots of 0.1 M acetic acid (lanes 8 and 9 contain half of the first and second fractions after TCA precipitation). Lane M contains high molecular weight markers. The samples were separated on a 10 % (w/v) polyacrylamide gel and stained with Coomassie blue [E3]. The positions of the molecular weight standards are indicated on the left hand side, in kDa.

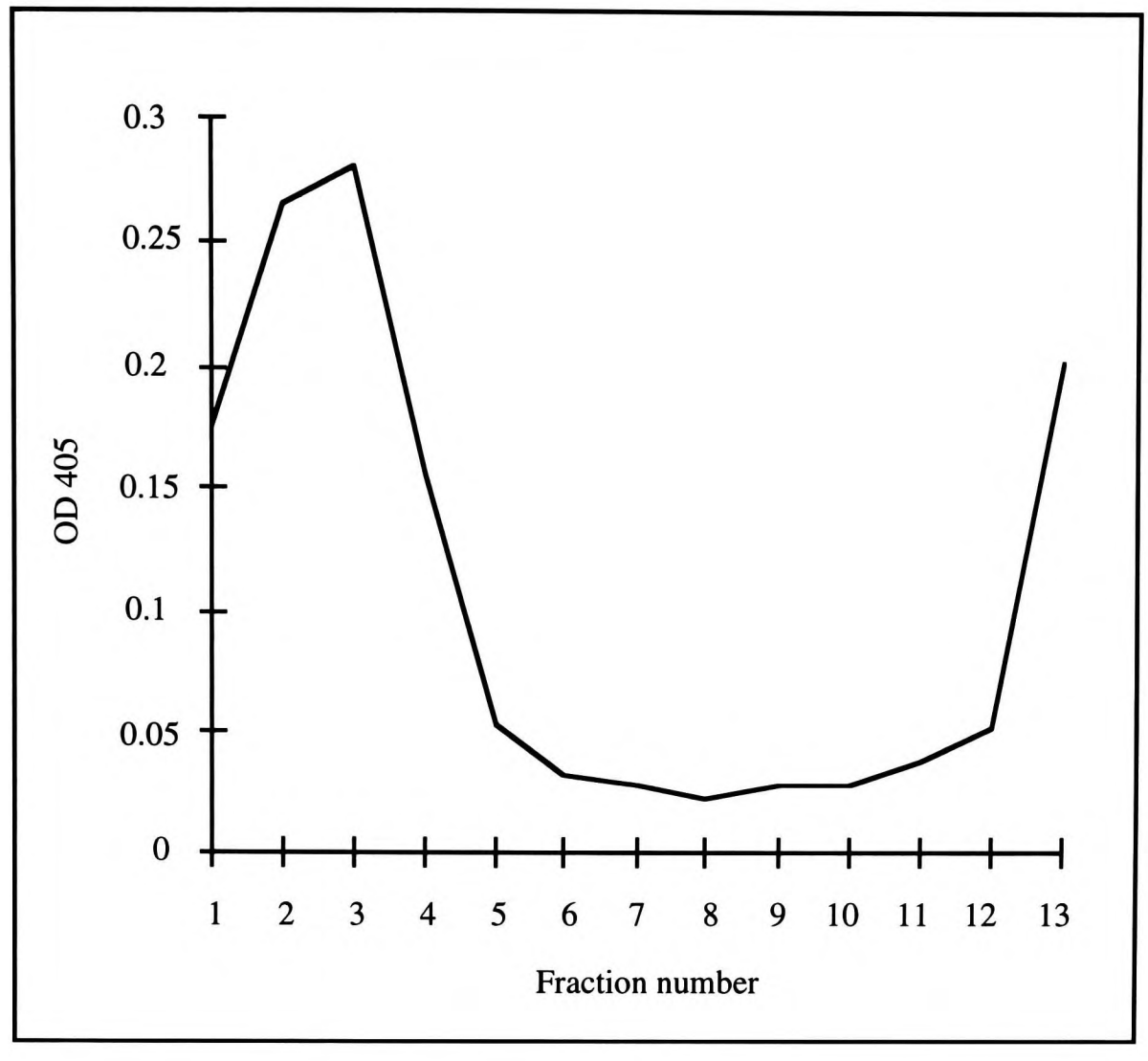

Figure 6-39: ß-hexosaminidase assay of a Percoll density gradient of microsomes from Raji cells. 10^9 Raji cells were homogenised with 80 strokes of a Dounce homogeniser in 10 ml of HB2 containing 1 mM phenylmethylsulphonyl fluoride, 10 µg/ml leupeptin and 5 mM iodoacetic acid [F5]. A post nuclear supernatant was prepared by centrifugation at 20 000 g for 30 minutes and was centrifuged at 100 000 g for 1 hour. The pelleted microsomes were resuspended in 5 ml of HB+ and loaded onto 10 ml of 20% (v/v) Percoll. After centrifugation at 25 000 g for 20 minutes, the gradient was fractionated and a sample of each fraction was assayed for ß-hexosaminidase activity [F4]. Low levels of ß-hexosaminidase can be detected in fractions 1-4 (endosomes and soluble material), and an even smaller amount is present in fraction 13 (lysosomes).

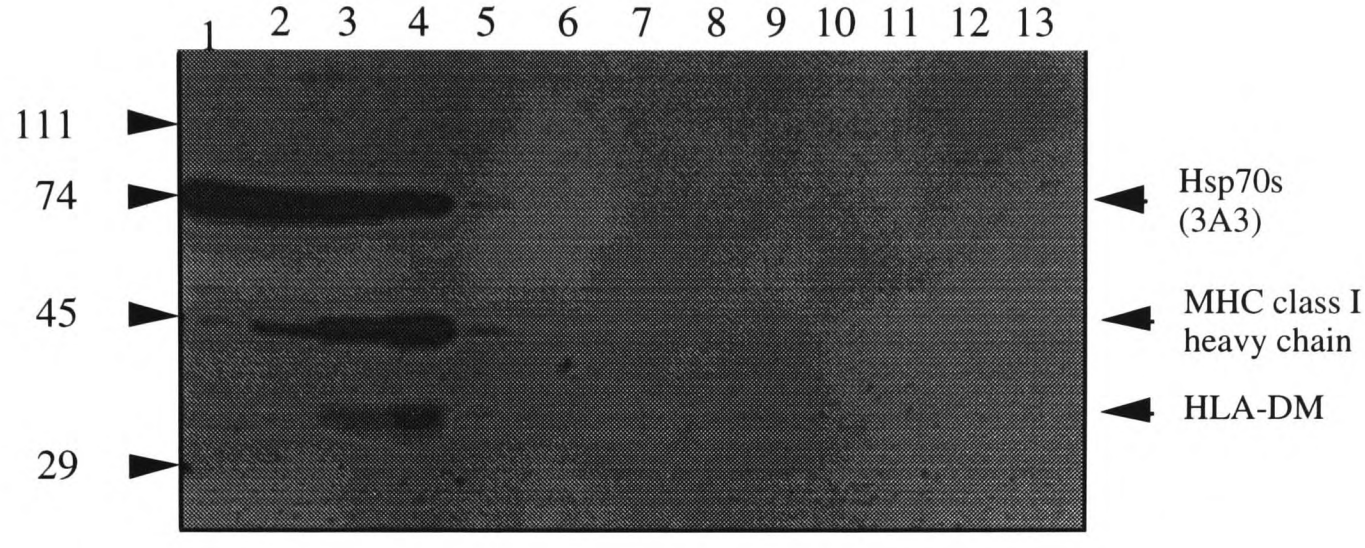

Figure 6-40: A density gradient of microsomes from Raji cells probed with antibodies against class I heavy chain, DM and hsp70s (antibody 3A3). Samples (10 µl) of the fractions prepared as described in Figure 6-39 were separated on 10% (w/v) polyacrylamide gels [E1], blotted [E4] and probed [E5] with antibodies against class I heavy chain, HLA-DM α-chain and hsp70s (3A3). Hsp70s can be detected in fractions 1-4, class I molecules in fractions 2-4 and DM in fractions 3 and 4. The positions of the molecular weight standards are indicated on the left hand side, in kDa.

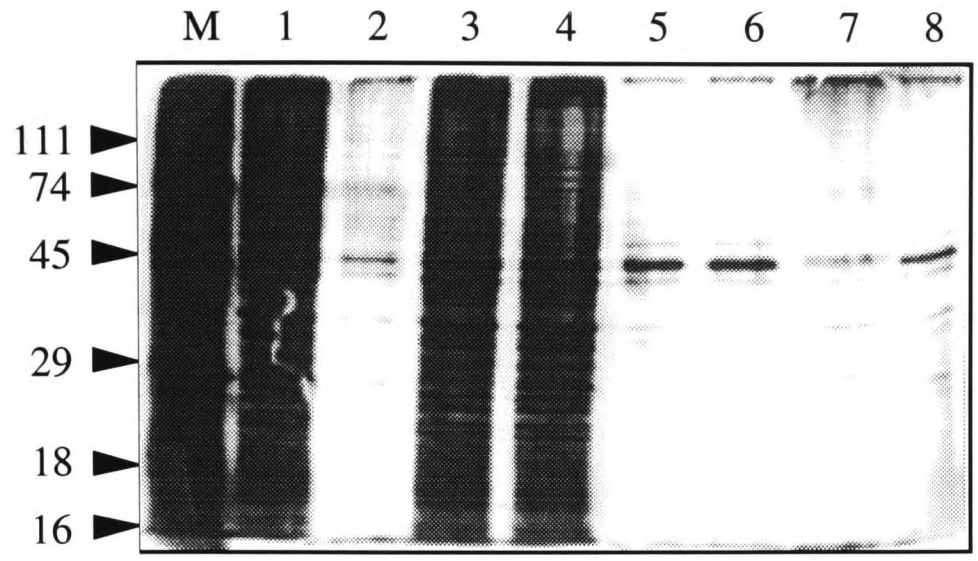

Figure 6-41: Unfolded protein affinity chromatography of proteins from ER fractions purified from Raji cells by density gradient centrifugation [F6]**.** Fractions 3 and 4 from two duplicate Percoll density gradients (described in Figures 6-39 and 6-40) contained both class I molecules and DM and, therefore, contained ER vesicles. They were pooled and lysed by addition of 0.5 % (v/v) Triton X100 (lane 1 contains 10 µl of 12 ml). The Percoll in the fractions was pelleted by centrifugation for 20 minutes at 100 000 g: lane 2 contains 10 µl of the pellet resuspended in 12 ml, and lane 3 contains 10 µl of the supernatant. This supernatant was added to the fetuin agarose column as described in Figure 6-38 (lane 4 contains 10 µl of the flow through). After washing the column, bound proteins were eluted with 1 mM ATP. Lane 5 contains half of the the first 1 ml ATP-eluted fraction and lane 6 contains half of the remaining 9 ml of eluate (after TCA precipitation). The column was then washed with 0.1 M acetic acid: lane 7 contains half of the first 1 ml fraction and lane 8 half of the remaining 9 ml (after TCA precipitation). Lane M contains high molecular weight markers. The samples were separated on 10% (w/v) polyacrylamide gels and proteins detected with silver stain [E3]. The positions of the molecular weight standards are indicated on the left hand side, in kDa.

clogging up the column. The supernatant was collected (lane 3) and added to the fetuin agarose column as before. As seen with unfolded protein affinity chromatography of microsomes (Figure 6-38), the major species eluted by ATP (lanes 5 and 6) or acetic acid (lanes 7 and 8) is a ~40 kDa protein. Other species could be detected with molecular weights of approximately 32 kDa, 37 kDa and 45 kDa. However, all the eluted proteins were only visible with silver staining and could not be detected with Coomassie blue. This contrasts with Figure 6-38, where the eluted proteins are detected strongly with Coomassie blue. Therefore, the unfolded protein affinity chromatography is much less efficient with ER microsomes that have been purified further by Percoll density gradient centrifugation. This suggests that components of the homogenisation buffer used for Percoll density gradient centrifugation interfere with the ability of molecular chaperones to bind to their substrates. The ER fractions from the density gradient are lysed in the same solution as the microsomes shown in Figure 6-38, except for the presence of 167 mM sucrose, 6.7 mM triethanolamine and 6.7 mM acetic acid.

It was not possible to reproduce the success of unfolded protein affinity chromatography when microsomes were purified by Percoll density gradient centrifugation. Therefore, it was decided not to carry on and apply the technique to lysosomes, as it is not possible to identify by N-terminal sequencing protein bands that are only visible by silver staining.

Discussion

The results presented in this chapter do not support evidence that hsp70s are located in the endocytic pathway. Firstly, PBP74, an hsp70 that was first described in early endosomes (VanBuskirk *et al.*, 1991), has been shown to reside exclusively in mitochondria. This finding has been confirmed by other studies (Dahlseid *et al.*, 1994; Webster *et al.*, 1994; Bhattacharyya *et al.*, 1995). Secondly, subcellular fractionation of a B cell line by Percoll density gradient centrifugation and subsequent probing with antibodies that each recognise a number of different hsp70s failed to detect any hsp70s in lysosomes. Hsp70s including the cytoplasmic hsp70s and BiP were detected exclusively at the top of the gradient, in fractions containing no vesicles as well as fractions containing ER, endosomes and plasma membrane. It is possible that some of the hsp70s detected represent an hsp70 inside endosomes, either a new location for an existing hsp70 or a novel member of the hsp70 family detected by the broad-specificity antibodies. However, it is more likely that hsp70 in these less dense fractions is soluble and cytoplasmic in origin. There remains the possibility that hsp70s not recognised by either of the antibodies used are found in the endocytic pathway, although this seems unlikely, given the astonishing conservation of the epitopes used between hsp70s from all known hsp70-containing compartments and from all eukaryotic species tested.

These findings are in contrast to the work of Dice and colleagues, who showed that hsc70 is found within lysosomes, particularly in serum starved fibroblasts (Terlecky and Dice, 1993) and in the liver of starved rats (Cuervo *et al.*, 1995). They demonstrated this localisation by metrizamide density gradient centrifugation and immunoelectron microscopy. In unstarved rats, lysosome-associated hsc70 was not detected by electron microscopy, and only weakly by subcellular fractionation, which is a less reliable technique. In other words, this paper does not provide strong evidence for hsp70s being

in lysosomes under normal conditions. During starvation, the amount of lysosome-associated hsc70 seen by both techniques increased dramatically. Hsc70 is unlike a typical lysosomal protein, since it lacks both a leader sequence (to direct its cotranslational translocation into the ER) and oligosaccharide groups (whose terminal mannose-6-phosphate groups could target it from the *trans*-Golgi to late endosomes and thence lysosomes). It is probably taken up as part of the non-specific degradation of cytoplasmic proteins by lysosomes during starvation of animals and serum starvation of cultured cells, which occurs by autophagy, a non-specific engulfment of cytoplasmic contents (Dunn, 1994), or by hsc70-mediated transport, since hsc70 contains a possible KFERQ lysosomal targeting motifs itself (Terlecky *et al.*, 1992). It is not known whether hsc70 still functions as a chaperone once it is inside lysosomes, but it seems unlikely as there is not known to be ATP in the endocytic pathway and the protein is likely to be degraded quickly.

Therefore, it seems likely that lysosomal degradation of cytoplasmic proteins during serum starvation does not occur in B lymphocytes. Perhaps it is not surprising that this pathway of degradation is restricted to selected tissues, such as liver, and does not occur in lymphocytes, which contain only limited cytoplasm in any case. It is likely to be advantageous for class II antigen processing cells in general to be exempted from this mechanism, because otherwise starvation would cause cytoplasmic antigens to be presented by class II molecules perhaps for the first time, breaking self-tolerance and causing auto-immunity. However, lysosomal import of cytoplasmic proteins has been seen in serum-starved fibroblasts, which express class II molecules in response to cytokines such as interferon-γ (Abbas *et al.*, 1996). Therefore, serum starvation might lead to the induction of cross-talk during an immune response.

Other evidence has also suggested that hsc70 is found inside organelles. Hsc70 coprecipitates with MHC class II molecules in lysosomal fractions of MHC-homozygous B lymphoblastoid cell lines (Auger *et al.*, 1996). It is interesting that this association occurs only with the product of a single allele (HLA-DRB1*0401), which is associated with

rheumatoid arthritis. The product of another allele (HLA-DRB1*1001), does not coprecipitate with hsc70 in lysosomal fractions under the same conditions, even though it can associate with hsc70 in immunoprecipitates from whole cell lysates. Since the same antibody against class II molecules was used in each immunoprecipitation, it seems that these experiments provide contradictory evidence, that hsc70 is both present in, and absent from, lysosomes of B lymphoblastoid cell lines. The association of hsc70 with MHC class II ß-chains depends on unknown factors or conditions, and may be an artefact that arises only once the cells and their organellar membranes have been lysed. The results presented here provide no evidence for hsc70 entering the ER (as suggested by Auger *et al.,* 1996) or lysosomes of either a lymphoblastoid cell line (Raji) or an osteosarcoma cell line (TK143B).

In summary, no hsp70s were consistently detected in fractions of density gradients that contained lysosomes or the lysosome-like MHC class II loading compartment (MIIC). Therefore, they are unlikely to help the assembly of MHC class II-peptide complexes by protecting antigenic peptides from complete degradation to amino acids, or chaperoning class II molecules themselves. It is unlikely that hsp70s are found in endosomes, where they might be involved in unfolding endocytosed antigens, but because these have the same density as ER and plasma membrane vesicles, it is not possible to say this definitively.

A broader strategy for isolating molecular chaperones from endocytic compartments was adopted. It is possible to identify chaperones by their ability to bind to unfolded proteins, by unfolded protein affinity chromatography. Such an approach was developed to identify ER chaperones from rat liver, and successfully purified many of them, including one novel species (Nigam *et al.*, 1994). Proteins from lysed ER vesicles were mixed with unfolded proteins immobilised on agarose or sepharose, washed and eluted with ATP (in the presence of Ca^{2+} and Mg^{2+}) or by acidic pH. This protocol was successfully applied to the antigen presenting Raji cell line when ER fractions they were purified by differential centrifugation as used by Nigam and colleagues. This showed that the ER of Raji cells

contains a major 40 kDa protein that appears to be novel, as well as several other less abundant putative chaperones. However, these proteins were purified much less efficiently from ER fractions that were prepared by Percoll density gradient centrifugation. As such density gradient centrifugation is necessary to purify lysosomes, it was not feasible to apply unfolded protein affinity chromatography to lysosomes. However, different centrifugation media and buffers might not interfere with the binding of chaperones to unfolded proteins, in which case this technique would be useful.

An alternative strategy to identify chaperones in endocytic compartments would be to purify proteins that bind to immobilised ATP. This approach is successful in purifying hsp70s from the cytoplasm of mammalian cells (Welch and Feramisco, 1985). However, lysosomes do not appear to contain hsp70s and other chaperones may not be ATP-dependent, as a mechanism for importing ATP into lysosomes is not known.

Chaperones are involved in the degradation of proteins in the cytoplasm, ER and mitochondria of eukaryotic cells and in the cytoplasm of bacteria (see Chapter 1), where they are involved in selecting substrates, unfolding them so they become accessible to proteases and preventing them from aggregating. All these considerations apply to substrates of proteolysis in the endocytic pathway as well. Chaperones may therefore be needed in endocytic compartments to unfold acid-stable proteins so that they become accessible to proteases and prevent chaperone- or acid-unfolded proteins from aggregating. They would therefore be involved in regulating proteolysis so that cellular endosomal and lysosomal proteins are prevented from being degraded. While the work presented in this chapter effectively discounts members of the hsp70 family in this story, there is a place for members of other, possibly novel, chaperone families in the MHC class II pathway of antigen processing and presentation.

Chapter 7: Regulation of the Expression of Hsp70s by Cytokines

Introduction

The proposed role of hsp70s in immunity suggests that their expression may be regulated during an immune response. Activation and regulation of the immune response is controlled by soluble glycoproteins called cytokines (reviewed by Abbas *et al.*, 1996). Each is a signal, secreted by particular cells in response to particular stimuli and interpreted by different cell types in different ways to provide a concerted attack on infections. An overview of the actions of several cytokines that may regulate the expression of hsp70s is given below.

The Actions of Cytokines

Type I interferons (IFN-α and -ß) are produced by many types of cell in response to viral infection and stimulation with hormones and cytokines such as tumour necrosis factor (TNF) (reviewed by Chelbi-Alix and Sripati, 1994). IFN-α and -ß inhibit viral replication in a wide range of cell types. They induce the expression of 2'5'-oligoadenylate synthetase, which is activated by the double stranded RNA that is a feature of viral infection to produce 2'5'-linked oligoadenylates. These inhibit the production of viral and cellular proteins by activating a cellular endonuclease to degrade mRNA.

Type II interferon (IFN-γ) is secreted by T lymphocytes in response to antigen stimulation, an effect enhanced by the T cell growth factor, IL-2. Like, the type I interferons, it inhibits viral replication and cell proliferation in a wide range of cell types. It also increases expression of MHC class I molecules and other components of this antigen

processing pathway (see below), and induces a diverse range of cell types to express MHC class II molecules. Since IFN-γ is produced by T lymphocytes and stimulates their activation by increasing the expression of MHC-peptide complexes, it amplifies the recognition phase of an immune response. It also promotes maturation of cytotoxic T cells and stimulates secretion of antibodies by B cells, although it inhibits B cell proliferation. IFN-γ is also powerful in innate immunity. It is a potent activator of mononuclear phagocytes, inducing them to synthesise enzymes of the respiratory burst to kill endocytosed micro-organisms. It acts in concert with lipopolysaccharide (LPS), a component of the bacterial cell wall, and perhaps TNF, to enable macrophages to kill tumour cells. It also activates neutrophils and NK cells.

Tumour necrosis factor (TNF) is the principal mediator of the host response to gram-negative bacteria and may also play a role in immune responses to other infections (Camussi *et al.*, 1991). It is produced by activated T cells, NK cells, macrophages (for example after LPS-stimulation) and mast cells. TNF is an inflammatory mediator with broad-ranging effects, and TNF receptors are present on almost all cell types examined. At low concentrations (~1 nM), TNF acts locally as a regulator of leukocytes and endothelial cells: it causes endothelial cells to adhere to neutrophils, monocytes and lymphocytes, attracting them to sites of infection; it activates inflammatory cells such as neutrophils, eosinophils and macrophages to kill micro-organisms; it stimulates macrophages to produce IL-1, IL-6 and TNF itself; and, like IFN-γ, it increases the expression of MHC molecules. TNF has systemic effects if it is produced in quantities sufficient to enter the blood stream: it activates the production of prostaglandins in the hypothalamus to cause fever; it stimulates macrophages and perhaps vascular endothelial cells to secrete IL-1 and IL-6 in the circulation; it induces the hepatic synthesis of serum proteins such as complement factors; and it acts on vascular endothelium to activate coagulation, and suppresses blood cell production in the bone marrow. Prolonged TNF treatment causes metabolic wasting (cachexia) and at very high levels, it is fatal. Since IFN-γ enhances the

production of TNF by activated macrophages and also augments many other of its effects, TNF provides a link between acquired and innate immunity.

Interleukin-1 (IL-1), like TNF, mediates inflammation in innate immune responses. It is mainly produced by macrophages activated by LPS or cytokines such as TNF or IL-1 itself, or by contact with helper T cells. It is also produced by epithelial and endothelial cells. IL-1 is synthesised in two forms, α and β, which have the same effects because they bind to the same receptor; most of the IL-1 activity found in the circulation is IL-1β. IL-1 enhances the proliferation of helper T cells and the growth and differentiation of B cells; it stimulates production of itself, IL-6 and IL-8 (which activates neutrophils) by phagocytes and vascular endothelium; it promotes coagulation; and it aids leukocyte adhesion. At high concentrations, IL-1 shares with TNF the ability to cause fever, induce production of plasma proteins by the liver and initiate metabolic wasting. However, unlike TNF, IL-1 does not affect the expression of MHC class I and II molecules.

Interleukin-6 (IL-6) is synthesised by macrophages, vascular endothelium, fibroblasts and other cell types in response to IL- 1 and, to a lesser extent, TNF. Like them, it causes hepatocytes to synthesise a unique pattern of plasma proteins that contribute to the acute phase response. It is also the principal growth factor of activated B cells and helps to stimulate T cells.

The Effects of Cytokines on the Expression of Hsp70s

The effects of cytokines on expression of hsp70s have mainly been studied *in vitro* with primary cultures of various cell types or, where indicated, in cell lines.

IFN-α and -ß inhibit hsp70 expression in human monocytes, although paradoxically they enhance the ability of prostaglandin PGA1 to stimulate it (D'Onofrio *et al.*, 1993). However, in human fibroblast and epithelial cell lines, both double-stranded RNA and insulin increase levels of hsp70(s), an effect that can be abolished with antibodies against

IFN-α and -ß (Chelbi-Alix and Sripati, 1994). IFN-ß has no effect on hsp70 expression by purified human oligodendrocytes (D'Souza *et al.*, 1994). Interestingly, stressing cells with heat or ethanol mimics the effects of IFN-α and -ß, by inducing the expression of 2'5'-oligoadenylate synthetase (Chelbi-Alix and Chousterman, 1992).

IFN-γ enhances the expression of hsp70 in human thyroid epithelial cells (Sztankay *et al.*, 1994) and cultured fibroblasts (Heufelder *et al.*, 1991). However, IFN-γ has no effect on hsp70 expression by human monocytes (Polla *et al.*, 1987; Fincato *et al.*, 1991) or human oligodendrocytes (D'Souza *et al.*, 1994).

TNF induces the production of prostaglandins by the hypothalamus, and several prostaglandins induce hsp70 expression in a range of cell types (reviewed by Santoro, 1994). In addition, TNF alters the expression of hsp70s in several cell types directly. TNF stimulates the expression of hsp70 in human monocytes, an effect mimicked by lipopolysaccharide (LPS), which elicits the secretion of cytokines including TNF from monocytes (Fincato *et al.*, 1991). This may be because TNF enhances phagocytosis (Klebanoff *et al.*, 1986), which is known to induce heat shock proteins in human monocytes and macrophages (Clerget and Polla, 1990). The heat shock response may be induced during phagocytosis to protect the phagocyte from the oxygen free radicals that are produced to kill phagocytosed organisms (Kantengwa *et al.*, 1991). Indeed, oxidative stress is known to mimic heat shock (Donati *et al.*, 1990), and transfected WEHI-S mouse tumour cells overexpressing hsp70 are resistant to the toxic effects of TNF (Jaattela *et al.*, 1992), and therefore are more tumourigenic (Jaattela, 1995). In non-monocyte cells, the effects of TNF on hsp70 expression are mixed. Hsp70 expression is stimulated by TNF in feline cardiac myocytes (Nakano *et al.*, 1996), but not in rat islets of Langerhans (Helqvist *et al.*, 1991) or human oligodendrocytes (D'Souza *et al.*, 1994). LPS-conditioned Raw medium (medium containing cytokines such as TNF secreted by LPS-activated Raw monocytes) enhanced hsc70 rather than hsp70 expression in human astrocytes (Hong-Brown and Brown, 1994).

IL-1α (but not IL-1ß) induces hsp70 expression in human oligodendrocytes (D'Souza *et al.*, 1994) and IL-1ß induces hsp70 expression in isolated rat islets of Langerhans (Helqvist *et al.*, 1989; Strandell *et al.*, 1995). This may be a mechanism to protect the cells against the toxic effects of IL-1ß, like the induction of hsp70 in monocytes and macrophages by TNF. Indeed, islet cells to which purified hsp70s have been delivered in liposomes are protected from the inhibitory effects of IL-1ß on insulin secretion (Margulis *et al.*, 1991). Heat shock proteins are not induced by IL-1ß in rat thyroid cells, rat mesangial cells or human monocytes (Helqvist *et al.*, 1991), and hsc70 rather than hsp70 is induced by IL-1ß in bovine chondrocytes (Cruz *et al.*, 1991) and cultured human astrocytes (Hong-Brown and Brown, 1994).

IL-6 has been shown to decrease hsc70 levels in human astrocytes, and this effect was opposed by insulin (Hong-Brown and Brown, 1994). It also induces the synthesis of hsp70s in HuH7 hepatoma cells (A. Stephanou, personal communication), but not blood monocytes (A. Stephanou, personal communication), or oligodendrocytes (D'Souza *et al.*, 1994).

An *in vivo* study has also been informative. Injection of lipopolysaccharide (LPS) into the peritoneum of mice increased the expression of hsp70 by peritoneal macrophages (but not thymocytes or spleen cells), with hsp70 levels reaching a peak 4 days after injection (Zhang *et al.*, 1994). This induction was markedly increased by TNF, slightly increased by IFN-γ, and opposed by IL-1, although none of these cytokines altered hsp70 levels when administered alone.

The effects of cytokines on the expression of hsp70s is therefore confusing, with different cytokines having very different effects on different cell types. Part of the problem may be the use of very different detection methods, ranging from detection of hsp70 mRNAs by Northern blotting to detection of the respective proteins by SDS-PAGE and Coomassie blue staining or antibodies, which although usually monoclonal may have

slightly different specificities for less well known members of the hsp70 family such as hsp70hom, hsp70B' and hsp70A2. Even different preparations of a given cell type can give different results. Thus IL-1α, IFN-γ and TNF-α induced hsp70 expression in oligodendrocytes grown in mixed glial cell cultures, but in purified oligodendrocytes, only IL-1α induced hsp70 expression. In mixed glial cell cultures, an IL-1 receptor antagonist abrogated hsp70 induction by IFN-γ and TNF-α as well as that due to IL-1α, confirming that the latter cytokine mediates the effects of the first two (D'Souza *et al.*, 1994). In addition, heat shock protein expression increases during cell division so, in cell lines, hsp70 levels may be higher than normal. Activated B lymphocytes (Spector *et al.*, 1989) and IL-2 stimulated T lymphocytes (Ferris *et al.*, 1988) have elevated hsp70 levels, although expression of hsc70 rather than hsp70 is induced by phorbol esters (stimulators of cell division) in bovine chondrocytes (Cruz *et al.*, 1991). Phorbol esters induce hsp70 expression in monocytes (Fincato *et al.*, 1991), but as these are terminally-differentiated, non-proliferative cells, they must do this other than by stimulating cell division. In addition, components of serum can alter expression of hsp70s, and their concentrations may vary between suppliers and even batches. Thus Transforming Growth Factor-ß (TGF-ß), though not PDGF, FGF and EGF, stimulates embryonic cells to proliferate and to express hsp70, hsc70, BiP and hsp90 (Takenaka and Hightower, 1993). This induction of a broad range of chaperones precedes the general increase in protein synthesis induced by TGF-ß and may be a preparatory event.

Cytokines and the MHC Class I Antigen Processing Pathway

It has been proposed that hsp70s are involved in the MHC class I pathway of antigen processing (see Chapter 1), and hsp70 genes may therefore be coregulated with other components of the pathway. IFN-β, IFN-γ and TNF increase the expression of MHC class I heavy chains (Johnson and Pober, 1990), $ß_2$-microglobulin (Johnson and Pober,

1990), TAP (Epperson *et al.*, 1992), LMP2 and LMP 7 (Roby *et al.*, 1995) in a range of cell types. Interferons and TNF act synergistically in stimulating the expression of these proteins (Epperson *et al.*, 1992). IFN-γ also induces the expression of gp96 (grp94), an ER-resident hsp90 that binds to antigenic peptides in the ER (Lammert *et al.*, 1997).

It was decided to focus on the cytokines interferon-γ (IFN-γ) and tumour necrosis factor (TNF), because of their effects on class I antigen processing, and interleukin-1ß (IL-1ß) and interleukin-6 (IL-6), which are known to have effects on the expression of hsp70s. As described above, IFN-γ is involved in cell-mediated immunity and is principally derived from activated T lymphocytes, whereas TNF, IL-1 and IL-6 are mediators of innate immune responses, and are produced by activated monocytes and macrophages.

While previous studies have demonstrated the induction of several different hsp70s by a range of cytokines, the aim of the present studies is to confirm these findings in well characterised cell lines and identify exactly which members of the hsp70 family are being induced. This study examines the effects of IFN-γ, TNF, IL-1ß and IL-6 on the expression of hsp70s in several human cell lines, using antibodies 3A3 and 5A5 (see Chapter 6), which each recognise several hsp70s, as well as antibodies specific for hsp70 and hsp70hom. In addition, expression of the three MHC-encoded hsp70 genes was detected at the RNA level, using locus specific probes.

Results

The Effects of IFN-γ on the Expression of Hsp70s Recognised by Antibodies 3A3 and 5A5

Preliminary experiments examined the effects of recombinant human IFN-γ on five human cell lines: HeLa (derived from an epitheloid carcinoma), HT1080 (fibrosarcoma), Raji (Burkitt's lymphoma), SW620 (colon adenocarcinoma) and TK143B (osteosarcoma). The cell lines were treated with 200 U/ml IFN-γ for 24 hours. Cell lysates were prepared and a sample of each was separated by SDS-PAGE [Chapter 2, Section E1], Western blotted [E4] and probed [E5] with monoclonal antibodies 3A3 (Figure 7-1a) and 5A5 (Figure 7-2a), which recognise mt hsp70 or BiP, respectively, as well as the human cytoplasmic hsp70s (Figure 6-15). An antibody against actin, the expression of which is not regulated by cytokines, was used as a control to check by eye that the loading of the wells was even (Figures 7-1b and 7-2b).

IFN-γ induces hsp70s recognised by antibody 3A3 in TK143B, HeLa, HT1080 and possibly SW620 cells, though not Raji cells (Figure 7-1). It possibly induces hsp70s recognised by antibody 5A5 in HeLa cells but strongly represses them in Raji (Figure 7-2). Since the two antibodies differ only in the recognition of mt hsp70 by 3A3 and the recognition of BiP by 5A5, these results suggests that IFN-γ induces mt hsp70 in a broad range of cell types and represses BiP in Raji cells. However, it is far from obvious what the biological significance of the induction of mitochondrial hsp70 by IFN-γ may be, so it is possible that IFN-γ induces one of the cytoplasmic hsp70s that is recognised by both antibodies, but that this is detected only weakly by antibody 5A5, perhaps because of the relative strength of the BiP signal in most cell lines.

MHC class I molecules are induced by IFN-γ, so an antibody against class I heavy chains (HC10) was used as a positive control to show that the cytokine was active in this

(a) Antibody 3A3

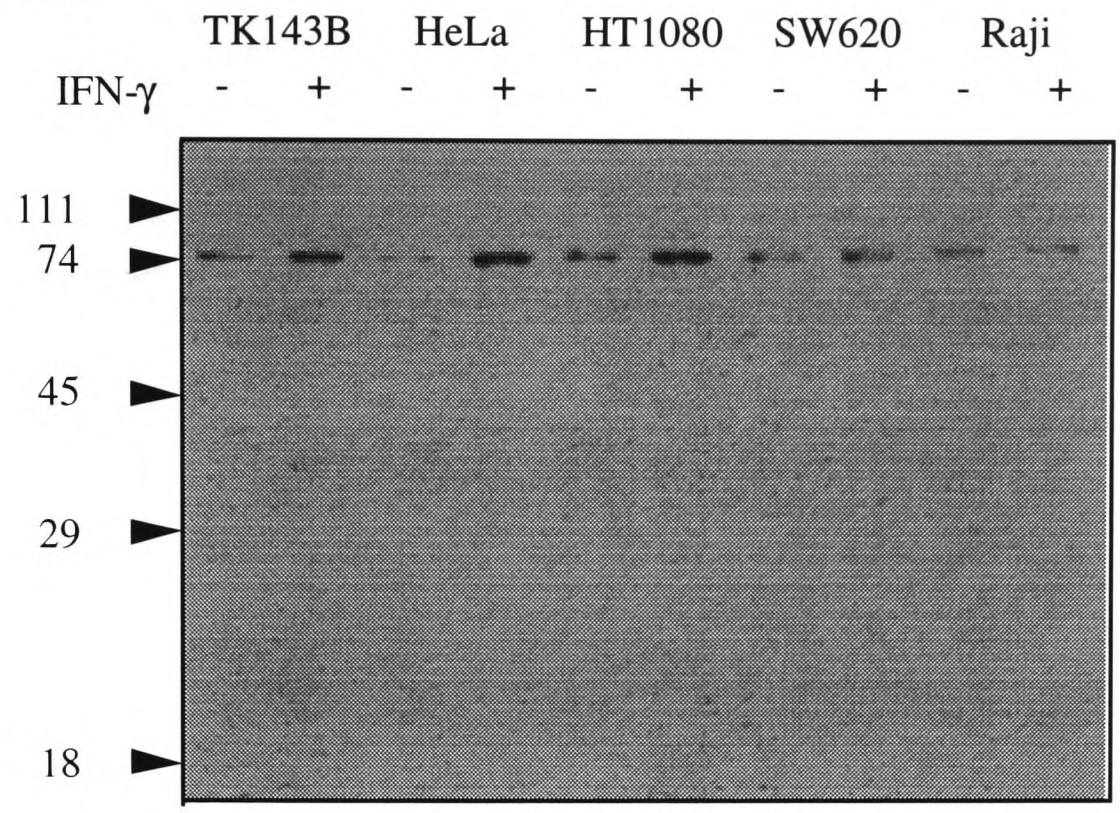

(b) Actin antibody

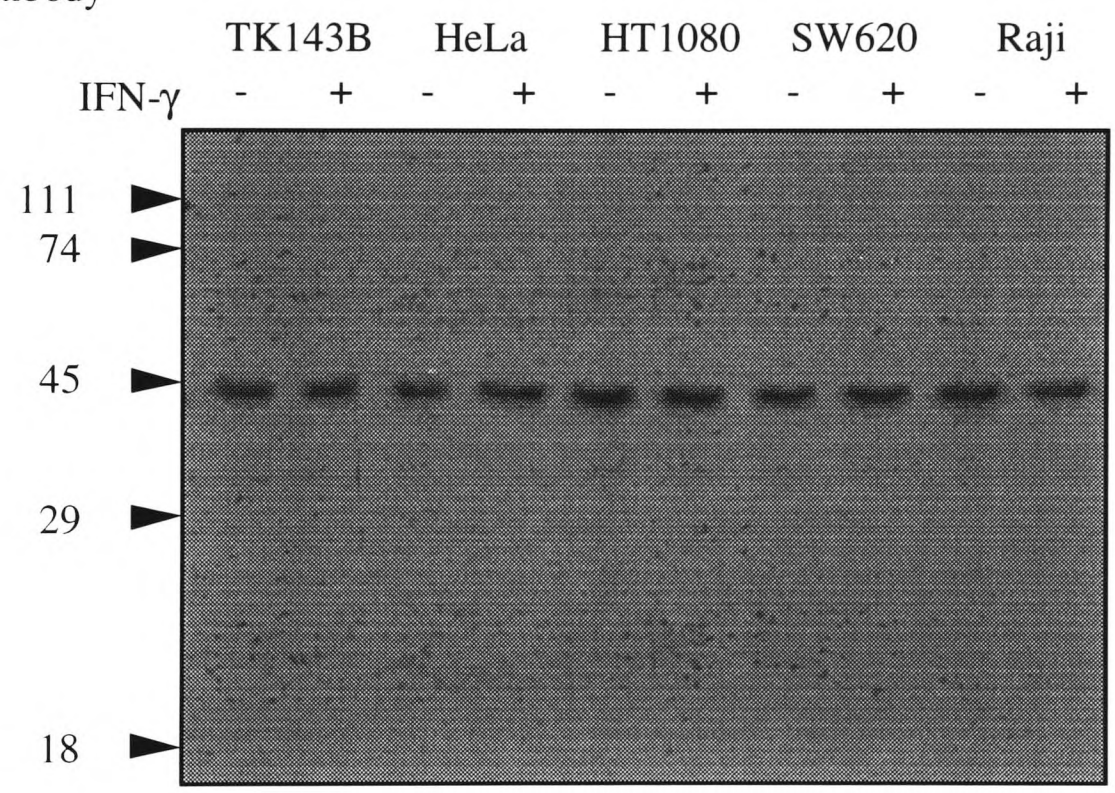

Figure 7-1: Effect of interferon-γ on the expression of hsp70s recognised by antibody 3A3. TK143B, HeLa, HT1080, SW620 and Raji cells (~10^7 cells each in an 80 cm^2 flask) were cultured for 24 hours in the presence (+) or absence (-) of 200 U/ml IFN-γ [A3]. The cells were harvested by scraping or by centrifugation at 2 000 g, then washed, and lysed by sonication in 600 µl of PBS. The insoluble material in the lysate was removed by centrifugation at 12 000 g for 5 minutes. A sample of each cell lysate (80 µg protein by BCA assay) was separated on a 12% (w/v) polyacrylamide gel [E1], blotted [E4] and probed with either (a) antibody 3A3 (cytoplasmic hsp70s + mt hsp70) or (b) an antibody against actin (45 kDa) [E5]. Antibodies bound to the blot were detected with a secondary antibody conjugated to alkaline phosphatase and enhanced chemiluminescence [E5]. The position of the molecular weight standards is indicated in kDa.

(a) Antibody 5A5

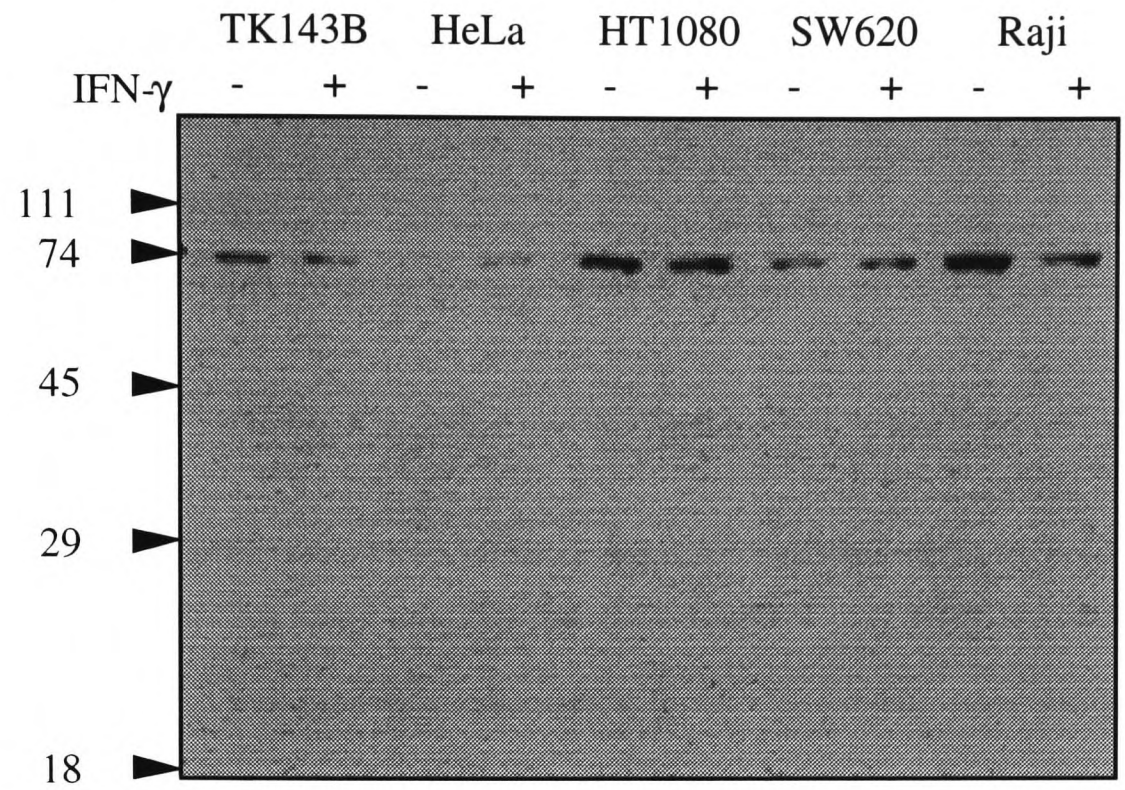

(b) Actin antibody

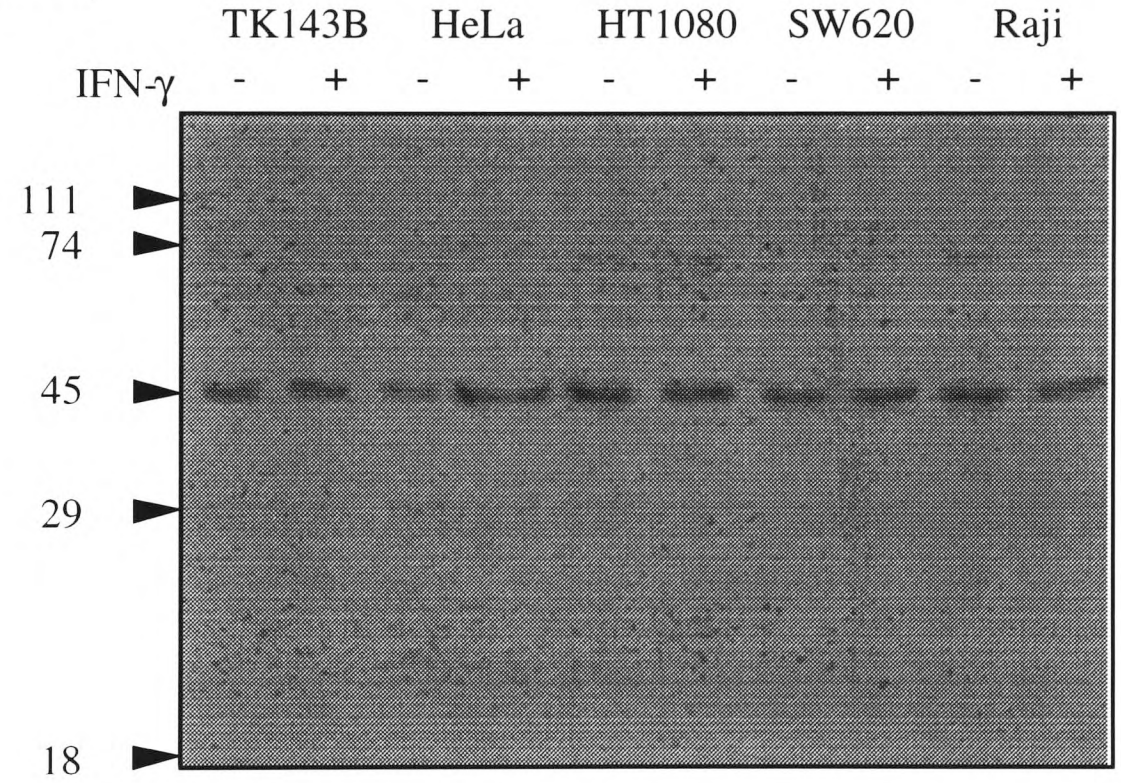

Figure 7-2: Effect of interferon-γ on the expression of hsp70s recognised by antibody 5A5. TK143B, HeLa, HT1080, SW620 and Raji cells were cultured for 24 hours in the presence or absence of 200 U/ml IFN-γ. Western blots were prepared as described in Figure 7-1, and probed with (a) antibody 5A5 (cytoplasmic hsp70s + BiP) and (b) an antibody against actin. The position of protein molecular weight standards is indicated on the left hand side, in kDa.

system. The induction of MHC class I heavy chains by IFN-γ (250 U/ml) and TNF (100 U/ml) is typically three-fold after 12 hours (Epperson *et al.*, 1992). However, only a small induction in the expression of class I molecules could be detected in this study (less than two-fold, data not shown).

The Effects of IFN-γ, TNF, IL-1 and IL-6 on the Expression of mRNAs of the MHC-encoded Hsp70s

It was interesting to determine whether the antibody 3A3 was detecting an induction by IFN-γ of one of the cytoplasmic MHC-encoded hsp70s. The MHC-encoded hsp70s are very similar to one another: two genes (hsp70-1 and hsp70-2) code for hsp70 and the third encodes hsp70hom, which is 89% identical to hsp70. To determine the expression levels of these three hsp70 genes independently, it is necessary to detect the expression of their mRNAs with locus-specific probes. Such probes, which hybridise with the unconserved 3' untranslated regions of the hsp70-1, hsp70-2 and hsp70hom genes, have been described previously (Milner and Campbell, 1990). The study was extended to look at the effects of TNF, IL-1 and IL-6 on the expression of these three genes.

Three human cell lines, HeLa, HepG2 (hepatocellular carcinoma), and 721.45 (Burkitt's lymphoma), were cultured in the presence of IFN-γ (20, 200 or 1000 U/ml), TNF (0.05, 1 or 20 ng/ml), IL-1 (0.1, 1 and 10 ng/ml) or IL-6 (0.1, 1 and 10 ng/ml), or in the absence of cytokines as a control [A3]. TNF, IL-1 and IL-6 had specific activities of > 10^7. Total RNA was harvested after 6, 12, 24 or 48 hours [D1]. Initially, RNA samples (15 μg of each) were separated by electrophoresis through 1% (w/v) agarose gels containing 1.9% (w/v) formaldehyde [D3] and transferred to nitrocellulose by Northern blotting [D4]. Probing the Northern blots with the hsp70-specific probes indicated that the RNA samples were not degraded and confirmed that the probes do not cross react with

(a) Hsp70-2

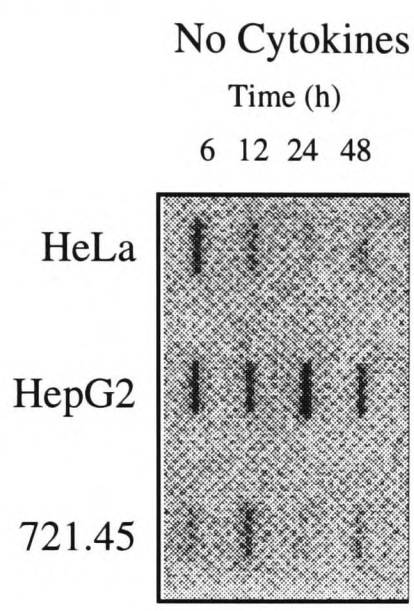

(b) Actin

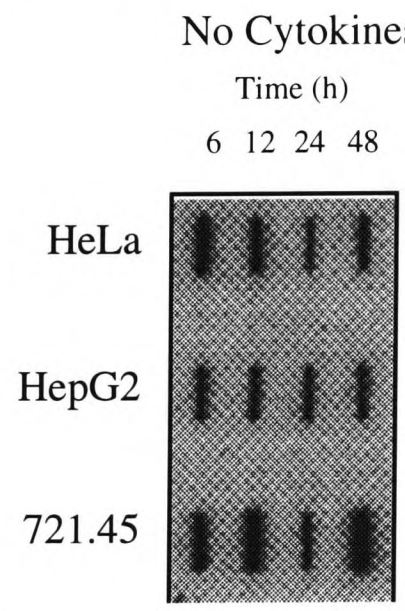

(c) Hsp70-2

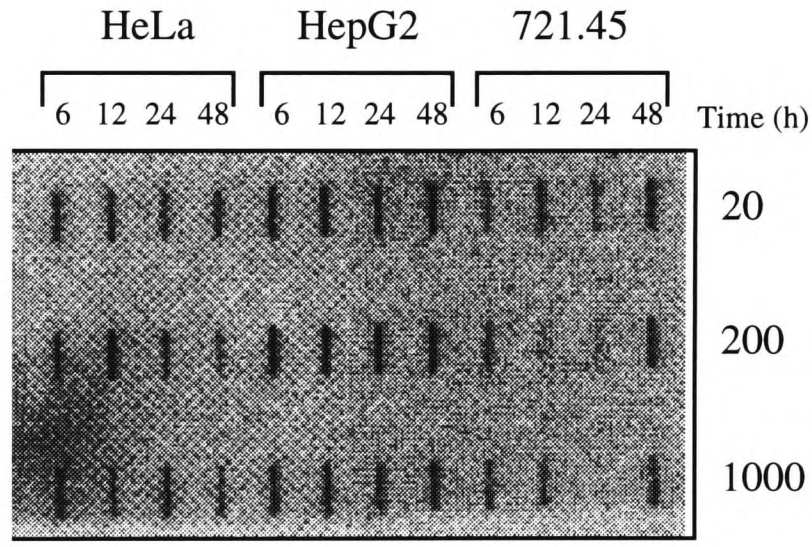

(d) Actin

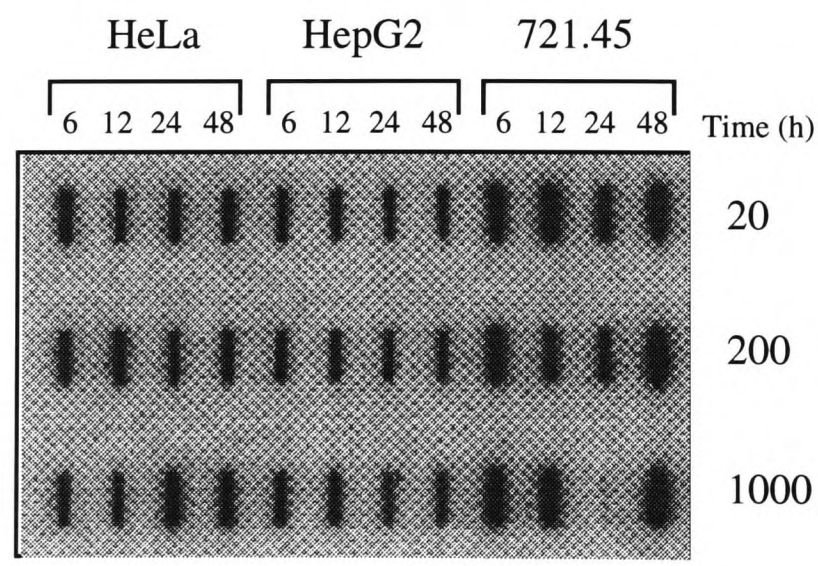

(e) Hsp70-2

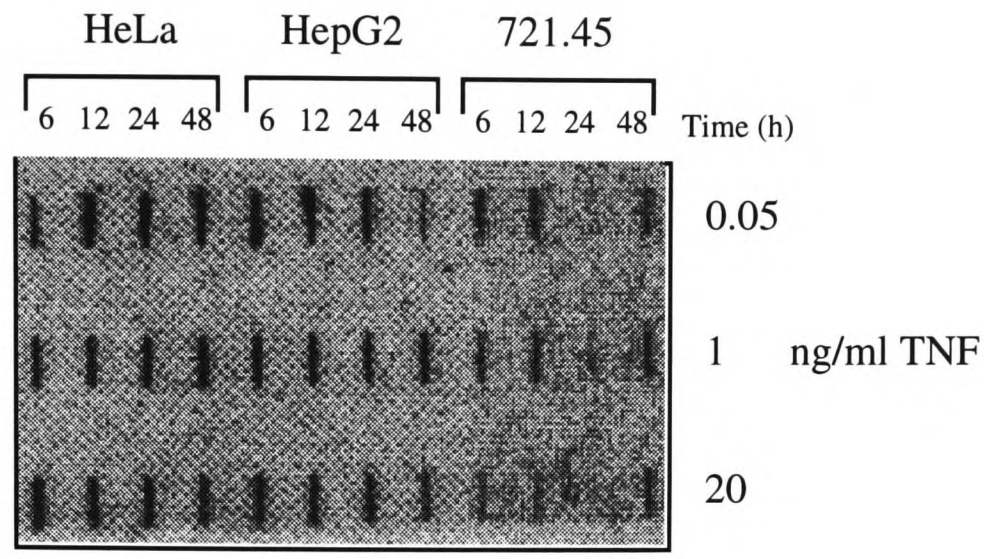

(f) Actin

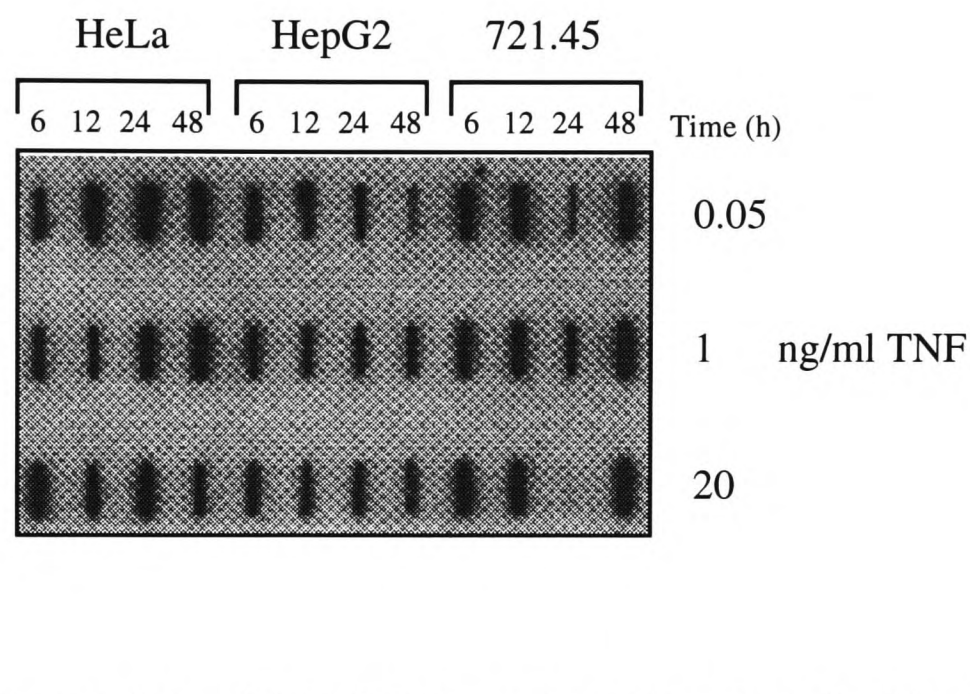

Figure 7-3: Expression of hsp70-2 (a, c and e) and actin (b, d and f) mRNAs in HeLa, HepG2 and 721.45 cell lines treated with no cytokine (a and b), IFN-γ (c and d) or TNF (e and f). Each cell line was cultured in a 9 cm^2 well to ~25% confluency and treated with 0, 20, 200 or 1000 U/ml of IFN-γ or 0, 0.05, 1 or 20 ng/ml of TNF. Total RNA was harvested after 6, 12, 24 and 48 hours [D1] and ~4 μg of each sample was transferred to nitrocellulose by slot blotting [D5]. Blots were hybridised with ^{32}P-labelled probes to detect hsp70-2 or actin. The hsp70-2 probe hybridises with the 3' untranslated region of the hsp70-2 mRNA and does not cross react with the mRNAs of other hsp70s (Milner and Campbell, 1990). It was prepared by digesting a clone of hsp70-2 with *Eco* 0109 and isolating the 600 bp fragment by gel purification [C4]. The actin probe hybridises to nucleotides 45-629 of actin mRNA (Ponte *et al.,* 1984) and was prepared by PCR [C12] from Raji reverse strand cDNA [D2] and gel purified. The hybridised probes were detected with phosphor screens and a Storm Imager.

other RNA species, since the sizes of the mRNAs of the hsp70 genes in the MHC are already known (Milner and Campbell, 1990).

Gel electrophoresis and Northern blotting are time consuming, and long exposure times (of at least a week) were required to detect the hybridisation of probes against the hsp70s. Therefore, a second technique was used thereafter, called slot blotting. In slot blotting, the denatured RNA samples are transferred directly to nitrocellulose using a vacuum manifold [D5]. Initially, the amount of RNA loaded in a slot was titrated (0.1, 0.2, 0.5, 1, 2, 5, 10, 20 and 30 μg of total RNA from Raji cells). Strong signals after overnight exposure were obtained from as little as 1 μg of RNA after probing with the hsp70hom probe. Slot blotting is more sensitive than Northern blotting because losses of RNA during gel electrophoresis and transfer to nitrocellulose are avoided. Furthermore, it is a shorter procedure, so there is less time for RNase contamination and resultant RNA degradation to occur, and it does not use ethidium bromide to visualise the RNA species, so another source of RNA damage is avoided.

Duplicate slot blots of the RNA samples from cytokine-treated cells were prepared. One was hybridised successively with probes against hsp70hom, hsp70-1 and actin (data not shown), while the other was hybridised with probes against hsp70-2 and actin (see Figure 7-3 for the results of IFN-γ and TNF treatment). The blots were stripped between each probing, and exposed to film to check the efficacy of stripping [D6]. The amount of probe hybridised to each sample was measured using a phosphorimager and quantified using Image Quant software [D6]. The signals for the hsp70s were divided by the actin signal to correct for any inequalities in loading, so it should be borne in mind that dividing one figure that includes a margin of error by another propagates the errors. Thus a 10% error in both readings would yield an error in the corrected hsp70 signal of up to 40%*.

---

* If the signals of both an hsp70 and actin were 1 ± 0.1 (10% error), the corrected hsp70 signal (hsp70 signal / actin signal) will be in the range 0.82 (0.9/1.1) to 1.22 (1.1/0.9).

As a result, in the analysis below, changes in the mRNA levels of the three hsp70s are only considered to be significant if they are greater than 50%.

In each cell line, the expression of the mRNAs encoding the three hsp70s was approximately the same at each time point and with each concentration of each cytokine. All three mRNAs were most strongly expressed in HepG2 cells and least abundant in the antigen presenting cell line 721.45. HepG2 cells are derived from hepatocytes, which may require abundant hsp70s to chaperone the large amounts of proteins they synthesise and secrete, but it is not clear why 721.45 cells should express lower levels of these proteins than HeLa cells. The strength of the signals detected for the mRNAs of the three hsp70s was hsp70-1 > hsp70hom > hsp70-2, but this may be accounted for by the relative specific activities of the probes used. When Milner and Campbell (1990) detected the levels of mRNA of these three hsp70s in HeLa cells by Northern blotting, the hsp70-1 message was also detected more strongly than the hsp70hom mRNA, but the hsp70-2 message could not be detected at all, using this less sensitive technique. The similarity of the actin signals for RNA from HeLa and HepG2 cells shows that these samples were quantified accurately by spectrophotometry, but there were clearly problems with the quantification of RNA from 721.45 cells, for which the strength of the actin signal varies significantly.

Interferon-γ had no effect on the expression of hsp70-1 mRNA in the three cell lines tested (data not shown). However, the levels of hsp70-2 mRNA in HeLa cells increased within 6 hours of exposure to IFN-γ and returned to little above normal by 24 hours (Figure 7-4). 1000 U/ml of IFN-γ had the most dramatic effect, stimulating levels of hsp70-2 five-fold within 6 hours, while levels were doubled by 200 U/ml of IFN-γ and increased by greater than 60% by 20 U/ml of IFN-γ over the same time range. Hsp70-2 mRNA expression was also increased in 721.45 cells. After 12, 24 and 48 hours, hsp70-2 mRNA levels were increased >60% by 1000 U/ml of IFN-γ and >70% by 20 U/ml of IFN-γ, with the induction reaching a peak after 24 hours with increases of 90% and 150%, respectively. Unlike the other concentrations, 200 U/ml of IFN-γ increased hsp70-2

(a)

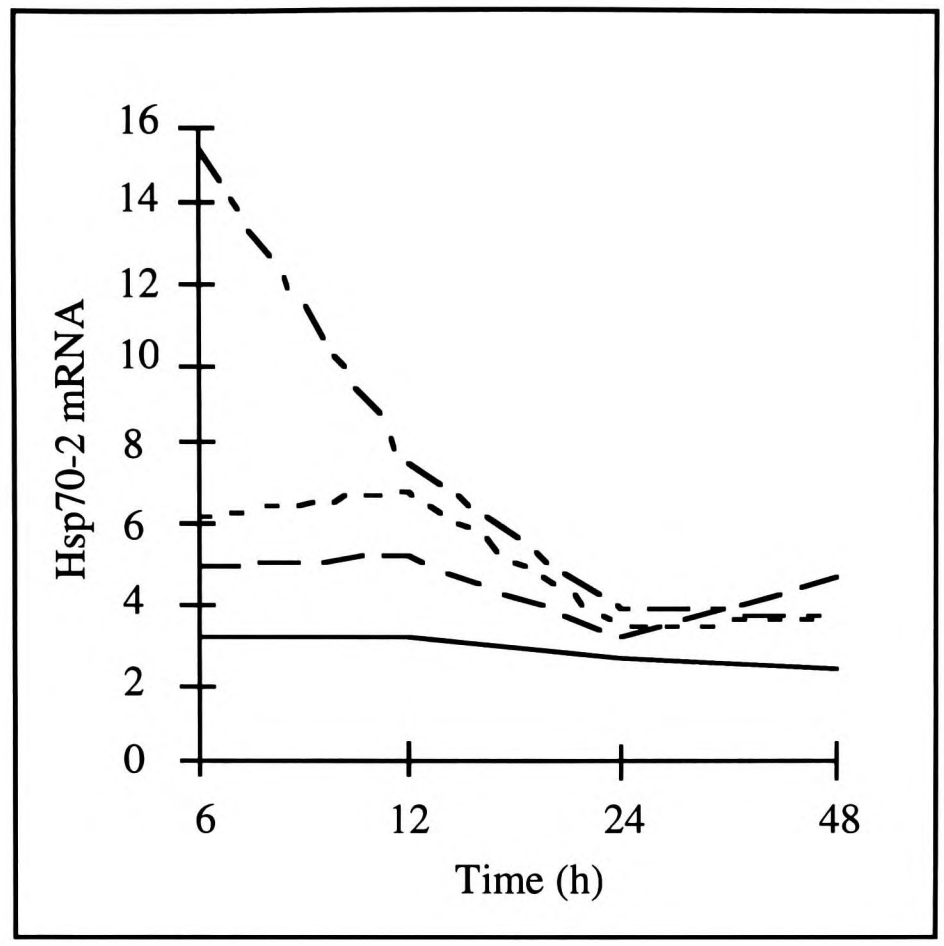

(b)

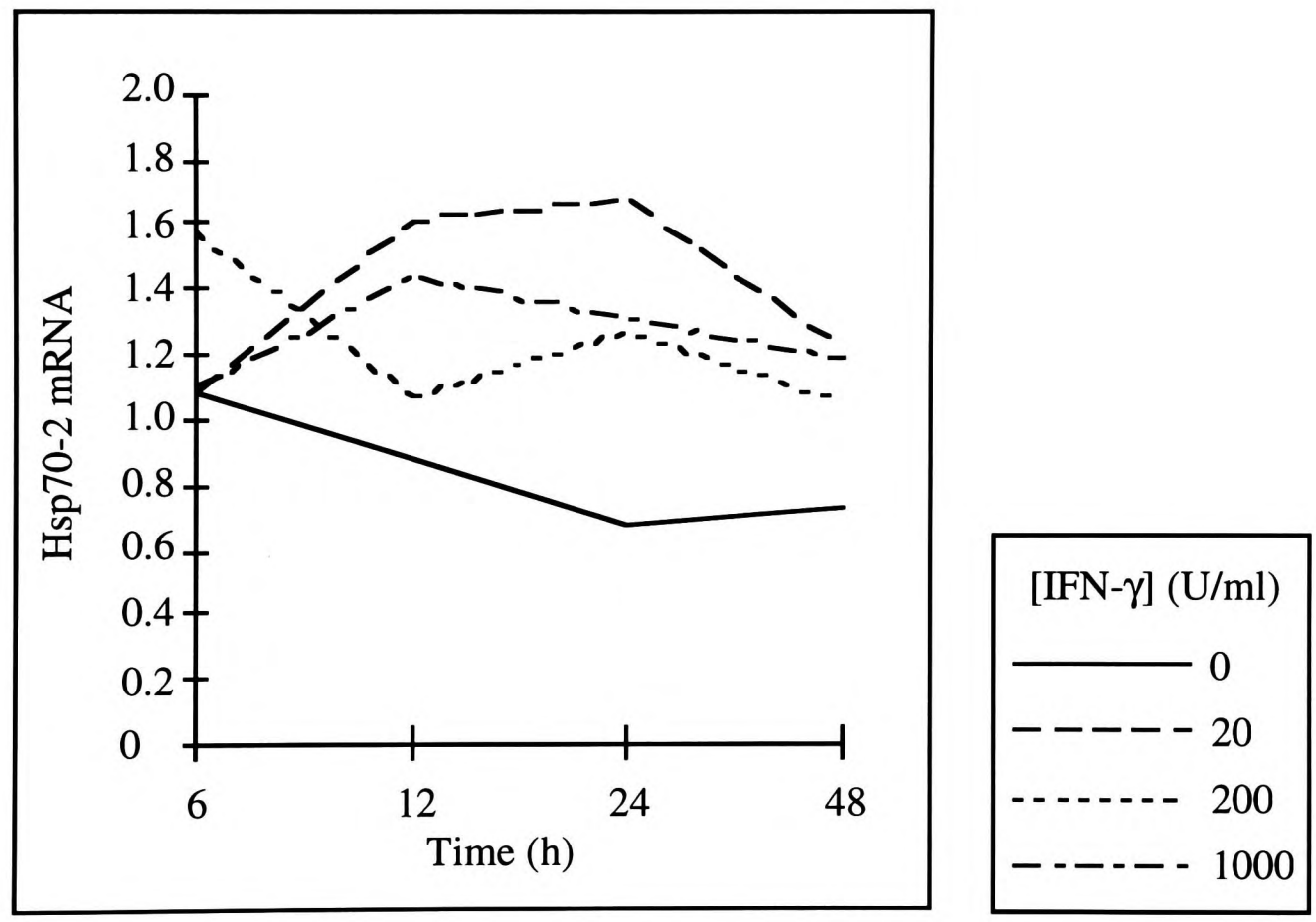

Figure 7-4: The influence of IFN-γ on hsp70-2 mRNA expression by (a) HeLa cells and (b) 721.45 cells. The amount of hsp70-2 and actin probes that hybridised to each slot was quantified using the Peak Finder and Area Report commands of Image Quant software. To correct for any unequal loading, the hsp70-2 signal was divided by the actin signal and multiplied by 100. The hsp70-2 signal obtained for 721.45 cells treated for 24 hours with 1000 U/ml IFN-γ is not included, because it was weak.

mRNA levels (by 40%) after only 6 hours, but at the other time points, the induction was less with this concentration of the cytokine. Hsp70-2 mRNA levels were unaffected by IFN-γ in HepG2 cells (data not shown). Furthermore, IFN-γ had no effect on the expression of hsp70hom mRNA in the three cell lines tested (data not shown).

TNF (0.05 or 1 ng/ml) almost doubled hsp70-1 levels in HeLa cells, after 12, 24 and 48 hours (Figure 7-5a), and 0.05 ng/ml TNF increased hsp70-1 levels three-fold in 721.45 cells after 12 and 24 hours (Figure 7-5b). After 6 hours, 20 ng/ml of TNF repressed hsp70-1 mRNA expression in 721.45 cells slightly, but this may represent an error in quantification. All three concentrations of TNF increased hsp70-2 mRNA levels in 721.45 and HeLa cells, almost doubling it after 12, 24 and 48 hours (Figure 7-6). TNF had no effect on hsp70hom expression in the three cell lines tested (data not shown).

IL-1 had no effect on the expression of hsp70-1 mRNA (data not shown). It also had no effect on the hsp70-2 mRNA levels in HeLa cells (data not shown). However, hsp70-2 mRNA levels in 721.45 cells were doubled by 10 ng/ml IL-1 after 12 and 24 hours and increased by all three concentrations of IL-1 after 12, 24 and 48 hours (Figure 7.7). After 6 hours, 0.1 and 1 ng/ml of IL-1 actually repressed hsp70-2 mRNA expression in 721.45 cells, but this may be due to errors in quantification. IL-1 did not alter expression of hsp70hom mRNA in any of the three cell lines tested (data not shown).

IL-6 had no effect on the expression of mRNAs encoding hsp70-1, hsp70-2 or hsp70hom in the three cell lines tested (data not shown).

In summary, at the RNA level, IFN-γ stimulated hsp70-2 expression in HeLa and 721.45 cells, TNF increased hsp70-1 and hsp70-2 expression in HeLa and 721.45 cells, and IL-1 increased hsp70-2 expression in 721.45 cells. None of the MHC-encoded hsp70s is induced by IL-6 in the cell lines tested, and HepG2 cells did not respond to any of the cytokines used. Therefore, expression of hsp70-2 was influenced by three of the cytokines and hsp70-1 by one of them, whereas hsp70hom expression is not affected by

(a)

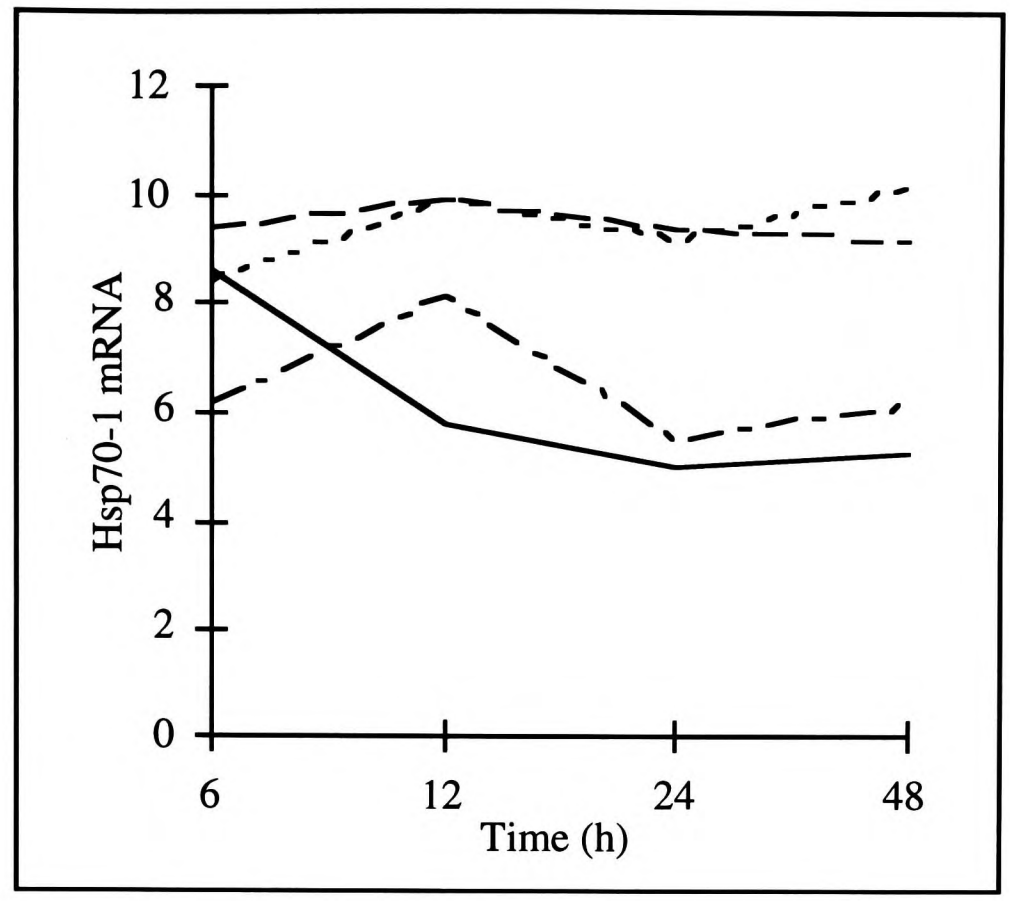

(b)

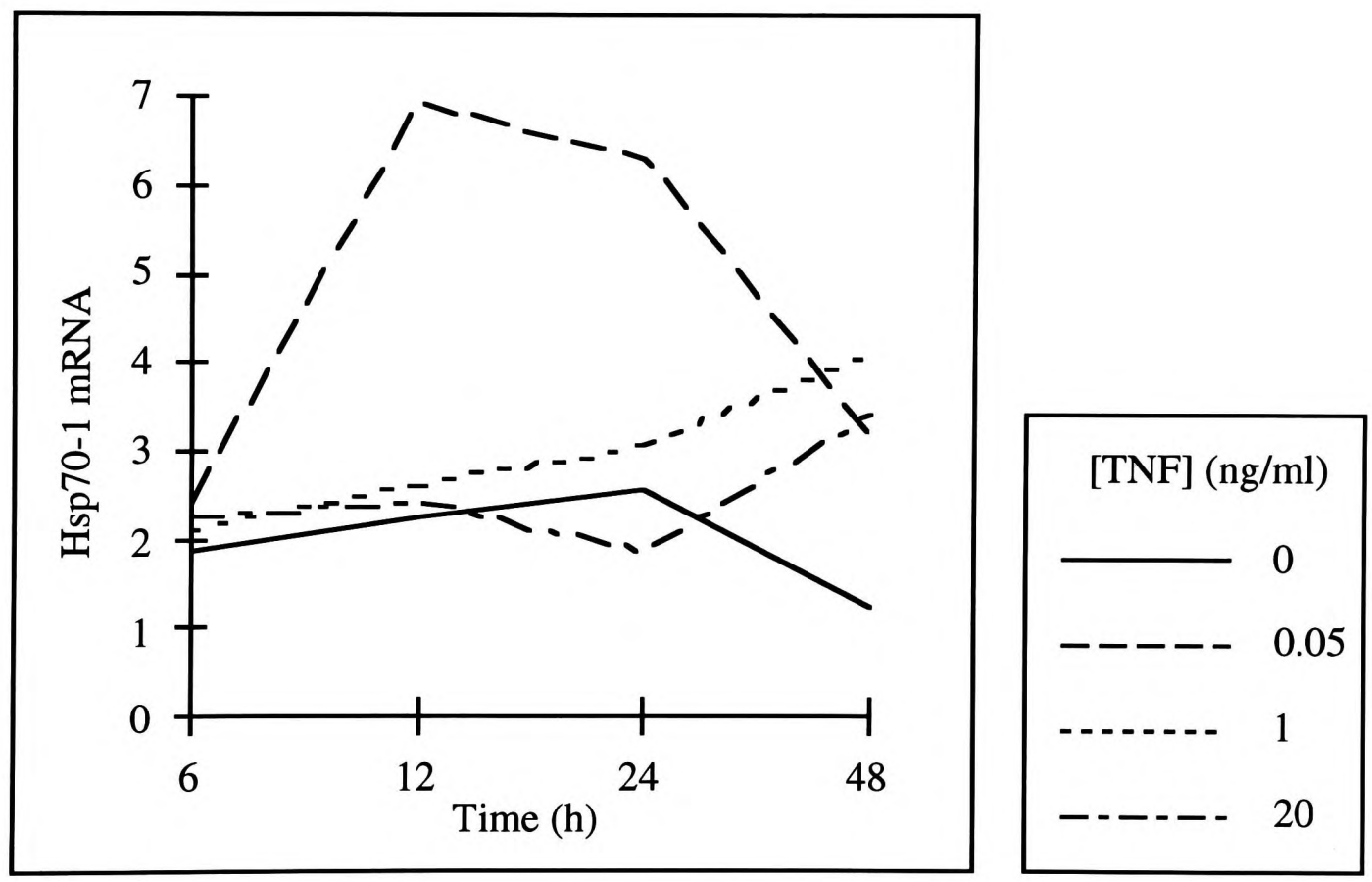

Figure 7-5: The influence of TNF on hsp70-1 mRNA expression by (a) HeLa cells and (b) 721.45 cells. The amount of hsp70-1 and actin probes that hybridised to each slot was quantified using the Peak Finder and Area Report commands of Image Quant software. To correct for any unequal loading, the hsp70-1 signal was divided by the actin signal and multiplied by 100.

(a)

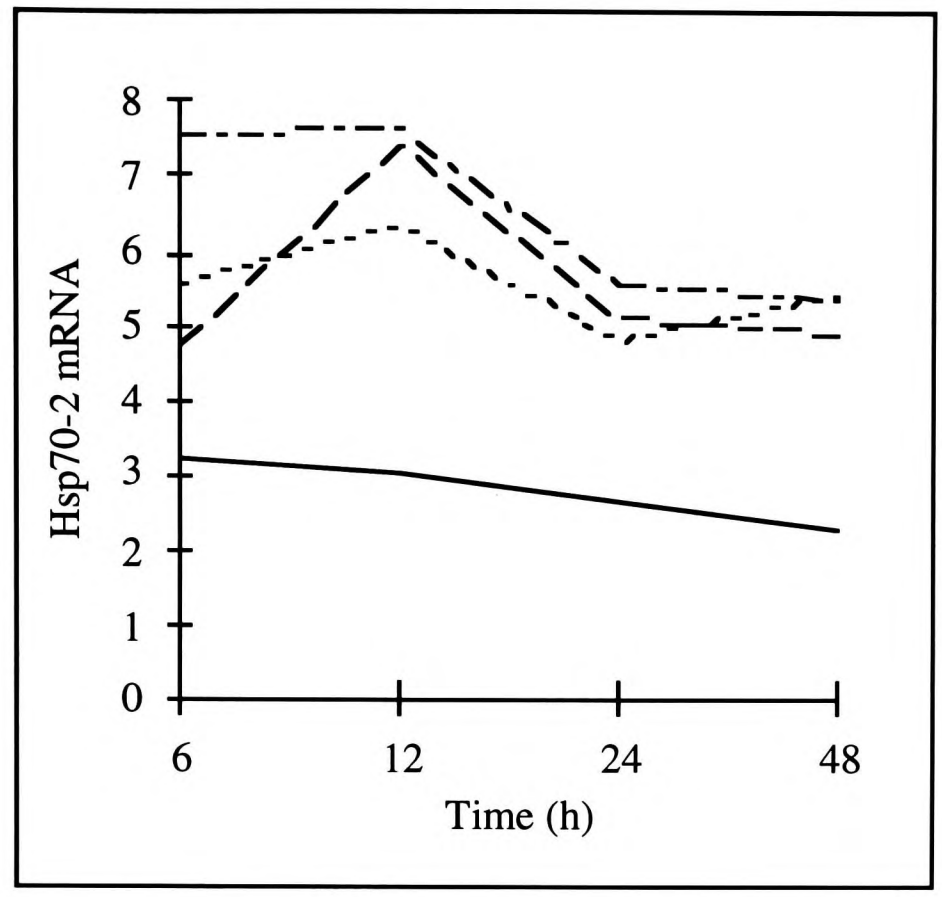

(b)

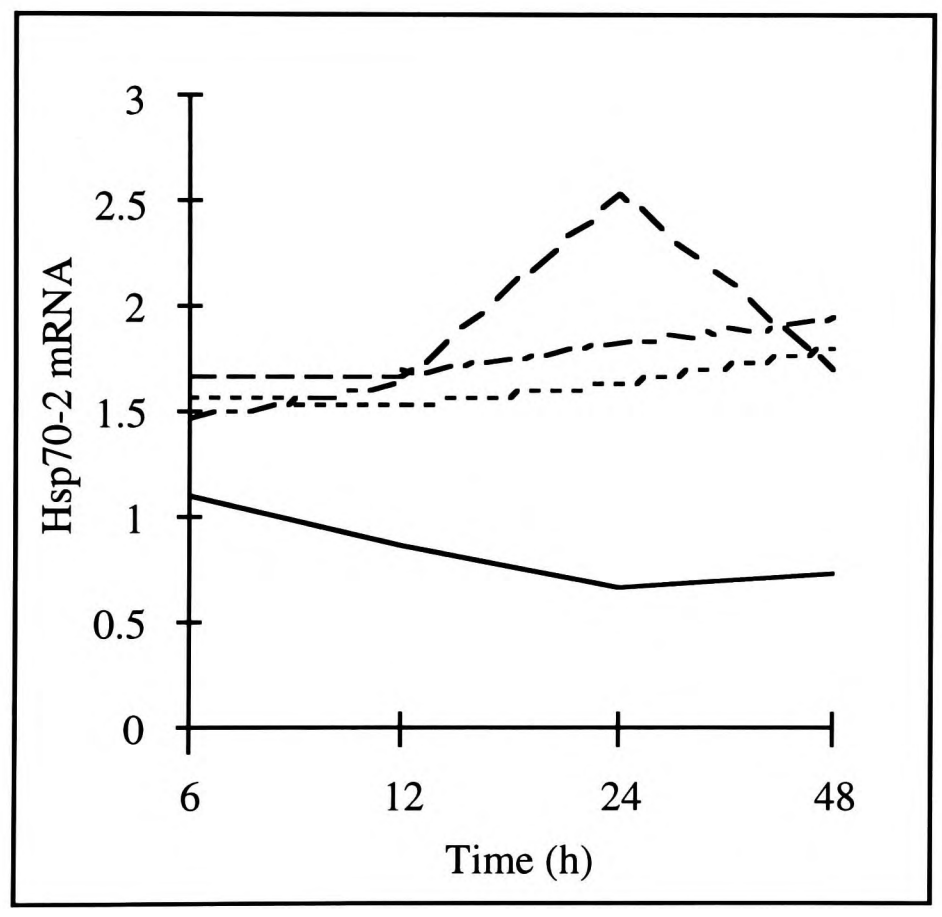

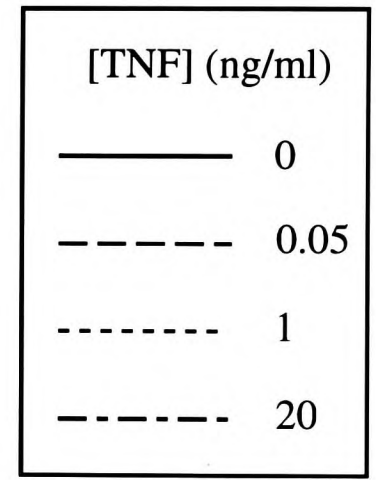

Figure 7-6: The influence of TNF on hsp70-2 mRNA expression by (a) HeLa cells and (b) 721.45 cells. The amount of hsp70-2 and actin probes that hybridised to each slot was quantified using the Peak Finder and Area Report commands of Image Quant software. To correct for any unequal loading, the hsp70-2 signal was divided by the actin signal and multiplied by 100. The hsp70-2 signal obtained for 721.45 cells treated for 24 hours with 20 μg/ml TNF is not included, because it was weak.

(a)

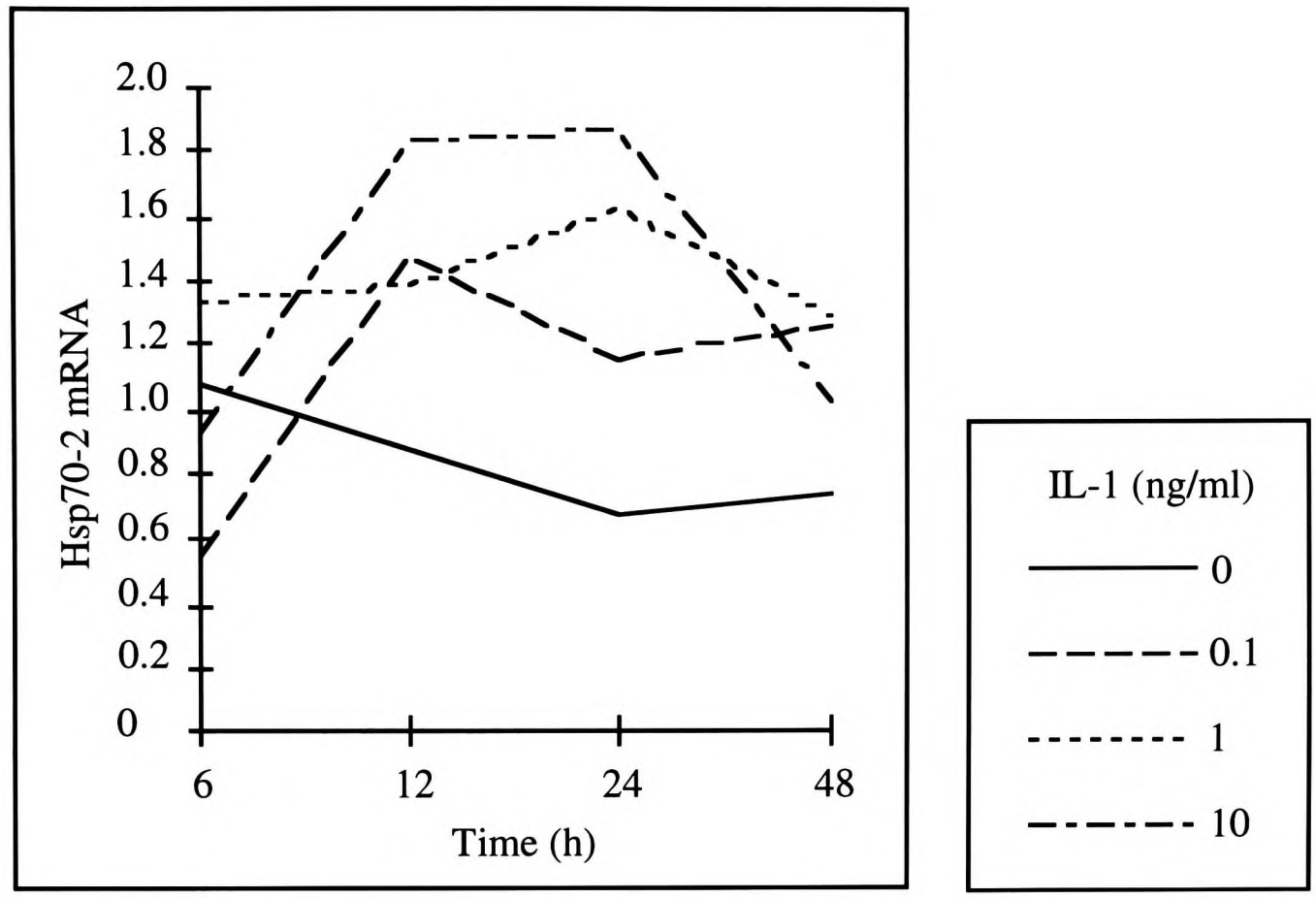

Figure 7-7: The influence of IL-1 on hsp70-2 mRNA expression by 721.45 cells. The amount of hsp70-2 and actin probes that hybridised to each slot was quantified using the Peak Finder and Area Report commands of Image Quant software. The hsp70-2 signal was divided by the actin signal and multiplied by 100, to correct for any unequal loading.

any of the cytokines investigated. The induction of mRNAs encoding the hsp70s was not always dose-dependent, i.e. the highest concentration of a cytokine did not always induce the greatest amount of mRNA. This is not entirely surprising, as high concentrations of cytokines can have inhibitory effects on cell functions (Abbas *et al.*, 1996). This was the reason for using a range of concentrations for each cytokine. The results of these experiments at the mRNA level suggest that at least some of the induction by IFN-γ of hsp70s detected by antibody 3A3 in several cell lines, including HeLa, is due to increased expression of the hsp70-2 gene.

The Effects of IFN-γ, TNF, IL-1 and IL-6 on the Expression of the MHC-encoded Hsp70s at the Protein Level

The first step in determining the biological significance of these findings was to show whether changes in the expression of hsp70-1 and hsp70-2 mRNAs alter the expression of the protein they encode. Furthermore, since the expression of hsp70s can be regulated translationally (reviewed by Sierra and Zapata, 1994), cytokines may have effects on the expression of hsp70s that are not reflected in changes in the expression of their mRNAs. Therefore, the effects of IFN-γ, TNF, IL-1 and IL-6 on the expression of the MHC-encoded hsp70s was examined by Western blotting, using monoclonal antibodies against hsp70 and hsp70hom (the generous gift of Dr. P. van Endert, Hôpital Necker Clin, Paris) [E4, E5]. To simplify the experiment, a single representative cell line and time-point were chosen. HeLa cells were treated with three concentrations of the four cytokines as before, and harvested after 24 hours. Western blots of the cell lysates were probed with monoclonal antibodies specific for hsp70 and hsp70hom, as well as antibody 3A3 that recognises the cytoplasmic hsp70s and mt hsp70. An antibody against actin was used as a control.

(a) IFN-γ

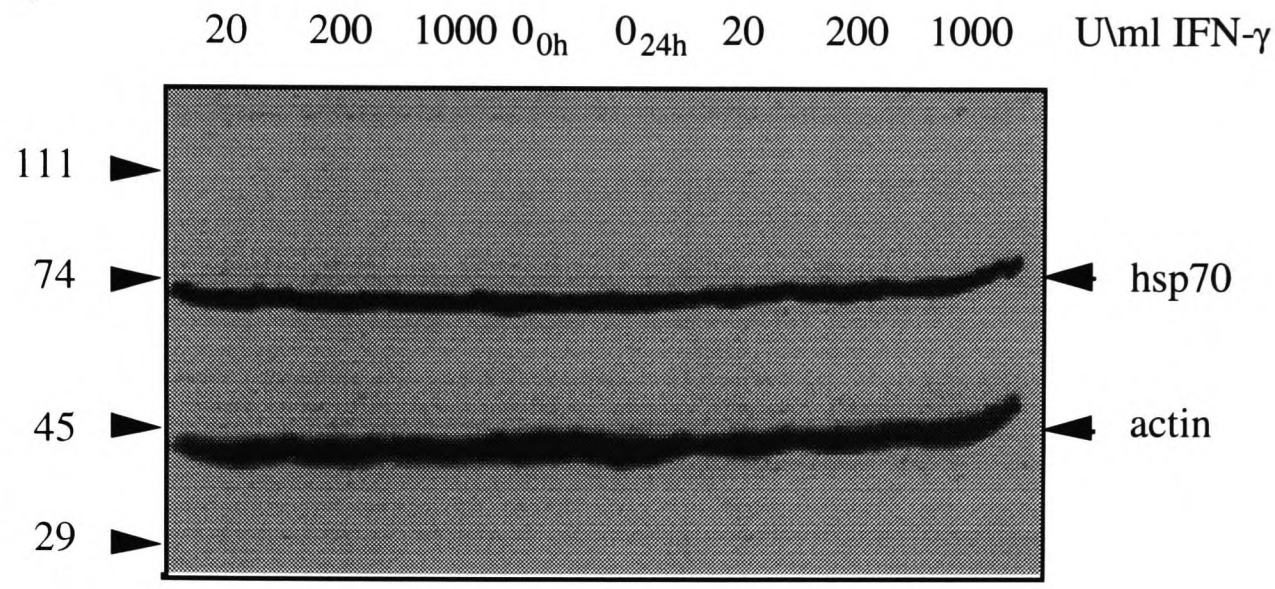

(b) TNF

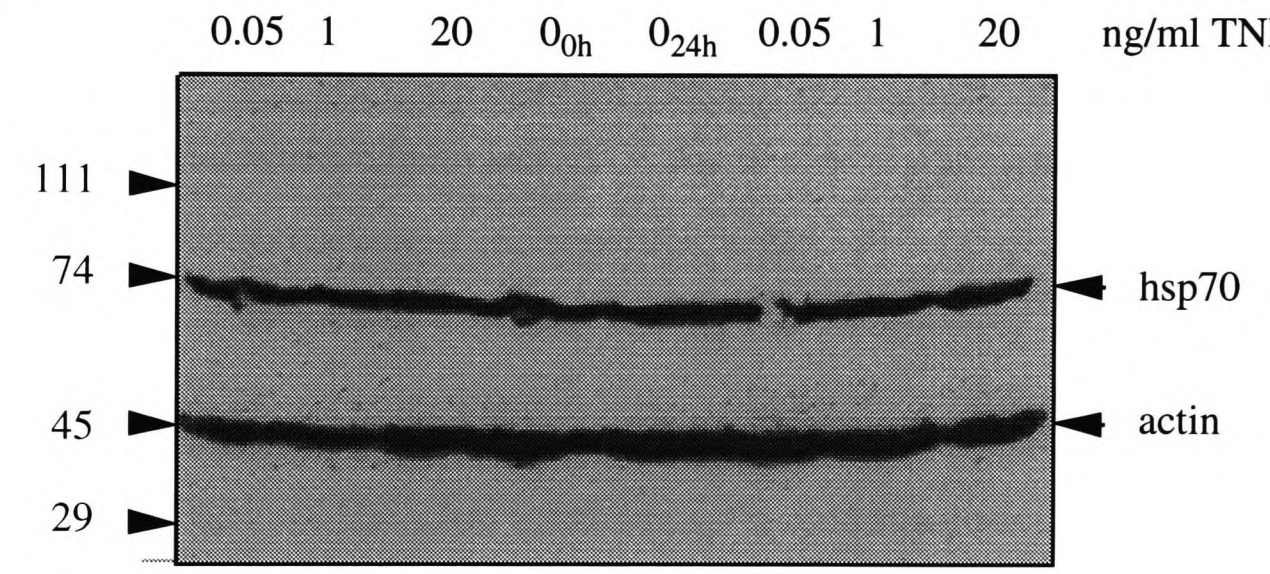

Figure 7-8: Effects of (a) IFN-γ and (b) TNF on the expression of hsp70 and actin in HeLa cells. HeLa cells were seeded in 6 well plates cells at ~25% confluency and grown for 24 hours, after which one well was harvested (0_{0h}). The cells were then treated with the concentrations of cytokines shown for a further 24 hours [A3]. The cells were harvested by incubation at 37 °C in PBS containing 0.5 mM EDTA and counted with a haemocytometer. 5 x 10^5 cells were loaded in each lane of a 10% (w/v) polyacrylamide gel [E1] which was blotted [E4] and probed [E5] with antibodies against hsp70 and actin. The bound antibody was detected by enhanced chemiluminescence as in Figure 7-1 and quantified by enhanced chemifluorescence, using a Storm imager [E5] (data not shown). The position of protein molecular weight standards is indicated in kDa.

Hsp70 protein was detected strongly in HeLa cells, but its expression was unaffected by any of the four cytokines used (Figure 7-9). This does not support the induction by IFN-γ, TNF and IL-1 of hsp70-1 and/or hsp70-2 mRNAs detected by slot blotting. However, it is possible either that the induction seen at the mRNA level is not sufficient to increase the levels of hsp70 protein significantly, or that there was sufficient hsp70 loaded onto the gel that its transfer to the membrane during western blotting was non-quantitative.

Hsp70hom could be detected only weakly in HeLa cells, making it difficult to quantify accurately (data not shown). However, there is no obvious induction of hsp70hom in response to the cytokines used. This is consistent with the results seen above at the mRNA level.

Hsp70s recognised by antibody 3A3 were detected strongly in HeLa cells but are not induced by treatment with IFN-γ, TNF, IL-1 or IL-6 for 24 hours (Figure 7-8). This is surprising, as in an earlier experiment, 200 U/ml of IFN-γ induced hsp70s recognised by this antibody in several cell lines, including HeLa cells, after 48 hours (Figure 7-1). This again suggests that the gel was sufficiently overloaded for the transfer of proteins to the blot not to be proportional to their abundance.

An antibody against MHC class I molecules was used as a positive control to detect the induction of these molecules by IFN-γ and TNF. As before, a weak induction could be seen in cells treated with these cytokines (data not shown), but this was not as dramatic as was expected from a study using a different antibody against class I molecules (Epperson *et al.*, 1992). Unfortunately, it was not possible to assemble a panel of antibodies that would act as positive controls in the three different cell lines for all four cytokines used.

(a) IFN

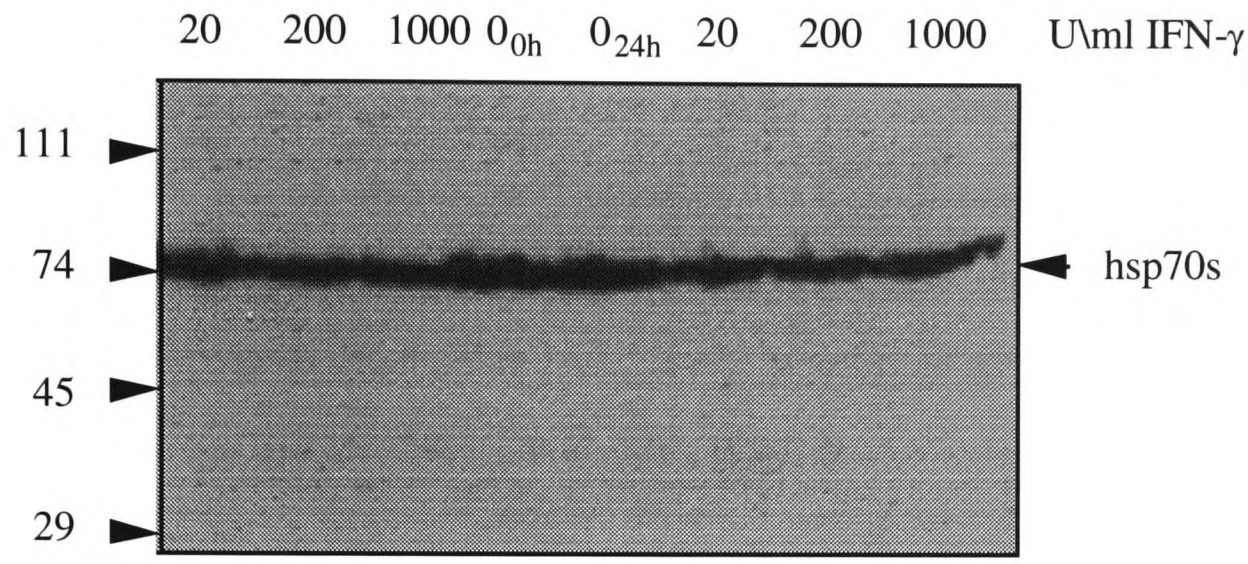

(b) TNF

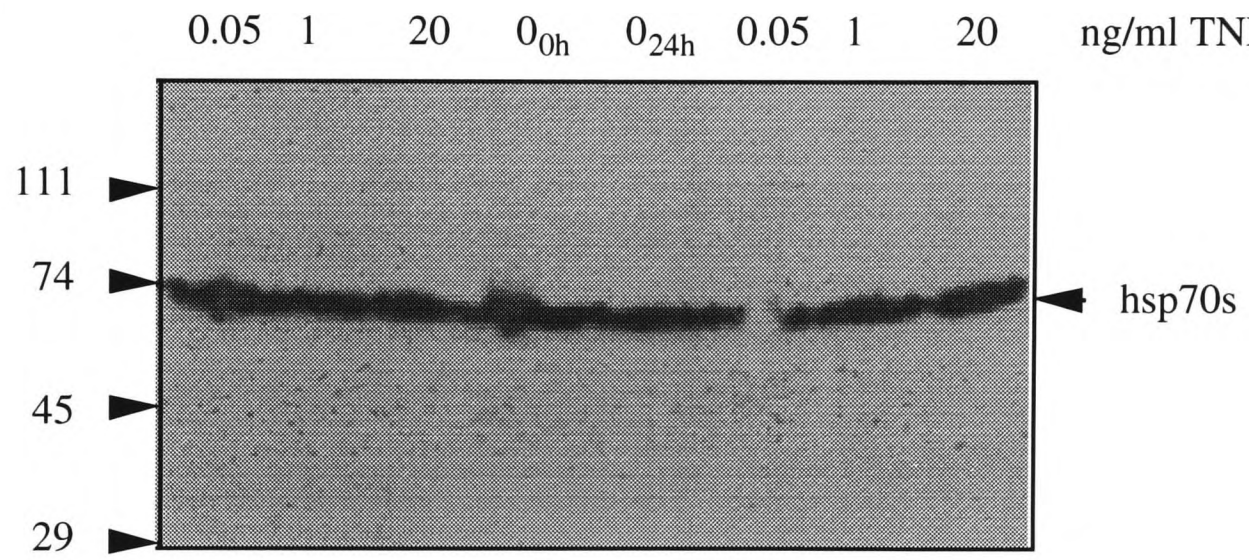

Figure 7-9: Effects of (a) IFN-γ and (b) TNF on the expression of hsp70s reactive with antibody 3A3 in HeLa cells. The blots described in Figure 7-8 were stripped [E5] and probed with antibody 3A3. The position of protein molecular weight standards is indicated on the left hand side, in kDa.

Analysis of the Promoter Regions of the MHC-encoded Hsp70s

The sequences upstream of the transcriptional start sites of the hsp70-1 and hsp70-2 genes (-1 to -274) were analysed for the presence of transcription factor binding sites using Transcription Element Search Software (Tess), version 3.1. No interferon-γ activated sites (GAS) or interferon-α stimulated response elements were identified (Schindler and Darnell, 1995). IL-1 and IL-6 both activate NF-IL6, and in addition, IL-1 activates NF-κB and IL-6 activates ISGF-like factor (Kishimoto *et al.*, 1994). A possible NF-κB binding site is found upstream of hsp70-1 (at -240), but no other relevant sites were identified. However, this does not exclude the possibility that sites for the induction of hsp70-1 and hsp70-2 by cytokines are found further upstream of the transcriptional start site. The sequence upstream of the hsp70hom gene has not been determined, and so was not available for analysis.

Discussion

The research described in this chapter shows that one or more hsp70s recognised by antibody 3A3, which is specific for mt hsp70 and the cytoplasmic hsp70s, are strongly induced by IFN-γ in a number of human cell lines, including HeLa, TK143B (osteosarcoma), HT1080 (fibrosarcoma) and possibly SW620 (colon adenocarcinoma). Since this induction is not detected by antibody 5A5, which recognises the cytoplasmic hsp70s and BiP, it seems likely that mt hsp70 is the induced species. It is surprising that the hsp70 of mitochondria is induced by IFN-γ, as mitochondria are not known to be involved in antiviral immunity. However, another mitochondrial molecular chaperone, hsp60, is induced by both IFN-γ and TNF in a monocytic cell line (Ferm *et al.*, 1992). Alternatively, antibody 3A3 may be detecting the induction of a novel member of the hsp70 family. Antibody 3A3 failed to detect any induction of hsp70s in HeLa, HepG2 or 721.45 cells by IFN-γ after 24 hours, but this may be because the western blots were overloaded with the protein. 5×10^5 cells were loaded per lane in Figures 7-7 and 7-8, compared with 80 μg of cell lysate (~3×10^4 cells) in Figures 7-1 and 7-2, when an induction of hsp70s was detected.

When the induction of the MHC-encoded hsp70s, hsp70-1, hsp70-2 and hsp70hom, was examined by slot blotting, IFN-γ was seen to increase levels of hsp70-2 mRNA in HeLa and 721.45 cells, TNF to increase hsp70-1 and hsp70-2 mRNA levels in HeLa and 721.45 cells and IL-1 to increase hsp70-2 mRNA levels in 721.45 cells. IL-6 had no effect on these hsp70s. Hsp70hom expression was unaffected by any of the four cytokines, and HepG2 cells appear to be unresponsive to the cytokines used. In summary, expression of the hsp70-2 gene is stimulated by one mediator of antiviral immunity (IFN-γ) and two inflammatory mediators (TNF and IL-1), while hsp70-1 mRNA expression is augmented by TNF alone. The levels of induction seen were relatively low (rarely greater

than three-fold), but the induction may not have been carried out under optimal conditions, as the induction of class I molecules by IFN-γ and TNF was less than has been previously reported (Epperson *et al.*, 1992).

These changes in the expression of the genes encoding hsp70 could not be detected at the protein level using an antibody against hsp70, perhaps because the western blots were overloaded. Hsp70hom (detected with an antibody) was expressed only at very low levels in the cell lines tested, and no induction in response to the cytokines used could be detected.

It is important to note that the results presented in this chapter must be treated with a degree of caution because the induction of MHC class I molecules by IFN-γ and TNF, which acted as a positive control for these cytokines in HeLa cells, was only weak. In addition, positive controls for the effects of IFN-γ and TNF on HepG2 and 721.45 cells, and IL-1 and IL-6 on all three cell lines were not carried out.

This is the first study of the effects of cytokines on the expression of hsp70hom at the protein and mRNA levels, and no induction could be detected. It is also the first investigation to look at the expression of the hsp70-1 and hsp70-2 genes independently. The mRNAs encoding hsp70 were induced in HeLa and 721.45 cells, by IFN-γ, TNF and IL-1, supporting the reported induction of hsp70 by IFN-γ in cultured fibroblasts (Heufelder *et al.*, 1991), by TNF in human monocytes (Fincato *et al.*, 1991) and feline cardiac myocytes (Nakano *et al.*, 1996) and by IL-1ß in isolated rat islets of Langerhans (Helqvist *et al.*, 1989; Strandell *et al.*, 1995). However, these studies, which were carried out at the mRNA (Fincato *et al.*, 1991) or protein level (Helqvist *et al.*, 1989; Heufelder *et al.*, 1991; Strandell *et al.*, 1995; Nakano *et al.*, 1996), show a greater degree of induction (often greater than five-fold) than was seen in this chapter for hsp70-1 or hsp70-2 mRNA (generally only two-fold) or protein (no induction detected).

The induction of hsp70 expression in the studies described in this chapter may be less dramatic than that seen in other studies because different cell lines were used. Alternatively, the cells used may have higher than normal expression of hsp70s in the absence of cytokines, because of differences in the medium, serum or incubator temperature used. Both elevated temperatures and components of serum, such as TGF-ß stimulate hsp70 expression (Heufelder *et al.*, 1991; Takenaka and Hightower, 1993). Furthermore, not all previous studies have used cell lines, which divide rapidly and may therefore have elevated levels of hsp70s (Granelli-Piperno *et al.*, 1986).

The results discussed in this chapter can be expanded in a number of ways. The effects of the four cytokines on levels of hsp70 protein should be re-examined using a less overloaded western blot, and on mt hsp70, with a specific monoclonal antibody or mRNA probe. It would be useful to examine a broader range of cell lines or, ideally, primary cell cultures, and establish positive controls for the effect of each cytokine on each cell line used. The use of serum-free media might enhance the induction of hsp70s by decreasing their expression under normal conditions. The induction of other members of the hsp70 family that may be induced by cytokines, such as hsc70 (Cruz *et al.*, 1991; Hong-Brown and Brown, 1994), could be investigated at the protein level using specific monoclonal antibodies and, at the mRNA level using specific probes.

It is also important to confirm results obtained with cell lines in whole animals, for example, investigating whether hsp70s are induced during infection or autoimmunity and, if so, whether their induction can be prevented by antibodies against particular cytokines. Research in our laboratory will be determining whether hsp70s are more highly expressed in lymphocytes and monocytes isolated from rheumatoid arthritis patients compared to healthy controls. If so, it will be interesting to elucidate the mechanism for this in animals.

The mechanisms that controls the expression of the genes encoding hsp70-1, hsp70-2 and any other hsp70s in response to IFN-γ, TNF and IL-1ß should be characterised; they

may be elements controlling mRNA transcription or stability. It will be interesting to discover if these control elements are influenced by the polymorphisms that have been identified in 5' flanking regions, 5' untranslated regions or coding sequences of the MHC-linked hsp70 genes (Milner and Campbell, 1991).

Chapter 8: Discussion

The ability of members of the hsp70 family to bind to antigenic peptides *in vivo* and *in vitro* suggests that they may be involved in the processing of antigens for binding to MHC class I and/or class II molecules (DeNagel and Pierce, 1992; Srivastava *et al.*, 1994). The aims of this thesis have been to investigate the involvement of hsp70s in antigen processing and characterise the binding of peptides by hsp70s.

Firstly, the peptide-binding domains of two hsp70s, hsp70hom and PBP74, which share 56% amino acid sequence identity, were expressed in isolation from the rest of the molecule, using the prokaryotic expression vector, pGEX-2T. Both of these hsp70s were implicated in antigen processing: hsp70hom in the class I pathway, due to its cytoplasmic localisation and constitutive expression, and the presence of its gene in the MHC; and PBP74 in the class II pathway because it was localised to endosomes and antibodies against it inhibited antigen processing. Both peptide-binding domains were expressed at high levels and could be purified easily by HPLC. However, their structures could not be determined by NMR spectroscopy or X-ray crystallography because they aggregated in solution.

Instead, the structure of the C-terminal region of hsp70hom, including its peptide-binding domain, was modelled based on the structure of the equivalent portion of the hsp70 of *E.coli,* dnaK (Zhu *et al.*, 1996). The resulting model is likely to be at least reasonably accurate, because hsp70hom and dnaK share 42% amino acid sequence identity over this region. The secondary structure and peptide-binding amino acids of dnaK are highly conserved in hsp70hom, and modelling studies with the peptide NRLLLTG, which was crystallised with the C-terminal region of dnaK, show that it may bind to these two hsp70s in a very similar manner. Hsp70hom was also modelled with another peptide, FYQLALT, bound in both possible orientations. The modelled complexes suggest that the peptide-

binding groove is very versatile, and able to interact with many peptides, in different ways. This would account for the broad peptide-binding specificity of members of the hsp70 family.

Peptide binding studies were carried out using several techniques. A biotinylated peptide, FYQLALT, was shown to bind to the peptide-binding domain (amino acids 384-554) and the C-terminal region of hsp70hom (amino acids 384-641), immobilised in plastic wells. The dissociation constants (Kds) of the complexes were <25 μM, which is within the range of Kds reported for other hsp70-peptide complexes (0.1-100 μM). Binding of the peptide-binding domain of PBP74 to a peptide from pigeon cytochrome c, and of the peptide-binding domain of hsp70hom to both this peptide and (unbiotinylated) FYQLALT was detected by isothermal titration calorimetry, although the heat change detected upon binding was too small to allow a Kd to be calculated. Assuming that the affinities of these interactions are typical for hsp70-peptide complexes (~10 μM), it can be concluded that they are entropically rather than enthalpically driven; in other words, the interactions of hsp70hom with the peptides with PBP74 and hsp70hom are predominantly hydrophobic. Thus, this result supports the conclusions of the modelling of the hsp70hom-peptide complex. In addition, binding of the C-terminal domain of hsp70hom to the unfolded protein substrate reduced, carboxymethylated α-lactalbumin (RCMLA), could be detected by native gel electrophoresis.

Secondly, PBP74, an hsp70 thought to be involved in the class II antigen processing pathway in endosomes was localised by immunofluorescence microscopy and shown to be a mitochondrial protein. Other researchers have shown that it is indeed identical to the mitochondrial hsp70 (Dahlseid *et al.*, 1994; Webster *et al.*, 1994; Bhattacharyya *et al.*, 1995). Therefore it is unlikely that PBP74 is involved in antigen processing. The presence of other members of the hsp70 family in lysosomes purified from a B cell line by Percoll density gradient centrifugation was, therefore, investigated using antibodies that reacted with many different members of the hsp70 family. No hsp70s were detected in these late

endocytic compartments, even after heat shock or serum starvation. This data does not support the localisation of hsc70 to lysosomes seen in rat liver after starvation (Cuervo *et al.*, 1995) or in fibroblasts after serum starvation (Terlecky, 1994). Auger *et al.*(1996) provided evidence that hsc70 is found in lysosomes from B cell lines with certain MHC class II haplotypes, but this work is difficult to interpret. Therefore, it seems likely that the accumulation of hsc70 in lysosomes during starvation or serum starvation is limited to certain cell types, not including antigen presenting B cells. However, the presence of hsp70s in endosomes of B cells, or of other chaperones in lysosomes cannot be ruled out.

A third approach investigated the induction of the three hsp70 genes found in the MHC by four cytokines, including two (IFN-γ and TNF) which increase the expression of components of the MHC class I antigen processing pathway (Abbas *et al.*, 1996). The hsp70-1 and hsp70-2 genes are induced at the mRNA level by TNF, while IFN-γ and IL-1 induces hsp70-2 alone. This data supports a role for the heat-inducible hsp70 in MHC class I antigen processing, as it appears to be coregulated with known members of this antigen processing pathway. The expression of hsp70hom was unaffected by any of the four cytokines examined. The mitochondrial hsp70 (which is not encoded in the MHC) appears to be induced by IFN-γ at the protein level. This is difficult to account for, but an induction of mitochondrial hsp60 has been reported under the same conditions (Ferm *et al.*, 1992), suggesting that IFN-γ may cause a generalised increase in the expression of molecular chaperones in mitochondria.

Several of the projects described in this thesis would reward further research. Thus, it may be possible to prevent the peptide-binding domains of PBP74 and hsp70hom from aggregating by binding a peptide (FYQLALT or possibly NRLLLTG) to them, as the aggregation of the C-terminal region of dnaK was reversed by addition of peptide (Dr. X. Zhu, personal communication). This would make them suitable for structure determination by NMR or X-ray crystallography. Alternatively, the structural work may be continued with the entire C-terminal region of hsp70hom, as prepared by Miss. S. Jenkins in our

laboratory. This would be the most effective test of the model of the C-terminal region of hsp70hom.

The nature of peptide binding to the hsp70 family is flexible, as revealed by molecular modelling and published peptide-binding studies. It is, therefore, unlikely that binding studies with synthetic peptides (Flynn *et al.*, 1989; Fourie *et al.*, 1994; Gragerov and Gottesman, 1994) would be useful in determining the specificities of the peptide-binding domains of PBP74 and hsp70hom. Even the use of peptide-phage display libraries is unlikely to produce clear conclusions (Blond-Elguindi *et al.*, 1993; Gragerov *et al.*, 1994; Takenaka *et al.*, 1995), as there is only one clear pocket for a peptide side chain (Leu 4 of NRLLLTG) and the lateral position of the peptide in the binding groove has the potential to vary.

Further studies are needed to confirm the induction of mt hsp70 by IFN-γ, using a more specific probe, and the responses to IFN-γ, TNF, IL-1 and IL-6 of the three hsp70 mRNAs encoded in the MHC using positive controls. The results for hsp70 and hsp70hom should be confirmed at the protein level. It would also be interesting to know whether hsc70, hsp70A2 or hsp70B' are induced by cytokines. It is important to note that the activity of hsp70s may be controlled in response to extracellular signals through post-translational modifications in addition to, or instead of, through expression levels. The activity of hsp70s is known to be regulated by phosphorylation (Leustek *et al.*, 1992; Panagiotidis *et al.*, 1994) and ADP-ribosylation in the case of BiP (Freiden *et al.*, 1992). It may also be controlled by calmodulin, a multipurpose intracellular Ca^{2+} receptor that binds to hsc70 (Stevenson and Calderwood, 1990).

None of the experiments in this thesis have addressed the potential roles of hsp70s in antigen processing directly. This is not straightforward, but a number of possibilities can be put forward. If hsp70s are important in the class I pathway of antigen processing, the presentation of cytoplasmic antigens and the cell surface expression of MHC class I

molecules may increase when hsp70s are induced and decrease when their expression is reduced. Herbimycin A, a benzoquinoid ansamycin antibiotic, is a specific inducer of cytoplasmic hsp70s, but not other chaperones (Morris *et al.*, 1996). It woud be interesting to see its effects on antigen presentation by cultured cells. A complementary approach would be to reduce the expression of individual hsp70s using antisense technology or by targeted gene disruption, in cultured cells or whole animals. However, if increasing the expression of hsp70s does not affect antigen presentation by MHC class I molecules, it does not necessarily mean that hsp70s are not involved. It may be that they are not a limiting factor. Conversely, reducing the expression of individual hsp70s would have little effect if several members of the hsp70 family played interchangeable roles in antigen processing.

Ideally, a role for hsp70s in antigen processing would be shown by reconstituting the antigen processing pathway *in vitro*. For instance, hsp70s may aid the degradation of intact antigens by proteasomes *in vitro*, or peptides complexed with hsp70s may be taken up more efficiently into purified microsomes by TAP. This could be investigated by adding peptides with or without hsp70s to purified microsomes, or by adding the peptides mixed with purified cytoplasm, from which different hsp70s have been depleted by immunoprecipitation.

If hsp70s were shown to interact physically with TAP, the proteasome or some other component of the class I antigen processing pathway, this would provide important circumstantial evidence for their involvement in this pathway. Such an interaction could be demonstrated by immunoprecipitation or by yeast two-hybrid screening. The latter approach has successfully found a novel partner protein for human hsc70 (HiP) (Frydman and Höhfeld, 1997), despite the danger of non-specific interactions between unfolded potential partners and the peptide-binding domain of the hsp70. Such an approach has the advantage of investigating potential roles for an hsp70 (such as hsp70hom) beyond antigen processing alone.

Srivastava and colleagues have shown that hsp70s are important in targeting antigenic peptides to macrophages and dendritic cells, where they are presented by class I molecules (Suto and Srivastava, 1995). Which members of the human hsp70 family are involved has not been determined. BiP is unlikely to be responsible, because it does not appear to bind to antigenic peptides transported into the ER by TAP (Lammert *et al.*, 1997). Furthermore, antigen presenting cells may endocytose the hsp70s of infectious micro-organisms and the peptides they carry, which would account for the adjuvancy of bacterial hsp70s in covalent or non-covalent complex with foreign antigens and explain why they are themselves prominent antigens in an immune response (Perraut *et al.*, 1993; Barrios *et al.*, 1994; Roman and Moreno, 1996).

The most interesting question about the potential roles of hsp70s in antigen processing is whether the specificity of hsp70s limit the repertoire of peptides presented by class I molecules. Unless naturally-occurring mutations in the peptide binding site of hsp70hom are found and shown to influence antigen presentation, this question will not be answered until our knowledge of the specificity of hsp70s for peptides, as well as the specificity of antigen processing (particularly in the selection of substrates for the proteasome) has improved significantly.

References

Abbas, A.K., Lichtman, A.H. and Pober, J.S. (1996). 'Cellular and Molecular Immunology.' W.B. Saunders Co.

Ahn, K., Meyer, T.H., Uebel, S., Sempe, P., Djaballah, H., Yang, Y., Peterson, P.A., Fruh, K. and Tampe, R. (1996a) 'Molecular mechanism and species specificity of TAP inhibition by herpes simplex virus ICP47.' *Embo J* **15**, 3247-55.

Ahn, K., Erlander, M., Leturcq, D., Peterson, P.A., Fruh, K. and Yang, Y. (1996b) 'In vivo characterization of the proteasome regulator PA28.' *J Biol Chem* **271**, 18237-42.

Ahn, K., Angulo, A., Ghazal, P., Peterson, P.A., Yang, Y. and Fruh, K. (1996c) 'Human cytomegalovirus inhibits antigen presentation by a sequential multistep process.' *Proc Natl Acad Sci U S A* **93**, 10990-5.

Aldrich, C.J., DeCloux, A., Woods, A.S., Cotter, R.J., Soloski, M.J. and Forman, J. (1994) 'Identification of a Tap-dependent leader peptide recognized by alloreactive T cells specific for a class Ib antigen.' *Cell* **79**, 649-58.

Allen, J.B., Walberg, M.W., Edwards, M.C. and Elledge, S.J. (1995) 'Finding prospective partners in the library: the two-hybrid system and phage display find a match.' *Trends Biochem Sci* **20**, 511-6.

Amigorena, S., Drake, J.R., Webster, P. and Mellman, I. (1994) 'Transient accumulation of new class II MHC molecules in a novel endocytic compartment in B lymphocytes.' *Nature* **369**, 113-20.

Androlewicz, M.J. and Cresswell, P. (1994) 'Human transporters associated with antigen processing possess a promiscuous peptide-binding site.' *Immunity* **1**, 7-14.

Anfinsen, C.B. (1973) *Science* **181**, 223-230.

Aronson, N., Jr. and Kuranda, M.J. (1989) 'Lysosomal degradation of Asn-linked glycoproteins.' *Faseb J* **3**, 2615-22.

Auger, I., Escola, J.M., Gorvel, J.P. and Roudier, J. (1996) 'HLA-DR4 and HLA-DR10 motifs that carry susceptibility to rheumatoid arthritis bind 70-kD heat shock proteins.' *Nat Med* **2**, 306-10.

Bachmann, M.F., Oxenius, A., Pircher, H., Hengartner, H., Ashton-Richardt, P.A., Tonegawa, S. and Zinkernagel, R.M. (1995) 'TAP1-independent loading of class I molecules by exogenous viral proteins.' *Eur J Immunol* **25**, 1739-43.

Bacik, I., Cox, J.H., Anderson, R., Yewdell, J.W. and Bennink, J.R. (1994) 'TAP (transporter associated with antigen processing)-independent presentation of endogenously synthesized peptides is enhanced by endoplasmic reticulum insertion sequences located at the amino- but not carboxyl-terminus of the peptide.' *J Immunol* **152**, 381-7.

Baron, M., Norman, D.G. and Campbell, I.D. (1991) 'Protein modules.' *Trends Biochem Sci* **16**, 13-7.

Barrios, C., Georgopoulos, C., Lambert, P.H. and Del-Giudice, G. (1994) 'Heat shock proteins as carrier molecules: in vivo helper effect mediated by Escherichia coli GroEL and DnaK proteins requires cross-linking with antigen.' *Clin Exp Immunol* **98**, 229-33.

Barton, G.J. (1990) 'Protein multiple sequence alignment and flexible pattern matching.' *Methods Enzymol* **183**, 403-28.

Barton, G.J. and Sternberg, M.J. (1987) 'A strategy for the rapid multiple alignment of protein sequences. Confidence levels from tertiary structure comparisons.' *J Mol Biol* **198**, 327-37.

Belich, M.P., Glynne, R.J., Senger, G., Sheer, D. and Trowsdale, J. (1994) 'Proteasome components with reciprocal expression to that of the MHC-encoded LMP proteins.' *Curr Biol* **4**, 769-76.

Bennett, K., Levine, T., Ellis, J.S., Peanasky, R.J., Samloff, I.M., Kay, J. and Chain, B.M. (1992) 'Antigen processing for presentation by class II major histocompatibility complex requires cleavage by cathepsin E.' *Eur J Immunol* **22**, 1519-24.

Berg, T., Gjoen, T. and Bakke, O. (1995) 'Physiological functions of endosomal proteolysis.' *Biochem J* **307**, 313-26.

Bevan, M.J. (1976) 'Cross-priming for a secondary cytotoxic response to minor H antigens with H-2 congenic cells which do not cross-react in the cytotoxic assay.' *J. Exp. Med.* **143**, 1283-1288.

Bevec, T., Stoka, V., Pungercic, G., Dolenc, I. and Turk, V. (1996) 'Major histocompatibility complex class II-associated p41 invariant chain fragment is a strong inhibitor of lysosomal cathepsin L.' *J Exp Med* **183**, 1331-8.

Bhattacharyya, T., Karnezis, A.N., Murphy, S.P., Hoang, T., Freeman, B.C., Phillips, B. and Morimoto, R.I. (1995) 'Cloning and subcellular localization of human mitochondrial hsp70.' *J Biol Chem* **270**, 1705-10.

Birnboim, H.C. and Doly, J. (1979) 'A rapid alkaline extraction procedure for screening recombinant plasmid DNA.' *Nucleic Acids Res* **7**, 1513-23.

Blond-Elguindi, S., Cwirla, S.E., Dower, W.J., Lipshutz, R.J., Sprang, S.R., Sambrook, J.F. and Gething, M.J. (1993) 'Affinity panning of a library of peptides displayed on bacteriophages reveals the binding specificity of BiP.' *Cell* **75**, 717-28.

Bodmer, J.G., Marsh, S.G., Albert, E.D., Bodmer, W.F., Dupont, B., Erlich, H.A., Mach, B., Mayr, W.R., Parham, P., Sasazuki, T. and et, a. (1994) 'Nomenclature for factors of the HLA system, 1994.' *Tissue Antigens* **44**, 1-18.

Bonnerot, C., Lankar, D., Hanau, D., Spehner, D., Davoust, J., Salamero, J. and Fridman, W.H. (1995) 'Role of B cell receptor Ig alpha and Ig beta subunits in MHC class II-restricted antigen presentation.' *Immunity* **3**, 335-47.

Bonnycastle, L.L.C., Yu, C.E., Hunt, C.R., Trask, B.J., Clancy, K.P., Weber, J.L., Patterson, D. and Schellenberg, G.D. (1994) 'Cloning, sequencing, and mapping of the human chromosome 14 heat shock protein gene (HSPA2).' *Genomics* **23**, 85-93.

Boorstein, W.R., Ziegelhoffer, T. and Craig, E.A. (1994) 'Molecular evolution of the HSP70 gene family.' *J Mol Evol* **38**, 1-17.

Brocklehurst, S.M. and Perham, R.N. (1993) 'Prediction of the three-dimensional structures of the biotinylated domain from yeast pyruvate carboxylase and of the lipoylated H-protein from the pea leaf glycine cleavage system: a new automated method for the prediction of protein tertiary structure.' *Protein Sci* **2**, 626-39.

Brodsky, F.M. (1992) 'Antigen processing and presentation: close encounters in the endocytic pathway.' *Trends in Cell Biology* **2**, 109-115.

Brodsky, J.L. (1996) 'Post-translational protein translocation: not all hsc70s are created equal.' *Trends Biochem Sci* **21**, 122-126.

Brodsky, J.L., Hamamoto, S., Feldheim, D. and Schekman, R. (1993) 'Reconstitution of protein translocation from solubilized yeast membranes reveals topologically distinct roles for BiP and cytosolic Hsc70.' *J Cell Biol* **120**, 95-102.

Brodsky, J.L. and McCracken, A.A. (1997) 'ER-associated and proteasome-mediated protein degradation: how two topologically restricted events came together.' *Trends Cell Biol* **7**, 151-156.

Brooks, B.R., Bruccoleri, R.E., Olafson, B.D., States, D.J., Swaminathan, S. and Karplus, M. (1983) 'CHARMM: A program for macromolecular energy minimization and dynamics calculations.' *J Comp Chem* **4**, 187-217.

Brown, J.H., Kardetzky, T.S., Gorga, J.C., Stern, L.J., Urban, R.G., Strominger, J.L. and Wiley, D.C. (1993) 'The three-dimensional structure of the human class II histocompatibility antigen HLA-DR.' *Nature* **364**, 33-39.

Bruschi, S.A., West, K.A., Crabb, J.W., Gupta, R.S. and Stevens, J.L. (1993) 'Mitochondrial HSP60 (P1 protein) and a HSP70-like protein (mortalin) are major targets for modification during S-(1,1,2,2-tetrafluoroethyl)-L-cysteine-induced nephrotoxicity.' *J Biol Chem* **268**, 23157-61.

Burkholder, W.F., Zhao, X., Zhu, X., Hendrickson, W.A., Gragerov, A. and Gottesman, M.E. (1996) 'Mutations in the C-terminal fragment of DnaK affecting peptide binding.' *Proc Natl Acad Sci U S A* **93**, 10632-7.

Burmeister, W.P., Huber, A.H. and Bjorkman, P.J. (1994) 'Crystal structure of the complex of rat neonatal Fc receptor with Fc.' *Nature* **372**, 379-83.

Calafat, J., Nijenhuis, M., Janssen, H., Tulp, A., Dusseljee, S., Wubbolts, R. and Neefjes, J. (1994) 'Major histocompatibility complex class II molecules induce the formation of endocytic MIIC-like structures.' *J Cell Biol* **126**, 967-77.

Campbell, I.D. and Downing, A.K. (1994) 'Building protein structure and function form modular units.' *Trends Biotechnol* **12**, 168-172.

Campbell, R.D. and Milner, C.M. (1993) 'MHC genes in autoimmunity.' *Curr Opin Immunol* **5**, 887-93.

Campbell, R.D. and Trowsdale, J. (1997) 'Map of the human MHC.' *Immunol Today* **18**, 43.

Camussi, G., Albano, E., Tetta, C. and Bussolino, F. (1991) 'The molecular action of tumor necrosis factor-alpha.' *Eur J Biochem* **202**, 3-14.

Castellino, F. and Germain, R.N. (1995) 'Extensive trafficking of MHC class II-invariant chain complexes in the endocytic pathway and appearance of peptide-loaded class II in multiple compartments.' *Immunity* **2**, 73-88.

Cella, M., Sallusto, F. and Lanzavecchia, A. (1997) 'Origin, maturation and antigen presenting function of dendritic cells.' *Curr Op Immunol* **9**, 10-16.

Chappell, T.G., Konforti, B.B., Schmidt, S.L. and Rothman, J.E. (1987) 'The ATPase core of a clathrin uncoating protein.' *J biol Chem* **262**, 746-751.

Chelbi-Alix, M.K. and Chousterman, S. (1992) 'Ethanol induces 2',5'-oligoadenylate synthetase and antiviral activities through interferon-beta production.' *J Biol Chem* **267**, 1741-5.

Chelbi-Alix, M.K. and Sripati, C.E. (1994) 'Ability of insulin and DsRNA to induce interferon system and Hsp 70 in fibroblast and epithelial cells in relation to their effects on cell growth.' *Exp Cell Res* **213**, 383-90.

Chiang, H.L., Terlecky, S.R., Plant, C.P. and Dice, J.F. (1989) 'A role for a 70-kilodalton heat shock protein in lysosomal degradation of intracellular proteins.' *Science* **246**, 382-5.

Chicz, R.M., Urban, R.G., Lane, W.S., Gorga, J.C., Stern, L.J., Vignali, D.A. and Strominger, J.L. (1992) 'Predominant naturally processed peptides bound to HLA-DR1 are derived from MHC-related molecules and are heterogeneous in size.' *Nature* **358**, 764-8.

Chomczynski, P. and Sacchi, N. (1987) 'Single-step method of RNA isolation by acid guanidinium thiocyanate-phenol-chloroform extraction.' *Anal Biochem* **162**, 156-9.

Chou, P.Y. and Fasman, G.D. (1978) 'Prediction of the secondary structure of proteins from their amino acid sequence.' *Adv Enzymol* **47**, 45-148.

Clerget, M. and Polla, B.S. (1990) 'Erythrophagocytosis induces heat shock protein synthesis by human monocytes-macrophages.' *Proc Natl Acad Sci U S A* **87**, 1081-5.

Collins, D.S., Unanue, E.R. and Harding, C.V. (1991) 'Reduction of disulfide bonds within lysosomes is a key step in antigen processing.' *J Immunol* **147**, 4054-9.

Collins, E.J., Garboczi, D.N. and Wiley, D.C. (1994) 'Three-dimensional structure of a peptide extending from one end of a class I MHC binding site.' *Nature* **371**, 626-9.

Cotner, T. and Pious, D. (1995) 'HLA-DR-beta chains enter into an aggregated complex containing GRP-78/BiP prior to their degradation by the pre-Golgi degradative pathway.' *Journal of Biological Chemistry* **270**, 2379-2386.

Counce, S., Smith, P., Barth, R. and Snell, G.D. (1956) 'Strong and weak histocompatibility gene differences in mice and their role in the rejection of homografts of tumour and skin.' *Ann Surg* **144**, 198-204.

Cox, J.H., Galardy, P., Bennink, J.R. and Yewdell, J.W. (1995) 'Presentation of endogenous and exogenous antigens is not affected by inactivation of E1 ubiquitin-activating enzyme in temperature-sensitive cell lines.' *J Immunol* **154**, 511-9.

Creighton, T.E. (1990) 'Protein folding.' *Biochem J* **270**, 1-16.

Creighton, T.E. (1991) 'Molecular chaperones. Unfolding protein folding.' *Nature* **352**, 17-8.

Cristau, B., Schafer, P.H. and Pierce, S.K. (1994) 'Heat shock enhances antigen processing and accelerates the formation of compact class II alpha beta dimers.' *J Immunol* **152**, 1546-56.

Cruz, T.F., Kandel, R.A. and Brown, I.R. (1991) 'Interleukin 1 induces the expression of a heat-shock gene in chondrocytes.' *Biochem J* **277**, 327-30.

Cuervo, A.M. and Dice, J.F. (1996) 'A receptor for the selective uptake and degradation of proteins by lysosomes.' *Science* **273**, 501-3.

Cuervo, A.M., Knecht, E., Terlecky, S.R. and Dice, J.F. (1995) 'Activation of a selective pathway of lysosomal proteolysis in rat liver by prolonged starvation.' *Am J Physiol* **269**, C1200-8.

Cuervo, A.M., Palmer, A., Rivett, A.J. and Knecht, E. (1995) 'Degradation of proteasomes by lysosomes in rat liver.' *Eur J Biochem* **227**, 792-800.

Cyr, D.M., Langer, T. and Douglas, D.M. (1994) 'DnaJ-like proteins: molecular chaperones and specific regulators of Hsp70s.' *Trends Biochem Sci* **19**, 176-181.

D'Onofrio, C., Franzese, O., Ricci, F. and Bonmassar, E. (1993) 'Combined treatments with interferon (alpha,beta) plus PGA1 to control early infection with HTLV-I in primary cord blood-derived mononuclear cells.' *Int J Immunopharmacol* **15**, 125-36.

D'Souza, S.D., Antel, J.P. and Freedman, M.S. (1994) 'Cytokine induction of heat shock protein expression in human oligodendrocytes: an interleukin-1-mediated mechanism.' *J Neuroimmunol* **50**, 17-24.

Dahlseid, J.N., Lill, R., Green, J.M., Xu, X., Qiu, Y. and Pierce, S.K. (1994) 'PBP74, a new member of the mammalian 70-kDa heat shock protein family, is a mitochondrial protein.' *Mol. biol. cell* **5**, 1265-1275.

Danpure, C.J. (1995) 'How can the products of a single gene be localised to more than one intracellular compartment?' *Trends Cell Biol* **5**, 230-238.

Davidson, H.W. and Watts, C. (1989) 'Epitope-directed processing of specific antigen by B lymphocytes.' *J Cell Biol* **109**, 85-92.

Dealtry, G.B. and Rickwood, D. (1992). 'Cell Biology Labfax.' Oxford, Blackwell Scientific Publications.

DeBruijn, M.L., Jackson, M.R. and Peterson, P.A. (1995) 'Phagocyte-induced antigen-specific activation of unprimed CD8+ T cells in vitro.' *Eur J Immunol* **25**, 1274-85.

DeCrouy-Chanel, A., Kohiyama, M. and Richarme, G. (1996) 'Specificity of DnaK for arginine/lysine and effect of DnaJ on the amino acid specificity of DnaK.' *J Biol Chem* **271**, 15486-90.

DeLuca-Flaherty, C., McKay, D.B., Parham, P. and Hill, B.L. (1990) 'Uncoating protein (hsc70) binds a conformationally labile domain of clathrin light chain LCa to stimulate ATP hydrolysis.' *Cell* **62**, 875-87.

DelVal, M., Hengel, H., Hacker, H., Hartlaub, U., Ruppert, T., Lucin, P. and Koszinowski, U.H. (1992) 'Cytomegalovirus prevents antigen presentation by blocking the transport of peptide-loaded major histocompatibility complex class I molecules into the medial-Golgi compartment.' *J Exp Med* **176**, 729-38.

DeNagel, D.C. and Pierce, S.K. (1992) 'A case for chaperones in antigen processing.' *Immunol Today* **13**, 86-9.

Dick, L.R., Aldrich, C., Jameson, S.C., Moomaw, C.R., Pramanik, B.C., Doyle, C.K., DeMartino, G.N., Bevan, M.J., Forman, J.M. and Slaughter, C.A. (1994) 'Proteolytic processing of ovalbumin and ß-galactosidase by the proteasome to yield antigenic peptides.' *J Immunol* **152**, 3884-3893.

Dick, T.P., Ruppert, T., Groettrup, M., Kloetzel, P.M., Kuehn, L., Koszinowski, U.H., Stevanovic, S., Schild, H. and Rammensee, H.G. (1996) 'Coordinated dual cleavages induced by the proteasome regulator PA28 lead to dominant MHC ligands.' *Cell* **86**, 253-62.

Diment, S. (1990) 'Different roles for thiol and aspartyl proteases in antigen presentation of ovalbumin.' *J Immunol* **145**, 417-22.

Dix, D.J., Allen, J.W., Collins, B.W., Mori, C., Nakamura, N., Poorman-Allen, P., Goulding, E.H. and Eddy, E.M. (1996) 'Targeted gene disruption of Hsp70-2 results in failed meiosis, germ cell apoptosis, and male infertility.' *Proc Natl Acad Sci U S A* **93**, 3264-8.

Domanico, S.Z., DeNagel, D.C., Dahlseid, J.N., Green, J.M. and Pierce, S.K. (1993) 'Cloning of the gene encoding peptide-binding protein 74 shows that it is a new member of the heat shock protein 70 family.' *Mol Cell Biol* **13**, 3598-610.

Donati, Y.R., Slosman, D.O. and Polla, B.S. (1990) 'Oxidative injury and the heat shock response.' *Biochem Pharmacol* **40**, 2571-7.

Driscoll, J., Brown, M.G., Finley, D. and Monaco, J.J. (1993) 'MHC-linked LMP gene products specifically alter peptidase activities of the proteasome.' *Nature* **365**, 262-4.

Dudler, T., Altmann, F., Carballido, J.M. and Blaser, K. (1995) 'Carbohydrate-dependent, HLA class II-restricted, human T cell response to the bee venom allergen phospholipase A2 in allergic patients.' *Eur J Immunol* **25**, 538-42.

Dunn, W.A. (1994) 'Autophagy and related mechanisms of lysosome-mediated protein degradation.' *Trends cell biol* **4**, 139-143.

Dworniczak, B. and Mirault, M.E. (1987) 'Structure and expression of a human gene coding for a 71 kd heat shock 'cognate' protein.' *Nucleic Acids Res* **15**, 5181-97.

Dyson, H.J. and Wright, P.E. (1991) 'Defining solution conformations of small linear peptides.' *Annu Rev Biophys Biophys Chem* **20**, 519-38.

Dyson, H.J. and Wright, P.E. (1995) 'Antigenic peptides.' *Faseb J* **9**, 37-42.

Ehrlich, R. (1995) 'Selective mechanisms utilized by persistent and oncogenic viruses to interfere with antigen processing and presentation.' *Immunol Res* **14**, 77-97.

Eisenlohr, L.C., Bacik, I., Bennink, J.R., Bernstein, K. and Yewdell, J.W. (1992) 'Expression of a membrane protease enhances presentation of endogenous antigens to MHC class I-restricted T lymphocytes.' *Cell* **71**, 963-72.

Elliott, T., Willis, A., Cerundolo, V. and Townsend, A. (1995) 'Processing of major histocompatibility class I-restricted antigens in the endoplasmic reticulum.' *J Exp Med* **181**, 1481-91.

Ellis, J. (1987) 'Proteins as molecular chaperones.' *Nature* **328**, 378-9.

Ellis, R.J. and Hartl, F.U. (1996) 'Protein folding in the cell: competing models of chaperonin function.' *Faseb J* **10**, 20-6.

Endo, T., Mitsui, S., Nakai, M. and Roise, D. (1996) 'Binding of mitochondrial presequences to yeast cytosolic heat shock protein 70 depends on the amphiphilicity of the presequence.' *J Biol Chem* **271**, 4161-7.

Epperson, D.E., Arnold, D., Spies, T., Cresswell, P., Pober, J.S. and Johnson, D.R. (1992) 'Cytokines increase transporter in antigen processing-1 expression more rapidly than HLA class I expression in endothelial cells.' *J Immunol* **149**, 3297-301.

Erlich, H.A., Gelfand, D. and Sninsky, J.J. (1991) 'Recent advances in the polymerase chain reaction.' *Science* **252**, 1643-51.

Evans, J.N.S. (1995). 'Biomolecular NMR.' Oxford University Press.

Fahnestock, M.L., Johnson, J.L., Feldman, R.M., Neveu, J.M., Lane, W.S. and Bjorkman, P.J. (1995) 'The MHC class I homolog encoded by human cytomegalovirus binds endogenous peptides.' *Immunity* **3**, 583-90.

Farr, C.D., Galiano, F.J. and Witt, S.N. (1995) 'Large activation energy barriers to chaperone-peptide complex formation and dissociation.' *Biochemistry* **34**, 15574-15582.

Farrell, H.E., Vally, H., Lynch, D.M., Fleming, P., Shellam, G.R., Scalzo, A.A. and Davis-Poynter, N.J. (1997) 'Inhibition of natural killer cells by a cytomegalovirus MHC class I homologue in vivo.' *Nature* **386**, 510-514.

Fehling, H.J., Swat, W., Laplace, C., Kuhn, R., Rajewsky, K., Muller, U. and von-Boehmer, H. (1994) 'MHC class I expression in mice lacking the proteasome subunit LMP-7.' *Science* **265**, 1234-7.

Feinberg, A.P. and Vogelstein, B. (1984) 'A technique for radiolabeling DNA restriction endonuclease fragments to high specific activity.' *Anal Biochem* **137**, 266-7.

Ferm, M.T., Soderstrom, K., Jindal, S., Gronberg, A., Ivanyi, J., Young, R. and Kiessling, R. (1992) 'Induction of human hsp60 expression in monocytic cell lines.' *Int Immunol* **4**, 305-11.

Ferris, D.K., Harel-Bellan, A., Morimoto, R.I., Welch, W.J. and Farrar, W.L. (1988) 'Mitogen and lymphokine stimulation of heat shock proteins in T lymphocytes.' *Proc natl Acad Sci USA* **85**, 3850-3854.

Fincato, G., Polentarutti, N., Sica, A., Mantovani, A. and Colotta, F. (1991) 'Expression of a heat-inducible gene of the HSP70 family in human myelomonocytic cells: regulation by bacterial products and cytokines.' *Blood* **77**, 579-86.

Finley, D., Özkaynak, E. and Varshavsky, A. (1987) 'The yeast polyubiquitin gene is essential for resistance to high temperatures, starvation and other stresses.' *Cell* **48**, 1035-46.

Fitzgerald, M.C. and Siuzdak, G. (1996) 'Biochemical mass spectrometry: worth the weight?' *Chemistry and Biology* **3**, 707-715.

Flaherty, K.M., DeLuca-Flaherty, C. and McKay, D.B. (1990) 'Three-dimensional structure of the ATPase fragment of a 70K heat-shock cognate protein.' *Nature* **346**, 623-8.

Flaherty, K.M., McKay, D.B., Kabsch, W. and Holmes, K.C. (1991) 'Similarity of the three-dimensional structures of actin and the ATPase fragment of a 70-kDa heat shock cognate protein.' *Proc Natl Acad Sci U S A* **88**, 5041-5.

Flajnik, M.F., Canel, C., Kramer, J. and Kasahara, M. (1991) 'Which came first, MHC class I or class II?' *Immunogenetics* **33**, 295-300.

Flynn, G.C., Chappell, T.G. and Rothman, J.E. (1989) 'Peptide binding and release by proteins implicated as catalysts of protein assembly.' *Science* **245**, 385-90.

Flynn, G.C., Pohl, J., Flocco, M.T. and Rothman, J.E. (1991) 'Peptide-binding specificity of the molecular chaperone BiP.' *Nature* **353**, 726-30.

Fourie, A.M., Sambrook, J.F. and Gething, M.J. (1994) 'Common and divergent peptide binding specificities of hsp70 molecular chaperones.' *J Biol Chem* **269**, 30470-8.

Fourney, R.M., Miyakoshi, J., Day, R.S. and Paterson, M.C. (1988) *Focus (Bethesda Research Laboratories)* **10**, 5-7.

Freeman, B.C., Myers, M.P., Schumacher, R. and Morimoto, R.I. (1995) 'Identification of a regulatory motif in Hsp70 that affects ATPase activity, substrate binding and interaction with HDJ-1.' *Embo J* **14**, 2281-92.

Freiden, P.J., Gaut, J.R. and Hendershot, L.M. (1992) 'Interconversion of three differentially modified and assembled forms of BiP.' *Embo J* **11**, 63-70.

Fremont, D.H., Matsumura, M., Stura, E.A., Peterson, P.A. and Wilson, I.A. (1992) 'Crystal structures of two viral peptides in complex with murine MHC class I H-2Kb.' *Science* **257**, 919-27.

Frydman, J. and Höhfeld, J. (1997) 'Chaperones get in touch: the Hip-Hop connection.' *Trends Biochem Sci* **22**, 87-92.

Gaczynska, M., Rock, K.L. and Goldberg, A.L. (1993) 'Gamma-interferon and expression of MHC genes regulate peptide hydrolysis by proteasomes.' *Nature* **365**, 264-7.

Gao, B.C., Biosca, J., Craig, E.A., Greene, L.E. and Eisenberg, E. (1991) 'Uncoating of coated vesicles by yeast hsp70 proteins.' *J Biol Chem* **266**, 19565-71.

Garboczi, D.N., Ghosh, P., Utz, U., Fan, Q.R., Biddison, W.E. and Wiley, D.C. (1996) 'Structure of the complex between human T-cell receptor, viral peptide and HLA-A2.' *Nature* 134-141.

Garcia, C., Degano, M., Stanfield, R.L., Brunmark, A., Jackson, M.R., Peterson, P.A., Teyton, L. & Wilson, I.A. (1996) 'An alpha-beta T cell receptor structure at 2.5 Å and its orientation in the TCR-MHC complex.' *Science* **274**, 209-219.

Garnier, J., Osguthorpe, D.J. and Robson, B. (1978) 'Analysis of the accuracy and implications of simple methods for predicting the secondary structures of globular proteins.' *J mol Biol* **120**, 97-129.

Genuardi, M. and Saunders, G.F. (1988) 'Localization of the HLA class II-associated invariant chain gene to human chromosome band 5q32.' *Immunogenetics* **28**, 53-6.

Germain, R.N. (1994) 'MHC-dependent antigen processing and peptide presentation: providing ligands for T lymphocyte activation.' *Cell* **76**, 287-299.

Germain, R.N. and Hendrix, L.R. (1991) 'MHC class II structure, occupancy and surface expression determined by post-endoplasmic reticulum antigen binding.' *Nature* **353**, 134-9.

Gething, M.J. and Sambrook, J. (1992) 'Protein folding in the cell.' *Nature* **355**, 33-45.

Ghosh, P., Amaya, M., Mellins, E. and Wiley, D.C. (1995) 'The structure of an intermediate in class II MHC maturation: CLIP bound to HLA-DR3.' *Nature* **378**, 457-62.

Gilbert, M.J., Riddell, S.R., Li, C.R. and Greenberg, P.D. (1993) 'Selective interference with class I major histocompatibility complex presentation of the major immediate-early protein following infection with human cytomegalovirus.' *J Virol* **67**, 3461-9.

Gorinsky, B., Laskowski, R.A., Lee, D.A. and Bomford, A. (1996) 'Conformational analysis of pentapeptide sequences matching a proposed recognition motif for lysosomal degradation.' *Biochim Biophys Acta* **1293**, 243-53.

Gragerov, A. and Gottesman, M.E. (1994) 'Different peptide binding specificities of hsp70 family members.' *J Mol Biol* **241**, 133-5.

Gragerov, A., Zeng, L., Zhao, X., Burkholder, W. and Gottesman, M.E. (1994) 'Specificity of DnaK-peptide binding.' *J Mol Biol* **235**, 848-54.

Grandea, A.3., Androlewicz, M.J., Athwal, R.S., Geraghty, D.E. and Spies, T. (1995) 'Dependence of peptide binding by MHC class I molecules on their interaction with TAP.' *Science* **270**, 105-8.

Granelli-Piperno, A., Andrus, L. and Steinman, R.M. (1986) 'Lymphokine and nonlymphokine mRNA levels in stimulated human T cells. Kinetics, mitogen requirements, and effects of cyclosporin A.' *J Exp Med* **163**, 922-37.

Grant, E.P., Michalek, M.T., Goldberg, A.L. and Rock, K.L. (1995) 'Rate of antigen degradation by the ubiquitin-proteasome pathway influences MHC class I presentation.' *J Immunol* **155**, 3750-8.

Gregori, L., Hainfeld, J.F., Simon, M.N. and Goldgaber, D. (1997) 'Binding of amyloid beta protein to the 20 S proteasome.' *J Biol Chem* **272**, 58-62.

Groettrup, M., Kraft, R., Kostka, S., Standera, S., Stohwasser, R. and Kloetzel, P.M. (1996a) 'A third interferon-gamma-induced subunit exchange in the 20S proteasome.' *Eur J Immunol* **26**, 863-9.

Groettrup, M., Soza, A., Eggers, M., Kuehn, L., Dick, T.P., Schild, H., Rammensee, H.G., Koszinowski, U.H. and Kloetzel, P.M. (1996b) 'A role for the proteasome regulator PA28alpha in antigen presentation.' *Nature* **381**, 166-8.

Groettrup, M., Soza, A., Kuckelkorn, U. and Kloetzel, P.M. (1996c) 'Peptide antigen production by the proteasome: complexity provides efficiency.' *Immunol Today* **17**, 429-435.

Groll, M., Ditzel, L., Löwe, J., Stock, D., Bochtler, M., Bartunik, H.D. and Huber, R. (1997) 'Structure of 20S proteasome from yeast at 2.4 Å resolution.' *Nature* **386**, 463-471.

Gueguen, M., Biddison, W.E. and Long, E.O. (1994) 'T cell recognition of an HLA-A2-restricted epitope derived from a cleaved signal sequence.' *J Exp Med* **180**, 1989-94.

Guo, H.C., Jardetzky, T.S., Garrett, T.P., Lane, W.S., Strominger, J.L. and Wiley, D.C. (1992) 'Different length peptides bind to HLA-Aw68 similarly at their ends but bulge out in the middle [see comments].' *Nature* **360**, 364-6.

Hammond, S.A., Bollinger, R.C., Tobery, T.W. and Silliciano, R.F. (1993) 'Transporter-independent processing of HIV-1 envelope protein for recognition by CD8+ T cells.' *Nature* **364**, 158-61.

Hammond, S.A., Johnson, R.P., Kalams, S.A., Walker, B.D., Takiguchi, M., Safrit, J.T., Koup, R.A. and Siliciano, R.F. (1995) 'An epitope-selective, transporter associated with antigen presentation (TAP)-1/2-independent pathway and a more general TAP-1/2-dependent antigen-processing pathway allow recognition of the HIV-1 envelope glycoprotein by CD8+ CTL.' *J Immunol* **154**, 6140-56.

Harding, C.V. (1995) 'Phagocytic processing of antigens for presentation by MHC molecules.' *Trends Cell Biol* **5**, 105-109.

Harding, C.V., Kihlberg, J., Elofsson, M., Magnusson, G. and Unanue, E.R. (1993) 'Glycopeptides bind MHC molecules and elicit specific T cell responses.' *J Immunol* **151**, 2419-25.

Hartl, F.U. (1996) 'Molecular chaperones in cellular protein folding.' *Nature* **381**, 571-580.

Heemels, M.T. and Ploegh, H.L. (1994) 'Substrate specificity of allelic variants of the TAP peptide transporter.' *Immunity* **1**, 775-84.

Heemels, M.T., Schumacher, T.N., Wonigeit, K. and Ploegh, H.L. (1993) 'Peptide translocation by variants of the transporter associated with antigen processing.' *Science* **262**, 2059-63.

Helqvist, S., Hansen, B.S., Johannesen, J., Andersen, H.U., Nielsen, H.J. and Nerup, J. (1989) 'Interleukin 1 induces new protein formation in isolated rat islets of Langerhans.' *Acta Endocrinol (Copenh)* **121**, 136-140.

Helqvist, S., Polla, B.S., Johannesen, J. and Nerup, J. (1991) 'Heat shock protein induction in rat pancreatic islets by recombinant human interleukin 1 beta.' *Diabetologia* **34**, 150-6.

Hendrick, J.P. and Hartl, F.U. (1993) 'Molecular chaperone functions of heat-shock proteins.' *Annu Rev Biochem* **62**, 349-84.

Heufelder, A.E., Wenzel, B.E., Gorman, C.A. and Bahn, R.S. (1991) 'Detection, cellular localization, and modulation of heat shock proteins in cultured fibroblasts from patients with extrathyroidal manifestations of Graves' disease.' *J Clin Endocrinol Metab* **73**, 739-45.

Hill, A.V., Elvin, J., Willis, A.C., Aidoo, M., Allsopp, C.E., Gotch, F.M., Gao, X.M., Takiguchi, M., Greenwood, B.M., Townsend, A.R. and et, a. (1992) 'Molecular analysis of the association of HLA-B53 and resistance to severe malaria [see comments].' *Nature* **360**, 434-9.

Hisamatsu, H., Shimbara, N., Saito, Y., Kristensen, P., Hendil, K.B., Fujiwara, T., Takahashi, E., Tanahashi, N., Tamura, T., Ichihara, A. and Tanaka, K. (1996) 'Newly identified pair of proteasomal subunits regulated reciprocally by interferon gamma.' *J Exp Med* **183**, 1807-16.

Hoeger, P.H., Tepper, M.A., Faith, A., Higgins, J.A., Lamb, J.R. and Geha, R.S. (1994) 'Immunosuppressant deoxyspergualin inhibits antigen processing in monocytes.' *J Immunol* **153**, 3908-16.

Hombach, J., Pircher, H., Tonegawa, S. and Zinkernagel, R.M. (1995) 'Strictly transporter of antigen presentation (TAP)-dependent presentation of an immunodominant cytotoxic T lymphocyte epitope in the signal sequence of a virus protein.' *J Exp Med* **182**, 1615-9.

Hong-Brown, L.Q. and Brown, C.R. (1994) 'Cytokine and insulin regulation of alpha 2 macroglobulin, angiotensinogen, and hsp 70 in primary cultured astrocytes.' *Glia* **12**, 211-8.

Hu, S.M. and Wang, C. (1996) 'Involvement of the 10-kDa C-terminal fragment of hsc70 in complexing with unfolded protein.' *Arch Biochem Biophys* **332**, 163-9.

Hubbard, T.J. and Sander, C. (1991) 'The role of heat-shock and chaperone proteins in protein folding: possible molecular mechanisms.' *Protein Eng* **4**, 711-7.

Hughes, A.L. and Nei, M. (1989) 'Nucleotide substitution at major histocompatibility complex class II loci: evidence for overdominant selection.' *Proc Natl Acad Sci U S A* **86**, 958-62.

Hunt, D.F., Michel, H., Dickinson, T.A., Shabanowitz, J., Cox, A.L., Sakaguchi, K., Appella, E., Grey, H.M. and Sette, A. (1992) 'Peptides presented to the immune system by the murine class II major histocompatibility complex molecule I-Ad.' *Science* **256**, 1817-20.

Imani, F. and Soloski, M.J. (1991) 'Heat shock proteins can regulate expression of the Tla region-encoded class Ib molecule Qa-1.' *Proc Natl Acad Sci U S A* **88**, 10475-9.

Jaattela, M. (1995) 'Over-expression of hsp70 confers tumorigenicity to mouse fibrosarcoma cells.' *Int J Cancer* **60**, 689-93.

Jaattela, M., Wissing, D., Bauer, P.A. and Li, G.C. (1992) 'Major heat shock protein hsp70 protects tumor cells from tumor necrosis factor cytotoxicity.' *Embo J* **11**, 3507-12.

Jaenicke, R. (1987) 'Folding and association of proteins.' *Prog Biophys Mol Biol* **49**, 117-237.

James, P., Pfund, C. and Craig, E.A. (1997) 'Functional specificity among hsp70 molecular chaperones.' *Science* **275**, 387-389.

Jancarik, J. and Kim, S.H. (1991) *J Appl Cryst* **24**, 409-411.

Jelachich, M.L., Grusby, M.J., Clark, D., Tasch, D., Margoliash, E. and Pierce, S.K. (1984) 'Synergistic effects of antigen and soluble T-cell factors in B-lymphocyte activation.' *Proc Natl Acad Sci U S A* **81,** 5537-41.

Jentsch, S. (1992) 'The ubiquitin-conjugation system.' *Annu Rev Genet* **26,** 179-207.

Johnson, D.R. and Pober, J.S. (1990) 'Tumour necrosis factor and immune interferon synergistically increase trasncription of HLA class I heavy and light chain genes in vascular endothelium.' *Proc Natl Acad Sci USA* **87,** 446-450.

Jordan, R. and McMacken, R. (1995) 'Modulation of the ATPase activity of the molecular chaperone DnaK by peptides and the DnaJ and GrpE heat shock proteins.' *J Biol Chem* **270,** 4563-9.

Jorgensen, W.L. and Tirado-Rives, J. (1988) *J Am Chem Soc* **110,** 1657-1666.

Kabsch, W. and Sander, C. (1983) 'Dictionary of protein secondary structure: pattern recognition of hydrogen-bonded and geometrical features.' *Biopolymers* **22,** 2577-637.

Kandil, E., Egashira, M., Miyosi, O., Niikawa, N., Ishibashi, T. and Kasahara, M. (1996) 'The human gene encoding the heavy chain of the major histocompatibility complex class I-like Fc receptor (FCGRT) maps to 19q13.3.' *Cytogenet Cell Genet* **73,** 97-8.

Kantengwa, S., Donati, Y.R., Clerget, M., Maridonneau-Parini, I., Sinclair, F., Mariethoz, E., Perin, M., Rees, A.D., Slosman, D.O. and Polla, B.S. (1991) 'Heat shock proteins: an autoprotective mechanism for inflammatory cells?' *Semin Immunol* **3,** 49-56.

Kauffman, S.H.E. (1990) 'Heat shock proteins and the immune response.' *Immunol Today* **11,** 129-136.

Kishimoto, T., Taga, T. and Akira, S. (1994) 'Cytokine signal transduction.' *Cell* **76,** 253-262.

Klebanoff, S.J., Vadas, M.A., Harlan, J.M., Sparks, L.H., Gamble, J.R., Agosti, J.M. and Waltersdorph, A.M. (1986) 'Stimulation of neutrophils by tumor necrosis factor.' *J Immunol* **136,** 4220-5.

Knittler, M.R., Dirks, S. and Haas, I.G. (1995) 'Molecular chaperones in protein degradation in the endoplasmic reticulum: Quantitative interaction of the heat shock cognate protein with partially folded immunoglobulin light chains that are degraded in the endoplasmic reticulum.' *Proc Natl Acad Sci USA* **92,** 1764-1768.

Koopmann, J.O., Hammerling, G.J. and Momburg, F. (1997) 'Generation, intracellular transport and loading of peptides associated with MHC molecules.' *Curr Op Immunol* **9,** 80-88.

Koopmann, J.O., Post, M., Neefjes, J.J., Hammerling, G.J. and Momburg, F. (1996) 'Translocation of long peptides by transporters associated with antigen processing (TAP).' *Eur J Immunol* **26,** 1720-8.

Koradi, R., Billeter, M. and Wuthrich, K. (1996) 'MOLMOL: a program for display and analysis of macromolecular structures.' *J Mol Graph* **14,** 51-5.

Kraulis, P. (1991) *J Appl Crystallogr* **24,** 946.

Kropshofer, H., Hämmerling, G.J. and Vogt, A.B. (1997) 'How HLA-DM edits the MHC class II peptide repertoire:survival of the fittest?' *Immunol Today* **18,** 77-82.

Kropshofer, H., Vogt, A.B., Stern, L.J. and Hammerling, G.J. (1995) 'Self-release of CLIP in peptide loading of HLA-DR molecules.' *Science* **270,** 1357-9.

Kuckelkorn, U., Frentzel, S., Kraft, R., Kostka, S., Groettrup, M. and Kloetzel, P.M. (1995) 'Incorporation of major histocompatibility complex-encoded subunits LMP2 and

LMP7 changes the quality of the 20S proteasome polypeptide processing products independent of interferon-gamma.' *Eur J Immunol* **25**, 2605-11.

Kuperberg, G., Ellis, J., Marcinkiewicz, J. and Chain, B.M. (1991) 'Temperature-induced stress abrogates co-stimulatory function in antigen-presenting cells.' *Eur J Immunol* **21**, 2791-5.

Kusabe, M., Yokoyama, M., Sakakura, T., Nomura, T., Hosick, H.L. and Nishizuka, Y. (1988) 'A novel methodology for analysis of cell distribution in chimeric mouse organs using a strain specific antibody.' *J Cell Biol* **107**, 257-265.

Ladbury, J.E. and Chowdhry, B.Z. (1996) 'Sensing the heat: the application of isothermal titration calorimetry to thermodynamic studies of biomolecular interactions.' *Chem Biol* **3**, 791-801.

Laemmli, U.K. (1970) 'Cleavage of structural proteins during the assembly of the head of bacteriophage T4.' *Nature* **227**, 680-5.

Lafuse, W.P., Brown, D., Castle, L. and Zwilling, B.S. (1995) 'IFN-gamma increases cathepsin H mRNA levels in mouse macrophages.' *J Leukoc Biol* **57**, 663-9.

Lah, T.T., Hawley, M., Rock, K.L. and Goldberg, A.L. (1995) 'Gamma-interferon causes a selective induction of the lysosomal proteases, cathepsins B and L, in macrophages.' *Febs Lett* **363**, 85-9.

Lakey, E.K., Margoliash, E. and Pierce, S.K. (1987) 'Identification of a peptide binding protein that plays a role in antigen presentation.' *Proc Natl Acad Sci U S A* **84**, 1659-63.

Lammert, E., Arnold, D., Nijenhuis, M., Momburg, F., Hämmerling, G.J., Brunner, J., Stevanovic, S., Rammensee, H.-G. and Schild, H. (1997) 'The endoplasmic reticulum-resident stress protein gp96 binds peptides translocated by TAP.' *Eur J Immunol* **27**, 923-927.

Landry, S.J., Jordan, R., McMacken, R. and Gierasch, L.M. (1992) 'Different conformations for the same polypeptide bound to chaperones DnaK and GroEL.' *Nature* **355**, 455-7.

Langer, T., Lu, C., Echols, H., Flanagan, J., Hayer, M.K. and Hartl, F.U. (1992) 'Successive action of DnaK, DnaJ and GroEL along the pathway of chaperone-mediated protein folding.' *Nature* **356**, 683-9.

Larsen, F., Solheim, J., Kristensen, T., Kolsto, A.B. and Prydz, H. (1993) 'A tight cluster of five unrelated human genes on chromosome 16q22.1.' *Hum Mol Genet* **2**, 1589-95.

Lawkowski, R.A., MacArthur, M.W., Moss, D.S. and Thornton, J. (1993) *J Appl Cryst* **26**, 283-291.

Lee, D.H., Sherman, M.Y. and Goldberg, A.L. (1996a) 'Involvement of the molecular chaperone Ydj1 in the ubiquitin-dependent degradation of short-lived and abnormal proteins in Saccharomyces cerevisiae.' *Mol Cell Biol* **16**, 4773-81.

Lee, S.P., Thomas, W.A., Blake, N.W. and Rickinson, A.B. (1996b) 'Transporter (TAP)-independent processing of a multiple membrane-spanning protein, the Epstein-Barr virus latent membrane protein 2.' *Eur J Immunol* **26**, 1875-83.

Lehner, P.J. and Cresswell, P. (1996) 'Processing and delivery of peptides presented by MHC class I molecules.' *Curr Opin Immunol* **8**, 59-67.

Leung, T.K., Rajendran, M.Y., Monfries, C., Hall, C. and Lim, L. (1990) 'The human heat-shock protein family. Expression of a novel heat-inducible HSP70 (HSP70B') and isolation of its cDNA and genomic DNA.' *Biochem J* **267**, 125-32.

Leustek, T., Amir-Shapira, D., Toledo, H., Brot, N. and Weissbach, H. (1992) 'Autophosphorylation of 70 kDa heat shock proteins.' *Cell Mol Biol* **38**, 1-10.

Leustek, T., Dalie, B., Amir-Shapira, D., Brot, N. and Weissbach, H. (1989) 'A member of the Hsp70 family is localized in mitochondria and resembles Escherichia coli DnaK.' *Proc Natl Acad Sci U S A* **86**, 7805-8.

Levitskaya, J., Coram, M., Levitsky, V., Imreh, S., Steigerwald-Mullen, P.M., Klein, G., Kurilla, M.G. and Masucci, M.G. (1995) 'Inhibition of antigen processing by the internal repeat region of the Epstein-Barr virus nuclear antigen-1.' *Nature* **375**, 685-8.

Liberek, K., Marszalek, J., Ang, D., Georgopoulos, C. and Zylicz, M. (1991) 'Escherichia coli DnaJ and GrpE heat shock proteins jointly stimulate ATPase activity of DnaK.' *Proc Natl Acad Sci U S A* **88**, 2874-8.

Lowe, J., Stock, D., Jap, B., Zwickl, P., Baumeister, W. and Huber, R. (1995) 'Crystal structure of the 20S proteasome from the archaeon T. acidophilum at 3.4 A resolution.' *Science* **268**, 533-9.

Lutz-Freyermuth, C., Query, C.C. and Keene, J.D. (1990) 'Quantitative determination that one of two potential RNA-binding domains of the A protein component of the U1 small nuclear ribonucleoprotein complex binds with high affinity to stem-loop II of U1 RNA.' *Proc Natl Acad Sci U S A* **87**, 6393-7.

Madden, D.R., Garboczi, D.N. and Wiley, D.C. (1993) 'The antigenic identity of peptide-MHC complexes: a comparison of the conformations of five viral peptides presented by HLA-A2 [published erratum appears in Cell 1994 Jan 28;76(2):following 410].' *Cell* **75**, 693-708.

Malnati, M.S., Marti, M., LaVaute, T., Jaraquemada, D., Biddison, W., DeMars, R. and Long, E.O. (1992) 'Processing pathways for presentation of cytosolic antigen to MHC class II-restricted T cells.' *Nature* **357**, 702-4.

Manara, G.C., Sansoni, P., Badiali-De-Giorgi, L., Gallinella, G., Ferrari, C., Brianti, V., Fagnoni, F.F., Ruegg, C.L., De-Panfilis, G. and Pasquinelli, G. (1993) 'New insights suggesting a possible role of a heat shock protein 70-kD family-related protein in antigen processing/presentation phenomenon in humans.' *Blood* **82**, 2865-71.

Margulis, I.A., Sandler, S., Eizirik, D.L., Welsh, N. and Welsh, M. (1991) 'Liposome delivery of purified hsp70 into rat pancreatic islets as protection against interleukin-1-beta induced impaired beta-cell function.' *Diabetes* **40**, 1418-1422.

Mariethoz, E., Tacchini-Cottier, F., Jacquier-Sarlin, M., Sinclair, F. and Polla, B.S. (1994) 'Exposure of monocytes to heat shock does not increase class II expression but modulates antigen-dependent T cell responses.' *Int Immunol* **6**, 925-30.

Marsh, M., Schmid, S., Kern, H., Harms, E., Male, P., Mellman, I. and Helenius, A. (1987) 'Rapid analytical and preparative isolation of functional endosomes by free flow electrophoresis.' *J Cell Biol* **104**, 875-86.

Martin, M., Mann, D. and Carrington, M. (1995) 'Recombination rates across the HLA complex: use of microsatellites as a rapid screen for recombinant chromosomes.' *Hum Mol Genet* **4**, 423-8.

Mehdi, S., Recktenwald, D.J., Smith, L.M., Li, G.C., Armour, E.P. and Hahn, G.M. (1984) 'Effect of hyperthermia on murine surface histocompatibility antigens.' *Cancer Res* **44**, 3394-3397.

Mellins, E., Smith, L., Arp, B., Cotner, T., Celis, E. and Pious, D. (1990) 'Defective processing and presentation of exogenous antigens in mutants with normal HLA class II genes.' *Nature* **343**, 71-4.

Michalek, M.T., Benacerraf, B. and Rock, K.L. (1992) 'The class II MHC-restricted presentation of endogenously synthesized ovalbumin displays clonal variation, requires endosomal/lysosomal processing, and is up-regulated by heat shock.' *J Immunol* **148,** 1016-24.

Michalek, M.T., Grant, E.P., Gramm, C., Goldberg, A.L. and Rock, K.L. (1993) 'A role for the ubiquitin-dependent proteolytic pathway in MHC class I-restricted antigen presentation.' *Nature* **363,** 552-4.

Michalek, M.T., Grant, E.P. and Rock, K.L. (1996) 'Chemical denaturation and modification of ovalbumin alters its dependence on ubiquitin conjugation for class I antigen presentation.' *J Immunol* **157,** 617-624.

Michikawa, Y., Baba, T., Arai, Y., Sakakura, T. and Kusakabe, M. (1993a) 'Structure and organization of the gene encoding a mouse mitochondrial stress-70 protein.' *Febs Lett* **336,** 27-33.

Michikawa, Y., Baba, T., Arai, Y., Sakakura, T., Tanaka, M. and Kusakabe, M. (1993b) 'Antigenic protein specific for C3H strain mouse is a mitochondrial stress-70 protein.' *Biochem Biophys Res Commun* **196,** 223-32.

Miller, R., DeTitta, G.T., Jones, R., Langs, D.A., Weeks, C.M. and Hauptman, H.A. (1993) 'On the application of the minimal principle to solve unknown structures.' *Science* **259,** 1430-3.

Milner, C.M. and Campbell, R.D. (1990) 'Structure and expression of the three MHC-linked HSP70 genes.' *Immunogenetics* **32,** 242-51.

Milner, C.M. and Campbell, R.D. (1992) 'Polymorphic analysis of the three MHC-linked HSP70 genes.' *Immunogenetics* **36,** 357-62.

Momburg, F., Roelse, J., Howard, J.C., Butcher, G.W., Hammerling, G.J. and Neefjes, J.J. (1994) 'Selectivity of MHC-encoded peptide transporters from human, mouse and rat.' *Nature* **367,** 648-51.

Morris, S.D., Cumming, D.V., Latchman, D.S. and Yellon, D.M. (1996) 'Specific induction of the 70-kD heat stress proteins by the tyrosine kinase inhibitor herbimycin-A protects rat neonatal cardiomyocytes. A new pharmacological route to stress protein expression?' *J Clin Invest* **97,** 706-12.

Morse, M.C., Bleau, G., Dabhi, V.M., Hetu, F., Drobetsky, E.A., Lindahl, K.F. and Perreault, C. (1996) 'The COI mitochondrial gene encodes a minor histocompatibility antigen presented by H2-M3.' *J Immunol* **156,** 3301-7.

Morshauser, R.C., Wang, H., Flynn, G.C. and Zuiderweg, E.R.P. (1995) 'The peptide-binding domain of hsc70 has an unusual secondary structure topology.' *Biochemistry* **34,** 6261-6.

Müller-Taubenberger, A., Hagmann, J., Noegel, A. and Gerisch, G. (1988) 'Ubiquitin gene expression in *Dictyostelium* is induced by heat and cold shock, cadmium and inhibitors of protein synthesis.' *J Cell Sci* **90,** 51-58.

Munro, S. and Pelham, H.R. (1986) 'An Hsp70-like protein in the ER: identity with the 78 kd glucose-regulated protein and immunoglobulin heavy chain binding protein.' *Cell* **46,** 291-300.

Munro, S. and Pelham, H.R. (1987) 'A C-terminal signal prevents secretion of luminal ER proteins.' *Cell* **48,** 899-907.

Murakami, Y., Matsufuji, S., Kameji, T., Hayashi, S., Igarashi, K., Tamura, T., Tanaka, K. and Ichihara, A. (1992) 'Ornithine decarboxylase is degraded by the 26S proteasome without ubiquitination.' *Nature* **360**, 597-9.

Nadeau, K., Nadler, S.G., Saulnier, M., Tepper, M.A. and Walsh, C.T. (1994) 'Quantitation of the interaction of the immunosuppressant deoxyspergualin and analogs with Hsc70 and Hsp90.' *Biochemistry* **33**, 2561-7.

Nadler, S.G., Tepper, M.A., Schacter, B. and Mazzucco, C.E. (1992) 'Interaction of the immunosuppressant deoxyspergualin with a member of the Hsp70 family of heat shock proteins.' *Science* **258**, 484-6.

Nakano, M., Knowlton, A.A., Yokoyama, T., Lesslauer, W. and Mann, D.L. (1996) 'Tumor necrosis factor-alpha-induced expression of heat shock protein 72 in adult feline cardiac myocytes.' *Am J Physiol* **270**, H1231-9.

Nandi, D., Jiang, H. and Monaco, J.J. (1996) 'Identification of MECL-1 (LMP-10) as the third IFN-gamma-inducible proteasome subunit.' *J Immunol* **156**, 2361-4.

Neefjes, J., Gottfried, E., Roelse, J., Gromme, M., Obst, R., Hammerling, G.J. and Momburg, F. (1995) 'Analysis of the fine specificity of rat, mouse and human TAP peptide transporters.' *Eur J Immunol* **25**, 1133-6.

Nelson, C.A., Roof, R.W., Mccourt, D.W. and Unanue, E.R. (1992) 'Identification of the naturally processed form of hen egg white lysozyme bound to the murine major histocompatibility complex class II molecule I-A-k.' *Proc Natl Acad Sci U S A* **89**, 7380-7383.

Newcomb, J.R. and Cresswell, P. (1993) 'Characterization of endogenous peptides bound to purified HLA-DR molecules and their absence from invariant chain-associated alpha beta dimers.' *J Immunol* **150**, 499-507.

Nicholls, A., K.A., S. and Honig, B. (1991) *Protein Struct Funct Genet* **11**, 281.

Niedermann, G., Butz, S., Ihlenfeldt, H.G., Grimm, R., Lucchiari, M., Hoschutzky, H., Jung, G., Maier, B. and Eichmann, K. (1995) 'Contribution of proteasome-mediated proteolysis to the hierarchy of epitopes presented by major histocompatibility complex class I molecules.' *Immunity* **2**, 289-99.

Nigam, S.K., Goldberg, A.L., Ho, S., Rohde, M.F., Bush, K.T. and Sherman, M. (1994) 'A set of endoplasmic reticulum proteins possessing properties of molecular chaperones includes Ca(2+)-binding proteins and members of the thioredoxin superfamily.' *J Biol Chem* **269**, 1744-9.

Nikolic-Paterson, D.J., Tesch, G.H., Lan, H.Y., Foti, R. and Atkins, R.C. (1995) 'Deoxyspergualin inhibits mesangial cell proliferation and major histocompatibility complex class II expression.' *J Am Soc Nephrol* **5**, 1895-902.

Ortiz, D.F., Ruscitti, T., McCue, K.F. and Ow, D.W. (1995) 'Transport of metal-binding peptides by HMT1, a fission yeast ABC-type vacuolar membrane protein.' *J Biol Chem* **270**, 4721-8.

Ortmann, B., Androlewicz, M.J. and Cresswell, P. (1994) 'MHC class I/beta 2-microglobulin complexes associate with TAP transporters before peptide binding.' *Nature* **368**, 864-7.

Palleros, D.R., Reid, K.L., Shi, L., Welch, W.J. and Fink, A.L. (1993) 'ATP-induced protein-Hsp70 complex dissociation requires K+ but not ATP hydrolysis.' *Nature* **365**, 664-6.

Palleros, D.R., Welch, W.J. and Fink, A.L. (1991) 'Interaction of hsp70 with unfolded proteins: effects of temperature and nucleotides on the kinetics of binding.' *Proc Natl Acad Sci U S A* **88**, 5719-23.

Panagiotidis, C.A., Burkholder, W.F., Gaitanaris, G.A., Gragerov, A., Gottesman, M.E. and Silverstein, S.J. (1994) 'Inhibition of DnaK autophosphorylation by heat shock proteins and polypeptide substrates.' *J Biol Chem* **269**, 16643-7.

Peace-Brewer, A.L., Tussey, L.G., Matsui, M., Li, G., Quinn, D.G. and Frelinger, J.A. (1996) 'A point mutation in HLA-A*0201 results in failure to bind the TAP complex and to present virus-derived peptides to CTL.' *Immunity* **4**, 505-14.

Pearson, W.R. and Lipman, D.J. (1988) 'Improved tools for biological sequence comparison.' *Proc Natl Acad Sci U S A* **85**, 2444-8.

Perraut, R., Lussow, A.R., Gavoille, S., Garraud, O., Matile, H., Tougne, C., van-Embden, J., van-der-Zee, R., Lambert, P.H., Gysin, J. and et, a. (1993) 'Successful primate immunization with peptides conjugated to purified protein derivative or mycobacterial heat shock proteins in the absence of adjuvants.' *Clin Exp Immunol* **93**, 382-6.

Peters, J.M., Franke, W.W. and Kleinschmidt, J.A. (1994) 'Distinct 19 S and 20 S subcomplexes of the 26 S proteasome and their distribution in the nucleus and the cytoplasm.' *J Biol Chem* **269**, 7709-18.

Phillips, G.J. and Silhavy, T.J. (1990) 'Heat-shock proteins DnaK and GroEL facilitate export of LacZ hybrid proteins in E. coli.' *Nature* **344**, 882-4.

Phillips, T.A., VanBogelen, R.A. and Neidhardt, F.C. (1984) 'lon gene product of Escherichia coli is a heat-shock protein.' *J Bacteriol* **159**, 283-7.

Pinet, V., Vergelli, M., Martin, R., Bakke, O. and Long, E.O. (1995) 'Antigen presentation mediated by recycling of surface HLA-DR molecules.' *Nature* **375**, 603-6.

Polla, B.S., Healy, A.M., Byrne, M. and Krane, S.M. (1987) 'Hormone 1 alpha, 25-dihydroxyvitamin D3 modulates heat shock response in monocytes.' *Am J Physiol* **252**, C640-C649.

Ponte, P., Ng, S., Engel, J., Gunning, P. and Kedes, L. (1984) 'Evolutionary conservation in the untranslated regions of actin mRNAs: DNA sequence of a human beta-actin cDNA.' *Nucleic Acids Res.* **12**, 1687-1696.

Potts, W.K. and Wakeland, E.K. (1993) 'Evolution of MHC genetic diversity: a tale of incest, pestilence and sexual preference.' *Trends Genet* **9**, 408-12.

Powis, S.J., Young, L.L., Joly, E., Barker, P.J., Richardson, L., Brandt, R.P., Melief, C.J., Howard, J.C. and Butcher, G.W. (1996) 'The rat cim effect: TAP allele-dependent changes in a class I MHC anchor motif and evidence against C-terminal trimming of peptides in the ER.' *Immunity* **4**, 159-65.

Qiu, Y., Xu, X., Wandinger-Ness, A., Dalke, D.P. and Pierce, S.K. (1994) 'Separation of subcellular compartments containing distinct functional forms of MHC class II.' *J Cell Biol* **125**, 595-605.

Raleigh, E.A., Murray, N.E., Revel, H., Blumenthal, R.M., Westaway, D., Reith, A.D., Rigby, P.W., Elhai, J. and Hanahan, D. (1988) 'McrA and McrB restriction phenotypes of some E. coli strains and implications for gene cloning [published erratum appears in Nucleic Acids Res 1995 Sep 11;23(17):3612].' *Nucleic Acids Res* **16**, 1563-75.

Rammensee, H.G., Falk, K. and Rotzschke, O. (1993) 'MHC molecules as peptide receptors.' *Curr Opin Immunol* **5**, 35-44.

Raposo, G., van-Santen, H.M., Leijendekker, R., Geuze, H.J. and Ploegh, H.L. (1995) 'Misfolded major histocompatibility complex class I molecules accumulate in an expanded ER-Golgi intermediate compartment.' *J Cell Biol* **131**, 1403-19.

Rassow, J., Voos, W. and Pfanner, N. (1995) 'Partner proteins determine multiple functions of Hsp70.' *Trends Cell Biol* **5**, 207-212.

Rawle, F.C., Tollefson, A.E., Wold, W.S. and Gooding, L.R. (1989) 'Mouse anti-adenovirus cytotoxic T lymphocytes. Inhibition of lysis by E3 gp19K but not E3 14.7K.' *J Immunol* **143**, 2031-7.

Rechsteiner, M. and Rogers, S.W. (1996) 'PEST sequences and regulation by proteolysis.' *Trends Biochem Sci* **21**, 267-271.

Rees, A.D., Donati, Y., Lombardi, G., Lamb, J., Polla, B. and Lechler, R. (1991) 'Stress-induced modulation of antigen-presenting cell function.' *Immunology* **74**, 386-92.

Reich, Z., Boniface, J.J., Lyons, D.S., Borochov, N., Wachtel, E.J. and Davis, M.M. (1997) 'Ligand-specific oligomerisation of T-cell receptor molecules.' *Nature* **387**, 617.

Retzlaff, C., Yamamoto, Y., Hoffman, P.S., Friedman, H. and Klein, T.W. (1994) 'Bacterial heat shock proteins directly induce cytokine mRNA and interleukin-1 secretion in macrophage cultures.' *Infect Immun* **62**, 5689-93.

Reyburn, H.T., Mandelboim, O., Vales-Gomez, M., Davis, D.M., Pazmany, L. and Strominger, J.L. (1997) 'The class I MHC homologue of human cytomegalovirus inhibits attack by natural killer cells.' *Nature* **386**, 514-517.

Richarme, G. and Kohiyama, M. (1993) 'Specificity of the Escherichia coli chaperone DnaK (70-kDa heat shock protein) for hydrophobic amino acids.' *J Biol Chem* **268**, 24074-7.

Riese, R.J., Wolf, P.R., Bromme, D., Natkin, L.R., Villadangos, J.A., Ploegh, H.L. and Chapman, H.A. (1996) 'Essential role for cathepsin S in MHC class II-associated invariant chain processing and peptide loading.' *Immunity* **4**, 357-66.

Rippmann, F., Taylor, W.R., Rothbard, J.B. and Green, N.M. (1991) 'A hypothetical model for the peptide binding domain of hsp70 based on the peptide binding domain of HLA.' *Embo J* **10**, 1053-9.

Roby, K.F., Yang, Y., Gershon, D. and Hunt, J.S. (1995) 'Cellular distribution of proteasome subunit Lmp7 mRNA and protein in human placentas.' *Immunology* **86**, 469-74.

Rock, K.L. (1996) 'A new foreign policy: MHC class I molecules monitor the outside world.' *Immunology Today* **17**, 131-137.

Roelse, J., Gromme, M., Momburg, F., Hammerling, G. and Neefjes, J. (1994) 'Trimming of TAP-translocated peptides in the endoplasmic reticulum and in the cytosol during recycling.' *J Exp Med* **180**, 1591-7.

Roman, E. and Moreno, C. (1996) 'Synthetic peptides non-covalently bound to bacterial hsp 70 elicit peptide-specific T-cell responses in vivo.' *Immunology* **88**, 487-92.

Roman, E., Moreno, C. and Young, D. (1994) 'Mapping of Hsp70-binding sites on protein antigens.' *Eur J Biochem* **222**, 65-73.

Romisch, K. and Schekman, R. (1992) 'Distinct processes mediate glycoprotein and glycopeptide export from the endoplasmic reticulum in Saccharomyces cerevisiae.' *Proc Natl Acad Sci U S A* **89**, 7227-31.

Rost, B. and Sander, C. (1993) 'Prediction of protein secondary structure at better than 70% accuracy.' *J Mol Biol* **232**, 584-99.

Rost, B. and Sander, C. (1994) 'Combining evolutionary information and neural networks to predict protein secondary structure.' *Proteins* **19**, 55-72.

Rotem-Yehudar, R., Groettrup, M., Soza, A., Kloetzel, P.M. and Ehrlich, R. (1996) 'LMP-associated proteolytic activities and TAP-dependent peptide transport for class 1 MHC molecules are suppressed in cell lines transformed by the highly oncogenic adenovirus 12.' *J Exp Med* **183**, 499-514.

Rudensky, A., Preston-Hurlburt, P., Hong, S.C., Barlow, A. and Janeway, C., Jr. (1991) 'Sequence analysis of peptides bound to MHC class II molecules.' *Nature* **353**, 622-7.

Rüdiger, S., Germeroth, L., Scheider-Mergener, J. and Bukau, B. (1997a) 'Substrate specificity of the dnaK chaperone determined by screening cellulose-bound peptide libraries.' *EMBO J* **16**, 1501-1507.

Rüdiger, S., A., B. and Bukau, B. (1997b) 'Interaction of Hsp70 chaperones with substrates.' *Nature Struct Biol* **4**, 342-349.

Sadasivan, B., Lehner, P.J., Ortmann, B., Spies, T. and Cresswell, P. (1996) 'Roles for Calreticulin and a novel glycoprotein, Tapasin, in the interaction of MHC class I molecules with TAP.' *Immunity* **5**, 103-114.

Sali, A. and Blundell, T.L. (1993) 'Comparative protein modelling by satisfaction of spatial restraints.' *J Mol Biol* **234**, 779-815.

Sali, A. and Overington, J.P. (1994) 'Derivation of rules for comparative protein modeling from a database of protein structure alignments.' *Protein Sci* **3**, 1582-96.

Sambrook, J., Fritsch, E.F. and Maniatis, T. (1989). 'Molecular cloning: a laboratory manual.' New York, Cold Spring Harbour Laboratory Press.

Sanderson, F., Thomas, C., Neefjes, J. and Trowsdale, J. (1996) 'Association between HLA-DM and HLA-DR in vivo.' *Immunity* **4**, 87-96.

Sanger, F., Nicklen, S. and Coulson, A.R. (1977) 'DNA sequencing with chain-terminating inhibitors.' *Proc Natl Acad Sci U S A* **74**, 5463-7.

Santoro, M.G. (1994) 'Heat shock proteins and virus replication: hsp70s as mediators of the antiviral effects of prostaglandins.' *Experientia* **50**, 1039-45.

Sayle, R.A. and Milner-White, E.J. (1995) 'RASMOL: biomolecular graphics for all.' *Trends Biochem Sci* **20**, 374.

Schindler, C. and Darnell, J.E. (1995) 'Transcriptional responses to polypeptide ligands: the JAK-STAT pathway.' *Annu Rev Biochem* **64**, 621-51.

Schirmbeck, R. and Reimann, J. (1994) 'Peptide transporter-independent, stress protein-mediated endosomal processing of endogenous protein antigens for major histocompatibility complex class I presentation.' *Eur J Immunol* **24**, 1478-86.

Schmid, D., Baici, A., Gehring, H. and Christen, P. (1994) 'Kinetics of molecular chaperone action.' *Science* **263**, 971-3.

Schneider, H.C., Berthold, J., Bauer, M.F., Dietmeier, K., Guiard, B., Brunner, M. and Neupert, W. (1994) 'Mitochondrial Hsp70/MIM44 complex facilitates protein import.' *Nature* **371**, 768-74.

Schneider, T.D. and Stephens, R.M. (1990) 'Sequence logos: a new way to display consensus sequences.' *Nucleic Acids Res* **18**, 6097-100.

Schumacher, T.N., Kantesaria, D.V., Heemels, M.T., Ashton-Rickardt, P.G., Shepherd, J.C., Fruh, K., Yang, Y., Peterson, P.A., Tonegawa, S. and Ploegh, H.L. (1994) 'Peptide length and sequence specificity of the mouse TAP1/TAP2 translocator.' *J Exp Med* **179**, 533-40.

Sealy, L., Mota, F., Rayment, N., Tatnell, P., Kay, J. and Chain, B. (1996) 'Regulation of cathepsin E expression during human B cell differentiation in vitro.' *Eur J Immunol* **26**, 1838-43.

Seemuller, E., Lupas, A., Stock, D., Lowe, J., Huber, R. and Baumeister, W. (1995) 'Proteasome from Thermoplasma acidophilum: a threonine protease.' *Science* **268**, 579-82.

Sette, A., Adorini, L., Colon, S.M., Buus, S. and Grey, H.M. . (1989) 'Capacity of intact proteins to bind to MHC class II molecules.' *J immunol* **143**, 1265-1267.

Seufert, W. and Jentsch, S. (1990) 'Ubiquitin-conjugating enzumes UBC4 and UBC5 mediate selective degradation of short-lived and abnormal proteins.' *EMBO J* **9** , 543-550.

Shawar, S.M., Cook, R.G., Rodgers, J.R. and Rich, R.R. (1990) 'Specialized functions of MHC class I molecules. I. An N-formyl peptide receptor is required for construction of the class I antigen Mta.' *J Exp Med* **171**, 897-912.

Shawar, S.M., Vyas, J.M., Rodgers, J.R., Cook, R.G. and Rich, R.R. (1991) 'Specialized functions of major histocompatibility complex class I molecules. II. Hmt binds N-formylated peptides of mitochondrial and prokaryotic origin.' *J Exp Med* **174**, 941-4.

Sherman, M.Y. and Goldberg, A.L. (1991) 'Formation in vitro of complexes between an abnormal fusion protein and the heat shock proteins from Escherichia coli and yeast mitochondria.' *Journal Of Bacteriology* **173**, 7249-7256.

Sherman, M.Y. and Goldberg, A.L. (1992) 'Involvement of the chaperonin dnaK in the rapid degradation of a mutant protein in Escherichia coli.' *Embo* **11**, 71-78.

Sherman, M.Y. and Goldberg, A.L. (1993) 'Heat shock of Escherichia coli increases binding of dnaK (the hsp70 homolog) to polypeptides by promoting its phosphorylation.' *Proceedings Of The National Academy Of Sciences Of The United States Of America* **90**, 8648-8652.

Shi, G.P., Webb, A.C., Foster, K.E., Knoll, J.H., Lemere, C.A., Munger, J.S. and Chapman, H.A. (1994) 'Human cathepsin S: chromosomal localization, gene structure, and tissue distribution.' *J Biol Chem* **269**, 11530-6.

Sierra, J.M. and Zapata, J.M. (1994) 'Translational regulation of the heat shock response.' *Mol Biol Rep* **19**, 211-220.

Sloan, V.S., Cameron, P., Porter, G., Gammon, M., Amaya, M., Mellins, E. and Zaller, D.M. (1995) 'Mediation by HLA-DM of dissociation of peptides from HLA-DR.' *Nature* **375**, 802-6.

Smith, D.B. and Johnson, K.S. (1988) 'Single-step purification of polypeptides expressed in Escherichia coli as fusions with glutathione S-transferase.' *Gene* **67**, 31-40.

Smith, G. (1994) 'Virus strategies for evasion of the host response to infection.' *Trends Microbiol* **2** , 81.

Smith, K.J., Reid, S.W., Stuart, D.I., McMichael, A.J., Jones, E.Y. and Bell, J.I. (1996) 'An altered position of the alpha 2 helix of MHC class I is revealed by the crystal structure of HLA-B*3501.' *Immunity* **4** , 203-13.

Smith, P.K., Krohn, R.I., Hermanson, G.T., Mallia, A.K., Gartner, F.H., Provenzano, M.D., Fujimoto, E.K., Goeke, N.M., Olson, B.J. and Klenk, D.C. (1985) 'Measurement

of protein using bicinchoninic acid [published erratum appears in Anal Biochem 1987 May 15;163(1):279].' *Anal Biochem* **150**, 76-85.

Snyder, H.L., Yewdell, J.W. and Bennink, J.R. (1994) 'Trimming of antigenic peptides in an early secretory compartment.' *J Exp Med* **180**, 2389-94.

Solinger, A.M., Ultee, M.E., Margoliash, E. and Schwartz, R.H. (1979) 'T-lymphocyte response to cytochrome c. I. Demonstration of a T-cell heteroclitic proliferative response and identification of a topographic antigenic determinant on pigeon cytochrome c whose immune recognition requires two complementing major histocompatibility complex-linked immune response genes.' *J Exp Med* **150**, 830-48.

Southern, E.M. (1975) 'Detection of specific sequences among DNA fragments separated by gel electrophoresis.' *J Mol Biol* **98**, 503-17.

Sozzani, S., Sallusto, F., Luini, W., Zhou, D., Piemonti, L., Allavena, P., Van-Damme, J., Valitutti, S., Lanzavecchia, A. and Mantovani, A. (1995) 'Migration of dendritic cells in response to formyl peptides, C5a, and a distinct set of chemokines.' *J Immunol* **155**, 3292-5.

Spector, N.L., Freedman, A.S., Freeman, G., Segil, J., Whitman, J.F., Welch, W.J. and Nadler, L.M. (1989) 'Activation primes human B lymphocytes to respond to heat shock.' *J Exp Med* **170**, 1763-8.

Srinivasan, M., Marsh, E.W. and Pierce, S.K. (1991) 'Characterization of naturally processed antigen bound to major histocompatibility complex class II molecules.' *Proc Natl Acad Sci U S A* **88**, 7928-32.

Srivastava, P.K. (1994) 'Heat shock proteins in immune response to cancer: the Fourth Paradigm.' *Experientia* **50**, 1054-1060.

Srivastava, P.K., Udono, H., Blachere, N.E. and Li, Z. (1994) 'Heat shock proteins transfer peptides during antigen processing and CTL priming.' *Immunogenetics* **39**, 93-8.

Stam, N.J., Spits, H. and Ploegh, H.L. (1986) 'Monoclonal antibodies raised against denatured HLA-B locus heavy chains permit biochemical characterization of certain HLA-C locus products.' *J Immunol* **137**, 2299-306.

Stanfield, R.L. and Wilson, I.A. (1995) 'Protein-peptide interactions.' *Curr Op Struct Biol* **5**, 103-113.

Stern, L.J., Brown, J.H., Jardetzky, R.S., Gorga, J.C., Urban, R.G., Strominder, J.L. and Wiley, D.C. (1994) 'Crystal structure of the human class II MHC protein HLA-DR1 complexed with an influenza virus peptide.' *Nature* **368**, 215-221.

Stevenson, M.A. and Calderwood, S.K. (1990) 'Members of the 70-kilodalton heat shock protein family contain a highly conserved calmodulin-binding domain.' *Mol Cell Biol* **10**, 1234-8.

Strandell, E., Buschard, K., Saldeen, J. and Welsh, N. (1995) 'Interleukin-1 beta induces the expression of hsp70, heme oxygenase and Mn-SOD in FACS-purified rat islet beta-cells, but not in alpha-cells.' *Immunol Lett* **48**, 145-8.

Straus, D.B., Walter, W.A. and Gross, C.A. (1988) 'Escherichia coli heat shock gene mutants are defective in proteolysis.' *Genes & Development* **2**, 1851-1858.

Suto, R. and Srivastava, P.K. (1995) 'A mechanism for the specific immunogenicity of heat shock protein-chaperoned peptides.' *Science* **269**, 1585-8.

Sztankay, A., Trieb, K., Lucciarini, P., Steiner, E. and Grubeck-Loebenstein, B. (1994) 'Interferon gamma and iodide increase the inducibility of the 72 kD heat shock protein in cultured human thyroid epithelial cells.' *J Autoimmun* **7**, 219-30.

Tabor, S. and Richardson, C.C. (1987) 'DNA sequence analysis with a modified bacteriophage T7 DNA polymerase.' *Proc Natl Acad Sci U S A* **84**, 4767-71.

Tabor, S. and Richardson, C.C. (1989) 'Selective inactivation of the exonuclease activity of bacteriophage T7 DNA polymerase by in vitro mutagenesis.' *J Biol Chem* **264**, 6447-58.

Takahashi, H., Cease, K.B. and Berzofsky, J.A. (1989) 'Identification of proteases that process distinct epitopes on the same protein.' *J Immunol* **142**, 2221-9.

Takenaka, I.M. and Hightower, L.E. (1993) 'Regulation of chicken Hsp70 and Hsp90 family gene expression by transforming growth factor-beta 1.' *J Cell Physiol* **155**, 54-62.

Takenaka, I.M., Leung, S.M., McAndrew, S.J., Brown, J.P. and Hightower, L.E. (1995) 'Hsc70-binding peptides selected from a phage display peptide library that resemble organellar targeting sequences.' *J Biol Chem* **270**, 19839-44.

Tavaria, M., Gabriele, T., Kola, I. and Anderson, R.L. (1996) 'A hitchhiker's guide to the human hsp70 family.' *Cell Stress & Chaperones* **1**, 23-28.

Terlecky, S.R. (1994) 'Hsp70s and lysosomal proteolysis.' *Experientia* **50**, 1021-1025.

Terlecky, S.R., Chiang, H.L., Olson, T.S. and Dice, J.F. (1992) 'Protein and peptide binding and stimulation of in vitro lysosomal proteolysis by the 73-kDa heat shock cognate protein.' *J Biol Chem* **267**, 9202-9.

Terlecky, S.R. and Dice, J.F. (1993) 'Polypeptide import and degradation by isolated lysosomes.' *J Biol Chem* **268**, 23490-5.

Theyssen, H., Schuster, H.P., Packschies, L., Bukau, B. and Reinstein, J. (1996) 'The second step of ATP binding to DnaK induces peptide release.' *J Mol Biol* **263**, 657-70.

Ting, J. and Lee, A.S. (1988) 'Human gene encoding the 78,000-dalton glucose-regulated protein and its pseudogene: structure, conservation, and regulation.' *Dna* **7**, 275-86.

Tomazin, R., Hill, A.B., Jugovic, P., York, I., van-Endert, P., Ploegh, H.L., Andrews, D.W. and Johnson, D.C. (1996) 'Stable binding of the herpes simplex virus ICP47 protein to the peptide binding site of TAP.' *Embo J* **15**, 3256-66.

Townsend, A., Bastin, J., Gould, K., Brownlee, G., Andrew, M., Coupar, B., Boyle, D., Chan, S. and Smith, G. (1988) 'Defective presentation to class I-restricted cytotoxic T lymphocytes in vaccinia-infected cells is overcome by enhanced degradation of antigen.' *J Exp Med* **168**, 1211-24.

Tsai, D.E., Kenan, D.J. and Keene, J.D. (1992) 'In vitro selection of an RNA epitope immunologically cross-reactive with a peptide.' *Proc Natl Acad Sci U S A* **89**, 8864-8.

Tulp, A., Verwoerd, D., Dobberstein, B., Ploegh, H.L. and Pieters, J. (1994) 'Isolation and characterisation of the intracellular MHC class II compartment.' *Nature* **369**, 120-126.

Udono, H. and Srivastava, P.K. (1993) 'Heat shock protein 70-associated peptides elicit specific cancer immunity.' *J Exp Med* **178**, 1391-6.

Urban, R.G., Chicz, R.M., Lane, W.S., Strominger, J.L., Rehm, A., Kenter, M.J., UytdeHaag, F.G., Ploegh, H., Uchanska-Ziegler, B. and Ziegler, A. (1994) 'A subset of HLA-B27 molecules contains peptides much longer than nonamers.' *Proc Natl Acad Sci U S A* **91**, 1534-8.

Ustrell, V., Pratt, G. and Rechsteiner, M. (1995) 'Effects of interferon gamma and major histocompatibility complex-encoded subunits on peptidase activities of human multicatalytic

proteases [published errata appear in Proc Natl Acad Sci U S A 1995 Apr 11;92(8):3632 and 1995 Aug 1;92(16):7605].' *Proc Natl Acad Sci U S A* **92**, 584-8.

VanBuskirk, A.M., DeNagel, D.C., Guagliardi, L.E., Brodsky, F.M. and Pierce, S.K. (1991) 'Cellular and subcellular distribution of PBP72/74, a peptide-binding protein that plays a role in antigen processing.' *J Immunol* **146**, 500-6.

VanEndert, P.M., Tampe, R., Meyer, T.H., Tisch, R., Bach, J.F. and McDevitt, H.O. (1994) 'A sequential model for peptide binding and transport by the transporters associated with antigen processing.' *Immunity* **1**, 491-500.

VanKaer, L., Ashton-Rickardt, P.G., Eichelberger, M., Gaczynska, M., Nagashima, K., Rock, K.L., Goldberg, A.L., Doherty, P.C. and Tonegawa, S. (1994) 'Altered peptidase and viral-specific T cell response in LMP2 mutant mice.' *Immunity* **1**, 533-41.

Varshavsky, A. (1992) 'The N-end rule.' *Cell* **69**, 725-735.

VonHeijne, G. (1988) 'Transcending the impenetrable: how proteins come to terms with membranes.' *Biochem. biophys. Acta* **947**, 307-333.

Vriend, G. (1990) 'WHAT IF: a molecular modeling and drug design program.' *J Mol Graph* **8**, 52-6.

Wadhwa, R., Kaul, S.C., Ikawa, Y. and Sugimoto, Y. (1993c) 'Identification of a novel member of mouse hsp70 family. Its association with cellular mortal phenotype.' *J Biol Chem* **268**, 6615-21.

Wadhwa, R., Kaul, S.C., Mitsui, Y. and Sugimoto, Y. (1993b) 'Differential subcellular distribution of mortalin in mortal and immortal mouse and human fibroblasts.' *Exp Cell Res* **207**, 442-8.

Wadhwa, R., Kaul, S.C., Sugimoto, Y. and Mitsui, Y. (1993a) 'Induction of cellular senescence by transfection of cytosolic mortalin cDNA in NIH 3T3 cells.' *J Biol Chem* **268**, 22239-42.

Wagner, I., Arlt, H., van-Dyck, L., Langer, T. and Neupert, W. (1994) 'Molecular chaperones cooperate with PIM1 protease in the degradation of misfolded proteins in mitochondria.' *Embo J* **13**, 5135-45.

Wang, T.F., Chang, J.H. and Wang, C. (1993) 'Identification of the peptide binding domain of hsc70. 18-Kilodalton fragment located immediately after ATPase domain is sufficient for high affinity binding.' *J Biol Chem* **268**, 26049-51.

Webster, T.J., Naylor, D.J., Hartman, D.J., Hoj, P.B. and Hoogenraad, N.J. (1994) 'cDNA cloning and efficient mitochondrial import of pre-mtHSP70 from rat liver.' *Dna Cell Biol* **13**, 1213-20.

Weeks, C.M., DeTitta, G.T., Miller, R. and Hauptman, H.A. (1993) *Acat Crystallogr D* **49**, 179.

Welch, W.J. and Feramisco, J.R. (1985) 'Rapid Purification of Mammalian 70,000-Dalton Stress Proteins: Affinity of the Proteins for Nucleotides.' *Mol Cell Biol* **5**, 1229-1237.

Wenzel, T. and Baumeister, W. (1995) 'Conformational constraints in protein degradation by the 20S proteasome.' *Nature struct Biol* **2**, 199-204.

West, M.A., Lucocq, J.M. and Watts, C. (1994) 'Antigen processing and class II MHC peptide-loading compartments in human B-lymphoblastoid cells.' *Nature* **369**, 147-151.

Wiech, H., Buchner, J., Zimmermann, M., Zimmermann, R. and Jakob, U. (1993) 'Hsc70, immunoglobulin heavy chain binding protein, and Hsp90 differ in their ability to

stimulate transport of precursor proteins into mammalian microsomes.' *J Biol Chem* **268**, 7414-21.

Wiertz, E.J., Jones, T.R., Sun, L., Bogyo, M., Geuze, H.J. and Ploegh, H.L. (1996) 'The human cytomegalovirus US11 gene product dislocates MHC class I heavy chains from the endoplasmic reticulum to the cytosol.' *Cell* **84**, 769-79.

Wubbolts, R., Fernandez-Borja, M. and Neefjes, J. (1997) 'MHC class II molecules: transport pathways for antigen presentation.' *Trends in cell biology* **7**, 115-118.

Xu, M., Capraro, G.A., Daibata, M., Reyes, V.E. and Humphreys, R.E. (1994) 'Cathepsin B cleavage and release of invariant chain from MHC class II molecules follow a staged pattern.' *Mol Immunol* **31**, 723-31.

Xu, X. and Pierce, S.K. (1995) 'The novelty of antigen-processing compartments.' *J. Immunol* **155**, 1652-4.

Yaglom, J.A., Goldberg, A.L., Finley, D. and Sherman, M.Y. (1996) 'The molecular chaperone Ydj1 is required for the p34CDC28-dependent phosphorylation of the cyclin Cln3 that signals its degradation.' *Mol Cell Biol* **16**, 3679-84.

Yang, B. and Braciale, T.J. (1995) 'Characteristics of ATP-dependent peptide transport in isolated microsomes.' *J Immunol* **155**, 3889-96.

Yang, S., Bergman, T., Veide, A. and Enfors, S.O. (1994) 'Effects of amino acid insertions on the proteolysis of a staphylococcal protein A derivative in Escherichia coli.' *Eur J Biochem* **226**, 847-52.

Yao, J., Dyson, H.J. and Wright, P.E. (1994) 'Three-dimensional structure of a type VI turn in a linear peptide in water solution. Evidence for stacking of aromatic rings as a major stabilizing factor.' *J Mol Biol* **243**, 754-66.

Zeigelhoffer, T., Johnson, J.L. and Craig, E.A. (1996) 'Protein folding: chaperones get Hip.' *Curr Biol* **6**, 272-275.

Zhang, J. and Walker, G.C. (1996) 'Identification of elements of the peptide binding site of DnaK by peptide cross-linking.' *J Biol Chem* **271**, 19668-74.

Zhang, Y.H., Takahashi, K., Jiang, G.Z., Zhang, X.M., Kawai, M., Fukada, M. and Yokochi, T. (1994) 'In vivo production of heat shock protein in mouse peritoneal macrophages by administration of lipopolysaccharide.' *Infect Immun* **62**, 4140-4.

Zhu, X., Zhao, X., Burkholder, W.F., Gragerov, A., Ogata, C.M., Gottesman, M.E. and Hendrickson, W.A. (1996) 'Structural analysis of substrate binding by the molecular chaperone DnaK.' *Science* **272**, 1606-14.

Zimmerman, S.B. and Trach, S.O. (1991) 'Estimation of macromolecule concentrations and excluded volume effects for the cytoplasm of Escherichia coli.' *J Mol Biol* **222**, 599-620.